







# KINETIC THEORY

OF

# ENGINEERING STRUCTURES

DEALING WITH

STRESSES, DEFORMATIONS AND WORK

FOR THE USE OF

*Blue*

STUDENTS AND PRACTITIONERS IN CIVIL ENGINEERING

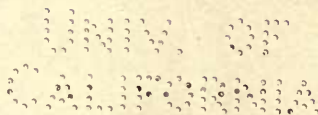
BY

DAVID A. MOLITOR, B.C.E., C.E.

AUTHOR "HYDRAULICS OF RIVERS, WEIRS AND SLUICES," ETC.; MEM. AM. SOC. C. E.; MEM. DETROIT  
ENGINEERING SOC.; MEM. SOC. FOR THE PROM. ENG. EDU.; MEM. A. A. A. S., ETC.;

FORMERLY DESIGNING ENGINEER ISTHMIAN CANAL COMMISSION;

PROFESSOR IN CIVIL ENGINEERING, CORNELL UNIVERSITY.



McGRAW-HILL BOOK COMPANY

239 WEST 39TH STREET, NEW YORK

6 BOUVERIE STREET, LONDON, E.C.

1911



TG 260  
M7

GENERAL

Copyright, 1910,  
BY  
DAVID A. MOLITOR

THE SCIENTIFIC PRESS  
ROBERT DRUMMOND AND COMPANY  
BROOKLYN, N. Y.

THE SCIENTIFIC PRESS  
ROBERT DRUMMOND AND COMPANY  
BROOKLYN, N. Y.

## PREFACE

"ALL that mankind has done, thought, gained, or been; it is lying in magic preservation in the pages of books"; and so in presenting this work for publication, the author hopes to preserve the results of many years of painstaking labors, study and experience, to civil engineering, his chosen profession.

The field of usefulness which it is proposed to supply is that of an advanced treatise on stresses and deformations in engineering structures, for the use of students and practitioners in civil engineering and particularly for specialists engaged in the design of so-called "higher structures" requiring more than the ordinary methods of statics for their analysis.

The reader is supposed to possess a thorough knowledge of higher mathematics, including the calculus; also, of the elements of statics, embracing the composition and resolution of forces, force and equilibrium polygons, etc. All these are usually given in the two first years of a Civil Engineering course in connection with mathematics and mechanics.

Details pertaining to the design of bridge members and connections are not dealt with.

The present volume might advantageously be employed as a text-book in bridge stresses with the aim of giving a more thorough training in the analysis of stresses and deformations by economizing somewhat on the time at present devoted to detailing and shop practice, which is not really justified in a four-year course of theoretical preparation.

In the opinion of the author this would be highly desirable, because details and shop practice can best be learned in the shop, where experience is the teacher. It devolves on the college to give to its students that thorough theoretical training which they cannot readily acquire in practice, a feature which must ultimately distinguish the college-bred engineer from the purely practical man.

The present work, which is the gradual evolution of years of labor, thus represents an effort to place before the profession a treatise on the analysis of engineering structures which is based on the most advanced theories and researches of the present time.

To enhance the educational value of the book, each subject is prefaced by a few brief historical remarks and all important theorems bear the names of their originators, a practice which has been shamefully neglected by many modern writers.

The author has made free use of any and all literature bearing on the various subjects treated and hereby expresses his grateful acknowledgment to all who have contributed to the sum total of our present knowledge. Prominent among these should be

mentioned Hooke, Bernoulli, Lagrange, Coulomb, Navier, Lamé, de Saint-Venant, Clapeyron, and Menabrea, as the founders of the theories of elasticity and virtual work.

To Clerk Maxwell, Castigliano, Mohr, Fraenkel, Culmann, Winkler, Mueller-Breslau, Engesser, Weyrauch, Manderla, Asimont, Landsberg, Melan, Zimmerman, Ritter, Land, and Mehrrens, we are indebted for advancing these theories to their present state of perfection and usefulness. Professor Otto Mohr enjoys the high distinction of being the foremost originator of novel principles in the analysis of engineering structures.

A bibliography of the works used by the author will be found at the end of this volume.

The author has avoided a sharp differentiation between analytic and graphic methods and uses both without discrimination, aiming always to secure the most practical solution for any problem in hand.

While this work was produced with very great care and diligence, hoping to eliminate typographical and other errors, it is certain that some have escaped detection. The author, therefore, invites the kind indulgence of the reader and will be truly thankful for having his or the publishers' attention called to any errors that may be discovered.

Finally, as the love liberated in our work is a true manifestation of character, so may the present production reflect the character of, the man, the engineer, the author.

ITHACA, N. Y., September 9, 1910.



## DEFINITIONS OF TERMS USED THROUGHOUT THIS WORK

FREQUENTLY some of the letters are employed in a special connection other than here defined, but in such cases the definitions locally given will prevent misunderstandings.

ART. 3.  $p$  = number of pin points of any frame.

$m$  = number of members of any frame.

$n$  = number of redundant conditions in any structure.

$n'$  = number of external redundants in any structure.

$n''$  = number of internal redundants in any structure.

$e$  = number of elements or simple frames in a structure.

$\Sigma r$  = number of necessary reaction conditions for any structure.

$\Sigma$  = the summation sign.

ART. 4.  $S$  = total stress in any member of a frame resulting from any loads  $P$  or other causes and  $+$  for tension.

$\bar{S}$  = the stress produced in any member by applied loads  $\bar{P}$ .

$f$  = the unit stress in any member,  $+$  for tension.

$l$  = length of any member or span of a structure for the condition of no stress.

$\Delta l$  = change in length of a member due to any cause, positive for elongation.

$F$  = cross-section of any member, prismatic in form.

$t$  = a uniform change in temperature in degrees,  $+$  for rise.

$\epsilon$  = coefficient of expansion per degree temperature.

$E$  = Young's modulus of elasticity for direct stress.

$\alpha$  = the angle which a member makes with the  $x$  axis of coordinates.

$\beta$  = the angle which a member makes with the  $y$  axis of coordinates.

$m$  = any point of a structure chosen for illustration.

$\rho = l/EF$  = the extensibility of a member employed for brevity.

$R$  = any reaction force, or condition, of a structure resulting from loads  $P$ .

$\bar{R}$  = any reaction force, or condition, of a structure resulting from loads  $\bar{P}$ .

$\Delta r$  = any displacement of the point of application of a force  $R$  in the direction of this force.

$P$  = any external load or force applied to a structure.

$\bar{P}$  = a load or force identical in position and point of application with the force  $P$  but having a different intensity.

ART. 5.  $\Delta$  = any displacement of a pin point.

$\delta$  = the displacement of the point of application of any force  $P$  in the direction of this force.

$A$  = actual work = force times distance through which the force moves.

$A_e$  = the positive or externally applied work of deformation of any structure.

$A_i$  = the negative or internally overcome work of deformation of any structure.

$W$  = a virtual work of deformation.

$\bar{W}$  = a virtual work of deformation produced by a conventional case of loading.

ART. 7.  $X_a, X_b, X_c$ , etc., are the stresses in redundant members or reactions  $A, B, C$ , etc.

$S_o$  = the stress in any member of a principal system, due entirely to loads  $P$  when all redundant conditions  $X$  are removed. This is known as condition  $X=0$ .

$S_a$  = the stress in any member of a principal system, due entirely to the conventional loading  $X_a=1$ , applied to the principal system. Condition  $X_a=1$ .

$S_b, S_c$ , etc., are similarly defined for conventional loadings  $X_b=1; X_c=1$ , etc.

$S_t$  = the stress in any member of a principal system produced by a uniform change in temperature.

$R_t$  = a reaction produced by a uniform change in temperature.

$M_t$  = a moment produced by a uniform change in temperature.

$R_o, R_a, R_b$ , etc., have definitions analogous to those given for  $S_o, S_a, S_b$ , etc.

$M_o, M_a, M_b$ , etc., are moments similarly defined for the conventional loadings.

$\delta_a, \delta_b, \delta_c$  are changes in the lengths of redundant members or supports  $X_a, X_b, X_c$ , respectively.

$L$  represents the length of span of a composite structure.

ART. 8.  $\delta_{ma}$  = the displacement of the point of application  $m$  of any load  $P_m$ , in the direction of this load, when the principal system is loaded only with  $X_a=1$ . Condition  $X_a=1$ .

$\delta_{mb}$  = a similar displacement of the point  $m$  for the conventional loading  $X_b=1$ . Condition  $X_b=1$ .

$\delta_{mc}$  = the same for condition  $X_c=1$ .

$\delta_{aa}$  = the change in length of the member  $a$  for condition  $X_a=1$ .

$\delta_{ab}$  = the change in length of the member  $a$  for condition  $X_b=1$ .

$\delta_{ba}$  = the change in length of the member  $b$  for condition  $X_a=1$ , etc.

$\delta_{at}$  = the change in length of the member  $a$  resulting from a change in temperature of  $t^\circ$ , when the principal system is not otherwise loaded, hence  $X=0, P=0$ .

$\delta_{bt}, \delta_{ct}$  are similarly defined for members  $b$  and  $c$  respectively.

ART. 13.  $f_x, f_y, f_z$  = the unit normal stresses in the directions  $X, Y$ , and  $Z$ , respectively, for any isotropic body.

$\tau_{xy}$  and  $\tau_{xz}$  = the unit tangential stresses in the  $YZ$  plane.

$\tau_{yx}$  and  $\tau_{yz}$  = the unit tangential stresses in the  $XZ$  plane.

$\tau_{zx}$  and  $\tau_{zy}$  = the unit tangential stresses in the  $XY$  plane.

$G$  = the modulus of tangential stress.

$m$  = the Poisson number or ratio of lateral to longitudinal deformation.

ART. 14.  $N$  = a normal thrust on any section.

$R$  = any oblique thrust.

$Q$  = a tangential force or shear.

$I$  = the moment of inertia of any cross-section.



$y$ =an ordinate usually the distance from the neutral axis to the extreme fiber of a cross-section.

$h$ =height of a section.

$b$ =base or breadth of a section.

$\beta$ =coefficient of shearing strain, Eq. (14L) and Eq. (14M).

ART. 16.  $\omega$ =weight of a moving body.

$H$ =height of fall. Later used to represent the horizontal thrust of an arch, also, the pole distance of a force polygon.

$v$ =velocity at instant of impact.

$g$ =acceleration due to gravity.

ART. 17.  $\eta$ =any ordinate to an influence line.

$d$ =a panel length.

$p$ =uniform moving load per unit of length.

ART. 18.  $m$ =a load point, being any one of the many possible points of application of a certain moving load.

$n$ =the point for which an influence line is drawn. Also, the location of a section under consideration.

ART. 20.  $i$ =the load divide for positive and negative effects. For arches the load divide is sometimes designated by  $d$ .

ART. 21.  $r$ =the lever arm of a member in the equation  $S=M/r$ .

$S_a$ =the stress in any member  $S$  due to a reaction unity at  $A$ , when the load producing this reaction is to the right of the section.

$S_b$ =the stress in the same member due to a reaction unity at  $B$ , when the load producing this reaction is to the left of the section.

ART. 28.  $e$ =the kernel point for the extreme fiber of the extrados of a solid web arch section.

$i$ =the kernel point for the extreme fiber of the intrados of the same arch section.

ART. 35.  $w$ =an elastic load, representing an abstract number without any particular unit of measure.

ART. 45.  $\bar{S}_o$ =the stress in any member of a statically indeterminate frame for the condition  $X=0$  and  $P=1$ .

$\bar{M}_o$ =a moment for the same conditions.

$\bar{A}_o$ =the reaction at  $A$  for the same conditions.

$\mu$ =an influence line factor by which all ordinates must be multiplied to obtain the actual influences.





# CONTENTS

---

	PAGE
PREFACE.....	v
DEFINITIONS OF TERMS.....	vii
INTRODUCTION.....	1

## CHAPTER I

### REACTIONS AND REDUNDANT CONDITIONS

1. Reaction Conditions.....	5
2. Structural Redundancy.....	6
3. Tests for Structural Redundancy.....	7

## CHAPTER II

### THEOREMS, LAWS, AND FORMULÆ FOR FRAMED STRUCTURES

4. Elastic Deformations, Fundamental Equations.....	11
5. General Work Equations for any Frame.....	14
6. Displacements of Points. Statically Determinate Structures.....	18
7. Indeterminate Structures, by Mohr's Work Equation.....	19
8. Indeterminate Structures, by Maxwell's Law.....	24
9. Prof. Maxwell's Theorem (1864).....	27
10. Theorems Relating to Work of Deformation.....	29
(a) Menabrea's law (1858). Theorem of least work.....	29
(b) Castigliano's law (1879). Derivative of the work equation.....	30
11. Temperature Stresses follow Menabrea's and Castigliano's Laws.....	31
12. Stresses Due to Abutment Displacements.....	32

## CHAPTER III

### THEOREMS, LAWS, AND FORMULÆ FOR ISOTROPIC BODIES

13. General Work Equations.....	34
14. Work of Deformation due to Shearing Stress.....	38
15. Work of Deformation for any Indeterminate Straight Beam.....	41
16. Work of Deformation due to Dynamic Impact.....	43



## CHAPTER IV

## INFLUENCE LINES AND AREAS FOR STATICALLY DETERMINATE STRUCTURES

	PAGE
17. Introductory .....	46
18. Influence Lines for Direct Loading .....	48
19. Influence Lines for Indirect Loading .....	50
20. The Load Divide for a Truss .....	51
21. Stress Influence Lines for Truss Members .....	52
22. Reaction Summation Influence Lines .....	54
23. Positions of a Moving Train for Maximum and Minimum Moments .....	57
24. Positions of a Moving Train for Maximum and Minimum Shears .....	62

## CHAPTER V

## SPECIAL APPLICATIONS OF INFLUENCE LINES TO STATICALLY DETERMINATE STRUCTURES

25. Double Intersection Trusses .....	65
26. Cantilever Bridges .....	67
27. Three-hinged Framed Arches .....	72
28. Three-hinged, Solid Web and Masonry Arches .....	78
29. Skew Plate Girder for Curved Double Track .....	80
30. Trusses with Sub-divided Panels .....	83

## CHAPTER VI

## DISTORTION OF A STATICALLY DETERMINATE FRAME BY GRAPHICS

31. Introductory .....	87
32. Distortions due to Changes in the Lengths of the Members .....	87
33. Rotation of a Rigid Frame about a Fixed Point .....	89
34. Special Applications of Williot-Mohr Diagrams .....	91

## CHAPTER VII

## DEFLECTION POLYGONS OF STATICALLY DETERMINATE STRUCTURES BY ANALYTICS AND GRAPHICS

35. Introductory .....	99
36. First Method, according to Prof. Mohr .....	100
(a) Influence on the deflections due to chord members .....	100
(b) Influence on the deflections due to web members .....	102
(c) The deflection polygon for the loaded chord .....	104
37. Second Method, according to Prof. Land .....	107
(a) The $w$ loads in terms of the unit stresses in the members .....	107
(b) To find the changes in the angles of a triangle .....	107
(c) To evaluate the elastic loads $w$ in terms of the angle changes .....	109
38. Horizontal Displacements .....	114
39. Deflections of Solid Web Beams .....	117



## CHAPTER VIII

## DEFLECTION INFLUENCE LINES FOR STATICALLY DETERMINATE STRUCTURES

	PAGE
40. Influence Lines for Elastic Displacements .....	122
41. Special Applications of Displacement Influence Lines .....	124
(a) Cantilever beam, deflection polygon .....	124
(b) Simple truss, displacement of any pin point in any direction .....	125
(c) Three-hinged arch, rotation between two lines .....	125

## CHAPTER IX

## INFLUENCE LINES FOR STATICALLY INDETERMINATE STRUCTURES

42. Influence Lines for One Redundant Condition .....	127
(a) When the redundant condition is internal .....	128
(b) When the redundant condition is external .....	128
43. Influence Lines for Two Redundant Conditions .....	130
44. Simplification of Influence Lines for Multiple Redundancy .....	132
(a) Structures having two redundant conditions .....	133
(b) Structures having three redundant conditions .....	135
45. Stress Influence Lines for Structures Involving Redundancy .....	137
(a) Multiple redundancy .....	137
(b) One redundant condition .....	139

## CHAPTER X

## SPECIAL APPLICATIONS OF INFLUENCE LINES TO STATICALLY INDETERMINATE STRUCTURES

46. Simple Beam with One End Fixed and Other End Supported .....	140
47. Plate Girder on Three Supports .....	143
48. Truss on Three Supports .....	148
49. Two-hinged Solid Web Arch or Arched Rib .....	153
50. Two-hinged Spandrel Braced Arch .....	166
51. Two-hinged Arch with Cantilever Side Spans .....	176
52. Fixed Framed Arches .....	178

## CHAPTER XI

## DESIGN OF STATICALLY INDETERMINATE STRUCTURES

53. Methods for Preliminary Designing .....	194
54. On the Choice of the Redundant Conditions .....	202
55. Solution of the General Case of Redundancy .....	203
56. Effect of Temperature on Indeterminate Structures .....	206
57. Effect of Shop Lengths and Abutment Displacements .....	208

## CHAPTER XII

## STRESSES IN STATICALLY DETERMINATE STRUCTURES

	PAGE
58. Dead Load Stresses .....	210
(a) General considerations .....	210
(b) Aug. Ritter's methods of moments (1860) .....	211
(c) The method of stress diagrams .....	213
59. Live Load Stresses .....	218
(a) The critical positions of a train of moving loads .....	218
(b) The method of influence lines .....	218
(c) Discussion of methods in common use .....	219
(d) The author's method .....	219

## CHAPTER XIII

## SECONDARY STRESSES

60. The Nature of Secondary Stresses .....	226
61. Secondary Stresses in the Plane of a Truss due to Riveted Connections .....	227
62. Secondary Stresses in Riveted Cross Frames of Trusses .....	244
(a) Dead and live load effects .....	244
(b) Wind effects .....	247
63. Secondary Stresses due to Various Causes .....	251
(a) Bending stresses in the members due to their own weight .....	251
(b) Secondary stresses in pin-connected structures .....	253
(c) The effect of eccentric connections .....	255
(d) Effect of temperature and erroneous shop lengths .....	256
64. Additional Stresses due to Dynamic Influences .....	256
(a) Forces acting longitudinally on a structure .....	256
(b) Forces acting transversely to a structure .....	258
(c) Forces acting vertically on a structure .....	262
(d) Fatigue of the material .....	265
(e) Unusual load effects .....	266
65. Concluding Remarks .....	267
(a) Features in design intended to diminish secondary and additional stresses .....	267
(b) Final combination of stresses as a basis for designing .....	268

## CHAPTER XIV

## MITERING LOCK GATES

66. The Nature of the Problem .....	271
67. The Theory of the Analysis .....	273
68. Example: Upper Gate, Erie Canal Lock No. 22 .....	279

## CHAPTER XV

## FIXED MASONRY ARCHES

	PAGE
69. General Considerations .....	298
70. Modern Methods of Construction .....	301
71. Preliminary Designs .....	304
72. Determination of the Redundant Conditions by the Theory of Elasticity .....	309
73. Co-ordinate Axes and Elastic Loads .....	314
74. Influence Lines for $X_a$ , $X_b$ , $X_c$ , and $M_m$ .....	317
75. Temperature Stresses .....	318
76. Stresses on any Normal Arch Section .....	320
77. Maximum Stresses and Critical Sections .....	322
78. Resultant Polygons .....	324
79. Example: 150-foot Concrete Arch .....	326
(a) Given data and preliminary design .....	326
(b) Analysis of the preliminary design by the theory of elasticity, treating the structure as symmetric .....	331
(c) Analysis as under (b), treating the structure as unsymmetric. ....	346

## BIBLIOGRAPHY

Theory of Elasticity .....	359
Graphostatics .....	359
General Treatises .....	360
Secondary and Additional Stresses .....	360
Special Treatises on Arches .....	361





# ENGINEERING STRUCTURES







# KINETIC THEORY

OF

# ENGINEERING STRUCTURES

---

## INTRODUCTION

**The work of deformation** constitutes the basis for the solution of all those problems which involve the elastic properties of the material and which are not susceptible to analysis by the methods of pure statics.

Work is the product of a constant force into the displacement of its point of application in the direction of the force.

When a prismatic body of length  $l$  and cross-section  $F$  is either lengthened or shortened a small amount  $\Delta l$  within the elastic limit, by a force  $S$  gradually produced without impact, then a certain amount of work or kinetic energy is stored up in the body. In the instant when the force ceases to alter the length a condition of static equilibrium is established and the total kinetic energy stored then assumes the form of potential energy or energy of position. When the force is gradually released and the body is allowed to resume its original length, the potential energy is liberated.

The work of deformation or applied kinetic energy may be thus expressed:

$$A = \int_0^{\Delta l} S d(\Delta l) = \frac{S}{\Delta l} \int_0^{\Delta l} \Delta l d(\Delta l) = \frac{S \Delta l^2}{2 \Delta l} = \frac{S \Delta l}{2} \dots \dots \dots (1)$$

**The principle of virtual work.** When a rigid body is set in motion by any group of forces, then the kinetic energy imparted is equal to the algebraic sum of all the work performed by the several applied forces.

A real displacement can never result in zero work, because motion cannot exist without the presence of a force, and the combination of force and motion constitutes work.

However, for a state of equilibrium wherein the applied forces do not actually alter the motion, a certain equilibrium proposition may be formulated by considering possible displacements that might be produced but may or may not be real. Such displacements are called *virtual*, and any work resulting therefrom is called *virtual work*.





taking advantage of some of the more advanced ideas presented in the earlier chapters. Special attention is directed to Art. 59, dealing with stresses due to concentrated live loads.

Chapter XIII gives a brief treatment of secondary stresses and the two last chapters are devoted to the problems of mitering lock gates and fixed masonry arches.

It is more than likely that the use of the word *kinetic* in the title of the present volume will be questioned by some. However, after long and careful consideration the author concluded that he was justified in employing the term without really departing from the best modern dictionary definitions. It is true that in hydraulics the term *kinetic energy* is exclusively confined to represent the static equivalent  $h = v^2/2g$  of a dynamic head. In mechanics generally, the expression is almost limited to the term  $Wv^2/2g = mv^2/2$ , representing the potential or kinetic energy of a moving mass. Otherwise the term is not met with.

While the author employs the term *kinetic* in connection with engineering structures which are, generally considered, at rest, it is precisely with the same idea above expressed in the mechanical sense. That is, a bridge or other structure composed of elastic material *ceases to be at rest* the moment it is acted upon by external forces. The distinction between the previous and present uses of the term is, therefore, only relative, being here applied in a different field and to a special class of bodies, where the displacements are small and follow certain empiric laws depending on the elastic properties of the material. Strictly speaking, then, we have no license to regard an elastic structure as statically at rest only when it is neither stressed nor distorted.

The equation of work is thus applied to a structure in the sense that the latter is a mechanical contrivance or machine in motion, instead of an inelastic body at rest. It is true that this motion prevails only while a change in the *static balance* is taking place, as when loads are added to, or removed from, the structure, but this may apply to any mechanism of interrupted activity.

Therefore, while we speak of a structure as in static equilibrium, we may also speak of it as in a state of dynamic equilibrium, a state which the structure assumes in the instant that the superimposed loads do not produce any further elastic deformations. The same would be true when all the loads are entirely removed, in which case the dynamic equilibrium returns to the special state of static equilibrium. This is merely a broader viewpoint of the subject, embracing at once all of the conditions as they really exist in a frame sustaining loads. The term *kinetic* thus appears quite appropriate to the use and application here made.

For the same structure the magnitude of the deformation of the deflection is a direct function of the loads, the unit stresses which they produce, and the elasticity of the material.

On the other hand, the stiffness of a given structure is independent of the magnitudes of the unit stresses, but depends entirely on the ability of the structure to resist stress and this in turn is a function of the elasticity of the material and the geometric shape of the structure.

Theoretically speaking, and disregarding economy, a structure of maximum stiffness is one of infinite height compared to its span, resulting in zero stress; and con-



versely, a structure of minimum stiffness is one of zero height involving infinite stress.

Maximum stress never occurs simultaneously in the chords and web of any structure. The maximum total load produces maximum chord stresses, but only a small fraction of the maximum web stress. Hence, the influence of the web on the total deflection of a bridge is always small as compared with that produced by the chords and is frequently negligible.

Throughout the present treatise, excepting Chapter XIII, all members of a frame are supposedly connected at their ends by frictionless pins, and no account is taken of the so-called secondary stresses occasioned in the members by friction on these pins or by the rigidity of riveted connections. Chapter XIII deals separately with the secondary stresses induced by riveted connections and friction on pins, etc.

Unless otherwise specifically stated, a clockwise moment of forces on the left of a section is regarded as positive, so also an upward shear on the left side of a section. Tensile stress and elongation are positive, while compressive stress and contraction are negative. Work is positive when the direction of a force coincides with the direction of the displacement of its point of application, independently of the algebraic signs of the forces or stresses and the displacements.

The nomenclature is uniform throughout, though in a few instances slight departures from American custom became necessary owing to conflicts encountered in combining so many subjects in one book. The definitions of terms are always given in appropriate places and also in summary form following the table of contents.

Equations and figures are designated by letters and numbers facilitating the matter of locating cross-references. The number refers to the article and the letter to the position of the equation, figure or table in that article. The article number appears in the heading of every page.

## CHAPTER I

### REACTIONS AND REDUNDANT CONDITIONS

#### ART. 1. REACTION CONDITIONS

The general purpose of engineering structures, of the class here considered, is to carry loads over otherwise impassable distances to certain fixed points.

The distances are called the spans, and the fixed points, to which the loads are finally transmitted, are called the supports or reactions.

It is thus clear that the sum total of the superimposed loads, together with the weight of the structure, must exactly equal the sum of the vertical reaction forces when equilibrium exists.

The nature and purpose of a structure determine the manner in which it must be supported to insure stability under all circumstances that are likely to occur.

This can always be accomplished by one of three types of supports known, respectively, as movable, hinged, and fixed. They are illustrated in Figs. 1A, 1B, and 1C.

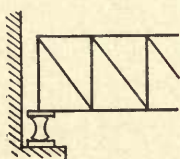


FIG. 1A.

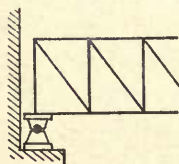


FIG. 1B.

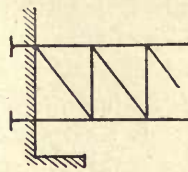


FIG. 1C.

Fig. 1A shows the type of support known as *movable*, which can exert a single upward reaction only. Any lateral force applied to such a support would result in horizontal displacement provided the roller is frictionless.

Fig. 1B shows a *hinged support* and can resist horizontal and vertical forces or any resultant of these.

Fig. 1C represents a *fixed support* which may be made to resist any direct forces and a bending moment.

Statically considered, the first type satisfies one stability condition, the second type offers two such conditions, and the third type supplies three stability conditions. These conditions may be represented by forces as shown in Figs. 1D, 1E, and 1F.

Let  $r$  represent a single vertical or horizontal force to be known as a *reaction condition*. Then the three types of supports will involve, respectively, one, two, and three such conditions. Each reaction condition may be represented by a short link, or member, which may transmit direct stress only; that is pure tension or compression.

Hence, for a single truss on two supports, with one end movable and the other end hinged, the number of reaction conditions is  $\Sigma r = 3$ . Also, for a two-hinged arch, with both ends on hinged supports,  $\Sigma r = 4$ ; and for an arch without hinged ends, commonly called a fixed arch,  $\Sigma r = 6$ .

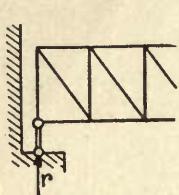


FIG. 1D.

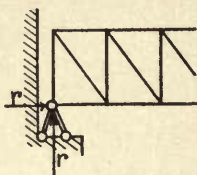


FIG. 1E.

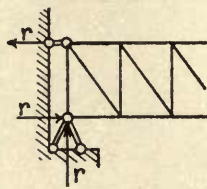


FIG. 1F.

## ART. 2. STRUCTURAL REDUNDANCY

Any structure, statically considered, may be classed as determinate or indeterminate, depending on the manner in which it is supported, and the arrangement of the members employed to form the structure.

A structure is **externally indeterminate** when it involves more than three reaction conditions for a single truss element or frame. This implies that the reactions are counted with the external forces.

A structure is **internally indeterminate** when it includes more members within its frame than are required for internal stability according to the conditions for static equilibrium, regardless of the reactions.

Hence external and internal redundancy may exist simultaneously. The terms *redundant* and *indeterminate*, as here used, are synonymous with impossible, only in so far as the laws of pure statics are concerned. However, the modifying term *static* may sometimes be omitted for the sake of brevity. Thus *indeterminate* will always mean *statically indeterminate*.

The conditions for static equilibrium applied to any structure as a whole are represented by the following equations:

$$\Sigma H = 0, \quad \Sigma V = 0, \quad \text{and} \quad \Sigma M = 0, \quad . . . . . (2A)$$

wherein  $\Sigma H$  is the sum of all the horizontal components of the external forces, including the reactions;  $\Sigma V$  is the sum of all the vertical components of these forces and reactions; and  $\Sigma M$  is the sum of the moments of these forces and reactions about any point in the plane of the structure. The sums are always algebraic sums.

These condition equations apply equally to all forces (externally applied and internal stresses) active about any pin point of any structure.

When the external forces are not thus balanced among themselves and with the internal stresses, then a structure is said to be *statically under determinate* or to be unstable.

A structure is, therefore, **externally determinate** when the three condition equations for static equilibrium suffice to determine the reactions.



**A structure is internally determinate** when its members are arranged to form triangles in such manner that the successive removal of pairs of members uniting in a point, finally reduces the structure to a single triangle. The triangle is thus seen to be the primary element of all determinate systems.

**A structure is in every sense determinate** when all reactions and stresses can be expressed purely as functions of the externally applied loads, unaffected by all temperature changes or temperature inequalities, and small reaction displacements.

### ART. 3. TESTS FOR STRUCTURAL REDUNDANCY

Let  $p$  = number of pin points of any given frame.

$m$  = number of members in the frame.

$n$  = total number of redundant conditions.

$n'$  = number of external redundant conditions.

$n''$  = number of internal redundant conditions.

$e$  = number of elements or simple frames in a structure.

$\Sigma r$  = number of necessary reaction conditions.

Then for any statically determinate structure

$$2p = m + \Sigma r, \quad . . . . . (3A)$$

which condition must be satisfied in any event, and when satisfied, the structure is always statically determinate but not always stable. This exception will be discussed below.

When

$$2p > m + \Sigma r, \quad . . . . . (3B)$$

then the structure is not in stable equilibrium and may be called statically insufficient.

When  $2p < m + \Sigma r$  then the structure involves redundant conditions or members, the total number of which is given by the equation,

$$n = m + \Sigma r - 2p, \quad . . . . . (3C)$$

wherein a negative  $n$  would indicate static insufficiency.

The number of necessary reaction conditions  $r$  for any structure depends on the number of frame elements or simple frames of which the structure may be composed. Hence in order to distinguish whether the  $n$  redundant conditions are external, internal, or both, it will be necessary to determine one or the other of these by a separate criterion. This criterion is readily established for the reactions. Thus in Art. 1,  $\Sigma r = 3$  was found to express the number of required reaction conditions for a simple truss on two supports.

A composite structure, which may be composed of any number  $e$  of simple truss frames, each one of which is directly supported by piers at one or two points, will always have more than three reaction conditions. The requisite number of reaction conditions for any statically determinate structure is

$$\Sigma r = 3 + e - 1 = e + 2. . . . . (3D)$$

The number of external redundant conditions  $n'$ , for any given structure of  $e$  elements, is thus:

$$n' = \Sigma r - e - 2, \quad \dots \dots \dots (3E)$$

and hence the number of internal redundant conditions must be

$$n'' = n - n' \dots \dots \dots (3F)$$

The number of elements entering into the makeup of any structure is thus an important consideration in establishing whether the redundant conditions, indicated by Eq. (3c), are external or internal. In general, a truss element may be defined as a frame or girder which in itself constitutes a simple truss or beam. The illustrations given below will serve to amplify this definition.

The exception to Eq. (3A), when a structure is apparently determinate but unstable, will now be discussed.

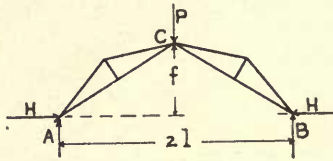


FIG. 3A.

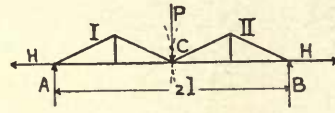


FIG. 3B.

The three-hinged arch, in Fig. 3A, is in every sense a determinate, stable structure for which the horizontal thrust  $H = Pl/2f$ . All the reactions  $A$ ,  $B$ , and  $H$  are finite quantities and the stresses in the several members are also finite. This will always remain true except when the middle ordinate  $f=0$ , whence  $H=\infty$ .

This special case is illustrated in Fig. 3B, where  $\overline{ACB}$  is a straight line and the load  $P$  cannot produce stress without causing a slight rotation of the two elements I and II about the points  $A$  and  $B$ . Hence equilibrium does not exist until rotation through a small arc  $ds$  has taken place and the stress along  $\overline{AC}$  and  $\overline{CB}$  is then infinite. Structures involving this peculiar feature of the well-known "toggle joint" are regarded temporarily unstable, and equilibrium in them can be established only after certain infinitesimally small displacements have taken place.

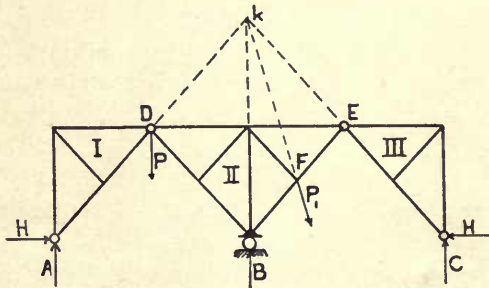


FIG. 3C.

Another striking example of this kind is shown in Fig. 3c, where the supports  $A$  and  $C$  are hinged, and the support  $B$  is movable, and hence  $\Sigma r=5$ . Also  $m=19$  and  $p=12$ , making  $n=m+\Sigma r-2p=0$ .

This structure is made up of three elements I, II and III, each one of which may be regarded as a simple frame in direct contact with a support. Hence  $e=3$  and  $n'=\Sigma r-e-2=0$ .

This proves the structure to be internally as well as externally statically determinate,

though a condition of temporary instability exists because the point  $k$  is common to the paths of the three elements in the first instant of rotation about their respective centers of rotation at  $A$ ,  $B$ , and  $C$ .

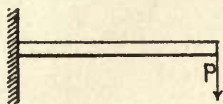


FIG. 3D.

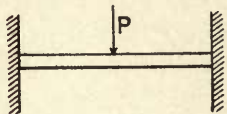


FIG. 3E.

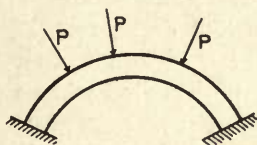


FIG. 3F.

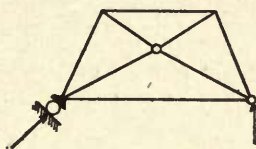


FIG. 3G.

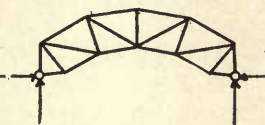


FIG. 3H.

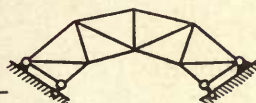


FIG. 3J.

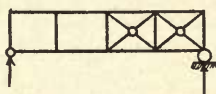


FIG. 3K.

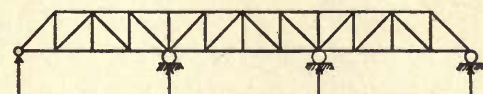


FIG. 3L.

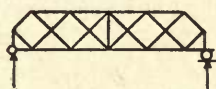


FIG. 3M.

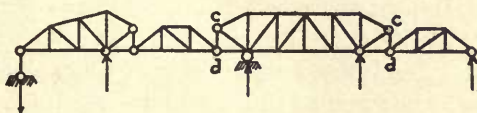


FIG. 3N.

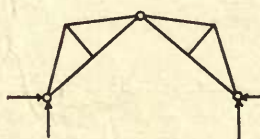


FIG. 3O.

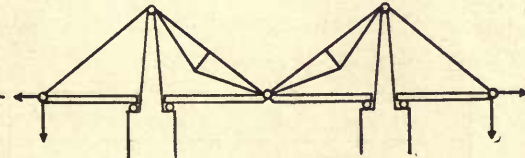


FIG. 3P.

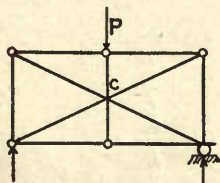


FIG. 3Q.



FIG. 3R.

The point  $k$  may thus be regarded as an imaginary crown hinge for a three-hinged arch  $\overline{AkC}$ . Hence a load  $P$ , acting at  $D$ , will cause a small rotation of the three elements before equilibrium is established and then the stresses become infinite.



The only loads which will not cause rotation are those passing through  $k$ , but for any of these loads, there will result an infinite number of conditions of equilibrium and as many different systems of stresses.

The following illustrations are presented for the purpose of showing various applications of Eqs. (3c) and (3E). Figs. 3D to 3M are all examples of simple truss elements for which  $e=1$ . Fig. 3N has six such elements counting the two suspenders  $\overline{cd}$ , which must always be included when the elements alone are regarded. For Fig. 3O,  $e=2$  and for Fig. 3P,  $e=8$ .

It should also be noted that Eq. (3c) is applicable to any structure as a whole, whether composed of one or many elements. This equation will apply when the individual members and pin points are counted and also when the elements and their connecting points only are considered.

For example, in Fig. 3N, there are 56 members, 32 pin points, and 8 reaction conditions, making  $n = \Sigma r + m - 2p = 8 + 56 - 2 \times 32 = 0$ , whence the structure is statically determinate. Now when the elements alone are considered, then  $e = m = 6$ ,  $p = 7$  and  $\Sigma r = 8$ , and Eq. (3c) again gives  $n = \Sigma r + m - 2p = 8 + 6 - 2 \times 7 = 0$ . Eq. (3E) gives  $n' = \Sigma r - e - 2 = 8 - 6 - 2 = 0$ . Hence, both equations may serve to test the external redundancy, when the elements alone are considered, but internal redundancy requires counting all members and pin points in the entire structure. It is thus important to understand the exact interpretation of these two test equations.

As a general rule it is best to count intersecting web members as four members instead of two, though the result is usually identical. Thus in Fig. 3K,  $n = \Sigma r + m - 2p = 3 + 17 - 20 = 3 + 21 - 24 = 0$ . But in this example the structure is not composed of a succession of triangles and when pairs of members, meeting in a point, are removed, the structure will not reduce to a single triangle, showing that it is not stable.

Fig. 3Q is another example of the toggle joint when the members at  $c$  are not connected.

The following table was arranged to illustrate all these points with reference to the several cases represented by Figs. 3D to 3R.

Fig.	$\Sigma r$	$m$	$p$	$e$	$n = \Sigma r + m - 2p$	$n' = \Sigma r - e - 2$	Remarks.
3D	3	1	2	1	$3 + 1 - 4 = 0$	$3 - 1 - 2 = 0$	Determinate.
3E	6	1	2	1	$6 + 1 - 4 = 3$	$6 - 1 - 2 = 3$	3 times ext. ind.
3F	6	1	2	1	$6 + 1 - 4 = 3$	$6 - 1 - 2 = 3$	3 times ext. ind.
3G	3	8	5	1	$3 + 8 - 10 = 1$	$3 - 1 - 2 = 0$	Once int. ind.
3H	4	21	12	1	$4 + 21 - 24 = 1$	$4 - 1 - 2 = 1$	Once ext. ind.
3J	6	17	10	1	$6 + 17 - 20 = 3$	$6 - 1 - 2 = 3$	Thrice ext. ind.
3K	3	21	12	1	$3 + 21 - 24 = 0$	$3 - 1 - 2 = 0$	Not stable.
3L	5	45	24	1	$5 + 45 - 48 = 2$	$5 - 1 - 2 = 2$	Twice ext. ind.
3M	3	33	18	1	$3 + 33 - 36 = 0$	$3 - 1 - 2 = 0$	Determinate
3N	8	56	32	6	$8 + 56 - 64 = 0$	$8 - 6 - 2 = 0$	Determinate.
3O	4	10	7	2	$4 + 10 - 14 = 0$	$4 - 2 - 2 = 0$	Determinate.
3P	10	16	13	8	$10 + 16 - 26 = 0$	$10 - 8 - 2 = 0$	Determinate.
3Q	3	9	6	1	$3 + 9 - 12 = 0$	$3 - 1 - 2 = 0$	Case of infinite stress.
3R	8	3	4	3	$8 + 3 - 8 = 3$	$8 - 3 - 2 = 3$	Thrice ext. ind.

## CHAPTER II

### THEOREMS, LAWS, AND FORMULÆ FOR FRAMED STRUCTURES

#### ART. 4. ELASTIC DEFORMATIONS, FUNDAMENTAL EQUATIONS

##### Elastic Deformations

Let  $S$  = total stress in any member of a frame resulting from any cause, or causes, designating tension by +.

$l$  = length of any member when its  $S = 0$ .

$\Delta l$  = change in  $l$  due to stress  $S$ , + for elongation.

$F$  = cross-section of any member, prismatic in form.

$t$  = a uniform change in temperature in degrees, + for rise.

$\epsilon$  = coefficient of expansion per degree of temperature.

$E$  = modulus of elasticity.

$f = S/F$  = unit stress in any member.

$\Delta l/l$  = relative elongation.

$l/FE = \rho$  = the extensibility, frequently employed for brevity.

Then according to Hooke's law and within the elastic limit of the material,

$$\frac{\Delta l}{l} = \frac{f}{E} + \epsilon t = \frac{S}{EF} + \epsilon t = \frac{f + E\epsilon t}{E},$$

from which

$$\Delta l = \frac{Sl}{EF} + \epsilon tl = S\rho + \epsilon tl. \quad \dots \dots \dots (4A)$$

This equation represents the elastic deformation for any member of any frame and is a fundamental elasticity condition.

Referring now to Fig. 4A, let  $\overline{AB}$  be any member of any frame which, as a result of elastic distortions of the frame, is made to undergo displacements  $\Delta_1$  at  $A$  and  $\Delta_2$  at  $B$  and a change in its original length of  $\Delta l$ . The new length of the member is then  $l + \Delta l$  and its new position may be shown as  $A_1B_1$ .

Since the displacements  $\Delta_1$  and  $\Delta_2$  are very small compared with the length  $\overline{AB}$ , the two lines  $\overline{AB}$  and  $\overline{A_1B_1}$  are assumed parallel for the present purpose. The member and its displacements are referred to rectangular axes in Fig. 4A. Then

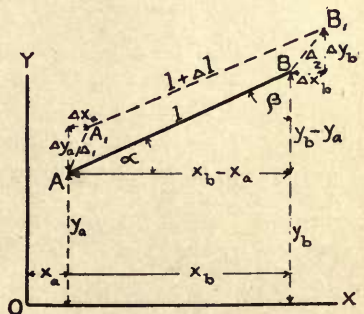


FIG. 4A.

$$l^2 = (x_b - x_a)^2 + (y_b - y_a)^2;$$



which, differentiated, gives

$$2l dl = 2(x_b - x_a)(dx_b - dx_a) + 2(y_b - y_a)(dy_b - dy_a).$$

Also from the figure  $x_b - x_a = l \cos \alpha$  and  $y_b - y_a = l \cos \beta$ , which values substituted in the previous equation, dividing through by  $2l$ , and replacing the differentials by small finite increments  $\Delta$ , gives

$$\Delta l = (\Delta x_b - \Delta x_a) \cos \alpha + (\Delta y_b - \Delta y_a) \cos \beta = \frac{Sl}{EF} + \epsilon l, \quad \dots \quad (4B)$$

which is a fundamental elasticity condition for any frame.

Hence, every frame will involve twice as many of the unknown, subscript-bearing displacements  $\Delta x$  and  $\Delta y$ , as there are pin points, while there will be as many equations of the form Eq. (4B), as there are members in the frame.

It will now be shown that any frame, whether involving redundancy or not, is capable of analysis by proving the following: *For any frame in stable equilibrium, there are as many possible condition equations as there are unknown quantities, provided the elasticity conditions Eq. (4B) are included.* This will be true of a statically determinate frame without including the elasticity conditions.

The ultimate analysis of any frame includes the determination of the reaction forces or conditions; the stresses in all the members; and the deformation of the frame as a result of these stresses. The deformation is considered solved when the displacements  $\Delta x$  and  $\Delta y$ , of all the pin points, are found.

It is assumed that for any structure under consideration, the externally applied loads  $P$ , the changes in temperature  $t$  and the abutment displacements  $\Delta r$  (if any exist) are all known and that wherever movable connections or roller bearings occur, these are frictionless.

Let  $S_1, S_2, S_3$ , etc., be the stresses in the several members meeting in some particular pin point  $m$ .

$\alpha_1, \alpha_2, \alpha_3$ , etc., be the angles which these members make with the  $x$  axis of coordinates.

$\beta_1, \beta_2, \beta_3$ , etc., be such angles with the  $y$  axis.

$P_x$  = the sum of the components parallel to the  $x$  axis, of all the external forces  $P$  acting on the point  $m$ .

$P_y$  = the sum of the components parallel to the  $y$  axis, of all these forces  $P$ .

$p, m$  and  $\Sigma r$  as previously defined in Art. 3. Then

$$\left. \begin{aligned} P_x + \Sigma S \cos \alpha &= 0 \\ P_y + \Sigma S \cos \beta &= 0 \end{aligned} \right\} \dots \dots \dots (4c)$$

because for a state of equilibrium, the sum of the horizontal and vertical components of all the forces acting on any one pin point must respectively equal zero.

Hence, for every pin point of a frame, two equations of the form of Eqs. (4c) may be written, expressing equilibrium of the internal and external forces for that point.



Also, one equation of the form of Eq. (4B) may be written for each member of a frame. Besides these, there will be one equilibrium equation for each reaction condition.

Therefore, every stable frame affords  $\Sigma r + m + 2p$  condition equations of the first degree, involving as many unknowns as there are equations, thus:

$2p$  equations of the form (4c) involving  $m$  unknowns  $S$ .  
 $m$  equations of the form (4B) involving  $2p$  unknowns  $\Delta x$  and  $\Delta y$ .  
 $\Sigma r$  equations for the reactions involving  $\Sigma r$  unknowns  $R$ .

Total  $2p + m + \Sigma r$  equations, involving  $2p + m + \Sigma r$  unknowns.

It follows then that the stresses  $S$ , the reactions  $R$  of known direction, and the  $\Delta x$  and  $\Delta y$  projections of the pin-point displacements, may all be represented as linear functions of the horizontal and vertical components of all the external forces  $P$ , plus similar functions of assumed temperature changes  $t$ , plus linear functions of the abutment displacements  $\Delta r$ ,  $\Delta r_2$ ,  $\Delta r_3$ , etc.

Thus any unknown function of *any frame* may be expressed by an equation of the form

$$Z = f(P_1, P_2, P_3, \text{etc.}) + f_1(t) + f_2(\Delta r_1, \Delta r_2, \Delta r_3, \text{etc.}), \dots \quad (4D)$$

in which the coefficients are independent of the values  $P$ ,  $t$  and  $\Delta r$ , but depend on the lengths and directions of the members also on  $E$ ,  $\epsilon$  and the manner in which the frame is supported.

**The law of the summation of similar partial effects.** In Eq. (4D), every set of causes or conditions  $P$ ,  $t$  and  $\Delta r$ , produces a partial value  $Z'$  for  $Z$  and the ultimate total value of  $Z = Z' + Z'' + Z'''$ , etc., is the sum of all the partial values or effects resulting from the respective sets of independent causes or conditions. *Thus each effect, such as a stress, whether due to loads, temperature or abutment displacements, may be ascertained or investigated by itself and the sum total effect  $Z$  will then be the sum of the several similar partial effects.* This is the law of the summation of similar partial effects resulting from various causes and is fundamental to the analysis of all structures involving redundancy.

**The law of proportionality between cause and effect.** Eq. (4D), being true for any set of effects, would remain true for any multiple of these effects. Hence, if the loads are doubled the resulting stresses will likewise be doubled, etc. Therefore, the law of proportionality holds true between the causes and their effects. Thus, if a set of loads  $P$  produces stresses  $S$  in the members of a frame then another set of parallel loads  $\bar{P}$ , acting at the same points, would produce stresses  $\bar{S}$  which are  $\bar{P}/P$  times as great as the stresses  $S$ . Or, if a single load unity, acting on a point  $m$  of any frame produces reactions  $R_1$ , and stresses  $S_1$ , then a load  $P_m$  acting at the same point will produce reactions  $R = P_m R_1$ , and stresses  $S = P_m S_1$ .

## ART. 5. GENERAL WORK EQUATIONS FOR ANY FRAME

**The general work equation, Clapeyron's law.** A loaded frame is a machine in equilibrium and within the limits of proportional elasticity its deformation varies directly with the magnitude of the superimposed loads.

The question of deformation does not enter into statics and hence a general and comprehensive treatment of the elastic frame must necessarily involve the principles of mechanics.

For example, given a frame with definite loading and supports, constituting a system in *external equilibrium*. The frame in turn will undergo certain deformations which will steadily increase in proportion to the internal stresses created in the members by the external forces as they are gradually applied. The final deformation will occur in the instant when the external forces are exactly balanced by the internal stresses, passing into the condition known as *static equilibrium*.

While this deformation is taking place the applied loads travel through certain distances which are the paths or displacements of the points of application of the loads. Thus a certain quantity of positive *work of deformation* is performed by the external forces.

The internal stresses in the members must accommodate themselves to the deformed condition of the frame and in resisting this action must produce *negative work of deformation*.

In the instant when static equilibrium is established between the loads and stresses the positive and negative work of deformation produced in the same interval of time must exactly balance.

Let  $A_e$  = the positive or externally applied work of deformation.

$A_i$  = the negative or internally overcome work of deformation.

$P$  = any externally applied loads including the reactions.

$S$  = the stress in any member due to the loads  $P$ .

$\Delta l$  = the change in length of any member due to the stress  $S$ .

$\delta$  = the displacement of the point of application of any force  $P$  measured in the direction of this force.

*A positive amount of work is always produced when the force and its displacement act in the same direction.*

The product  $\frac{1}{2}P\delta$  represents the actual work produced by a force gradually applied and increasing from its initial zero value to a certain end value  $P$ , thus exerting only its average intensity during the entire time of traversing the path  $\delta$  to perform this work. Hence, for all the external forces acting on any frame, the total *positive external work of deformation* would be  $A_e = \frac{1}{2}\Sigma P\delta$ .

Similarly  $\frac{1}{2}S\Delta l$  represents the actual work in any member subjected to a gradually increasing stress of end value  $S$ , with an average intensity  $S/2$  during the entire time while producing a change in its length of  $\Delta l$ . Hence for all internal stresses in any frame the total *negative work of deformation* would be  $A_i = \frac{1}{2}\Sigma S\Delta l$ .

By the "doctrine of the conservation of energy," the applied work must equal the work overcome, hence

$$\left. \begin{aligned} A_e &= A_i = \frac{1}{2}\Sigma P\delta = \frac{1}{2}\Sigma S\Delta l \\ A_e - A_i &= 0 \text{ and } \frac{1}{2}\Sigma P\delta - \frac{1}{2}\Sigma S\Delta l = 0 \end{aligned} \right\}, \dots \dots \dots (5A)$$

or



which is Clapeyron's law (1833), and may be stated as follows: *For any frame of constant temperature, and acted on by loads which are gradually applied, the actual work produced during deformation is independent of the manner in which these loads are created and is always half as great as the work otherwise produced by forces retaining their full end values during the entire act of deformation.*

By regarding any elastic body as composed of an infinite multiplicity of members, it is readily seen that Clapeyron's law applies equally to frames and solid web elastic structures when properly supported. Clapeyron's law finds extensive application in problems dealing with deformations of framed structures.

Cases involving dynamic impact would imply a certain amount of kinetic energy in excess of the applied work of deformation. That is, the applied forces have some initial value, greater than zero, while the stresses are still zero. This would not be represented by the work Eq. (5A), wherein  $A_e - A_i = 0$ , but would give rise to the following equation:

[illegible]

indicating a state of accelerated motion instead of one of equilibrium. For problems under this heading see Art. 16.

The law of virtual work will now be considered. It is a general law, permitting of more varied application than does Clapeyron's law.

The law of virtual work was first enunciated by Galilei and Stevin, and in its more general form by Joh. Bernoulli. Lagrange (1788) reduced the law to an algebraic expression for which the following derivation may be given.

According to the general law expressed by Eqs. (4c), all forces (and stresses) acting on a pin point of any structure in equilibrium will have components parallel to any axis and the sum of such a set of parallel components must be zero. Calling  $\alpha$  the angle which any force or stress  $P$  makes with the axis chosen, then for any pin point

$$\Sigma P \cos \alpha = 0.$$

Now if a displacement  $\Delta$ , parallel to the axis, be arbitrarily assigned to this pin point and assuming equilibrium to continue, then the product of  $\Delta$  with the sum of the components must still be zero. This is equivalent to multiplying the above equation by  $\Delta$  to obtain

$$\Sigma(P \cos \alpha) \Delta = 0.$$

But the displacements  $\Delta \cos \alpha = \delta$  are the projections of the displacements  $\Delta$  on the directions of the several forces, hence

[illegible]

wherein  $\overline{P}$  signifies that the forces are in every sense independent of the displacements  $\delta$ .

This is the law of *virtual work*, and is applicable to any point or group of points and hence to any frame or group of bodies. The displacements  $\delta$  may be any possible displacements whether or not subject to the law of elastic deformation, provided equilibrium exists.



Stated in words this law implies *that for any point, frame or body acted on by loads  $\bar{P}$  in an established state of equilibrium, the sum total work performed by these forces, in moving over any small arbitrary but possible displacements  $\delta$ , must always be equal to zero.*

If the time element is introduced into Eq. (5c) giving  $\Sigma \bar{P} \delta / t = 0$ , the law of *virtual velocities* is obtained.

**Professor Otto Mohr's work equations.** Proceeding from Eq. (5c), Professor Mohr, in 1874, developed two equations which furnish the most comprehensive laws for framed structures. These equations are now derived.

Given any frame carrying the arbitrarily assumed loads  $\bar{P}_1, \bar{P}_2, \bar{P}_3$ , etc., which in combination with temperature changes produce stresses  $\bar{S}_1, \bar{S}_2, \bar{S}_3$ , etc., in the several members of the frame and thus constituting a system of forces in static equilibrium.

All the pin points of the frame are now supposed to be subjected to small, arbitrarily assigned displacements  $\Delta_1, \Delta_2, \Delta_3$ , etc., which may have been produced by some other system of actual loads  $P_1, P_2, P_3$ , etc., entirely independent of the loads  $\bar{P}$ . The  $\Delta$ 's will naturally vary in amount and direction for each pin point.

According to the laws for static equilibrium, the sum of the components, taken in any fixed direction, of all forces acting on any pin point of a frame must equal zero.

Choosing for the fixed direction the displacement  $\Delta_1$ , then for any particular pin point, Fig. 5A, the following equation may be written:

$$\bar{P}_1 \cos \theta_1 + \Sigma \bar{S} \cos \phi = 0;$$

which multiplied through by  $\Delta_1$  gives

$$\Delta_1 \bar{P}_1 \cos \theta_1 + \Delta_1 \Sigma \bar{S} \cos \phi = 0.$$

But from the figure,  $\Delta_1 \cos \theta_1 = \delta_1$ , which value substituted in the above equation gives

$$\bar{P}_1 \delta_1 + \Delta_1 \Sigma \bar{S} \cos \phi = 0. \quad (5d)$$

Eq. (5d) represents the virtual work of all forces acting on the pin point 1, in accordance with Eq. (5c).

One such Eq. (5d) may be written for each pin point and the sum of all these equations would furnish the total virtual work for the whole frame.

In this sum equation, each load  $\bar{P}$  will occur only once, while each stress  $\bar{S}$  will occur twice, being involved once for each end of the same member.

The terms containing the forces  $\bar{P}$  will give the sum

$$\bar{P}_1 \delta_1 + \bar{P}_2 \delta_2 + \bar{P}_3 \delta_3 + \dots = \Sigma \bar{P} \delta.$$

The sum terms involving the same stress  $\bar{S}$  may be found for each member as

$$\bar{S} \Delta = \bar{S} (\Delta_n \cos \phi_m + \Delta_p \cos \phi_q),$$

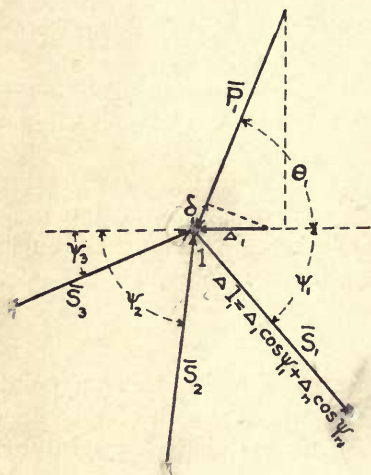


FIG. 5A.

since the two displacements  $\Delta \cos \psi$  for the two ends of the same member give the sum  $\Delta l$ , or actual change in the length of such member.

Hence, the terms containing the stresses  $\bar{S}$  will give the sum

$$-\bar{S}_1 \Delta l_1 - \bar{S}_2 \Delta l_2 - \bar{S}_3 \Delta l_3 - \dots = -\Sigma \bar{S} \Delta l,$$

where the minus sign is due to the fact that the stresses applied to pin points as external forces are always opposite in direction with their respective  $\Delta l$ 's.

The final sum equation for all pin points then becomes

$$\Sigma \bar{P} \delta - \Sigma \bar{S} \Delta l = 0;$$

or

$$\Sigma \bar{P} \delta = \Sigma \bar{S} \Delta l, \quad . . . . . (5E)$$

which may be said to represent a condition of *elastic equilibrium* as distinguished from *static equilibrium*. The law thus expresses the equality between the external and internal virtual work of deformation for real displacements and arbitrary cases of loading, provided elastic equilibrium exists.

The external forces  $\bar{P}$  necessarily include the reactions due to the applied loads  $\bar{P}$ . However, the work of the reactions is always zero when the abutments are immovable. In the general case involving abutment displacements  $\Delta r$  in the directions of the reactions  $\bar{R}$  produced by loads  $\bar{P}$ , Eq. (5E) may be written

$$\Sigma \bar{P} \delta + \Sigma \bar{R} \Delta r = \Sigma \bar{S} \Delta l. \quad . . . . . (5F)$$

It should be repeated that the displacements  $\delta$ ,  $\Delta r$  and  $\Delta l$  are actual and mutually dependent on the same causes, such as the actual loads  $P$  and temperature changes. The arbitrary loads  $\bar{P}$ , reactions  $\bar{R}$  and stresses  $\bar{S}$  form a system in elastic equilibrium which is independent of the actual loads  $P$ , reactions  $R$  and stresses  $S$ , and hence independent of the actual displacements.

In the special case where the forces  $P$ ,  $S$  and  $R$  become identical with the forces  $\bar{P}$ ,  $\bar{S}$  and  $\bar{R}$ , Eq. (5F) becomes

$$\Sigma P \delta + \Sigma R \Delta r = \Sigma S \Delta l = \Sigma \frac{S^2 l}{E F}, \quad . . . . . (5G)$$

which is in accordance with Clapeyron's law.

Eq. (5F) is the fundamental law of framed structures and includes all conditions of equilibrium of the external forces; of the external forces and internal stresses; and of all relations existing between the stresses and the distortions of any frame.

**Professor Mohr's second work equation** serves the purpose of determining any displacement  $\delta_m$  produced by any case of loading. It follows from Eq. (5F) by allowing all the arbitrary loads to vanish and substituting therefor a single load unity and the stresses  $S_1$  and reactions  $R_1$  resulting from such unit load. The new work equation then becomes

$$1 \cdot \delta + \Sigma R_1 \Delta r = \Sigma S_1 \Delta l, \quad . . . . . (5H)$$



wherein the unit loading, henceforth called the *conventional loading*, may be a single force unity or a moment equal to unity. In the latter case the  $\delta$  will represent a rotation measured in arc. By dividing Eq. (5H) by unity the stresses  $S_1$  become abstract numbers and the equation will read

$$\delta + \Sigma R_1 \Delta r = \Sigma S_1 \Delta l. \quad (5i)$$

The applications of this law, universally known as *Mohr's work equation*, will be shown in the following articles 6 and 7. The work represented by the *conventional loading* will generally be designated by  $\bar{W}$ .

#### ART. 6. DISPLACEMENTS OF POINTS. STATICALLY DETERMINATE STRUCTURES BY PROFESSOR MOHR'S WORK EQUATION

The relative displacement  $\delta_m$  between any two pin points  $m_1$  and  $m$ , of any frame Fig. 6A, when  $\Delta l$  is given for each member of the frame, may be found by applying Eq. (5i).

If the abutments undergo known displacements  $\Delta r$ , as a result of the given actual loading, this effect on the required  $\delta_m$  must be included.

Likewise temperature displacements may be considered, but the problem will first be treated by neglecting this effect.

Now assume two unit forces, applied at the points  $m_1$  and  $m$  respectively, and, acting in opposite directions along the line  $m_1m$ . The directions of these unit forces should be so chosen as to make the conventional work  $1 \cdot \delta_m$  a positive quantity. This means that if  $\delta_m$  is an elongation, then the unit forces must be so applied as to elongate the distance  $m_1m$ . This rule will be universally applied to determinate structures as well as to indeterminate for redundant members or conditions. A negative result will indicate an erroneous assumption in the direction of the unit conventional load.

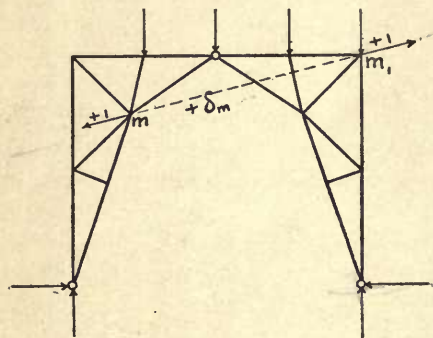


FIG. 6A.

The stresses  $S_1$  and abutment reactions  $R_1$  resulting from the two unit loads acting at  $m_1$  and  $m$  are now determined from a Maxwell diagram or by computation.

The work Eq. (5H) applied to this assumed or *conventional loading* then gives, after substitution of values  $\Delta l = S_1 l / EF$ , excluding temperature effect,

$$+1 \cdot \delta_m = \Sigma S_1 \Delta l - \Sigma R_1 \Delta r = \Sigma \frac{S_1 S l}{EF} - \Sigma R_1 \Delta r. \quad (6A)$$

The stresses  $S$  are those produced in the structure by any real case of loading, as loads  $P$ , temperature changes or abutment displacements, giving rise to the actual changes  $\Delta l$  in the lengths of the members.



Eq. (6A) then offers a solution to the above problem, because all the quantities except  $\delta_m$  are known or can be found from the given data.

If temperature effects are to be included then Eq. (4A) gives the value for  $\Delta l$ , thus furnishing the final equation

$$+1 \cdot \delta_m = \Sigma S_1 \left( \frac{Sl}{EF} + \epsilon ll \right) - \Sigma R_1 \Delta r. \quad \dots \dots \dots (6B)$$

In a similar manner the relative displacement of any pair of points, the deflection of any point, or the angular change between any pair of lines of any frame, resulting from given changes  $\Delta l$  of all the members of the frame, may be found by assigning such *conventional loads* as will produce the conventional work  $1 \cdot \delta$  on the frame at the point or points in question. See also Art. 9 for other examples of this class.

## ART. 7. INDETERMINATE STRUCTURES BY PROFESSOR MOHR'S WORK EQUATION

A truss, according to Chapter I, may include more than the statically necessary number of members or reaction conditions, and is then called statically indeterminate. It is now proposed to show the manner in which Mohr's work equation may be employed to find the stresses and reactions in such a structure, loaded by any system of loads  $P$  concentrated at the several pin points of the frame.

The structure must be so constituted that when all *redundant* members and reaction forces are removed, the remaining frame will represent a statically determinate structure, including the necessary conditions for proper support. This determinate frame will always be called the *principal frame or system*.

Now let  $X_a, X_b, X_c$ , etc., represent the stresses produced by the applied loads in any redundant members or supports, as the case may demand. When these stresses are applied to the *principal system*, together with the external loads, the resulting stresses in all the *principal members* will be identical with those produced in these same members by the original loading of the whole indeterminate frame. This will also be true of the deformations.

It follows then that the loads  $P$  applied to the *indeterminate frame*, and the loads  $P$  and  $X$  applied to the *principal frame* produce identical stresses and deformations in the principal members. Also, the deformations are in each case definitely fixed by the elastic changes  $\Delta l$  of the *necessary* members of the *principal system*. Hence, for applied loads only (without temperature effects) the work of the stresses in the principal frame is always greater when a redundant member is omitted. The work which a redundant member can do must necessarily lessen the work otherwise required of the principal system.

If, then, the elastic displacements of the several pin points representing the points of application of the redundant forces  $X$ , are found for the principal system, these displacements will suffice to solve one elasticity equation for each unknown  $X$ . This may be done in two ways: (1) By applying Mohr's work equation to the indeterminate system, and (2) by finding the requisite elastic displacements of the principal system from Maxwell's law. The solution by Mohr's work equation will now be given.

The following definitions of terms will be strictly adhered to in all succeeding discussions.

Let  $S$  = the stress in any member of the principal system.

$S_o$  = the stress in this member due to the loads  $P$  when the several redundants  $X$  and  $t$  are all zero, to be known as condition  $X=0$ .

$S_a$  = the stress in this member of the principal system when no load other than  $X_a=1$  is active. Condition  $X_a=1$ .

$S_b$  = the same when no load other than  $X_b=1$  is active on the principal system.

$S_c$  = the same when no load other than  $X_c=1$  is active on the principal system.

$S_t$  = the stress in the same member caused by a uniform change in temperature.

$R_t$  = a reaction produced by a uniform change in temperature.

$M_t$  = a moment produced by a uniform change in temperature.

$X_a, X_b, X_c$ , etc., the stresses in the redundant members or reactions.

$R_o, R_a, R_b, R_c$ , etc., are defined like the  $S$ 's with like subscripts, but represent reaction forces instead of stresses.

$\delta_a, \delta_b, \delta_c$ , are changes in the lengths of the redundant members  $X_a, X_b, X_c$ , respectively.

The forces  $X_a, X_b, X_c$ , etc., may be the stresses in redundant members or they may be redundant reactions as in the case of fixed arches or continuous girders, etc.

Each of the above cases of *conventional loading* will be known as *conditions*. Thus condition  $X=0$  will mean that all the redundant conditions are removed, while *condition*  $X_a=1$  will signify that this force alone is applied to the principal system and all other  $X$ 's,  $S_t$ , and  $P$ 's are removed.

The stress  $S$ , in any member of a frame involving redundant conditions, is a linear function of the loads  $P, X_a, X_b, X_c$ , etc., all treated as external forces applied to the principal system. This follows because all conditions of equilibrium are represented by linear equations.

Hence, according to the law of the summation of effects expressed by Eq. (4b), the general equation for stress in any member of a truss involving redundancy, would have the form

$$S = S_o - S_{ax} - S_{bx} - S_{cx}, \text{ etc.}, + S_t;$$

wherein  $S_{ax}$  = the stress in any member due to the external force  $X_a$  acting alone on the principal system. Similarly  $S_{bx}$  = the stress in the same member due to the external force  $X_b$  acting alone on the principal system, etc.

But by the law of proportionality  $S_{ax} = S_a X_a$ ,  $S_{bx} = S_b X_b$  and  $S_{cx} = S_c X_c$ , etc. Hence, the general equation for any case of redundancy may be written:

for the stress in any principal member

$$S = S_o - S_a X_a - S_b X_b - S_c X_c, \text{ etc.}, + S_t$$

for any reaction of the principal system

$$R = R_o - R_a X_a - R_b X_b - R_c X_c, \text{ etc.}, + R_t \quad \dots \dots \dots (7A)$$

and for any moment on the principal system

$$M = M_o - M_a X_a - M_b X_b - M_c X_c, \text{ etc.}, + M_t$$



In these equations the quantities  $S_o$ ,  $R_o$  and  $M_o$  are all linear functions of the externally applied loads  $P$ , while all the stresses, reactions, and moments bearing subscripts  $a$ ,  $b$ ,  $c$ , etc., are constants due to conventional loadings and are absolutely independent of all external loads  $P$  and  $X$ .

The work of any member or reaction is obtained from Eqs. (7A) by multiplying both sides of these equations by the deformation which each sustains. Thus, neglecting temperature effects, the work equations are

$$\left. \begin{aligned} S\Delta l &= [S_o - S_a X_a - S_b X_b - S_c X_c, \text{ etc.}] \Delta l \\ R\Delta r &= [R_o - R_a X_a - R_b X_b - R_c X_c, \text{ etc.}] \Delta r \end{aligned} \right\} \dots \dots \dots (7B)$$

The negative signs in Eqs. (7A) and (7B), indicate that the quantities involving the redundants  $X$  must always be of opposite sign to the stress  $S_o$  resulting from the loads  $P$ , for reasons above stated in this article.

Hence the increment of work performed by the redundants  $X$ , as shown by Eqs. (7B), is always negative with respect to the work performed by the stress  $S_o$  because the forces  $X$  are classed with the external forces.

The conventional unit loadings are always applied in the opposite direction to the forces they replace, and this in turn puts these (negative) unit forces in the same direction as the displacements  $\delta$  which they accompany. Hence the work  $1 \cdot \delta$  is always positive.

This is exactly the same as the case illustrated in Art. 2, where the unit load was independent of all redundant conditions.

Therefore, whenever in the following a *conventional unit load* represents a redundant condition, the direction of this unit load must be taken in a direction opposite to the force representing the stress in such member. This is equivalent to saying that when a member  $X$  elongates under stress, then the unit load  $X=1$  must be so applied as to move the adjacent pin points apart, and the converse when the member shortens under stress.

Whenever the direction of a redundant force cannot be correctly foreseen, then some assumption is made which, if it be erroneous, will result in a negative value for such redundant  $X$ .

The following illustration is given to make these points clear and to avoid confusion of ideas in all future problems.

Figures 7A to 7E represent an indeterminate structure involving three redundant conditions as may be verified by applying Eq. (3c) to the problem in Fig. 7A.

The truss is supported by hinged bearings at  $A$  and  $D$  and by columns at  $B$  and  $C$ , all of which may be subjected to certain displacements which may be estimated from the conditions of the problem.

Figure 7B, then, represents the principal system carrying loads  $P$ , when all redundant conditions are removed and shows condition  $X=0$ . The other figures represent, respectively, the conventional loadings  $X_a=1$ ,  $X_b=1$  and  $X_c=1$ , the three  $X$ 's being the redundant conditions. Note here the directions which the unit forces take. They are negative



with respect to the forces they replace, but in the same directions as the displacements which their points of application undergo as a result of the loads  $P$ .

The reaction displacements are assumed to be downward by amounts  $\Delta A$ ,  $\Delta B$ ,  $\Delta C$ , and  $\Delta D$  for these supports respectively, and it is also assumed that  $A$  and  $D$  move apart by an amount  $\Delta L$ . Temperature effects will be taken up later being omitted for the present.

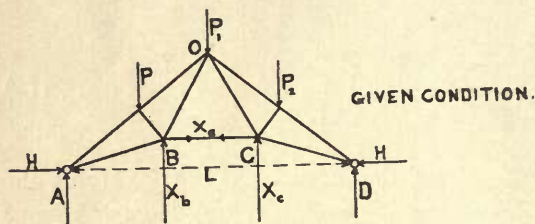


FIG. 7A.

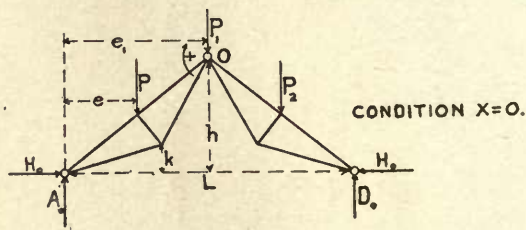


FIG. 7B.

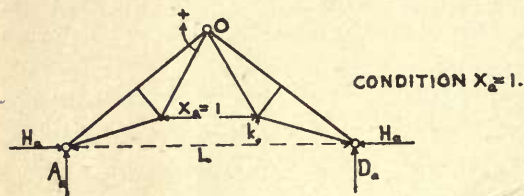


FIG. 7C.

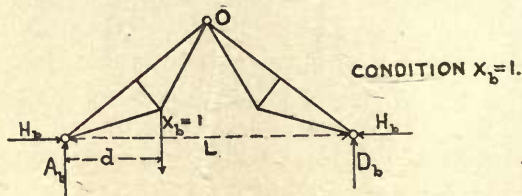


FIG. 7D.

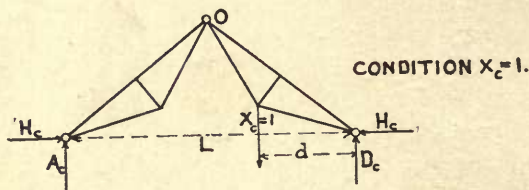


FIG. 7E.

The various reactions in the following table, given for the four conventional loadings, are now found for the principal system, which in this case is a three-hinged arch.

For Condition.	A	B	C	D	H*
$X=0$	$A_o = \frac{\Sigma P(L-e)}{L}$	$B_o=0$	$C_o=0$	$D_o = \frac{\Sigma P e}{L}$	$H_o = \frac{A_o L - P(L-2e)}{2h}$
$X_a=1$	$A_a=0$	$B_a=0$	$C_a=0$	$D_a=0$	$H_a = \frac{1(h-k)}{h}$
$X_b=1$	$A_b = \frac{1(L-d)}{L}$	$B_b=0$	$C_b=0$	$D_b = \frac{1 \cdot d}{L}$	$H_b = \frac{1 \cdot d}{2h}$
$X_c=1$	$A_c = \frac{1 \cdot d}{L}$	$B_c=0$	$C_c=0$	$D_c = \frac{1(L-d)}{L}$	$H_c = \frac{1 \cdot d}{2h}$

\* Obtained by taking moment equation about the middle hinge O, in a clockwise direction.

Hence from Eq. (7A) for reactions, these values give:

$$\left. \begin{aligned} A &= A_o - A_a X_a - A_b X_b - A_c X_c = \frac{\Sigma P(L-e)}{L} - \frac{L-d}{L} X_b - \frac{d}{L} X_c \\ B &= 0 \\ C &= 0 \\ D &= D_o - D_a X_a - D_b X_b - D_c X_c = \frac{\Sigma P e}{L} - \frac{d}{L} X_b - \frac{L-d}{L} X_c \\ H &= H_o - H_a X_a - H_b X_b - H_c X_c = H_o - \frac{h-k}{h} X_a - \frac{d}{2h} X_b - \frac{d}{2h} X_c \\ S &= S_o - S_a X_a - S_b X_b - S_c X_c \end{aligned} \right\} \dots \dots \dots (7c)$$

and

The work equation (6A), when applied to each of the three redundant forces  $X_a$ ,  $X_b$  and  $X_c$  and observing that the conventional work  $1 \cdot \delta$  in each case is positive, gives

$$\left. \begin{aligned} 1 \cdot \delta_a &= \Sigma S_a \Delta l - \Sigma R_a \Delta r = +1 \cdot \Delta L \left( \frac{h-k}{h} \right) \\ 1 \cdot \delta_b &= \Sigma S_b \Delta l - \Sigma R_b \Delta r = +1 \cdot \Delta B \\ 1 \cdot \delta_c &= \Sigma S_c \Delta l - \Sigma R_c \Delta r = +1 \cdot \Delta C \end{aligned} \right\} \dots \dots \dots (7d)$$

The values for  $\Sigma R \Delta r$ , in each of the Eqs. (7d), may also be written out from the above tabulated quantities for the three conventional loadings  $X_a=1$ ,  $X_b=1$  and  $X_c=1$ . They are:

$$\left. \begin{aligned} \Sigma R_a \Delta r &= -H_a \Delta L = -\Delta L \left( \frac{h-k}{h} \right) \\ \Sigma R_b \Delta r &= -A_b \Delta A - D_b \Delta D - H_b \Delta L \\ &= -\frac{L-d}{L} \Delta A - \frac{d}{L} \Delta D - \frac{d}{2h} \Delta L \\ \Sigma R_c \Delta r &= -A_c \Delta A - D_c \Delta D - H_c \Delta L \\ &= -\frac{d}{L} \Delta A - \frac{L-d}{L} \Delta D - \frac{d}{2h} \Delta L \end{aligned} \right\} \dots \dots \dots (7e)$$

It should be observed that when the direction of a force is opposite to the direction of the displacement over which the force travels, then the product which represents work is always negative. This is the case with all the work quantities in Eqs. (7e). Hence, when these are substituted into Eqs. (7d) they become positive.

The quantities  $\Sigma S_a \Delta l$ ,  $\Sigma S_b \Delta l$  and  $\Sigma S_c \Delta l$  still remain to be evaluated. Eq. (4A) gives  $\Delta l = S \rho + \epsilon t l$ , where  $S = S_o - S_a X_a - S_b X_b - S_c X_c$  from Eq. (7A). Then by substitution

$$\Delta l = [S_o - S_a X_a - S_b X_b - S_c X_c] \rho + \epsilon t l, \dots \dots \dots (7f)$$

which gives the final value

$$\Sigma S_a \Delta l = \Sigma S_a S_o \rho - X_a \Sigma S_a^2 \rho - X_b \Sigma S_a S_b \rho - X_c \Sigma S_a S_c \rho + \Sigma S_a \epsilon t l. \dots \dots (7g)$$

Similar expressions follow for  $\Sigma S_b dl$  and  $\Sigma S_c dl$ , and these substituted in Eqs. (7D) give for the values  $\delta$ :

$$\left. \begin{aligned} \delta_a &= \Sigma S_a S_o \rho - X_a \Sigma S_a^2 \rho - X_b \Sigma S_a S_b \rho - X_c \Sigma S_a S_c \rho - \Sigma R_a dr + \Sigma S_a \epsilon t l \\ \delta_b &= \Sigma S_b S_o \rho - X_a \Sigma S_b S_a \rho - X_b \Sigma S_b^2 \rho - X_c \Sigma S_b S_c \rho - \Sigma R_b dr + \Sigma S_b \epsilon t l \\ \delta_c &= \Sigma S_c S_o \rho - X_a \Sigma S_c S_a \rho - X_b \Sigma S_c S_b \rho - X_c \Sigma S_c^2 \rho - \Sigma R_c dr + \Sigma S_c \epsilon t l \end{aligned} \right\} \quad (7H)$$

wherein the summations, except those of the reactions, include only the members of the principal system.

Now  $\delta_a$ ,  $\delta_b$ , and  $\delta_c$  being the changes in the lengths of the three redundants, these may be evaluated from Eq. (4A) in terms of the lengths, areas and stresses of these members (or reactions) and become

$$\delta_a = \frac{X_a l_a}{EF_a} + \epsilon t l_a; \quad \delta_b = \frac{X_b l_b}{EF_b} + \epsilon t l_b; \quad \delta_c = \frac{X_c l_c}{EF_c} + \epsilon t l_c. \quad (7J)$$

Hence all the terms in Eq. (7H) are now known except the three redundant forces  $X_a$ ,  $X_b$  and  $X_c$ , and having three elasticity equations involving only these unknowns, the latter may be found by solving Eqs. (7H) for simultaneous values of the  $X$ 's, with the aid of Eqs. (7E) and (7J).

It is thus seen that the abutment displacements are of vital importance in determining the magnitudes of the stresses in any statically indeterminate structure. Whenever these displacements cannot be determined with any degree of certainty, or when small displacements indicate large resulting stresses, then such structures should not be built. This applies particularly to fixed arches and continuous girders.

Eqs. (7H), based on Professor Mohr's work equation, thus furnish a means for the analysis of any statically indeterminate structure.

## ART. 8. INDETERMINATE STRUCTURES BY MAXWELL'S LAW

The application of Maxwell's law to the same analysis will now be given by expressing the summations in Eqs. (7H) in terms of the elastic deformations of the structure instead of the stresses in the members.

Let  $\delta_{ma}$  = the displacement of the point of application  $m$  of any load  $P_m$ , in the direction of this load, when the principal system is loaded with only  $X_a = 1$ .

$\delta_{mb}$  = a similar displacement of the same point  $m$  for the conventional loading  $X_b = 1$ .

$\delta_{mc}$  = the same for condition  $X_c = 1$ .

$\delta_{aa}$  = the change in length of the member  $a$  for condition  $X_a = 1$ .

$\delta_{ab}$  = the change in length of the same member  $a$  for condition  $X_b = 1$ .

$\delta_{ac}$  = the similar change for condition  $X_c = 1$ .

$\delta_{ba}$  = the change in length of the member  $b$  for condition  $X_a = 1$ .

$\delta_{bb}$  = the change in length of the member  $b$  for condition  $X_b = 1$ .



- $\delta_{bc}$  =the change in length of the member  $b$  for condition  $X_c=1$ .
- $\delta_{ca}$  =the change in length of the member  $c$  for condition  $X_a=1$ .
- $\delta_{cb}$  =the change in length of the member  $c$  for condition  $X_b=1$ .
- $\delta_{cc}$  =the change in length of the member  $c$  for condition  $X_c=1$ .
- $\delta_{at}$  =the change in length of the member  $a$  resulting from a change in temperature  $t^\circ$ , when the principal system is otherwise not loaded, hence  $X=0, P=0$ .
- $\delta_{bt}$  =the same for the member  $b$ .
- $\delta_{ct}$  =the same for the member  $c$ .

For the sake of simplicity, the abutments will be assumed immovable, thus making all  $\Delta r=0$ . This part of the previous problem remains unchanged.

The work Eq. (5E) for the condition  $X=0$ , (when the loads  $P$  only are acting on the principal system and producing the stresses  $S_o$ ) now becomes for the three cases of displacements

$$\left. \begin{aligned} \Sigma P_m \delta_{ma} &= \Sigma S_o \Delta l_a = \Sigma S_o S_{a\rho} \\ \Sigma P_m \delta_{mb} &= \Sigma S_o \Delta l_b = \Sigma S_o S_{b\rho} \\ \Sigma P_m \delta_{mc} &= \Sigma S_o \Delta l_c = \Sigma S_o S_{c\rho} \end{aligned} \right\} \dots \dots \dots (8A)$$

Similarly applying the work Eq. (6A) to the conditions  $X_a=1, X_b=1$  and  $X_c=1$ , the various displacements become

$$1 \cdot \delta_{aa} = \Sigma S_a \Delta l_a; \quad 1 \cdot \delta_{ab} = \Sigma S_a \Delta l_b \text{ and } 1 \cdot \delta_{ac} = \Sigma S_a \Delta l_c;$$

and by inserting values for  $\Delta l_a, \Delta l_b$  and  $\Delta l_c$  from Eq. (4A) then

$$\left. \begin{aligned} \Sigma S_a S_{a\rho} &= \delta_{aa}; \quad \Sigma S_a S_{b\rho} = \delta_{ab}; \quad \Sigma S_a S_{c\rho} = \delta_{ac} \\ \text{and similarly for conditions } X_b=1 \text{ and } X_c=1 \\ \Sigma S_b S_{a\rho} &= \delta_{ba}; \quad \Sigma S_b S_{b\rho} = \delta_{bb}; \quad \Sigma S_b S_{c\rho} = \delta_{bc} \\ \Sigma S_c S_{a\rho} &= \delta_{ca}; \quad \Sigma S_c S_{b\rho} = \delta_{cb}; \quad \Sigma S_c S_{c\rho} = \delta_{cc} \end{aligned} \right\} \dots \dots \dots (8B)$$

Finally the work Eq. (6B), for temperature displacements for each of the conventional unit loadings, gives

$$\Sigma S_a \epsilon t l = 1 \cdot \delta_{at}; \quad \Sigma S_b \epsilon t l = 1 \cdot \delta_{bt} \text{ and } \Sigma S_c \epsilon t l = 1 \cdot \delta_{ct}. \quad \dots \dots \dots (8C)$$

Substituting all these values from Eqs. (8A), (8B), and (8C) into Eqs. (7H), the following important equations are obtained:

$$\left. \begin{aligned} \delta_a &= \Sigma P_m \delta_{ma} - X_a \delta_{aa} - X_b \delta_{ab} - X_c \delta_{ac} - \Sigma R_a \Delta r + \delta_{at} \\ \delta_b &= \Sigma P_m \delta_{mb} - X_a \delta_{ba} - X_b \delta_{bb} - X_c \delta_{bc} - \Sigma R_b \Delta r + \delta_{bt} \\ \delta_c &= \Sigma P_m \delta_{mc} - X_a \delta_{ca} - X_b \delta_{cb} - X_c \delta_{cc} - \Sigma R_c \Delta r + \delta_{ct} \end{aligned} \right\} \dots \dots \dots (8D)$$

It should be noted that for the quantities on the *right-hand* side of Eqs. (8D), the single subscripts and the second one of the double subscripts always refer to the con-

ventional loadings  $X_a=1$ ,  $X_b=1$  and  $X_c=1$ , while the first of the double subscripts always refers to a point or member of the structure.

According to *Maxwell's law* (proven in Art. 9) the following equalities exist in Eqs. (8d):

$$\delta_{ab}=\delta_{ba}; \quad \delta_{ac}=\delta_{ca} \quad \text{and} \quad \delta_{bc}=\delta_{cb}.$$

This means that the order of the subscripts may be interchanged at will without altering the equations, thus greatly simplifying the solution of problems.

All of the displacements  $\delta$ , in Eqs. (8d), may now be determined by four Williot-Mohr displacement diagrams (see Chapter VI), drawn respectively for the conditions  $X_a=1$ ,  $X_b=1$ ,  $X_c=1$  and  $t=1$  acting on the principal system. Hence, the three redundant conditions  $X$  are again found by solving Eqs. (8d) for simultaneous values.

It is thus seen that any indeterminate structure may be analyzed in either of two ways, by Eqs. (7h) or (8d), according to the choice of the designer or the nature of the problem.

The redundants  $X$  being found by either of the above methods, all the stresses  $S$  and reactions  $R$  may now be determined from Eqs. (7A). In these the  $X$ 's are the redundant forces from Eqs. (7h) or (8d) and the stresses  $S_o$ ,  $S_a$ ,  $S_b$  and  $S_c$  are those found for the conventional loadings on the principal system and are independent of the values  $X$  and of each other.

The summations in all the previous equations include only the members of the principal frame. However, an equation of the form (7h) may be written to cover all members, including the redundant, and this form is frequently very useful.

The work Eqs. (7d) when made to cover all members of an indeterminate frame become

$$\Sigma R_a dr = \Sigma S_a dl; \quad \Sigma R_b dr = \Sigma S_b dl; \quad \Sigma R_c dr = \Sigma S_c dl. \quad \dots \quad (8e)$$

These values inserted into Eq. (7g), and others of that form, give

$$\left. \begin{aligned} \Sigma R_a dr &= \Sigma S_a S_o \rho - X_a \Sigma S_a^2 \rho - X_b \Sigma S_a S_b \rho - X_c \Sigma S_a S_c \rho + \Sigma S_a \epsilon t l \\ \Sigma R_b dr &= \Sigma S_b S_o \rho - X_a \Sigma S_b S_a \rho - X_b \Sigma S_b^2 \rho - X_c \Sigma S_b S_c \rho + \Sigma S_b \epsilon t l \\ \Sigma R_c dr &= \Sigma S_c S_o \rho - X_a \Sigma S_c S_a \rho - X_b \Sigma S_c S_b \rho - X_c \Sigma S_c^2 \rho + \Sigma S_c \epsilon t l \end{aligned} \right\}, \quad \dots \quad (8f)$$

wherein the summations extend over all the members including the redundant, and all the terms retain their previous significance. Therefore, when  $X_a=1$ , then  $S_o=0$ ,  $S_a=1=X_a$ ,  $S_b=0$ , and  $S_c=0$ .

The first terms of the right-hand side of each of the Eqs. (8f), according to Eqs. (8a), may be expressed in terms of the external loads as follows:

$$\Sigma S_o S_a \rho = \Sigma P_m \delta_{ma}; \quad \Sigma S_o S_b \rho = \Sigma P_m \delta_{mb}; \quad \Sigma S_o S_c \rho = \Sigma P_m \delta_{mc}, \quad \dots \quad (8g)$$

and may be evaluated from Williot-Mohr displacement diagrams, Chapter VI. All the other summations may be determined once for all either from Maxwell stress diagrams, or in terms of displacements by employing Eqs. (8b).

Problems of the kind treated in Art. 6 can now be solved for any indeterminate structure by following precisely the same method there indicated except that the redundants



must first be found by one of the two methods just given, finally employing Eq. (7A), to ascertain the stresses. These stresses being found, the elastic changes in all the members are computed. Then by applying a conventional unit load to the point for which the displacement is desired, determine the stresses in the principal system for this unit load and proceed as before by using Eq. (6A).

It may be well to mention in closing this subject that there is usually a wide latitude in the choice of the redundant conditions. Thus, in Fig. 7A, one abutment might have been placed on rollers, thus making the principal system a simple truss on two supports. Then  $X_a$  would have become the horizontal thrust instead of the stress in a member.

### ART. 9. PROF. MAXWELL'S THEOREM (1864)

This theorem, known as the law of reciprocal displacements, and previously mentioned in discussing Eqs. (8D), establishes the mutual relation between the elastic displacements of a pair of points, or a pair of lines, whenever these displacements result from simultaneous conditions of loading; provided that the arrangement of the members remains unchanged and the supports are immovable.

For the sake of simplicity it is assumed that the frame is in a condition of no stress and that there are no temperature changes.

Clapeyron's law then applies and the equation for *actual work* becomes

$$A = \frac{\sum S \Delta l}{2} = \frac{\sum P \delta}{2} = \frac{1}{2} [P_1 \delta_1 + P_2 \delta_2 + P_3 \delta_3 + \text{etc.}], \dots \dots \dots (9A)$$

wherein the  $P$ 's are concentrated loads, and the  $\delta$ 's are the deflections of the points on which the loads act in the respective directions of these loads.

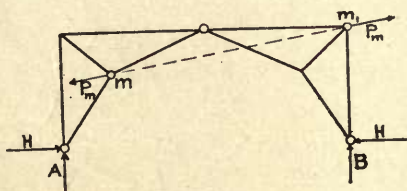


FIG. 9A.

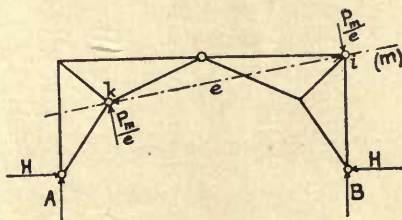


FIG. 9B.

Each of the products  $\frac{1}{2} P_m \delta_m$  may now be regarded as a summation of work produced by some group of loads such that the work of the group is exactly identical with the work represented by  $\frac{1}{2} P_m \delta_m$ . Figs. 9A, 9B, and 9C will illustrate just what is meant by such groups of loads.

If in Fig. 9A, two equal and opposite forces  $P_m$  are applied at the points  $m_1$  and  $m$ , then the resulting  $\delta_m$  represents the relative displacement between these two points. We call this case the *loading of a pair of points* corresponding to the case illustrated in Fig. 6A, where the loads  $P$  are each equal to unity.

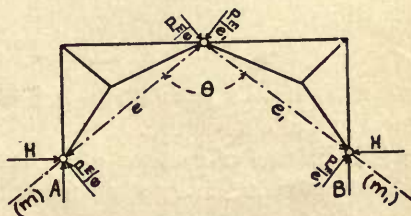


FIG. 9C.



Fig. 9B shows a pair of equal and opposite forces perpendicular to a line  $\overline{ik}$  and producing a couple of moment  $1 \cdot P_m$ . This represents the *loading of a line*. The resulting  $\delta_m$  represents the angular change in the line  $\overline{ik}$  expressed in arc. This case may be designated as the loading of a line  $m$  and, when  $P=1$ , it becomes the unit loading of this line.

Fig. 9c represents the *loading of a pair of lines*  $m_1$  and  $m$ . The  $\delta_m$  of this group of loads is the relative angular change between the two lines, or it is the change in the angle  $\theta$ , which results from the conventional loading.

The three groups of loadings are typical, and any particular load applied to a frame may become one load of such a group, but not of two or more groups simultaneously.

For brevity, any such group of loads will be known as a *loading* and the corresponding  $\delta$  will be the *path* or elastic displacement of the loading.

The several  $\delta$ 's are always linear functions of the applied loads  $P$  and can be expressed as follows:

$$\left. \begin{aligned} \delta_a &= \delta_{aa}P_a + \delta_{ab}P_b + \dots \delta_{am}P_m; \\ \delta_b &= \delta_{ba}P_a + \delta_{bb}P_b + \dots \delta_{bm}P_m; \\ \delta_m &= \delta_{ma}P_a + \delta_{mb}P_b + \dots \delta_{mm}P_m, \end{aligned} \right\} \dots \dots \dots (9B)$$

wherein the  $\delta$ 's with the double subscripts are independent of the loads  $P$ , and for example  $\delta_{am}$  represents the special value of  $\delta_a$  when  $P_m=1$  and all the other loads  $P$  are zero, all in accordance with the nomenclature employed in Art. 8.

Now apply loads  $P_m$  to any frame, producing stresses  $S_m$  in the several members, and changes in their lengths  $\Delta l_m = S_m l / EF$ .

Likewise for a system of loads  $P_n$ , producing stresses  $S_n$ , and changes  $\Delta l_n = S_n l / EF$ .

Let  $\delta'_{mn}$  = the value of  $\delta_m$ , for the point  $m$ , when certain loads  $P_n$  only are active. Also, let  $\delta'_{nm}$  = the special value of  $\delta_n$  for the point  $n$ , when a certain set of loads  $P_m$  only are active. Then note that  $\delta'_{mn} = \delta_{mn}$  when  $\Sigma P_n = 1$  and  $\delta'_{nm} = \delta_{nm}$  when  $\Sigma P_m = 1$ .

The work equation for the loads  $P_m$ , stresses  $S_m$  and displacements  $\delta'_{mn}$  and  $\Delta l_n$  due the loads  $P_n$  only, is according to Eq. (5E)

$$\Sigma P_m \delta'_{mn} = \Sigma S_m \Delta l_n = \Sigma S_m \frac{S_n l}{EF}.$$

Similarly

$$\Sigma P_n \delta'_{nm} = \Sigma S_n \Delta l_m = \Sigma S_n \frac{S_m l}{EF},$$

therefore,

$$\Sigma P_m \delta'_{mn} = \Sigma P_n \delta'_{nm}, \dots \dots \dots (9C)$$

which is Betti's law (1872) and which extends Maxwell's law to the summation of all members of a structure.

If instead of systems of loads  $P_m$  and  $P_n$  as above, only the unit loads  $P_m=1$  and  $P_n=1$  are successively applied to the frame, then Eq. (9c) becomes

$$\delta_{mn} = \delta_{nm}, \dots \dots \dots (9D)$$

which is Maxwell's law (1864) and may be stated thus:

1. The relative displacement  $\delta_{mn}$  of a pair of points  $m_1$  and  $m$ , resulting from a unit loading of another pair of points  $n_1$  and  $n$ , is equal to the relative displacement  $\delta_{nm}$  of the pair of points  $n_1$  and  $n$ , caused by a unit loading of the pair of points  $m_1$  and  $m$ .

2. The same equality exists between the relative angular changes of two pairs of lines, successively loaded with a unit loading.

3. The same equality also exists between the linear change in a pair of points resulting from a unit loading of a pair of lines, and the angular change (expressed in arc) of the pair of lines, resulting from a unit loading of the pair of points.

The practical value of Maxwell's law when applied to redundant conditions was shown in Art. 8. Its application to displacement influence lines is given in Chapter VIII.

ART. 10. THEOREMS RELATING TO WORK OF DEFORMATION

(a) **Menabrea's law (1858), or theorem of least work.** Given a statically indeterminate framework in an initial condition of no stress for which the temperature is known and remains constant; also, assuming that the supports are either rigidly fixed or permit frictionless movements, such that  $\Sigma R \Delta r = 0$  for the entire structure, then the changes in the lengths of the members are expressed by the formula  $\Delta l = Sl/EF$ , and the work equations for the several statically indeterminate quantities  $X_a, X_b, X_c$ , etc., are, according to Eqs. (8E),

$$\left. \begin{aligned} \Sigma R_a \Delta r &= \Sigma S_a \Delta l = \frac{\Sigma S_a Sl}{EF} = 0; \\ \Sigma R_b \Delta r &= \Sigma S_b \Delta l = \frac{\Sigma S_b Sl}{EF} = 0; \\ \Sigma R_c \Delta r &= \Sigma S_c \Delta l = \frac{\Sigma S_c Sl}{EF} = 0; \\ &\text{etc.,} \end{aligned} \right\} \dots \dots \dots (10A)$$

the value  $S$  in which is given by Eq. (7A) as

$$S = S_o - S_a X_a - S_b X_b - S_c X_c, \text{ etc.} \dots \dots \dots (10B)$$

The partial differentiation of  $S$  with respect to  $X_a$  gives

likewise for the other  $X$ 's,

$$\left. \begin{aligned} \frac{\partial S}{\partial X_a} &= -S_a; \\ \frac{\partial S}{\partial X_b} &= -S_b; \\ \frac{\partial S}{\partial X_c} &= -S_c. \end{aligned} \right\} \dots \dots \dots (10C)$$

The actual work of deformation for the entire frame, including redundant members as external forces, becomes by Clapeyron's law or Eq. (5A)

$$A = \frac{1}{2} \Sigma \frac{S^2 l}{EF} = \frac{1}{2} \Sigma P \delta, \dots \dots \dots (10D)$$

which when differentiated gives

$$\partial A = \frac{\Sigma S \partial S l}{EF},$$

and by dividing through by  $\partial X_a$  this becomes, after substitution of values from Eqs. (10c),

$$\frac{\partial A}{\partial X_a} = \Sigma S \frac{\partial S l}{\partial X_a EF} = - \frac{\Sigma S_a S l}{EF},$$

which by Eq. (10A) must equal zero. Hence,

$$\frac{\partial A}{\partial X_a} = 0 \quad \text{and similarly} \quad \frac{\partial A}{\partial X_b} = 0 \quad \text{and} \quad \frac{\partial A}{\partial X_c} = 0, \quad . . . . \quad (10E)$$

which proves that *the redundant or indeterminate conditions, reduce the actual work of deformation of the frame to a minimum.* This is the theorem of least work.

(b) **Castigliano's law (1879), or derivative of the work equation.** This law deals with the displacement of the point of application of a force.

Any external load  $P_m$  acting on a framework will, by Clapeyron's law, produce the *actual applied work of deformation*

$$A = \frac{1}{2} P_m \delta_m, \quad . . . . . \quad (10F)$$

when  $\delta_m$  is the displacement of the point of application of  $P_m$  in the direction of  $P_m$  and within range of proportionality, or within the elastic limit of the material.

Also, the *actual internal work of deformation*, for the entire frame, becomes, according to Eq. (10D)

$$A = \frac{1}{2} \Sigma \frac{S^2 l}{EF}, \quad . . . . . \quad (10D)$$

The partial differential derivative of  $A$  with respect to any certain external load  $P_m$  is

$$\frac{\partial A}{\partial P_m} = \frac{1}{2} \Sigma \frac{\partial}{\partial P_m} \left( \frac{S^2 l}{EF} \right) = \Sigma S \frac{\partial S}{\partial P_m} \cdot \frac{l}{EF}, \quad . . . . . \quad (10H)$$

wherein  $\partial S / \partial P_m$  is the derivative of the stress  $S$  in any member of a determinate or indeterminate structure.

The general expression for  $S$ , from Eq. (10B), by substituting for  $S_o$  its equivalent value in terms of external loads, becomes

$$S = S_1 P_1 + S_2 P_2, \text{ etc.}, + S_m P_m - S_a X_a - S_b X_b - S_c X_c, \text{ etc.}, \quad . . . \quad (10J)$$

in which  $S_1$  is the stress in the member  $S$  for  $P_1 = 1$ , while  $S_a$  is that stress when  $X_a = 1$ , etc.; finally  $S$  is the stress in any particular member caused by the combined effects of all  $P$ 's and  $X$ 's.

The several values  $S_1$  to  $S_m$  are thus independent of the loads  $P$  and  $X$ . Also, the loads  $P$  and  $X$  are independent of each other. Hence,  $S$  may be partially differentiated with respect to  $P_m$  or  $X$  and Eq. (10J) when so treated gives

$$\frac{\partial S}{\partial P_m} = S_m \quad \text{and} \quad \frac{\partial S}{\partial X_a} = -S_a, \text{ etc.} \quad . . . . . \quad (10K)$$



Substituting this value in Eq. (10H) then

$$\frac{\partial A}{\partial P_m} = \Sigma S_m S \left( \frac{l}{EF} \right). \quad \dots \quad (10L)$$

but, according to Mohr's law, Eq. (6A), when abutment displacements are zero, then

$$1 \cdot \delta_m = \Sigma S_m S \left( \frac{l}{EF} \right). \quad \dots \quad (10M)$$

In Eqs. (10L) and (10M) the summation extends to all the members, including the redundant conditions, and hence

$$1 \cdot \delta_m = \frac{\partial A}{\partial P_m}, \quad \dots \quad (10N)$$

which, expressed in words, means that *the path  $\delta_m$  of a load  $P_m$  is equal to the partial differential derivitave of the actual work of the frame with respect to  $P_m$ .*

Castigliano's law thus expressed is equivalent to Mohr's work equation, that is, leading to the identical result by a more circuitous process.

In similar manner the same law may be deduced for girders with solid webs.

Mohr's law thus offers the most direct method of finding any displacement which may result from any specific cause. Castigliano's law will lead to the same conclusions by a somewhat less direct method.

ART. 11. TEMPERATURE STRESSES FOLLOW MENABREA'S AND CASTIGLIANO'S LAWS

When a structure is subjected to a uniform change in temperature  $t$  then, from Eq. (4A),

$$\Delta l = \frac{Sl}{EF} + \epsilon t l.$$

This value of  $\Delta l$  when substituted into Eq. (10D) for  $Sl/EF$ , gives

$$A = \frac{\Sigma S^2 l}{2EF} + \Sigma \epsilon t S l, \quad \dots \quad (11A)$$

and the differential of  $A$  with respect to  $S$  is

$$\partial A = \frac{\Sigma S \partial S l}{EF} + \Sigma \epsilon t l \partial S. \quad \dots \quad (11B)$$

Similarly when the temperature effect is introduced into Eqs. (10A) then for immovable abutments as before

$$\Sigma S_a \Delta l = \frac{\Sigma S_a S l}{EF} + S_a \epsilon t l = 0. \quad \dots \quad (11C)$$

Also, Eqs. (10c) apply equally when temperature effects are included, hence by dividing Eq. (11B) by  $\partial X_a$ , and substituting values from Eqs. (10c), then Eq. (11B) becomes

$$\frac{\partial A}{\partial X_a} = \frac{\Sigma S \partial S l}{\partial X_a E F} + \Sigma \epsilon t l \frac{\partial S}{\partial X_a} = \frac{\Sigma S_a S l}{E F} + \Sigma S_a \epsilon t l. \quad (11D)$$

But, by Eq. (11c) this expression is equal to zero, hence, as before

$$\frac{\partial A}{\partial X_a} = 0 \quad \text{and similarly} \quad \frac{\partial A}{\partial X_b} = 0, \text{ etc.}, \quad (11E)$$

which proves Menabrea's law applicable to the general case of stress from temperature and applied loads, provided the abutments are rigid and immovable.

The introduction of the temperature factor  $\Sigma \epsilon t S l$  from Eq. (11A) into Eqs. (10G), to (10N) will suffice to prove that Castigliano's law also applies to the general case including temperature effects. It is not deemed necessary to repeat the transformations here.

## ART. 12. STRESSES DUE TO ABUTMENT DISPLACEMENTS

Abutment displacements produce stresses which follow Menabrea's and Castigliano's laws.

This is readily seen when it is considered that the supporting elements may always be replaced by linked members which take up these displacements and undergo elastic deformations. The immovable supports are then outside of these *connecting links* as illustrated in Figs. 1D, 1E and 1F, and the links are counted with the structural members.

If then the abutment displacements are defined as distortions  $\Delta r$  in these several *links*, which are in every way equal to the former displacements, the resulting effect on the structure remains unchanged.

Therefore, when the distortions  $\Delta r$  must be considered in the computation of the  $X$ 's and  $\delta$ 's, it is only necessary to extend the work equations to include these *links*. It is also clear that these links may have any desired sections, lengths or values of  $E$ , as may be required for metal or masonry supports.

Thus, let  $r$  be the length of a supporting link;

$R$  the load which the link carries;

$\Delta r$  the change in length of this link;

$F_r$  the cross-section of this link;

$\epsilon_r$  the coefficient of expansion;

$t$  the change in temperature from the normal;

$E_r$  the modulus of elasticity for any material.

then from Eq. (4A)

$$\Delta r = \frac{Rr}{E_r F_r} + \epsilon_r t r. \quad (12A)$$

The general work Eq. (11A) then becomes

$$A = \frac{\Sigma S^2 l}{2EF} + \Sigma \epsilon t S l + \Sigma R \Delta r = 0, \quad (12B)$$



wherein  $\mathcal{A}r$  may be regarded as a constant and Menabrea's and Castigliano's laws again apply.

For the case of one external indeterminate,  $R$  becomes  $X_a$  and  $\mathcal{A}r$  becomes  $\delta_a$ , then from Eq. (12B)

$$A = \frac{\Sigma S^2 l}{2EF} + \Sigma \epsilon t S l + X_a \delta_a.$$

By differentiating for  $S$  with respect to  $X_a$  and imposing the condition for minimum this becomes

$$\frac{\Sigma S \partial S l}{\partial X_a EF} + \Sigma \epsilon t l \frac{\partial S}{\partial X_a} + \delta_a = 0. \quad (12c)$$

Also,  $S = S_o - S_a X_a$  and its differential is

$$\frac{\partial S}{\partial X_a} = -S_a. \quad (12d)$$

Substituting the value from Eq. (12d) into Eq. (12c) and solving for  $X_a$  then the latter becomes

$$X_a = \frac{\Sigma S_o S_a \frac{l}{EF} + \Sigma \epsilon t l S_a - \delta_a}{\frac{\Sigma S_a^2 l}{EF}}, \quad (12e)$$

which might be used as the expression for the horizontal thrust of a two-hinged arch where  $X_a$  is the redundant thrust.

## CHAPTER III

### THEOREMS, LAWS, AND FORMULÆ FOR ISOTROPIC SOLIDS

#### ART. 13. GENERAL WORK EQUATIONS

In the previous chapters no consideration was given to solid web structures or other isotropic solid bodies only in so far as was necessary in demonstrating the general laws and theorems of framed structures.

While it is true that the foregoing discussion is generally applicable to all isotropic solid bodies which are supported in any of the ways given in Chapter I, and stressed within the elastic limit by externally applied loads, yet the formulæ previously given will require some modifications to better adapt them to solid web and other massive and homogeneous structures. Also, the introduction of shearing stress now enters as a further complication.

As was previously mentioned, all structures which are purely isotropic can involve only external redundancy. It is, therefore, desirable to take up this subject to the

extent, at least, of giving the special formulæ applicable to any solid in which the physical properties of the material are presumably uniform in any and all directions. Such bodies are called isotropic solids.

It will scarcely be necessary to prove at length all of the theorems and laws previously given for frames, but a passing reference at the proper time will be deemed sufficient proof of their general acceptance.

The elastic deformation resulting from given stresses in an infinitesimally small particle of a body is a certain and definitely measurable quantity and is dependent only on the magnitude of the given stresses and the physical properties of the material.

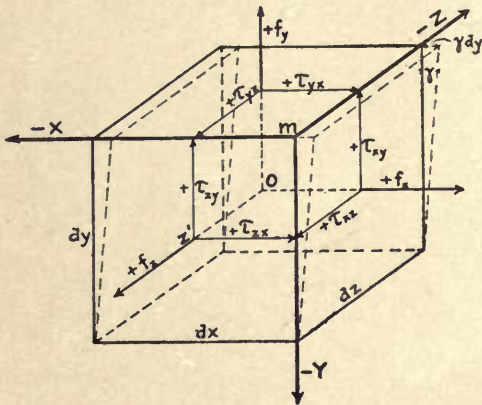


FIG. 13A.

If then Fig. 13A represents a small parallelepiped of mass, referred to axes  $X$ ,  $Y$  and  $Z$ , and having dimensions  $dx$ ,  $dy$  and  $dz$ , coincident with these axes respectively, then the stress acting at the corner  $m$  is determined in magnitude and direction by nine components, viz., three normal stresses and six tangential stresses acting in the three coordinate planes and positive in the directions of the arrows.

Let  $f_x, f_y$  and  $f_z$  be the unit normal stresses (tension or compression) in the directions  $X, Y$  and  $Z$ , respectively. Also, let  $\tau_{xy}$  and  $\tau_{xz}$  be the unit tangential stresses in the  $\overline{YZ}$  plane;  $\tau_{yx}$  and  $\tau_{yz}$  those in the  $\overline{XZ}$  plane; and  $\tau_{zx}$  and  $\tau_{zy}$  those in the  $\overline{XY}$  plane. The first subscript indicating the normal stress to which they belong, and the second subscript referring to the axis.

The two unit tangential stresses intersecting in any one point are equal, in each case, otherwise the body would rotate about its center of gravity, which is the intersection  $O$  of the three normal unit stresses. Also, because the three normal stresses and four tangential stresses,  $\tau_{yz}, \tau_{xz}, \tau_{zy}$  and  $\tau_{zx}$ , cannot have any moment about such a gravity axis  $\overline{OZ'}$ , hence, the moment of the two remaining stresses  $\tau_{yx}$  and  $\tau_{xy}$  must equal zero. But, the latter having equal lever arms must be equal to each other.

Therefore,

$$\tau_{xy} = \tau_{yx} = \tau_x; \quad \tau_{yz} = \tau_{zy} = \tau_y; \quad \tau_{zx} = \tau_{xz} = \tau_z. \quad (13A)$$

The resulting stress at the point  $m$  is then determined by the three normal stresses  $f_x, f_y, f_z$  and the three tangential stresses  $\tau_x, \tau_y$ , and  $\tau_z$  in Eqs. (13A), and these in turn determine the deformation of the parallelopiped.

Let  $\Delta dx, \Delta dy$  and  $\Delta dz$  represent small elastic changes which the lengths  $dx, dy$  and  $dz$  undergo, then the forces represented by the unit normal stresses  $f$  will produce the following virtual work:

$$dW_f = f_x dydz \Delta dx + f_y dzdx \Delta dy + f_z dxdy \Delta dz = \left( f_x \frac{\Delta dx}{dx} + f_y \frac{\Delta dy}{dy} + f_z \frac{\Delta dz}{dz} \right) dx dy dz. \quad (13B)$$

Also, let  $\gamma_x, \gamma_y$  and  $\gamma_z$  be the tangents of small angular distortions of the parallelopiped such that  $+\gamma_x$  is an increase in the angle between the  $Y$  and  $Z$  axes;  $\gamma_y$  the change in the angle between the  $X$  and  $Z$  axes, etc. Then the virtual work of the tangential forces is found thus: For the distortion of the  $\overline{YZ}$  plane, the path is  $\gamma_x dy$  and the force is  $\tau_x dx dz$ , and since the vertical force  $\tau_x$  can do no work in this direction then the work of the tangential stress for the plane  $\overline{XZ}$  becomes  $\tau_x dx dz \gamma_x dy$ , and similarly for the other two planes, whence the total work becomes

$$dW_\tau = \tau_x dx dz \gamma_x dy + \tau_y dy dx \gamma_y dz + \tau_z dz dy \gamma_z dx. \quad (13C)$$

The expressions  $\Delta dx/dx, \Delta dy/dy$ , and  $\Delta dz/dz$  in Eqs. (13B) are rates of elongation, or coefficients, for which the values  $\alpha_x, \alpha_y$  and  $\alpha_z$  may be substituted. Then by making  $dx dy dz = dV$ , and combining Eqs. (13B) and (13C), the total internal virtual work is obtained. Also, since by Clapeyron's law, this must be equal to the virtual work of the externally applied forces, then the fundamental work equation for isotropic bodies becomes:

$$W = \Sigma P \delta + \Sigma R \Delta r = \int [f_x \alpha_x + f_y \alpha_y + f_z \alpha_z + \tau_x \gamma_x + \tau_y \gamma_y + \tau_z \gamma_z] dV. \quad (13D)$$

This equation is applicable to any case of related displacements and elastic deformations  $\delta, \Delta r, \alpha$ , and  $\gamma$ , so long as these are small in comparison with the dimensions of the structure. The external forces must include dead loads and all frictional resistances which may be active at points of support.



As was previously shown for indeterminate frames, so also the various elements in Eq. (13D) may now be expressed as linear functions of the applied loads and any redundant conditions, thus:

$$\left. \begin{aligned} R &= R_o - R_a X_a - R_b X_b, \text{ etc.} \\ f_x &= f_{xo} - f_{xa} X_a - f_{xb} X_b, \text{ etc.} \\ f_y &= f_{yo} - f_{ya} X_a - f_{yb} X_b, \text{ etc.} \\ f_z &= f_{zo} - f_{za} X_a - f_{zb} X_b, \text{ etc.} \\ \tau_x &= \tau_{xo} - \tau_{xa} X_a - \tau_{xb} X_b, \text{ etc.} \\ &\text{etc.,} \quad \text{etc.} \end{aligned} \right\} \dots \dots \dots (13E)$$

Also, the virtual work of the reactions for each of the conventional loadings becomes, (see Eqs. (7E)):

$$\left. \begin{aligned} \Sigma R_a \Delta r &= \int [f_{xa} \alpha_x + f_{ya} \alpha_y + f_{za} \alpha_z + \tau_{xa} \gamma_x + \tau_{ya} \gamma_y + \tau_{za} \gamma_z] dV \\ \Sigma R_b \Delta r &= \int [f_{xb} \alpha_x + f_{yb} \alpha_y + f_{zb} \alpha_z + \tau_{xb} \gamma_x + \tau_{yb} \gamma_y + \tau_{zb} \gamma_z] dV \end{aligned} \right\} \dots \dots \dots (13F)$$

etc.

Then by writing Eq. (13D) for a load  $P_a = 1$  the following is obtained:

$$1 \cdot \delta_m = \int [f_{xa} \alpha_x + f_{ya} \alpha_y + f_{za} \alpha_z + \tau_{xa} \gamma_x + \tau_{ya} \gamma_y + \tau_{za} \gamma_z] dV - \Sigma R_a \Delta r. \dots (13G)$$

from which problems of the kind described in Art. 6 may be solved.

Since the redundants  $X$  in Eqs. (13E) may be treated as independent variables, their differentiation furnishes

$$\frac{\partial f_x}{\partial X_a} = -f_{xa}; \quad \frac{\partial f_y}{\partial X_a} = -f_{ya}; \quad \text{etc., and} \quad \frac{\partial \tau_x}{\partial X_a} = -\tau_{xa}; \quad \text{etc.,}$$

which by substitution into Eqs. (13F) give

$$\begin{aligned} -\Sigma R_a \Delta r &= \int \left[ \alpha_x \left( \frac{\partial f_x}{\partial X_a} \right) + \alpha_y \left( \frac{\partial f_y}{\partial X_a} \right) + \alpha_z \left( \frac{\partial f_z}{\partial X_a} \right) + \gamma_x \left( \frac{\partial \tau_x}{\partial X_a} \right) \right. \\ &\quad \left. + \gamma_y \left( \frac{\partial \tau_y}{\partial X_a} \right) + \gamma_z \left( \frac{\partial \tau_z}{\partial X_a} \right) \right] dV. \dots (13H) \end{aligned}$$

Similar expressions result for  $\Sigma R_b \Delta r$ , etc.

The general work equation is now found by inserting for the actual distortions  $\alpha$  and  $\gamma$  their values in terms of stresses and the moduli of elasticity for direct and tangential stress.

The length  $dx$  subjected to the unit stress  $f_x$  and a rise in temperature of  $t$  degrees, will be changed by an amount

$$\alpha_x = \frac{\Delta dx}{dx} = \frac{f_x}{E} + \epsilon t.$$

The two other unit stresses  $f_y$  and  $f_z$  will diminish the effect on  $\alpha_x$  by an amount

$$\frac{f_y + f_z}{mE},$$

wherein  $m$  is the "Poisson number" (1829) which is given as 3.33 for structural steel and 3.5 for high steel. Professor F. E. Turneaure gives 0.1 to 0.125 for concrete. This quantity  $m$  is also defined as the ratio of lateral to longitudinal deformation and is determined by experiment.

Hence,  $\alpha_x$  and similarly  $\alpha_y$  and  $\alpha_z$ , also,  $\gamma_x$ ,  $\gamma_y$  and  $\gamma_z$  may be evaluated as follows:

$$\left. \begin{aligned} \alpha_x &= \frac{1}{E} \left[ f_x - \frac{f_y + f_z}{m} + E\epsilon t \right], & \text{and} & \quad \gamma_x = \frac{\tau_x}{G} \\ \alpha_y &= \frac{1}{E} \left[ f_y - \frac{f_z + f_x}{m} + E\epsilon t \right], & \text{and} & \quad \gamma_y = \frac{\tau_y}{G} \\ \alpha_z &= \frac{1}{E} \left[ f_z - \frac{f_x + f_y}{m} + E\epsilon t \right], & \text{and} & \quad \gamma_z = \frac{\tau_z}{G} \end{aligned} \right\}, \dots \dots \dots (13j)$$

wherein  $G$  is the modulus of tangential stress or shear and has the value  $G = \frac{mE}{2(m+1)}$ ,

while  $m$  is the "Poisson number" just given.

Inserting the values given by Eqs. (13j) into Eq. (13d), the following equation is obtained for the *actual work* of an isotropic body:

$$A = \frac{W}{2} = \int \left[ f_x^2 + f_y^2 + f_z^2 - \frac{2}{m}(f_x f_y + f_x f_z + f_y f_z) \right] \frac{dV}{2E} \\ + \int \left[ \tau_x^2 + \tau_y^2 + \tau_z^2 \right] \frac{dV}{2G} + \int [f_x + f_y + f_z] \epsilon t dV. \quad (13k)$$

Also, by substituting the values from Eqs. (13j) into Eq. (13h), reducing and integrating the expressions  $f_x \partial f_x$ , etc., the following simple form is obtained by inserting the value from Eq. (13k), when temperature effect is neglected, thus:

$$\Sigma R_a \Delta r = \frac{\partial A}{\partial X_a} \quad \text{and similarly} \quad \Sigma R_b \Delta r = \frac{\partial A}{\partial X_b}, \text{ etc.} \dots \dots \dots (13l)$$

When the abutments are immovable and no temperature effects exist then

$$\frac{\partial A}{\partial X_a} = 0 \quad \text{and} \quad \frac{\partial A}{\partial X_b} = 0, \text{ etc.}, \dots \dots \dots (13m)$$

which again proves Menabrea's law.

Proceeding from Eq. (13g) in the same manner above applied to Eq. (13f) to obtain Eq. (13h), and then substituting values from Eqs. (13j), reducing and integrating as before, the following important fundamental equation is obtained for any load  $P_m$ , or redundant  $X_m$ :

$$\delta_m = \frac{\partial A}{\partial P_m} - \Sigma \frac{\partial R}{\partial P_m} \Delta r. \quad \dots \dots \dots (13n)$$

The value of  $A$  in all the Eqs. (13L) to (13N) is that given by Eq. (13K).

When the abutments are immovable the last term of Eq. (13N), becomes zero and Castigliano's law is again established.

Proceeding from Eq. (13G), and writing same for two related conditions of unit loading, it is easily shown that Maxwell's law likewise applies here.

#### ART. 14. WORK OF DEFORMATION DUE TO SHEARING STRESS

For a beam of any section and any loading applied in the vertical plane  $\overline{YY}$ , Figs. 14A and 14B, the resultant of the external forces on one side of any section  $\overline{AA}$  may be represented by a force  $R$  which may in turn be resolved into a normal force  $N$  and a tangential force  $Q$  acting at the point of application of  $R$  on the section  $\overline{AA}$ .

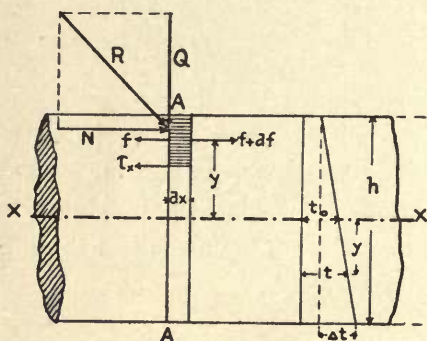


FIG. 14A.

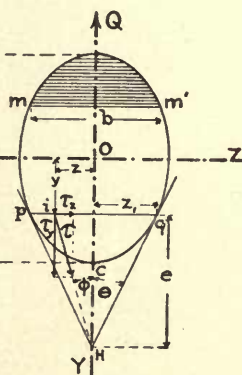


FIG. 14B.

Let  $M$  be the static moment of the normal force  $N$  about the  $Z$  axis and  $I_z$  the moment of inertia of the section about this same axis.

Then the unit stress  $f$  at any point of the section is by Navier's law:

$$f = \frac{N}{F} + \frac{My}{I_z} \quad \dots \dots \dots (14A)$$

If now this stress undergoes a small change  $df$  due to the differential change in  $R$  for a neighboring section, distant  $dx$  from the first, then the shear on the area  $2z_1dx$  becomes

$$2\tau_x z_1 dx = \int (f + df) dF - \int f dF = \int df dF \quad \dots \dots \dots (14B)$$

where  $\tau_x$  is the unit shear on the differential area  $dF$ .

Assuming  $N$  constant in Eq. (14A), and treating  $M$  as a variable, then by differentiation

$$df = \frac{y dM}{I_z} \quad \dots \dots \dots (14C)$$



Also, since the shear is the differential of the bending moment, then

$$dM = Qdx. \quad (14D)$$

Combining Eqs. (14B), (14C) and (14D), then

$$2\tau_x z_1 dx = \int \frac{y dM dF}{I_z} = \frac{Q dx}{I_z} \int y dF, \quad (14E)$$

and since  $\int y dF$  is the static moment  $M_s$  of the cross-section, this integration may be considered performed to obtain

$$\tau_x = \frac{QM_s}{2z_1 I_z} = \frac{Q}{b I_z} \int y dF. \quad (14F)$$

Return now to Fig. 14B, take any section  $\overline{pq}$  perpendicular to the  $y$  axis and let  $Q$  produce a unit shear  $\tau$  in any point  $i$  of this section. The line of this shear intersects the  $y$  axis in a point  $H$ , which is determined by the tangent  $\overline{pH}$ . This is a pure assumption, but from the nature of the case it is the most rational assumption to make.

The shear  $\tau$  may now be resolved into components  $\tau_y$  and  $\tau_z$ , while  $\tau_x$ , for this sectional plane, must be zero. However,  $\tau_y$  now has the same value as previously found for  $\tau_x$ , and hence

$$\tau_y = \frac{QM_s}{2I_z z_1} = \frac{Q}{b I_z} \int y dF. \quad (14G)$$

Again, from Fig. 14B,  $\tan \phi = \frac{\tau_z}{\tau_y} = \frac{z}{e}$  from which  $\tau_z = \frac{z}{e} \tau_y$ . But  $\tan \theta = \frac{z_1}{e}$ , therefore,

$$\tau_z = \tau_y \left( \frac{z}{z_1} \right) \tan \theta. \quad (14H)$$

For  $\theta = 0$ ,  $\tau_z = 0$ , which is the case for any surface point, the tangent to which is parallel to the  $y$  axis.

From Eqs. (14F) and (14G) it follows that for a given loading and section, the shearing stresses depend only on  $M_s$  and attain a maximum when the section coincides with a gravity axis parallel to the neutral axis. In practical cases it is usually sufficient to consider the shearing stress of a section as extending only over a unit length of the beam, as given by Eq. (14F). The actual work produced by shearing stress alone is then found from Eq. (13K) as

$$A = \frac{1}{2} \int (\tau_y^2 + \tau_z^2) \frac{dV}{G} = \frac{1}{2} \int \frac{dx}{G} \int \int (\tau_y^2 + \tau_z^2) dy dz. \quad (14J)$$

By substituting the value of  $\tau_z$  from Eq. (14H), into Eq. (14J), the latter becomes

$$\begin{aligned} A &= \frac{1}{2} \int \frac{dx}{G} \int \int \tau_y^2 \left( 1 + \tan^2 \theta \frac{z^2}{z_1^2} \right) dy dz, \\ A &= \frac{1}{2} \int \frac{dx}{G} \int \tau_y^2 dy \int_{-z_1}^{+z_1} \left( 1 + \tan^2 \theta \frac{z^2}{z_1^2} \right) dz, \\ A &= \int \frac{dx}{G} \int \tau_y^2 \left( 1 + \frac{1}{3} \tan^2 \theta \right) z_1 dy, \quad (14K) \end{aligned}$$

and by substituting for  $\tau_y$  its value from Eq. (14c), then Eq. (14k) may be solved for any special section. This gives in general for any section

$$\left. \begin{aligned} A &= \beta \int \frac{Q^2 dx}{2GF} \\ \beta &= \frac{F}{Q^2} \int \tau_y^2 dF \\ \tau_y &= \frac{Q}{bI_z} \int y dF \end{aligned} \right\} \dots \dots \dots (14L)$$

In Eqs. (14L)  $\beta$  is an involved function of the shape of the section, called by German authors the “*distribution number*” of the section, or “coefficient of shearing strain.”

This number  $\beta$  is 1.2 for any solid square or rectangular section, and 1.111 for a solid circular or elliptic section. Other values will be given after illustrating the computation of this number by the use of Eq. (14L).

**For a rectangle** of height  $h$  and breadth  $b=2z_1$ , then  $I_z=\frac{bh^3}{12}$ ;  $F=bh$ ; and  $dF=bdy$ , hence,

$$\tau_y = \frac{Q}{2z_1 I_z} \int_y^{\frac{h}{2}} y dF = \frac{3Qh^2}{2bh^3} \left(1 - \frac{4y^2}{h^2}\right)$$

and

$$\beta = \frac{bh}{Q^2} \int_{-\frac{h}{2}}^{+\frac{h}{2}} \tau_y^2 dF = 2 \left( \frac{9b^2h^5Q^2}{4b^2h^6Q^2} \right) \int_0^{\frac{h}{2}} \left(1 - \frac{4y^2}{h^2}\right)^2 dy = 2 \left( \frac{9}{4} \right) \left( \frac{1}{2} - \frac{1}{3} + \frac{1}{16} \right) = \frac{6}{5} = 1.20.$$

**For any I section**, Professor Mehrtens finds the general formula for  $\beta$  as follows:

$$\beta = \frac{F}{Q^2} \int \tau^2 dF = \frac{F}{I^2} \left[ \frac{h^2d}{6} (8b^3 - 12b^2t - t^3 + 6bt^2) + \frac{t}{2} \left( \frac{8a^5}{15} + \frac{4ia^3}{3} + i^2a \right) \right], \dots \dots (14M)$$

wherein  $i = \frac{4db_1h}{t}$  and the special dimensions here used are shown in Fig. 14c.

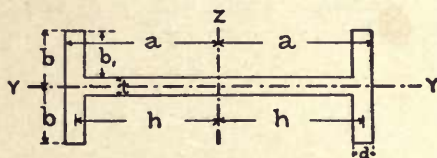


FIG. 14c.

Professor L. von Tetmajer, in his “*Elastizitaets und Festigkeitslehre*,” 1905, p. 49, gives a table of values for  $\beta$  for I beams ranging from  $3\frac{3}{8}''$ —4 lbs. to  $19\frac{3}{4}''$ —95 lbs., for which  $\beta=2.39$  to 2.03 respectively. Also for riveted girders made of  $\frac{3}{8}''$  webs, 4 L’s  $3\frac{9}{16}'' \times 3\frac{9}{16}'' \times \frac{3}{8}''$  each, and 2 plates  $8\frac{5}{8}'' \times \frac{3}{8}''$  on each chord. Then for

$2a=15\frac{3}{4}''$	$19\frac{1}{16}''$	$23\frac{5}{8}''$	$27\frac{9}{16}''$
$\beta=2.96$	2.71	2.49	2.35

The value  $\beta$  is independent of the unit of length and is, therefore, the same for metric and U. S. measures.

# ART. 15. WORK OF DEFORMATION FOR ANY INDETERMINATE STRAIGHT BEAM

**Direct stress.** For axial or direct stress only, Eq. (13κ) gives

$$A = \int \frac{f_x^2}{2E} dV + \int f_x \epsilon t dV. \quad (15A)$$

Also, by observing that  $\alpha_x = f_x/E$ , then Eq. (13H) becomes for direct stress alone,

$$\Sigma R_a dr = \int \frac{f_x \partial f_x}{E \partial X_a} dV + \int \frac{\epsilon t \partial f_x}{\partial X_a} dV = \frac{\partial A}{\partial X_a}. \quad (15B)$$

Now  $\int f_x dF = N$ , the normal direct stress, and, as  $dV = dF dx$ , then from Eq. (15A)

$$\int \frac{f_x^2}{2E} dV = \int \frac{N f_x dx}{2E} = \int \frac{N f_x F dx}{2EF} = \int \frac{N^2 dx}{2EF}, \quad (15C)$$

and similarly from Eq. (15B)

$$\int \frac{f_x \partial f_x}{E \partial X_a} dV = \int \frac{N \partial f_x dx}{E \partial X_a} = \int \frac{N \partial f_x F dx}{EF \partial X_a} = \int \frac{N \partial N dx}{EF \partial X_a}. \quad (15D)$$

**The temperature effects** in Eqs. (15A) and (15B) will now be determined on the supposition that the effect is not uniform, but as shown on Fig. 14A, where

$t_0$  = the change in temperature from normal at the gravity axis of the section;

$\Delta t$  = the difference in temperature of the two extreme fibers;

$h$  = height of the section;

$y$  = any ordinate;

$t$  = the temperature above normal, of any point of the section then

$$t = t_0 + \Delta t \frac{y}{h}. \quad (15E)$$

Substituting this value for  $t$  into the temperature element of Eq. (15A), the latter becomes

$$\int f_x \epsilon t dV = \int \int f_x \left( t_0 + \Delta t \frac{y}{h} \right) \epsilon dx dF = \int \epsilon t_0 dx \int f_x dF + \int \frac{\epsilon \Delta t}{h} dx \int f_x y dF.$$

But  $\int f_x dF = N$  and  $\int f_x y dF = M$  = moment of resistance of the section, therefore,

$$\int f_x \epsilon t dV = \int \epsilon t_0 N dx + \int \epsilon \Delta t \frac{M}{h} dx. \quad (15F)$$

By differentiating Eq. (15F), and dividing through by  $\partial X_a$ , the value of the temperature element for Eq. (15B), is obtained thus:

$$\int \frac{\epsilon t \partial f_x}{\partial X_a} dV = \int \epsilon t_0 \frac{\partial N}{\partial X_a} dx + \int \frac{\epsilon \Delta t}{h} \frac{\partial M}{\partial X_a} dx. \quad (15G)$$



**The bending moment.** From Eq. (14A),  $f_x = My/I_z$  and  $I_z = \int y^2 dF$ . With these values and neglecting the temperature element, Eq. (15A) becomes

$$A = \int \frac{f_x^2}{2E} dV = \int \frac{M^2 y^2}{2EI_z^2} dV = \int \frac{M^2 dx}{2EI_z^2} \int y^2 dF = \int \frac{M^2}{2EI_z} dx. \quad (15H)$$

By differentiating Eq. (15H) and dividing through by  $\partial X_a$  then

$$\frac{\partial A}{\partial X_a} = \int \frac{M}{EI_z} \frac{\partial M}{\partial X_a} dx = \Sigma R_a \Delta r. \quad (15J)$$

**The general work equation**, including all effects, may now be written out by collecting the several Eqs. (14L), (15A), (15C), (15H), and (15F) into the following, representing the *total actual work* for any isotropic body by

$$A = \int \frac{N^2 dx}{2EF} + \int \frac{M^2 dx}{2EI_z} + \beta \int \frac{Q^2 dx}{2GF} + \int \epsilon t_0 N dx + \int \epsilon \Delta t \frac{M}{h} dx. \quad (15K)$$

Similarly the following differential expression of Eq. (15K) is obtained from Eqs. (14L), (15B), (15D), (15J) and (15G) or directly by differentiating Eq. (15K) and dividing through by  $\partial X_a$ , thus:

$$1 \cdot \partial_a = \frac{\partial A}{\partial X_a} = \Sigma R_a \Delta r = \int \frac{N}{EF} \frac{\partial N}{\partial X_a} dx + \int \frac{M}{EI} \frac{\partial M}{\partial X_a} dx + \beta \int \frac{Q}{GF} \frac{\partial Q}{\partial X_a} dx \\ + \int \epsilon t_0 \frac{\partial N}{\partial X_a} dx + \int \frac{\epsilon \Delta t}{h} \frac{\partial M}{\partial X_a} dx. \quad (15L)$$

Equation (15L) being true for any force  $X_a$  is, of course, true for a force  $P_m$ , hence by substitution of the latter value and then inserting the value  $\partial A / \partial P_m$ , thus obtained from Eq. (15L) into Eq. (13N) the following equation for elastic deflection is obtained:

$$\delta_m = \int \frac{N}{EF} \frac{\partial N}{\partial P_m} dx + \int \frac{M}{EI} \frac{\partial M}{\partial P_m} dx + \beta \int \frac{Q}{GF} \frac{\partial Q}{\partial P_m} dx + \int \epsilon t_0 \frac{\partial N}{\partial P_m} dx \\ + \int \frac{\epsilon \Delta t}{h} \frac{\partial M}{\partial P_m} dx - \Sigma \frac{\partial R}{\partial P_m} \Delta r. \quad (15M)$$

The last three equations (15K), (15L) and (15M) are the three fundamentals from which all cases of redundancy for isotropic bodies can be solved. There are always as many of these equations as there are redundant conditions  $X$ .

*In each of these the first term expresses the effect due to direct or normal stress; the second term that due to pure bending; the third term that due to shearing stress; the fourth term gives the effect due to a uniform rise in temperature  $t_0$ ; and the fifth term that due to a difference  $\Delta t$  in the temperature of opposite extreme fibers.*

The object in presenting these rather long fundamental equations is not to make the subject appear complicated, but rather with a view to showing once for all the combined effect from all causes, thus permitting the easy choice in combining any effects or in omitting such as may seem negligible in any specific problem.

Equation (15κ) may also be derived from Eq. (5H) for virtual work and offers very useful applications.

Thus assuming a column subjected to a thrust  $N_m$  and a bending moment  $M_m$  the virtual work on the column from Eq. (5H) becomes

$$1 \cdot \delta_m = \sum_0^l N_a \Delta l + \int_0^l M_a \Delta d\phi;$$

where  $N_a$  and  $M_a$  are due to the usual conventional loadings. But

$$\Delta l = \int_0^l \frac{N_m dx}{EF} \quad \text{and} \quad \Delta d\phi = \frac{M_m dx}{EI},$$

hence,

$$\overline{W} = 1 \cdot \delta_m = \int_0^l \frac{N_m N_a dx}{EF} + \int_0^l \frac{M_m M_a dx}{EI}, \quad \dots \dots \dots (15\pi)$$

When the virtual work becomes the actual work  $A$  then Eq. (15π) becomes identical with Eq. (15κ) term for term.

## ART. 16. WORK OF DEFORMATION DUE TO DYNAMIC IMPACT

Problems involving the deflection or strength of a structure subjected to impact, are frequently met with, and their treatment is here considered as properly belonging to the subject of the present chapter.

Let  $\omega$  = weight of a moving body;

$H$  = height of a fall;

$v$  = velocity at instant of impact;

$g$  = acceleration due to gravity;

$\delta$  = any elastic displacement produced by the moving body in some structure.

Then the work expended by the moving mass is represented either in terms of velocity or height of fall as follows:

$$A = \omega(H + \delta) = \omega \frac{v^2}{2g}, \quad \dots \dots \dots (16A)$$

wherein  $v^2/2g$  represents the velocity height or height through which a body falls in acquiring a velocity  $v$ . When the body moves with a velocity  $v$  along a horizontal path, then  $v^2/2g$  will be the height to which the body would raise itself in order to expend its energy and come to a state of rest.

The work thus produced by kinetic energy, when it is instantly taken up by a quiescent body or structure, is twice as great as the work of the same moving body gradually applied, and hence produces twice the internal work in the body struck as would result from an equivalent static load.

**Problem 1.** The weight  $w$  falls on top of a column, stressing the column normally what sectional area is required in order that the unit compressive stress does not exceed  $f$ ?

From Eq. (15κ) the work due to direct stress is given by the first term, where  $N$  is the total static load, and to balance the dynamic energy, twice this amount is taken; hence

$$A = 2 \int_0^l \frac{N^2 dx}{2EF} = \frac{N^2 l}{EF} = \frac{f^2 l F}{E} = \omega(H + \delta), \quad \dots \dots \dots (16B)$$

and since  $\delta = \frac{fl}{E}$  this gives for  $F$ ,

$$F = \omega \left( H + \frac{fl}{E} \right) \frac{E}{f^2 l} = \frac{\omega}{f} \left( \frac{HE}{fl} + 1 \right). \quad \dots \dots \dots (16C)$$

**Problem 2.** A weight  $w$  falls from some height striking a beam resting on two supports. The weight strikes the center of the beam with a velocity  $v$ ; what will be the stress  $f$  in the extreme fiber for a given beam section? Shear and bending resistances are to be considered.

From Eq. (15κ) the actual internal work is

$$A = \int \frac{M^2 dx}{2EI} + \beta \int \frac{Q^2 dx}{2GF}. \quad \dots \dots \dots (16D)$$

Let  $P$  = an equivalent static load producing the same stress  $f$  in the given beam. Then, for any point of the beam of depth  $h$  and span  $l$ ,

$$M = \frac{P}{2} x; \quad \text{also} \quad f = \frac{My}{I} = \frac{Plh}{8I} \quad \text{or} \quad P = \frac{8fI}{lh}. \quad \dots \dots \dots (16E)$$

Hence

$$\int_{-\frac{l}{2}}^{+\frac{l}{2}} \frac{M^2 dx}{2EI} = \frac{P^2}{4EI} \int_0^{\frac{l}{2}} x^2 dx = \frac{P^2 l^3}{96EI} = \frac{2f^2 l I}{3Eh^2}. \quad \dots \dots \dots (16F)$$

Also, for  $Q = \frac{P}{2}$  the second term of Eq. (16D) becomes

$$\beta \int_{-\frac{l}{2}}^{+\frac{l}{2}} \frac{Q^2 dx}{2GF} = \frac{\beta P^2}{4GF} \int_0^{\frac{l}{2}} dx = \frac{\beta P^2 l}{8GF} = \frac{8\beta f^2 l^2}{GFh^2}. \quad \dots \dots \dots (16G)$$

The sum of Eqs. (16F) and (16G) gives  $A$ , according to Eq. (16D), and this must equal  $\omega v^2/2g$ . Therefore,

$$\frac{\omega v^2}{2g} = \omega H = \frac{2f^2 l I}{3Eh^2} + \frac{8\beta f^2 l^2}{GFh^2} = \frac{2f^2 l}{h^2} \left( \frac{l}{3E} + \frac{8\beta l}{GF} \right). \quad \dots \dots \dots (16H)$$



Here  $G$  = modulus of shear  $= \frac{mE}{2(m+1)} = 0.385 E$  for structural steel (see Eqs. (13j)).

The coefficient of shearing strain  $\beta$  is given by Eqs. (14L) and (14M).

By applying Eq. (16H) to a steel beam  $2.5 \times 2.5$  inches by 78 inches long, it is found that when shear is included, the stress  $f$  is about  $\frac{3}{4}$  per cent smaller than when this term is omitted, showing that the internal resistance due to shear is very small and usually negligible. This is also true when computing deflections.

In the same manner all problems involving impact may be solved.

Suppose a ship weighing  $w$  tons, and moving with a velocity of  $v$  feet per second were to collide with a fixed structure, then the work which the ship is capable of expending is represented by  $\omega v^2/2g$  ft.tons. This work may be expended in injuring the structure or the ship itself, a condition depending on the relative strength of the two bodies, which must be ascertained from the design and construction of each.

## CHAPTER IV

### INFLUENCE LINES AND AREAS FOR STATICALLY DETERMINATE STRUCTURES

#### ART. 17. INTRODUCTORY

Professors MOHR and WINKLER, in 1868, published simultaneously the first treatises on influence lines describing, at that early date, practically all the uses and applications of these lines known at the present time. Professor J. Weyrauch, in 1873, introduces the name *influence line* not used by Mohr and Winkler in their earlier work. Professor Mohr, in a series of articles published from 1870 to 1877, was the first to apply influence lines to deflections and to redundant conditions.

Professor Geo. F. Swain, in 1887, gave the first treatise on the subject in English.

**An influence line** is the graphic representation of some particular effect produced, at a certain point of a structure, by a single moving load occupying, successively, all possible positions over the entire span. The effect may be the shear, the bending moment or the deflection at any certain point of the structure; it may also represent any reaction force or the stress in any member. The single moving load is usually taken equal to unity, though in certain special cases it may be desirable to use any load  $P$ .

An influence line represents a certain effect for a certain point or member of a structure and for any position of a moving load, while a shear or moment diagram represents effects due to a single position of the load or loads for all points of a structure.

**The ordinate** to any influence line is thus an influence number or factor, usually designated by  $\eta$  when stresses are dealt with and sometimes by  $\delta$  when deflections are under consideration.

As a matter of convention, all positive influence line ordinates will be laid off downward from the axis of abscissæ.

**A load point** is any particular one of the many possible positions of the moving load.

**A summation influence line** is one which gives the *total effect* at some particular point due to a train of concentrated loads. The actual loads are here employed and each influence ordinate is made to represent the summation of influences of the same kind for a certain position of the train of loads. Usually this position is taken so that the first load is over the point for which the influence line is constructed.

**An influence area** is the area included between the influence line, the axis of abscissæ and the two end ordinates.

**The maximum effect** is always produced when the load point coincides with the maximum ordinate of the influence area. Hence influence lines are eminently suited

to the solution of all problems relating to position of moving loads for maximum and minimum effects and stresses.

The **load divide** is such a load point, the ordinates to either side of which have opposite signs. Hence, the influence ordinate at a load divide passes through zero and the influence line intersects the axis of abscissæ at such *load divide*.

It is assumed that if a unit load produces some effect  $\eta$  at a certain point of a given structure, then a load  $P$  will produce the effect  $P\eta$  at this same point, so long as the material is not stressed beyond the elastic limit. This follows from the law of proportionality stated at the end of Art. 4.

Hence, the total effect  $Z$  produced by a system of moving loads,  $P_1, P_2$ , etc., will be the sum of the effects  $P\eta$  of all the loads and the maximum and minimum value of  $Z$  will be determined by the position of the moving loads.

The total effect is thus expressed by the following equation when the case of loading is simultaneous and within working limits:

$$Z = P_1\eta_1 + P_2\eta_2 + P_3\eta_3, \text{ etc.} = \Sigma P\eta. \quad . \quad . \quad . \quad . \quad . \quad (17A)$$

Therefore, having given the influence line for a certain effect on some structure, then the total effect, due to any system of loading, is easily found by a summation of the products of loads into corresponding *influence ordinates or numbers* for any desired positions of the loads.

For a **uniform moving load**  $p$  per foot of length, Eq. (17A) becomes

$$Z = p \int \eta dx, \quad . \quad . \quad . \quad . \quad . \quad . \quad . \quad . \quad . \quad . \quad (17B)$$

wherein the integral represents the area of the influence polygon between the end ordinates of the uniform load.

The **equation of any influence line** may be written out by expressing the desired function for a particular point in question in terms of a moving load unity acting at any variable distance  $x$  from one end of the structure taken as origin.

Since influence lines represent all possible effects it is readily seen that maximum and minimum stresses may be found from the same lines. Therefore, only one half of a symmetric structure requires analysis. The left half is usually treated, as a matter of conventional uniformity.

**Direct and indirect loading.** In the above it was assumed that the loads were directly applied to the beam, which is rather the exception. Usually they are taken up by the floor system and then transferred to the panel points as load concentrations. The former case of loading will be known as *direct loading* and the latter as *indirect loading*.

The **influence line between two successive panel points** is always a straight line, regardless of the system of loading or the particular influence.

Let Fig. 17A represent two successive floor beams of any truss and the load  $P = 1$

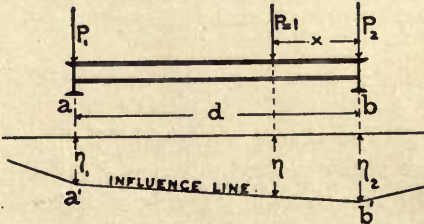


FIG. 17A.



is transferred to the points  $a$  and  $b$  by the floor stringer  $\overline{ab}$ . The load effects  $P_1$  and  $P_2$ , which are carried to the panel points  $a$  and  $b$ , are

$$P_1 = \frac{Px}{d} \quad \text{and} \quad P_2 = P \left( \frac{d-x}{d} \right).$$

Now the total influence of  $P_1$  and  $P_2$ , on the structure as a whole, must be exactly equal to that produced by the resultant  $P$ .

But the influence line  $\overline{a'b'}$ , extending over the panel  $\overline{ab}$ , must give, by Eq. (17A),

$$P\eta = P_1\eta_1 + P_2\eta_2 = P\eta_1 \left( \frac{x}{d} \right) + P\eta_2 \left( \frac{d-x}{d} \right),$$

from which

$$\eta = \eta_1 \left( \frac{x}{d} \right) + \eta_2 \left( \frac{d-x}{d} \right). \quad \dots \dots \dots (17c)$$

For any influence line,  $\eta_1$ ,  $\eta_2$  and  $d$  are constants, hence Eq. (17c) represents a straight line, which was to be proven.

## ART. 18. INFLUENCE LINES FOR DIRECT LOADING

The several influence lines for reactions, shears, moments and deflections for a beam with direct loading will now be given. They will always be known by the names indicated in Fig. 18A. Thus the  $A$  line is the influence line for the reaction  $A$ .

The influence line for a reaction is of the first importance, because the other lines are generally derived from the reaction influence line. This is really seen from the circumstance that for the unloaded portion of a beam or truss, the shear is always equal to the end reaction and the moment is equal to this reaction into the distance from the section in question to the end of the beam.

Hence, in drawing influence lines it is always best to consider the unloaded portion of the span to the right or left of the section as the case may be, because the only external force on that side of the section will then be the reaction.

In the following the moving load will always be assumed as coming on the span from the right end and the effect produced on the left half of the span only, is considered.

(a) **Reaction influence lines  $A$  and  $B$ .** Using the dimensions indicated in Fig. 18A, the two reactions become

$$A = \frac{Px'}{l} \quad \text{and} \quad B = \frac{Px}{l}. \quad \dots \dots \dots (18A)$$

For  $x'$  and  $x$  variable, both expressions represent equations of straight lines which are easily plotted. When  $P=1$  and  $x'=l$  then  $A=1$  and for  $x'=0$ ,  $A=0$ . Hence, the  $A$  line is drawn by laying off a distance unity down from  $A$  and joining this point with  $B$ . The reaction  $A$  for any load  $P$  acting at the load point  $m$  is then  $A_m = P\eta_m$ .

In like manner the  $B$  line is found, and the corresponding reaction  $B_m$  for a load  $P$  at  $m$  becomes  $B_m = P\eta'_m$ , and  $\eta_m + \eta'_m = 1$  for every point of the span.

(b) **Shear influence lines.** The shear  $Q_n$  for a certain point  $n$  to the left of the load point  $m$  is always equal to the reaction  $A$ . But for a load point to the left of  $n$  (not shown) the shear is  $Q_n = A - P = -B$ , because  $P = A + B$ .

The influence line for  $Q_n$  is thus derived from the influence lines for  $A$  and  $-B$  as indicated in Fig. 18A, and consists of the polygon  $\overline{An'n''B}$ .

The point  $n$  becomes the *load divide* for shears at  $n$  and hence there will always be a maximum and a minimum value for  $Q_n$  depending on whether the positive or the negative influence area is fully loaded. The shear due to any single load  $P$  must change sign in passing the point  $n$ .

(c) **Moment influence lines.** The moment for the point  $n$  is now found when the moving load is to the right or left of the section at  $n$ . Then for

$$x > a, \quad M_n = Aa; \text{ and for } x < a, \quad M_n = B(l-a).$$

Thus the moment influence line is also derived from the reaction lines because the ordinates of the latter, when multiplied by  $a$  or  $(l-a)$  as the case may be, give the ordinates to the moment line. Hence the bounding lines of the moment influence line are easily found.

Since  $A$  and  $B$  are both unity, then the ordinate  $\overline{AA'} = a$  and the ordinate  $\overline{BB'} = l-a$  and the lines  $\overline{AB'}$  and  $\overline{A'B}$  inclose the required moment influence line. Also, the ordinate at  $n$  is the ordinate of the intersection  $n'$  between the two bounding lines. Hence, if  $\overline{BB'}$  should fall off the drawing, then the line  $\overline{AB'}$  may be drawn from  $A$  to  $n'$  without finding  $B'$ .

In either case the moment influence line is then the polygon  $\overline{An'B}$  with all ordinates positive so long as the point  $n$  is not outside the span, a case which will be given later. The maximum ordinate is always under  $n$  and has the value  $1 \cdot a(l-a)/l$ , which offers still another construction for this influence line. The middle ordinate of the  $\overline{AB'}$  line  $= \frac{1}{2}(l-a)$  which furnishes a convenient construction for this line when  $B'$  falls off the drawing.

It is clearly seen that if a single load is placed at  $n$  over the maximum ordinate, then a maximum moment is produced.

(d) **Deflection influence lines.** The deflection for a point  $n$ , produced by a single load at any point  $m$ , is given in terms of the moment of inertia of the beam section and the modulus of elasticity, as follows:

$$\delta_n = \frac{ax'}{6EI} (l^2 - x'^2 - a^2) P = \frac{a(l-x)}{6EI} (2lx - x^2 - a^2) P. \quad \dots \quad (18B)$$

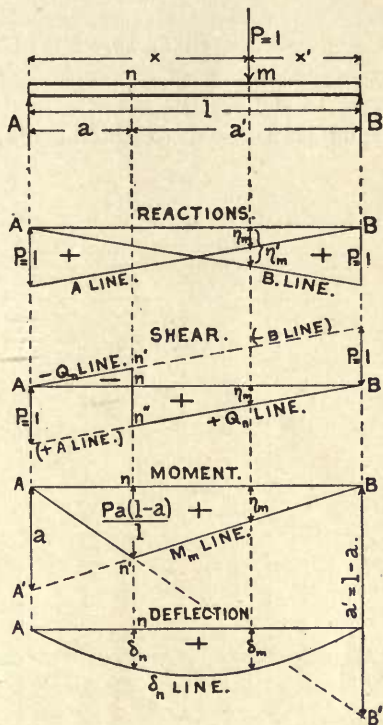


FIG. 18A

This is a cubic equation and when plotted for all values of  $x$  and making  $P=1$ , the influence line for deflections is obtained.

In general, any deflection polygon, drawn for a load unity acting on a fixed point  $n$  of any structure, is the deflection influence line for the point  $n$  of that structure. This follows from Maxwell's law.

As the subject of deflection influence lines is fully treated in Chapter VIII, no further consideration is given to it now.

### ART. 19. INFLUENCE LINES FOR INDIRECT LOADING

In the present case the loads are applied to a stringer and floor-beam system and are thus transferred to the beam at certain panel points as load concentrations. The beam is then *indirectly loaded* and since an influence line was shown to be a straight line between panel points the present case will require some slight modification of the influence lines just found for direct loading. See Fig. 19A.

However, all that was said for cases of *direct loading* applies here and the modifications made necessary by the *indirect loading* occur only in the panel wherein the point  $n$  is located. As before,  $n$  is the point for which the influence line is drawn and  $m$  is any one of the possible load points for the moving load  $P=1$ .

(a) **Reaction influence lines** remain the same whether the loading is direct or indirect, since the point for which the influence is sought is always at  $A$  or  $B$ , which are also panel points.

Furthermore, the reaction influence lines being straight over the length of the span will always be straight between successive panel points.

(b) **Shear influence lines.** The  $Q$  line, outside of the panel  $\bar{ce}$  and containing the point  $n$ , remains the same as for direct loading. But since the influence line within a panel must be a straight line, therefore, the points  $c'$  and  $e'$  must determine the influence line for the panel  $\bar{ce}$  regardless of the location of the

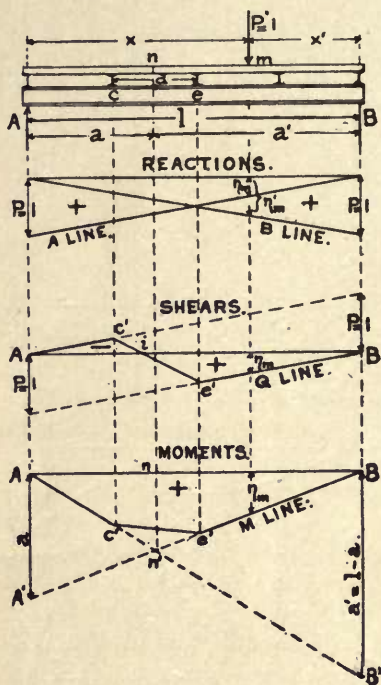


FIG. 19A.

point  $n$  so long as this point is within the panel  $\bar{ce}$ .

Hence, the polygon  $Ac'e'B$  is the shear influence line for the panel  $\bar{ce}$  and the point  $i$  is the *load divide* for this panel. The limiting values for shear are thus the same for any point  $n$  of the same panel.

(c) **Moment influence lines.** Here again the influence line within the panel  $\bar{ce}$  is all that requires modification in the case of indirect loading.



Hence for the same reasons just given to determine the modified  $Q$  line, the  $M$  line for the point  $n$  is now the polygon  $Ac'e'B$ , instead of the triangle  $An'B$  for direct loading. The point  $n$  is the center of moments.

## ART. 20. THE LOAD DIVIDE FOR A TRUSS

In constructing influence lines for truss web members it frequently happens that one or the other end ordinate falls outside the limits of the drawing.

There is a very simple way of locating the *load divide*  $i$  and thus facilitating the construction of any influence line. The method is given first and the proof follows:

Let Fig. 20A represent a truss arranged for bottom chord loading, but no loads are shown. Required to find the *load divide*  $i$  for the panel  $\overline{fg}$  necessary to determine the stress in the diagonal  $\overline{eg}$  cut by the section  $\overline{tt}$ .

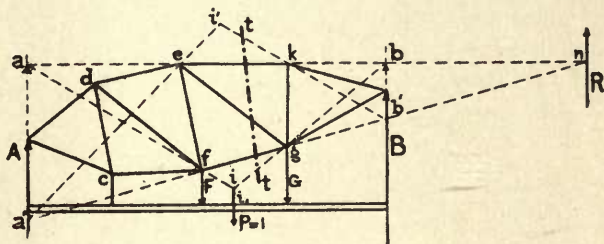


FIG. 20A.

**Construction.** Prolong the unloaded chord member  $\overline{ek}$  in the panel  $\overline{fg}$  until it intersects the verticals through the end reactions in  $a$  and  $b$ . Then the intersection  $i$  of the two lines  $\overline{af}$  and  $\overline{bg}$  will be the required load divide.

**Proof.** Suppose the unit moving load is now located in the vertical through  $i$ . Then if  $i$  is the desired load divide, the unit load for the load point  $i_1$  will produce zero stress in the member  $\overline{eg}$  and the influence line ordinate for the point  $i$  must be zero.

Let  $F$  and  $G$  be the panel concentrations in the points  $f$  and  $g$  due to the load  $P=1$  at  $i$ .

Then the polygon  $\overline{abfg}$  may be regarded as the equilibrium polygon for the forces  $A$ ,  $B$ ,  $F$  and  $G$ . Also, the resultant  $R$  of all forces on one side of the section  $\overline{tt}$  must pass through the intersection  $n$  of the two included sides of the equilibrium polygon.

But, the point  $n$  is the intersection of the two chords  $\overline{fg}$  and  $\overline{ek}$ , which point is also the center of moments for the diagonal  $\overline{eg}$ .

Hence the moment of this resultant  $R$  about  $n$  must be zero and cannot produce stress in the member  $\overline{eg}$ , thus proving that the load  $P=1$  is actually located in the load divide.

When the top chord is the loaded chord, a similar construction furnishes the point  $i'$ , as the load divide for the member  $\overline{eg}$ , according to the same proof above given.

This construction applies to any structure even when one or both chords are straight.

When the center of moments  $n$  falls inside the span then there is no load divide and all loads on the entire span will produce the same kind of stress in any particular web member.



$\overline{EG}$  and hence the line  $\overline{E'G'}$  must be drawn to complete the influence line. Here  $F$  is the center of moments for the member  $U$ .

The influence line for the diagonal  $D$  is similarly drawn and the load divide  $i'$ , found in the lower diagram, is seen to coincide with the point  $i$  found on the truss diagram by the method previously given. Also the intersection  $O'$ , between the limiting rays  $\overline{AE'}$  and  $\overline{G'B}$  of the  $D$  line, is vertically under the center of moments  $O$  for the member  $D$ .

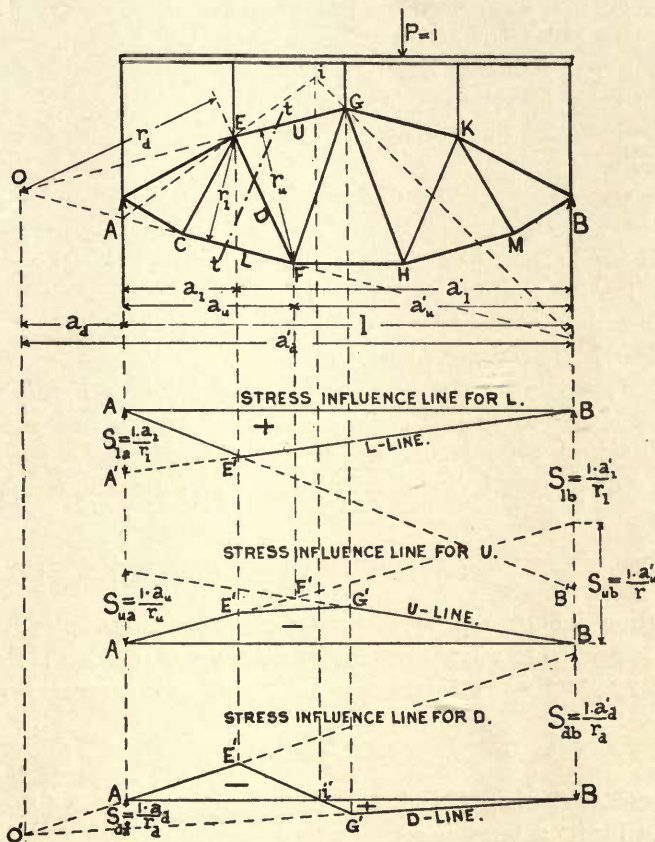


FIG. 21A.

It should be observed that in all three influence lines, Fig. 21A, the limiting rays intersect on the vertical through the center of moments for the particular member. This then serves as a check on the diagram.

Regarding the sign of the influence area the following rule should be observed: When the center of moments is located between the supports A and B then all ordinates of that particular stress influence line will be of the same sign; when the center of moments is off the span, then there exists a load divide and there will be positive and negative influence areas giving rise to stresses of opposite signs.



The criterion for position of a moving load for maximum and minimum stresses in any member is thus clearly shown by influence lines and the maximum effect of any load is always produced when that load is situated over the maximum influence ordinate. This subject is more fully treated in another article.

It is sometimes necessary to construct influence lines without the divisor  $r$ , and dividing the final stress thus found by  $r$ . Either method is employed as circumstances may demand, though it is always better to avoid the divisor and follow the method given in Fig. 21A, unless there is some very good reason for doing otherwise.

Attention is also called to the fact that moment and shear influence lines are not required when the stress influence lines are used. The former were given to render the treatment complete and may be employed to find stresses, but it is usually preferable to draw the stress influence lines directly. The final result of an analysis will be more satisfactory when this is done.

Influence lines are seldom used for finding dead load stresses, though such a procedure may sometimes be warranted, and then the following points must be observed: For direct loading and for beams, it makes no difference whether the influence lines be used for dead or live loads, but in dealing with framed structures an error might be committed because then the influence lines are always drawn for a certain loaded chord while the dead loads act along both chords.

This is easily remedied by drawing the influence lines for both chords loaded and applying the dead loads to the proper lines. These influence lines are identical except in the panel containing the member in question. Hence by observing this circumstance, dead load stresses may be found from the same influence lines without difficulty.

## ART. 22. REACTION SUMMATION INFLUENCE LINES

Most summation influence lines become rather complicated and, therefore, their use is practically restricted to a few cases for which the construction is simple.

In general, any ordinate to a summation influence line is expressed by Eq. (17A), as

$$Z = \Sigma P\eta,$$

and it is readily seen that when  $P$  and  $\eta$  are both variables, such a line would ordinarily require much labor for its determination.

However, the summation influence line for an end reaction of a simple truss is very easily constructed and serves a most valuable purpose in finding the end shears for a system of moving loads. This influence line will be called simply the *sum A line* to distinguish it from the ordinary *A line* in Figs. 18A and 19A.

The general usefulness, of the *sum A line* originated by Professor Winkler, will be shown later; suffice it to say here that it affords a ready means of finding stresses in the web members of any truss, because, as previously shown, the shears and moments for any point of a truss are easily found when the end reaction for the particular loading is known.

The *sum A line* for a system of concentrated wheel loads will now be demonstrated, using but five loads for simplicity, though the method applies to any number of loads.

Given the train of moving loads  $P_1, P_2$ , etc., in kips of 1000 lbs., and spaced as shown in Fig. 22A, to construct the *sum A line* for a span of 25 ft.

Since a reaction influence line is the same both for direct and indirect loading, the *sum A line* is independent of the number and location of panel points.

For standard position of loads on a truss, the train is always assumed as coming on the span from the right end and moving toward the left, but the above loads are placed in exactly the reverse order, with the first load  $P_1$  over the support  $B$ . The reason for this will appear later.

The loads are applied consecutively from  $P_1$  up on the vertical through  $A$ , using any convenient scale.

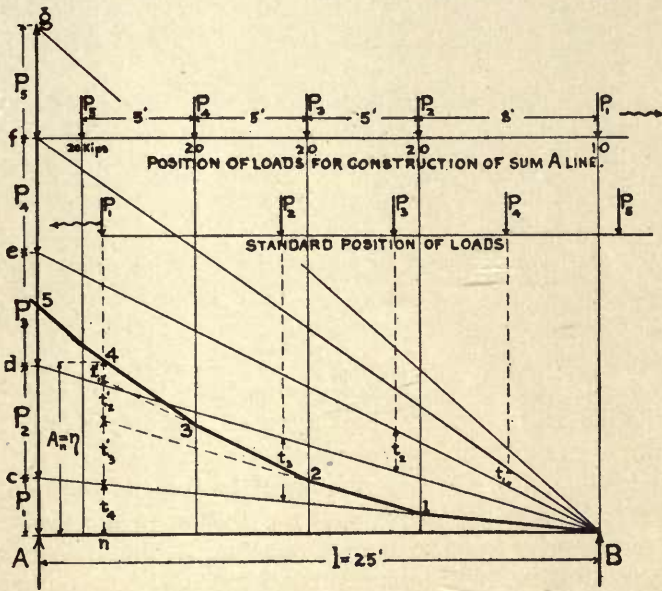


FIG. 22A.

The several rays drawn from  $B$  to the respective load points  $c, d, e$ , etc., form a force polygon with pole distance  $H=l$ . The *sum A line* is then drawn as the equilibrium polygon for this force polygon and the loads  $P$ , by making  $1-2 \parallel Bc, 2-3 \parallel Bd, 3-4 \parallel Be$ , etc.

It will now be shown that the equilibrium polygon so obtained is really the summation influence line for the end reaction  $A$ .

Referring again to Fig. 22A, the line  $Bc$  is easily recognized as the influence line for  $A$  due to a moving load  $P_1$ . Also, the influence line for  $A$  when the moving load is  $P_2$ , may be represented by the line  $Bd$  when  $Bc$  is the axis of the abscissæ. Similarly  $Be$  represents the  $A$  line for  $P_3$ , and so on for any other loads. The summation of all ordinates should then represent the desired summation influence line.

For the train coming on the span from right to left, the ordinate  $\eta$ , under the forward load  $P_1$ , always represents the reaction  $A$ . Thus when the train has advanced



to the point  $n$ , Fig. 22A, the ordinate  $\eta$  represents the sum of the ordinates  $t$ , and  $\eta = A_n = t_4 + t_3 + t_2 + t_1$  which is readily seen by inspection. The ordinates  $t$  are the contributions to  $A$  from the several loads on the span. It is now seen why the train was first placed in reverse position for the construction of the equilibrium polygon.

Hence the *sum A line* for direct or indirect loading is an equilibrium polygon drawn for a pole distance equal to the length of span and any system of train loads placed in reverse order on the span with the forward load at  $B$ .

The reaction  $A$  for any position of loading is then the ordinate to the *sum A line* measured under the forward load when the train approaches from right to left. The greatest possible reaction  $A$  will always be the end ordinate  $A5$ , Fig. 22A.

When extraordinary accuracy is required the end ordinate  $A5$  can be readily checked by computation.

The *sum A line* for uniformly distributed loads may be constructed in precisely the same manner as above illustrated for concentrated loads, merely by laying off the load line  $\overline{Ag}$  to represent the total load on the span  $=pl$  and dividing this into some convenient number of equal parts. The greater this number the more accurate will be the result, and the polygon finally becomes a parabola.

The application of the *sum A line*, to finding the shear at any point of a beam or truss, will now be presented.

The shear at any point  $n$  of a beam, for a case of direct loading, is equal to the reaction  $A$  minus the loads between  $A$  and  $n$ . Hence, the *sum A line* gives a complete solution for this case. The subtraction of any loads to the left of  $n$  can be performed graphically on the diagram, Fig. 22A, by taking off the proper ordinate less the loads between  $A$  and  $n$ .

For indirect loading, the shear at  $n$  is equal to the end reaction  $A$ , provided the forward load is exactly over the panel point  $n$ . But when the load extends over into the panel, then the shear is equal to the end reaction  $A$ , minus the panel reaction  $a$  at the left hand pin point of the loaded panel. See Fig. 22B.

The values of  $a$  for all possible positions of loads in a single panel may be found by drawing a *sum a line* noe for one panel, using as many of the loads from the forward end of the train as may be placed into one panel. If this auxiliary *sum a line* is drawn on tracing paper, it will also serve a ready means for finding the position of the train for maximum shear in any panel  $\overline{mn}$ .

The method of finding the *sum a line* is exactly the same as for the *sum A line* only the pole distance for the former is the panel length  $d$ .

When the forward wheel of the train is at  $n$ , then the shear is the ordinate  $\eta_n$ . When the forward wheel is at  $r$  the shear in the panel  $\overline{mn}$  is  $Q_r = \overline{rc} - \overline{re} = \overline{ec}$  where  $\overline{re} = \eta_a =$  the panel reaction  $a$  for loads  $P_1$  and  $P_2$  in the panel and load  $P_3$  at  $n$ . Similarly when the forward wheel is at  $s$  and the second wheel is at  $n$  the shear  $Q_s = \overline{sf} - \overline{os}$ .

The position of the train for *max. Q* in the panel  $\overline{mn}$  is then easily found by selecting such a point  $s$  for which the ordinate  $\overline{of} = \eta$  *max.* This maximum  $\eta$  is easily found with a pair of dividers and will always occur when some one of the forward wheels is at the panel  $n$ .



If the *sum a line* is drawn on tracing cloth, it may be superimposed on any panel of the *sum A line* and  $\eta$  *max.* can be quickly determined.

It sometimes happens that two positions of the train give the same maximum shear, in which case either may be used. In Fig. 22B this would be true if  $\overline{oe} \parallel \overline{cf}$  then  $\overline{ec} = \overline{of}$  and both  $Q_r$  and  $Q_s$  would thus be equal.

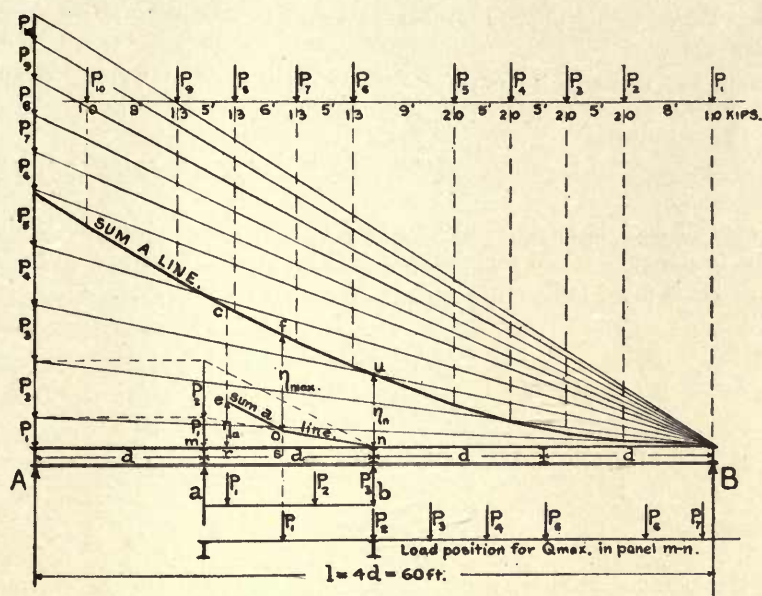


FIG. 22B.

ART. 23. POSITIONS OF A MOVING TRAIN FOR MAXIMUM AND MINIMUM MOMENTS

(a) **Point of greatest moment for direct loading.** Given a span of certain length  $l$ , loaded with a train of loads,  $P_1, P_2, P_3$ , etc., to find the point  $n$  which is subjected to the greatest bending moment. It is assumed that all loads remain on the span. See Fig. 23A.

- Let  $R$  =resultant of all loads  $P$  on the span.
- $R_1$  =resultant of all loads to the left of  $n$ .
- $R_2$  =resultant of all loads to the right of  $n$ .
- $A$  and  $B$  are the end reactions for  $R$ .
- $n$  =the point of maximum moments to be found.

Then the moment about  $n$  is

$$M = Ax - R_1a_1 = \frac{Rx}{l}(l - x - a) - R_1a_1. . . . . (22A)$$

By differentiating and equating to zero, the abscissa for the point of maximum moments is found thus:

$$\frac{dM}{dx} = \frac{R}{l}(l-2x-a) = 0 \quad \text{or} \quad x + \frac{a}{2} = \frac{l}{2} \quad \dots \dots \dots (23B)$$

Eq. (23B) signifies that *the maximum moment under any system of loads occurs for a point  $n$  when the center of gravity of the system and the point  $n$  are equidistant from the center of the beam.*

Introducing the value of  $x$  from Eq. (23B) into Eq. (23A) the value of *max.  $M$*  is obtained as

$$\text{max. } M = R \frac{x^2}{l} - R_1 a_1. \quad \dots \dots \dots (23C)$$

In any special case it is necessary to find the particular load  $P_n$  which must act at the point  $n$  to produce a real maximum. The moment influence line clearly indicates that one of the loads must fall at  $n$  to obtain *the maximum moment.*



FIG. 23A.

Usually the point  $n$  falls very near the center of the beam and in most practical problems it will suffice to place that load at  $n$  which falls nearest the center of gravity of the system of loads.

When dealing with floor stringers it frequently happens that the stringer is long enough to carry three wheel loads but that the *max.  $M$*  so found is less than when only two of the loads are on the stringer. A few of these special cases are here given.

**Case I.** When there is only one load  $P$  on the span, then  $x=l/2$  and  $a=0$ . Hence Eq. (23c) gives

$$\text{max. } M = \frac{Pl}{4}. \quad \dots \dots \dots (23D)$$

**Case II.** When there are two equal loads  $P$  on the span, distant  $e$  from each other, then  $R=2P$  and  $\frac{a}{2} = \frac{e}{4}$ , hence  $x = \frac{l}{2} - \frac{a}{2} = \frac{l}{2} - \frac{e}{4}$  which gives, from Eq. (23c),

$$\text{max. } M = \frac{2P}{l} \left( \frac{l}{2} - \frac{e}{4} \right)^2. \quad \dots \dots \dots (23E)$$

Equating Eqs. (23D) and (23E) to find when one or two loads give equal maxima, this results in the condition  $e=0.5858l$ . Hence, when  $e>0.5858l$ , then one load gives a greater moment than two loads, all loads being of same magnitude.

**Case III.** When there are three equal loads  $P$  on the span, distant  $e$  from each other, then  $R=3P$  and  $x=l/2$  making  $a=0$ . Also  $R_1=P$  and  $a_1=e$ , hence

$$\max. M = \frac{3Pl}{4} - Pe = P\left(\frac{3l}{4} - e\right). \quad (23f)$$

From Eqs. (23e) and (23f) it is found that when  $e > 0.4494l$ , then two loads give a greater  $\max. M$  than do three loads, all loads being equal.

**Case IV.** For four equal loads on the span  $\max. M$  occurs under the second load and Eq. (23c) gives

$$\max. M = P\left(l + \frac{e^2}{4l} - 2e\right). \quad (23g)$$

Here again it is found that when  $e > 0.2679l$ , then three loads give a greater maximum than four loads.

(b) **Critical loading for maximum moments. Direct loading.** In this case the moment influence line for any point  $n$  is a triangle and the discussion is, therefore, applicable to any beam or truss for which the moment influence line is a triangle. See Fig. 23B.

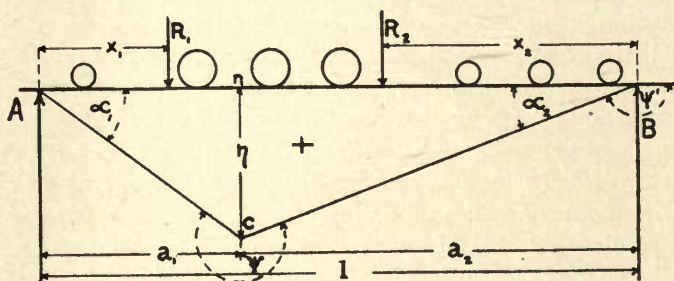


FIG. 23B.

Let  $R = \Sigma P =$  the total load, or resultant of loads on the span.

$R_1 =$  the resultant of all loads between  $A$  and  $n$  for a certain position of a train of loads.

$R_2 =$  the resultant of all loads between  $n$  and  $B$  for the same position of the train of loads.

Calling  $\eta_1$  and  $\eta_2$  the influence ordinates for the load points of  $R_1$  and  $R_2$  respectively, then the moment for the point  $n$  may be written as

$$M_n = R_1\eta_1 + R_2\eta_2 = R_1x_1 \tan \alpha_1 + R_2x_2 \tan \alpha_2. \quad (23h)$$

Suppose now that the train is moved to the right by a small distance  $dx$ , producing the change  $+dx$  in  $x_1$  and the change  $-dx$  in  $x_2$ , then the change in  $M_n$  is  $dM_n$  and the differential coefficient thus obtained is equated to zero for maximum and minimum, thus:

$$\frac{dM_n}{dx} = R_1 \tan \alpha_1 - R_2 \tan \alpha_2 = 0. \quad (23i)$$



But since  $\tan \alpha_1 = \frac{\eta}{a_1}$ , and  $\tan \alpha_2 = \frac{\eta}{a_2}$ , Eq. (23j) gives, by substitution,

$$\frac{R_1}{a_1} = \frac{R_2}{a_2} \quad (23k)$$

By observing that  $a_1 + a_2 = l$  and  $R_1 + R_2 = R$ , then by composition, Eq. (23k) gives:

$$\frac{R_1 + R_2}{a_1 + a_2} = \frac{R_1}{a_1} = \frac{R}{l} \quad (23l)$$

Either Eq. (23k) or Eq. (23l) may serve as a criterion for the critical position of the train load on the span. The load  $P_n$ , falling at  $n$ , is divided equally between  $R_1$  and  $R_2$ .

In the first instance the criterion would be satisfied *when the average unit loads on both sides of the point  $n$  are equal*, a condition which is absolutely fulfilled by a uniformly distributed load.

According to Eq. (23l) the criterion for *max.  $M$*  would be *that the average unit load to the left of the point  $n$  must equal the average unit load on the whole span*.

Also, since the maximum ordinate  $\eta$  is under the load point  $n$ , *no position of loads can give a real maximum unless one of the loads is directly over  $n$* . Hence it is readily understood that there are usually two or more maxima for any point  $n$ , depending on which load is placed over this point. Therefore, so long as the criterion is fulfilled, all positions giving such a *max.  $M_n$*  must be used to determine *the real maximum*.

In general for any moment influence line, Fig. 23B, the moment will be maximum for a point  $n$  when a load  $P$  is applied at  $n$  and when the angle  $\phi$  of the influence line exceeds  $180^\circ$ . The moment at  $n$  will be minimum only when there is a load at some point  $B$  for which  $\phi' < 180^\circ$ , that is where the angle between two successive elements of the influence line is convex upward. Hence all angles in a moment influence line represent critical load points and correspond to maxima or minima accordingly as these angles are convex downward or upward, respectively.

(c) **Critical loading for maximum moments. Indirect loading.** For any point  $n$ , other than a panel point, the moment influence line is a quadrilateral, hence all cases for which this is true are included here.

Let  $R_1$  = the resultant of all loads acting between  $A$  and  $c$ .

$R_2$  = the resultant of all loads acting in the panel  $\overline{ce}$ .

$R_3$  = the resultant of all loads acting between  $e$  and  $B$ .

Other notation, as shown in Fig. 23C, which represents a beam or girder with four panels, each of length  $d$ .

From Eq. (23h) the general expression for an influence line of any number of sides may be written as

$$M = \Sigma R x \tan \alpha, \quad (23m)$$

and the differential coefficient, equated to zero for maximum and minimum, becomes

$$\frac{dM}{dx} = \Sigma R \tan \alpha = 0. \quad (23n)$$

The various values of  $R \tan \alpha$  are now found from the special case in hand, using the notation and illustration in Fig. 23c. Three such terms are here required and these are evaluated as follows:

$$\tan \alpha_1 = \frac{\eta}{a_1}; \quad \tan \alpha_3 = \frac{\eta}{a_2}; \quad \text{also} \quad \frac{\eta_c}{\eta} = \frac{a_1 - d_1}{a_1}; \quad \frac{\eta_e}{\eta} = \frac{a_2 - d_2}{a_2},$$

from which  $\tan \alpha_2 = \frac{\eta_e - \eta_c}{d} = \frac{\eta}{d} \left( \frac{d_1}{a_1} - \frac{d_2}{a_2} \right)$ .

With  $R_1$ ,  $R_2$  and  $R_3$  and these values of  $\alpha_1$ ,  $\alpha_2$  and  $\alpha_3$ , and observing that for  $dx$  to the right the value  $R_3 \tan \alpha_3$  must be negative, then Eq. (23N) becomes

$$\frac{dM}{dx} = \eta \left[ \frac{R_1}{a_1} + \frac{R_2}{d} \left( \frac{d_1}{a_1} - \frac{d_2}{a_2} \right) + \frac{R_3}{a_2} \right] = 0, \quad \dots \dots \dots (23O)$$

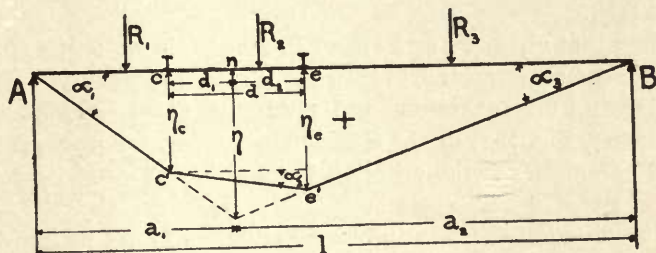


FIG. 23c.

which may be reduced to give the criterion

$$\frac{R_1 + R_2 \frac{d_1}{d}}{a_1} = \frac{R_3 + R_2 \frac{d_2}{d}}{a_2}. \quad \dots \dots \dots (23P)$$

Observing that  $R = R_1 + R_2 + R_3$  as before; also that  $d = d_1 + d_2$  and that  $l = a_1 + a_2$ , then by composition of Eq. (23P) and substitution of these values the second form of criterion is obtained as

$$\frac{R_1 + R_2 \frac{d_1}{d}}{a_1} = \frac{R}{l}. \quad \dots \dots \dots (23Q)$$

Eq. (23P) expresses the criterion for max.  $M_n$  when the average unit loads on both sides of the point  $n$  are equal, provided the resultant  $R_2$  is distributed between  $R_1$  and  $R_3$  in the proportion  $d_1 : d_2$ .

Eq. (23Q) stipulates that the average unit load over the distance  $a_1$  must be equal to the average unit load over the whole span, provided the portion  $R_2 d_1 / d$  is added to the resultant  $R_1$ .

The question of finding which particular load must be placed at either  $c$  or  $e$  to fulfill either of the above criteria may be solved, by trial, as for the case of direct loading.

## ART. 24. POSITIONS OF A MOVING TRAIN FOR MAXIMUM AND MINIMUM SHEARS

(a) **Critical loading for maximum and minimum shear.** **Direct loading.** The shear influence line is then as shown in Fig. 18A and the  $\max. +Q_n$  is obviously produced by a full loading of the entire span between  $B$  and the load divide  $n$ . The  $\min. -Q_n$  is produced by a full loading over the distance  $\overline{An}$ , which corresponds to the negative influence area. This is absolutely correct for uniformly distributed loads.

For a concentrated load system, the train must cover the portion of span between  $n$  and  $B$ , with the first load just to the right of  $n$  so that its influence ordinate is  $nn''$  without any negative effect from the ordinate  $nn'$ . However, if the first load is small compared with the second load, it may necessitate placing the second wheel at  $n$  to attain the real  $\max. +Q_n = A - P_1$ .

Hence, it is clear that either  $P_1$  or  $P_2$  must be just to the right of  $n$  to obtain  $\max. +Q$ , and whichever gives the greater value is then the real maximum.

(b) **Critical loading for maximum and minimum shear.** **Indirect loading.** The influence line for shear, Fig. 19A, or the stress influence line for a web member, Fig. 21A, are both included here. Hence the criterion for position of loads for a  $\max. Q$  will also serve for maximum stress in a web member.

For uniformly distributed loads the load divide, as found in Fig. 20A, will always establish the point at which the head end of the load must be located for  $\max. +Q$  or  $\min. -Q$ .

When dealing with concentrated load systems the position for maximum and minimum shear is most advantageously found by graphics, as illustrated in Fig. 22B, where the magnitude of these shears is at once determined, together with the critical position of loads.

When analytic methods are employed, the following criterion may serve a useful purpose.

Let Fig. 24A represent a truss with bottom chord loaded and  $i$  is the load divide for the diagonal  $D$ . The train of loads covers the span from  $B$  to  $i$ , making  $R_1$  the resultant of the loads in the panel  $\overline{CF}$  and  $R_2$  the resultant of the loads between  $B$  and  $F$ . The line  $\overline{A'C'F'B'}$  is the stress influence line for the member  $D$ .

Then the stress in the member  $D$  is

$$S_D = R_1\eta_1 + R_2\eta_2 = R_1\eta\left(\frac{d_2 - x_1}{d_2}\right) + R_2\eta\left(\frac{x}{a_2 - d_2}\right). \quad (24A)$$

By shifting the train  $dx$  to the right, both  $x_1$  and  $x$  are diminished by this amount  $dx$ . Hence the stress now becomes

$$S'_D = R_1\eta\left(\frac{d_2 - x_1 + dx}{d_2}\right) + R_2\eta\left(\frac{x - dx}{a_2 - d_2}\right). \quad (24B)$$



Subtracting Eq. (24B) from Eq. (24A) the differential change in  $S_D$  is obtained thus

$$dS = S_D - S_{D'} = \eta \left[ -\frac{R_1 dx}{d_2} + \frac{R_2 dx}{a_2 - d_2} \right] \dots \dots \dots (24c)$$

From Eq. (24c) the value  $dS/dx$  is found and equated to zero for maximum value of  $S_D$ . This gives

$$\frac{R_1}{d_2} = \frac{R_2}{a_2 - d_2}, \quad \text{or by composition} \quad \frac{R_1 + R_2}{a_2} = \frac{R_1}{d_2} = \frac{R}{a_2}, \quad \dots \dots (24d)$$

where  $R$  is the resultant of all loads between  $B$  and  $i$ . This furnishes the criterion, provided no additional loads have entered the panel  $\overline{CF}$  and no other loads have come on the span in making the shift.

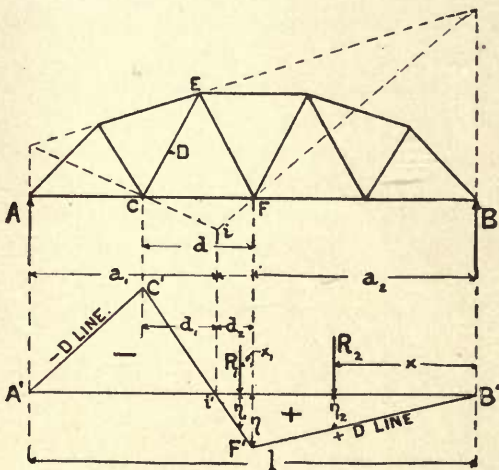


FIG. 24A.

It is evident from the influence line, Fig. 24A, that any loads to the left of  $i$  would produce a negative influence on  $S_D$ , so that the minimum value of  $S_D$  may be found by loading the left portion  $\overline{Ai}$  of the span, and the criterion then becomes

$$\frac{R_1}{d_1} = \frac{R}{a_1} \dots \dots \dots (24E)$$

This criterion expresses exactly the same condition as previously found for moments in Eq. (23L), but the span now becomes the length  $a_1$  or  $a_2$ , as the case may be, covering only that portion of the stress influence line  $D$ , which has the same sign.

As previously found, by the graphic method, it is always necessary to place a load at the panel point  $F$  for  $\max. D$  and one at  $C$  for  $\min. D$ , allowing as many loads inside the panel  $\overline{CF}$  as may be required to satisfy the criterion.

The above discussion of the various criteria for position of moving loads to produce maximum and minimum stresses in any member of a statically determinate structure is ample demonstration of the high value and practical use of influence lines.

It was not deemed advisable to extend this discussion to cover the various types of special and composite structures, as the influence lines themselves, when used for the determination of stresses, will give complete and comprehensive answers in all cases without special analytic treatment. However, when such is desirable, the methods previously employed will indicate the procedure to be followed for any particular influence line.

The subject of influence lines for statically indeterminate structures and for deflections will be treated after presenting the general subject of distortions and deflection polygons of framed structures.



## CHAPTER V

### SPECIAL APPLICATIONS OF INFLUENCE LINES TO STATICALLY DETERMINATE STRUCTURES

#### ART. 25. DOUBLE INTERSECTION TRUSSES

Usually trusses of this type are analyzed as two separate systems, dividing the loads between them in such manner as may seem most probable.

The stresses found for the separate systems are then combined for the double system wherever the same member forms part of each system, provided simultaneous cases of loading were used.

The method of influence lines has advantages especially in the distribution of simultaneous load effects, and the combined stress in a member belonging to both systems is at once found for the same position of loads.

Double intersection trusses should always be designed with an even number of panels, thus retaining symmetry of both systems with respect to the center of the span. Otherwise the loading carried by one system in the left half span must go to the other system in the right half span, which is not desirable.

Fig. 25A represents a double intersection truss for which stress influence lines will now be drawn.

**Bottom chord member  $\overline{DE}$ .** A section  $\bar{tt}$ , passed through the panel  $\overline{DE}$ , cuts the diagonals  $\overline{FE}$  and  $\overline{GK}$ , hence the chord  $\overline{DE}$  forms part of two panels for which there are two centers of moments,  $F$  and  $G$ . Therefore, each system gives rise to a stress influence line for the member  $\overline{DE}$ , shown in Fig. 25A, by the two dotted triangles  $\overline{A'C'B'}$  and  $\overline{A'D'B'}$ . The top chord members are regarded straight between alternate pin points for each system in question.

Loads acting at panel points are supposed to be carried by the system to which each such point belongs except at the panel  $O$  where the load is divided equally between the two systems.

Hence a load at  $D$  goes entirely to one system and its influence is represented by the ordinate  $\overline{DD'}$ , of the influence line  $\overline{A'D'B'}$ ; while a load at  $E$  is carried by the other system and its influence ordinate becomes  $\overline{EE'}$  in the influence line  $\overline{A'C'B'}$ . This same reasoning applies to all panel points.

Since influence lines between successive panel points must be straight lines, the actual influence line for  $\overline{DE}$  is represented by the shaded area  $\overline{A'O'C'D'E'K'}$  to  $\overline{B'}$ . The point  $O'$  must lie midway between the two ordinates for  $O$  because at this point the load is carried equally by both systems. This is not the case at  $M$ , where the entire load goes to one system.



**Top chord member  $\overline{LF}$ .** The influence line for  $\overline{DE}$  is like the influence line for  $\overline{LF}$ , except that the end ordinates are slightly different. Here the lever arms are measured normally to the members  $\overline{LF}$  and  $\overline{FG}$ .

**Diagonal member  $\overline{FE}$ .** The method of reasoning just applied to chord members answers in every sense for the web members.

The influence line for  $\overline{FE}$  is constructed as indicated in the figure. The stresses in  $\overline{FE}$ , due first to a unit load at  $A$  and then at  $B$ , are found for the system to which  $\overline{FE}$  belongs.

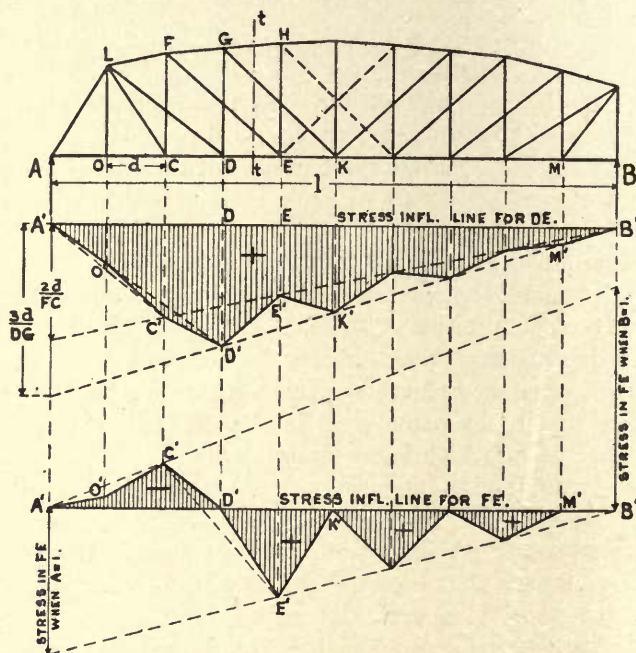


FIG. 25A.

Since loads at the panel points of the other system cannot cause stress in  $\overline{FE}$ , the influence line ordinates for these points must be zero. This means that the other influence line is the base line  $\overline{A'B'}$ . Observing again that the required influence line must be straight between successive panel points the final line becomes  $\overline{A'O'C'D'E'K'}$  to  $\overline{B'}$ . The point  $O'$ , as before, is midway between the ordinates under  $O$ .

The influence line indicates clearly that when loads are spaced  $2d$  apart, then the entire web stress goes into one system, making the design very uneconomical. This would easily happen for 50 ft. locomotives and 25 ft. panels.

ART. 26. CANTILEVER BRIDGES

Any statically determinate structure extending over more than two supports (piers or abutments), when continuous over  $r-2$  of these supports, may be regarded as a cantilever. If  $r$  is the total number of supports, then such a structure must be provided with  $r-2$  intermediate hinges such that the bending moments at these hinged points are zero for any system of loads.

The reaction and typical stress influence lines for such a cantilever will now be drawn.

**Reaction influence lines** for all simple structures are independent of the panels and may, therefore, be illustrated on a simple cantilever beam, Fig. 26A.

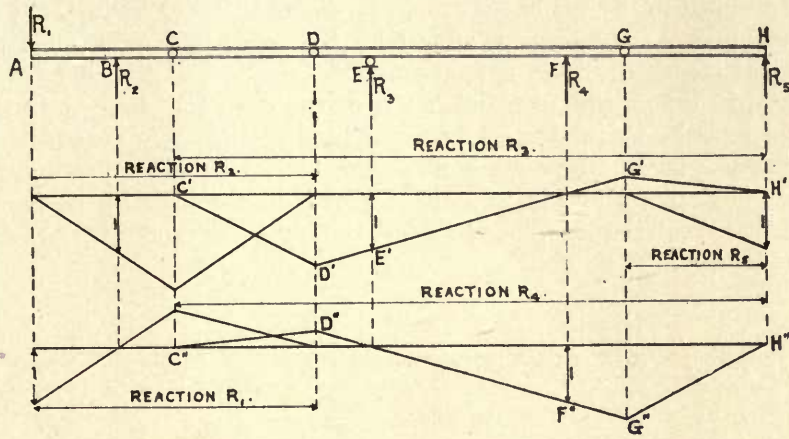


FIG. 26A.

The illustration represents an anchor arm  $\overline{AB}$  with a downward reaction or anchorage at A and an upward pier support at B. The span  $\overline{EF}$  is a simple beam on two supports E and F, with an overhanging cantilever arm at each end. A similar arm projects out from the anchor arm, making three cantilevers,  $\overline{BC}$ ,  $\overline{DE}$  and  $\overline{FG}$ , in the whole system.

The two spans  $\overline{CD}$  and  $\overline{GH}$  are known as intermediate spans and are supported on hinged ends which permit of horizontal displacements. Hence, there is only one roller bearing at E, and the anchorage at A also admits of slight horizontal motion.

The whole system is, therefore, determinate and can have no temperature stresses, neither will slight displacements of the supports cause any internal stresses.

The reaction influence lines thus involve no principles other than those already elucidated for simple beams on two supports.

The central span  $\overline{EF}$  is a suitable beginning, as it rests on two supports  $R_3$  and  $R_4$  with a roller bearing at E. Hence the influence lines for these two reactions are drawn precisely as for a simple beam between the points E and F. But the two arms at the ends of this span must also be considered.

Regarding first the influence line for  $R_3$ , it is seen that a load at F has zero effect,

and as the load proceeds to the left its effect on  $R_3$  is uniformly increasing and this continues to be the case until the load reaches the point  $D$ , where the effect becomes a maximum.

The same is true for a load between  $F$  and  $G$ , hence the ordinate unity at  $E'$  determines the  $R_3$  influence line from  $D'$  to  $G'$ . A load at  $C$  or at  $H$  produces zero effect on  $R_3$  and loads outside the span  $\overline{CH}$  have no influence, hence the line  $\overline{C'D'G'H}$  is the influence line for  $R_3$ . Further proof will scarcely be needed, though the several moment equations for the separate spans  $\overline{CD}$  and  $\overline{GH}$  will readily supply this.

Similarly the line  $\overline{C''D''G''H''}$  represents the influence line for  $R_4$ , based on the unit ordinate at  $F''$ .

The influence line for  $R_5$  is the same as for a simple beam  $\overline{GH}$ .

Precisely the same reasoning applies to the reactions  $R_1$  and  $R_2$ , the influence lines for which are shown to the left in Fig. 26A. It should be noted with regard to  $R_1$  that the negative influence area being greater than the positive, provision must be made for a downward reaction. When the upward reaction  $R_1$ , due to live load from  $A$  to  $B$ , is greater than the downward reaction  $R'_1$ , due to dead load from  $A$  to  $D$ , then the fastening at  $A$  must be designed to take stress in both up and down directions.

**Shear influence lines.** These are readily deduced from the reaction influence lines, as may be seen by comparing Fig. 26B with Fig. 26A. Four typical panels are assumed. One each for the central span  $\overline{EF}$ , the cantilever arms  $\overline{BC}$  and  $\overline{FG}$ , and the anchor arm  $\overline{AB}$ , respectively.

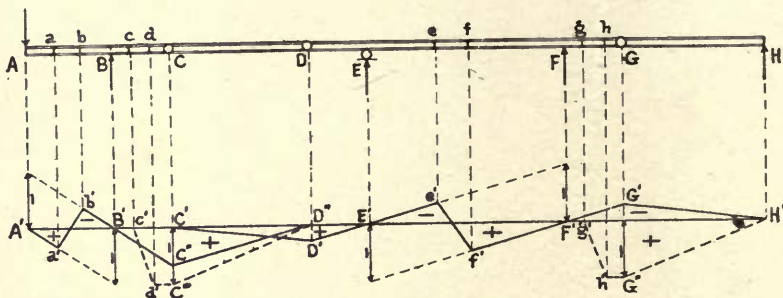


FIG. 26B.

For the panel  $\overline{ef}$  the shear influence line within the span is precisely as for any simple beam on two supports, while outside the span these lines are continued to the intersections  $D'$  and  $G'$  with the verticals through the hinges  $D$  and  $G$ , respectively. The shear influence line for the panel  $\overline{ef}$  is thus found as  $\overline{C'D'e'f'G'H'}$ .

For the panel  $\overline{ab}$  the same construction is applied as for a span on two supports  $A$  and  $B$  followed by a cantilever to the right of  $B$  exactly as for the previous case. The shear influence line for the panel  $\overline{ab}$  is the polygon  $\overline{A'a'b'B'C''D''}$ .

When the panel is located in one of the cantilever arms as for  $\overline{gh}$ , then the circumstances are slightly different, because the shear in any cantilever arm is always equal to the sum of the applied forces between the section and the outer end of the arm.



Accordingly the shear must be composed of the end reaction from the intermediate truss  $\overline{GH}$  and the constant effect of loads between  $h$  and  $G$ . Hence the influence line for the panel  $\overline{gh}$  is easily found to be the polygon  $\overline{g'h'G''H'}$ . It should be noted that loads to the left of  $g$ , even on the next span  $\overline{EF}$ , can have no effect on the shear in the panel  $\overline{gh}$ .

The shear influence line for the panel  $\overline{cd}$  is similarly found to be the polygon  $\overline{c'd'C''D''}$ .

Any panel located within either of the intermediate spans  $\overline{CD}$  and  $\overline{GH}$ , is treated precisely as for a span on two supports, since no load outside these spans can produce any effect on these trusses.

**Moment influence lines.** These offer very little difficulty and follow directly from the methods previously given.

In Fig. 26c the anchor arm was omitted, as the portion of the structure from  $C$  to  $H$  affords all the illustration required.

Here, again, the central span  $\overline{EF}$  is treated exactly like a simple beam and the negative effects of the adjoining cantilever arms are found by prolonging the lines so

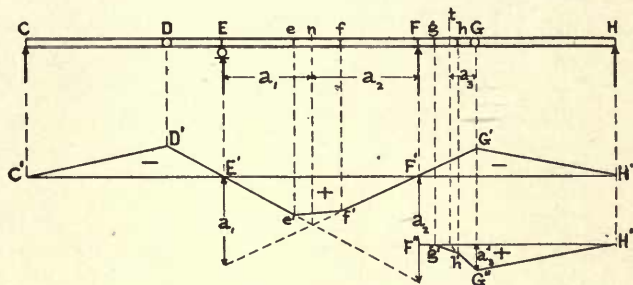


FIG. 26c.

obtained to the intersections  $D'$  and  $G'$  with the verticals through the hinged points. The moment influence line for the point  $n$ , in the panel  $\overline{EF}$ , thus becomes  $\overline{C'D'E'e'f'F'G'H'}$ , and it is readily seen that a load on any portion of the structure  $\overline{CH}$  affects the moment at  $n$ .

For the section  $t$ , in the panel  $\overline{gh}$ , the moment is the reaction at  $G$  into the lever arm  $a_3$ , hence for a unit load, the ordinate at  $G$  must be  $1 \cdot a_3$ , and observing that the influence line must be straight over the panel  $\overline{gh}$ , the required moment influence line for the section  $t$  becomes  $\overline{F''g'h'G''H''}$ .

**Stress influence lines.** The general method for stress influence lines, illustrated in Fig. 21A, serves every purpose in connection with cantilevers.

In every determinate structure the stress in any member may be expressed as  $S=M/r$  and from this it follows that the stress influence line for any truss member is similar to the moment influence line drawn for the center of moments pertaining to the member. The difference between the stress and moment influence lines is only the constant divisor  $r$  applied to the ordinates of the latter to obtain the ordinates for the stress influence line.

For convenience, the central span  $\overline{CE}$ , Fig. 26d, will be treated first, because this

portion of the structure is exactly like a simple truss on two supports, and all the rules previously given apply here.

Regarding the web members it should be observed that the center of moments may fall inside or outside the limits of the span. In the former case there will be no load divide within the span. Both cases are illustrated in Fig. 26d, where the stress influence lines for members  $U$ ,  $L$ ,  $D$ , and  $D'$  are presented.

The designations regarding the stresses in these members for unit reactions at  $C$  and  $E$ , will be as previously adopted in describing Fig. 21A, viz.,  $S_{uc}$  = the stress in the member  $U$  for a reaction unity acting at  $C$ .

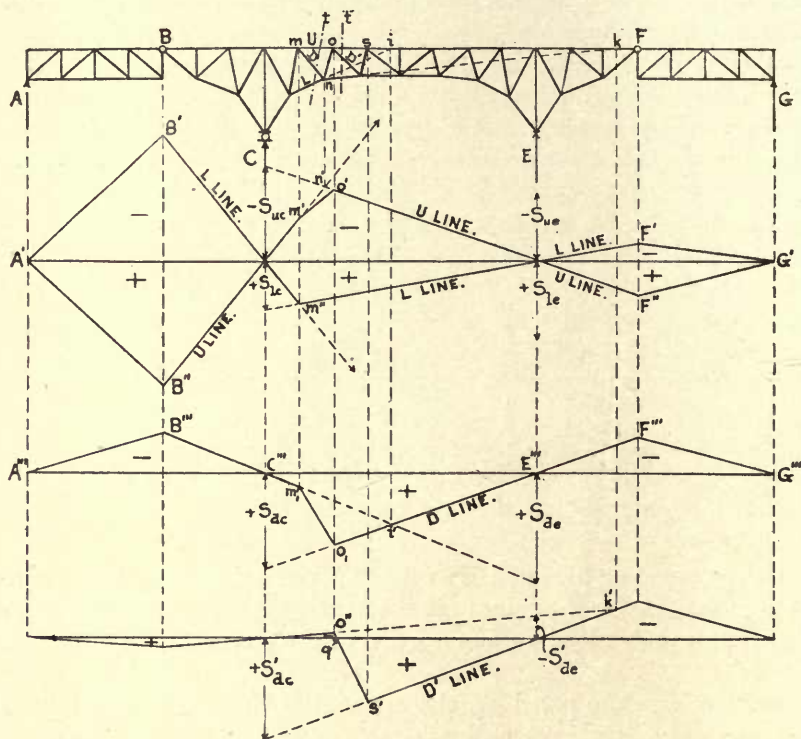


FIG. 26d.

Since these stresses are always necessary in constructing influence lines; it is best to find them for all members of the structure before proceeding to draw any influence lines. These stresses are very easily found either by slide rule, using Ritter's moment method, or by drawing a Maxwell diagram.

**Stress influence line for  $U$ , central span.** This being a top chord member, and in compression, its influence line is negative between  $C$  and  $E$ , which is also recognized by the stresses  $-S_{uc}$  and  $-S_{ue}$  found for this member for the reactions unity, acting first at  $C$  and then at  $E$ .

These stresses are laid off from  $\overline{A'B'}$ , Fig. 26d, upward and on the verticals through

$C$  and  $E$ , respectively. The stress influence line is then easily drawn, observing that the intersection  $n'$  must fall under the center of moments  $n$  for the member  $U$ . Hence this is a check and may also be used as a shorter method of finding the  $U$  line, when only  $-S_{uc}$  is known. Between the panel points  $m$  and  $o$  the influence line must be straight, hence  $m'o'$  is drawn.

To complete the influence line over the side spans, the  $U$  line, just found, is continued to intersections  $B''$  and  $F''$  with the verticals through the hinged points  $B$  and  $F$  and the final  $U$  line is then found to be  $A'B''m'o'F''G'$ . The portions below the base line  $A'G'$  are positive and the upper portion is negative. The positions of loads to produce *max.*  $U$  and *min.*  $U$  are thus clearly indicated and no other criterion is required.

**Stress influence line  $L$ , central span.** This is constructed in precisely the same manner as the  $U$  line, but  $L$  being in tension, as found for  $C=1$ , the stress  $+S_{lc}$  is laid off downward under  $C$ . The point  $m''$ , vertically under the center of moments  $m$  for the member  $L$ , is thus found and may serve to complete the  $L$  line without using the stress  $S_{lc}$ . The  $L$  line is then obtained as  $A'B'm''F'G'$  and is positive over the span  $CE$  and negative over the two cantilever spans  $AC$  and  $EG$ .

**Stress influence line  $D$ , central span.** The center of moments for this member is at  $i$ , which is within the supports, and hence this member has no load divide. The stress influence line is constructed exactly as was done for the  $U$  line, by laying off the positive stresses  $S_{dc}$  and  $S_{de}$  to obtain the two limiting rays, with intersection  $i'$  under the point  $i$ .

However, since the rate of increase in the stress  $D$  must be uniform for a load advancing from  $E$  to  $o$ , the ray  $E'''i'$  must be continued to  $o_1$ , finally drawing the line  $m_1o_1$  to complete the polygon.

Over the two side spans the  $D$  line is drawn as for the two previous cases, giving the complete line  $A'''B'''C'''m_1o_1E'''F'''G'''$ .

**Stress influence line  $D'$ , central span.** The center of moments for  $D'$  is outside the span at  $k$ , hence the influence line must show a load divide. The stresses  $+S'_{dc}$  and  $-S'_{de}$  serve to construct the stress influence line for  $D'$  which is in all other respects like the  $D$  line. The limiting rays intersect in  $k'$  and the load divide is at  $q$ .

**Stress influence line  $U$ , cantilever arm, Fig. 26E.** The effect of a moving load, coming on the span from left to right, begins when the load is just to the right of  $A$  and increases uniformly until the load reaches  $B$ . From  $B$  toward  $m$  the effect is uniformly decreasing and becomes zero when the load is over  $n$ , which is the center of moments for  $U$ . The stress in  $U$  for a load  $P=1$  at  $B$  is  $-S_{ub}$ , and laying this off from the base  $A'o'$ , the negative  $U$  line is easily drawn. For the effect due to loads in the panel  $m\bar{o}$  draw  $m'o'$  to complete the influence line. Loads to the right of  $o$  or to the left of  $A$  have no influence on  $U$ .

**Stress influence line  $L$ , cantilever arm.** The center of moments for  $L$  is at  $o$  and the stress in  $L$  for a load  $P=1$  at  $B$  is  $+S_{lb}$ . Hence the influence line becomes  $A''B''o''$  and is positive.

**Stress influence line  $D'$ , cantilever arm.** The center of moments for this diagonal is at  $i$ , which is inside the cantilever arm. The rule for load divide is now reversed because loads on opposite sides of  $i$  produce opposite stresses in  $D'$ , and a load at  $i$  cannot produce any stress. Hence  $i$  is the load divide for  $D'$ .



The stress in  $D'$  due to a unit load at  $F$  is  $-S'_{df}$ , hence making the ordinate under  $F$  equal to this stress the influence line  $s'i'F''G'$  is obtained.

Since loads to the left of  $h$  cannot affect  $D'$ , and since the influence line is a straight line over a panel, the influence line is completed by drawing  $h's'$ .

**Stress influence line D, cantilever arm.** The center of moments now falls off the arm at  $k$  and hence all loads produce the same kind of stress in  $D$ . Lay off the stress  $+S_{df}$  on the vertical through  $F$  and complete the influence line as shown in Fig. 26E, obtaining  $s''v'F'''G''$  for the  $D$  line.

The intermediate spans  $\overline{AB}$  and  $\overline{FG}$  are simple trusses on two supports and require no further consideration.

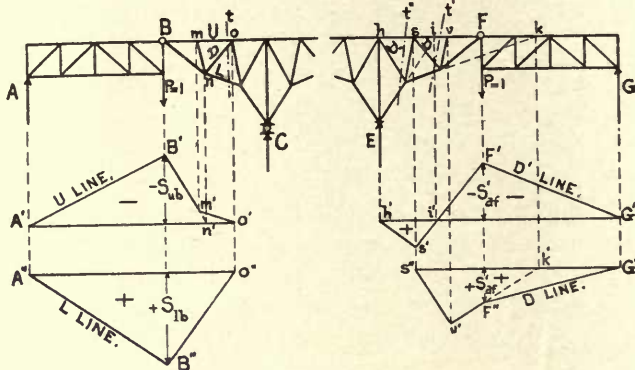


FIG. 26E.

## ART. 27. THREE-HINGED FRAMED ARCHES

In taking up this subject it is necessary to show briefly the general relations between the reactions and external loads.

Let Fig. 27A represent any three-hinged arch  $\overline{ACB}$ , which may be framed or solid. The single load  $P$  may be applied at any point  $m$ .

For all positions of  $P$  between  $A$  and  $C$ , the reaction  $R_2$  will always have the direction  $\overline{BC}$  and the two reactions  $R_1$  and  $R_2$  must be components of  $P$ . Similarly for all positions of the load  $P$  between  $C$  and  $B$ , these reactions will have the directions  $\overline{AC}$  and  $\overline{CB}$ , respectively. Hence for any position of the load  $P$ , the reactions at  $A$  and  $B$  are found by resolving  $P$  into two components as shown, and the points of application of all possible positions of  $P$  will lie on the prolongation of either  $\overline{AC}$  or  $\overline{BC}$ .

If the reactions  $R_1$  and  $R_2$  be resolved, each into a vertical component and one along  $\overline{AB}$ , the two last-named components  $H'$  will be equal and opposite, while the two vertical components  $A$  and  $B$  will be precisely the same as for a simple beam on two supports  $A$  and  $B$ , because the forces acting at  $C$  are in equilibrium among themselves.

Therefore,

$$A + B = P; \quad A = \frac{Pa_2}{l}, \quad \text{and} \quad B = \frac{Pa_1}{l}. \quad \dots \dots \dots (27A)$$

The horizontal component of  $H'$  is known as the horizontal thrust of the arch and is found from

$$H = H' \cos \alpha. \quad \dots \dots \dots (27B)$$

If the reactions  $R_1$  and  $R_2$  had been decomposed into components  $A'$ ,  $B'$  and  $H$ , then the former would no longer be the reactions for a simple beam  $\overline{AB}$ . However, when  $\alpha=0$  and the end supports are on a horizontal line, then the vertical end reactions are always as for a beam on two supports.

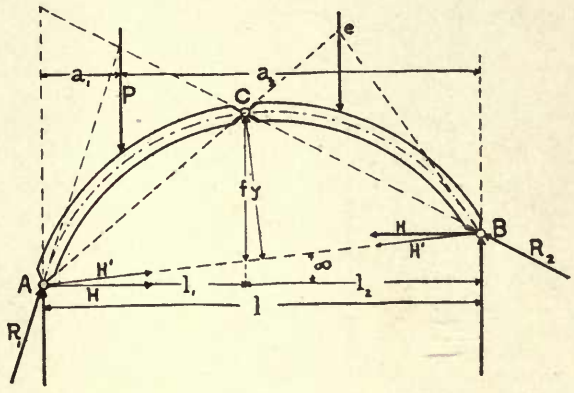


FIG. 27A.

Taking moments about the hinge C, when P alone is acting, then for condition of equilibrium at C

$$M = Al_1 - H'y = Al_1 - H'f \cos \alpha = 0,$$

and substituting values from Eqs. (27A) and (27B) this gives

$$\frac{Pa_2l_1}{l} = Hf \quad \text{or} \quad H = \frac{Pa_2l_1}{fl}. \quad \dots \dots \dots (27C)$$

When  $P=1$  is applied at C the value  $H_c$  becomes the ordinate vertically under C for the influence line for *horizontal thrust*.

Hence,

$$\eta_c = H_c = \frac{Pl_1l_2}{fl} \quad \text{and when} \quad l_1 = l_2 = \frac{l}{2}, \quad \text{then} \quad \eta_c = \frac{l}{4f}, \quad \dots \dots (27D)$$

making the  $H$  influence line a triangle with middle ordinate  $\eta_c$  under C, as given by Eq. (27D).

The influence lines for the vertical end reactions are found exactly as for a simple beam  $\overline{AB}$ .

**The stress influence line for any member** of a three-hinged framed arch will now be developed.

When the structure is symmetric, the half arch only requires analysis, but for unsymmetric arches the entire structure must be treated, though the method remains the same as would appear from the previous discussion.

In Fig. 27B, the half arch is shown with a load  $P$  producing reactions  $R_1$  and  $R_2$ , and since the latter must be transmitted to the point  $C$ , the right half of the span may be considered removed and its effect replaced by  $R_2$  acting at  $C$ . The left half of the span is then held in equilibrium by the two reactions  $R_1$  and  $R_2$ , the latter applied at  $C$ .

The reaction  $R_1$  is now resolved into  $A$  and  $K$  and the reaction  $R_2$  is similarly replaced by a vertical reaction  $C$  and a reaction  $K$  which is equal and opposite to the first  $K$ .

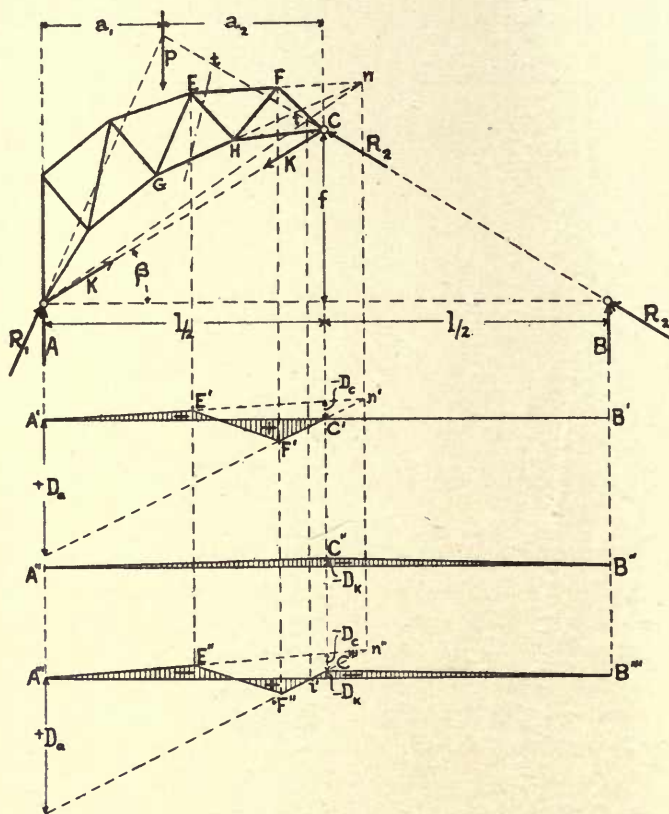


FIG. 27B.

If the forces  $K$  were zero, then the half span would represent a simple truss on two supports, with vertical reactions  $A$  and  $C$  and the influence line for any member could be found by the method previously given. Thus, the influence line for any member is easily drawn when the stresses, first for  $A=1$ , and then for  $B=1$  are known. Such an influence line is drawn for the diagonal  $D$ , and is shown as the polygon  $A'E'F'C'$ , Fig. 27B, where the stress  $D_a$ , due to  $A=1$  is positive, and the stress  $D_c$ , resulting from  $C=1$ , is negative. In each case the half span is supposed to be held first at  $C$  and then at  $A$  in order to find these stresses.





Typical stress influence lines will now be given for the three-hinged, framed arch, Fig. 27c, treating the top chord as the loaded chord.

The example will be taken up in such manner as to indicate a complete solution for all stresses in the several members by the method of influence lines.

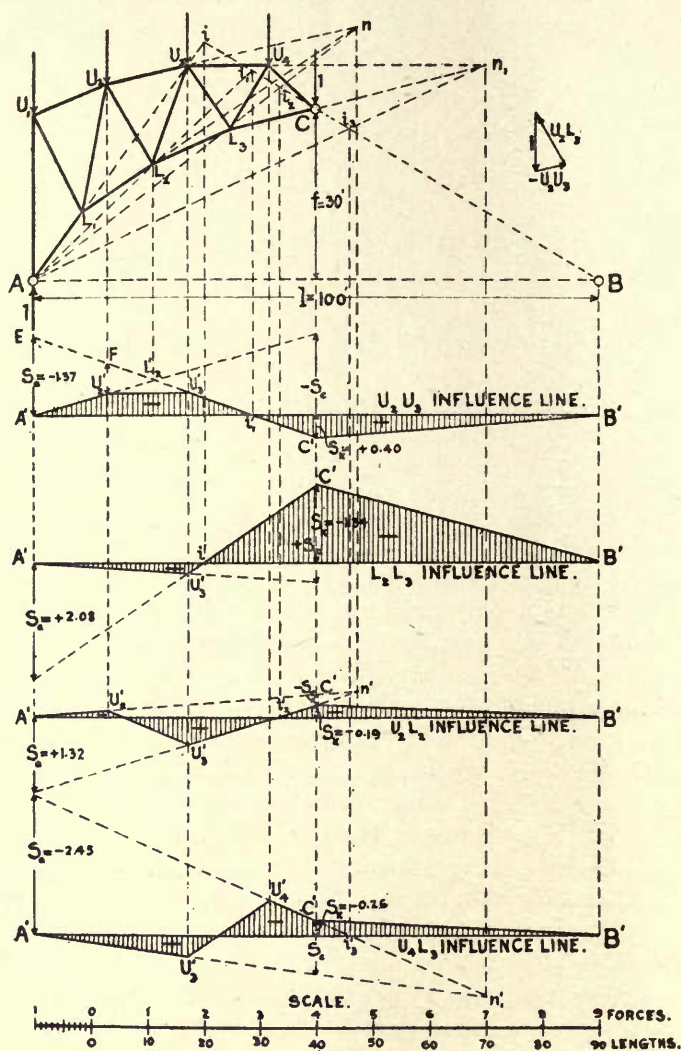


FIG. 27c.

The first step will be to determine the stresses  $S_a$  and  $S_k$  for all the members and this will be done analytically by Ritter's method of moments, being very careful about the sign of each stress.

The same stresses could also be found in a very convenient way by drawing two Maxwell diagrams, one for  $A = 1$ , supposing the half truss  $AC$  fixed at  $C$ ; and the other

for a load  $P=1$  acting vertically downward at  $C$  and producing the horizontal thrust  $H=1 \cdot l/4f=0.833$ , which is again applied at  $A$ , supposing the half truss fixed at  $C$ .

The following table contains the stresses  $S_a$  and  $S_H$  thus obtained and the stresses  $S_k=\frac{1}{2}S_a+S_H$  are then easily found.

MEMBER.	STRESSES.			MEMBER.	STRESSES.		
	$S_a$	$S_H$	$S_k$		$S_a$	$S_H$	$S_k$
$U_1A$	-1.00	+1.02	+0.52	$U_1U_2$	-0.45	+0.52	+0.30
$U_1L_1$	+0.93	-0.57	-0.11	$U_3U_3$	-1.37	+1.08	+0.40
$U_2L_1$	-1.29	+0.79	+0.15	$U_3U_4$	-3.11	+1.97	+0.42
$U_2L_2$	+1.32	-0.85	-0.19	$AL_1$	0.00	-1.44	-1.44
$U_3L_2$	-1.65	+0.77	-0.05	$L_1L_2$	+0.85	-1.87	-1.45
$U_3L_3$	+2.19	-1.15	-0.06	$L_2L_3$	+2.08	-2.38	-1.34
$U_4L_3$	-2.45	+0.96	-0.26	$L_3C$	+4.40	-3.35	-1.15
$U_4C$	+3.05	-1.19	+0.33	+ for tension and - for compression.			

The values in this table will suffice for the construction of all the stress influence lines, but only those for  $\overline{U_2U_3}$ ,  $\overline{L_2L_3}$ ,  $\overline{U_2L_2}$  and  $\overline{U_4L_3}$  will be drawn, as shown in Fig. 27c.

**Stress influence line  $\overline{U_2U_3}$ .** The stress  $S_a = -1.37$  is laid off, to a convenient scale, upward from  $A'$  and the stress  $S_k = +0.40$  is laid off downward from  $A'B'$ , vertically under  $C$ . The lines  $\overline{EC'}$  and  $\overline{C'B'}$  are then drawn.

The center of moments for  $\overline{U_2U_3}$  is at  $L_2$ , hence find  $L'_2$  vertically under  $L_2$  and draw  $\overline{A'L'_2}$ . Finally since the influence line must be straight over the loaded panel  $\overline{U_2U_3}$ , draw  $\overline{U'_2U'_3}$  to complete the influence line  $\overline{A'U'_2U'_3C'B'}$ . As a check observe that the load divide  $i'_1$  falls vertically under  $i'$ , which latter is the intersection of  $\overline{AL_2}$  with  $\overline{BC}$  produced. Still another check may be had by resolving a unit load at  $U_2$  into components parallel to  $\overline{U_2U_3}$  and  $\overline{U_2L_2}$  as was done to the right of the truss diagram. The stress thus found for  $\overline{U_2U_3}$  must equal the ordinate  $\overline{U'_2F}$ . Lastly, the ordinate  $-S_c$  is the stress in  $\overline{U_2U_3}$  for a load unity at  $C$  when the half truss  $\overline{AC}$  is fixed at  $A$  and the half span  $\overline{CB}$  is removed.

**Stress influence line  $\overline{L_2L_3}$ .** The method is precisely as for the previous case, being careful to observe the signs of the stresses  $S_a$  and  $S_k$  in laying them off from the base line  $\overline{A'B'}$ . The point  $U'_3$ , vertically under the center of moments for this member, again serves to complete the stress influence line, with all the checks just mentioned for the upper chord member.

**Stress influence lines  $\overline{U_2L_2}$  and  $\overline{U_4L_3}$ .** The same method again applies and the two lines illustrate the effects of the signs of the stresses  $S_a$  and  $S_k$ . The center of moments  $n$ , for the member  $\overline{U_2L_2}$  now falls outside the span, but the same relations hold good as before. Similarly for the center  $n_1$  of the member  $\overline{U_4L_3}$ . In this last case the load divide  $i_3$  falls below the middle hinge  $C$  and is no longer a real load divide, as the influence line for  $\overline{U_4L_3}$  indicates, but all other relations continue to exist as before.



## ART. 28. THREE-HINGED, SOLID-WEB AND MASONRY ARCHES

Fig. 28A illustrates a three-hinged, solid-web arch, which may be built of masonry or steel, according to circumstances. If of masonry, then the section will be rectangular, and if of steel, then the section will resemble that of a plate girder.

Whenever the depth of the section is small compared with the radius of the arch center line, then the effects of curvature are very minute and the stresses in the arch rib may always be found by the well known beam formula of Navier. This condition always prevails in bridges and all larger arches, but when dealing with small arched culverts and structures of that class, then the effects of curvature may require special consideration.

For any girder section then, the stress on the extreme fiber is derived from

$$\pm f = \frac{N}{F} \pm \frac{My}{I} = \frac{M_k y}{I} = \frac{M_k}{W}, \quad \dots \dots \dots (28A)$$

wherein  $M$  is the bending moment,  $N$  the normal axial thrust,  $F$  the cross-section,  $I$  the moment of inertia of the section and  $y$  the distance from the center of gravity of the section to the extreme fiber.  $M_k$  is the total bending moment of the external forces about one of the outer kernel points  $e$  or  $i$  (Fig. 28A) and  $W$  is the moment of resistance of the section.

Calling  $r$  the radius of gyration of the section, then

$$W = \frac{I}{y} = \frac{Fr^2}{y} = Fk \quad \text{where} \quad k = -\frac{r^2}{y} = -\frac{I}{Fy}. \quad \dots \dots \dots (28B)$$

The quantity  $k$  is the distance from the gravity axis to a kernel point and the negative sign indicates that it is measured in the opposite direction from  $y$  for all sections.

Hence, the influence lines for the kernel moments  $M_e$  and  $M_i$  will serve to find the stresses  $f_e$  and  $f_i$  for the extreme fibers of extrados and intrados of any particular section  $\bar{tt}$ , by using the multiplier  $\mu = 1/W = 1/Fk$ . For unsymmetric sections the two kernel distances are not equal so that  $\mu_e = 1/Fk_e$  for extrados and  $\mu_i = 1/Fk_i$  for intrados.

For each section the stresses on the extreme fibers thus become

$$f_e = \frac{M_e}{Fk_e} \quad \text{and} \quad f_i = -\frac{M_i}{Fk_i}, \quad \dots \dots \dots (28C)$$

where  $M_e = K_{ac}e$  and  $M_i = K_{ac}i$ , and  $K_{ac}$  is the end reaction at  $A$  for a load unity at  $C$  found by resolving the vertical reaction  $A$  along  $\bar{AC}$  and  $\bar{AB}$ . See also Art. 49 on two-hinged arches.

The moment influence lines  $M_e$  and  $M_i$  are now found by the method previously outlined for framed arches.

Each of these moments becomes zero when the unit moving load passes through a load divide  $d$ . Hence the load divides are easily located for each case.

Also since moments and not stresses are now considered, the end ordinate for the influence line at  $A$  is equal to  $x_e$  or  $x_i$  as the case may be.

Hence to draw the influence line  $M_i$ , lay off  $x_i$  at  $A$  and project the point  $d$  down to  $d'$ , draw  $\overline{Gd'C'}$  and after projecting down the center of moments  $i$  to find  $i'$ , finally complete the influence line by drawing  $\overline{A'i'}$  and  $\overline{C'B'}$ . Now find as a check, that  $\overline{C'D} = x'_i$ .

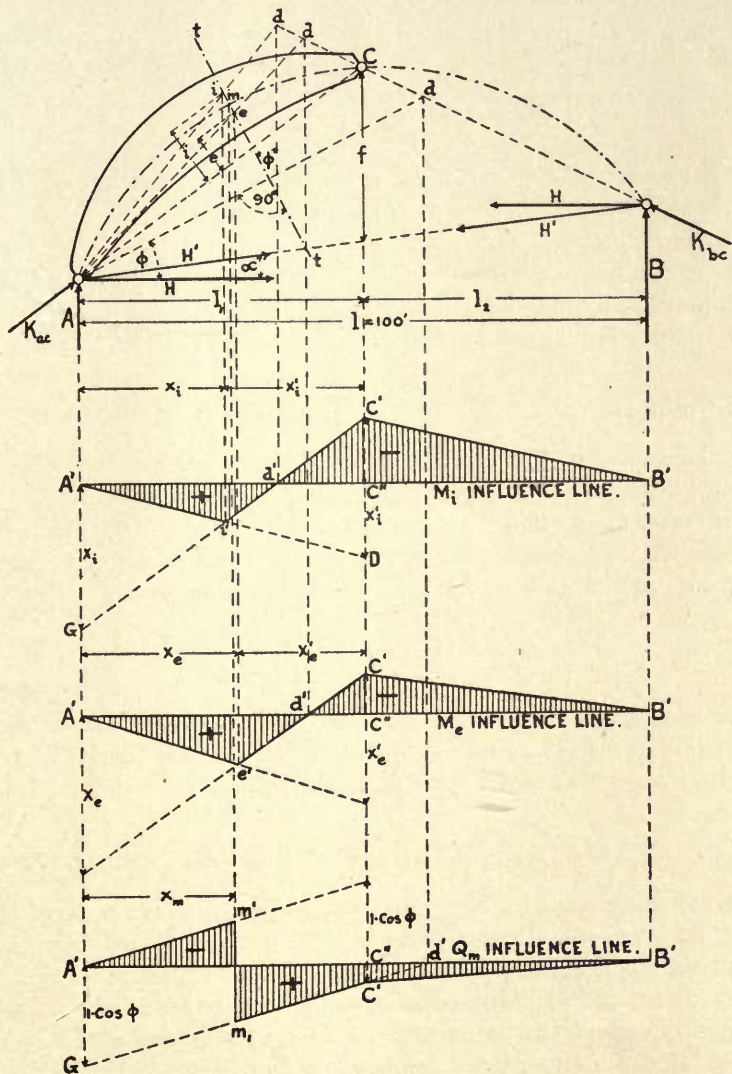


FIG. 28A.

The  $M_i$  influence line becomes the  $f_i$  influence line with a factor  $\mu_i = 1/Fk_i$ .

The influence line  $M_e$  is found in precisely the same manner.

In both cases the ordinate  $\overline{C'C''}$  is equal to  $M_i$  or  $M_e$  as given by Eq. (28c) for a unit load at C. The  $M_e$  influence line becomes the  $f_e$  influence line with a factor  $\mu_e = 1/Fk_e$ .

The shear influence line  $Q_m$  is found by a similar process. Here the center of moments, for a web member at  $m$ , would be practically at an infinite distance because the chords are parallel or nearly so. Hence the line  $\overline{Ad} \perp \overline{tt}$  will intersect the chord  $\overline{CB}$  in the load divide  $d$ , which in this case is only imaginary, but serves the purpose as before.

The equation for shear along the section  $\overline{tt}$  is easily found to be

$$Q_m = A \cos \phi - H \left( \frac{\sin (\phi - \alpha)}{\cos \alpha} \right), \quad \dots \dots \dots (28D)$$

and this gives, for a unit reaction at  $A$ , when the half arch is fixed at  $C$ , the end ordinate  $\overline{A'G} = 1 \cdot \cos \phi$ . Also since the shear is constant between  $A$  and  $m$ , the limiting lines  $\overline{A'm'}$  and  $\overline{Gd'}$  must be parallel.

Hence the shear influence line is easily constructed by drawing  $\overline{GC'd'}$ , and then completing the polygon by drawing  $\overline{A'm'} \parallel \overline{Gd'}$  and joining  $C'$  with  $B'$ .

Since the loading is directly applied the line  $\overline{m_1m'}$ , vertically under  $m$ , completes the  $Q_m$  line.

Finally the ordinate  $\overline{C'C''} = H \left( \frac{\sin (\phi - \alpha)}{\cos \alpha} \right)$  wherein  $H = 1 \cdot \frac{l_1 l_2}{fl}$  for a unit load at  $C$ .

When the loads are indirectly applied, then the condition that the influence line must be straight between load or panel points must be carefully observed.

For masonry arches the section is always rectangular and  $I = bD^3/12$ , hence  $k = -r^2/y = \mp \frac{1}{6}D$ , where  $D$  is the thickness of the arch ring. The points  $e$  and  $i$  thus become the middle third points of the arch section and Eqs. (28C) become

$$f_e = \frac{6M_e}{D^2} \quad \text{and} \quad f_i = -\frac{6M_i}{D^2}, \quad \dots \dots \dots (28E)$$

from which the stresses in a masonry arch section are readily found in terms of the moments about the kernel points of the section. The stress influence lines thus become moment influence lines with a factor  $6/D^2$  for each section.

## ART. 29. SKEW PLATE GIRDER FOR CURVED DOUBLE TRACK

In general, influence lines for skew bridges are drawn in all respects like those for any simple truss or beam with the exception that at one end of the span the load always leaves the span before it is entirely outside of the limits of the longer truss. This merely calls for a slight correction in the end panel of the influence line as ordinarily drawn.

At the opposite end of such truss some load comes on the end floor beam before the moving load is on the truss, but since the end floor beam transmits its load directly to the bridge support and not to the truss, this last-named circumstance does not affect the influence line. These points will be brought out in connection with the following problem.

It may seem inappropriate to apply influence lines to plate girders, but the practical designer who has dealt with problems of skew plate girders on curved double track will readily appreciate the advantages of the method there presented.



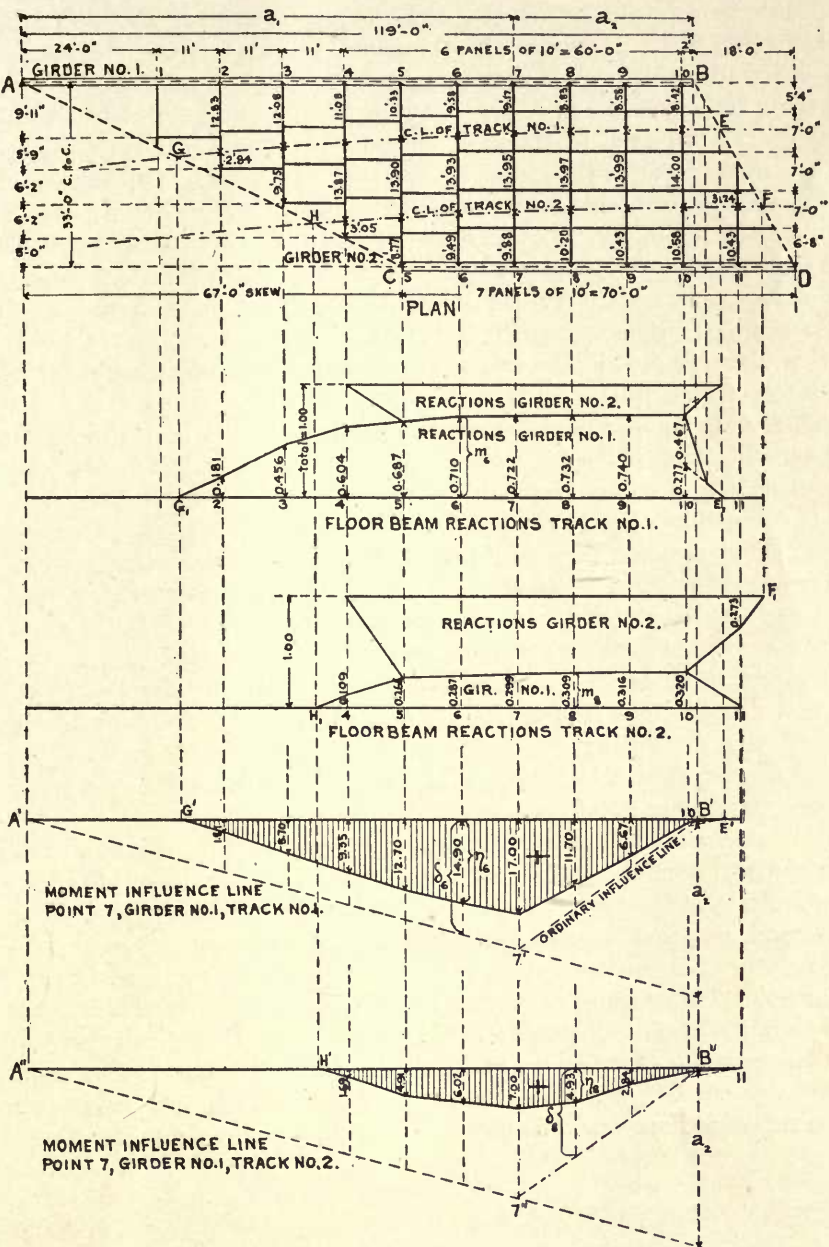


FIG. 29A.

This method was first suggested and used by Mr. T. B. Moenniche, C. E., in designing a skew double-track girder of 125 ft. span for the Virginian Ry. Co., in 1906. The author is indebted to Mr. Moenniche for the solution which follows.

The principal advantage in the present application of influence lines consists in reducing the solution of this rather complicated problem to a method instead of a time consuming process of experimentation.

The principle of the method may be outlined as follows: The floor-beam reactions are first determined for a unit load situated on track No. 1, and then for a unit load on track No. 2, which requires a careful computation of the coordinates or intersection points of each track on each floor beam. These floor beam reactions are then used as influence or reduction factors for the ordinates to any particular influence line, because the factors represent the proportion of a total load which can reach either girder at any panel point. This will give two influence lines for each panel point of a girder, one separately for each track.

In Fig. 29A, the upper diagram represents the structure in plan and the two succeeding figures show the floor beam reactions graphically. The last two diagrams are the moment influence lines for point 7, girder No. 1, for tracks No. 1 and 2, respectively.

The two reaction diagrams were drawn merely as a convenient way of showing the figures and in practice they would serve the same purpose, though they might be dispensed with entirely. The reactions appearing as ordinates are plotted to some convenient scale making the sum of two reactions for each floor beam equal to unity except at the ends where the floor beams do not connect with both girders.

**The moment influence lines for point 7** are drawn in the usual manner by laying off  $a_2$  vertically down from  $B$  and drawing  $\overline{A'7'}$  and  $\overline{7'B'}$ . Since the load on track No. 1, when coming on from the right, begins to affect girder No. 1 as soon as it passes the abutment at  $E$ , therefore, the distance  $\overline{E10}$  must be treated as a panel and the influence line is drawn straight from 10 to  $B'$ .

The ordinates  $\delta$  of the influence line are now successively reduced by multiplying them with the corresponding ordinates or factors  $m$  of the reaction diagram to obtain the real ordinates  $\eta$  of the required moment influence line. Thus  $\eta_6 = \delta_6 m_6$  and similarly for the influence line point 7, girder 1, track No. 2, the ordinate  $\eta_8 = \delta_8 m_8$ .

With the use of these two influence lines, represented by shaded areas, the actual moment for point 7 may be found for any case of loading for each track and the sum of the two gives the combined  $max. M_7$ .

Shear influence lines may be drawn in a similar manner, though they would scarcely serve a useful purpose except when dealing with a truss. In the above example only the reaction influence lines would be useful to determine the end shears.

## ART. 30. TRUSSES WITH SUBDIVIDED PANELS

From a point of economy, large trusses must have long panels, but with the increase in panel length the stringers of the floor system soon attain such proportions as to impose a practical limitation on the panel length.

To overcome this difficulty, modern practice has developed a new type of truss especially adapted to long spans, wherein the stringers are supported by floor beams placed at the half-panel points. These intermediate floor beams are carried at the ends by a secondary set of truss members, which latter serve to carry the loads, thus locally applied, to the main truss system. This has given rise to the truss with subdivided panels.

In the analysis of these truss types, it is not always a simple matter to determine the criterion for maximum stresses in the members, and it is believed that the following treatment by influence lines will serve to clear up the doubts usually encountered.

Fig. 30A shows a truss of 200 ft. span with four different forms of subdivided panels. These are all combined in the one structure, though in practice only one form should be used in the same structure excepting in the first panels  $\overline{AL_1L_2}$ , where the several compression members shown offer distinct advantages in stiffening the ends of the truss. Otherwise the panel  $\overline{L_2L_3}$ , Case I, is the best and most economical type for adoption, as will appear later.

In general, all primary members in the structure will receive stresses which are at least equal to those which would exist if the secondary members were all removed and in addition to these primary stresses nearly all of the members, excepting the verticals, will receive increased stresses due to local loads from the secondary members. This local loading is transmitted to the truss through the vertical  $\overline{M_3K}$  which never acts as a primary member and gets no stress other than that due to a full panel load, besides the dead weight of bridge floor and bottom chords.

It is the load, locally transferred to the points  $M$ , which enters as a disturbing element, and the four cases here treated will illustrate about all the practical points.

To make the four cases directly comparable, the same panel  $\overline{L_2L_3}$  was retained, but the diagonals were successively rearranged. The stress influence line for the primary stress in  $\overline{U_2L_3}$  remains the same in each case, hence it is drawn only once and is then modified according to local conditions in the panel  $\overline{L_2L_3}$  for each case.

**The Diagonal Member  $\overline{U_2L_3}$ .**

**Case I.** The stress influence line for  $\overline{U_2L_3}$ , when acting only as a principal truss member, is drawn by laying off the end ordinate  $\overline{A'A''} = +0.568$  which is the stress  $\overline{U_2L_3}$  for a reaction unity at  $A$ . The ordinate  $\overline{B'B''}$  (not shown) is  $-2.790$  and is the stress in the same member for a unit reaction at  $B$ . By drawing  $\overline{A''B'}$  and  $\overline{A'B''}$  the points  $U'_2$  and  $L'_3$  are found and the line  $\overline{U'_2L'_3}$  completes the influence line  $\overline{A'U'_2L'_3B'}$  with load divide at  $i$ .

This gives the maximum stress for  $\overline{M_3L_3}$  but not for  $\overline{U_2M_3}$ , because a load at  $K$  would produce additional stress in the latter member without affecting the former.

Hence to find the influence line for  $\overline{U_2M_3}$ , it is necessary to determine the stress



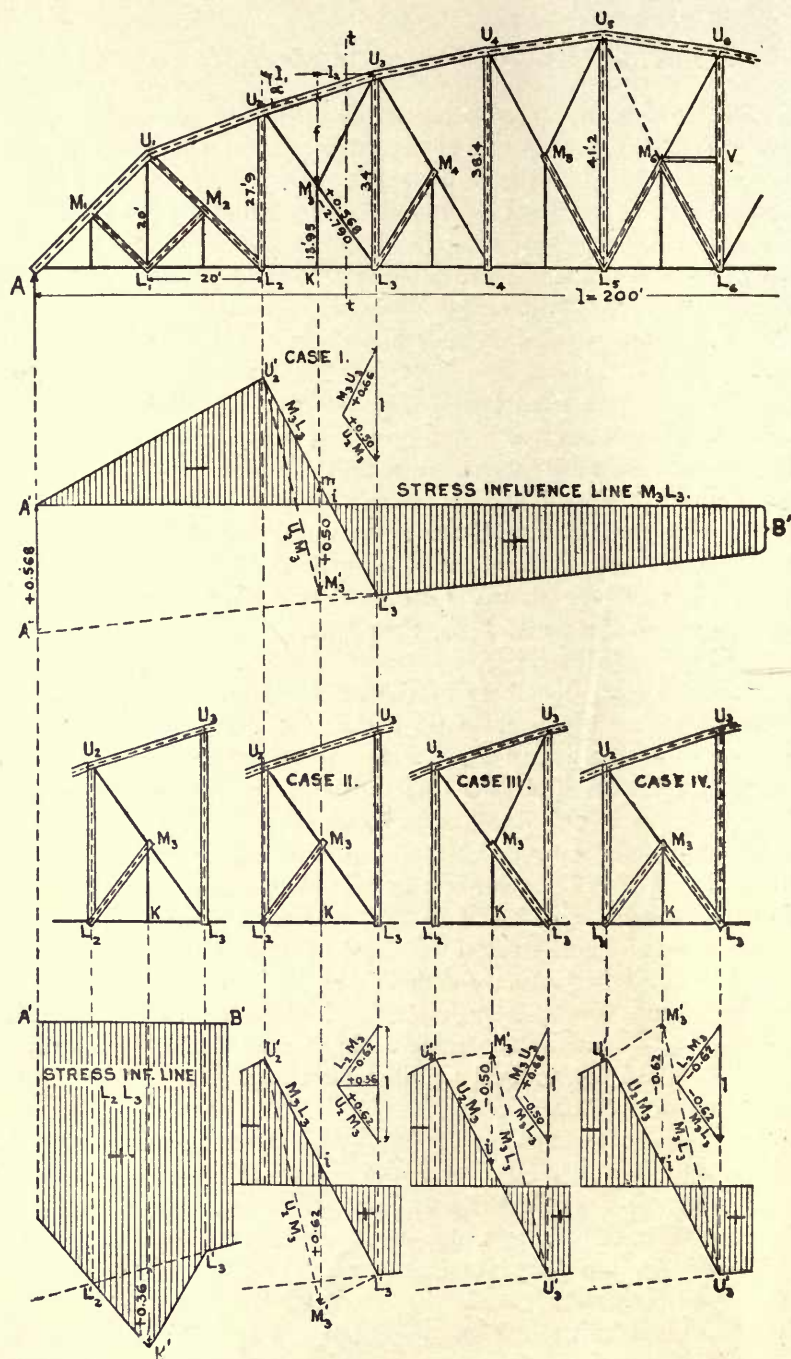


FIG. 30A.

in this member due to a local load unity at  $M_3$  which gives the total ordinate  $\overline{mM_3'}$  under  $M_3$ .

A load at  $M_3$  will be carried entirely by  $\overline{U_2M_3}$  and  $\overline{M_3U_3}$ , hence the stress due to a unit load is readily found by resolving the unit load into components parallel to these two members as indicated by the triangle of forces in the figure for Case I, drawn to half the scale of the influence line ordinates. The stress in  $\overline{U_2M_3}$  is thus found to be +0.5, which is laid off from  $m$  to complete the influence line  $\overline{A'U_2'M_3'L_3'B'}$  for the member  $\overline{U_2M_3}$ . It is seen that the point  $M_3'$  does not fall on the line  $\overline{B'A''}$  as usually assumed by authors on this subject. The error from this assumption is more apparent in Case II, and is not always on the safe side.

**Case II.** The influence line for the primary stress in  $\overline{U_2L_3}$  is as before, and again gives maximum for the lower portion  $\overline{M_3L_3}$ . However, a unit load at  $M_3$  is now carried to the members  $\overline{U_2M_3}$  and  $\overline{L_2M_3}$ , and these stresses are again found by a triangle of forces drawn in the figure for Case II.

The stress thus produced in  $\overline{U_2M_3}$  is now +0.62, from which the new influence line for  $\overline{U_2M_3}$  is readily obtained as  $\overline{A'U_2'M_3'L_3'B'}$ .

**Case III.** Here the primary stress holds good for the upper portion  $\overline{U_2M_3}$  and the stress in the lower portion  $\overline{M_3L_3}$  is diminished by the compression due to local loading at  $M_3$ . A unit load at  $M_3$  is now carried by  $\overline{M_3L_3}$  and  $\overline{M_3U_3}$  and the triangle of forces again gives the ordinate  $\overline{iM_3'}$ , which is here negative.

**Case IV.** This is like Case III, but a local load at  $M_3$  is now carried by  $\overline{L_2M_3}$  and  $\overline{M_3L_3}$  equally. Hence the stress in  $\overline{M_3L_3}$  due to a unit load at  $M_3$  is found as -0.62, which gives the ordinate  $\overline{iM_3'}$ .

**Members  $\overline{L_2M_3}$  and  $\overline{M_3U_3}$ ,** whenever they occur alone, can act only as secondary members to carry the portion of load locally applied at  $M_3$ . When the panel is subject to counter stress as in panels  $\overline{L_4L_5}$  and  $\overline{L_5L_6}$ , then the local stress must be combined with the counter stress when a counter  $\overline{U_5M_6}$  is employed. However, it is usually preferable to omit the counter member and design the main diagonal to take both the direct and counter stresses.

**The verticals  $\overline{U_2L_2}$ ,  $\overline{U_3L_3}$ ,** etc., may be treated entirely as primary members assuming the panels to be  $\overline{L_2L_3}$ ,  $\overline{L_3L_4}$ , etc.

**The vertical  $\overline{U_1L_1}$**  is merely a suspender for the double panel  $\overline{AL_2}$  and its maximum stress will occur when the span is fully loaded from  $A$  to  $L_2$ .

**The member  $\overline{M_6V}$ ,** and others of similar character often employed in large bridges, are entirely secondary and perform no work as truss members. The sole purpose of these members is to stiffen certain long compression members.

**Bottom chord member  $\overline{L_2L_3}$ .** The influence line for this member is easily drawn. The center of moments is at  $U_2$  and the end ordinate at  $A$  is the stress in the member for a unit reaction at  $A$ . The influence line thus becomes a triangle  $\overline{A'L_2'B'}$ .

**Case I.** With the diagonals all as tension members the local loads at the middle points cannot affect the bottom chord stresses and the influence line just described gives maximum stress.

**Case II.** Here the bottom chord stress is increased by the local load transmitted from  $M_3$  to  $L_2$ . This is shown in Fig. 30A. For a unit load at  $M_3$  the stress in the

bottom chord is the horizontal component in  $\overline{L_2M_3}$  found in the small force diagram for Case II. This stress, equal to +0.36, must then be the additional plus ordinate under  $M_3$  and the stress influence line for  $\overline{L_2L_3}$  thus becomes  $\overline{A'L_2'K'L_3'B'}$ , as shown.

**Case III** is exactly like Case II, and the horizontal component of  $\overline{M_3L_3}$  due to a unit load at  $M_3$  will be the positive ordinate to be added to the ordinary influence line under  $K$ .

**Case IV.** Here the two members  $\overline{L_2M_3}$  and  $\overline{M_3L_3}$  will transmit the unit load from  $M_3$  after the manner of a three-hinged arch. The local stress in the bottom chord then becomes  $\frac{\overline{L_2L_3}}{4M_3K} = \frac{20}{4 \times 13.95} = +0.358$  for a unit load at  $M_3$ .

Hence the positive ordinate under  $K$  must be increased by 0.358 to determine the proper influence ordinate under  $K$ .

**Top chord member  $\overline{U_2U_3}$**  has four cases as just described for the bottom chord.

**Case I.** Here the local load at  $M_3$  produces a compression in the top chord like a suspension system. The amount of this compression for a unit load at  $M_3$  is readily found from the Eq. (27D) given for three-hinged arches and is  $H' = l_1l_2/fd \cos \alpha$ , where  $l_1 + l_2 = d = \text{panel length}$ , see the truss diagram Fig. 30A.

This will give the negative stress ordinate to be added to the negative stress ordinate under  $M_3$  for the final influence line.

**Cases II and III** are similar and here the local effect in the top chord is the component in  $\overline{U_2M_3}$  or  $\overline{M_3U_3}$  parallel to  $\overline{U_2U_3}$ .

**Case IV** does not influence the top chord for local load at  $M_3$ . It is similar to Case I for bottom chord.

It is thus seen that the best criterion for trusses of this type is obtained from influence lines and the ease and clearness with which any case is solvable speaks greatly in favor of this method of analysis, where critical positions of loads and stresses are all given from the one solution.

In conclusion it may be remarked that the type of panel illustrated in Case I is in all respects preferable to the others. The type Case II deserves second choice, and the others, especially Case IV, should be avoided whenever possible.

The panel  $\overline{L_1L_2}$  is in a certain sense indeterminate and should never be used except in end panels as here illustrated, where the several posts tend to steady the shock of trains coming on the structure.



## CHAPTER VI

### DISTORTION OF A STATICALLY DETERMINATE FRAME BY GRAPHICS

#### ART. 31. INTRODUCTORY

The displacement between any two points or pairs of lines of any determinate frame may be found analytically as shown in Arts. 6 and 9. However, many problems, to be considered later, require a complete solution for every pin point of a structure, and then the analytic method would become quite laborious.

The graphic solution here given includes the two following problems: (1) To find the distortion, or change in form, of a frame resulting from changes in the lengths of its members, first published in 1877 by the French engineer Williot; and (2) to find the effect on this distortion produced by a yielding of the supports, or reaction displacements. This latter contribution came from Professor Otto Mohr in 1887, and without it the Williot diagram had little real value. Hence it is proper to call the complete diagram a Williot-Mohr displacement diagram, contrary to the position taken by Professor Mueller-Breslau, who erroneously credits the entire subject to Williot.

Having given the changes in the lengths of all the members of a structure, by Eq. (4B), when the stresses and cross-sections are known, let it be required to find the horizontal and vertical displacements of all the pin points.

The Williot diagram, to be presented first, offers a partial solution of this problem, which is completed by Mohr's rotation diagram.

#### ART. 32. DISTORTIONS DUE TO CHANGES IN THE LENGTHS OF THE MEMBERS BY A WILLIOT DIAGRAM

Since any determinate frame is formed by a succession of triangles, this elementary frame is first examined. The process may then be extended to include any number of such triangles or a complete frame.

In Fig. 32A suppose the point  $c$  to be connected with the points  $a$  and  $b$  by members 1 and 2, and that the lengths of these members also undergo changes  $-41$  and  $+42$ , respectively, while the points  $a$  and  $b$  move to new positions  $a'$  and  $b'$ . It is now required to find the direction and amount of displacement resulting for the point  $c$ .

Both members are first moved parallel to themselves until they occupy the positions  $\overline{a'c_2}$  and  $\overline{b'c_1}$ , respectively. The length of member 1 is now shortened by the amount  $41$  because this is a negative change; similarly the member 2 is lengthened by the amount  $42$ , giving the new lengths  $\overline{a'c_4}$  and  $\overline{b'c_3}$ , respectively.

With  $a'$  and  $b'$  as centers and corrected lengths  $a'c_4$  and  $b'c_3$  as radii, describe arcs which may intersect in a point  $c'$  representing the new position of the point  $c$ . But because  $\Delta 1$  and  $\Delta 2$  are always very minute compared with the lengths of the members to which they belong, the arcs  $c_4c'$  and  $c_3c'$  are replaced by their tangents, drawn respectively perpendicular to the original directions of the members. The diagram shows these displacements several hundred times larger than they actually are compared with the real lengths of the members  $\overline{ac}$  and  $\overline{bc}$ .

It is clear that the point  $c'$  might have been determined in a separate figure, without including the members themselves, by dealing exclusively with the directions and changes in the lengths of these members. Thus, in Fig. 32B, the  $\Delta l$ 's are plotted on a very large scale, affording greater accuracy in the results.

If the point  $O$  is regarded as a fixed point or pole, and if from this pole the displacements of the points  $a$  and  $b$  are drawn, making  $\overline{Oa'} = \overline{aa'}$  and  $\overline{Ob'} = \overline{bb'}$ , both in magnitude and direction; also, applying at  $a'$  the shortening  $-\Delta 1$  in the length of the member 1; and at  $b'$  the lengthening  $+\Delta 2$  of the member 2; then the perpendiculars

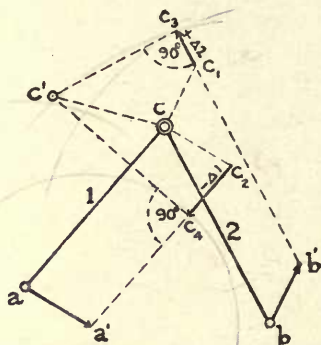


FIG. 32A.

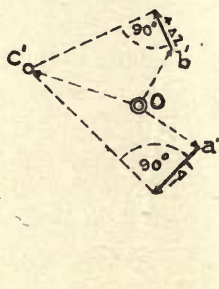


FIG. 32B.

erected at the extremities of  $\Delta 1$  and  $\Delta 2$  will intersect in  $c'$ , which is the new position of  $c$ . The displacement of  $c$  is then represented in direction and amount by the ray  $\overline{Oc'}$ .

In laying off the values of  $\Delta l$ , in Fig. 32B, the following rule must be observed with regard to signs: If  $a'$  is regarded as fixed, then  $-\Delta 1$  representing the *shortening* of  $\overline{ac}$ , it follows that  $c$  moves in the direction from  $c$  toward  $a$ , and hence  $-\Delta 1$  must be drawn from  $a'$  in the direction of  $c$  to  $a$ . Likewise, if  $b'$  is regarded fixed, then since  $+\Delta 2$  represents a *lengthening* of  $\overline{bc}$ , it follows that  $c$  moves *away* from  $b$  and hence  $+\Delta 2$  must be drawn from  $b'$  in the direction of  $b$  to  $c$ .

Any succession of triangles, as in Fig. 32c, may be treated in the same manner. It is necessary, however, to assume that one of the members, as  $\overline{ab}$ , retains its direction, and that some point of  $\overline{ab}$ , as  $a$ , remains fixed. The changes  $\Delta l$  in the several members being given, the construction is carried out as follows:

The point  $O$ , Fig. 32b, is the assumed pole, and since the point  $a$  is considered fixed it must coincide with  $O$ . Also, since the member  $\overline{ab}$  does not change in direction, then  $-\Delta 1$  is drawn parallel to  $\overline{ab}$  and, being negative, it must be applied in the direction of  $b$  toward  $a$ . The displacement of the point  $b$  is thus given by  $\overline{Ob'}$ .

The point  $c$  recedes from  $a$  by an amount  $+43$ , and approaches  $b$  by an amount  $-42$ . If, therefore,  $42$  be drawn from  $b'$  in the direction of  $c$  toward  $b$  and parallel to  $\overline{cb}$ , and if  $43$  be drawn from  $O$  or  $a'$ , in the direction of  $a$  toward  $c$  and parallel to  $\overline{ac}$ , then the intersection  $c'$  of the perpendiculars, to the extremities of  $42$  and  $43$ , will determine the new position of  $c$ . The displacement of  $c$  is thus given, both in direction and amount, by a ray  $\overline{Oc'}$  not drawn in the figure.

The point  $d$  is joined to  $a$  and  $c$  by the members  $\overline{ad}$  and  $\overline{dc}$ , Fig. 32c. Its displacement  $\overline{Od'}$  is now found, in Fig. 32d, by drawing  $+44$  parallel to  $\overline{ad}$  from  $O$  and in the direction  $a$  to  $d$ ; also by drawing  $-45$  parallel to  $\overline{cd}$  from  $c'$  in the direction  $d$  to  $c$ . The intersection  $d'$ , of the two perpendiculars to the extremities of  $44$  and  $45$ , is the new position of  $d$ . Finally the new position  $e'$  of the point  $e$  is similarly found by applying the same method.

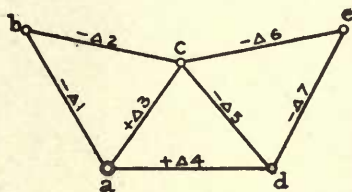


FIG. 32c.

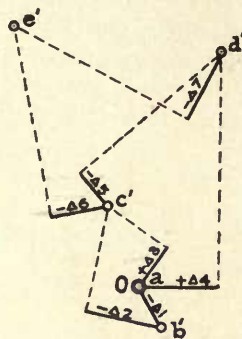


FIG. 32d.

Fig. 32d, whose polar rays  $\overline{Ob'}$ ,  $\overline{Oc'}$ ,  $\overline{Od'}$ , and  $\overline{Oe'}$  give the displacements of the several points  $b$ ,  $c$ ,  $d$  and  $e$ , both in direction and magnitude, is called the "Williot displacement diagram," for the frame  $\overline{abcde}$ , giving credit to the name of its originator.

### ART. 33. ROTATION OF A RIGID FRAME ABOUT A FIXED POINT—PROFESSOR MOHR'S ROTATION DIAGRAM

In the Williot diagram it was assumed that the member  $\overline{ab}$  did not alter its position, but merely changed its length. However, this is not always the case and more frequently this member  $\overline{ab}$  is also subjected to a rotation about some instantaneous center. In the latter event, the elastic displacements, given by the Williot diagram, will require further changes to make them comply with the initial change in the position of the member  $\overline{ab}$ . It is supposed, for the present, that the frame has undergone its elastic deformation and has passed into a rigid state.

The solution of this phase of the problem was first proposed by Professor Mohr and is based on the following theorem in mechanics: *The motion of a rigid body, at any given instant, may be defined as a rotation about a certain point called the instantaneous center of rotation, and the direction of motion of any point of this body, at the instant in*



question, will be perpendicular to the line joining such point with the instantaneous center of rotation.

Thus, if  $\overline{abcde}$ , Fig. 33A, represents a rigid frame rotating about the instantaneous center  $P$ , each arrow, perpendicular to its respective ray, will then represent the direction of motion of the point to which the ray is drawn.

Now, if from any pole  $O$ , Fig. 33B, a series of radial rays be drawn respectively parallel to the arrows representing the motions of the several points, then these rays  $\overline{Oa''}$ ,  $\overline{Ob''}$ ,  $\overline{Oc''}$ ,  $\overline{Od''}$ , and  $\overline{Oe''}$  will in turn represent, both in magnitude and direction, the several displacements of the several points,  $a$ ,  $b$ ,  $c$ ,  $d$  and  $e$ . The figure  $\overline{a''b''c''d''e''}$  will be the new position of the rigid frame  $\overline{abcde}$ .

For,  $\overline{a''O} \perp \overline{aP}$ ;  $\overline{b''O} \perp \overline{bP}$ ;  $\overline{c''O} \perp \overline{cP}$ ; etc., because the direction of motion of each such point of the rigid frame was perpendicular to the ray joining this point with the instantaneous center of rotation.

Also,  $\overline{a''O} : \overline{b''O} : \overline{c''O}$ , etc. =  $\overline{aP} : \overline{bP} : \overline{cP}$ , etc., because the displacements of the several points  $a$ ,  $b$ ,  $c$ , etc., are respectively proportional to their velocities, and these in turn

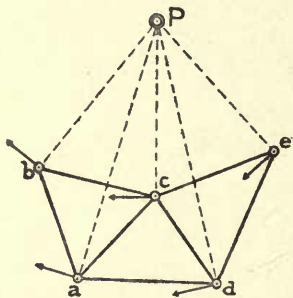


FIG. 33A.

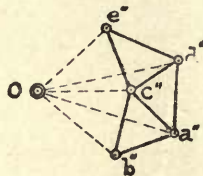


FIG. 33B.

are proportional to the distances of the several points from the instantaneous center of rotation.

From these conditions it follows that:

(a) If the points  $a''$ ,  $b''$ ,  $c''$ , etc., of the diagram Fig. 33B, are joined by straight lines, so that for every member  $\overline{ab}$  of the frame, there will be a corresponding line  $\overline{a''b''}$  in the displacement diagram, then these latter lines will produce a figure  $\overline{a''b''c''d''e''}$  which will be similar to the rigid frame.

(b) Also, the line joining any two points of the rigid frame, as  $\overline{ab}$ , will be perpendicular to the corresponding line  $\overline{a''b''}$  of the displacement diagram.

Hence, if it is possible to determine the position of any two of the points  $a''$ ,  $b''$ ,  $c''$ , etc., of the displacement diagram, then the figure  $\overline{a''b''c''d''e''}$  can be drawn by similarity with the figure  $\overline{abcde}$ . The method of determining two such points  $a''$ ,  $b''$  will be illustrated in the examples.

Therefore, the secondary displacements, due to rotation of the rigid frame, are found by inserting in the Williot displacement diagram a figure  $\overline{a''b''c''d''e''}$  similar to the frame  $\overline{abcde}$ , and having its sides respectively perpendicular to the sides of the

latter frame. The original displacements  $\overline{Ob'}$ ,  $\overline{Oc'}$ , etc., are then combined with the displacements  $\overline{Ob''}$ ,  $\overline{Oc''}$ , etc., due to rotation to produce the resultant displacements  $\overline{b''b'}$ ,  $\overline{c''c'}$ , etc.

The complete solution for the displacement of the pin points of any framed structure, definitely supported, may then be outlined in the three following steps:

(a) Assume any member and a point on the axis of this member as fixed and construct a Williot displacement diagram.

(b) Then assume the frame as rigid and subjected to a rotation such as will conform to the actual conditions of the supports.

(c) The displacements of the several pin points may then be found, in magnitude and direction, by scaling the distances between the  $m''$  and  $m'$  points. The direction of any displacement will always be from  $m''$  toward  $m'$ .

The complete diagram, combining the *Williot displacement diagram* with the *Mohr rotation diagram*, will hereafter be known as a *Williot-Mohr diagram*.

The analytic solution of deflection problems is conducted with the aid of Professor Mohr's work, Eq. (6A), and may be advantageously employed when only one point of the structure is to be treated, or when great accuracy is required in the solution.

This method is fully discussed in Art. 6 and, in combination with Maxwell's theorem given in Art. 9, offers the most accurate analytic solution of a great variety of problems dealing with displacements of points and lines.

However, all problems requiring a complete solution for all the pin points of a structure, may be solved by a Williot-Mohr displacement diagram when extreme accuracy is not necessary.

Attention is called to the fact that the value for  $E$ , in all deflection problems, should be chosen low rather than high, because there is always a slight amount of lost motion and permanent set, which follows the first loading of a new structure and which is not truly an elastic deformation. This can be compensated for in the calculations by assuming a small  $E$ .

As a general rule, the changes  $\Delta l$ , in the lengths of the members, are best figured on gross sections rather than on net sections. Experience indicates that this gives results nearer the truth. Also the stresses in the members must be simultaneous and not maximum.

#### ART. 34. SPECIAL APPLICATIONS OF WILLIOT-MOHR DIAGRAMS

(1) **Distortion of a simple truss.** Fig. 34A has been solved in three ways, for the purpose of illustrating that the displacements are not affected by the choice of the member and point which are regarded as fixed in position, and also in order to show how to select the most convenient of the possible forms of solution.

The truss is supported on rollers at  $e$  and is fixed at  $a$ . The extensions (+) and contractions (−) of the members are assumed to be as marked upon them.

The solution given in diagram  $b$  is made under the supposition that the direction of the member  $\overline{af}$  and the point  $a$  remain fixed.

According to the method outlined in Art. 32, a displacement diagram is constructed

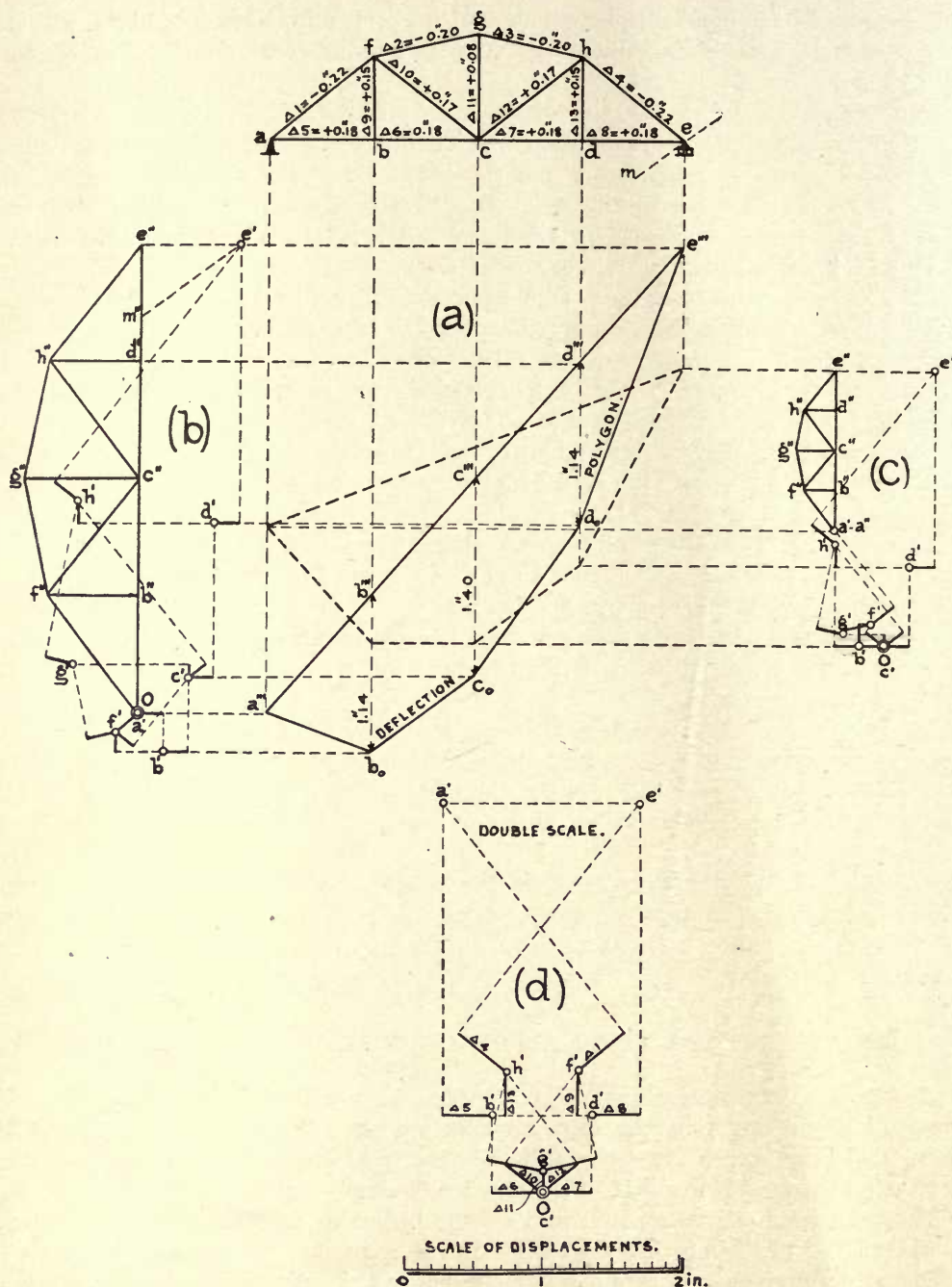


FIG. 34A.



with pole at  $O$ . Since  $a$  is now supposed to remain fixed, the point  $a'$  coincides with  $O$ , and the displacements of the various points  $b, c, d, e$  and  $f$  are obtained by scaling the distances  $\overline{Ob'}$ ,  $\overline{Oc'}$ ,  $\overline{Od'}$  . . .  $\overline{Of'}$ .

In reality, however, the direction of the member  $\overline{af}$  does not remain fixed, for the member revolves about the point  $a$ . Therefore, the displacements just found must be combined with those displacements  $\overline{Ob''}$ ,  $\overline{Oc''}$ ,  $\overline{Od''}$ , etc., which are caused by revolving the rigid frame, or truss,  $\overline{abge}$  about the point  $a$  until the point  $e$  shows a resulting displacement,  $\overline{e'e''}$ , parallel to the direction of motion of the roller bed at  $e$ .

In other words, the resultant movement of the point  $e$  will be horizontal when the roller bed is horizontal. If the bed were inclined, as  $\overline{em}$ , diagram a, then the point  $e$  would move parallel to  $\overline{em}$ .

The figure  $\overline{a''b''c''d''e''f''g''h''}$ , similar to the figure of the truss, can then be constructed, making the sides respectively perpendicular to the members of the truss. This figure is definite and can be drawn when the points  $a''$  and  $e''$  are found. The point  $a''$  will coincide with  $a'$  or  $O$ , since it remains fixed and  $\overline{a''e''}$  will be perpendicular to  $\overline{ae}$ . Also  $\overline{e'e''}$  will be parallel to the roller bed, which is horizontal in the present case, but may be in any direction, as  $\overline{e'm''}$ , for a skew-back.

The actual displacements of the points  $b, c, d$ , etc., will then be given in direction and in amount by the distances  $\overline{b''b'}$ ,  $\overline{c''c'}$ ,  $\overline{d''d'}$ , etc., but the horizontal and vertical projections of these displacements are more generally desired and may be scaled from the drawing.

The deflection polygon of the bottom chord is found graphically by projecting the points  $a', a'', b', b''$ , etc., on to the verticals through the panel points  $a, b$ , etc. The points  $a'', b'', c''$ , etc., will be projected in  $a'''$ ,  $b'''$ ,  $c'''$ , etc., and will form a straight line  $\overline{a'''e'''}$ . The points  $b', c', d'$ , etc., will fall in  $b_0, c_0, d_0$ , etc., and the ordinates  $\overline{b_0b''}$ ,  $\overline{c_0c''}$ , etc., will give the vertical deflections of the panel points  $b, c$ , etc.

In diagram c the direction  $\overline{cb}$  is assumed and the point  $c$  is fixed. All that has been said regarding the first solution applies here. It will be seen that this solution gives exactly the same displacements as previously found, while it occupies only about half the space of the first diagram because the member  $\overline{bc}$  has a lesser angular motion than the member  $\overline{af}$ .

The third solution, diagram d, is the simplest of all, and its diagram covers the least area; for the member  $\overline{cg}$ , which is now assumed as fixed, really has no angular motion, but simply drops vertically. The relative displacement  $\overline{b'g'}$  of any two points,  $b$  and  $g$ , may be scaled off directly. Although this displacement diagram was drawn on the assumption that the line  $\overline{cg}$  and the point  $c$  remained fixed, nevertheless any two points may be directly compared. Hence, any point may be chosen as the origin of coordinates from which to scale the horizontal and vertical displacements of all other points relatively to this origin. Naturally the displacements desired would be those with respect to the point  $a$ , for this is the fixed point, giving for the point  $e$  a horizontal movement from  $a'$  to  $e'$ . All other points move to the right and down from their original positions by amounts which may be scaled from the diagram, taking  $a'$  for the origin.

Hence it may be concluded that if a truss contains a member which will move

parallel to itself, or which has no angular motion, then this member is the best one to choose as the fixed member in constructing the displacement diagram. The rotation displacements are thereby eliminated.

(2) **A French roof truss.** Fig. 34B. In this example the stresses were found from a Maxwell diagram, and the corresponding changes in the lengths of the members were obtained by means of the formula  $\Delta l = Sl/EF$ , taking  $E$  at 25,600,000 pounds per square inch for wrought iron. Changes of length, due to temperature, are neglected. The values of  $\Delta l$  being very small, ten times these values were taken. All the data necessary in the solution of this truss are given in the following table:

TABLE OF THE VALUES OF  $S$ ,  $F$ ,  $l$ , AND  $10\Delta l$  IN FIG. 34B

Member.	Stress, Lbs. $S$	Area, Sq. in. $F$	Length, Inches, $l$	$10(\Delta l)$ , Inches.	Member.	Stress, Lbs. $S$	Area, Sq. in. $F$	Length, inches. $l$	$10(\Delta l)$ , Inches.
1	-21,800	6.82	83.53	-0.106	15	-20,970	6.82	83.53	-0.102
2	-20,040	6.82	83.53	-0.094	16	-19,210	6.82	83.53	-0.091
3	-18,300	6.82	83.53	-0.087	17	-17,470	6.82	83.53	-0.083
4	-16,540	6.82	83.53	-0.079	18	-15,710	6.82	83.53	-0.075
5	+19,730	2.02	96.53	+0.370	19	+15,330	2.02	96.53	+0.288
6	+16,430	2.02	96.53	+0.307	20	+13,570	2.02	96.53	+0.256
7	+9,040	1.86	100.08	+0.189	..	.....	.....	.....	.....
8	+9,260	1.86	96.53	+0.189	22	+6,200	1.86	96.53	+0.126
9	+12,560	1.86	96.53	+0.256	23	+7,960	1.86	96.53	+0.161
10	-3,300	1.40	48.07	-0.043	24	-1,680	1.40	48.07	-0.024
11	+3,300	0.78	96.53	+0.162	25	+1,680	0.78	96.53	+0.087
12	-6,600	2.48	96.53	-0.102	26	-3,520	2.48	96.53	-0.055
13	+3,300	0.78	96.53	+0.162	27	+1,680	0.78	96.53	+0.087
14	-3,300	1.40	48.07	-0.043	28	-1,680	1.40	48.07	-0.024

The truss is composed of the two frames  $\overline{aeh}$  and  $\overline{sqh}$ , designated as I and II. These are connected by the member  $\overline{as}$  and by the pin at  $h$ .

The displacement diagram of frame I is first drawn, assuming as fixed the direction of any member, as  $\overline{ab}$ , and the position of a point, as  $a$ , of this member. The point  $a'$  then coincides with the pole  $O$ , and the displacement  $\overline{Ob'}$ , of the point  $b$  will be equal to  $\Delta l_2$ . The points  $c'$ ,  $d'$ ,  $e'$ ,  $f'$ ,  $g'$  and  $h'$  are then found as directed in Art. 32.

The displacement diagram of frame II is next drawn, assuming as fixed the direction of the member  $\overline{sk}$  and the position of the point  $s$ .

Having thus determined the points  $k'$ ,  $l'$ ,  $m'$ ,  $q'$ ,  $n'$ ,  $p'$  and  $h'$  in diagram II, the relative changes in the positions of the points  $h$ ,  $s$  and  $q$ , parallel to the straight lines joining the points  $h$  and  $s$ ,  $h$  and  $q$ , and  $s$  and  $q$ , may be found. These changes are called  $\Delta \overline{hs}$ ,  $\Delta \overline{hq}$  and  $\Delta \overline{sq}$ .

Diagram I may now be completed by inserting the values  $\Delta \overline{hs}$ ,  $\Delta \overline{hq}$  and  $\Delta \overline{sq}$  previously found from diagram II. The point  $s'$  is found from  $\Delta l_7$  and  $\Delta \overline{hs}$ , and the point  $q'$  is found from  $\Delta \overline{hq}$  and  $\Delta \overline{sq}$ . Since  $q$  moves on a horizontal roller bed and since  $e$  is fixed, the figure  $\overline{c'd''b''g''h''f''a''s''q''}$  can be drawn as in the preceding problem. This figure gives the displacements of all the points of frame I, and those of the points  $s$  and  $q$ .



The displacement diagram of frame II may now be completed by transferring the displacements of the points  $h$  and  $q$  from diagram I into diagram II, thus determining

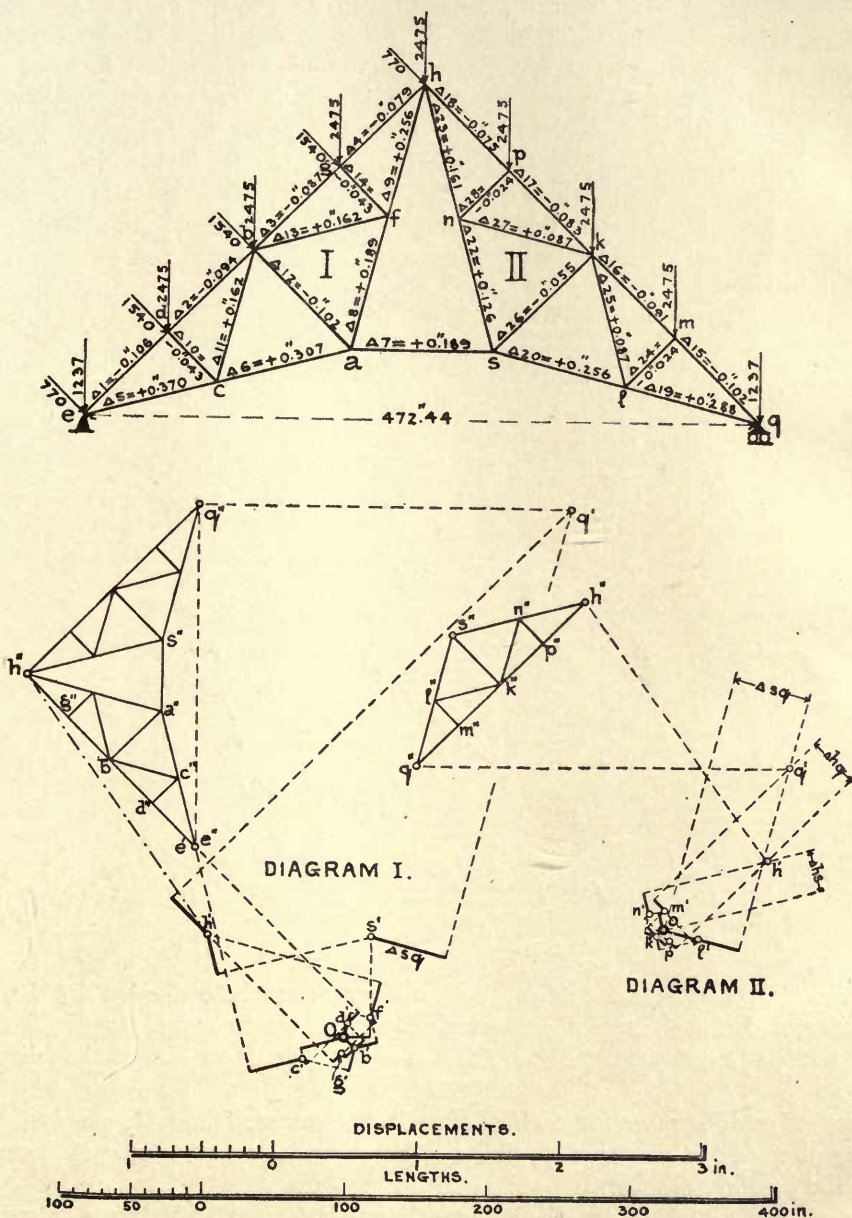


FIG. 34B.

the points  $q''$  and  $h''$  from which the figure  $q''v''s''n''h''m''k''p''$  can be drawn.

As a check, it should be remembered that the line  $q''h''$  in diagram II must be



perpendicular to the line  $\overline{hq}$ , and that the displacement  $\overline{s's''}$  of the point  $s$  must be the same, both in direction and in amount, in both diagrams.

Diagram II might have been dispensed with in the present case, as the values  $\Delta\overline{hs}$ ,  $\Delta\overline{hq}$  and  $\Delta\overline{sq}$  might have been found directly by summing the  $\Delta l$ 's. However, the use of diagram II is general, and it becomes necessary when the points  $h$ ,  $p$ ,  $k$ ,  $m$  and  $q$  or  $h$ ,  $n$  and  $s$ , or  $l$ ,  $s$  and  $q$ , are not in straight lines, as in the case of a curved top chord.

Measurements from diagram I show that the point  $g$  undergoes the greatest displacement, having a horizontal movement of  $1.93/10 = 0.193$  inch to the right, a vertical downward movement of  $2.33/10 = 0.233$  inch, or a resultant movement of  $\overline{g'g''} = 3.02/10 = 0.302$  inch. The horizontal movement of the point  $q$  is  $= q'q'' = 2.61/10 =$

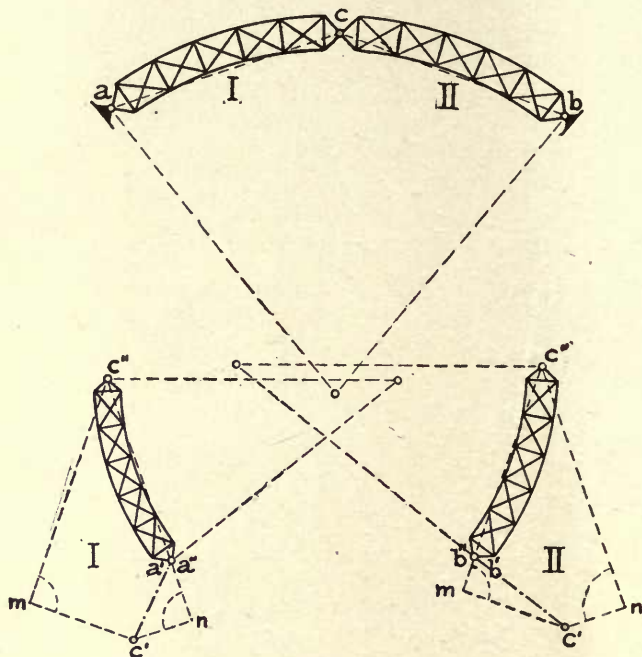


FIG. 34c.

0.261 inch. The displacements given by the diagram are here divided by 10, because, as already stated, the changes  $\Delta l$  were originally taken ten times too large.

(3) **A three-hinged arch.** Fig. 34c. It is required to draw the displacement diagram.

Independent diagrams for each of the elastic frames, I and II, are first drawn by assuming as fixed the direction of, and a point on, some member of each frame, as was done in the previous problem.

The frames I and II are then regarded as rigid, and each frame is supposed to revolve in such a way as to satisfy the conditions imposed by the supports.

The displacement diagrams are omitted and only the second part of the problem is solved.

Supposing that the points  $a'$  and  $c'$  in Fig. 34c, diagram I, and the points  $b'$  and  $c'$ , diagram II, have been found from the corresponding displacement diagrams (not shown), let it be required to complete the solution by adding Mohr's rotation diagram.

The following conditions must exist between the figures  $\overline{a''c''}$  and  $\overline{b''c''}$ , which are to be similar to the frames I and II respectively:

- a. The displacement of the point  $a$  is zero, hence  $a''$  will coincide with  $a'$ .
- b. Similarly  $b''$  will coincide with  $b'$ .
- c. The line  $\overline{a''c''}$ , in diagram I, must be perpendicular to the line  $\overline{ac}$ .
- d. The line  $\overline{b''c''}$ , in diagram II, must be perpendicular to the line  $\overline{bc}$ .
- e. Both diagrams, I and II, must give the same displacement  $\overline{c'c''}$  for the point  $c$ .

Hence  $\overline{a''c''}$  is drawn through  $a'$ , perpendicular to  $\overline{ac}$ , also  $\overline{b''c''}$  through  $b'$  perpendicular to  $\overline{bc}$ . Now, in diagram I,  $\overline{c'n}$  is drawn parallel to  $\overline{ac}$ , intersecting  $\overline{a''c''}$  in  $n$ , and the projection of the required displacement  $\overline{c'c''}$ , parallel to  $\overline{ac}$ , is thus obtained. Likewise, in diagram II,  $\overline{c'm}$  is drawn parallel to  $\overline{cb}$ , intersecting  $\overline{b''c''}$  in  $m$ , giving  $\overline{c'm}$ , the projection of  $\overline{c'c''}$  parallel to  $\overline{cb}$ .

Diagram I may now be completed by transferring  $\overline{c'm}$  from diagram II and erecting a perpendicular to  $\overline{c'm}$  at  $m$ . This perpendicular will intersect  $\overline{na''c''}$  in  $c''$ , and the figure  $\overline{a''c''}$  can now be drawn by similarity with the frame I, since the members in the two figures are respectively perpendicular.

In like manner diagram II may be completed by transferring  $\overline{c'n}$  from diagram I and drawing  $\overline{nc''}$  perpendicular to  $\overline{c'n}$ , thus determining  $c''$ . As a check, the displacements  $\overline{c'c''}$  must be equal and parallel in the two diagrams.

(4) **A cantilever bridge**, similar in principle to the Memphis bridge, is represented in Fig. 34d.

It is assumed, as in the two preceding problems, that separate displacement diagrams have been made for each of the elastic frames, I, II, III, and IV, and of these, the diagrams for I and III can be completely solved, as was done with the example in Fig. 34A, since each is a determinate framed structure on two supports.

It is here deemed necessary only to complete the rotation diagrams of the frames II and IV. The displacements of these frames depend on those of the points  $c$  and  $m$  and upon that of the point  $s$ , respectively.

Let it be assumed that the points  $d'$  and  $n'$  have been determined for the elastic frame II as in diagram II, and let it be required to find the figure  $\overline{d''n''}$  which shall be similar to frame II.

The members  $\overline{cd}$  and  $\overline{mn}$  are elongated by  $\Delta 1$  and  $\Delta 2$  respectively, and their elongations must be applied to the points  $d'$  and  $n'$  in diagram II, giving the points  $c'$  and  $m'$ . Now if the displacements  $\overline{c'c''}$  and  $\overline{m'm''}$  be drawn as found by diagrams I and III (not shown), the points  $c''$  and  $m''$  are obtained. These represent the original positions of the points  $c$  and  $m$ . The point  $n''$  must have originally occupied the same relative level with  $m''$ , also  $d''$  must have been at the same relative level with  $c''$ . Lastly, the line  $\overline{d''n''}$  must be perpendicular to  $\overline{dn}$ . Hence, if the distance  $x$ , or the horizontal distance between  $d'$  and  $d''$ , can be found, then the figure  $\overline{d''n''}$  becomes determinable and the diagram can be completed. If it is granted that the point  $w$  will always be midway between the points  $c$  and  $m$ , this problem becomes definite, and the value  $x$





## CHAPTER VII

### DEFLECTION POLYGONS OF STATICALLY DETERMINATE STRUCTURES BY ANALYTICS AND GRAPHICS

#### ART. 35. INTRODUCTORY

The deflection polygon for any series of panel points, either of the top or bottom chord, may be found from a Williot-Mohr diagram as shown in the previous chapter.

However, when the deflections, so obtained, are intended to form the basis for stress computations, then greater accuracy is actually required than that obtainable from the above method of solution. This is especially true of large structures, because the error committed by substituting the tangent of an arc for the arc itself is of a cumulative nature, always giving excessive values. This fact has been overlooked by most authors treating of indeterminate structures.

Professor Mohr, in 1875, established a very important relation between deflection polygons and equilibrium polygons drawn for simultaneous cases of loading. Accordingly a deflection polygon may be derived from a moment diagram by dividing the ordinates of the latter by a certain constant which depends on the geometric shape of the structure.

The elastic deformation in the angle included between two successive chord members can always be expressed in terms of the coexisting changes in the lengths of the truss members or in terms of the stresses in these members for any simultaneous case of loading. Such an angular change may be regarded as an *elastic load*  $w$ , which designation will always be used in the following chapters.

The several elastic loads  $w$  for all pin points of an entire chord will then suffice to determine the deflection polygon for that chord precisely as the external loads  $P$  will determine an equilibrium polygon from which moments and stresses in the chords may be found.

Naturally such a deflection polygon will furnish displacements in one fixed direction only, and this is usually all that is required. However, two such polygons, for horizontal and vertical deflections, respectively, would, if drawn for the same pin points and same loading, determine actual displacements.

Since the total deflection of a truss is almost entirely due to the deformation in the chords, it is often admissible to neglect the web system. For arches with parallel chords this is always true.

The deflection polygon is usually drawn for the loaded chord only. If the loaded chord is straight, as is often the case, then the computations are greatly simplified.

In the following, two methods will be given for finding such deflection polygons. In the first method the elastic loads  $w$  are derived from the changes  $\Delta l$  of all members

of the structure, according to Professor Mohr. The second method is a modification of the first, given by Professor Land, in 1887, and expresses the  $w$  loads in terms of the unit stresses of the several truss members.

### ART. 36. FIRST METHOD, ACCORDING TO PROFESSOR MOHR

(a) **Influence on the deflections due to chord members.** For any particular case of loading, the stresses and changes in the lengths of the several members are supposed to be known. Neglecting the web members for the present, by regarding their changes  $\Delta l$  all zero, the influence of a single chord member is first considered. See Fig. 36A.

The deflection  $y_m$  of any lower chord point  $m$ , due to a shortening in the upper chord member opposite the point  $m$ , may be found from Mohr's work equation. Let a unit force act downward from  $m$  (if vertical deflections are desired). Then from Eq. (6A),  $1 \cdot y_m = S_{ma} \Delta l_m$ , when there are no abutment displacements.

Let  $M_{ma}$  represent the static moment about the point  $m$  when only the unit load at  $m$  is acting. This is easily found from either one of the reactions, resulting from the unit load, multiplied by the distance from  $m$  to that reaction. Then the stress  $S_{ma} = M_{ma}/r_m$  as may be seen from Fig. 36A.

Now if  $1 \cdot y_m$  be regarded as a moment  $M_{mw}$  due to a load  $w$  hung at the point  $m$ , then by proportion

$$\frac{w_m}{1} = \frac{M_{mw}}{M_{ma}} \quad \text{or} \quad w_m = \frac{1 \cdot y_m}{M_{ma}} = \frac{S_{ma} \Delta l_m}{S_{ma} r_m} = \frac{\Delta l_m}{r_m} \quad \dots \quad (36A)$$

The load  $w$ , thus expressed, will be known as an *elastic load*.

Hence, a moment diagram drawn for the elastic load  $w_m$  acting at  $m$ , will give the ordinate  $M_{mw} = y_m$  under the point  $m$ . Laying off  $w_m$  on the load line to the right and with a pole distance  $H=1$ , to scale of forces, drawing the moment diagram  $A'm'B'$ , then the ordinate  $y_m$  represents the deflection of the point  $m$  due to a change  $\Delta l_m$  in the length of the member  $\overline{fg}$  opposite the point  $m$ , because

$$M_{mw} = 1 \cdot y_m = S_{ma} \Delta l_m.$$

Now the polygon  $A'm'B'$  is also the *influence line of deflections for the point  $m$*  for any moving load  $w_m$ . Hence, the deflection  $y_{nm}$ , at the point  $n$ , is that due to a load  $w_m$  at the point  $m$ , and so on for any pin point of the chords.

In like manner the deflection  $y_n$  is obtained for a load  $w_n = \Delta l_n/r_n$  and the polygon  $A'n'B'$  is then the influence line of deflections for the point  $n$  for a moving load  $w_n$ . The ordinate  $y_{mn}$ , under the point  $m$ , is now the deflection at  $m$  for a load  $w_n$  at  $n$ . But, by Maxwell's law  $y_{mn} = y_{nm}$ .

By drawing these influence lines successively for all the pin points of the top and bottom chords, the several partial effects of all the elastic loads  $w$  on any particular point as  $m$  may be found, and the summation of these effects  $\Sigma y_{mn}$  will be the total deflection  $\delta_m$  for the point  $m$  resulting from the given case of actual loading.

The summation, however, is more easily performed by combining the several loads  $w$  into a load line  $\Sigma w$  and with a pole  $H=1$ , drawing the force and equilibrium polygons.

The latter is a moment polygon and also a summation deflection polygon, any ordinate  $\delta_m$  of which represents the actual deflection of the corresponding pin point  $m$  for that particular case of loading and is measured to the scale of lengths. This does not include the effect of the web members.

If the external loads are applied to the lower chord pin points then the true deflection polygon for the lower chord is the inscribed dotted polygon  $A'c''m''n''B'$ , because the deflection polygon between the successive floor beams must be a straight line.

When the loads  $w$  are multiplied by  $E$  and the scale of lengths is chosen  $1:a$ , then by making the pole distance  $H=E$  to the scale of forces, the deflections will have the scale  $1:a$ . When the deflections are desired  $m$  times actual to the scale  $1:a$ , then the pole should be chosen  $E/m$  to the scale of forces.

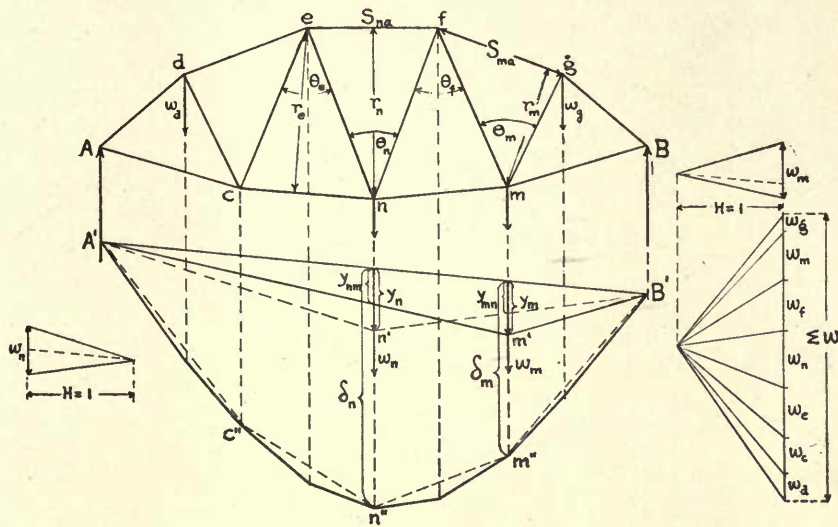


FIG. 36A.

As is seen from the above, the elastic loads  $w$  are ratios; that is, they have no dimension but depend on the unit stresses in the members and the geometric shape of the structure. From this and the real value  $w = \Delta l / r$ , it follows that these elastic loads may also be defined as tangents of the angular changes in the angles  $\theta$ , or simply  $w_m = \Delta \theta_m$  from Fig. 36A.

For a top chord point, the angular change  $\Delta \theta$  is positive, while for a lower chord point it is negative, but in either case the angular change produces downward deflection.

For a top chord point

$$+\Delta l = \frac{Sl}{EF} = S\rho \quad \text{and} \quad S = \frac{M}{r}, \quad \text{hence} \quad w = +\frac{\Delta l}{r} = +\frac{M\rho}{r^2},$$

and for a bottom chord point

$$-\Delta l = S\rho \quad \text{and} \quad S = -\frac{M}{r}, \quad \text{hence again} \quad w = +\frac{M\rho}{r^2}.$$





This elastic load produces reactions  $A_a$  and  $B_a$  and, as previously shown, the moment  $M_{wo}$  (for all the forces on one side of the section and for the center of moments  $o$ ) is found to be  $M_{wo} = S_a \Delta l = 1 \cdot y_c$ .

Hence the influence line for the moment  $M_{wo}$ , for a moving load  $w = \Delta l/r$ , may be found. By laying off  $y_c = \overline{c'c''}$  as an ordinate from  $\overline{a'b'}$  under the point  $c$  to any convenient scale, and drawing a line  $\overline{a'c''}$  to intersect the vertical through  $o$  in the point  $o'$ , the two limiting lines of the influence area are determined. Thus,  $\overline{a'u'o'}$  represents the influence of  $B_a$  and  $\overline{o'b'a''}$  the influence of  $A_a$ . Between the panel points  $n$  and  $u$  the influence line is a straight line  $\overline{n'u'}$ .

Also, for any other position of this elastic load the same influence line will be found. Hence the most suitable point of application for this elastic load will be the load divide  $i'$  for the panel whose section is under consideration. This would make any line through the load divide  $i'$  an influence line for the elastic load  $w$ . Such a line would intersect the verticals through the two adjacent panel points in points  $n'$  and  $u'$  and the two limiting lines  $\overline{n'b'}$  and  $\overline{a'u'}$  must be made to intersect in the point  $o'$  which is any convenient point in the vertical through  $o$ . These two limiting lines cut off the closing line  $\overline{a'b'}$  on the verticals through  $A$  and  $B$ . Then any load  $w = \Delta l/r$ , applied at the load divide  $i$ , will produce a zero deflection in the corresponding point  $c$  and a zero moment  $M_{wo}$  about the point  $o$ .

Now the elastic load  $w$  may be replaced by two such loads  $w_n$  and  $w_u$ , acting at the points  $n$  and  $u$ , respectively. These may be determined graphically by drawing the force polygon Fig. 36B, corresponding to the moment diagram  $\overline{a'u'n'b'}$ .

The analytic method for finding  $w_n$  and  $w_u$  is as follows: The position of  $w$  is evidently immaterial, because the resulting loads  $w_n$  and  $w_u$  will be the same for any position of  $w$ . If the load divide is chosen as the point of application, then the moment  $M_{wo} = 0$  and the sum of the moments produced by the loads  $w_n$  and  $w_u$  must likewise be zero. Hence, the resultant of the two components must pass through the center of moments  $o$ .

Also, by drawing a line  $\overline{nh} \parallel \overline{um}$ , Fig. 36B, and remembering that the resultant of  $w_n$  and  $w_u$  must equal  $w$ , then by taking moments about  $n$

$$w_u \times \overline{un} = \frac{\Delta l}{r} \cdot \overline{no} \quad \text{or} \quad w_u = \frac{\Delta l}{r} \cdot \frac{\overline{no}}{\overline{un}} = \frac{\Delta l}{r_u} \quad \text{because} \quad \frac{\overline{no}}{\overline{un}} = \frac{r}{r_u}.$$

Similarly by taking moments about  $u$ , and noting that  $\frac{\overline{mo}}{\overline{mh}} = \frac{r}{r_n}$ , then

$$w_n \times \overline{un} = \frac{\Delta l}{r} \cdot \overline{uo} \quad \text{or} \quad w_n = \frac{\Delta l}{r} \cdot \frac{\overline{uc}}{\overline{un}} = \frac{\Delta l}{r} \cdot \frac{\overline{mo}}{\overline{mh}} = \frac{\Delta l}{r_n}.$$

The two new elastic loads, which were substituted for  $w$ , may now be evaluated from the following equations, without involving the lever arm  $r$ , thus:

$$w_u = \frac{\Delta l}{r_u} \quad \text{and} \quad w_n = \frac{\Delta l}{r_n} \quad \dots \dots \dots (36c)$$

In most cases this simple relation proves of valuable assistance, because  $r$  is frequently outside the limits of the drawing.

Regarding the signs of the two elastic loads  $w_u$  and  $w_n$  it is discerned from the above that the signs must always be opposite and it is necessary to distinguish which of the two is the positive load and then call the other one negative. The sign of  $\Delta l$  alone determines this without regard to the sign of the work  $S_a \Delta l$  and Professor Mohr gives the following simple rule, which will always identify the positive elastic load  $w$ .

*Calling all top chord members negative and all bottom chord members positive and giving the proper sign to  $\Delta l$  for the web member in question, then the positive  $w$  is found on that side of the section or panel where the sign of  $\Delta l$  coincides with that of the adjacent chord.*

The same result is obtained from the force polygon, Fig. 36B, drawn for the three loads  $w$ . This is also seen when the distortion in the quadrilateral  $mgun$ , due to the change  $\Delta l$  in the member  $\overline{mn}$ , is considered. Assuming the top chord  $mg$  immovable, then  $-\Delta l$  in  $\overline{mn}$  will cause the point  $u$  to drop, hence  $w_u$  is positive when the bottom chord is the loaded chord. Were the top chord the loaded chord, then  $\overline{un}$  would be considered immovable in applying this reasoning.

**When the center of moments  $o$  falls inside the span** there is no load divide, whence the deflection influence line for a web member can have only a positive area. The maximum stress is then due to the total span loaded, the same as for maximum moments.

However, this in no wise affects the previous discussion, but some proof of the identity of the effects of the substitute loads  $w_u$  and  $w_n$  with that of  $w$  must be furnished for this case.

Thus the elastic load  $w = \Delta l / r$ , acting at  $c$ , is in equilibrium with the reactions  $A$  and  $B$  resulting from  $w$ , and it is also the resultant of the two substitute loads  $w_u$  and  $w_n$ . Hence the sum of the moments of the forces,  $A$ ,  $B$ ,  $w_u$  and  $w_n$  about any point  $o$  in the plane of forces, must be zero. But the resultant  $w$  of  $w_u$  and  $w_n$ , always passes through the center of moments  $o$ , hence this resultant must be equal and opposite to the resultant of  $A$  and  $B$ . The method is thus general and applies equally to cases of  $o$  inside and outside the span.

The elastic loads  $w_u$  and  $w_n$  may also be expressed in terms of the moments of the external forces, as was previously done for the chords, and the following general expressions are thus obtained:

$$w_u = \frac{\Delta l}{r_u} = \pm \frac{M\rho}{r_u r} \quad \text{and} \quad w_n = \frac{\Delta l}{r_n} = \mp \frac{M\rho}{r_n r}; \quad \dots \dots \dots (36D)$$

also

$$w = \frac{\Delta l}{r} = \pm \frac{\Delta l}{r_u} \mp \frac{\Delta l}{r_n} = \frac{M\rho}{r^2}, \quad \text{hence} \quad \frac{1}{r} = \pm \frac{1}{r_u} \mp \frac{1}{r_n} \dots \dots \dots (36E)$$

This condition is easily seen directly from Fig. 36B.

**(c) The deflection polygon for the loaded chord.** This deflection polygon may be found by applying the formulæ (36B) and (36D) to any given frame. The elastic loads  $w$  are now computed for each chord and each web member and all those acting at the same pin point are algebraically added for total effects.

The deflection polygon is then found by combining the loads  $w$  into a force polygon and drawing the moment or equilibrium polygon exactly as shown in Fig. 36A, following



the description relating thereto. These moments may also be computed to obtain the deflections analytically.

Before concluding this subject a few special cases will be illustrated.

(1) **When there is no end post**, as in Fig. 36B, then Ritter's section cuts only two members  $\overline{ad}$  and  $\overline{ac}$  and some doubt may exist regarding the application of the formula for  $w$ .

To overcome this difficulty, add a member  $\overline{ak} \parallel \overline{cd}$  and of any convenient length. Then the center of moments  $o_1$  will be the center for the member  $\overline{ad}$  treated as a web member. The two imaginary members  $\overline{ak}$  and  $\overline{kd}$  are assumed rigid and Eqs. (36D) again apply. The load  $w$  thus found for the point  $a$  will have no effect, and the result is the same as would be found by applying Eq. (36B) to the center of moments at  $c$  with the lever  $r'_1$ .

(2) **When there is a vertical end post** and the deflection polygon for the lower chord is required, then a load applied at  $a$ , Fig. 36C, will not produce stress in the verticals nor end post. The end chord section, and these members, therefore, do not influence the deflection polygon of the lower chord.

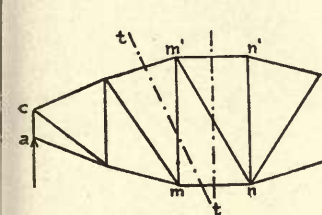


FIG. 36C.

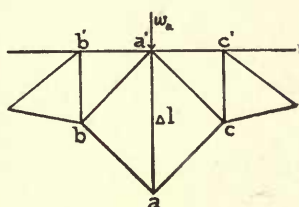


FIG. 36D.

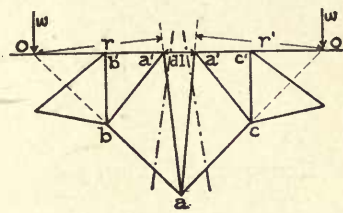


FIG. 36E.

If the load is applied at the upper point  $c$ , then it is best to construct the deflection polygon by regarding the  $\Delta l = 0$  for the two end posts. Now since the whole top chord is lowered by amounts  $-\Delta l$  and  $-\Delta l_1$  of these vertical end posts, it is merely necessary to raise the closing line of the deflection polygon by these amounts at the two respective ends. The deflection ordinates are thus corrected by the addition of the end post effects.

(3) **Frames with vertical posts**, as in Figs. 36C and 36D.

When the center of moments cannot be ascertained by a section through three members, as for the member  $\overline{aa'}$ , Fig. 36D, the elastic load for the point  $a'$  cannot be directly found.

To overcome this difficulty assume the disposition in Fig. 36E, where the small chord  $dl$  is interposed at  $a'$  and the vertical  $\overline{aa'}$  is split into two posts such that the deflection remains the same as for the original case. Then the original solution is again applicable by passing two sections as indicated and cutting three members by each section.

The vertical post is now made up of two substitute posts for which the work must be equal to that of the original post, thus:

$$S\Delta l = 2 \frac{S}{2} \left( \frac{\frac{Sl}{2}}{\frac{EF}{2}} \right).$$

Also for each substitute there will be a load  $w$  active at the center of moments  $o$  and the resultant of these two loads will be  $w_a$ , Fig. 36d.

Hence,

$$w_a = \frac{Al}{r} + \frac{Al}{r'}.$$

In the ordinary case, Fig. 36c, the deflection polygons for top and bottom chords are alike when the web system is neglected. When the latter is included it is best to construct the deflection polygon of the chord which ends in the supports (the lower chord in this instance) and the deflection of the other chord is then found by simply correcting the first polygon by the  $\pm Al$  of the verticals, being careful to regard the sign.

(4) **Trusses with parallel chords** become very much simplified because the height of the truss and the inclination of the web members are then uniform, Fig. 36f.

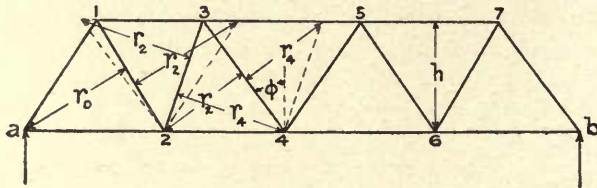


FIG. 36f.

Hence for all chord members, Eq. (36b) gives

$$w = \frac{Al}{h} \dots \dots \dots (36f)$$

For the web members, the center of moments is at infinity, making the elastic loads equal and opposite for the same section. Each pair thus constitutes a moment which is balanced by an infinitesimally small force acting at an infinite distance. For this and other reasons it is better to determine the elastic loads for the web members directly from the shear. Calling the shear  $Q$ , Eq. (36d) then gives

$$\left. \begin{aligned} \pm w_u &= \frac{Al}{r_u} = \frac{Sl}{EFr_u} = \frac{Ql}{EFr_u \cos \phi} \\ \mp w_n &= \frac{Al}{r_n} = \frac{Sl}{EFr_n} = \frac{Ql}{EFr_n \cos \phi} \end{aligned} \right\} \dots \dots \dots (36g)$$

Here  $r_u = r_n$  for each panel and  $\phi$  is the angle of the diagonal with the vertical. The figure shows the case where the  $w$  loads are desired for the bottom chord panel points.

When  $\phi$  is constant for all web members then the factor  $l/Er$  becomes constant and may be applied to the scale of the elastic loads  $w$ , which are then  $l/Er$  times natural size. Thus by making the pole distance  $Er/l$  times larger, the resulting deflection polygon for web members will be unchanged.

(5) **Composite structures**, like three-hinged arches and cantilever systems, may likewise be treated by the above method.

For any position of the moving elastic load  $w$  and any panel, the same work equation applies and also Eq. (36B).

Hence, with due regard to signs, the influence area of a deflection  $y$  is again the influence area for the moment  $M_{w0}$  and also the influence area of the particular member under consideration. It is only necessary to observe the signs of the loads  $w$  and the corresponding position of the closing line of the deflection polygon.

The  $w$  loads which result from the chord members will have the same sign as the moment influence line for that panel. When the moment changes sign in any particular panel, as might be the case in cantilever systems, then the  $w$  loads of the adjacent pin points must be of opposite signs.

The  $w$  load resulting from the diagonals will always be of opposite signs according to the rule above given, no matter whether the center of moments for such diagonals falls inside or outside the span.

(6) **For indeterminate systems** the foregoing method is made applicable by removing the redundant members or reaction conditions and replacing these by external forces  $X$  acting on the principal system in the manner described in Art. 7.

The deflection of an indeterminate system under certain loads  $P$  is the same as the deflection of the statically determinate frame subjected to the loads  $P$  and  $X$  and the work Eq. (6A) is in like manner applicable to this principal system, so loaded.

An example showing the application of the above method may be found in Table 50B.

ART. 37. SECOND METHOD, ACCORDING TO PROFESSOR LAND

(a) **The  $w$  loads in terms of the unit stresses in the members.**

This method is sometimes preferable to the former when the deflection polygon of any succession of members is desired without regard to the remaining members of the structure. The first method is, however, preferable when a more general solution is required.

Here, any succession of members or rods is treated purely as a "kinematic chain" involving only the angular changes occurring in the angles included between successive members and the changes  $\Delta l$  in the lengths of these members.

The problem resolves itself into two parts: (a) to find the changes in the angles of any triangle resulting from changes  $\Delta l$  in the lengths of the sides, and (b) to evaluate the loads  $w$  in terms of these changes and finally to construct the deflection polygon.

(b) **To find the changes in the angles of a triangle.**

Let  $\alpha, \beta$  and  $\gamma$  be the three angles of a triangle  $\overline{ABC}$  and  $f_a, f_b$  and  $f_c$  the unit stresses respectively in the three members opposite these angles, as given in Fig. 37A. Also let

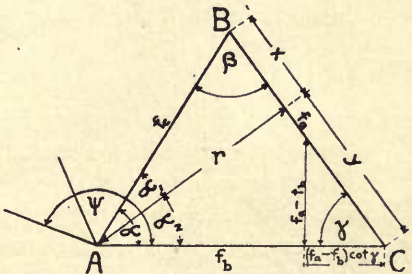


FIG. 37A.



$\Delta\alpha$ ,  $\Delta\beta$  and  $\Delta\gamma$  be the changes in the three angles resulting from the changes  $\Delta l_a$ ,  $\Delta l_b$  and  $\Delta l_c$  in the lengths of the three sides.

Then from the figure,  $\sin \alpha_1 = x/l_c$  and  $\sin \alpha_2 = y/l_b$ , and by differentiation and treating all quantities as variables,

$$\cos \alpha_1 \Delta \alpha_1 = \frac{l_c \Delta x - x \Delta l_c}{l_c^2} \quad \text{and} \quad \cos \alpha_2 \Delta \alpha_2 = \frac{l_b \Delta y - y \Delta l_b}{l_b^2}.$$

Adding these expressions and solving for  $\Delta \alpha_1 + \Delta \alpha_2 = \Delta \alpha$  gives

$$\Delta \alpha = \Delta \alpha_1 + \Delta \alpha_2 = \frac{\Delta x - x \frac{\Delta l_c}{l_c}}{l_c \cos \alpha_1} + \frac{\Delta y - y \frac{\Delta l_b}{l_b}}{l_b \cos \alpha_2}. \quad \dots \dots \dots (37A)$$

But  $l_c \cos \alpha_1 = l_b \cos \alpha_2 = r$ , hence Eq. (37A) becomes

$$\Delta \alpha = \frac{x}{r} \left( \frac{\Delta x}{x} - \frac{\Delta l_c}{l_c} \right) + \frac{y}{r} \left( \frac{\Delta y}{y} - \frac{\Delta l_b}{l_b} \right). \quad \dots \dots \dots (37B)$$

Now from Fig. 37A,

$$\frac{\Delta x}{x} = \frac{\Delta y}{y} = \frac{f_a}{E}, \quad \frac{\Delta l_c}{l_c} = \frac{f_c}{E}, \quad \frac{\Delta l_b}{l_b} = \frac{f_b}{E}, \quad \frac{x}{r} = \cot \beta; \quad \text{and} \quad \frac{y}{r} = \cot \gamma,$$

which values substituted into Eq. (37B) give

$$E \Delta \alpha = (f_a - f_b) \cot \gamma + (f_a - f_c) \cot \beta. \quad \dots \dots \dots (37C)$$

The values  $E \Delta \beta$  and  $E \Delta \gamma$  can be derived in the same way to obtain the following:

$$\left. \begin{aligned} E \Delta \alpha &= (f_a - f_b) \cot \gamma - (f_c - f_a) \cot \beta \\ E \Delta \beta &= (f_b - f_c) \cot \alpha - (f_a - f_b) \cot \gamma \\ E \Delta \gamma &= (f_c - f_a) \cot \beta - (f_b - f_c) \cot \alpha \end{aligned} \right\} \dots \dots \dots (37D)$$

wherein tensile stresses  $f$  are positive and compressive stresses are negative.

Since the sum of the three angles of a triangle is always constant, therefore,

$$E \Delta \alpha + E \Delta \beta + E \Delta \gamma = 0 \quad \dots \dots \dots (37E)$$

whence the third value is easily found after having computed any two from Eqs. (37D).

The above formulæ are extensively used in Art. 61 dealing with secondary stresses.

When temperature changes are to be included then the unit stresses  $f$  must be corrected by  $\epsilon t E$ . A positive  $t$  produces elongation in all members, hence  $\epsilon t E$  must then be positively applied to all values  $f$ . The contrary is true for  $-t$ .

The change in any peripheral angle  $\phi$  of a frame is easily found by summing the changes  $\Delta \alpha$  occurring in the several angles  $\alpha$  whose apices meet in that angle  $\phi$ . Then  $\phi = \Sigma \alpha$  and  $\Delta \phi = \Sigma \Delta \alpha$ , making

$$\pm E \Delta \phi = E \Sigma \Delta \alpha \quad \dots \dots \dots (37F)$$

using the minus sign when  $\phi=360^{\circ}-\Sigma\alpha$  which is the case when the vertices of the angles  $\alpha$  are on the opposite side of the kinematic chain from the peripheral angle  $\phi$ . The values  $E\Delta\alpha$  are obtained from Eqs. (37D).

The products of the form  $(f_a-f_b)\cot\gamma$  in Eq. (37D) may be graphically found from a large scale truss diagram as indicated in Fig. 37A. The quantity  $(f_a-f_b)$  is laid off perpendicular to either  $\overline{AC}$  or  $\overline{BC}$  so as to include the angle  $\gamma$ . The base, to scale of forces  $f$ , will then be the desired quantity. The sign is easily found by inspection of the given data and depends on the sign of  $(f_a-f_b)$  and the sign of the  $\cot\gamma$ .

(c) To evaluate the elastic loads  $w$  in terms of the angle changes  $\Delta\psi$  and the changes  $\Delta l$  in the lengths of the members, and finally to construct the deflection polygon for the kinematic chain.

In Fig. 37B such a chain of chord members is shown and the  $\Delta\psi$  and  $\Delta l$  are now supposed to be given. The system is referred to coordinate axes  $(x, y)$ .

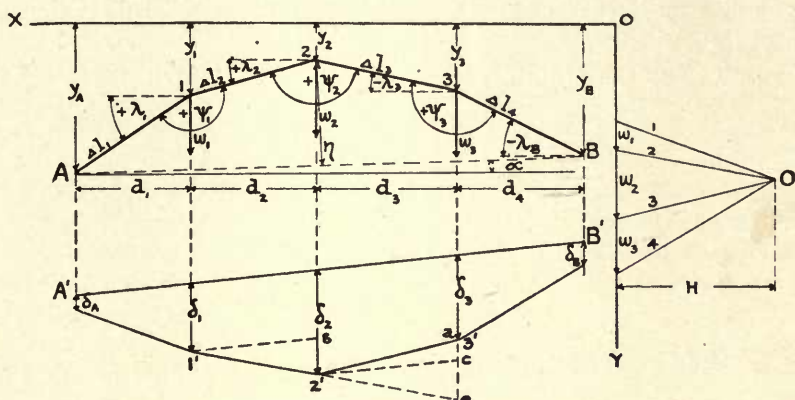


FIG. 37B.

Now let  $\lambda$ =the angle which any member makes with a line parallel to the  $x$  axis and through the right-hand end of the member. See Fig. 37B regarding the sign of  $\lambda$  for different members.

$\delta_A, \delta_1, \delta_2$  are the displacements of the points  $A, 1, 2$ , etc., respectively, measured from the closing line  $\overline{A'B'}$  and parallel to the given  $y$  axis.

$w_1, w_2, w_3$  are the elastic loads, the moment polygon for which represents the deflection polygon  $\overline{A'1'2'3'}$  with closing line  $\overline{A'B'}$ . These loads are now to be found and then the polygon is easily constructed as for the first method above given. The loads  $w$ , parallel to the  $y$  axis, are applied, as before, in the direction in which the deflections are to be measured.

In the figure  $\overline{1's} \parallel \overline{A'B'} \parallel \overline{2'c}$ , hence it follows that  $\overline{ce}=(\delta_2-\delta_1)\frac{d_3}{d_2}$  and  $ac=\delta_2-\delta_3$  and by addition of these equations,  $\overline{ae}$  is obtained as

$$\overline{ae}=(\delta_2-\delta_1)\frac{d_3}{d_2}+(\delta_2-\delta_3)\dots\dots\dots (37G)$$

But since the sides of the deflection polygon are respectively parallel to the rays of the force polygon, then  $\frac{ae}{d_3} = \frac{w_2}{H}$ . This value of  $ae$  inserted in Eq. (37g) gives

$$w_2 = H \left( \frac{\delta_2 - \delta_1}{d_2} - \frac{\delta_3 - \delta_2}{d_3} \right) \quad \dots \quad (37h)$$

Also from Fig. 37B,

$$y_1 - y_2 = l_2 \sin \lambda_2 \quad \dots \quad (37j)$$

The differential of Eq. (37j) gives

$$\Delta y_1 - \Delta y_2 = \Delta l_2 \sin \lambda_2 + l_2 \cos \lambda_2 \Delta \lambda_2 = \delta_1 - \delta_2 \quad \dots \quad (37k)$$

which must equal  $\delta_1 - \delta_2$  because both expressions represent the deflection of the point 2 with respect to the point 1.

Also from the figure  $d_2 = l_2 \cos \lambda_2$  which divided into Eq. (37k) gives

$$-\frac{\delta_2 - \delta_1}{d_2} = \frac{\Delta l_2}{l_2} \tan \lambda_2 + \Delta \lambda_2,$$

and in like manner is found for  $+\lambda_3$

$$-\frac{\delta_3 - \delta_2}{d_3} = \frac{\Delta l_3}{l_3} \tan \lambda_3 + \Delta \lambda_3.$$

Making  $H=1$  and substituting these values into Eqs. (37h) then

$$w_2 = -\Delta \lambda_2 + \Delta \lambda_3 - \frac{\Delta l_2}{l_2} \tan \lambda_2 + \frac{\Delta l_3}{l_3} \tan \lambda_3 \quad \dots \quad (37l)$$

But  $180^\circ - \lambda_2 + \lambda_3 = \phi_2$  then  $-\Delta \lambda_2 + \Delta \lambda_3 = \Delta \phi_2$ .

Also  $\frac{\Delta l_2}{l_2} = \frac{f_2}{E}$  and  $\frac{\Delta l_3}{l_3} = \frac{f_3}{E}$ , whence Eq. (37l) becomes

$$Ew_2 = \pm E \Delta \phi_2 - f_2 \tan \lambda_2 + f_3 \tan \lambda_3 \quad \dots \quad (37m)$$

The general expression for any pin point  $n$  is then

$$Ew_n = \pm E \Delta \phi_n - f_n \tan \lambda_n + f_{n+1} \tan \lambda_{n+1} \quad \dots \quad (37n)$$

in which  $E \Delta \phi_n$  is given by Eq. (37f) for top chords, using the  $-$  sign for bottom chords.

For any negative angle  $\lambda$  (see Fig. 37B)  $\tan \lambda$  also becomes negative. Similarly the signs of the unit stresses  $f$  must be considered in substituting values in Eqs. (37f) and (37n). The equations as they stand are written for positive values in all cases.

*If the elastic loads  $w$  are multiplied by  $E$  and the force polygon be constructed to any*



convenient scale of forces with a pole  $H=E$  to scale of forces, when the scale of the truss diagram is  $1:a$ , then the deflections will be actual to the scale  $1:a$ . But if the deflections should appear  $m$  times actual when measured with the scale  $1:a$ , then the pole distance must be made  $E/m$  to the scale of forces.

Finally the closing line  $\overline{A'B'}$  is found from the reaction displacements. If these are zero, then  $\delta_A$  and  $\delta_B$  are zero and the closing line must join the ends of the equilibrium polygon. Otherwise  $\delta_A$  and  $\delta_B$  must be ascertained from the conditions of the supports.

When the web system does not include vertical members then it is preferable to choose these web members for the kinematic chain rather than a chain of chords, because the deflection polygon will then furnish the deflections of all the pin points instead of only those belonging to one chord.

When the deflections in one direction only are required, then the above polygon affords a complete solution, but for a general determination of displacements in the plane of the truss, a second deflection polygon would be required, giving deflections perpendicular to the direction chosen for the first polygon. In the above illustration this would be parallel to the  $x$  axis and the resultant displacement of any point would be the resultant of the horizontal and vertical displacements of that point.

The displacements in the  $x$  direction could be computed from the same Eq. (37N) by substituting  $-\cot \lambda$  for  $+\tan \lambda$  in each case, but a better solution is given below.

The method fails when any angle  $\lambda=90^\circ$ , hence no member of the kinematic chain should be parallel to the direction of the deflections. If this occurs then a pair of substitute members must be employed as was done in Fig. 36B. For this reason also, the  $w$  loads from Eq. (37N) cannot usually be employed for finding horizontal displacements as per Art. 38.

For a straight chord, the Eqs. (37F) and (37N) give the following simple formula for  $w_n$

$$Ew_n = E\Delta\psi_n = E\Sigma\Delta\alpha \quad . \quad . \quad . \quad . \quad . \quad . \quad . \quad . \quad (37o)$$

**Example.** The above method will now be illustrated by the following example of a two-hinged framed arch as shown in Fig. 37c. The same problem is also solved in Art. 50, using the method given in Art. 36.

The unit stresses and angle functions appear in the truss diagram of Fig. 37c and the nomenclature used in Eqs. (37D) as indicated on a small triangle, is successively applied to all the triangles of the frame.

The deflection polygons are drawn first for the bottom chord and then for the top chord, both for the conventional loading  $X_a=1$ , and the computations of the  $Ew$  loads are given in detail for the bottom chord only, because these represent the general case necessitating the use of Eqs. (37D), Eq. (37F) and Eq. (37N). For the top chord, the computations do not require the use of Eq. (37N) and the resulting values of the loads  $Ew$  only are given without the details of the figuring.

In the present problem, the method would not apply to the kinematic chain  $U_0L_1U_1L_2U_2$ , etc., because the verticals are parallel to the direction of the vertical deflections. Hence, the chords are treated separately, thus avoiding all vertical members in the chains.

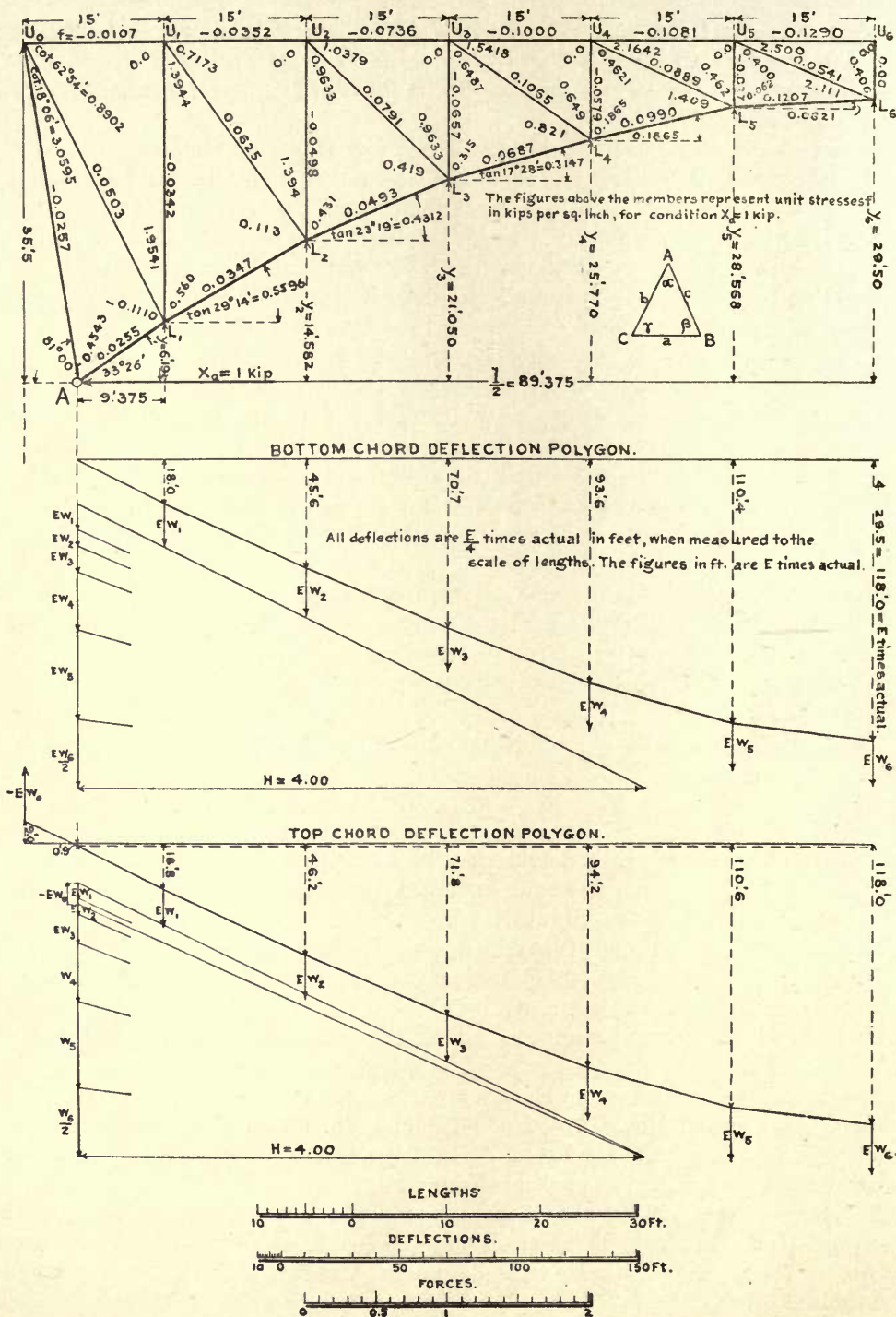


FIG. 37c.

The elastic load  $Ew_0$  for the bottom chord has no effect on the deflection of this chord and is, therefore, neglected.

Computation of the elastic loads  $Ew$  for the bottom chord panel points.

**For panel point  $L_1$ :**

$$\begin{aligned} \text{By Eqs. (37D), } E\Delta\alpha_1 &= (-0.0257 - 0.0503)3.059 - (0.0255 + 0.0257)0.454 = -0.2557 \\ E\Delta\alpha_2 &= 0.0 - (0.0503 + 0.0107)0.890 = -0.0543 \\ E\Delta\alpha_3 &= (0.0625 - 0.0347)0.1125 - (-0.0342 - 0.0625)1.394 = +0.1379 \end{aligned}$$

$$\text{By Eq. (37F), } -E\Delta\psi_1 = E\Sigma\Delta\alpha = -0.1721$$

$$\text{By Eq. (37N), } Ew_1 = 0.1721 - 0.0255 \times 0.660 + 0.0347 \times 0.5596 = +0.175$$

**For panel point  $L_2$ :**

$$\begin{aligned} \text{By Eqs. (37D), } E\Delta\alpha_1 &= (-0.0342 - 0.0625)1.394 - (0.0347 + 0.0342)0.5596 = -0.1733 \\ E\Delta\alpha_2 &= 0.0 - (0.0625 + 0.0352)0.7173 = -0.0701 \\ E\Delta\alpha_3 &= (0.0791 - 0.0493)0.4192 - (-0.0498 - 0.0791)0.963 = +0.1366 \end{aligned}$$

$$\text{By Eq. (37F), } -E\Delta\psi_2 = E\Sigma\Delta\alpha = -0.1068$$

$$\text{By Eq. (37N), } Ew_2 = 0.1068 - 0.0347 \times 0.5596 + 0.0493 \times 0.4312 = +0.109$$

**For panel point  $L_3$ :**

$$\begin{aligned} \text{By Eqs. (37D), } E\Delta\alpha_1 &= (-0.0498 - 0.0791)0.963 - (0.0493 + 0.0498)0.431 = -0.1668 \\ E\Delta\alpha_2 &= 0.0 - (0.0791 + 0.0736)1.038 = -0.1585 \\ E\Delta\alpha_3 &= (0.1065 - 0.0687)0.821 - (-0.0657 - 0.1065)0.649 = +0.1428 \end{aligned}$$

$$\text{By Eq. (37F), } -E\Delta\psi_3 = E\Sigma\Delta\alpha = -0.1825$$

$$\text{By Eq. (37N), } Ew_3 = 0.1825 - 0.0493 \times 0.4312 + 0.0687 \times 0.3147 = +0.183$$

**For panel point  $L_4$ :**

$$\begin{aligned} \text{By Eqs. (37D), } E\Delta\alpha_1 &= (-0.0657 - 0.1065)0.6487 - (0.0687 + 0.0657)0.3147 = -0.1540 \\ E\Delta\alpha_2 &= 0.0 - (0.1065 + 0.1000)1.542 = -0.3184 \\ E\Delta\alpha_3 &= (0.0889 - 0.0990)1.409 - (-0.0579 - 0.0889)0.462 = +0.0536 \end{aligned}$$

$$\text{By Eq. (37F), } -E\Delta\psi_4 = E\Sigma\Delta\alpha = -0.4188$$

$$\text{By Eq. (37N), } Ew_4 = 0.4188 - 0.0687 \times 0.3147 + 0.0990 \times 0.1865 = +0.416$$

**For panel point  $L_5$ :**

$$\begin{aligned} \text{By Eqs. (37D), } E\Delta\alpha_1 &= (-0.0579 - 0.0889)0.462 - (0.0990 + 0.0579)0.1865 = -0.0971 \\ E\Delta\alpha_2 &= 0.0 - (0.0889 + 0.1081)2.164 = -0.4263 \\ E\Delta\alpha_3 &= (0.0541 - 0.1207)2.111 - (-0.0270 - 0.0541)0.400 = -0.1082 \end{aligned}$$

$$\text{By Eq. (37F), } -E\Delta\psi_5 = E\Sigma\Delta\alpha = -0.6316$$

$$\text{By Eq. (37N), } Ew_5 = 0.6316 - 0.0990 \times 0.1865 + 0.1207 \times 0.0621 = +0.621$$

**For panel point  $L_6$ :**

$$\begin{aligned} \text{By Eqs. (37D), } E\Delta\alpha_1 &= (-0.0270 - 0.0541)0.400 - (0.1207 + 0.0270)0.062 = -0.0416 \\ E\Delta\alpha_2 &= 0.0 - (0.0541 + 0.1290)2.500 = -0.4578 \end{aligned}$$

$$\text{By Eq. (37F), } -\frac{1}{2}E\Delta\psi_6 = \frac{1}{2}E\Sigma\Delta\alpha = -0.4994$$

$$\text{By Eq. (37N), } \frac{1}{2}Ew_6 = 0.4994 - 0.1207 \times 0.0621 = +0.492$$



The minus sign in Eq. (37F) applies here because the angles  $\alpha$  are on the side of the chord opposite to the angle  $\phi$ .

The  $Ew$  elastic loads are now combined into a force polygon and the equilibrium polygon drawn for these loads acting through the several lower chord panel points will then represent the deflection polygon for the lower chord.

If the pole distance  $H$  were made equal to  $E$  then the deflections would be actual to the scale of lengths according to the rule above given. However, this would be too small a scale for accurate results and therefore, the pole distance was made equal to  $4w$  units, giving deflections  $E/4$  times actual to the scale of lengths of the drawing. By constructing a scale four times smaller than the scale of lengths, the deflection ordinates  $E$  times actual may be scaled directly from the drawing, and these values are written on the ordinates.

The same problem is solved by the graphic method in Fig. 50B and again by the method of Art. 36 in Table 50B.

Using the  $Ew$  loads computed for the top chord panel points the top chord deflection polygon is obtained in precisely the same manner and these loads and the deflections found for the top chord are comparable with the values in Art. 50 just referred to.

The numerical values of the  $Ew$  loads for the top chord panel points are as follows:

$$\begin{array}{llll} Ew_0 = -0.139 & Ew_2 = +0.117 & Ew_4 = +0.415 & \frac{1}{2}Ew_6 = +0.479 \\ Ew_1 = +0.098 & Ew_3 = +0.203 & Ew_5 = +0.608 & \end{array}$$

The details for the computation of the load  $Ew_2$  are given for illustration. Thus:

$$\begin{array}{l} \text{By Eqs. (37D), } E\Delta\alpha_1 = (0.0625 + 0.0352)0.7173 - (-0.0498 - 0.0625)1.394 = +0.2266 \\ E\Delta\alpha_2 = (0.0493 + 0.0498)0.431 - (0.0791 - 0.0493)0.419 = +0.0302 \\ E\Delta\alpha_3 = (-0.0657 - 0.0791)0.963 - 0.0 = -0.1394 \end{array}$$

$$\text{By Eqs. (37F) and (37O)} \qquad Ew_2 = E\Delta\phi_2 = E\Sigma\Delta\alpha = +0.1174$$

which follows for a straight chord when the angles  $\alpha$  and  $\phi$  are on the same side of the chord.

### ART. 38. HORIZONTAL DISPLACEMENTS

To find the displacements in a horizontal direction when the deflection polygon for vertical deflections is given.

It is readily seen, from the previous description, that the elastic loads  $w$  are independent of the direction of the deflections because in every instance their value is dependent on the shape of the truss and the changes in the lengths of the members, regardless of how these were produced. See Eqs. (36B) and (36C). Hence, the same elastic loads may be employed to find deflections in any direction.

The force polygon, used for the deflection polygon for vertical deflections, will thus be the same for any other direction of deflections when revolved through an angle equal to the angle included between these two directions. When horizontal and vertical

deflections are under consideration this angle is  $90^\circ$  and the same force polygon may readily serve both purposes, since the rays for horizontal deflections are then perpendicular to the rays drawn for the vertical deflections.

In Fig. 38A, let the succession of members  $A$  to  $B$  represent the *bottom or tension chord* of some structure, fixed at  $A$  and supported by a roller bearing on a horizontal plane at  $B$ . Also given the deflection polygon  $A'c'd'e'f'B'$  to find the deflection polygon  $A''c''d''e''f''B''$  for horizontal deflections. The loads  $w$  are all multiplied by  $E$  and the deflections are  $m$  times natural.

The left-hand end of the chord having no horizontal motion, it is most convenient to call all horizontal deflections positive to the right.

The pin points are horizontally projected on to the closing line  $A''e_0$ , which latter is perpendicular to the closing line  $A'B'$ . The polygon  $A''c''d''e''f''B''$  is then drawn

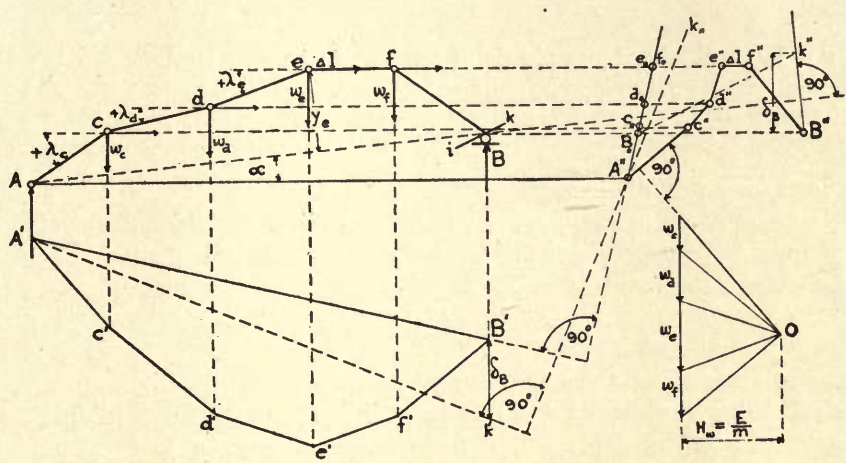


FIG. 38A.

by making the sides perpendicular to the respective rays of the force polygon and maintaining the same order of succession in the pin points formerly used in constructing the deflection polygon for vertical deflections. The horizontal abscissa  $\overline{B_0B''}$  is then the horizontal displacement of the point  $B$ . Similarly the abscissa  $\overline{a_0d''}$  is the horizontal displacement of the point  $d$ , etc.

For any horizontal member, as  $\overline{ef}$ , the horizontal displacement of the point  $f$  with respect to  $e$  must naturally be the  $\Delta l$  for that member. Hence since the scale of deflections is  $m$  times actual to the scale of lengths the displacement  $\overline{e''f''} = m\Delta l$  to the scale of lengths used.

If the point  $B$  is made to roll on some inclined plane  $\overline{ik}$  instead of the horizontal, then a new closing line  $\overline{A''k_0}$  must be determined for the two deflection polygons, as follows: draw a line  $\overline{B_0k''} \parallel \overline{ik}$  and erect a perpendicular to  $\overline{AB}$  prolonged, and passing through  $B''$ . The intersection of these two lines gives  $k''$  and the vertical ordinate  $\delta_B$  represents the vertical displacement of the support  $B$ .



Hence, making  $\overline{B'k'} = \delta_B$  the closing line  $\overline{A'k'}$  may be drawn. Also a line  $\overline{A''k_0} \perp \overline{A'k'}$  becomes the required closing line for the horizontal deflection polygon.

The same solution will apply to deflections in any direction other than  $90^\circ$  with the vertical. Also, when the deflection polygon for vertical deflections of all points of a truss is given, as in Fig. 36A, then the horizontal deflections of all pin points are found precisely as above by adhering strictly to the sequence in which these points occur on the given deflection polygon.

The change  $\delta_{AB}$  in the length of the chord  $\overline{AB}$ , Fig. 38A, may easily be found by taking the loads  $w$  parallel to  $\overline{AB}$ . In this case the displacement  $\delta_{AB}$  becomes the intercept on  $\overline{AB}$  produced and included between the extreme rays of the equilibrium polygon. Hence this displacement is equal to

$$\delta_{AB} = \sum \frac{wy}{H_w} \quad \dots \quad (38A)$$

wherein  $y$  is the ordinate of any pin point measured normally to  $\overline{AB}$ .

This same result may also be found by computation from

$$\delta_{AB} = \sum wy, \quad \dots \quad (38B)$$

which follows for a pole distance of unity.

For the case given in Fig. 37B, where the angle changes  $\Delta\phi$  and the changes in the lengths of the members are given, the total effect on the length of span  $\overline{AB}$  then becomes for  $n$  members,

$$\delta_{AB} = \sum_1^{n-1} y \Delta\phi + \sum_1^n \Delta l \cos (\lambda - \alpha), \quad \dots \quad (38C)$$

where  $\alpha$  is the angle which the span  $\overline{AB}$  makes with the horizontal.

**Example.** The lengthening  $\delta_{AB}$  for the span  $\overline{AB}$  due to the loading  $X_a=1$  in Fig. 37o is computed from Eq. (38C), using the values  $E\Delta l$  as given in Fig. 50A. The value  $\frac{1}{2}E\delta_{AB}$  was found to check the value determined graphically in Fig. 50B. The values  $E\Delta\phi$  are those above computed for the bottom chord panel points and  $\alpha=0$  because the span is symmetric.

Point.	$E\Delta\phi$	$y$ Feet.	$Ey\Delta\phi$	$E\Delta l$ Fig. 50A. Feet.	$\cos \lambda$	$E\Delta l \cos \lambda$
$L_1$	0.1721	6.188	1.0649	0.286	0.834	0.2385
$L_2$	0.1068	14.58	1.5571	0.597	0.873	0.5212
$L_3$	0.1825	21.05	3.8416	0.805	0.918	0.7390
$L_4$	0.4188	25.77	10.7925	1.080	0.954	1.0303
$L_5$	0.6316	28.568	18.0435	1.511	0.983	1.4853
$L_6$	$\frac{1}{2}=0.4994$	29.50	14.7323	1.814	0.998	1.8104

$$\frac{1}{2}E\sum y\Delta\phi = 50.0319$$

$$\frac{1}{2}E\sum \Delta l \cos \lambda = 5.8247 \text{ ft.}$$

These values substituted into Eq. (38C) give for a lengthening  $E$  times actual,  $\frac{1}{2}E\delta_{AB} = \frac{1}{2}E\sum y\Delta\phi + \frac{1}{2}E\sum \Delta l \cos \lambda = 50.0319 + 5.8247 = 55.8566$  ft., where  $E=29000$  kips per sq. inch.



## ART. 39. DEFLECTION OF SOLID WEB BEAMS

(a) **Deflection due to moments.** The differential equation of the elastic curve is

$$\frac{d^2y}{dx^2} = \frac{M}{EI} \quad \dots \dots \dots (39A)$$

Eq. (36B) gives the elastic loads  $w$ , for only one chord, in terms of moment and truss dimensions as

$$w = \frac{M\rho}{r^2} = \frac{Ml}{EFr^2}.$$

Considering both chords, each of area  $F$ , and neglecting the web effect, which is usually quite small, then for a unit length of girder

$$w = \frac{2Ml}{EFr^2} = \frac{1 \cdot M}{EI}.$$

Hence Eq. (39A) gives directly the elastic loads  $w$  per unit length of girder as

$$w = \frac{d^2y}{dx^2} = \frac{M}{EI} \quad \dots \dots \dots (39B)$$

An equilibrium polygon drawn for these loads, with pole distance equal to unity, gives deflections to the scale of lengths chosen for the drawing.

By treating the moments  $M$  per unit length of girder, as loads which now become  $EI$  times too large, and constructing an equilibrium polygon for these loads  $M$  with a pole distance  $H = EI$ , the same deflection polygon is again obtained, giving deflections to the scale of lengths of the drawing. In other words the moment polygon for any case of loading becomes the load line for the deflection polygon corresponding to such case of loading.

Deflections are usually drawn several times actual size, in which case the pole must be divided by as many times the scale of the drawing. Thus, if the scale of lengths is  $1:n$  and the deflections should appear twice actual, then the pole  $H = EI/2n$ .

When the value  $I$  is variable, the pole distance is made to vary as a function of  $I$ , as illustrated in the example below. See also Art. 47.

(b) **Deflection due to shear.** From Eq. (15M) the deflection of a straight beam when acted on by shearing forces only, is

$$\delta_m = \frac{\beta}{GF} \int_0^m Q \frac{\partial Q}{\partial P_m} dx. \quad \dots \dots \dots (39C)$$

Disregarding all unnecessary refinements, since shear deflections are small compared to the total deflection, the value  $\beta$  may be taken as constant and  $Q$  will be assumed uniformly distributed over the web plate of sectional area  $F_1 = F/3$ .

For a single concentrated load  $\partial Q/\partial P_m=1$  and  $Q=R$ =the end reaction, hence

$$\delta_m = \frac{\beta}{GF} = \int_0^m Q \frac{\partial Q}{\partial P_m} dx = \frac{\beta}{GF} \int_0^m R dx = \frac{\beta M}{GF}.$$

Taking  $G=0.333E$  and  $F_1=F/3$  and assuming an average value for  $\beta=2.5$  for ordinary girder sections, then approximately

$$\delta_m = \beta \frac{M}{GF} = \frac{5M}{2EF_1}. \quad (39D)$$

(c) **Deflection due to combined shear and moments.** Ordinarily it will suffice to figure the deflection due to shear for a point at or near the point of maximum moments and to determine the percentage which this  $\delta_m$  is of the moment deflection ordinate at the same point. All other moment deflection ordinates may then be increased in the same proportion to obtain the deflection polygon for combined shear and moment effects.

For a uniformly loaded beam or constant  $I$  and neglecting shear effect, the deflection becomes

$$\delta = \frac{1}{EI} \int_0^l \left( \frac{pl}{2}x - \frac{px^2}{2} \right) x dx = \frac{5pl^4}{384EI} = \frac{5M_{\max}l^2}{48EI}. \quad (39E)$$

When the depth of a girder is constant, but the moment of inertia varies so as to maintain a constant stress on the extreme fiber at all sections, then the ratio  $M/EI$  becomes constant and the deflection for such a case would be

$$\delta = \frac{M}{EI} \int_0^l x dx = \frac{6M_{\max}l^2}{48EI_m}, \quad (39F)$$

where  $I_m$  is the moment of inertia at the section of maximum stress.

When the moment of inertia varies abruptly the deflection may be expected to fall between the two above values, making the numerical coefficient close to  $1/9$ . Taking in the shear effect, the approximate formula for maximum deflection, of a beam of variable  $I$ , becomes

$$\delta = \frac{M_{\max}l^2}{9EI} + \frac{5M_{\max}}{2EF_1}. \quad (39G)$$

However, for general cases of loading and variable  $I$  the graphic solution, above given under Art. 39A, should be employed.

(d) **Example.** Given a plate girder of variable section and uniformly varying water load as shown in Fig. 39A, required to find its deflection polygon. The girder is designed as a double web beam and normally occupies a vertical position so that there are no dead load stresses.

These girders are spaced 9.175 ft. center to center so that each will carry a full water load  $P=31.25 \times 9.175(l-a)^2$  giving rise to the end reactions  $A$  and  $B$ , and moments  $M$ , all as indicated in the diagrams, Fig. 39A.





The moments of inertia were computed for the various sections on gross areas, and are plotted in the upper diagram.

The bending moments were also computed, using the formula

$$M = \frac{P}{3l}(l-a)x - \frac{P}{3} \frac{(x-a)^2}{(l-a)^3}, \quad \dots \quad (39H)$$

and the results were plotted in millions of foot-pounds in the second diagram.

The  $w$  loads were then taken as the moments  $M$  over certain convenient lengths  $\Delta x$ , instead of unit lengths according to the formula (39B), whence

$$w = \frac{M \Delta x}{EI} \quad \dots \quad (39J)$$

The lengths  $\Delta x$  are usually chosen with respect to the girder sections, so that  $I$  is constant over each length  $\Delta x$ . Where the depth of section is variable the mean value of  $I$  is taken for each length  $\Delta x$ .

Since  $M$  and  $\Delta x$  are both expressed in feet, while  $E$  and  $I$  are both for inches, the factor  $12 \times 12 = 144$  is introduced into Eq. (39J) to establish a true ratio between like units. Also,  $M$  and  $E$  are both expressed in millions of pounds, making the unit weight one million pounds. This furnishes the true values for  $w$  in terms of the given data as

$$w = \frac{144 M \Delta x}{28 I} = \frac{M \Delta x}{28 I} = \frac{M \Delta x}{H}, \quad \dots \quad (39K)$$

wherein  $E = 28$  is chosen low rather than high.

Now the scale of lengths was taken as 1:120, and if the deflections are to appear twice actual size then the pole must be made equal to

$$H = \frac{28 I}{2 \times 120 \times 144} = 0.00081 I. \quad \dots \quad (39L)$$

The pole distances are thus a constant function of  $I$  and may be found for all values of  $I$ .

The force polygon is now easily drawn to any convenient scale of forces, using the same scale for the loads  $w$  and the pole distances  $H$ . This scale has no influence on the deflection polygon, but merely affects the size of the force polygon.

The deflection polygon is then constructed as the equilibrium polygon of the  $w$  loads with the various pole distances, and the ordinates included between this polygon and the closing line  $\overline{A'B'}$  will represent the deflections to twice natural scale. Had the pole distances been taken twice as long, then the deflections would have been actual.

The deflection due to shear, at the point of maximum moments, is found from Eq. (39D) as  $\delta_m = \frac{5M}{2EF_1} = \frac{5 \times 5.37 \times 12}{2 \times 28 \times 58.5} = 0.098$  inch which is 10.5 per cent of the maximum deflection due to bending alone.

The total deflection of the girder is therefore 10.5 per cent greater than the amounts given on the deflection polygon of Fig. 39A. The maximum deflection due to combined shear and bending effect is thus  $0.93 + 0.098 = 1.028$  inches, for the point 7.

The approximate formula (39G) gives for this same point

$$\delta_7 = \frac{5.37 \times 12 \times \overline{56.5^2} \times \overline{12^2}}{9 \times 28 \times 134000} + 0.098 = 0.978 \text{ inch.}$$

See Art. 47 for another method of dealing with variable moment of inertia, by treating the quantities  $M\Delta x/I$  as elastic loads and making the pole distance equal to  $E$ .

## CHAPTER VIII

### DISPLACEMENT INFLUENCE LINES FOR STATICALLY DETERMINATE STRUCTURES

#### ART. 40. INFLUENCE LINES FOR ELASTIC DISPLACEMENTS

Deflection influence lines could not receive adequate treatment in Chapter IV because these depended on a knowledge of deflection polygons. The latter were taken up in Chapters VI and VII. The subject is now treated from the most general aspect covering the influence line for any elastic displacement.

Proceeding from Maxwell's law, Professor Mohr, in 1875, first developed displacement influence lines. The application results from a consideration of two conventional loadings, of unit work each, applied to any frame so that one of the loadings represents the desired influence at some point  $n$ , and the other loading is a vertical moving load  $P=1$  applied at any load point  $m$  of the loaded chord. This includes all cases of conventional loadings given in Art. 9, besides the simpler problems pertaining to displacements of points.

As applied to any simple beam or truss, the following theorem is now established: *A deflection polygon, drawn for a load unity acting in a fixed direction on some definite point  $n$  of any frame, is the deflection influence line for the deflection of the point  $n$ , in the fixed direction for any system of parallel moving loads applied to the loaded chord.* When the system of moving loads does not consist of parallel loads, then, of course, no influence line is possible.

To prove this theorem, the simple beam, Fig. 40A, is loaded with a vertical load  $P_n=1$  applied at the point  $n$ . A deflection polygon, drawn for this case of loading will then be the *deflection influence line* for the point  $n$ , according to the following demonstration. The method of drawing the deflection polygon is given in Art. 39.

The moment diagram is first drawn for the conventional loading  $P_n=1$  kip, applied at  $n$  and thus making the maximum ordinate under  $n$  equal to  $\bar{M}_n=1 \cdot aa'/l=4.8$  kip ft. The symbol  $\bar{M}$  is used to indicate a moment due to a conventional unit load.

This diagram is divided into suitable sections (2 ft. apart) and the moment areas  $\bar{M}\Delta x$  are computed and treated as elastic loads  $w$ , for which the deflection polygon  $A''B''$  is finally drawn, all as shown in Fig. 40A.

Assume the modulus  $E=28000$  kips per sq. inch,  $I=2087$ , in inches,  $\bar{M}$  in kip feet, and  $\Delta x$  in feet. Then the pole distance for the force polygon becomes  $H=EI/144$  when the  $w$  loads are made equal to  $\bar{M}\Delta x$ , by Eq. (39j), for deflections of actual size. However, the scale of lengths of the drawing was made 1:36 and the deflections should appear 200 times actual, hence  $H$  must be made  $EI/200 \times 36 \times 144=56.35$   $w$  units.



With a pole  $H=56.35$  and the  $w$  loads  $\bar{M}dx$ , construct the force and equilibrium polygons as shown, and the deflection polygon so found represents the *deflection influence line* for the point  $n$  according to the following application of Maxwell's law.

The vertical deflection of any point  $m$ , for the given load  $P_n=1$ , is represented by the vertical ordinate  $\eta_m$  of the deflection polygon  $A''B''$ , vertically under the point  $m$ . For, by Maxwell's law,  $\eta_m = \delta_{mn} = \delta_{nm}$ , or in words,  $\eta_m$  equals the elastic displacement of the point  $n$  for a unit load  $P_m$  acting at the point  $m$ . Hence  $m$  being any position

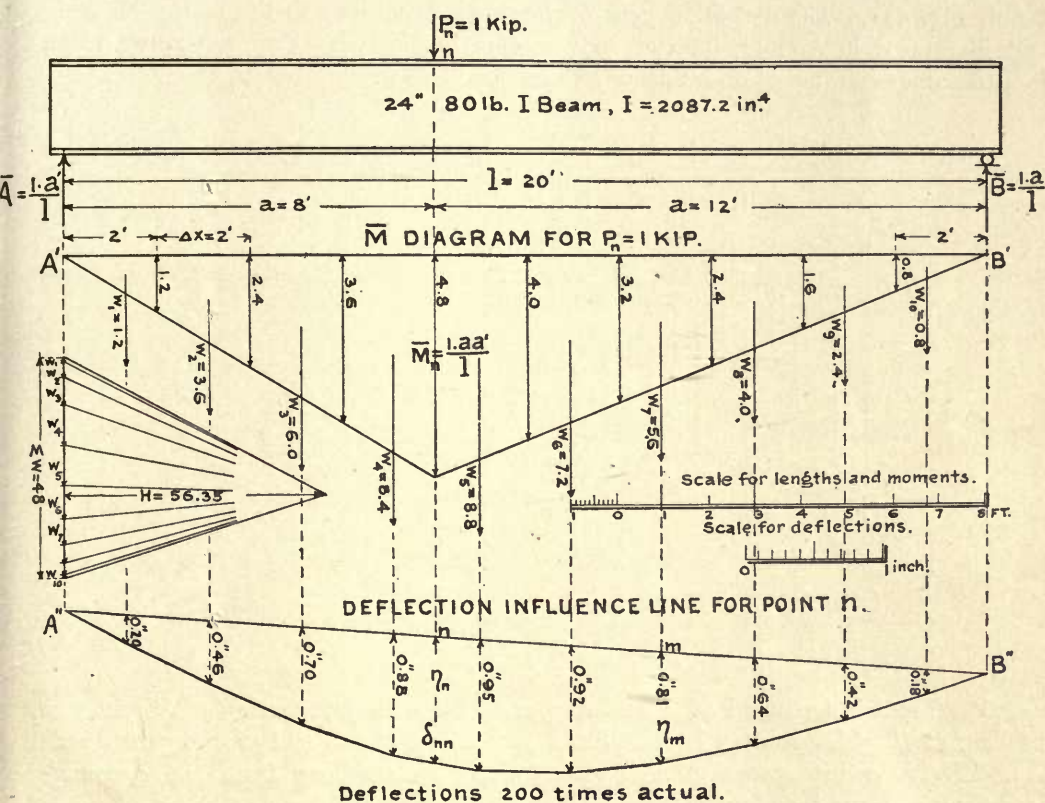


FIG. 40A.

of the moving load point, it follows that all ordinates  $\eta_m$  represent deflections for the point  $n$  due to a unit load at the variable point  $m$ . This makes the polygon  $A''B''$  the desired deflection influence line for the point  $n$ .

Therefore, for any train of moving loads, the deflection at the point  $n$  becomes

$$\delta_n = P_1\eta_1 + P_2\eta_2 + P_3\eta_3 + \dots = \Sigma P\eta \quad (40A)$$

Since Maxwell's law is generally applicable to any case of conventional loading, whether for a single point, a pair of points or a pair of lines, as illustrated in Art. 9,

therefore, the above application affords a solution for any displacement influence line other than those for simple vertical deflections. However, the train of loads must consist of parallel forces  $P$ , as otherwise no influence line is possible.

#### ART. 41. SPECIAL APPLICATIONS OF DISPLACEMENT INFLUENCE LINES

(a) Required the deflection influence line for the point  $n$  of the simple cantilever beam, Fig. 41A. The deflection polygon is drawn according to the method of Art. 39 and illustrated in Art. 40, for the conventional loading  $P_n=1$  at the point  $n$ . This then becomes the deflection influence line for the point  $n$ .

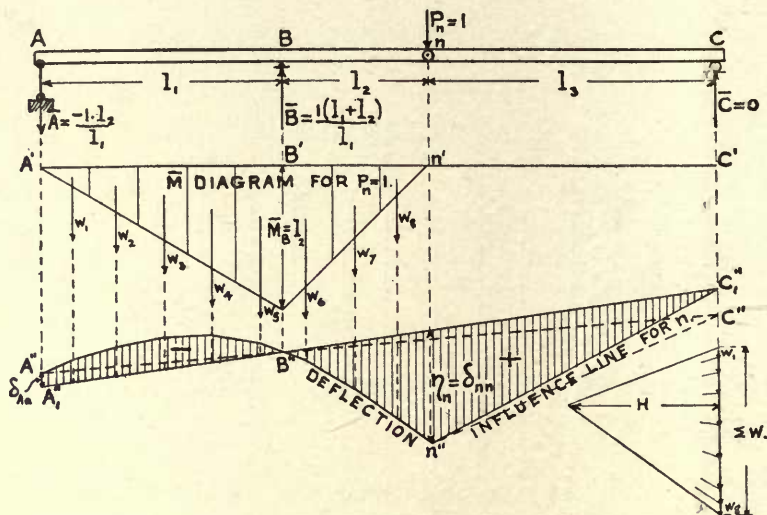


FIG. 41A.

The beam is anchored at  $A$  and supported by a hinged bearing at  $B$  and a roller bearing at  $C$ . The point  $n$  is the hinged connection at the end of the cantilever arm  $Bn$ . The following moments  $\bar{M}$  and reactions  $\bar{R}$ , resulting from the conventional loading  $P_n=1$ , are then found:

$$\begin{aligned}\bar{A} &= -\frac{1 \cdot l_2}{l_1}, & \bar{B} &= \frac{1(l_1 + l_2)}{l_1}, & \bar{C} &= 0, \\ \bar{M}_A &= 0, & \bar{M}_B &= 1 \cdot l_2, & \bar{M}_n &= 0.\end{aligned}$$

The  $\bar{M}$  diagram is constructed by making the ordinate at  $B'$  equal to  $l_2$ , and after dividing this diagram into suitable sections and computing the loads  $w_1$  to  $w_8$ , the deflection polygon is easily drawn, observing the method followed in Art. 40.

The closing line of the deflection polygon is then found to be  $A''B''C''$ , which completes the influence line. The point  $B''$  is the intersection of the deflection line

with the vertical through  $B$  and  $\overline{n''C''}$  is a straight line. Upward deflections are negative.

The support at  $A$  is elastic and its displacement  $\delta_{Aa}$ , due to the conventional loading  $P_n=1$ , should be computed from Eq. (4A) including temperature effect if desirable. This displacement is then applied at the point  $A''$  and the final closing line  $\overline{A_1''B''C_1''}$  is thus made to include this effect. By applying any train of loads the resulting actual deflection of the point  $n$ , according to Eq. (40A) becomes  $\delta_n = \Sigma P\eta$ .

For any case of variable moment of inertia of the given beam the pole distance  $H$  is made variable, as was done in Fig. 39A.

(b) Given a simple truss, Fig. 41B, on two supports, to find the displacement influence line for any panel point  $n$  for displacements  $\delta_n$  in the fixed direction  $\overline{nn'}$ . The loading is to consist of a system of vertical concentrated loads  $P$  acting on the bottom chord.

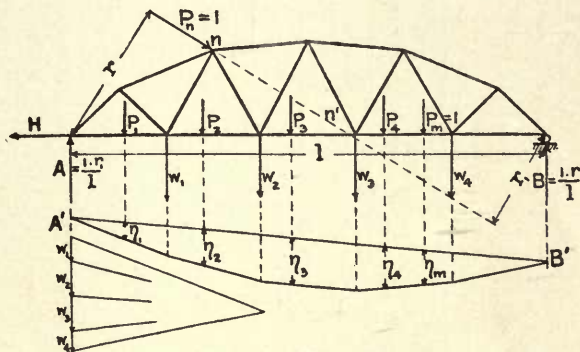


FIG. 41B.

Apply the conventional loading  $P_n=1$  in the given direction  $\overline{nn'}$  and compute the reactions  $H$ ,  $A$  and  $B$  for this load, then determine the stress  $S_1$  and resulting change  $\Delta l$  in length, for each member. Finally compute the  $w$  loads for the several panel points and draw the deflection polygon for the loaded chord (here the bottom chord) using any of the methods of Chapter VI, but preferably the one given in Art. 36 (c). The direction of the  $w$  loads is always taken parallel to the system of loads  $P$ , hence the displacement influence ordinates  $\eta$  will be vertical ordinates, measured vertically under the respective loads  $P$ . This is necessary because the direction of the deflections is determined by the direction assigned to the  $w$  loads.

The proof that the polygon  $\overline{A'B'}$  is the desired influence line again follows from Maxwell's law, viz., for any ordinate  $\eta_m = \delta_{mn} = \delta_{nm}$ .

The displacement  $\delta_n$  of the point  $n$  in the direction  $\overline{nn'}$ , caused by the system of vertical loads  $P$  is then

$$\delta_n = P_1\eta_1 + P_2\eta_2 + P_3\eta_3 + P_4\eta_4 = \Sigma P\eta.$$

(c) Given the three-hinged arch, Fig. 41C, to find the influence line for the angular rotation  $\delta_n$  between the two lines  $\overline{An}$  and  $\overline{Bn}$ . The train loads are to be carried by the top chord.





## CHAPTER IX

### INFLUENCE LINES FOR STATICALLY INDETERMINATE STRUCTURES

#### ART. 42. INFLUENCE LINES FOR ONE REDUNDANT CONDITION

The principle, illustrated in Chapter VIII, for drawing deflection influence lines, is easily applied to the construction of the influence line for any external or internal redundant condition.

Eqs. (7H) and (8D) for one redundant condition and a single external force  $P=1$  become

$$\left. \begin{aligned} \delta_a &= \Sigma S_a S_o \rho - X_a \Sigma S_a^2 \rho = \frac{X_a l_a}{EF_a} = X_a \rho_a \\ \delta_a &= 1 \cdot \delta_{ma} - X_a \delta_{aa} = X_a \rho_a \end{aligned} \right\}, \dots \dots \dots (42A)$$

after substituting the value  $\delta_a$  as obtained from Eq. (4A) and neglecting temperature and abutment displacements.

This gives  $X_a$  in terms of displacements or stresses, whichever is preferred, as

$$X_a = \frac{\Sigma S_o S_a \rho}{\Sigma S_a^2 \rho + \rho_a} = \frac{1 \cdot \delta_{ma}}{\delta_{aa} + \rho_a}, \dots \dots \dots (42B)$$

where the redundant may be external or internal.

If the single load  $P=1$  is vertical and applied to some panel point of the *loaded chord* then Eq. (42B) represents the influence line for  $X_a$  for a unit load applied at any panel point  $m$ .

A deflection polygon, drawn for the conventional loading or condition  $X_a=1$ , will give the ordinates  $\eta_m = \delta_{ma} = \delta_{am} = \Sigma S_o S_a \rho$  for the displacement of the point  $a$ , for a unit load at any point  $m$  of the loaded chord. Hence the deflection polygon drawn for condition  $X_a=1$  is the  $X_a$  influence line provided all the ordinates are divided by the constant denominator  $\delta_{aa} + \rho_a = \Sigma S_a^2 \rho + \rho_a$ . The constant displacement  $\delta_{aa} = \Sigma S_a^2 \rho$  is found by computation or otherwise, and  $\rho_a$  is a given constant depending on the length and section of the redundant member. When  $X_a$  is a reaction then  $\rho_a=0$  for the case of immovable supports.

Accordingly the following theorem may be stated: *The ordinates to the influence line of any redundant  $X_a$  are some constant factor  $\mu = 1 \div (\delta_{aa} + \rho_a)$  times the ordinates to a deflection polygon drawn for the loaded chord, for the conventional loading  $X_a=1$  ( $P=0$ ), applied to the principal system.*

(a) **When the redundant  $X_a$  is an internal condition**, as illustrated in Fig. 42A, the above theorem is applied as follows: If the direction of stress in the redundant can be anticipated, then this should be done, otherwise an arbitrary assumption must be made and, if it was erroneous, the resulting value of the redundant  $X_a$  will turn out negative with respect to  $S_o$ . In any case the conventional loading  $X_a=1$ , being external work, should be so applied as to produce positive work when the redundant member is removed. In the illustration, the member  $X_a$  will be assumed in tension so that  $\Delta l_a$  is a positive elongation. Hence, the unit forces  $X_a=1$  must be applied so as to move the points  $n$  and  $n_1$  apart. The principal system is the entire frame exclusive of the member  $X_a$ .

The stresses  $S_a$  are computed or found from a Maxwell diagram and from these the  $w$  loads and deflection polygon for the loaded chord (which was taken to be the bottom chord in the illustration) are determined by one of the methods in Chapter VII.

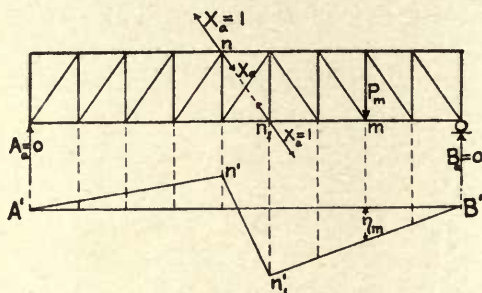


FIG. 42A.

The deflection polygon so obtained may be represented by the broken line  $\overline{A'n'n_1'B'}$ , with ordinates  $\eta_m = \delta_{ma} = \delta_{am}$ , which, according to Eq. (42B) are  $(\delta_{aa} + \rho_a)$  times the actual influence line ordinates for the redundant stress  $X_a$ . Hence the stress  $X_a$ , for any system of moving loads, becomes

$$X_a = \left( \frac{1}{\delta_{aa} + \rho_a} \right) \Sigma P \eta = \mu \Sigma P \eta. \quad (42c)$$

(b) **When the redundant  $X_a$  is an external condition**, the quantity  $\rho_a$  becomes zero for the assumption  $\delta_a = 0$  for immovable supports, and this gives rise to a slight simplification in the solution of problems of this class.

Eq. (42B) then becomes in general

$$X_a = \frac{\Sigma S_o S_a \rho}{\Sigma S_a^2 \rho} = \frac{1 \cdot \delta_{ma}}{\delta_{aa}}. \quad (42d)$$

The illustration of a simple beam on three supports is given, in Fig. 42B, as a case of one external redundant condition  $X_c$ . Any one of the three supports might be treated as the redundant one, but the middle support  $C$  is here chosen.

The conventional loading  $X_c=1$  is again chosen so as to produce a positive quantity of applied work. The deflection polygon  $A''C''B''$  of the simple determinate beam  $\overline{AB}$ ,



which now becomes the principal system, is found for this load  $X_c=1$  exactly as was done in Art. 40, Fig. 40A. The unit load is applied at  $C$  in a downward direction because the deflection of this point of the principal system is also downward when the support is removed.

Any ordinate  $\eta_m$  of this deflection polygon is equal to the deflection  $\delta_{mc}=\delta_{cm}$ , which is  $\delta_{cc}$  times the  $X_c$  influence line ordinate according to Eq. (42D). Also the special ordinate  $\eta_c=\delta_{cc}$  is given by the same deflection polygon and is a constant quantity. Hence the factor  $\mu$  for the influence line  $X_c$  is equal to  $1/\delta_{cc}$  and the ratio  $\delta_{mc}/\delta_{cc}$  determines the value of the influence line ordinate for any point  $m$ .

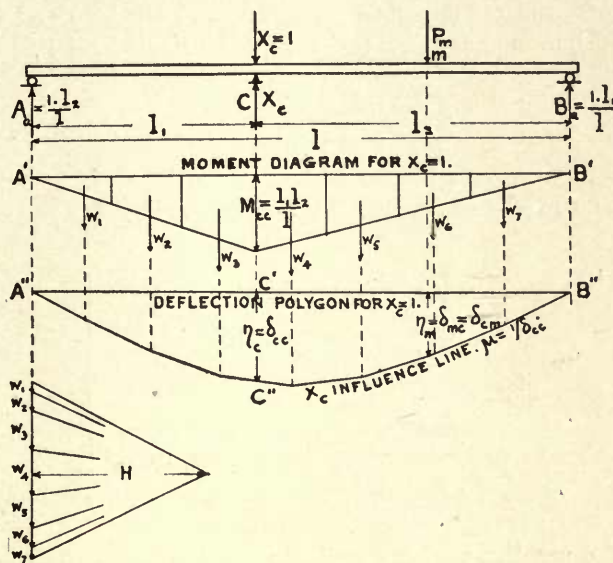


FIG. 42B.

It is thus seen that for the case of a single external redundant  $X_c$  the magnitude of the moment  $M_{cc}=l_1 l_2 / l$  and the pole distance  $H$  of the deflection polygon, do not affect the influence line ordinates  $\eta_m=\delta_{mc}/\delta_{cc}$ , though they do affect each of the ordinates  $\delta_{mc}$  and  $\delta_{cc}$  separately.

For any system of moving loads the required redundant reaction becomes

$$X_c = \frac{1}{\delta_{cc}} \Sigma P \eta = \mu \Sigma P \eta. \quad (42E)$$

## ART. 43. INFLUENCE LINES FOR TWO REDUNDANT CONDITIONS

When there are two redundants, then two deflection polygons may be drawn for the loaded chord of the principal system; one for condition  $X_a=1$  and one for condition  $X_b=1$ . These polygons are then combined into an influence area for  $X_a$  the ordinates to which, times a certain factor  $\mu_a$ , will give the influence line ordinates for the  $X_a$  influence line. Another combination similarly made for  $X_b$  will give ordinates which when multiplied by a factor  $\mu_b$ , will give the ordinates for the  $X_b$  influence line. The analytic solution for these influence lines is derived from Eqs. (8d).

Thus for two external redundants with  $\delta_a$  and  $\delta_b$  both zero and neglecting temperature and reaction displacements, Eqs. (8d) give, for a single load  $P$ ,

$$\left. \begin{aligned} P\delta_{ma} &= X_a\delta_{aa} + X_b\delta_{ba} \\ P\delta_{mb} &= X_a\delta_{ab} + X_b\delta_{bb} \end{aligned} \right\} \dots \dots \dots (43A)$$

These equations solved for  $X_a$  and  $X_b$  and observing that  $\delta_{ba}=\delta_{ab}$  by Maxwell's law, give

$$\left. \begin{aligned} X_a &= \frac{\delta_{ma} - \delta_{mb} \frac{\delta_{ab}}{\delta_{bb}}}{\delta_{aa} - \delta_{ab} \frac{\delta_{ab}}{\delta_{bb}}} P = \frac{\eta_{ma} P}{\eta_a} = \mu_a \eta_{ma} P \\ X_b &= \frac{\delta_{mb} - \delta_{ma} \frac{\delta_{ab}}{\delta_{aa}}}{\delta_{bb} - \delta_{ab} \frac{\delta_{ab}}{\delta_{aa}}} P = \frac{\eta_{mb} P}{\eta_b} = \mu_b \eta_{mb} P \end{aligned} \right\} \dots \dots \dots (43B)$$

wherein  $\delta_{ma}$  and  $\delta_{mb}$  are the variable ordinates to the two deflection polygons  $X_a=1$  and  $X_b=1$ , respectively, for any panel point  $m$ . The other quantities are all constants given by the same deflection polygons.

These equations for a load  $P=1$ , are the equations for the influence lines  $X_a$  and  $X_b$ . Their numerators then give variable ordinates which may be called  $\eta_{ma}$  and  $\eta_{mb}$  while the constant denominators  $\eta_a$  and  $\eta_b$  may be used as influence factors  $\mu_a=1/\eta_a$  and  $\mu_b=1/\eta_b$  for the two influence lines  $X_a$  and  $X_b$  respectively.

For any train of moving loads the redundant reactions are expressed by

$$\left. \begin{aligned} X_a &= \mu_a \Sigma P_m \eta_{ma} \\ X_b &= \mu_b \Sigma P_m \eta_{mb} \end{aligned} \right\} \dots \dots \dots (43C)$$

The problem of a simple beam, Fig. 43A, continuous over four supports, is chosen to illustrate this case.

The redundant supports are considered removed and the principal system then becomes a simple beam on two supports. In the present case the supports  $X_a$  and  $X_b$  are treated as redundants, although any two of the four reactions could be thus regarded.

The moment diagrams for the two conventional loadings  $X_a=1$  and  $X_b=1$  are now drawn and from these the deflection polygons are constructed precisely as illustrated in Fig. 40A. The two poles  $H$  are made equal and as a check on the drawing  $\delta_{ab}$  must equal  $\delta_{ba}$ . When the structure is a frame, then the deflection polygons for the loaded chord are drawn as described in Art. 37.

The deflection polygons so obtained are the influence lines for the deflections  $\delta_a$

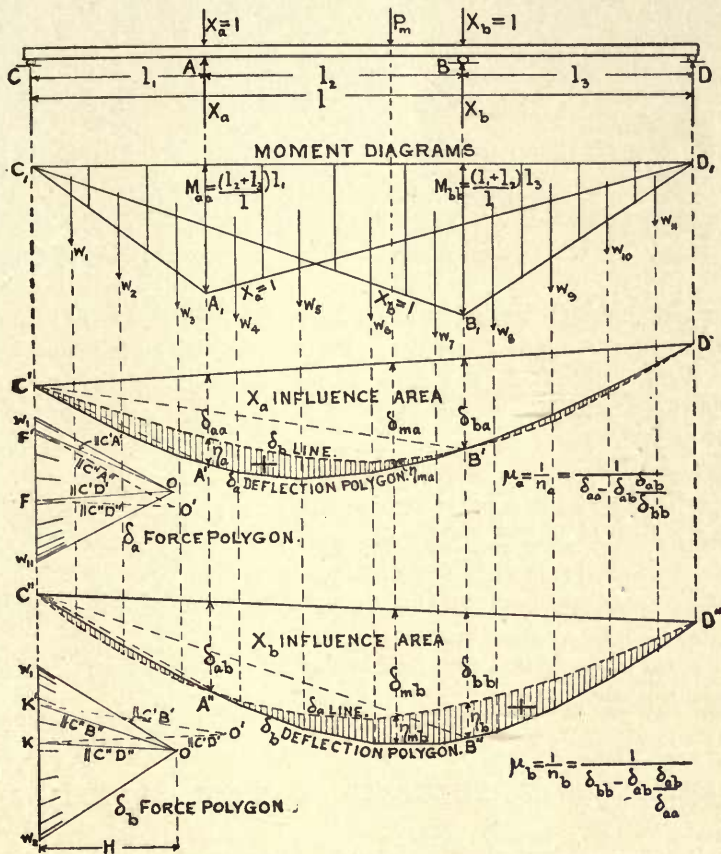


FIG. 43A.

and  $\delta_b$  of the two redundant supports. For immovable supports these are zero and Eqs. (43A) apply to any case of loading.

To obtain the influence areas for the redundants, the two deflection polygons are combined into two influence areas by computing the ordinates from Eqs. (43B) as follows:

$$\left. \begin{aligned} \eta_{ma} &= \delta_{ma} - \delta_{mb} \frac{\delta_{ab}}{\delta_{bb}} \\ \eta_{mb} &= \delta_{mb} - \delta_{ma} \frac{\delta_{ab}}{\delta_{aa}} \end{aligned} \right\} \dots \dots \dots (43D)$$



The factors  $\mu_a$  and  $\mu_b$  are the reciprocals of the denominators of Eqs. (43B) all the values for which are given on the two deflection polygons. The ordinates  $\eta_{ma}$  give, when plotted, the shaded area  $\overline{C'D'}$ , which is the influence area for  $X_a$ . The ordinate  $\eta_a$ , under the support  $X_a$ , gives the influence factor  $\mu_a = 1/\eta_a$ . In similar manner the ordinates  $\eta_{mb}$  furnish the shaded area  $\overline{C''D''}$ , which is the influence area for  $X_b$  with the factor  $\mu_b = 1/\eta_b$ , obtained from the ordinate  $\eta_b$  under the support  $X_b$ .

**A purely graphic construction** of the influence area  $X_a$  is given by Mueller-Breslau as follows: Draw the  $\delta_a$  deflection polygon for the  $w_a$  loads, using any convenient pole  $H$ . Then for the  $w_b$  loads draw an equilibrium polygon passing through the three points  $C'$ ,  $B'$  and  $D'$ . This is perhaps the best and most convenient solution and is also illustrated in Fig. 43A.

The  $\delta_a$  and  $\delta_b$  deflection polygons are first drawn as above described with any assumed pole distance which may be the same for each polygon. Then draw the  $\delta_b$  line through the three points  $C'$ ,  $B'$  and  $D'$ , and also draw the  $\delta_a$  line through the three points  $C''$ ,  $A''$  and  $D''$ . The shaded areas thus formed represent the  $X_a$  and  $X_b$  influence areas.

To find the new poles  $O'$  in the two force polygons, which are necessary in drawing an equilibrium polygon through three given points, proceed as follows: In the  $\delta_b$  force polygon, draw  $\overline{OK} \parallel \overline{C''D''}$  and  $\overline{OK'} \parallel \overline{C''B''}$  thus determining the points  $K$  and  $K'$ . Then draw  $\overline{KO'} \parallel \overline{C'D'}$  and  $\overline{K'O'} \parallel \overline{C'B'}$  and the new point  $O'$ , thus found by the intersection of  $\overline{K'O'}$  and  $\overline{KO'}$ , will be the required pole for drawing the  $\delta_b$  line through  $C'$ ,  $B'$  and  $D'$ .

The pole  $O'$  in the  $\delta_a$  force polygon is found in a similar way as indicated in the figure, using the points  $F$  and  $F'$ . The new pole  $O'$ , found by the intersection of  $\overline{FO'}$  and  $\overline{F'O'}$ , serves to draw the  $\delta_a$  line through the points  $C''$ ,  $A''$  and  $D''$ .

This construction is based on the fact that the influence of a load at  $B$  on  $X_a$  must be zero, likewise for a load at  $A$  on  $X_b$ .

The above methods are not practicable for more than two redundants, and the following method of simplification is given for multiple redundancy.

#### ART. 44. SIMPLIFICATION OF INFLUENCE LINES FOR MULTIPLE REDUNDANCY

In many problems of this class it is possible to so choose the redundant forces  $X$  that they will have a common point of application. Then for certain directions of the  $X$ 's the  $\delta$  coefficients bearing different subscripts and appearing as factors of the  $X$ 's in Eqs. (8d) may be reduced to zero. Whenever this is possible then  $\delta_{a0} = \delta_{ba} = 0$ ,  $\delta_{ac} = \delta_{ca} = 0$ ,  $\delta_{bc} = \delta_{cb} = 0$ ; etc.; and the following simple equations are obtained:

$$\left. \begin{aligned} \delta_a &= \Sigma P_m \delta_{ma} - X_a \delta_{aa} - \Sigma R_a \Delta r + \delta_{at} \\ \delta_b &= \Sigma P_m \delta_{mb} - X_b \delta_{bb} - \Sigma R_b \Delta r + \delta_{bt} \\ \delta_c &= \Sigma P_m \delta_{mc} - X_c \delta_{cc} - \Sigma R_c \Delta r + \delta_{ct} \end{aligned} \right\}, \dots \dots \dots (44A)$$

involving only one redundant  $X$  in each equation. The same assumptions may be applied to Eqs. (7H).

This method of analysis was first introduced by Professor Mueller-Breslau, and serves a most valuable purpose, especially when applied to fixed arches.

As will be shown presently, this disposition of the redundants is easily made when their number does not exceed three. Beyond this number the analysis leads to many complications. Fortunately, the important cases of redundancy are nearly always limited to from one to three redundants, and then there is no difficulty in following the scheme here proposed.

The solution of Eqs. (8D) for simultaneous values of the  $X$ 's is thus avoided and the other chances for serious errors are greatly lessened.

It is usually expedient to treat temperature stresses and abutment displacements separately from the primary stresses, and then Eqs. (44A) become for load effects only and immovable abutments,

$$X_a = \frac{\Sigma P_m \delta_{ma}}{\delta_{aa}}; \quad X_b = \frac{\Sigma P_m \delta_{mb}}{\delta_{bb}}; \quad \text{etc.} \quad (44B)$$

and for temperature effects only,

$$X_{at} = 1 \cdot \frac{\delta_{at}}{\delta_{aa}}; \quad X_{bt} = 1 \cdot \frac{\delta_{bt}}{\delta_{bb}}; \quad \text{etc.} \quad (44C)$$

By placing  $\Sigma R_a \Delta r = 0$ ,  $\delta_a$  also becomes zero, likewise for  $\Sigma R_b \Delta r$  and  $\delta_b$ , a circumstance which should be noted in writing Eqs. (44B) and Eqs. (44C).

In all of the following investigations, the  $X$ 's will represent either a single force or a couple applied to a *principal system*. The  $\delta$ 's in the first case will then represent linear displacements and in the second case they will be angular distortions expressed in arc. Thus, if a redundant  $X_a$  is applied to the point  $a$  then  $\delta_{aa}$  is the displacement of the point  $a$  in the direction of  $X_a$  for a force  $X_a = 1$ . When  $X_a$  is a moment or couple, then  $\delta_{aa}$  becomes the angular rotation of a rigid principal system as produced by a couple  $X_a = 1$ . The displacements  $\delta_a$ ,  $\delta_b$ , etc., and the *conventional loadings*  $X_a = 1$ ;  $X_b = 1$ , etc., are always positive in the opposite sense in which the redundants  $X_a$ ,  $X_b$ , etc., are supposed to act.

It should also be noted that in all cases here considered, the points  $a$  and  $b$  are coincident and these designations are retained merely to distinguish the particular forces from each other.

The Eqs. (44A) to (44C) are equally applicable to graphic and analytic solutions, but the latter method is useful only when there are not more than three redundant conditions, and great accuracy is desired. The graphic method is less laborious and leads to a more comprehensive presentation.

The above will now be applied to general cases of two and three redundants.

(a) **Structures having two redundant conditions.** Here the two redundant forces can always be applied at the same point and the case can be solved by applying Eqs. (44B) and (44C), provided the directions of  $X_a$  and  $X_b$  are so chosen that  $\delta_{ba} = \delta_{ab} = 0$ .

To accomplish this, assume the direction of  $X_a$  as may seem most convenient, and find the displacement  $\overline{a_1a}$  of the point  $a$  for a load  $X_a=1$ , Fig. 44A. Now take  $X_b$  acting at the same point  $a$  and at right angles with  $\overline{a_1a}$ .

Then  $\delta_{ba}=0$ , because it represents the displacement of the point  $b$  in the direction of  $X_b$  when only the force  $X_a=1$  is active. Therefore,  $\delta_{ab}$  also becomes zero by Maxwell's law. If then the displacement  $\overline{b_1b}$  of  $X_b$  is found for the load  $X_b=1$ , this in turn must be perpendicular to  $X_a$  because  $\delta_{ab}$  is zero. This always furnishes a valuable check on the solution when the graphic method is employed.

The example of a two-hinged arch with a column support at the center, Figs. 44B to 44D, is used to illustrate the application of the method to two redundants.

Fig. 44B shows the given structure with hinged supports at  $A$ ,  $B$  and  $C$ , thus involving two external redundants. By removing the support at  $A$  the structure becomes determinate, involving a simple truss on supports  $B$  and  $C$ , and an overhanging cantilever  $\overline{AC'}$ . The redun-

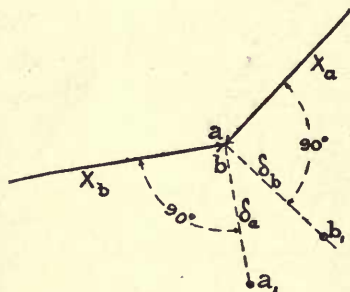
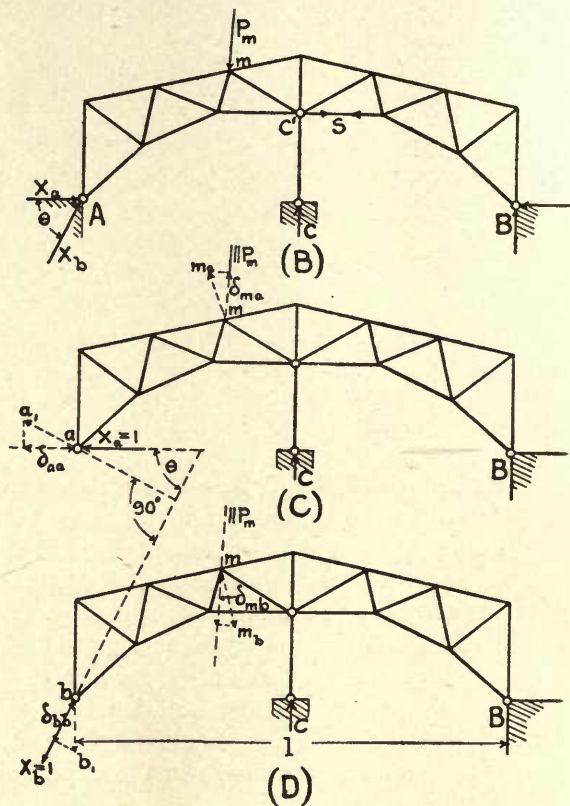


FIG. 44A.



FIGS. 44B, C, D.

dant forces  $X_a$  and  $X_b$  are then applied to the principal system at  $A$  and are treated as external forces.

The first redundant  $X_a$  is assumed to act horizontally and the second redundant  $X_b$  is applied at the same point and making the angle  $\theta$  with  $X_a$ , such that  $\delta_{ab}=\delta_{ba}=0$ .

Fig. 44C represents the conventional loading  $X_a=1$  and a Williot-Mohr displacement diagram, drawn for this loading, will furnish the displacement  $\overline{aa_1}$  for the point  $A$  and the displacement  $\overline{mm_a}$  for the point  $m$ . Hence  $\delta_{aa}$  becomes the projection of  $\overline{aa_1}$  on the direction of  $X_a$  and  $\delta_{ma}$  is the projection of  $\overline{mm_a}$  on the direction of the force  $P_m$ .



Similarly in Fig. 44D, another displacement diagram drawn for the conventional loading  $X_b=1$  and acting at  $90^\circ$  with the displacement  $\overline{aa_1}$ , gives the displacements  $\overline{bb_1}$  and  $\overline{mm_b}$  from which the values  $\delta_{bb}$  and  $\delta_{mb}$  are found by projecting the displacements on the directions of their respective forces  $X_b$  and  $P_m$ .

The angle  $\theta$  is thus graphically determined, and as a check, the displacement  $\overline{bb_1}$  must be perpendicular to  $X_a$ .

Thus having the constants  $\delta_{aa}$  and  $\delta_{bb}$  and the displacements  $\delta_{ma}$  and  $\delta_{mb}$  for any pin point  $m$ , the influence produced by any load  $P_m$ , according to Eqs. (44B) becomes

$$X_a = \frac{P_m \delta_{ma}}{\delta_{aa}} \quad \text{and} \quad X_b = \frac{P_m \delta_{mb}}{\delta_{bb}}, \dots \dots \dots (44D)$$

where  $\delta_{ma}$  is negative with respect to the force  $P_m$ , as may be seen from Fig. 44C.

The values  $X_a$  and  $X_b$  for any set of loads become

$$X_a = \frac{\Sigma P_m \delta_{ma}}{\delta_{aa}} \quad \text{and} \quad X_b = \frac{\Sigma P_m \delta_{mb}}{\delta_{bb}} \dots \dots \dots (44E)$$

and the several values  $\delta_{ma}$  and  $\delta_{mb}$  are found from the two displacement diagrams above described.

When the load  $P=1$  is vertical then the values in Eqs. (44D) represent influence line ordinates for any point  $m$  for the redundants  $X_a$  and  $X_b$ . The same displacement diagrams will furnish all values  $\delta_{ma}$  and  $\delta_{mb}$  for finding all the influence line ordinates for both redundants.

For a uniform rise in temperature of  $t^\circ$ , the point  $A$  will move horizontally an amount  $\epsilon t l$  and the projections of this displacement on the directions of  $X_a$  and  $X_b$  will then be respectively  $\delta_{at} = \epsilon t l$  and  $\delta_{bt} = \epsilon t l \cos \theta$ , whence

$$X_{at} = 1 \cdot \frac{\epsilon t l}{\delta_{aa}} \quad \text{and} \quad X_{bt} = 1 \cdot \frac{\epsilon t l \cos \theta}{\delta_{bb}} \dots \dots \dots (44F)$$

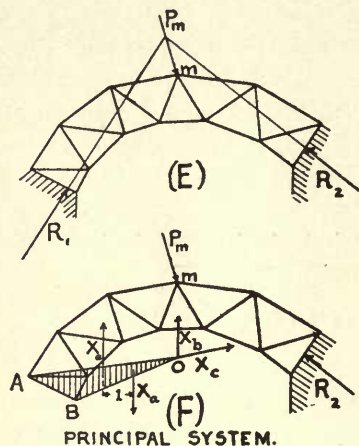
**(b) Structures having three redundant conditions.** The most prevalent case of three redundants is a fixed arch, and hence this style of structure is chosen, as an illustration, see Figs. 44E to 44J.

Fig. 44E represents any general arch with fixed supports. It is transformed into a determinate structure by removing one fixed support and converting the frame into a cantilever arm to be treated as the principal system.

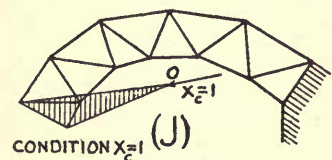
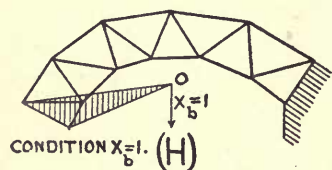
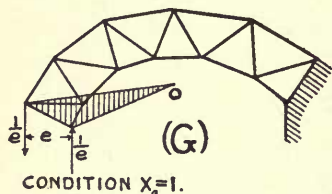
If, now, this support is replaced by three redundant conditions, a moment  $1 \cdot X_a$  and forces  $X_b$  and  $X_c$ , all acting on the rigid disc  $\overline{ABO}$ , Fig. 44F, the stresses in the structure will remain exactly the same as in the original fixed condition.

Then  $\delta_a$  will be the angular rotation of the rigid disc  $\overline{ABO}$  about some pole  $O$ ;  $\delta_b$  will be the linear displacement of the point  $O$  in the direction of  $X_b$ ; and  $\delta_c$  will be that

displacement in the direction of  $X_c$ . These displacements are supposed to be so chosen that the moment  $X_a$  and the forces  $X_b$  and  $X_c$ , all applied to the rigid disc  $\overline{ABO}$ , will exert precisely the same effect on the principal system as was previously produced by the redundancy.



PRINCIPAL SYSTEM.



FIGS. 44E, F, G, H, J.

The pole  $O$  is taken as the instantaneous center of rotation of the disc, when acted upon by a moment  $X_a = 1$ . If this pole is chosen as the point of application for the redundants  $X_b$  and  $X_c$ , then  $\delta_{ba} = 0$  and  $\delta_{ca} = 0$ . From this it follows that the angular displacements  $\delta_{ab}$  and  $\delta_{ac}$  produced by the loadings  $X_b = 1$  and  $X_c = 1$  acting on the disc, must likewise be zero if the drawing or computation is correct. Finally, if  $X_b$  is arbitrarily chosen in a vertical direction and  $X_c$  is taken perpendicular to the displacement which the point  $b$  (pole  $O$ ) undergoes as a result of the loading  $X_b = 1$ , then  $\delta_{cb} = 0 = \delta_{bc}$ .

Hence this disposition of the redundant conditions will cause all the quantities  $\delta$  bearing double subscripts of different letters, to become zero, and the simplified Eqs. (44A) will now apply.

When the abutments are considered immovable,  $\delta_a$ ,  $\delta_b$ , and  $\delta_c$  become zero and Eqs. (44B) and (44C) will suffice to solve the fixed arch. For vertical loads these same equations furnish the ordinates for the  $X_a$ ,  $X_b$  and  $X_c$  influence lines by inserting a single load  $P_m = 1$ .

In proceeding to a solution it is best to apply a unit moment  $e \cdot 1/e$ , Fig. 44G, to the points  $A$  and  $B$ , representing the conventional loading  $X_a = 1$  acting on the principal system. A Williot-Mohr displacement diagram, drawn for this condition, will furnish the displacements  $\overline{A_1A}$  and  $\overline{B_1B}$  of the two points  $A$  and  $B$ . The pole  $O$ , being the instantaneous center of rotation of the rigid disc, is found by the intersection of two lines  $\overline{OA} \perp \overline{A_1A}$  and  $\overline{OB} \perp \overline{B_1B}$ . Then  $X_b$  is applied at  $O$  in a vertical direction and  $X_c$  is made active at  $O$  and in a direction perpendicular to the displacement found for  $O$  from the displacement diagram drawn for the condition  $X_b = 1$ . See Figs. 44H and 44J for the conventional loadings  $X_b = 1$  and  $X_c = 1$ .

See Figs. 44H and 44J for the conventional loadings  $X_b = 1$  and  $X_c = 1$ .

# ART. 45. STRESS INFLUENCE LINES FOR STRUCTURES INVOLVING REDUNDANCY

(a) **Multiple redundancy.** The previous articles 42 to 44 show how influence lines for redundant conditions may be determined. In the present article it is proposed to present the methods of drawing stress influence lines for the members of any structure involving redundant conditions.

The general equation for the stress in any member of the principal system of a statically indeterminate structure is Eq. (7A). This equation, if written for a single external load  $P_m=1$ , will represent the stress influence line ordinate, under the point  $m$ , for the member  $S$ . Hence, if  $\bar{S}_o$  represents the stress in the member for condition  $X=0$  and  $P_m=1$ , then Eq. (7A) gives the desired influence ordinate for any point  $m$  as

$$\eta_m = S = \bar{S}_o - S_a X_a - S_b X_b - S_c X_c, \text{ etc.}, \quad . \quad . \quad . \quad . \quad . \quad . \quad (45A)$$

where  $\eta_m$  is the algebraic sum of the partial influences  $\bar{S}_o$ ,  $X_a$ ,  $X_b$ ,  $X_c$ , etc., on the stress of a certain member  $S$ , due to a load  $P_m=1$  acting at the panel point  $m$ . In other words, a separate influence line may be drawn for each term of Eq. (45A) and the algebraic sum of the several influence ordinates under a certain load point  $m$  becomes the stress influence ordinate  $\eta_m$  for that particular load point. Such an influence line may be regarded as a *summation influence line* of partial stress effects instead of a summation load effect as originally implied by the definition in Art. 17.

Accordingly, for any system of external parallel loads, the total stress in any member is represented by

$$S = P_1 \eta_1 + P_2 \eta_2 + P_3 \eta_3, \text{ etc.} = \Sigma P \eta \quad . \quad . \quad . \quad . \quad . \quad . \quad (45B)$$

As may be seen from Eq. (45A) such a stress influence line will always necessitate drawing as many influence lines as there are redundants, plus one for the  $\bar{S}_o$  stress. However, the influence lines for the redundants remain unchanged for all members of the same structure and hence need be drawn only once. Also the stresses  $S_a$ ,  $S_b$  and  $S_c$  are constants for a given member but vary for different members. The  $\bar{S}_o$  influence line is the same as the stress influence line for any member of a determinate frame and will be different for each member. See Chapter IV.

Therefore, it is advisable to draw the influence lines for the redundants without the  $S_a$ ,  $S_b$ ,  $S_c$ , etc., factors and then draw the  $\bar{S}_o$  stress influence line for any particular member  $S$ . Finally insert for the  $X$ 's the values for any set of ordinates, as for point  $k$ , and these combined with the stresses  $S_a$ ,  $S_b$ ,  $S_c$  in Eq. (45A) give the required ordinate  $\eta_k$  for the stress influence line  $S$ . The several ordinates  $\eta$  for all panel points furnish the required influence line. However, much of this work is done graphically as illustrated in Fig. 45A.

**The example is a two-hinged framed arch** with a column supporting the crown, thus involving two external redundant conditions  $X_a$  and  $X_b$  as indicated in Fig. 45A. The loads are vertical and applied to the top chord. Required to find the stress influence line for the chord  $\bar{ik}$ .



The influence lines for  $X_a$  and  $X_b$  are drawn supposedly by the method given in Art. 43. The ordinary stress influence line for the chord  $ik$  is then drawn as indicated and called the  $S_o$  line, meaning that it is the influence line for condition  $X=0$  with  $P=1$ . This line  $A'i'k'B'$  incloses a negative area representing compressive stress in the top chord of a simple truss  $AB$ .

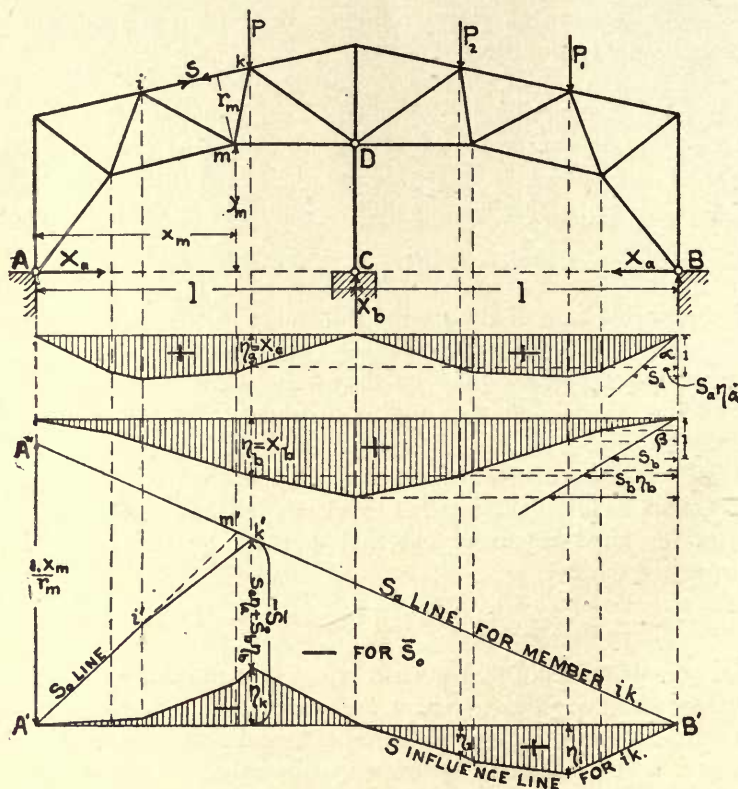


FIG. 45A.

The influence lines  $X_a$  and  $X_b$  are both positive and the stresses  $S_a$  and  $S_b$ , for the member  $ik$ , are found to be negative. The ordinate  $\eta_k$  for the panel point  $k$  is found from Eq. (45A) as

$$\eta_k = -\bar{S}_o + S_a\eta_a + S_b\eta_b, \dots \dots \dots (45c)$$

giving a negative residual for  $\eta_k$ .

In like manner all ordinates for the  $S$  influence line may be found and plotted to give the shaded area  $A'B'$ , which is the influence area for the chord  $ik$ .

The multiplications  $S_a\eta_a$ , etc., can be performed graphically by laying off angles corresponding to  $\tan \alpha = S_a$  and  $\tan \beta = S_b$  as indicated in the figure. The products  $S_a\eta_a$  and  $S_b\eta_b$  are then taken off directly for any ordinate, added or subtracted graphically and the sum  $S_a\eta_a + S_b\eta_b$  is then applied to the ordinate  $\bar{S}_o$  in the proper direction. The angles  $\alpha$  and  $\beta$  are constant for the same member but vary for different members.

The stresses  $S_a = \tan \alpha$  and  $S_b = \tan \beta$  are found from Maxwell diagrams or by computation. It is thus seen that all loads between  $A$  and  $C$  produce compression in the member  $\bar{ik}$ , while all loads between  $C$  and  $B$  will produce tension. The stress resulting from any system of loads is then

$$S = P_1 \eta_1 + P_2 \eta_2, \quad \text{etc.} = \Sigma P \eta, \quad . . . . . (45D)$$

observing the sign of  $\eta$  for each particular point.

Since the large majority of practical problems of redundancy do not, and should not, involve more than one redundant condition, the general case is here treated in less comprehensive manner. For a special method of deriving the influence line for a web member from those of two adjacent chords, see Art. 52.

(b) **One redundant condition** according to Eq. (45A) gives rise to the simple stress equation

$$\eta_m = S = \bar{S}_o - S_a X_a = S_a \left( \frac{\bar{S}_o}{S_a} - X_a \right), \quad . . . . . (45E)$$

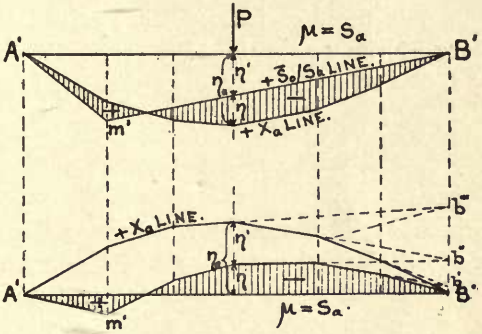
which makes it possible to represent the  $S$  influence area as the area inclosed between the  $X_a$  influence line and the  $\bar{S}_o/S_a$  influence line, which latter is drawn with as much ease as the simple  $\bar{S}_o$  line. The resulting  $S$  influence area will then require a factor  $S_a$  applied to all its ordinates.

These influence areas may be drawn in either of two ways: *First*, by plotting both the  $X_a$  and the  $\bar{S}_o/S_a$  lines from a common straight base, observing the rule that areas above this base are negative, see Fig. 45B. The  $S$  line ordinates  $\eta$  will then be measured between the  $X_a$  line and the  $\bar{S}_o/S_a$  line and these ordinates will be positive when measured down from the  $X_a$  line. *Second*, by first plotting the  $X_a$  line from a straight base and then constructing the  $S$  area by applying the  $+\bar{S}_o/S_a$  ordinates  $\eta'$  down from the  $X_a$  line, see Fig. 45C. In this case the  $+X_a$  ordinates are best plotted above the base so that the  $+\eta$  ordinates of the  $S$  area will appear below the base in the customary way.

The first method is more generally used, though the second leads to a very interesting property by which the  $S$  line may be derived from the  $X_a$  line when one point of the  $S$  line and its zero points are known.

This property is shown in Fig. 45C, where it is seen that over any distance, as  $m'B'$ , for which the  $\bar{S}_o/S_a$  line is straight, the corresponding elements of the  $S$  line and the  $X_a$  line will intersect in points  $b', b'', b'''$  which are in a straight line parallel to  $P$  and passing through the end zero point of the  $\bar{S}_o/S_a$  line.

Further details and applications are not given here, as these will be illustrated in connection with specific problems in Chapter X.



FIGS. 45B, c.

## CHAPTER X

### SPECIAL APPLICATIONS OF INFLUENCE LINES TO STATICALLY INDETERMINATE STRUCTURES

#### ART. 46. SIMPLE BEAM WITH ONE END FIXED AND OTHER END SUPPORTED

The solution by influence lines is illustrated by Figs. 46A, using the general method developed in Art. 45B.

Applying the criterion of Eq. (3c) to this structure, where  $m=1$ ,  $\Sigma r=4$  and  $2p=4$ , gives  $m+\Sigma r-2p=1$ . Hence there is one redundant condition and by Eq. (3E) this condition must be external.

Accordingly, the reaction  $X_a$ , acting at the expansion end  $B$ , is chosen as the redundant support, reducing the beam to a simple cantilever arm as the *principal determinate system*.

The problem is considered solved when the shear and moment influence lines are found for any point  $n$  of the beam. The case of direct loading is assumed.

**The  $X_a$  influence line** is represented by Eq. (42D) as

$$X_a = \frac{1 \cdot \delta_{ma}}{\delta_{aa}}, \dots \dots \dots (46A)$$

where  $\delta_{ma}$  is the variable influence line ordinate at any point  $m$  with  $\mu=1/\delta_{aa}$  is the constant factor, when  $\delta_{ma}$  and  $\delta_{aa}$  may be acutal or measured to the same scale.

The equations for moment and shear at any point  $n$  and for the vertical reaction  $A$ , are given by Eqs. (7A) written in the form of Eq. (45E) as

$$\left. \begin{aligned} M_n &= \overline{M}_o - M_a X_a = M_a \left[ \frac{\overline{M}_o}{\overline{M}_a} - X_a \right] \\ Q_n &= \overline{Q}_o - Q_a X_a = Q_a \left[ \frac{\overline{Q}_o}{\overline{Q}_a} - X_a \right] \\ A &= \overline{A}_o - A_a X_a = A_a \left[ \frac{\overline{A}_o}{\overline{A}_a} - X_a \right] \end{aligned} \right\}, \dots \dots \dots (46B)$$

wherein  $\overline{M}_o$  is the moment about the point  $n$  produced in the principal system by a load unity acting at any point  $m$  of the structure.  $M_a$  is the moment at the point  $n$  due to the conventional loading  $X_a=1$ . Similar definitions follow for  $\overline{Q}_o$ ,  $Q_a$ , also  $\overline{A}_o$  and  $A_a$ .



The following solution by influence lines is based on these Eqs. (46B), when the influence line for  $X_a$  is known or found from Eq. (46A).

The ordinates  $\delta_{ma}$  are ordinates of a deflection polygon drawn for the conventional loading  $X_a=1$  kip, being a load unity acting downward at the point  $B$  when the beam is treated as a cantilever. This deflection polygon is drawn as described in Art. 40, and as shown in Fig. 46Aa.

The  $\overline{M}$  moment diagram for the conventional loading  $X_a=1$ , is drawn by making the end ordinate  $\overline{A'C'}=l$  and drawing  $\overline{C'B'}$ . This end ordinate may be measured to any convenient scale and was drawn to half the scale of lengths, making all the moment ordinates to half scale of lengths. The figured ordinates represent moments, in kip feet, and are scaled at points  $\Delta x=2$  ft. apart.

The areas  $w=\overline{M}\Delta x$  are now computed and treated as elastic loads for the construction of the force polygon (a) and the deflection polygon (b) when the pole distance  $H=EI$

Taking  $E=28000$  kips and  $I=2087$  in.<sup>4</sup> and reducing  $\Delta x$  to inches and  $\overline{M}$  to kip inches, then the pole would be  $\frac{28000 \times 2087}{144}$ . When the scale of lengths is 1:60 then, for deflections 25 times actual, this pole becomes  $H=\frac{28000 \times 2087}{144 \times 60 \times 25}=270.5$   $w$  units. When  $I$  is variable the pole is made variable as was done in Fig. 39A, or the  $w$  loads may be divided by  $I$  as is done in Art. 47.

The force and equilibrium polygons are now drawn, using any convenient scale for the  $w$  forces and the same scale for  $H$ . This gives the deflection polygon  $\overline{A'C'}$ , Fig. 46Ab, with ordinates 25 times actual. Thus the actual end ordinate  $\delta_{aa}=1.96/25$  inches. This same polygon is also the  $X_a$  influence line with a factor  $\mu=1/\eta_B$  irrespective of the scale of ordinates, since all ordinates  $\eta_m$  and  $\eta_B$  are measured with the same scale. To obtain the  $X_a$  influence line with a factor  $\mu=1$ , divide all the ordinates of Fig. 46Ab by the end ordinate  $\eta_B$ , whence the curve  $\overline{A'C'}$ , in Fig. 46Ac, is obtained with the end ordinate  $\overline{B'C'}=1$ , drawn to any convenient scale of ordinates. The redundant reaction  $X_a$  can thus be found for any case of concentrated loads  $P$  and is  $X_a=\Sigma P\eta/\eta_B$ .

**To obtain the  $M_n$  influence area** for moments about the point  $n$ , the  $X_a$  influence line is now combined with the  $\overline{M}_o/M_a$  influence line, with a factor  $\mu=M_a$  according to Eq. (46B).

In Fig. b, the line  $\overline{n'C'}$  represents the  $\overline{M}_o$  influence line provided the end ordinate  $\overline{B'C'}$  is made equal to  $z$ , but this end ordinate is actually  $\eta_B$ , hence the line in question must have a factor  $\mu=z/\eta_B$ . But since  $M_a=z$ , therefore, the same line  $\overline{n'C'}$  becomes the  $\overline{M}_o/M_a$  influence line with a factor  $\mu=1/\eta_B$  which is the same as the factor for the  $X_a$  line. Hence the area  $\overline{A'n'C'}$  represents the  $M_n$  influence area with a factor  $\mu=M_a/\eta_B=z/\eta_B$ .

Similarly in Fig. c, the area  $\overline{A'n'C'}$  represents the  $M_n$  influence area with the factor  $\mu=M_a=z$ , because  $\eta'_B$  was here made equal to unity. This was done to show the two solutions and to illustrate the fact that the second step of drawing the  $X_a$  influence line with  $\mu=1$  is really unnecessary and adds nothing except to simplify the final factor.

The algebraic sign of the  $M_n$  area is derived from Eq. (46B) since the larger  $X_a$  area (which is positive) is subtracted from the positive  $\overline{M}_o/M_a$  area, leaving a negative area as the remainder.



The moment area  $M_m$ , for moments about a point  $m$ , is indicated to show a case where a portion of the area below the  $X_a$  line is positive, creating a load divide at the point  $i$ .

The moment area  $M_A$ , for moments about the abutment  $A$ , is also shown. It is the area between the line  $A'C'$  and the  $X_a$  line, which is entirely a positive area.

In all of these moment influence areas, the moments obtained will be expressed in the same units as the applied loads  $P$  and the ordinate  $z$ . Thus for  $P$  in lbs. and  $z$  in feet the moments will be ft. lbs. The scale of the ordinates  $\eta$  is immaterial and is eliminated in the factor  $\mu$ . Thus if Fig. b is used, the moment about  $n$  for any train of loads would be

$$M_n = -\frac{z}{\eta_B} \Sigma P \eta;$$

and using Fig. c it would be

$$M_n = -z \Sigma P \eta$$

and the units would depend solely on those chosen for  $z$  and the loads  $P$ .

To obtain the  $Q_n$  influence area for shear at the point  $n$ , the  $X_a$  influence line is now combined with the  $\overline{Q_o}/Q_a$  line, with a factor  $\mu=Q_a=1$ , according to Eq. (46B), see Fig. 46Ad.

For a load unity to the right of  $n$ , the shear in the principal system would be  $\overline{Q_o}=1$  and for  $X_a=1$  the shear  $Q_a=1$ , hence  $\overline{Q_o}/Q_a=1$  so that the broken line  $A'n'DC'$  represents the  $\overline{Q_o}/Q_a$  influence line with a factor unity, and the  $Q_n$  influence area is the shaded area with a factor  $\mu=Q_a=1$ , with the portion below the  $X_a$  line positive, as before. Were Fig. b used, the factor would be  $\mu=Q_a/\eta_B=1/\eta_B$ .

The point  $n$  is always a load divide for  $Q_n$ .

The end reaction  $A$  for any system of loads is simply  $\Sigma P - X_a$ , from Eq. (46B), because  $A_o=\Sigma P$  and  $A_a=1$ .

A uniform live load covering the whole span would give  $X_a=3pl/8$ , as may be found from Eq. (15j). The graphic diagram, Fig. 46Ab, gave  $X_a=7.412p=0.372pl$ .

ART. 47. PLATE GIRDER ON THREE SUPPORTS

The example chosen is a general case of unequal spans and variable moment of inertia as illustrated in Figs. 47A. All dimensions in inches, and the loads are directly applied to the girder.

According to the criterion of Eq. (3c) this structure involves one external redundant condition. Any one of the three supports may be taken as the redundant condition, but it is generally most convenient to assume the middle support at  $C$  and thus obtain the principal system as a simple beam on two supports  $A$  and  $B$ .

The  $X_c$  influence line for the redundant support is again given by Eq. (42d) as

$$X_c = \frac{1 \cdot \delta_{mc}}{\delta_{cc}}, \quad \dots \dots \dots (47A)$$

where  $\delta_{mc}$  is the variable influence line ordinate at any point  $m$  with the constant factor  $\mu=1/\delta_{cc}$ , and  $\delta_{mc}$  and  $\delta_{cc}$  must be measured to the same scale. The ordinates  $\delta_{mc}$  are



the ordinates of a deflection polygon drawn for the conventional loading  $X_c=1$  kip, acting downward at  $C$  on the principal system or simple beam  $\overline{AB}$ .

This deflection polygon is the equilibrium polygon drawn for a series of elastic loads  $w = \overline{M} \Delta x / I$  when the pole  $H=E$ . The variable moment of inertia is not taken care of in the manner previously given, by varying the pole distance, but the alternative method of involving  $I$  in the  $w$  loads is here employed. The moments of inertia are given for the various sections of the beam in Fig. 47Aa. The  $\overline{M}_o$  diagram for  $X_c=1000$  lbs. is drawn in Fig. 47Ab, with an ordinate under the point  $C$  equal to  $1000 l_1 l_2 / l = 175,000$  in. lbs.

The several  $\overline{M}$  ordinates are scaled from the diagram or computed, and these values divided by the corresponding  $I$ 's furnish the figures for plotting the  $\overline{M}/I$  diagram. Thus the ordinate at  $C$  is  $175000 \div 34982 = 5.00$ . The  $w$  loads are then computed as the areas of the  $\overline{M}/I$  diagram using the horizontal distances between the ordinates in inches. These loads are applied at the centers of gravity of the respective areas.

The  $w$  loads are now combined into a force polygon, Fig. 47Ac, with pole  $H=E/100 \times 120 = 2333$   $w$  units, all drawn to the same scale, but this scale may be taken as any convenient one without regard to the deflections. The particular pole will then give deflections one hundred times actual, because the scale of lengths for the girder span was chosen 1:120 and the pole was made  $100 \times 120 = 12000$  times too small.  $E = 28,000,000$  lbs. per sq. inch. The resulting equilibrium polygon  $\overline{A'C'B'}$ , Fig. 47Ac, is the deflection polygon for the load  $X_c=1000$  lbs. with ordinates 100 times actual and it is also the  $X_c$  influence line with a factor  $1/c$  where  $c$  is the ordinate under  $C$  measured to the same scale as the other influence ordinates.

It is clear from Eq. (47A) that the scale of the influence ordinates is immaterial so long as the same scale is used for the ordinate  $c$ , but when actual deflections are sought then a natural scale, as inches, must be employed.

The reaction  $X_c$  for any case of concentrated loads may then be found from Fig. 47Ac, by multiplying the loads by the  $\delta$  ordinates and dividing the sum of these products by  $c$ , thus  $X_c = \Sigma P \delta / c$ , where  $c$  and the  $\delta$ 's are measured to the same convenient scale.

**The A and B influence areas** are easily found when the  $X_c$  line is given. Thus in Fig. 47Ac, the line  $\overline{B'C'A''}$  represents the  $\overline{A_o}/A_a$  influence line with some factor, and the shaded area is the  $A$  influence area with a factor  $1/\eta_A$  to be proven.

For this proof the end ordinate  $\overline{A'A''}$  is evaluated according to Eq. (46B), and the factor required for this ordinate will be the factor for all ordinates  $\eta$  of the  $A$  influence area.

For the point  $A$ ,  $\overline{A_o}=1$  and  $A_c=1 \cdot l_2/l$  and  $X_c$  has the factor  $1/c$ . Hence  $\overline{A_o}/A_c = l/l_2$  and the end ordinate should be

$$A = A_c \left[ \frac{\overline{A_o}}{A_c} - X_c \right] = \frac{l_2}{l} \left[ \frac{l}{l_2} - \frac{X_c}{c} \right] = \frac{l_2}{cl} \left[ \frac{cl}{l_2} - X_c \right], \quad \dots \quad (47B)$$

where the factor is  $l_2/cl$ .

But  $\frac{l_2}{cl} = \frac{A_c}{c} = \frac{1}{\eta_A}$ , hence the factor is simply  $1/\eta_A$ .

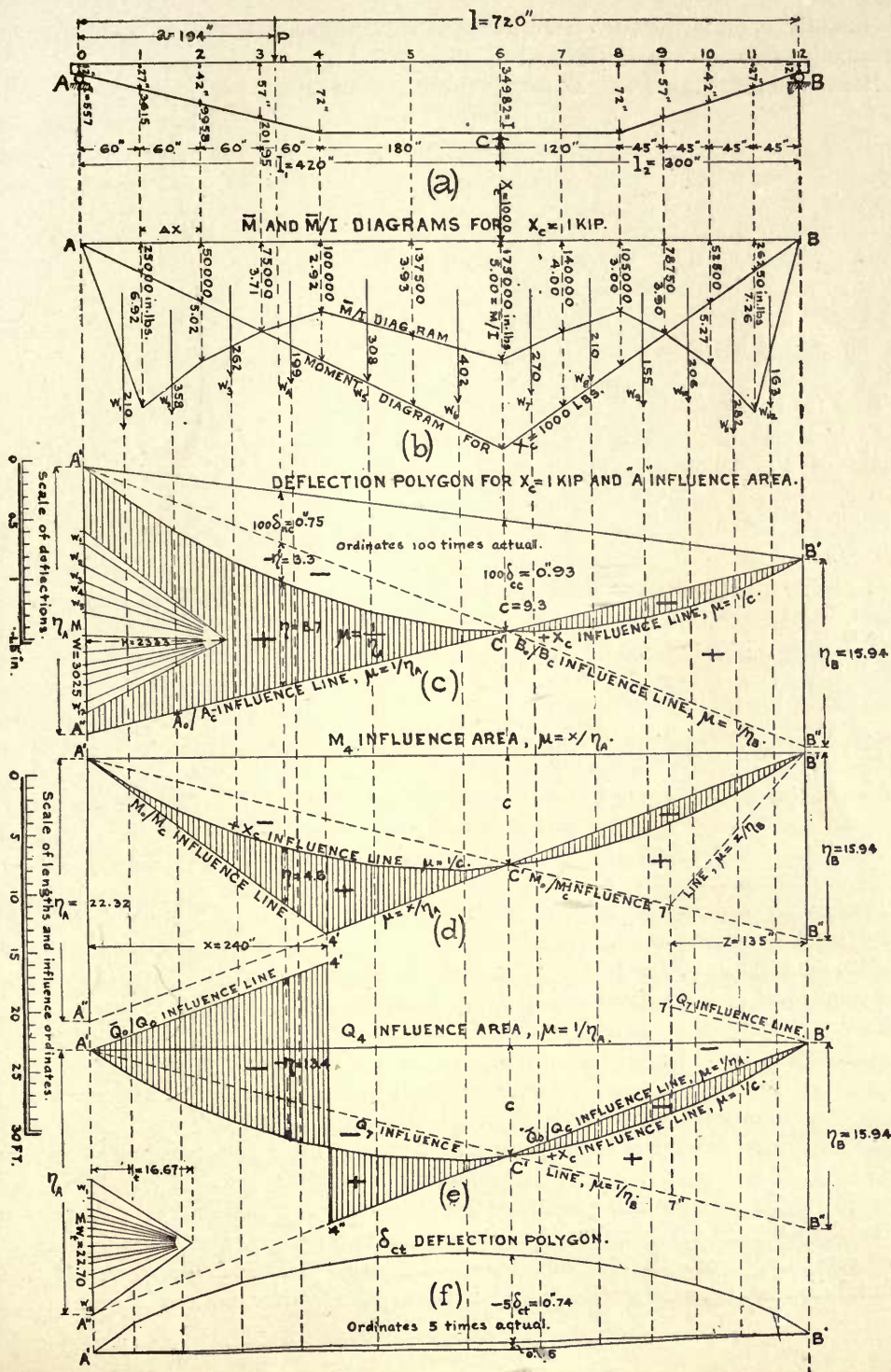


FIG. 47A.



Similarly  $1/\eta_B$  is the factor for the  $B$  influence area indicated in Fig. 47Ac as the area included between the  $X_c$  line and the line  $\overline{A'C'B''}$ .

Hence the reactions  $A$  and  $B$ , for any train of concentrated loads, become

$$A = \frac{1}{\eta_A} \sum P \eta \quad \text{and} \quad B = \frac{1}{\eta_B} \sum P \eta'. \quad (47c)$$

The algebraic signs of the areas are determined as before. All areas below the  $X_c$  line are positive and those above this line are negative. The ordinates may be measured with any scale so long as the same scale is used for all.

**The  $M$  influence area** is a portion of the  $A$  area for all points between  $A$  and  $C$ , while for points between  $C$  and  $B$  the  $M$  area is a portion of the  $B$  area. See Fig. 47Ad.

Thus for the point 4 the  $M_4$  influence area is shown as the shaded area between the  $X_c$  line and the broken line  $\overline{A'4'B'}$ . The factor is  $M_c/c = x/\eta_A$ , where  $x$  is the ordinate of the point 4. When  $x$  is expressed in feet the resulting moment is in ft. lbs.

Similarly the  $M_7$  influence area is indicated by dotted lines and the factor is  $M_c/c = x/\eta_B$ .

The usual directions as to algebraic signs and scales apply as before.

**The  $Q$  influence area** for shear is shown, in Fig. 47Ae, for the point 4 as the shaded area with a factor  $Q_c/c = 1/\eta_A$  the same as for the  $A$  influence area. The line  $\overline{A'4'}$  is parallel to  $\overline{B'C'4''}$ .

Similarly the  $Q_7$  influence area is indicated by dotted lines and has a factor  $Q_c/c = 1/\eta_B$ .  $\overline{B'7'}$  is parallel to  $\overline{A'C'7''}$ . The signs are again determined with reference to the areas above and below the  $X_c$  line.

All of these influence areas have a load divide at the point  $C'$  and the  $Q$  areas have two load divides each. This determines the positions of train loads for positive and negative effects, and to obtain maximum effects, the heaviest loads should be placed over the maximum ordinates.

**Temperature effects.** A uniform change in temperature will expand the girder equally in all directions and will produce a slight lifting of the ends  $A$  and  $B$  equal to  $\epsilon t(72-12) = 0.0105$  inch, for  $t = 25^\circ$  F. and  $\epsilon = 0.000007$ . When the three supports are on the same level then no stress will be produced by uniform temperature changes.

However, when the sun shines down on such a structure experience teaches that the top flange is heated much more than the bottom flange and this difference in temperature may become quite considerable and will cause the girder to assume a curved position, convex upward, when the top flange is warmer than the bottom.

The maximum difference in temperature between the two flanges is bound to remain somewhat problematic, but observations indicate that differences of  $30^\circ$  F. are quite common. In the present example  $\Delta t = +20^\circ$  F. will be assumed and on this basis and that the temperature varies uniformly between the two flanges, a set of  $w_t$  elastic loads is now computed from the formula  $w_t = -\epsilon \Delta t \Delta x / h = -0.00014 \Delta x / h$ , where  $\Delta x$  is the horizontal distance between sections and  $h$  is the depth of girder, both in inches.



The following table gives the  $w_t$  loads:

Point.	$\Delta x$ Inches.	$h$ Inches.	$w_t$	$10,000w_t$	Point.	$\Delta x$ Inches.	$h$ Inches.	$w_t$	$10,000w_t$
1	60	19.5	0.00043	4.3	7	60	72	0.000117	1.17
2	60	34.5	0.00024	2.4	8	60	72	0.000117	1.17
3	60	49.5	0.00017	1.7	9	45	64.5	0.000098	0.98
4	60	64.5	0.000115	1.15	10	45	49.5	0.000127	1.27
5	90	72	0.000175	1.75	11	45	34.5	0.000183	1.83
6	90	72	0.000175	1.75	12	45	19.5	0.000323	3.23

An equilibrium polygon drawn for these  $w_t$  loads with a pole distance unity, would represent the deflection curve of the beam due to  $\Delta t$ . However, for convenience it is better to multiply these small loads  $w_t$  by some factor as 10,000 and then make the pole distance 10,000 instead of unity.

The scale of lengths for the girder was made 1:120 and if the ordinates are to appear say 5 times actual, the pole distance should be made equal to  $H=10,000/5 \times 120 = 16.67$ , using the scale chosen for the  $w_t$  loads.

Fig. 47Af shows the force and equilibrium polygons for the  $w_t$  loads, with ordinates *five* times actual. Since these  $w_t$  loads are all negative for  $+\Delta t$ , the  $\delta_{ct}$  deflection curve was drawn above the closing line  $\overline{A'B'}$ . The ordinate under the point  $C$  represents  $5\delta_{ct}$  and this must be increased by the small ordinate  $5 \times 0.0105$ , previously found for the uniform rise in temperature to obtain total effect.

According to Eq. (44c), the redundant reaction produced by this temperature effect is  $X_{ct} = \delta_{ct} / \delta_{cc}$ . The deflection polygon for  $X_c = 1$  kip, gives  $100\delta_{cc} = 0''.93$ , whence  $+\delta_{cc} = 0''.0093$ , and the  $\delta_{ct}$  deflection polygon gives  $-5\delta_{ct} = 0''.74 + 0.05 = 0''.79$ , making  $\delta_{ct} = -0''.16$ .

Hence  $X_{ct} = \delta_{ct} / \delta_{cc} = -0.16 / 0.0093 = -17.2$  kips, which indicates a downward reaction at  $C$  to maintain the girder on the middle support. As the entire girder has an approximate weight of 7440 lbs. the above temperature effect would lift the girder off the center support and cause the beam to carry itself on two supports, producing a compression of about 3100 lbs. per sq.in. on the extreme fiber. This temperature stress would not, however, be fully developed unless the span is loaded down in contact with the center support.

The dead and live load stresses must finally be combined with the temperature effect to obtain the real stress at any point.

**The application of these influence areas** is illustrated by placing a single load  $P_n$  at any point  $n$  of the span and showing the values of the several functions. The same process is followed for each load of a train of loads and the total effect of the train is the sum of the individual load effects.

The ordinates  $\eta$  under the point  $n$ , in each of the influence areas, are all scaled to the same scale to which  $\eta_A$  and  $\eta_B$  are measured. This may be any convenient scale, which is universally used for all ordinates of the drawing.

The values of the various functions for the load  $P_n$  are

$$X_c = \frac{P_n \delta_n}{c} = \frac{7.5}{9.3} P_n = 0.807 P_n;$$

$$A = \frac{P_n \eta}{\eta_A} = \frac{8.7}{22.32} P_n = 0.390 P_n;$$

$$B = -\frac{P_n \eta'}{\eta_B} = -\frac{3.3}{15.94} P_n = -0.207 P_n;$$

$X_c + A + B = P$ , which checks to 1 per cent.

$$M_4 = \frac{\eta x P_n}{\eta_A} = \frac{4.6 \times 240}{22.32} P_n = 49.4 P_n \text{ in.lbs. for } P_n \text{ lbs.}$$

$$Q_4 = -\frac{\eta P_n}{\eta_A} = -\frac{13.4}{22.32} P_n = -0.600 P_n;$$

$$M_{4t} = \frac{X_c l_2 a}{l} = \frac{17200 \times 300 \times 194}{720} = 1,390,330 \text{ in.lbs.}$$

#### ART. 48. TRUSS ON THREE SUPPORTS

Figs. 48A illustrate the analysis by influence lines of a truss on three supports. The bottom chord is the loaded chord and the lengths and cross-sections of the members are written over the members in Fig. a, while the stress  $S_A$ , produced by a unit reaction at  $A$  on the simple span  $\overline{AB}$ , are written below the members. The stress diagram, from which the  $S_A$  stresses are found, is shown in Fig. b. The solution is similar to that given in Art. 47.

As in the previous problem, Art. 47, the present structure involves one external redundant condition, which is again taken as the middle support  $C$ , reducing the truss to a principal system on two supports,  $A$  and  $B$ .

The  $X_c$  influence line is derived from Eq. (42D) as in the previous problem and becomes

$$X_c = \frac{1 \cdot \delta_{mc}}{\delta_{cc}}, \quad \dots \dots \dots (48A)$$

where the variable influence line ordinate  $\delta_{mc}$  is the ordinate for a deflection polygon, drawn for the loaded chord and for the conventional loading  $X_c = 1$  kip acting downward at  $C$  on the principal system or simple truss  $\overline{AB}$ . The influence line factor  $\mu = 1/\delta_{cc}$ .

The elastic loads for this deflection polygon are found from Eqs. (36B) as:

$$w = \frac{\overline{M}_c l}{EFr^2}, \quad \dots \dots \dots (48B)$$

for each pin point of the top and bottom chords. The effect of the web members is usually neglected as being insignificant, but when it is desired to include their effect, Eqs. (36c) will give the  $w$  loads due to the web members and these are added to the

chord loads found from Eq. (48B). See Art. 36, for a complete discussion of this method, and Art. 50 for a complete problem.

A Williot-Mohr diagram might also be employed to obtain this deflection polygon. See also the example in Art. 50, Fig. 50B.

In the present example the web system will be neglected and the  $w$  loads are found for the chords, using Eq. (48B). The moments  $\overline{M}$  are those produced by the conventional loading  $X_c=1000$  lbs. and are represented in the moment diagram, Fig. b, expressed in inch-lbs. The ordinate at the point  $C$  will be  $Pl/4=528,000$  in. lbs.

Using these moments and the values for  $l$ ,  $F$  and  $r$  given, in Fig. a, for each member, the following computation of the  $w$  forces is made:

$w$	Member.	$\overline{M}_c$ Inch-lbs.	$l$ Inch.	$F$ Square Inches.	$r$ Inch.	$\frac{\overline{M}_c l}{Fr^2}$
1	$L_0L_2$	127,125	508.5	22.7	384	14.8
2	$U_1U_3$	254,250	509.0	42.0	384	20.8
3	$L_2L_4$	381,375	508.5	22.7	384	57.7
4	$U_3U_5$	528,000	299.3	44.7	434.9	$2 \times 18.7$
5	$L_4L_6$	381,375	508.5	22.7	384	57.7
6	$U_5U_7$	254,250	509.0	42.0	384	20.8
7	$L_6L_8$	127,125	508.5	22.7	384	14.8
$\Sigma w =$						224.0

The modulus  $E=29,000,000$  lbs. per sq. inch, was not embodied in the tabulated values, hence the  $w$  loads are  $E$  times too large and the deflections would be natural size for a pole  $H=E$ . But the scale of lengths of the drawing was 1:300, and wishing to make the deflections 400 times actual the pole must be made equal to  $E/300 \times 400 = 241.7w$  units.

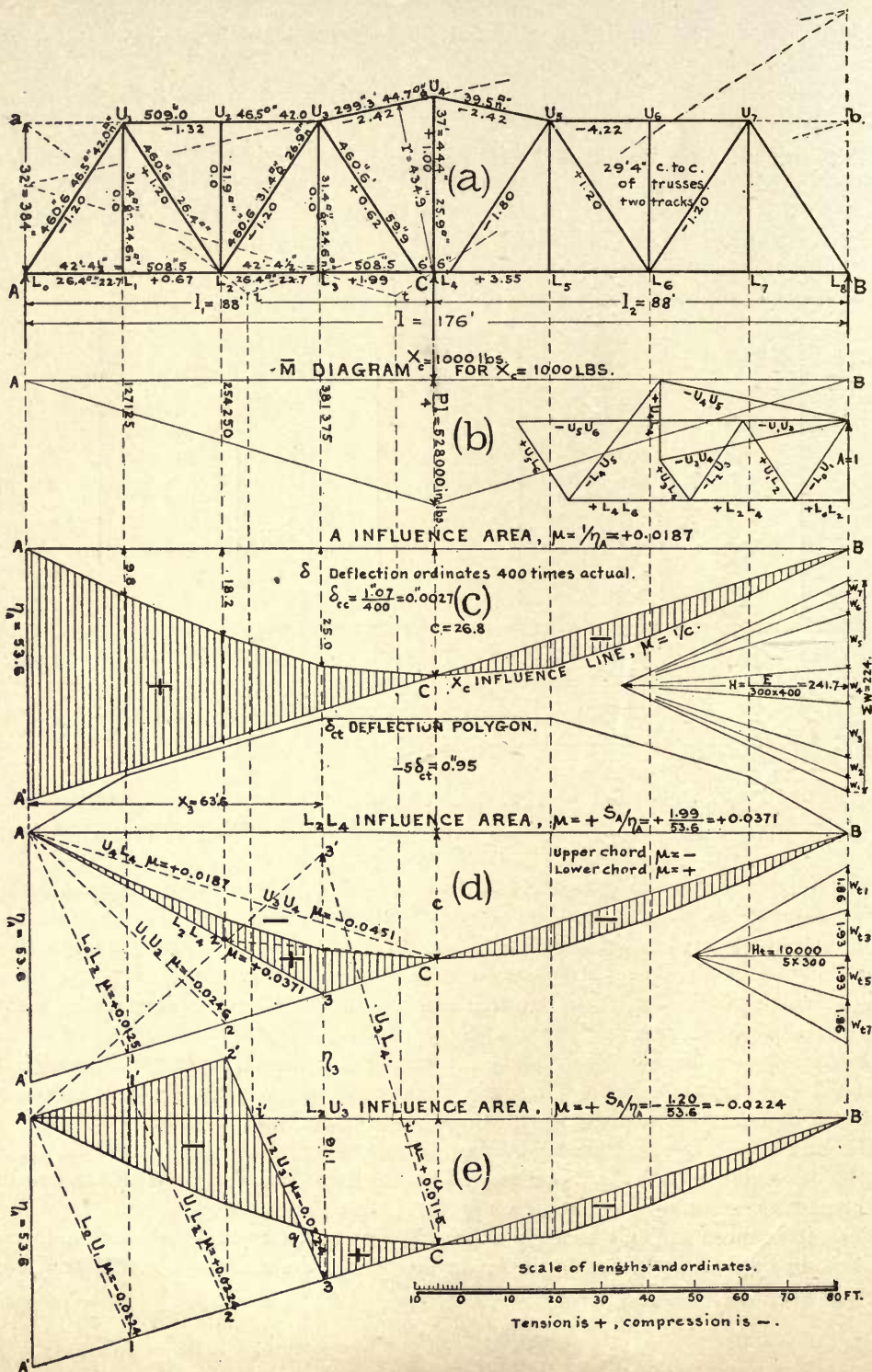
The force and equilibrium polygons, Fig. c, are then drawn, using any convenient scale for  $w$  forces. The  $X_c$  influence line is thus found as the polygon  $ACB$ , with a factor  $\mu=1/c$ . The actual deflection of the point  $C$  is  $\delta_{cc}=1''.07/400=0''.0027$ , obtained by measuring the ordinate  $c$  in inches. All influence ordinates are measured with the same scale, which may, however, be any convenient scale, because the factor  $\mu$  makes the quotients  $\delta_{mc}/\delta_{cc}$  independent of an absolute scale. For this same reason the  $\overline{M}$  diagram might have been drawn with any middle ordinate as unity, though when the actual deflection  $\delta_{cc}$  is wanted for temperature investigations, the method here given is less confusing.

The **A influence area** is now found by combining the  $X_c$  influence line with the ordinary  $A$  line for the span  $AB$ , in such manner as to make the ordinate at  $C$  equal to zero and then finding the factor  $\mu$  which reduces the ordinate at  $A$  to unity.

The line  $A'CB$ , Fig. c, is the ordinary  $A$  influence line with a factor  $1/\eta_A$ , and when this is combined with the  $X_c$  influence line, the areas included between the two lines will represent the  $A$  influence area with a factor  $\mu=1/\eta_A=0.0187$ .

Since it is more difficult to redraw the  $X_c$  line so as to make the ordinate  $c=1$ , than it is to apply the factor  $\mu$ , the latter method is decidedly preferable to the one frequently given.





The point  $C$  is a load divide for both reactions  $A$  and  $B$ , and in the present case the same influence area will serve for both these reactions, because  $l_1 = l_2$ . When the spans are unequal, then the  $B$  influence area is included between the  $X_c$  line and the line  $\overline{AC}$  prolonged to the vertical through  $B$  and the factor then becomes  $\mu_B = 1/\eta_B$ .

**The influence area for a chord member  $L_2L_4$**  is obtained by combining the ordinary  $S_o$  stress influence line of the member for the principal system with the  $X_c$  influence line, Fig. d.

A load at  $C$  can produce no stress in any member of the indeterminate truss, hence the ordinate under  $C$ , for every stress influence line, must be zero. Therefore, the line  $\overline{BCA'}$  must be common to all stress influence lines of the members between  $A$  and  $C$ , web members included. The point  $C$  must be a load divide for all members.

The center of moments for the chord  $L_2L_4$  is at  $U_3$ , hence the line  $\overline{A3}$ , Fig. d, completes the  $S_o$  stress influence line with a factor  $S_A/\eta_A$ , where  $S_A$  is the stress in the chord  $L_2L_4$  for a unit reaction at  $A$ .

The area included between the  $X_c$  polygon and the  $S_o$  influence line is thus the required influence area for the chord  $L_2L_4$  with the factor  $\mu = S_A/\eta_A$ . The area below the  $X_c$  polygon is positive as usual. The stress  $S_A = +1.99$ , hence the factor  $\mu = +1.99/53.6 = +0.0371$ .

If the vertical  $L_3U_3$  were absent, then the  $S_o$  line would have to be straight over the panel  $L_2L_4$  and a line  $\overline{2C}$  would be necessary to complete the  $S_o$  influence line. With the member  $L_3U_3$  acting, the chord stress  $L_2L_4$  is, therefore, greater than when the vertical is omitted.

The  $S_o$  influence lines and their factors for all chord members are shown by dotted lines in Fig. d, and the final influence areas are always positive below the  $X_c$  line. The factors  $\mu$  are negative for the top chords because  $S_A$  is then negative.

The stress in the member  $L_2L_4$ , for any train of moving loads, is expressed by

$$S = \frac{S_A}{\eta_A} [P_1\eta_1 + P_2\eta_2 + P_3\eta_3, \dots] \dots \dots \dots (48c)$$

where each  $\eta$  is the ordinate of the shaded influence area vertically under its respective load  $P$  and  $S_A$  is given in the same units as the loads.

This influence area is also the  $M_3$  influence area with a factor  $\mu = x_3/\eta_A$  and gives moments in foot units when  $x_3$  is measured in feet as indicated.

The scale of the influence ordinates is immaterial so long as all ordinates are measured with the same scale. This is apparent from Eq. (48a).

**The influence area for a web member  $L_2U_3$**  is found from exactly similar considerations as those shown to exist for the chords. The shaded area in Fig. e is the influence area for the web member  $L_2U_3$ . The  $S_o$  lines for the other web members are indicated by dotted lines.

The line  $\overline{BCA'}$ , Fig. e, is again one of the limiting lines of the  $S_o$  influence line for each web member, and when the chords are parallel in the panel containing the particular web member, then the other limiting line  $\overline{A2'}$  will be parallel to  $\overline{BC}$  and the line  $\overline{2'3}$  completes the  $S_o$  line for the member  $L_2U_3$ .

The load divide  $i$  for this member, considering the principal system, must fall



vertically over the point  $i'$  where the line  $\overline{2'3}$  intersects the base line  $\overline{AB}$ . This serves as a check or when the chords are not parallel, as in the panel  $L_3L_4$ , then it may be used to complete the  $S_o$  line as indicated for the member  $U_3L_4$  with the load divide  $t$ .

In case the chords are not parallel and the center of moments for the diagonal falls outside the drawing, then the ordinate  $\eta_3$  as for the member  $U_3L_4$ , may be computed from the formula

$$\frac{\eta_3}{\eta_A} = \frac{x_3 + a_3}{a_3} \quad \text{or} \quad \eta_3 = \left( \frac{x_3 + a_3}{a_3} \right) \eta_A = \left( \frac{63.6 + 91}{91} \right) 53.6, \quad \dots \quad (48D)$$

where  $x_3$  is the distance  $L_0L_3$  from  $A$  to the panel containing the web member, and  $a_3$  is the distance from  $A$  to the center of moments of the member, both in the same units, as feet.

The factor  $\mu = S_A/\eta_A$  again applies and the sign of  $S_A$  determines the sign for  $\mu$ .

**Stresses due to temperature.** When the three supports  $A$ ,  $B$  and  $C$  are on the same level then a uniform change in temperature produces no stresses in the structure. However, when the sun illuminates the bridge from above, there is usually a difference in the temperature of the two chords. Assuming this difference as  $\Delta t = 20^\circ$  F. as in Art. 47, then the bottom chord would be cooler than the top chord by this amount and the changes in the lengths of the bottom chord members would be  $-\epsilon \Delta t l$  and the  $w_t$  elastic loads would be

$$w_t = -\frac{\Delta l}{r} = -\frac{\epsilon \Delta t l}{r}, \quad \dots \quad (48E)$$

These loads being extremely small, it is well to multiply them by say 10,000 and then using a pole distance of 10,000, the  $\delta_{ct}$  deflections would be natural size. However, the scale of lengths on the drawing was 1:300 and for deflections five times natural the pole becomes

$$H_t = \frac{10000}{5 \times 300} = 6.67 w_t \text{ units.}$$

The loads  $w_t$  are figured for the panel points 1, 3, 5 and 7, taking  $\epsilon = 0.000007$ ,  $\Delta t = 20^\circ$  F. and  $r = 384$  inches. The  $\delta_{ct}$  deflection polygon is shown in Fig. d, and has negative deflections, five times actual. Hence  $\delta_{ct} = 0''.95/5 = 0''.19$  and  $\delta_{cc}$  was previously found from Fig. e, as  $0''.0027$ , hence from Eq. (44c)

$$X_{ct} = -\frac{\delta_{ct}}{\delta_{cc}} = -\frac{0.19}{0.0027} = -70.4 \text{ kips.} \quad \dots \quad (48F)$$

This value is in kips because  $\delta_{cc}$  is the actual deflection for one kip, and  $X_{ct}$  being negative produces the same effect on the principal system as a load  $X_{ct}$  hung at the point  $C$ . The reaction at  $A$ , due to a load of 70.4 kips at  $C$ , would then be  $A_t = 70.4 l_2 / (l_1 + l_2) = +35.2$  kips.

The stresses in the members are then  $S_t = S_A A_t = 35.2 S_A$  kips. The stresses  $S_A$ , due to a unit reaction at  $A$ , are already found in Fig. b, hence the temperature stresses are readily determined. Thus for the member  $U_3U_4$ ,  $S_A = -2.42$ , hence  $S_t = -2.42 \times 35.2 = -85.2$  kips. The negative sign indicates compression.



## ART. 49. TWO-HINGED SOLID WEB ARCH OR ARCHED RIB

This and the two-hinged framed arch are perhaps the most common structures involving external redundancy which are met with in practice. They will receive special attention here as deserving a prominent place among commendable structures. The external redundancy may be said to offer less objection here than in any other class of structures.

The present theory will be developed in its most general application to unsymmetric arches and will be equally applicable to masonry, concrete or steel arched ribs.

Fig. 49A represents an unsymmetric two-hinged arched rib of any cross-section and the lettered dimensions are in general the same as those previously employed for three-hinged arches in Art. 28.

The arch thrust along  $\overline{AB}$  is treated as the external redundant condition. When it is removed, by replacing the hinged support at  $A$  by a roller bearing, the simple beam  $\overline{AB}$  (though curved) on two supports, then becomes the principal system.

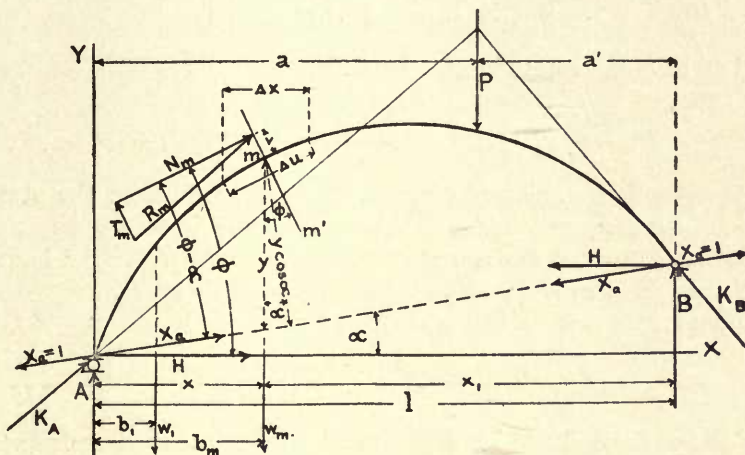


FIG. 49A.

According to Eqs. (7A), the following values for the reactions, thrusts and moment for any point  $m$  may be written:

$$\left. \begin{aligned} A &= A_o - A_a X_a, \quad \text{where} \quad A_o = \frac{\sum P a'}{l} \quad \text{and} \quad A_a = -1 \cdot \sin \alpha \\ B &= B_o - B_a X_a, \quad \text{where} \quad B_o = \frac{\sum P a}{l} \quad \text{and} \quad B_a = 1 \cdot \sin \alpha \\ M_m &= M_o - M_a X_a, \quad \text{where} \quad M_o = A_o x - \sum_0^x P(a' - x') \quad \text{and} \quad M_a = 1 \cdot y \cos \alpha \\ N_m &= N_o - N_a X_a, \quad \text{where} \quad N_o = Q_o \sin \phi; \quad N_a = -1 \cdot \cos(\phi - \alpha) \\ T_m &= T_o - T_a X_a, \quad \text{where} \quad T_o = Q_o \cos \phi = (A_o - \sum_0^x P) \cos \phi; \quad T_a = 1 \cdot \sin(\phi - \alpha) \end{aligned} \right\} \quad (49A)$$

in which  $A$  and  $B$  are the vertical end reactions;  $M_m$  is the moment of the external forces about any axial point  $m$ ;  $R_m$  is the resultant thrust, on the normal section  $mm'$ , produced by all the external forces acting on one side of this section;  $N_m$  is the component of  $R_m$ , normal to the section  $mm'$ ; and  $T_m$  is the tangential component of  $R_m$  in the section  $mm'$ .  $Q_o$  is the vertical shear at any point  $m$  produced by all the loads  $P$  acting on a simple beam  $\overline{AB}$ . The conventional loading  $X_a=1$  is applied as indicated in the opposite direction of  $X_a$ .

Eqs. (49A), with the special values inserted, thus become

$$\left. \begin{aligned} A &= \frac{\Sigma Pa'}{l} + X_a \sin \alpha \\ B &= \frac{\Sigma Pa}{l} - X_a \sin \alpha \\ M_m &= M_o - X_a y \cos \alpha \\ N_m &= Q_o \sin \phi + X_a \cos (\phi - \alpha) \\ T_m &= Q_o \cos \phi - X_a \sin (\phi - \alpha) \end{aligned} \right\}, \quad \dots \dots \dots (49B)$$

where  $M_o$  and  $Q_o$  have the values in Eqs. (49A).

From Fig. 49A,

$$M_m = N_m v; \quad R_m = \sqrt{N_m^2 + T_m^2}; \quad H = X_a \cos \alpha. \quad \dots \dots (49C)$$

In the above equations, all terms except  $X_a$  are derived from the static conditions and the solution becomes possible when  $X_a$  is determined.

**The  $X_a$  influence line for the redundant haunch thrust.** When the haunches are on the same level then this thrust  $X_a$  becomes the horizontal thrust  $H$ .

The equation for  $X_a$  is given by Eq. (42D) as

$$X_a = \frac{1 \cdot \delta_{ma}}{\delta_{aa}}, \quad \dots \dots \dots (49D)$$

where  $\delta_{ma}$  is the vertical deflection ordinate of any point  $m$  of a deflection polygon, drawn for the loaded chord and for the conventional loading  $X_a=1$  applied to the principal system; and  $\delta_{aa}$  is the change in the length  $\overline{AB}$ , due to  $X_a=1$  acting on the principal system.

Since  $\delta_{ma}$  and  $\delta_{aa}$  are not parallel displacements, they cannot be obtained from the same deflection polygon as in the previous examples, Arts. 46–48. This circumstance necessitates the construction of an extra displacement polygon for  $\delta_{aa}$ , if the graphic solution is strictly followed, or of finding  $\delta_{aa}$  by computation, which is usually advisable.

The  $X_a$  influence line thus becomes the  $\delta_{ma}$  deflection polygon with a factor  $\mu=1/\delta_{aa}$ . Should this deflection polygon be constructed for a pole distance  $H=\delta_{aa}$  then the factor  $\mu=1$ .

According to Art. 40, the  $\delta_{ma}$  deflection polygon is the equilibrium polygon drawn for a set of elastic loads  $w$  with a pole distance  $H=1$ . These elastic loads represent partial areas of a moment diagram drawn for the conventional loading  $X_a=1$ .





which is the effect due to  $N_a$  only, and this added to the displacement previously found for moments only, gives the total displacement

$$\delta_{aa} = \sum_0^l wy \cos \alpha + \sum_0^l \frac{\cos^2 (\phi - \alpha) \Delta x}{\cos \phi EF} \quad (49\text{HH})$$

Hence, when axial thrust is to be considered in Eq. (49H), then the value  $\delta_{aa}$  should be computed from Eq. (49HH) and used as the pole distance  $H$  in drawing the equilibrium polygon for the elastic loads  $w$ . When the loads  $w$  are taken  $E$  times actual, then the  $E$  in the second term of Eq. (49HH) is omitted.

**Temperature stress.** For any change in temperature above or below the normal,  $X_{at}$  is expressed by Eq. (44c) as

$$X_{at} = \frac{1 \cdot \delta_{at}}{\delta_{aa}}, \quad (49\text{I})$$

wherein  $\delta_{at}$  is the change in the distance  $\overline{AB}$  due to any change in temperature of  $\pm t^\circ$  acting on the principal system.

**When the structure retains a uniform temperature** then the change  $\pm t^\circ$  will be uniform in all directions so that the shape of the structure will always be similar to its normal geometric shape. Hence, the distance  $\overline{AB}$  will change as for any case of linear expansion and

$$\delta_{at} = \pm \frac{\epsilon t l}{\cos \alpha} = \pm \frac{0.000488 l}{\cos \alpha}, \quad (49\text{J})$$

for  $\epsilon = 0.0000065$  per  $1^\circ\text{F}$ ., and  $t = \pm 75^\circ$ .

**When the change in temperature is not uniform**, as when the upper flange is  $+t^\circ$  warmer than the lower flange, then  $\delta_{at}$  must be found from a deflection polygon drawn for a set of  $w_t$  elastic loads computed from the formula  $w_t = -\epsilon \Delta t \Delta u / D$ , where  $D$  is the depth of section and  $\Delta u$  is the length between sections measured along the axis. The pole distance, if made equal to unity, will give the actual  $\delta_{at}$ , and if the pole be made equal to  $\delta_{aa} = \sum wy \cos \alpha$  as for  $X_a$ , then the displacement found will be  $X_{at}$  measured parallel to  $\overline{AB}$ . The  $w_t$  loads must likewise be taken parallel to  $\overline{AB}$  in drawing the force and equilibrium polygons since  $\delta_{at}$  is a displacement along  $\overline{AB}$ .

$X_{at}$  will be positive for  $+t$ , while for  $-t$  the  $w_t$  loads are negative and  $X_{at}$  would also be negative.

In any case, when  $X_{at}$  is determined, then the quantities  $M_{mt}$ ,  $N_{mt}$ , and  $T_{mt}$  are found from Eqs. (49B) by omitting all the terms involving the effects of the loads  $P$ , thus:

$$\left. \begin{aligned} M_{mt} &= -X_{at} y \cos \alpha = N_{mt} v \\ N_{mt} &= X_{at} \cos (\phi - \alpha) \\ T_{mt} &= -X_{at} \sin (\phi - \alpha) \end{aligned} \right\} \quad (49\text{K})$$

**Abutment displacements.** When the abutments undergo displacements  $\Delta r$  in the directions of the reaction forces  $R$ , then, for the case of external redundancy where  $\delta_a = 0$ , Eq. (8D) gives for  $P = 0$ ,

$$X_{ar} \delta_{aa} = -\sum R_a \Delta r,$$







When the section is symmetric about a horizontal gravity axis, which is usually the case, then these equations give, for  $e=i=D/2$ , or the half depth between extreme fibers,

$$\left. \begin{aligned} k &= k_e = k_i = \frac{r^2}{e} = \frac{I}{Fe} = \frac{2I}{FD} \\ f_e &= -\frac{M_e}{Fk} \quad \text{and} \quad f_i = \frac{M_i}{Fk} \\ N &= \frac{M_e - M_i}{2k} \quad \text{and} \quad v = \frac{k(M_e + M_i)}{M_e - M_i} = \frac{M_e + M_i}{2N} \end{aligned} \right\} \dots \dots \dots (49R)$$

For a rectangular section of unit thickness and of depth  $D$ , making  $e=i=D/2$ .

$$\left. \begin{aligned} k &= \frac{r^2}{e} = \frac{D}{6}, \quad F = 1 \cdot D, \quad I = \frac{1 \cdot D^3}{12} \\ f_e &= -\frac{6M_e}{D^2}, \quad f_i = \frac{6M_i}{D^2} \\ N &= \frac{3}{D}(M_e - M_i) \quad \text{and} \quad v = \frac{M_e + M_i}{2N} \end{aligned} \right\} \dots \dots \dots (49S)$$

In all the above formulæ  $M_e$  and  $M_i$  have opposite signs when  $N$  acts between the two kernel points  $e$  and  $i$ . When  $v > k_i$ , both moments are negative and when  $v$  is negative and larger than  $k_e$ , both moments are positive. The figure shows  $v$  to be positive when measured from the gravity axis at  $c$  toward the extrados. The stresses  $f_e$  and  $f_i$  take their signs from  $M_e$  and  $M_i$  respectively, and compression is regarded as a negative stress.

The stresses on any arch section  $\overline{mm'}$  may, therefore, be found for any simultaneous position of a moving train of loads when the influence areas for  $M_e$ ,  $M_i$  and  $T_m$  have been drawn.

The resultant polygon for any simultaneous case of loading may also be drawn by plotting the offsets  $v$  from the gravity axis of each section examined, observing that  $+v$  is toward the extrados and  $-v$  is toward the intrados.

The method of combining the  $X_a$  influence line with ordinary moment and shear influence lines to obtain the  $M_e$ ,  $M_i$  and  $T_m$  influence areas for any section  $\overline{mm'}$  will now be illustrated.

**Kernel moment influence areas.** The moment equations for the kernel points according to Eq. (49B) are

$$\left. \begin{aligned} M_{me} &= M_{ae} \left[ \frac{M_{oe}}{M_{ae}} - X_a \right] = y_e \cos \alpha \left[ \frac{M_{oe}}{y_e \cos \alpha} - X_a \right] \\ M_{mi} &= M_{ai} \left[ \frac{M_{oi}}{M_{ai}} - X_a \right] = y_i \cos \alpha \left[ \frac{M_{oi}}{y_i \cos \alpha} - X_a \right] \end{aligned} \right\} \dots \dots \dots (49T)$$

The intercept of the  $M_{oe}$  influence line on the vertical through  $A$  is simply the ordinate  $x_e$  of the point  $e$ . Similarly for the  $M_{oi}$  influence line this intercept is the ordinate

$x_i$  of the point  $i$ . Hence the positive intercepts on the vertical through  $A$ , of the  $M_{oe}/y_e \cos \alpha$  and of the  $M_{oi}/y_i \cos \alpha$  influence lines, are easily computed when the coordinates of the kernel points  $e$  and  $i$  are given, provided the  $X_a$  influence line was drawn for a factor  $\mu = 1$ .

The coordinates of the kernel points are derived from the coordinates  $(x_m, y_m)$  of the axial point for the same section, when the kernel distances  $k$  and the angle  $\phi$  are known for that section. From Fig. 49B,

$$\left. \begin{aligned} x_e &= x_m + k_e \sin \phi, & y_e &= y_m - k_e \cos \phi \\ x_i &= x_m - k_i \sin \phi, & y_i &= y_m + k_i \cos \phi \end{aligned} \right\}, \quad \dots \dots \dots (49U)$$

which apply to all points from  $A$  to the crown, and from there to the abutment  $B$  the signs of the last terms are reversed. By using the  $l-x$  ordinates the intercepts on the vertical through  $B$  are found.

One intercept only need be computed as the two limiting rays of the  $M_o/y \cos \alpha$  line must intersect on the vertical through the center of moments. See Fig. 49c.

By constructing the  $X_a$  influence area for  $\mu = 1$ , which may always be done by making the pole distance  $H = \Sigma wy \cos \alpha$ , and since both the  $X_a$  and the  $M_o/y \cos \alpha$  lines are positive, then by applying them below the closing line  $\overline{A'B'}$ , the area included between the two lines will represent the  $M_m$  influence area. The portion below the  $X_a$  line will be the positive area because  $X_a$  is subtractive in Eqs. (49T). The entire  $M_m$  influence area has a factor  $\mu = y \cos \alpha = M_a$ .

**The  $T_m$  influence area for tangential force on any section  $mm'$ .** From Eqs. (49B) the following equation for  $T_m$  is obtained.

$$T_m = \sin (\phi - \alpha) \left[ \frac{Q_o \cos \phi}{\sin (\phi - \alpha)} - X_a \right]. \quad \dots \dots \dots (49V)$$

From this the end ordinate at  $A$ , for the  $T_o/T_a$  line, becomes  $1 \cdot \cos \phi \div \sin (\phi - \alpha)$  because the end ordinate for the  $Q_o$  line is unity. In this case the end ordinate at  $B$  is numerically the same but negative. For axial points to the right of the crown the end ordinate at  $B$  is positive and the one at  $A$  is negative. Other details are illustrated in connection with the example. The final  $T_m$  influence area has a factor  $\mu = \sin (\phi - \alpha)$ .

**Example.** A two-hinged arched rib, modeled after the Chagrin River Bridge near Bentleyville, O., was selected to illustrate the application of the previous theory. The structure was made unsymmetric by shortening the span at the right-hand end as shown in Figs. 49c. The clear span thus became 164 ft. and the rise 27.89 ft. This bridge was designed to carry a live load of 24 kips per truss per panel. The arch section is composed of a  $\frac{3}{8}$ -inch web plate and  $4-6'' \times 6'' \times 11/16''$  angles, with  $2-14'' \times 7/16''$  flange plates on each flange. Besides these there is one  $14'' \times \frac{3}{8}''$  plate on each flange extending from sections 2 to 5 and 7 to 10. The sections are all symmetric about the gravity axis and all general dimensions are given on the drawing and in Table 49a.

The bridge consists of two steel arched ribs 27 ft. between centers and carrying a total dead load of 1,058,000 pounds. The following values are assumed as a basis

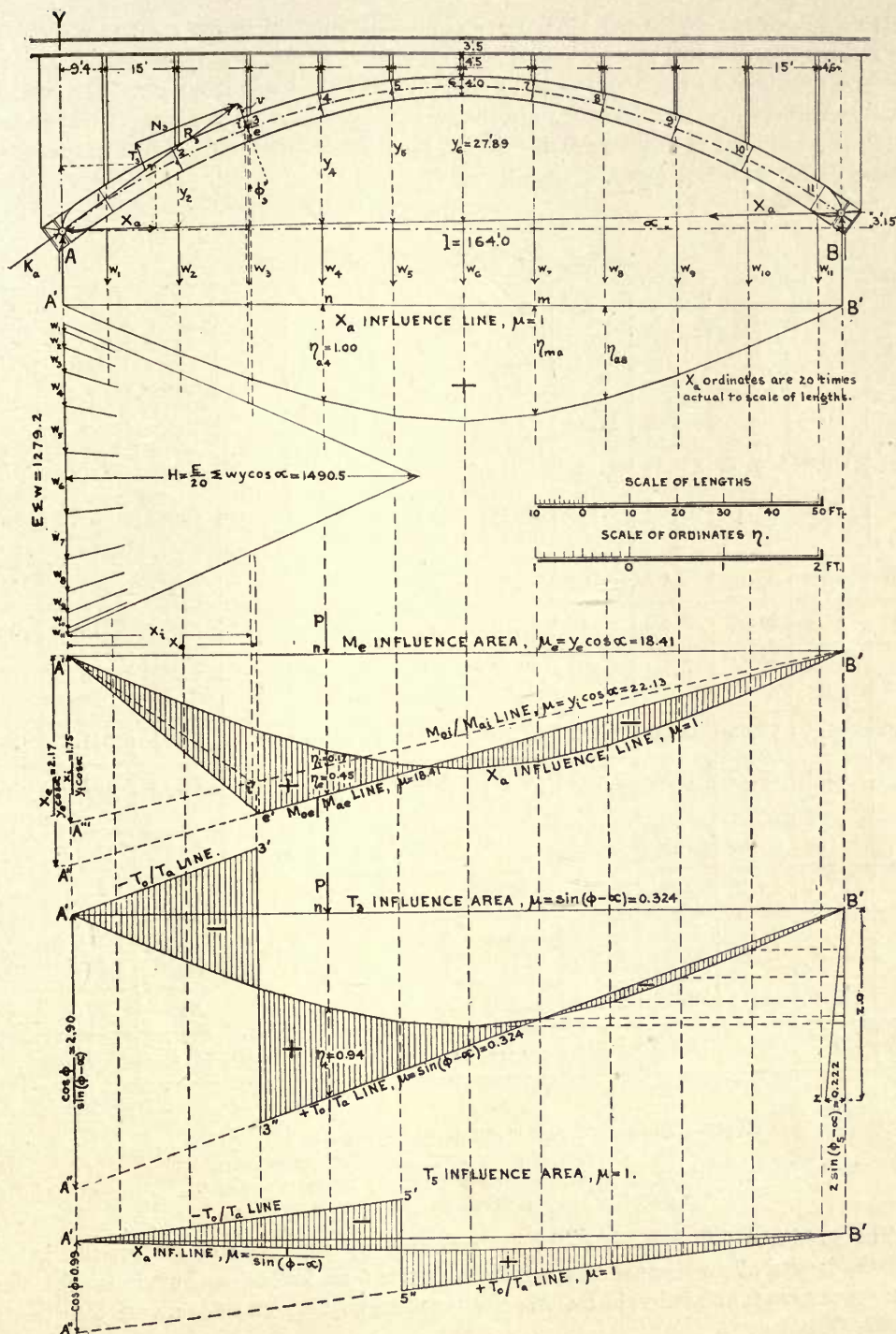


FIG. 49c.



for the analysis:  $E=29,000$  kips per sq.in.  $=4,176,000$  kips per sq.ft.;  $\epsilon=0.0000065$  per  $1^\circ\text{F}$ .; and  $t=\pm 75^\circ\text{F}$ .

The first step in the analysis is to compute the  $Ew$  loads from Eq. (49F) using the tabulated dimensions in Table 49A. In the same table the values  $Ewy \cos \alpha$  are computed, giving the required pole distance  $H=E\Sigma wy \cos \alpha$  for constructing the  $X_a$  influence line in accordance with Eq. (49H).

TABLE 49A  
 $X_a$  INFLUENCE LINE

Section.	Coordinates of Gravity Axis.		$\phi$	$\frac{1}{\cos \phi}$	$I$ in. <sup>4</sup>	$I$ ft. <sup>4</sup>	$\theta = \frac{1}{\cos \phi}$ ft.	$\Delta x$ ft.	$\frac{\theta \Delta x = \frac{\Delta x}{I \cos \phi}}{I \cos \phi}$ ft.	$\frac{Ew = \frac{\Delta xy \cos \alpha}{I \cos \phi}}{I \cos \phi}$ ft.	$Ewy \cos \alpha$
	$x$ ft.	$y$ ft.									
0	0	0	36° 15'	1.240	74,180	3.578	0.3466	9.4	0.652	0	0
1	9.4	6.01	32 15	1.182	74,180	3.578	0.3260		4.954	29.8	179
2	24.4	14.12	26 00	1.113	64,710 76,530	3.121 3.691	0.3567 0.3017	15	4.939	69.7	984
3	39.4	20.30	20 00	1.064	66,170	3.191	0.3332	15	5.014	101.8	2065
4	54.4	24.73	14 15	1.032	56,750	2.737	0.3770	15	5.673	140.3	3468
5	69.4	27.24	7 30	1.009	48,160 40,420	2.323 1.949	0.4352 0.5176	15	7.198	196.0	5339
6	84.4	27.89	0 00	1.000	33,590	1.620	0.6173	15	9.011	251.3	7007
7	99.4	26.77	7 30	1.009	40,420 48,160	1.949 2.323	0.5176 0.4352	15	7.198	192.6	5156
8	114.4	23.58	14 15	1.032	56,750	2.737	0.3770	15	5.673	133.7	3153
9	129.4	18.58	20 00	1.064	66,170	3.191	0.3332	15	5.014	93.1	1730
10	144.4	11.82	26 00	1.113	76,530 64,710	3.691 3.121	0.3017 0.3567	15	4.939	58.4	690
11	159.4	3.14	32 15	1.182	74,180	3.578	0.3260	15	3.983	12.5	39
12	164.0	0	34 20	1.211	.....	.....	0.3260	4.6	0.0	0	0

$$E\Sigma wy \cos \alpha = 29,810$$

NOTE. The  $x$  abscissæ are measured horizontally from  $A$ .

The  $y$  ordinates are measured vertically from  $AB$ .

The  $\Delta x$  are measured horizontally between sections.

$$\alpha = 1^\circ 06', \cos \alpha = 0.9998, \sin \alpha = 0.0192.$$

The products  $\theta \Delta x$  in Table 49A are summed by the prismoidal formula treating  $\Delta x$  as the length of a prismoid whose middle area is  $\theta$  and whose end areas are the means of the successive tabulated values of  $\theta$ . This is necessary because  $\theta$  is a variable quantity.

Calling  $\theta_{0-1}$  the mean between  $\theta_0$  and  $\theta_1$ , and  $\theta_{1-2}$  the mean between  $\theta_1$  and  $\theta_2$  etc., then the values  $\theta_1 x$  become:

$$\theta_0 x = \frac{1x}{3}[2\theta_0 + \theta_{0-1}] = \frac{1.9}{3}[0.6932 + 0.3363] = 0.652;$$

$$\theta_1 x = \frac{4x}{6}[\theta_{0-1} + 4\theta_1 + \theta_{1-2}] = \frac{15}{6}[0.3363 + 1.3040 + 0.3413] = 4.954.$$

$$\theta_2 x = \frac{4x}{6}[\theta_{1-2} + 2\theta_2 + 2\theta_2' + \theta_{2-3}] = \frac{15}{6}[0.3413 + 0.7134 + 0.6034 + 0.3174] = 4.939.$$

$$\theta_3 x = \frac{4x}{6}[\theta_{2-3} + 4\theta_3 + \theta_{3-4}] = \frac{15}{6}[0.3174 + 1.3328 + 0.3551] = 5.014,$$

etc.,            etc.

After collecting the tabulated data from the drawing, Fig. 49c, the remaining computations are quite simple and no further comment is necessary here, as the several operations are indicated in Table 49A.

**The  $X_a$  influence line** is now drawn by combining the  $Ew$  loads into a force polygon and making the pole distance equal to  $E\Sigma wy \cos \alpha$ . The resulting equilibrium polygon represents the  $X_a$  influence line with ordinates to the scale of lengths and  $\mu=1$ , in accordance with Eq. (49H).

In the drawing, the pole distance was made  $1/20$  of the actual length so that the ordinates  $\eta_a$  are twenty times too large. For this reason a special scale of ordinates, twenty times the scale of lengths, was constructed and used for all influence ordinates.

The scale of forces for the force polygon may be any convenient scale, so long as the pole distance is measured with the same scale as the forces.

**The influence areas for the kernel moments and tangential force** are now drawn by combining the  $M_o/M_a$  lines and the  $T_o/T_a$  line each with the  $X_a$  line. According to Eqs. (49r), (49u), (49v), this will require computing the kernel distances  $k$ , and the coordinates of the kernel points and finally the end ordinates at  $A$  of all influence lines. The end ordinates at  $B$  may be obtained by substituting for the abscissæ  $x$  the values  $l-x$ . These computations are given in Table 49B, which is self-explanatory.

In Fig. 49c the influence areas  $M_e$  and  $M_i$  are constructed for section 3. The  $X_a$  polygon is copied from the original one by transferring down the several  $\eta_a$  ordinates from a horizontal base  $A'B'$ . The  $M_o/M_a$  lines are constructed from the end ordinates  $\overline{A'A''} = x_c/y_e \cos \alpha$  and  $\overline{A'A'''} = x_i/y_i \cos \alpha$ , using the coordinates for the two kernel points as given in Table 49B. The lines  $\overline{B'A''}$  and  $\overline{B'A'''}$  are thus determined.

The kernel points  $e$  and  $i$  are the centers of moments and have the abscissæ  $x_e$  and  $x_i$ , as given in the table, and from these the points  $e'$  and  $i'$  are located.

The two moment influence lines are completed by drawing the lines  $\overline{A'e'}$  and  $\overline{A'i'}$ . The  $M_{oe}/M_{ae}$  influence line is thus found to be the broken line  $A'e'B'$  and the shaded area included between it and the  $X_a$  line is the  $M_e$  influence area for section 3. The factor for the ordinates  $\eta_e$ , when measured to the same scale as the  $\eta_a$  ordinates, is  $\mu_e = y_e \cos \alpha = 18.41$ .





For the  $A$  ordinate  $Q_o=1$ , hence this ordinate is simply  $\cos \phi$  and by reducing all the  $\eta_a$  ordinates by multiplying them by  $\sin (\phi-\alpha)$ , the  $T_5$  area is found with a factor  $\mu=1$ .

The  $\eta_a$  ordinates are easily reduced by graphics, laying off the line  $\overline{B'z}$  such that its deviation from the vertical is  $\sin (\phi-\alpha)$  in a distance unity. The  $\eta_a$  ordinates projected over horizontally are then reduced to the small horizontal intercepts between  $\overline{B'z}$  and the vertical.

The  $T_5$  influence area is thus constructed and is represented by the shaded area included between the broken line  $\overline{A'5'5''B'}$  and the reduced  $X_a$  line. The factor  $\mu=1$ .

The tangential force for section 3, for any train of moving loads is expressed by

$$T_3=\mu_t \Sigma P \eta_t,$$

. . . . . (49x)

and the tangential stress by  $T_3/F_3$ , where  $\eta_t$  is any ordinate to the  $T_3$  area under some particular load  $P$ .

The stress due to a uniform change in temperature is found from Eqs. (49i) and (49j) whence for  $t=\pm 75^\circ \text{ F.}$ ,

$$X_{at}=\frac{1 \cdot \delta_{at}}{\delta_{aa}}=\pm \frac{\epsilon t l}{\delta_{aa} \cos \alpha}=\pm \frac{0.000488 l}{\delta_{aa} \cos \alpha}.$$

Eq. (49G) gives  $\delta_{aa}=\Sigma w y \cos \alpha$  and Table 49A furnishes  $E \Sigma w y \cos \phi=29810$ , hence  $\delta_{aa}=29810 / E$  ft. for  $X_a=1$  kip. Making  $E=4,176,000$  kips per sq.ft.,  $l=164$  ft. and  $\cos \alpha=0.9998$ , then  $\delta_{aa}=0.00714$  ft. and  $X_{at}=\pm \frac{0.000488 \times 164}{0.00714 \times 0.9998}=\pm 11.21$  kips.

Eqs. (49k), will furnish the means of finding the values  $M_{mt}, N_{mt}, T_{mt}$ , and  $v=M_{mt} / N_{mt}$  and with these and Eqs. (49p) the temperature stresses  $f_e$  and  $f_i$  may be computed for any section  $\overline{mm'}$ .

**Stress due to abutment displacements.** Eq. (49L) furnishes the haunch thrust  $X_{ar}$  for any change  $\Delta l$  in the length of span. The quantity  $\Delta l$  must be estimated from the elastic properties of the abutments and is always more or less problematic, though it is well to investigate the probable stress which might be created by such a displacement.

In the present example it is assumed that for the maximum case of loading the haunches will spread an amount  $\Delta l=0.03$  ft., then for  $\delta_{aa}=0.00714$  ft.,  $X_a=1$  kip, and  $\cos \alpha=0.9998$ , Eq. (49L) gives

$$X_{ar}=-\frac{\Delta l}{\delta_{aa} \cos \alpha}=-\frac{0.03}{0.00714 \times 0.9998}=-4.20 \text{ kips.}$$

The stresses  $f_e$  and  $f_i$  may then be found in precisely the same manner as was just described for the case of temperature stresses.

The stresses due to temperature and abutment displacements should be separately investigated for several typical sections, especially the crown section, so as to enable the designer to judge of the relative importance which these may have in comparison with the combined dead and live load stresses.

**The live load stresses for section 3** will now be found for a single load  $P$  acting at section 4, merely to illustrate the use of the influence areas shown in Fig. 49c.

$$M_{e3} = \mu_e \eta_{e4} P = 18.41 \times 0.45 P = 8.285 P.$$

$$M_{i3} = \mu_i \eta_{i4} P = 22.13 \times 0.17 P = 3.762 P.$$

$$N_3 = \left( \frac{M_e - M_i}{2k} \right) P = \frac{4.523}{3.98} P = 1.136 P.$$

$$v = \frac{M_e + M_i}{2N} = \frac{12.047}{2.272} = 5.30 \text{ ft.}$$

$$f_e = -\frac{M_e}{Fk} = -\frac{8.285 P}{\frac{87.8}{144} \times 1.99} = -6.84 P \text{ per sq.ft.} = -0.0474 P \text{ per sq.in.}$$

$$f_i = \frac{M_i}{Fk} = \frac{3.762 P}{87.8 \times 1.99} = 0.0216 P \text{ per sq.in.}$$

$$X_a = 1.00 P; \quad T_3 = \mu_t \eta_{t4} P = 0.324 \times 0.94 P = 0.305 P.$$

$$R_3 = P \sqrt{N_3^2 + T_3^2} = 1.18 P; \quad A = \frac{109.6}{164} P + X_a \sin \alpha = 0.684 P.$$

The resultant  $K_A$ , of  $A$  and  $X_a$ , is found graphically to be  $1.19 P$ , which, for a single load to the right of section 3, should check  $R_3$ , as it does.

#### ART. 50. TWO-HINGED SPANDREL BRACED ARCH OR FRAMED ARCH

The analysis of the two-hinged frame arch is accomplished in the same general manner followed in the previous article, where the corresponding solid web arch was treated, only that the frame is usually simpler.

The general Eqs. (49B) for the reactions  $A$ ,  $B$ , and moment  $M_m$  apply equally to an unsymmetric framed arch, and the influence line for the redundant haunch thrust  $X_a$  is determined precisely as in the previous problem except that the  $w$  loads are found by the method given in Art. 36.

The stress in any member then becomes

$$S = S_o - S_a X_a = S_a \left[ \frac{S_o}{S_a} - X_a \right], \quad . . . . . (50A)$$

according to Eq. (45E) for one external redundant condition. This equation is later employed to construct the stress influence lines for the members.

The  $X_a$  influence line for the haunch thrust is represented by Eq. (49H) as

$$X_a = \frac{1 \cdot \delta_{ma}}{\delta_{aa}} = \frac{1 \cdot \delta_{ma}}{\sum w y \cos \alpha} = \eta_a, \quad . . . . . (50B)$$

where  $\delta_{ma}$  is the vertical deflection ordinate of any point  $m$  of a deflection polygon, drawn for the loaded chord and for the conventional loading  $X_a=1$  applied to the principal system; and  $\delta_{aa} = \sum w y \cos \alpha$  is the change in the span  $\overline{AB}$ , due to  $X_a=1$  acting on the principal system.

According to Art. 40, the  $\delta_{ma}$  deflection polygon is the equilibrium polygon drawn for a set of elastic loads  $w$ , with a pole distance  $H=1$ , according to the method given in Art. 36c.

The elastic loads  $w$  are functions of the changes in the lengths of all the members of the frame as given by Eqs. (36B) and (36c). These are algebraically summed for all the panel points to obtain the total loads  $w$ . Thus the elastic loads for the chords alone are  $w_c = \Delta l / r$  and each web member contributes two elastic loads  $w_u = \Delta l / r_u$  and  $w_n = \Delta l / r_n$ , acting at the two adjacent panel points  $u$  and  $n$  of the loaded chord. Hence when the loads  $P$  are to be applied to the top chord, then the  $w_u$  and  $w_n$  elastic loads are computed for the top chord panel points. The lever arms  $r$  for the chords are measured as shown in Fig. 36A and the lever arms  $r_u$  and  $r_n$  for the web members are measured as explained in Figs. 36B and 36F. The details of the computation of the  $w$  loads are illustrated in Table 50B, and Fig. 50A, in connection with a complete example.

For any braced arch with parallel chords, the  $w$  loads for the web members may always be neglected.

The displacement  $\delta_{aa} = \Sigma w y \cos \alpha$  is computed for the same  $w$  loads by taking the sum of their moments about the line  $\overline{AB}$  joining the haunches. The lever arms for an unsymmetric span thus become the vertical ordinates of the respective pin points times  $\cos \alpha$ . See also Table 50A.

The  $X_a$  influence line thus becomes the equilibrium polygon drawn for the elastic loads  $w$  with a pole distance  $\delta_{aa} = \Sigma w y \cos \alpha$ .

Still another method of finding this influence line consists in drawing the deflection polygon for the loaded chord by means of a Williot-Mohr displacement diagram, which also furnishes the value  $\delta_{aa}$  from which the influence line ordinates  $\eta_a$  may be computed and plotted. This solution is illustrated in Fig. 50B.

Since the modulus  $E$  does not affect the  $X_a$  influence line it is more convenient to compute all displacements and the  $w$  loads  $E$  times too large, thus avoiding the small quantities resulting in many decimals.

**Temperature Stress.** Calling  $\Delta l_t$  the change in the length of any member due to any temperature effect, then from Mohr's work Eq. (5H) the change  $\delta_{at}$  in the length of the span  $\overline{AB}$  becomes

$$1 \cdot \delta_{at} = \Sigma S_a \Delta l_t = \Sigma S_a \epsilon t l. \quad \dots \dots \dots (50c)$$

The redundant thrust  $X_{at}$ , due to any temperature effect, is found from Eq. (44c) as

$$X_{at} = \frac{1 \cdot \delta_{at}}{\delta_{aa}} = \frac{\Sigma S_a \Delta l_t}{\delta_{aa}} = \frac{E \Sigma S_a \Delta l_t}{E \Sigma w y \cos \alpha} \quad \dots \dots \dots (50d)$$

For a uniform change in temperature of  $\pm t^\circ$ , above or below a certain normal, the change  $\delta_{at}$  in the length of the span  $\overline{AB}$ , is found from Eq. (49j) as

$$\delta_{at} = \pm \frac{\epsilon t \overline{AB}}{\cos \alpha} \quad \dots \dots \dots (50e)$$

In any case the stresses in the members are best found from  $S_t = \mp S_a X_{at}$  for  $\pm X_{at}$ , or from a Maxwell diagram drawn for the external loading  $X_{at}$ , acting on the principal system.

For a uniform change of  $t^\circ$  from the normal temperature, the resulting stresses become  $S_t = \mp S_a X_{at}$ . The effect on the final stresses  $\pm S$  for full loading, will then be additive or  $\pm S_{max} = \pm (S + S_t)$



**Abutment displacements** will affect the stresses in the members by producing a redundant thrust  $-X_{ar}$  as found from Eq. (49L) when  $\Delta l$  is an increase in the length of span  $\overline{AB}$ . The stresses  $S_r$  would be found from a Maxwell diagram drawn for  $-X_{ar}$  acting on the principal system. They could also be found as  $S_r = \mp S_a X_{ar}$ , for  $\pm X_{ar}$ , since  $S_a$  is the stress produced in any member  $S$  by  $X_a = 1$  acting outward.

**The stress influence area for any member  $S$**  is derived from the previous Eq. (50A) from which any stress influence ordinate  $\eta$  becomes

$$S = S_a \left[ \frac{\bar{S}_o}{\bar{S}_a} - X_a \right] = \eta. \quad \dots \dots \dots (50F)$$

These influence areas are alike in principle for all members, whether chords or web members, and represent the area inclosed between the  $X_a$  influence line and the  $\bar{S}_o/S_a$  influence line, times a factor  $S_a$ .

The  $\bar{S}_o/S_a$  influence line is the ordinary stress influence line  $S_o$  for any determinate frame, multiplied by the factor  $1/S_a$ . Hence the end ordinates for the  $S_o$  line may be found in the usual way. Thus the stress  $S_A$  in the member  $S$  due to the upward reaction  $A = 1$  is the end ordinate of the  $S_o$  line at the point  $A$ , and this ordinate divided by  $S_a$  becomes the required end ordinate  $\eta_A = S_A/S_a$  of the  $\bar{S}_o/S_a$  line at  $A$ . Similarly the end ordinate of the  $\bar{S}_o/S_a$  line at  $B$  is  $\eta_B = S_B/S_a$ , where  $S_B$  is the stress in the member due to the upward reaction  $B = 1$  acting on the principal system.

Hence if the stresses  $S_A$ ,  $S_B$  and  $S_a$ , for all the members of the principal system, are found either by computation or from three Maxwell diagrams, then all the data for the several stress influence lines are at hand provided the  $X_a$  influence line is known.

In drawing the  $\bar{S}_o/S_a$  influence lines the following points should be observed: 1, That the end bounding lines must always intersect in a point  $i'$  on the vertical through the center of moments  $i$  of the particular member treated. 2, that this  $\bar{S}_o/S_a$  line must be a straight line between adjacent panel points of the loaded chord. 3, that when one of the end ordinates is too large to be conveniently measured, then half this ordinate may be laid off at the center of the span. This is frequently done as in the example which follows, see Figs. 50c.

The signs of the end ordinates and of the factors  $\mu = S_a$  all follow from the signs of the stresses  $S_A$ ,  $S_B$  and  $S_a$ .

**Deflection of any point  $m$ .** Applying Mohr's work equation (6B) the deflection  $\delta_m$  of any point  $m$ , becomes

$$\left. \begin{aligned} \delta_m &= \Sigma S_1 \left( \frac{Sl}{EF} + \epsilon tl \right) - \Sigma R \Delta r \\ &= \frac{1}{E} \Sigma S_1 \left( \frac{Sl}{F} + \epsilon l E \right) - \Sigma R \Delta r \end{aligned} \right\}, \quad \dots \dots \dots (50G)$$

wherein  $S_1$  is the stress in any member due to a load  $P = 1$ , applied at the point  $m$  in the direction of the desired deflection; and  $S$  is the corresponding stress due to any cause or actual condition of simultaneous loading for which the deflection is sought, including load effects as well as temperature changes and abutment displacements. The summation covers all the members of the principal system.

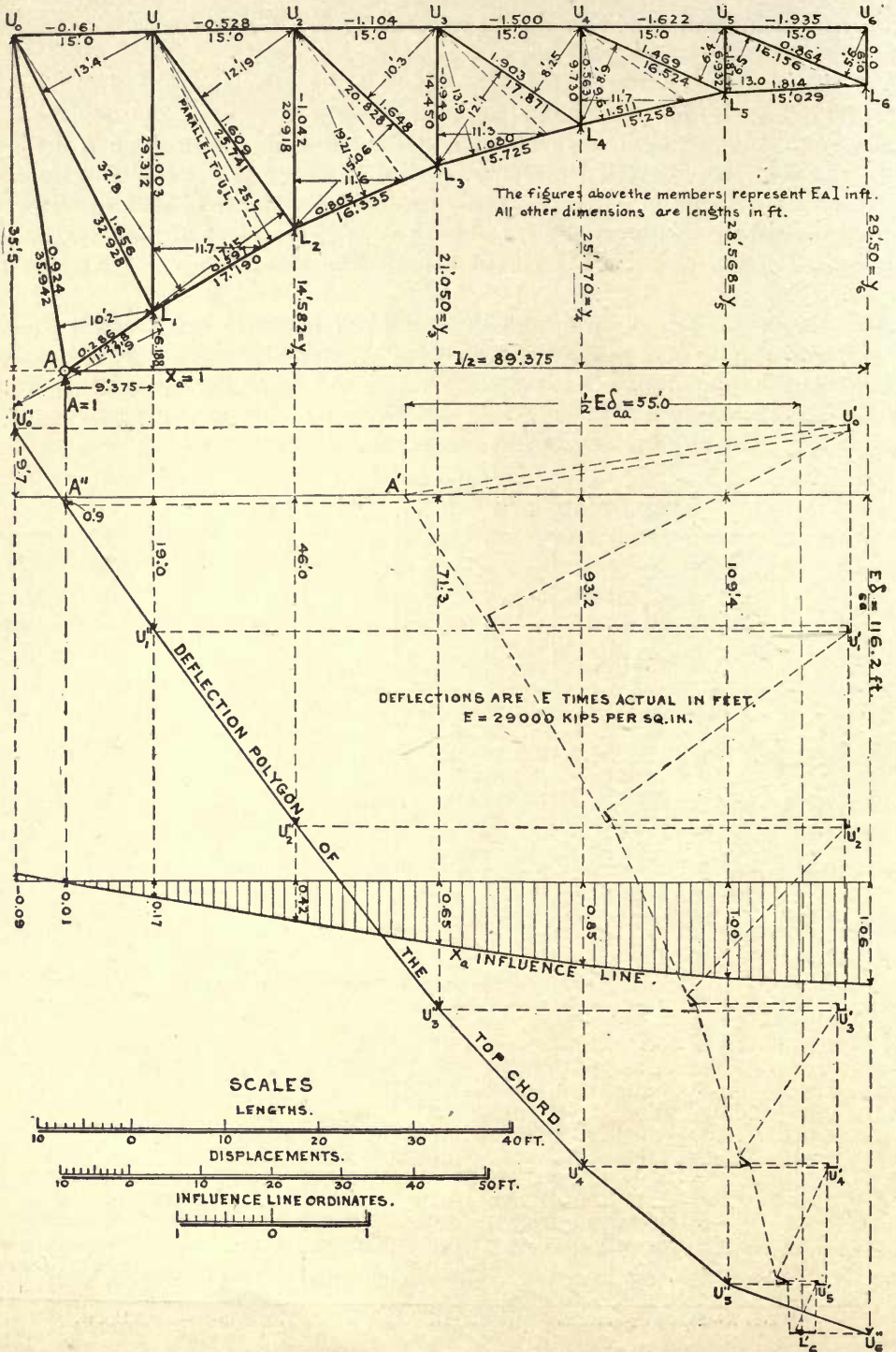
[illegible]

The arch has a span of 168.75 ft. between pin supports, a rise of 29.5 ft., and weighs 1,060,320 lbs. without abutment shoes, making a uniform dead load of 43.2 kips per truss per panel. The top chord is the loaded chord. The abutments are symmetric and, therefore,  $\alpha = 0$ .

Fig. 50A shows the half span with the lengths of members in feet below the lines, and the values  $E\Delta l$ , in feet, as found from Table 50A, above the lines. The various lever arms used in the computation of the stresses  $S_A$ ,  $S_B$  and  $S_a$ , and of the  $w$  loads, are also shown. The actual values  $\Delta l$  in feet  $= E\Delta l \div 29000$ , because the areas  $F$  were not reduced to square feet. See also the example in Art. 52, where  $\Delta l$  is actual.

Member	Stresses in Kips.			Area, $F$ Sq.in.	Length $l$ ft.	Unit Stress, $f = \frac{S_a}{F}$ Kips.sq.in.	$*E\Delta l = \frac{S_a l}{F}$ ft.	End Ordinates, $\frac{S_o}{S_a}$ Infl. Lines.		Temperature Effect.		
	$S_A$ for $A=1$	$S_B$ for $B=1$	$S_a$ for $X_a=1$					$*E\Delta l_t$ $= \epsilon l E$ ft.	$*ES_o\Delta l_t$			
									+	-		
$U_0 U_1$	- 0.320	- 5.437	- 0.211	19.80	15.000	- 0.0107	- 0.1605	1.517	25.770	197.9	.....	41.
$U_1 U_2$	- 1.165	- 6.902	- 0.697	19.80	15.000	- 0.0352	- 0.5280	1.671	9.917	197.9	.....	137.
$U_2 U_3$	- 2.725	- 8.953	- 1.457	19.80	15.000	- 0.0736	- 1.1040	1.870	6.145	197.9	.....	288.
$U_3 U_4$	- 5.588	- 11.755	- 2.649	26.48	15.000	- 0.1000	- 1.5000	2.109	4.438	197.9	.....	524.
$U_4 U_5$	- 10.008	- 14.336	- 4.121	38.11	15.000	- 0.1081	- 1.6215	2.429	3.479	197.9	.....	815.
$U_5 U_0$	- 14.062	- 14.062	- 4.917	38.11	15.000	- 0.1290	- 1.9350	2.859	2.859	197.9	.....	973.
$L_0 L_1$	- 0.172	.....	+ 1.085	42.50	11.228	+ 0.0255	0.2863	- 0.159	.....	88.9	96.5	
$L_1 L_2$	0.366	6.231	1.388	40.00	17.190	0.0347	0.5965	0.263	4.481	136.1	188.9	
$L_2 L_3$	1.269	7.516	1.848	37.50	16.335	0.0493	0.8053	0.687	4.067	129.4	239.1	
$L_3 L_4$	2.857	9.386	2.575	37.50	15.725	0.0687	1.0803	1.109	3.645	124.5	320.6	
$L_4 L_5$	5.685	11.958	3.712	37.50	15.258	0.0990	1.5105	1.532	3.221	120.8	448.4	
$L_5 L_0$	10.027	14.363	5.131	42.50	15.029	0.1207	1.8140	1.954	2.799	119.0	610.6	
$U_0 L_0$	- 0.917	.....	- 0.605	23.52	35.942	- 0.0257	- 0.9237	1.516	.....	379.5	.....	229.
$U_1 L_1$	- 1.179	- 2.043	- 0.678	19.80	29.312	- 0.0342	- 1.0025	1.739	3.014	309.5	.....	209.
$U_2 L_2$	- 1.502	- 1.976	- 0.732	14.70	20.918	- 0.0498	- 1.0417	2.052	2.700	220.9	.....	161.
$U_3 L_3$	- 1.857	- 1.817	- 0.773	11.76	14.450	- 0.0657	- 0.9494	2.402	2.351	152.6	.....	118.
$U_4 L_4$	- 2.042	- 1.193	- 0.681	11.76	9.730	- 0.0579	- 0.5634	2.999	1.752	102.7	.....	70.
$U_5 L_5$	- 1.622	+ 0.109	- 0.318	11.76	6.932	- 0.0270	- 0.1872	5.101	- 0.343	73.2	.....	23.
$U_0 L_0$	- 0.0	0.0	0.0	11.76	6.000	0.0	0.0	0.0	0.0	63.4	.....	0.
$U_0 L_1$	1.017	.....	+ 0.671	13.34	32.928	0.0503	1.6563	1.515	.....	347.7	233.3	
$U_1 L_2$	1.451	2.514	0.834	13.34	25.741	0.0625	1.6088	1.740	3.015	271.8	226.7	
$U_2 L_3$	2.166	2.848	1.055	13.34	20.828	0.0791	1.6475	2.053	2.700	220.0	232.1	
$U_3 L_4$	3.413	3.339	1.421	13.34	17.871	0.1065	1.9033	2.402	2.350	188.7	268.1	
$U_4 L_5$	4.869	2.843	1.622	18.25	16.524	0.0889	1.4690	3.002	1.753	174.4	282.9	
$U_5 L_0$	4.367	- 0.294	0.857	15.84	16.156							

\* Where  $E=29,000$  kips instead of  $29,000 \times 144$ .  $\frac{1}{2} E \Sigma S_a \Delta l_i = -299.8$  kip. ft.



FIGS 50A, B



Table 50A gives these stresses, in kips, as found by computation, also the areas  $F$  of the members, being gross for compression and net for tension members. The lengths  $l$  of the members, unit stresses  $f$  and quantities  $E\Delta l$  ( $-$ for shortening) are also included in this table, and finally the end ordinates of the  $\bar{S}_o/S_a$  influence lines are obtained.

The  $X_a$  influence line is now found by two different methods to illustrate the applications frequently referred to elsewhere.

The first method is by constructing a deflection polygon of the top chord by means of a Williot-Mohr displacement diagram, Fig. 50b, using the quantities  $E\Delta l$ , in feet, as the changes in the lengths of the members for the conventional loading  $X_a=1$ , producing stresses  $S_a$ . The second method is by finding this deflection polygon from the  $w$  loads.

**The first method** requires little description other than to say that the displacement diagram Fig. 50B is drawn for displacements  $E\Delta l$ , Table 50A, on the assumption that the point  $L_6$  and the direction of the member  $L_6U_6$  remain fixed and since the span is symmetric about this member and the point  $L_6$ , therefore no rotation diagram is necessary. The deflection polygon of the top chord is then found by projecting the vertical deflections of the top chord panel points onto the verticals through these points, furnishing the polygon  $\overline{A''U_6''}$  with a closing line  $\overline{A'A''}$ , horizontally through  $A'$ . These deflections are  $E$  times actual, in feet, measured to the scale of displacements.

The horizontal displacement  $\frac{1}{2}E\delta_{aa}$  between  $A$  and  $L_6$  is also obtained from the same diagram as the horizontal distance between  $A'$  and  $L'_6$ .

The vertical ordinates of the deflection polygon are values of  $\delta_{ma}$ , and hence the  $X_a$  influence line ordinates  $\eta_a$  are found by dividing the several deflection ordinates  $E\delta_{ma}$  by the constant  $E\delta_{aa}$  according to Eq. (50B), giving

$$X_a = \frac{E\delta_{ma}}{E\delta_{aa}} = \frac{\delta_{ma}}{\delta_{aa}} = \eta_a. \quad \cdot \cdot \cdot \cdot \cdot \cdot \cdot \cdot \cdot (50I)$$

This shows that the factor  $E$  and the scale of the ordinates do not affect  $X_a$ . The ordinates  $\eta_a$ , for all panel points, are plotted to any convenient scale to obtain the  $X_a$  influence line.

**Second method.** The same displacements  $Edl$ , in feet, are here employed to compute the elastic loads  $Ew$ , using the lever arms, also in feet, as given on Fig. 50A. See Table 50B.

In the present example all the members are included and the table indicates exactly how much each member contributes to the several total  $Ew$  loads. The method of Art. 35 is rigidly followed. By using displacements  $E\Delta$  which are  $E$  times too large, the  $w$  loads are also multiplied by  $E$ .

Each chord member furnishes one  $w$  load which acts at the center of moments for that chord while each web member contributes two loads  $w_u$  and  $w_n$  acting at the two adjacent panel points  $u$  and  $n$  of the loaded chord or the chord for which the deflection polygon is to be drawn.

The  $w_e$  loads resulting from the chord members are always positive as found by Eq. (36B), thus:

$$w_c = \frac{\Delta l}{r} \quad \text{or} \quad Ew_c = \frac{E\Delta l}{r} \quad . \quad . \quad . \quad . \quad . \quad . \quad . \quad . \quad (50\kappa)$$

The negative and positive loads for a web member are

$$w_u = \frac{\Delta l}{r_u} \quad \text{and} \quad w_n = \frac{\Delta l}{r_n} \quad \text{or} \quad Ew_u = \frac{E\Delta l}{r_u} \quad \text{and} \quad Ew_n = \frac{E\Delta l}{r_n}, \quad . \quad . \quad (50L)$$

as given by Eq. (36D).

The lever arm  $r$  for a chord, is the distance from the center of the moments for such chord and perpendicular to the chord. The lever arms  $r_u$  and  $r_n$  are perpendicular distances onto a web member as described in Figs. 36B, and 36F. They may be identified by comparing the values in Table 50B with the dimensioned lever arms on Fig. 50A.

The rule for the signs of the two loads for any web member was stated in Art. 36, and is as follows: *Calling all top chord members negative and all bottom chord members positive, and giving the proper sign to  $\Delta l$  for the web member in question, then the positive  $w$  load is found on that side of the panel where the sign of  $\Delta l$  coincides with the sign of the adjacent chord.*

For the panel point  $U_0$  the total load  $Ew_0$  (Table 50B) is made up of the positive load produced by the chord  $L_0L_1$  and one of the loads from each of the web members  $U_0L_1$  and  $U_1L_1$ , the signs of which are negative according to the above rule.

The  $w$  load for point  $A$  produces zero effect on the deflection and need not be considered.

For the panel point  $U_1$  the total load  $Ew_1$  becomes

$$\frac{\Delta L_1 L_2}{25.7} + \frac{\Delta U_0 L_1}{13.4} - \frac{\Delta U_1 L_2}{17.15} + \frac{\Delta U_1 L_1}{11.7} - \frac{\Delta U_2 L_2}{15} = 0.069,$$

and similarly for the other panel points of the loaded (top) chord.

The bottom chord points receive only the loads produced by the top chord members except at  $L_1$  where the member  $U_0L_0$ , being the end post, contributes a load  $\Delta U_0 L_0 / 10'2$ .

The total  $Ew$  loads acting in the same vertical are then summed for the seven panel points of the half span and used in constructing the deflection polygon with a pole distance  $H = E\Sigma yw$ .

The  $y$  ordinates are measured vertically from the line  $\overline{AB}$  to the points of application of the respective  $Ew$  loads, distinguishing between the loads acting at the top and bottom panel points.

In order that the  $X_a$  influence line ordinates may appear to a scale twenty times as large as the scale of lengths, the pole distance was made equal to  $E\Sigma yw/20$ , see Fig. 50c. Note the agreement of the ordinates here found with those obtained in Fig. 50B.

**Stress influence areas.** The end ordinates  $\eta_A$  and  $\eta_B$  of the  $\overline{S}_o/S_a$  lines are computed in Table 50A and these serve to construct all stress influence areas for the several members.

Fig. 50c shows stress influence areas for six typical members, and each one has a factor  $S_a$  as per Eq. (50A). The end ordinates are applied down from the closing line when positive and up when negative. The signs of the influence areas are uniformly + for areas below the  $X_a$  influence line and the factor  $\mu$  takes the sign of  $S_a$ .



Pt.	Ew LOADS.				Total * Ew Loads.	y ft.	* E <sub>yw</sub>	Total * Ew load through Each Vertical for	Ew
	Diagonals.		Verticals.						
U <sub>0</sub>	$\frac{\Delta L_0 L_1}{32.8} = 0.0087$	$\frac{\Delta U_0 L_1}{17.9} = -0.0925$	.....	$\frac{\Delta U_1 L_1}{15} = -0.0668$	-0.151	35.5	-5.361	U <sub>0</sub>	Ew <sub>0</sub> = -0.151
U <sub>1</sub>	$\frac{\Delta L_1 L_2}{25.7} = 0.0232$	$\frac{\Delta U_1 L_2}{17.15} = -0.0938$	$\frac{\Delta U_1 L_1}{11.7} = 0.0857$	$\frac{\Delta U_2 L_2}{15} = -0.0694$	0.069	35.5	+2.450	U <sub>1</sub> L <sub>1</sub>	Ew <sub>1</sub> = +0.165
U <sub>2</sub>	$\frac{\Delta L_2 L_3}{19.21} = 0.0419$	$\frac{\Delta U_2 L_3}{12.19} = 0.1318$	$\frac{\Delta U_2 L_2}{11.6} = 0.0898$	$\frac{\Delta U_3 L_3}{15} = -0.0633$	0.091	35.5	3.231	U <sub>2</sub> L <sub>2</sub>	Ew <sub>2</sub> = 0.116
U <sub>3</sub>	$\frac{\Delta L_3 L_4}{13.9} = 0.0777$	$\frac{\Delta U_3 L_4}{10.3} = 0.1599$	$\frac{\Delta U_3 L_3}{11.3} = 0.0840$	$\frac{\Delta U_4 L_4}{15} = -0.0376$	0.127	35.5	4.508	U <sub>3</sub> L <sub>3</sub>	Ew <sub>3</sub> = 0.203
U <sub>4</sub>	$\frac{\Delta L_4 L_5}{9.6} = 0.1573$	$\frac{\Delta U_4 L_5}{8.25} = 0.2307$	$\frac{\Delta U_4 L_4}{11.7} = 0.0482$	$\frac{\Delta U_5 L_5}{15} = -0.0125$	0.238	35.5	8.449	U <sub>4</sub> L <sub>4</sub>	Ew <sub>4</sub> = 0.393
U <sub>5</sub>	$\frac{\Delta L_5 L_6}{6.9} = 0.2629$	$\frac{\Delta U_5 L_6}{6.4} = 0.2296$	$\frac{\Delta U_5 L_5}{13.0} = 0.0144$	$\frac{\Delta U_6 L_6}{15} = 0.0$	0.374	35.5	13.277	U <sub>5</sub> L <sub>5</sub>	Ew <sub>5</sub> = 0.608
U <sub>6</sub> 2	.....	$\frac{\Delta U_6 L_6}{5.6} = 0.1543$	.....	.....	0.154	35.5	5.467	$\frac{1}{2} U_6 L_6$	$\frac{1}{2} Ew_6 = 0.477$
L <sub>1</sub>	$\frac{\Delta U_0 L_1}{29.31} = 0.0055$	.....	$\frac{\Delta U_0 L_0}{10.2} = 0.0905$	.....	0.096	6.19	0.594	$\frac{1}{2} E \Sigma w = 1.811$	
L <sub>2</sub>	$\frac{\Delta U_1 U_2}{20.92} = 0.0252$	.....	.....	.....	0.025	14.58	0.365	For a pole distance H = EΣyw = 109.526 the X <sub>a</sub> in- fluence line ordi- nates are natural to the scale of lengths. Making H = 109.526/20 = 5.476 gives ordi- nates 20 times nat- ural to the scale of lengths.	
L <sub>3</sub>	$\frac{\Delta U_2 U_3}{14.45} = 0.0764$	.....	.....	.....	0.076	21.05	1.600		
L <sub>4</sub>	$\frac{\Delta U_3 U_4}{9.73} = 0.1542$	.....	.....	.....	0.154	25.77	3.969		
L <sub>5</sub>	$\frac{\Delta U_4 U_5}{6.93} = 0.2340$	.....	.....	.....	0.234	28.57	6.685		
L <sub>6</sub> 2	$\frac{\Delta U_5 U_6}{6.00} = 0.3225$	.....	.....	.....	0.323	29.50	9.529		

1. EFW = 54.763

 $\frac{1}{2} E \Sigma \psi w = 54.763.$ 

 \* Where  $E = 29,000$  kips instead of  $29,000 \times 144$ .





The method of computing stresses for any train of loads need not be repeated here except to call attention to the load divides, which must be carefully observed for each member in placing the loads on the span.

**Temperature effects.** For a general case of unequal temperatures in the several members the following assumptions are made:

Let the normal temperature be  $65^{\circ}\text{ F.}$ , for which the structure has no temperature stresses. Then assume a case where the top chord is heated to  $130^{\circ}\text{ F.}$ ; the bottom chord to  $104^{\circ}\text{ F.}$ , and the web system to  $117^{\circ}\text{ F.}$  For  $\epsilon=0.000007$ , and  $E=29000$  kips per sq.in. the values of  $E\epsilon t$  become

$$\begin{aligned}\text{Top chord} \quad t &= 130^{\circ} - 65^{\circ} = 65^{\circ}, & E\epsilon t &= 13.20; \\ \text{Web system} \quad t &= 117^{\circ} - 65^{\circ} = 52^{\circ}, & E\epsilon t &= 10.56; \\ \text{Bottom chord} \quad t &= 104^{\circ} - 65^{\circ} = 39^{\circ}, & E\epsilon t &= 7.92.\end{aligned}$$

The values  $E\Delta l_t = \epsilon l E$  and  $ES_a \Delta l_t$  are computed in Table 50A, using  $l$  in feet and  $E$  in kip feet. Finally the half sum  $E\Sigma S_a \Delta l_t$  is found to be  $3293.4 - 3593.2 = -299.8$  kip feet. Table 50B gives  $\frac{1}{2}E\Sigma yw = 54.76$  and from Eq. (50D) for  $\cos \alpha = 1$ ,

$$X_{at} = -\frac{299.8}{54.76} = -5.475 \text{ kips, . . . . . (50M)}$$

which is a thrust acting outward the same as the conventional loading  $X_a = 1$ .

Hence the temperature stress in any member becomes

$$S_t = S_a X_{at},$$

wherein  $S_t$  has the same sign as  $S_a$ .

A more severe stress would be produced when the top chord is colder than the bottom chord, or when the top chord has a temperature of  $+10^{\circ}\text{ F.}$  at the same time that the bottom chord has a temperature of  $-16^{\circ}\text{ F.}$  a case which might occur on a clear, cold day. The stresses  $S_t$  produced by such a condition would have the opposite sign of  $S_a$  when found from  $+X_{at}$ .

For a uniform rise of  $65^{\circ}$  above the normal, the elongation for the whole span becomes, by Eq. (50E),

$$E\delta_{at} = \frac{\epsilon t \overline{AB} \cdot E}{\cos \alpha} = 2226.6 \text{ ft.},$$

and from Eq. (50D),

$$X_{at} = \frac{E\delta_{at}}{E\delta_{aa}} = \frac{2226.6}{2 \times 54.76} = +20.33 \text{ kips,}$$

giving stresses  $S_t = -S_a X_{at}$ .

For a uniform fall of  $65^{\circ}$  below the normal  $\delta_{at} = -2226.6 \text{ ft.}$  and  $X_{at} = -20.33 \text{ kips,}$  giving stresses  $S_t = S_a X_{at}$ .

Compare these results with those of the example in Art. 59, for a solid web arch of about the same dimensions.

**Abutment displacements.** Assuming that as a result of yielding abutments the length of span is increased an amount  $\Delta l = 0.03$  ft. then from Eq. (49L)

$$X_{ar} = -\frac{E\Delta l}{E\Sigma yw} = -\frac{0.03 \times 29,000}{109.53} = -7.95 \text{ kips.}$$

Comparing this result with the one obtained for the solid web arch in Art. 49, it is clear that the framed arch is almost twice as stiff.

**Deflection of the crown** due to the temperature effect producing  $X_{at} = -5.48$  kips, Table 50A, and Eq. (50M). In this case the abutments are assumed rigid making  $\Delta r = 0$ , and the stresses  $S_o$  are not included, since temperature effects alone are desired. This reduces Eq. (50G) to

$$\delta_6 = \frac{1}{E} \Sigma S_1 \left( \frac{S_t l}{F} + \epsilon l E \right),$$

where  $S_t = -S_a X_{at}$  and  $\frac{S_t l}{F} = -\frac{S_a l X_{at}}{F} = -E \Delta l X_{at}$ ; also  $S_1 = \frac{S_A}{2}$  for a load unity at the center of a symmetric span, and  $\epsilon l E = E \Delta l_t$ . Hence

$$\delta_6 = \frac{1}{2E} \Sigma S_A (-E \Delta l X_{at} + E \Delta l_t),$$

which can easily be computed for any  $X_{at}$  using the values  $S_A$ ,  $E \Delta l$  and  $E \Delta l_t$  given in Table 50A.

## ART. 51. TWO-HINGED ARCH WITH CANTILEVER SIDE SPANS

Occasionally a structure of this type is peculiarly adapted to certain sites as the one at High Bridge, Ky. Its application has, however, received adverse criticism because the analysis of stresses was considered too complicated.

This objection might apply to any of the ordinary methods of analysis, but not when the problem is solved by influence areas.

As a type of bridge it is commendable and deserves careful consideration whenever a particular site offers a suitable profile and good foundations for the center span.

Fig. 51A represents one of several forms which might be employed. The center span is the same as the arch in the previous article with the exception of the end posts which are here made vertical, thus increasing the span to 180 ft. Owing to this difference, the computations in Tables 50A and 50B no longer apply because the stresses  $S_A$ ,  $S_B$  and  $S_a$  are now slightly changed. Otherwise the preliminary computations would be precisely the same in both structures.

The difference between the two-hinged arch and the present structure with cantilever side spans is entirely in the principal system which results when the redundant thrust  $X_a$  is removed. In the first case the principal system is a simple truss on two supports  $A$  and  $B$ , while in Fig. 51A the principal system becomes a cantilever when the hinged support at  $A$  is made movable for the purpose of analysis. The supports at  $D$  and  $F$  are roller bearings and the simple trusses  $\overline{DC}$  and  $\overline{EF}$  are hinged at  $C$  and  $E$  respectively.



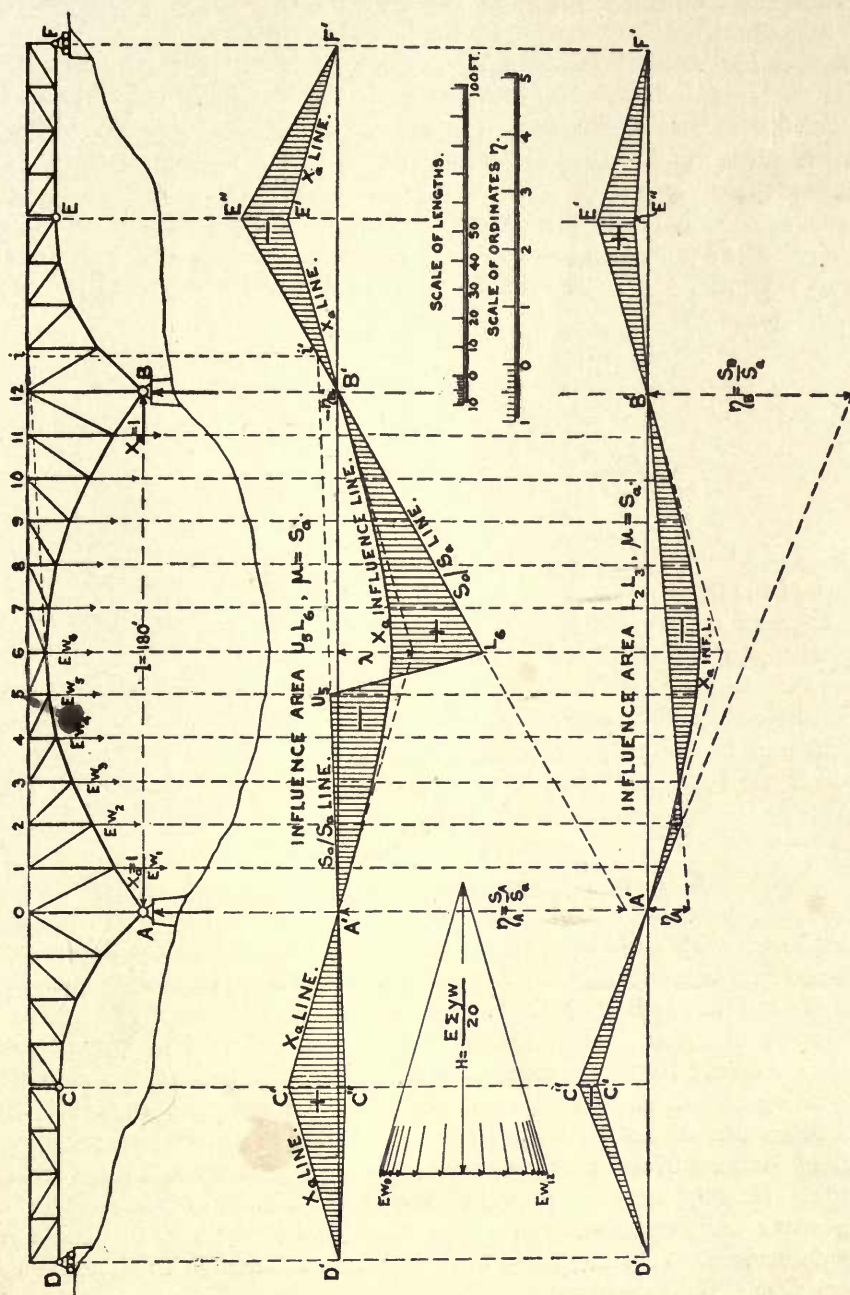


Fig. 51A.

The two-hinged central span, as in any ordinary two-hinged arch, is made determinate by substituting a roller bearing for the hinged bearing at  $A$ .

The  $X_a$  influence line is found as in the previous problem and the computation of the  $Ew$  loads is not repeated here. However, the loads  $Ew_0$  and  $Ew_{12}$ , must now be included because these loads affect the directions of the extreme rays  $C'A'$  and  $B'E'$  of the equilibrium polygon outside of the span  $\overline{AB}$  while they have no bearing on the  $X_a$  influence line within this span.

The complete  $X_a$  influence line for the whole span  $\overline{DF}$  is found by prolonging the extreme rays of the equilibrium polygon  $A'B'$  to the points  $C'$  and  $E'$  and finally drawing the lines  $D'C'$  and  $E'F'$ . The middle ordinate  $\lambda$  may be computed from the force polygon as follows:

$$\lambda = \frac{El \Sigma_0^{12} w}{4H} \text{ measured to scale of lengths,}$$

or

$$\lambda = \frac{El \Sigma_0^{12} w}{4E \Sigma y w} \text{ measured to scale of ordinates.}$$

The lines  $\overline{A'C'}$  and  $\overline{B'E'}$ , found by laying off  $\lambda$ , are respectively parallel to the extreme rays of the force polygon.

**Stress influence areas.** These are found precisely as in Art. 50, so far as the span  $\overline{AB}$  is concerned, by laying off end ordinates  $\eta_A = S_A/S_a$  and  $\eta_B = S_B/S_a$  and the factor becomes  $\mu = S_a$ . In each case the two end rays so determined will intersect in a point  $i'$ , which is vertically under the center of moments  $i$  of the member in question. Also the  $\overline{S_o/S_a}$  influence lines must be straight over the panel containing the member.

Outside of the span  $\overline{AB}$  the  $\overline{S_o/S_a}$  lines are drawn as for any cantilever system as per Art. 26.

## ART. 52. FIXED FRAMED ARCHES

A framed arch with fixed ends has three external redundant conditions according to Eq. (3c) and Fig. 3j, and hence requires for its analysis three elasticity equations either of the form of Eqs. (7h) or Eqs. (8d).

Temperature changes and abutment displacements come into prominence here. These effects are bound to remain more or less problematic because the actual circumstances attending the construction and later life of the structure cannot be foretold with any high degree of certainty. Therefore, it would seem unnecessary to attempt the analysis of the load effects with any extraordinary refinement and some assumptions may be made to simplify the work, provided they are on the side of safety.

It is nearly always permissible to neglect the effect of the web system in computing the elastic loads  $w$ . In preliminary work it is also admissible to choose a constant cross-section for the chord members.

As a general criticism it might be added that fixed framed arches are not commendable for the flat type, since the temperature and reaction effects produce very considerable

stresses which increase as the rise diminishes. Good rock foundations must be available under all circumstances, otherwise the fixed arch is prohibitive.

It is always advisable to separate the computation of the load stresses from the temperature and reaction displacement stresses so as to determine the relative importance of the latter.

**General relations between the external forces and the principal system.** There are several ways in which the three external redundant conditions may be applied, depending on the choice of the principal system. One of these was illustrated in Figs. 44E to J, where the principal system was a cantilever fixed at one end. Another assumption might be made by cutting the arch at the crown and creating two cantilevers fixed at the respective abutments of the arch.

However, the simplest determinate structure is always a truss on two supports, and in the present case that disposition will be made, as it affords the most comprehensive solution.

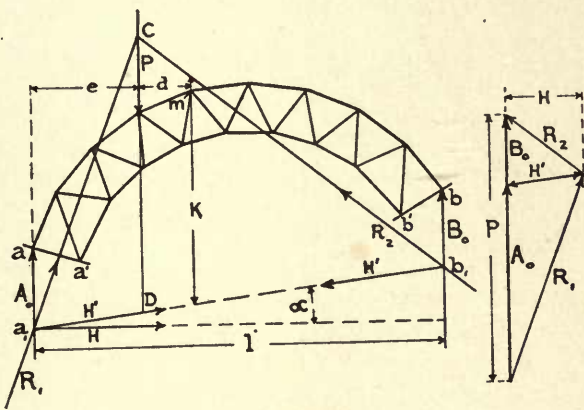


FIG. 52A.

All three methods have been used by Professor Mueller-Breslau and others, and the final results are identical and involve about the same amount of labor. In each case the external redundant conditions may be so chosen that the application of the simplified Eqs. (44A) becomes possible in accordance with the discussion in Art. 44.

Fig. 52A illustrates the relation of the external forces for a single applied load  $P$ , producing reactions  $R_1$  and  $R_2$ , intersecting in the point  $C$  on this load. This fixes the points  $a_1$  and  $b_1$  on the verticals through the outer supports  $a$  and  $b$  with span  $l$ . The triangle  $a_1cb_1$  thus becomes a resultant polygon with the closing line  $a_1b_1$ . The reaction  $R_1$  may be resolved into the vertical component  $A_o$  and the haunch thrust  $H'$  along  $a_1b_1$ . The reaction  $R_2$  may similarly be resolved into the vertical reaction  $B_o$  and the thrust  $H'$ , which latter is equal and opposite to the  $H'$  acting at  $a_1$ .

The vertical reactions  $A_o$  and  $B_o$  are the same as for a simple beam  $\overline{ab}$  with determinate supports  $A_o$  and  $B_o$ . Hence  $A_o = P(l - e) / l$  and  $B_o = Pe / l$ . Also the moment, for any point  $m$  of the simple beam, equals  $M_{om} = KH$ , where  $H$  is the horizontal component of  $H'$  and  $K$  is the vertical ordinate of the triangle  $a_1cb_1$  through the point  $m$ . Hence



$K = M_{om}/H = M_{om}/H' \cos \alpha$ . Therefore, the resultant polygon  $\overline{a_1 C b_1}$  is determined when  $H'$  and the closing line  $\overline{a_1 b_1}$  are found.

The external redundant conditions are now removed by relieving the fixed ends and resting the curved structure on two determinate supports at the extreme outer points  $a$  and  $b$ , Fig. 52B. This simple truss of span  $l$ , provided with a hinged bearing at  $a$  and a roller bearing at  $b$ , constitutes the principal system.

To each end of the principal system an imaginary rigid disk is attached as shown in the figure by the two shaded triangles. The redundant conditions are now applied to these disks as external forces or moments, thereby re-establishing conditions of stress in the principal system which are identical with those produced in the original structure while the redundant conditions were active. The two disks are not connected at  $O$ , but are free to transmit a set of forces independently to each abutment.

The equal and opposite forces  $X_b$  are chosen vertically, and the one acting upward is supposed to act on the disk  $\overline{OA}$ . The forces  $X_c$  are equal and opposite, but of unknown direction  $\beta$  with the horizontal, the one acting to the right is applied to the disk  $\overline{OA}$ . The

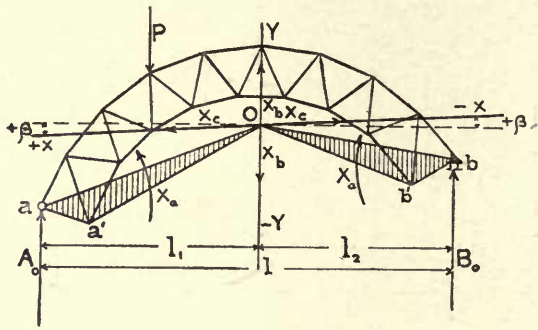


FIG. 52B.

two moments  $X_a$  are also equal and opposite and act separately, one on each disk. The pole  $O$  is not yet determined, but will be fixed by certain geometric conditions to be established later.

To determine the exact relations between these redundant forces and the principal system it is preferable to discuss only the forces acting on one end of the span. In Fig. 52c, the left-hand abutment is shown with the redundant forces which are active at that end only. A similar set, not shown, would be active at the right-hand abutment.

The structure is now referred to coordinate axes  $(x, y)$  with origin at  $O$ . The  $y$  axis is made vertical, and the  $x$  axis is coincident with the redundant  $X_c$  making the angle  $\beta$  with the horizontal. The location of  $O$  and the angle  $\beta$  are still unknown. The ordinate  $y_m$  of any point  $m$  is measured vertically from the  $x$  axis, while the abscissa  $x_m$  of this point is measured horizontally from the  $y$  axis instead of parallel to the  $x$  axis. This is more convenient in the considerations which follow.

The rigid disk  $\overline{aa'O}$  connects the origin  $O$  with the arch along  $\overline{aa'}$ , and to this origin are applied two equal and opposite forces  $H'$ , which are equal and parallel to the original haunch thrust acting at  $a_1$ . The equilibrium of the principal system and of the fixed

arch thus remains undisturbed. In the original fixed condition the force  $P$  produced the reactions  $R_1$  and  $R_2$  and these were resolved into components  $A_o$  and  $H'$  acting at  $a_1$  and  $B_o$  and  $H'$  acting at  $b_1$ .

Suppose now that all the external forces to the left of a section  $\bar{u}$  act on the principal system only, and that the three forces  $H'$  and the vertical reaction  $A_o$  are applied to the rigid disk  $\bar{a}'\bar{O}$  and are thence transmitted to the principal system. Then the force  $H'$  at  $a_1$  and the force  $H'$ , in opposite direction at  $O$ , form a couple with lever arm  $z_o \cos \alpha$  producing a moment  $X_a = H'z_o \cos \alpha$ . The other force  $H'$ , acting at  $O$  and to the right, may be resolved into two components  $X_b$  and  $X_c$ , where  $X_b$  is vertical along the  $y$  axis, and  $X_c$  acts along the  $x$  axis. The external forces to the left of the section and acting on the principal system, are then  $P$ ,  $A_o$ ,  $X_b$ ,  $X_c$  and a moment  $X_a = H'z_o \cos \alpha = Hz_o$ . Of these the two forces  $X_b$  and  $X_c$  and the moment  $X_a$  constitute the redundant conditions while the forces  $P$  and  $A_o$  are known and all are applied to the principal system

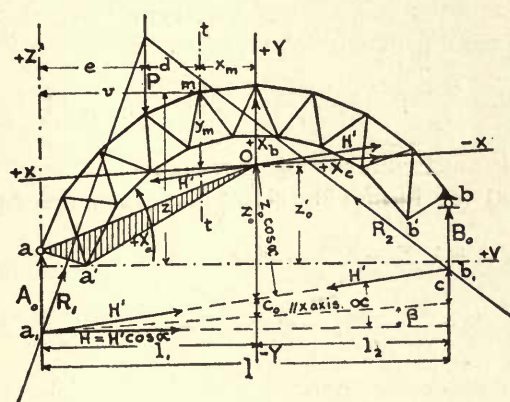


FIG. 52c.

to the left of the section  $\bar{t}\bar{t}$ . A similar set of external forces acts on the principal system to the right of the section, but these are not shown in Fig. 52c.

The moment of all external forces about any point  $m$  of any frame, involving three redundant conditions, is expressed by Eq. (7A) as

$$M_m = M_{om} - M_a X_a - M_b X_b - M_c X_c \quad . . . . . (52A)$$

wherein  $M_{om} = A_o(l_1 - x_m) - Pd$  = the moment about  $m$  due to the load  $P$  acting on the principal system. This is condition  $X = 0$ .

$M_a = 1$  = the moment about  $m$  due to the moment  $X_a = 1$  applied to the principal system. Condition  $X_a = 1$ .

$M_b = 1 \cdot x_m$  = the moment about  $m$  due to the force  $X_b = 1$  acting on the principal system. Condition  $X_b = 1$ .

$M_c = 1 \cdot y_m \cos \beta$  = the moment about  $m$  due to the force  $X_c = 1$  acting on the principal system. Condition  $X_c = 1$ .

Substituting these values into Eq. (52A) gives the following fundamental moment equation for fixed arches:

$$M_m = M_{om} - 1 \cdot X_a - x_m X_b - y_m \cos \beta X_c. \quad (52B)$$

Before  $M_m$  can be determined for any point  $m$  of the arch, the three redundants  $X_a$ ,  $X_b$  and  $X_c$  must be evaluated from three simultaneous work equations of the form of Eqs. (44B), which equations may be made to apply to the present problem by so locating the  $(x, y)$  axes that  $\delta_{ab}$ ,  $\delta_{ac}$  and  $\delta_{bc}$  all become zero.

Since there are as many values for the redundants as there are panel points on the arch, and for each point there will be as many values as there are positions of the moving loads requiring investigation, the only practical solution of the problem is by means of influence lines, first for the three redundants and then for the moment  $M_m$  for each member of the arch.

The stress  $S$  in any member may always be found from the moment  $M_m$  about the center of moments  $m$  for that member and the lever arm  $r_m$  measured from this moment center perpendicular to the direction of the member. Hence

$$S = \frac{M_m}{r_m}; \quad S_o = \frac{M_{om}}{r_m}; \quad S_a = \frac{M_a}{r_m}; \quad S_b = \frac{M_b}{r_m}; \quad \text{and} \quad S_c = \frac{M_c}{r_m}, \quad (52C)$$

where the lever arm  $r_m$  is constant for the same member.

Therefore, Eq. (52B) will furnish the stress in any member as

$$S = \frac{M_m}{r_m} = \frac{1}{r_m} [M_{om} - 1 \cdot X_a - x_m X_b - y_m \cos \beta X_c] = S_o - S_a X_a - S_b X_b - S_c X_c, \quad (52D)$$

where 
$$S_a = \frac{M_a}{r_m} = \frac{1}{r_m}; \quad S_b = \frac{M_b}{r_m} = \frac{x_m}{r_m}; \quad \text{and} \quad S_c = \frac{M_c}{r_m} = \frac{y_m \cos \beta}{r_m}. \quad (52E)$$

**Location of the coordinate axes.** According to the conditions imposed by the simplifying process of Eqs. (8D), discussed in Art. 44, the coordinate axes must be so located that the displacements  $\delta$ , bearing different double subscripts, must be made zero.

These displacements  $\delta$  as given by Eqs. (8B), then become

$$\delta_{ab} = \delta_{ba} = \Sigma S_a S_b \rho = \Sigma S_a S_b \frac{l}{EF} = 0;$$

$$\delta_{ac} = \delta_{ca} = \Sigma S_a S_c \rho = \Sigma S_a S_c \frac{l}{EF} = 0;$$

$$\delta_{bc} = \delta_{cb} = \Sigma S_b S_c \rho = \Sigma S_b S_c \frac{l}{EF} = 0;$$

and substituting the values for the stresses from Eqs. (52E) then

$$\left. \begin{aligned} \delta_{ab} = \delta_{ba} &= \Sigma \frac{x l}{EF r^2} = \Sigma x w_a = 0 \\ \delta_{ac} = \delta_{ca} &= \Sigma \frac{y \cos \beta l}{EF r^2} = \cos \beta \Sigma y w_a = 0 \\ \delta_{bc} = \delta_{cb} &= \Sigma \frac{x y \cos \beta l}{EF r^2} = \cos \beta \Sigma x y w_a = 0 \end{aligned} \right\}, \quad (52F)$$



where  $w_a = 1 \cdot l / EFr^2$  for a moment unity, according to Eqs. (36B) and (36D), giving  $w_a = Al/r = Sl/EFr = Ml/EFr^2$  and representing a certain geometric function called an elastic load for some particular pin point with coordinates  $(x, y)$ .

Eqs. (52F) then represent the conditions which determine the location of the coordinate axes such that the simple work Eqs. (44A) become applicable.

The first two conditions (52F) imply that the origin  $O$  of the  $(x, y)$  coordinate axes is the center of gravity of the several elastic loads of all panel points of the principal system. This must be so because the moments  $\Sigma xw_a$  and  $\Sigma yw_a$  could not be zero unless the resultant  $\Sigma w_a$  passes through the origin. According to the third condition, the angle between the axes must be such that the centrifugal moment  $\Sigma xyw_a = 0$ , which is true when the axes are related as conjugate axes.

The origin  $O$  may then be located with respect to any assumed pair of axes as the  $(z, v)$  axes in Fig. 52C, where the  $z$  axis is taken vertically through the point  $a$  and the  $v$  axis is any horizontal axis conveniently located say through  $a'$ . The coordinates  $z, v$ , of all the panel points, are then determined from the arch diagram and tabulated. The  $w_a$  elastic loads are computed from Eq. (36B) (and Eqs. (36D) if the web members are included) for each pin point. See the problem in Art. 51. Finally the moments  $zw_a$  and  $vw_a$  are found and from these the coordinates  $l_1$  and  $z_o'$  for the origin  $O$  are obtained from

$$l_1 = \frac{\Sigma vw_a}{\Sigma w_a} \quad \text{and} \quad z_o' = \frac{\Sigma zw_a}{\Sigma w_a} \quad (52G)$$

This fixes the  $y$  axis, which is parallel to the vertical  $z$  axis through the center of gravity  $O$ . The  $x$  axis, while passing through  $O$ , makes some angle  $\beta$  with the horizontal such that  $\Sigma xyw_a = 0$ , according to the last of Eqs. (52F).

The  $(x, y)$  coordinates are derived from the  $(z, v)$  coordinates when the angle  $\beta$  is determined. Taking  $\beta$  positive when measured to the left of the origin and below the horizontal, or to the right and above the horizontal as shown in Fig. 52C, then

$$x = l_1 - v \quad \text{and} \quad y = z - z_o' + x \tan \beta \quad (52H)$$

The angle  $\beta$  is found by substituting the value for  $y$  from Eqs. (52H) into the condition equation, giving

$$\Sigma xyw_a = \Sigma x[z - z_o' + x \tan \beta]w_a = 0;$$

or

$$\Sigma xzw_a - z_o' \Sigma xw_a + \tan \beta \Sigma x^2w_a = 0;$$

and noting that  $\Sigma xw_a = 0$ , then

$$\tan \beta = - \frac{\Sigma xzw_a}{\Sigma x^2w_a} \quad (52J)$$

The abscissæ  $x$  being known from Eqs. (52H) the values  $\Sigma xzw_a$  and  $\Sigma x^2w_a$  are readily found and  $\tan \beta$  is then obtained from Eq. (52J). Finally, the  $y$  ordinates are computed by the second Eq. (52H) and the new axes and  $(x, y)$  coordinates are thus determined.

For symmetric arches the  $x$  axis is horizontal and  $\tan \beta = 0$ , thus greatly lessening the foregoing computations.

**Influence lines for  $X_a$ ,  $X_b$ ,  $X_c$  and  $M_m$ .** The coordinate axes  $(x, y)$  having been located to fulfill the requirements making  $\delta_{ab}=\delta_{ba}=0$ ,  $\delta_{ac}=\delta_{ca}=0$  and  $\delta_{bc}=\delta_{cb}=0$ , the simplified Eqs. (44A) become applicable to the present problem.

Since it is desirable to investigate separately the effects due to loads, temperature and abutment displacements, the load effect will be considered first for immovable abutments. Eqs. (44A) then take the simple form of Eqs. (44B), as

$$X_a = \frac{\Sigma P_m \delta_{ma}}{\delta_{aa}}; \quad X_b = \frac{\Sigma P_m \delta_{mb}}{\delta_{bb}} \quad \text{and} \quad X_c = \frac{\Sigma P_m \delta_{mc}}{\delta_{cc}}. \quad (52K)$$

Eqs. (8B) give the displacements  $\delta_{aa}$ ,  $\delta_{bb}$  and  $\delta_{cc}$  in terms of the stresses in the members. Noting that  $\rho = l/EF$ , and substituting the values for  $S_a$ ,  $S_b$  and  $S_c$  from Eqs. (52E), then Eqs. (8B) give

$$\delta_{aa} = \Sigma S_a^2 \frac{l}{EF} = \Sigma \frac{l}{EFr^2}; \quad \delta_{bb} = \Sigma S_b^2 \frac{l}{EF} = \Sigma \frac{x^2 l}{EFr^2}; \quad \delta_{cc} = \Sigma S_c^2 \frac{l}{EF} = \cos^2 \beta \Sigma \frac{y^2 l}{EFr^2}$$

and calling  $l/EFr^2 = w_a$ ;  $x^2 l/EFr^2 = x^2 w_a = xw_b$  and  $y^2 l/EFr^2 = y^2 w_a = yw_c$  then Eqs. (52K) become for a single load unity at any point  $m$ :

$$\left. \begin{aligned} X_a &= \frac{1 \cdot \delta_{ma}}{\Sigma w_a} \\ X_b &= \frac{1 \cdot \delta_{mb}}{\Sigma x^2 w_a} = \frac{1 \cdot \delta_{mb}}{\Sigma xw_b} \\ X_c &= \frac{1 \cdot \delta_{mc}}{\cos^2 \beta \Sigma y^2 w_a} = \frac{1 \cdot \delta_{mc}}{\cos^2 \beta \Sigma yw_c} \end{aligned} \right\} \dots \dots \dots (52L)$$

Eqs. (52L) furnish the values  $X_a$ ,  $X_b$  and  $X_c$  for any position  $m$  of a single moving load  $P_m=1$ , as functions of the deflections  $\delta_{ma}$ ,  $\delta_{mb}$  and  $\delta_{mc}$  of the point  $m$  resulting from the conventional loadings  $X_a=1$ ,  $X_b=1$ , and  $X_c=1$ .

The exact significance of the deflections  $\delta_{ma}$ ,  $\delta_{mb}$  and  $\delta_{mc}$  may be determined from their values as given by Eqs. (8A), noting that  $S_o = M_{om}/r_m$  for a load  $P_m=1$  applied at  $m$  from Eqs. (52c), also using the values given by Eqs. (52E). Hence

$$\left. \begin{aligned} 1 \cdot \delta_{ma} &= \Sigma S_o S_a \frac{l}{EF} = \Sigma \frac{M_{om} l}{EFr_m^2} = \Sigma M_{om} w_a \\ 1 \cdot \delta_{mb} &= \Sigma S_o S_b \frac{l}{EF} = \Sigma \frac{M_{om} xl}{EFr_m^2} = \Sigma M_{om} w_b \\ 1 \cdot \delta_{mc} &= \Sigma S_o S_c \frac{l}{EF} = \cos \beta \Sigma \frac{M_{om} yl}{EFr_m^2} = \cos \beta \Sigma M_{om} w_c \end{aligned} \right\} \dots \dots \dots (52M)$$

Now  $\delta_{ma}$  is the deflection of a point  $m$  due to  $X_a=1$  and  $P_m=0$ , and by Eqs. (52M) it is equal to the sum of the moments  $M_{om} w_a$  of the loads  $w_a$  about  $m$ . Hence  $\delta_{ma}$  must represent the ordinate to a moment digram drawn for the loads  $w_a$  with a pole unity. Also, if this moment diagram be drawn with a pole  $H_a = \Sigma w_a$ , then the resulting ordinates  $\eta_a$  will represent ordinates of the  $X_a$  influence line according to Eqs. (52L).

Similarly the moment diagram drawn for the loads  $w_b = xw_a$  with a pole  $H_b = \Sigma xw_b$  will furnish ordinates  $\eta_b$  for the  $X_b$  influence line and a third moment diagram drawn for the loads  $w_c = yw_a$  with a pole  $H_c = \cos \beta \Sigma yw_c$  will give ordinates  $\eta_c$  for the  $X_c$  influence line, noting that one of the  $\cos \beta$  factors cancels.

Hence the equations for the influence lines of the three redundant conditions from Eqs. (52L), become

$$\left. \begin{aligned} X_a &= \frac{1 \cdot \delta_{ma}}{\Sigma w_a} = \frac{\delta_{ma}}{H_a} = \eta_{am} \\ X_b &= \frac{1 \cdot \delta_{mb}}{\Sigma xw_b} = \frac{\delta_{mb}}{H_b} = \eta_{bm} \\ X_c &= \frac{1 \cdot \delta_{mc}}{\cos \beta \Sigma yw_c} = \frac{\delta_{mc}}{H_c} = \eta_{cm} \end{aligned} \right\} \dots \dots \dots (52N)$$

These influence lines remain the same for the same structure and hence are drawn only once.

The moment influence line  $M_m$ , for any point  $m$  with coordinates  $x_m$  and  $y_m$ , is derived from Eq. (52B), giving any moment ordinate as

$$\eta_m = M_m = \overline{M}_{om} - [X_a + x_m X_b + y_m \cos \beta X_c] = \eta_{om} - [\eta_a + x_m \eta_b + y_m \cos \beta \eta_c], \quad (52O)$$

where  $\eta_{om}$  is any ordinate of the ordinary moment influence line  $\overline{M}_{om}$ , drawn for the point  $m$  of a simple beam on two determinate supports  $A_o$  and  $B_o$ , which is a different line for each point  $m$ . The ordinates  $\eta_a$ ,  $\eta_b$  and  $\eta_c$  are those respectively of the  $X_a$ ,  $X_b$  and  $X_c$  influence lines all under the same panel point of the truss.

Hence, the moment influence line  $M_m$  for any point  $m$  is drawn by computing the ordinates  $-(\eta_a + x_m \eta_b + y_m \cos \beta \eta_c)$  for all panel points of the loaded cord and plotting these ordinates negatively from the  $\overline{M}_{om}$  influence line. Positive areas thus correspond to positive moments.

This  $M_m$  influence line will serve to find the maximum and minimum bending moments for the point  $m$  due to any system of concentrated loads. The influence line gives the load divides.

**The stress influence line for any member** may be derived from the moment influence line drawn for the center of moments  $m$  for that particular member. Thus if  $r_m$  is the lever arm for a certain member  $S$  with center of moments  $m$ , then  $S = M_m/r_m$ , and the ordinates  $\eta_s$  for this stress influence line by Eq. (52O) become

$$\eta_s = \frac{M_m}{r_m} = \frac{1}{r_m} [\eta_{om} - (\eta_a + x_m \eta_b + y_m \cos \beta \eta_c)], \quad \dots \dots \dots (52P)$$

where the several  $\eta$  ordinates are as above defined and all measured under the same panel point. Positive areas then give positive or tensile stress. The moment influence line for the center of moments for any member may be directly used by applying the factor  $1/r_m$  to obtain the stress.

The rather lengthy operation of computing all these ordinates for the several stress influence lines for all the members may be considerably shortened by employing the



following suggestions: Thus the multiplications  $x_m \eta_b$  and  $y_m \cos \beta \eta_c$ , may be performed graphically by laying off angles whose tangents are respectively  $x_m$  and  $y_m \cos \beta$ , as illustrated in Fig. 52d, using the scale of the  $\eta$  ordinates. Two such diagrams are required for each  $M_m$  or  $S$  line.

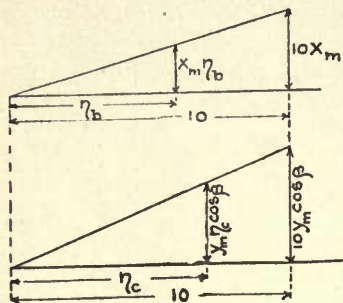


FIG. 52d.

If a proportional divider is at hand, then it may be used to perform these multiplications by setting the dividers first for the ratio  $1:x_m$  and then for  $1:y_m \cos \beta$ .

Aside from the above methods, the stress influence line for any web member may be derived from the influence lines of two adjacent chords by using the following method given by Professor Mueller-Breslau.

When the top chord is the *loaded chord*, then the adjacent members of the bottom chord are used, and vice versa.

In Fig. 52E, assume a unit positive stress in  $L_1$  and resolve the same into components  $-\epsilon_1$  parallel to  $D_1$  and  $+\epsilon_2$  parallel to  $D_2$ .

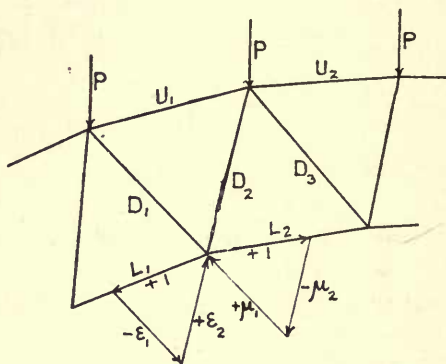


FIG. 52E.

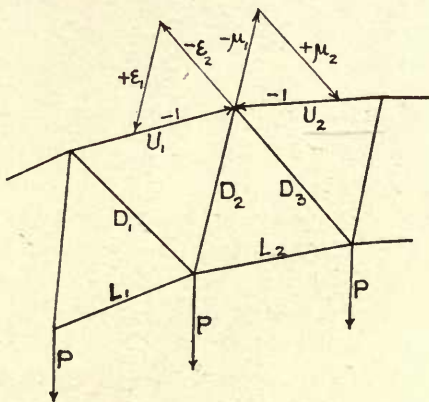


FIG. 52F.

Then assume a unit positive stress in  $L_2$  and resolve this into components  $+\mu_1$  parallel to  $D_1$  and  $-\mu_2$  parallel to  $D_2$ . Then for the top chord loaded and no load at  $m$ , the stresses  $D_1$  and  $D_2$  become

$$\left. \begin{aligned} D_1 &= -\epsilon_1 L_1 + \mu_1 L_2 = \mu_1 \left( -\frac{\epsilon_1 L_1}{\mu_1} + L_2 \right) \\ D_2 &= +\epsilon_2 L_1 - \mu_2 L_2 = \mu_2 \left( +\frac{\epsilon_2 L_1}{\mu_2} - L_2 \right) \end{aligned} \right\} \dots \dots \dots (52q)$$

By substituting influence ordinates for the stresses  $D$  and  $L$  this furnishes a ready means of deducing a  $D$  influence line from the two influence lines of the adjacent chords. Thus the  $D_1$  influence area is the area between the  $L_2$  line and the  $\epsilon_1 L_1 / \mu_1$  line and the

final  $D_1$  area thus obtained will have a factor  $\mu_1$ . The ordinates to be used in the equations are always under the same load point.

When the bottom chord is the loaded chord and there is no load at the point  $n$ , then using the stresses as indicated in Fig. 52F, the diagonals  $D_2$  and  $D_3$  become

$$\left. \begin{aligned} D_2 &= +\varepsilon_1 U_1 - \mu_1 U_2 = \mu_1 \left( \frac{\varepsilon_1 U_1}{\mu_1} - U_2 \right) \\ D_3 &= -\varepsilon_2 U_1 + \mu_2 U_2 = \mu_2 \left( -\frac{\varepsilon_2 U_1}{\mu_2} + U_2 \right) \end{aligned} \right\} \dots \dots \dots (52R)$$

The value of  $D_2$  will be the same in both equations Q and R and the signs will come alike by noting that the influence ordinates for the  $L$  and  $U$  lines have opposite signs and hence the coefficients  $\varepsilon$  and  $\mu$  have opposite signs from those used in Eqs. (52Q).

The resultant polygon for any case of applied loads  $P$  may be located by finding the corresponding values of  $X_a$ ,  $X_b$ , and  $X_c$  from the three influence lines for these redundants, having previously located the  $(x, y)$  axes.

The redundants  $X_c$  and  $X_b$ , Fig. 52C, were taken as the components of  $H'$ , respectively coincident with the  $x$  and  $y$  axes. The angle  $\beta$ , which the  $x$  axis makes with the horizontal is given by Eq. (52J) and the  $y$  axis was taken vertically. Hence the horizontal component  $H$  of  $X_c$  is

$$\left. \begin{aligned} H &= X_c \cos \beta, \quad \text{and from Fig. 52C,} \\ \tan \alpha &= \tan \beta + \frac{X_b}{H} \\ H' &= \frac{H}{\cos \alpha} = \frac{X_c \cos \beta}{\cos \alpha} \\ z_o &= \frac{X_a}{H' \cos \alpha} = \frac{X_a}{H} \\ c &= \frac{X_b l}{H} = l(\tan \alpha - \tan \beta) \\ c_o &= \frac{X_b l_1}{H} = l_1(\tan \alpha - \tan \beta) \\ X_a &= X_c z_o \cos \beta = X_b z_o \frac{l}{c} \end{aligned} \right\} \dots \dots \dots (52S)$$

These dimensions fix the location of the closing line  $\overline{a_1 b_1}$  on the two end verticals of the abutments, also the haunch thrust  $H'$ , all in terms of  $X_a$ ,  $X_b$  and  $X_c$ .

The reactions  $R_1$  and  $R_2$  may be found from the vertical reactions  $A_o$  and  $B_o$  and the thrust  $H'$ . The vertical reactions are those due to loads  $P$  acting on a simple beam  $\overline{a_1 b_1}$  and may be computed from  $A_o = \Sigma P(l-e)/l$  and  $B_o = \Sigma P e/l$ . The reactions  $R_1$  and  $R_2$  must then intersect on the line of the resultant  $R$  of all the applied loads  $P$ .

A force polygon is drawn by laying off all the loads  $P$  in proper succession, dividing this load line into the parts  $A_o$  and  $B_o$  and at the dividing point draw a line parallel to  $\overline{a_1b_1}$  of length equal to  $H'$ . This determines the pole of the force polygon from which the reactions  $R_1$  and  $R_2$  and the resultant polygon through  $a_1$  and  $b_1$  are easily drawn. See also the force polygon in Fig. 52A, showing how the pole  $O$  is located when  $H'$ ,  $A_o$  and  $B_o$  are given.

**Temperature stresses.** For the general case of temperature effects, each member may be supposed to undergo some change  $\pm \Delta l_t = \epsilon t l$  in its length. These changes will produce a deformation in the frame, giving rise to external redundant forces  $X_{at}$ ,  $X_{bt}$  and  $X_{ct}$ , which may be found from Eqs. (44c), where abutment displacements and load effects are excluded.

Using the values of  $\delta_{at}$ ,  $\delta_{bt}$  and  $\delta_{ct}$  as given by Eqs. (8c) and then noting the substitutions for  $\delta_{aa} = \Sigma w_a$ ,  $\delta_{bb} = \Sigma xw_b$  and  $\delta_{cc} = \Sigma yw_c$  made in Eqs. (52N), the Eqs. (44c) become

$$\left. \begin{aligned} X_{at} &= \frac{\delta_{at}}{\delta_{aa}} = \frac{\Sigma S_a \Delta l_t}{\Sigma w_a} \\ X_{bt} &= \frac{\delta_{bt}}{\delta_{bb}} = \frac{\Sigma S_b \Delta l_t}{\Sigma xw_b} \\ X_{ct} &= \frac{\delta_{ct}}{\delta_{cc}} = \frac{\Sigma S_c \Delta l_t}{\cos \beta \Sigma yw_c} \end{aligned} \right\}, \quad \dots \dots \dots (52T)$$

where  $\delta_{at}$  represents a rotation measured in arc, while  $\delta_{bt}$  and  $\delta_{ct}$  are the displacements of the origin  $O$ , due to the assumed temperature changes measured in the directions of the  $y$  and  $x$  axes respectively.

These redundant conditions would then produce a moment  $M_{mt}$  about any point  $m$  as given from Eq. (52B), where  $M_{om} = 0$ , thus

$$-M_{mt} = X_{at} + x_m X_{bt} + y_m \cos \beta X_{ct}. \quad \dots \dots \dots (52U)$$

Since the changes  $\Delta l_t$  in the lengths of the members represent a simultaneous condition and the stresses  $S_a$ ,  $S_b$  and  $S_c$  were previously found in computing the  $w$  loads, it is best to solve Eqs. (52T) analytically, using the denominators previously found for the pole distances of the  $X$  influence lines. The moment Eq. (52U) can then be solved for any moment point to obtain the stress in a corresponding member.

For a uniform change in temperature of  $\pm t^\circ$  from the normal, an approximate determination of temperature stresses may be obtained for arches of high rise. For flat arches this assumption would not be permissible. When the effect of the redundants  $X_a$  and  $X_b$  is neglected then the stresses may be found from Eqs. (52T) and (52U) as

$$-M_{mt} = y_m \cos \beta X_{ct} = y_m \left( \frac{\Sigma S_c \Delta l_t}{\Sigma yw_c} \right). \quad \dots \dots \dots (52V)$$

**The effect of abutment displacements** may be investigated in a similar manner, using Eqs. (44A) and omitting the terms representing the loads  $P$  and the temperature. The



displacements  $\Delta r$  must then be assumed or estimated and  $\delta_a$ ,  $\delta_b$  and  $\delta_c$  become zero. Hence the redundants and moments may be found in precisely the same manner above illustrated for temperature effects, thus

$$\left. \begin{aligned} X_{ar} &= \frac{\Sigma R_a \Delta r}{\delta_{aa}} \\ X_{br} &= \frac{\Sigma R_b \Delta r}{\delta_{bb}} \\ X_{cr} &= \frac{\Sigma R_c \Delta r}{\delta_{cc}} \end{aligned} \right\}, \dots \dots \dots (52w)$$

where the  $\delta$ 's in the denominators are those used in Eqs. (52t).

**Example.** Owing to the comparatively few fixed arches of the framed type in existence, it was difficult to find a suitable example to use in illustrating the above method of analysis. For this reason the present example, Figs. 52g, was taken with slight modification, from the one given by Professor Mehrrens in his "Statik der Baukonstruktionen," Vol. III, p. 343.

The bridge has a clear span of 162 ft. and rise of 23.69 ft. The roadway is 30 ft. wide and the estimated weight is about 400,000 lbs., making 20 kips per truss per panel. The uniform live load is taken at 110 lbs. per sq.ft. of roadway or 30 kips per truss per panel, for medium highway loading. The top chord is the loaded chord and the arch is symmetric, making  $\beta=0$ .

The top chord panel points are on the arc of a circle whose radius is  $R_u=163.7$  ft. The chords are parallel and the radius for the bottom chord points is  $R_l=148.7$  ft.

Ordinarily the computation might be carried out by neglecting the effect of the web members, but for the sake of completeness all members will be included.

The cross-sections  $F$ , lengths  $l$ , and lever arms  $r$  of all the members, are tabulated in Tables 52A and 52B, and the  $Ew_a$  loads are computed by successive steps indicated by the headings of the columns. The lever arms  $r_u$  and  $r_n$  are found as described in Figs. 36B and 36F. In the present solution the areas were converted into sq.ft. in computing  $\Delta l$  so that the modulus  $E$  enters with its real value of 4,176,000 kips per sq.ft. instead of 29,000 kips per sq.in. as used in the problem of Art. 51. The stresses  $S_a$  due to a moment  $X_a=1$  kip ft., are easily found, as the reciprocals of the lever arms  $r$ , being careful to observe the signs of the stresses.

The arch being symmetric, the  $y$  axis is known to be the vertical axis of symmetry, and the angle  $\beta$ , which the  $x$  axis makes with the horizontal, becomes zero. Hence, the  $(x, y)$  axes are located by computing the ordinate  $z_o'=E\Sigma zw_a/E\Sigma w_a=21.927$  ft., thus determining the distance from the  $v$  axis to the center of gravity  $O$  of the  $w_a$  loads. See Table 52c. The  $y$  ordinates then become  $y=z-z_o'$ . The  $(x, z)$  coordinates must of course be determined from the arch dimensions or the equations of the chord curves.

Table 52c then gives the functions  $Ew_b=Exw_a$ ,  $Ew_c=Eyw_a$ ,  $Exw_b$  and  $Eyw_c$  all in terms of the  $w_a$  loads. The sums  $E\Sigma w_a$ ,  $E\Sigma xw_b$  and  $E\Sigma yw_c$  represent the pole distances for the  $X_a$ ,  $X_b$  and  $X_c$  influence lines such that the influence ordinates will be actual when measured to the scale of lengths.

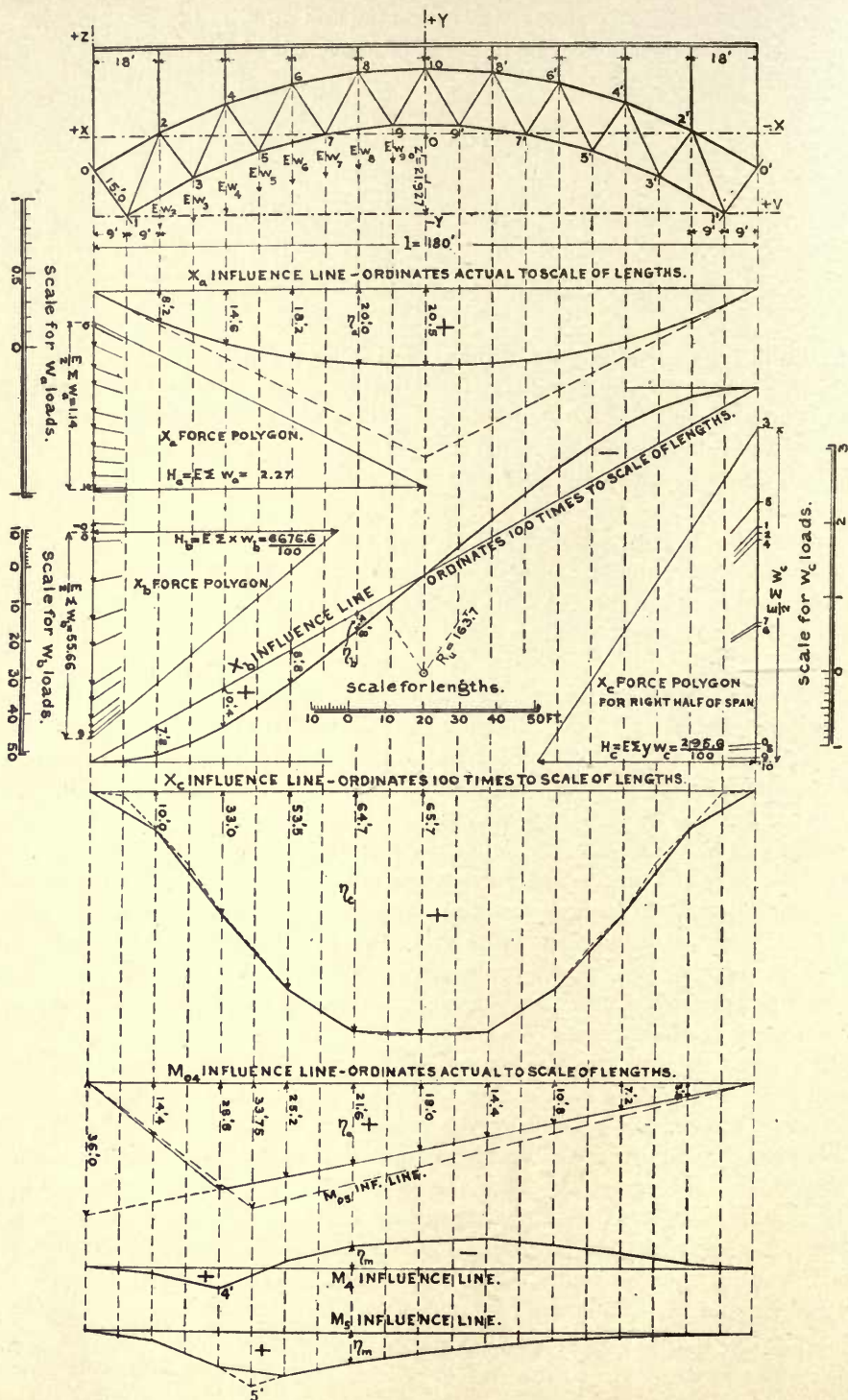


FIG. 52g.

TABLE 52A

$w_a$  LOADS FOR CHORD MEMBERS

Chord.	$F$ Sq.in.	$l$ ft.	$r$ ft.	$S_a=\frac{1}{r}$ Kips.	$f=\frac{S_a}{F}$ Kips sq.ft.	$*E\delta l=\frac{S_a l}{F}$ ft.	$*Ew_a=\frac{E\delta l}{r}$	Panel Point.
0-2	100	20.73	14.92	-0.0670	-0.0965	-2.002	0.1341	1
2-4	110	19.51	14.84	-0.0674	-0.0883	-1.728	0.1165	3
4-6	120	18.72	14.79	-0.0676	-0.0811	-1.512	0.1022	5
6-8	124	18.25	14.77	-0.0677	-0.0786	-1.440	0.0975	7
8-10	130	18.03	14.79	-0.0676	-0.0737	-1.325	0.0896	9
1-3	82	20.59	15.14	0.0661	0.1161	2.390	0.1580	2
3-5	94	19.33	15.21	0.0657	0.1008	1.944	0.1277	4
5-7	100	18.55	15.25	0.0656	0.0945	1.757	0.1152	6
7-9	104	18.13	15.28	0.0654	0.0906	1.642	0.1074	8
$\frac{1}{2}(9-9')$	128	9.00	15.31	0.0653	0.0734	0.662	0.0432	10

\* Above  $w_a$  loads are for  $E=29,000 \times 144=4,176,000$  kips per sq.ft.

TABLE 52B

$w_a$  LOADS FOR WEB MEMBERS

Member.	$F$	$l$	$r$	$S_a=\frac{1}{r}$	$f=\frac{S_a}{F}$	$*E\delta l=\frac{S_a l}{F}$	$\tau_u$ and $\tau_n$	$*Ew_a=\frac{*E\delta l}{r}$ For loaded panel Points.		At Panel Point.
	Sq.in.	ft.	ft.	Kips.	Kips. sq.ft.	ft.	ft.	+	-	
0-1	8	15.03	.....	.....	.....	.....	{ 12.81	0.0248	.....	0
1-2	14	24.06	780.87	+0.00128	+0.0132	+0.3176	{ 13.05	.....	0.0243	2
							{ 21.90	.....	0.0419	2
2-3	18	15.26	132.91	0.00752	0.0602	0.9186	{ 18.96	0.0485	.....	4
							{ 13.26	0.0533	.....	2
3-4	10	21.79	443.54	0.00225	0.0324	0.7060	{ 13.65	.....	0.0517	4
							{ 19.98	.....	0.0407	4
4-5	18	15.66	154.04	0.00649	0.0519	0.8128	{ 17.70	0.0459	.....	6
							{ 13.80	0.1055	.....	4
5-6	6	20.09	331.25	0.00302	0.0725	1.4565	{ 14.40	.....	0.1011	6
							{ 18.45	.....	0.0513	6
6-7	14	16.19	175.75	0.00569	0.0585	0.9471	{ 16.62	0.0570	.....	8
							{ 14.37	0.1205	.....	6
7-8	6	18.78	260.26	0.00384	0.0922	1.7315	{ 15.18	.....	0.1141	8
							{ 17.10	.....	0.0688	8
8-9	10	16.91	206.93	0.00483	0.0696	1.1769	{ 15.84	0.0743	.....	10
							{ 15.03	0.1225	.....	8
9-10	6	17.76	231.40	0.00432	0.1037	1.8417	{ 16.05	.....	0.1148	10

\* Above  $w_a$  loads are for  $E=29,000 \times 144=4,176,000$  kips per sq.ft.



TABLE 52C

COMPUTATION OF *w* LOADS AND POLE DISTANCES

Pin Points.	Total <i>Ew<sub>a</sub></i> Loads.	<i>z</i> ft.	<i>Ezw<sub>a</sub></i>	<i>x</i> ft.	<i>y</i> = <i>z</i> - <i>z</i> <sub>o</sub> ' ft.	<i>Ew<sub>b</sub></i> = <i>Exw<sub>a</sub></i>	<i>Ew<sub>c</sub></i> = <i>Eyw<sub>a</sub></i>	<i>Exw<sub>b</sub></i>	<i>Eyw<sub>c</sub></i>	Pin Points.
0	0.0248	12.03	0.2983	90	- 9.897	2.232	-0.245	200.88	2.429	0
1	0.1341	0.00	0.0	81	-21.927	10.862	-2.940	879.83	64.474	1
2	0.1451	22.31	3.2372	72	+ 0.383	10.447	+0.056	752.20	0.021	2
3	0.1165	9.99	1.1638	63	-11.937	7.340	-1.391	462.39	16.601	3
4	0.1893	29.83	5.6468	54	+ 7.903	10.222	+1.496	552.00	11.823	4
5	0.1022	17.03	1.7405	45	- 4.897	4.599	-0.501	211.55	2.451	5
6	0.1292	34.99	4.5207	36	+13.063	4.651	+1.688	167.44	22.046	6
7	0.0975	21.53	2.0992	27	- 0.397	2.633	-0.039	71.08	0.015	7
8	0.1040	38.01	3.9530	18	+16.083	1.872	+1.673	33.70	26.900	8
9	0.0896	23.69	2.1226	9	+ 1.763	0.806	+0.158	7.26	0.279	9
$\frac{1}{2}(10)$	0.0027	39.00	0.1053	0	+17.073	0.0	+0.046	0.00	0.787	$\frac{1}{2}(10)$
	$\frac{E}{2} \Sigma w_a =$ 1.1350  <i>H<sub>a</sub></i> = 2.270	..... .....  <i>z</i> <sub>o</sub> ' =	$\frac{E}{2} \Sigma zw_a =$ 24.8874 24.8874 $\frac{24.8874}{1.135} = 21.92$	..... .....  7 ft.		$\frac{E}{2} \Sigma w_b =$ 55.664	$\frac{E}{2} \Sigma w_c = 0$ + 5.117 - 5.116	$\frac{E}{2} \Sigma xw_b =$ 3338.33	$\frac{E}{2} \Sigma yw_c =$ 147.826	  <i>H<sub>b</sub></i> = 6676.6 <i>H<sub>c</sub></i> = 295.65

TABLE 52D

ORDINATES FOR MOMENT INFLUENCE LINES

Panel Point.	$\eta_a$ ft.	$\eta_b$ ft.	$\eta_c$ ft.	<i>M<sub>4</sub></i> Influence Line, $\eta_m = \eta_{om} - [\eta_a + 54\eta_b + 7.9\eta_c]$				<i>M<sub>5</sub></i> Influence Line. $\eta_m = \eta_{om} - [\eta_a + 45\eta_b - 4.897\eta_c]$			
				$\eta_o$	$54\eta_b$	$7.9\eta_c$	$\eta_m$	$\eta_o$	$45\eta_b$	$4.897\eta_c$	$\eta_m$
2	8.2	0.078	0.100	14.4	4.21	0.79	1.20	13.5	3.51	0.49	2.28
4	14.6	0.104	0.330	28.8	5.62	2.61	5.97	27.0	4.68	1.62	9.34
6	18.2	0.088	0.535	25.2	4.75	4.23	-1.98	31.5	3.96	2.62	11.96
8	20.0	0.048	0.647	21.6	2.59	5.11	-6.10	27.0	2.16	3.17	8.01
10	20.5	0.000	0.657	18.0	0.00	5.19	-7.69	22.5	0.00	3.22	5.22
8'	20.0	-0.048	0.647	14.4	-2.59	5.11	-8.12	18.0	-2.16	3.17	3.33
6'	18.2	-0.088	0.535	10.8	-4.75	4.23	-6.88	13.5	-3.96	2.62	1.88
4'	14.6	-0.104	0.330	7.2	-5.62	2.61	-4.39	9.0	-4.68	1.62	0.70
2'	8.2	-0.078	0.100	3.6	-4.21	0.79	-1.18	4.5	-3.51	0.49	0.30

All ordinates are in feet.

The three influence lines for the redundants are now drawn by constructing the force polygons, using the  $w_a$ ,  $w_b$  and  $w_c$  forces in the order of the loaded panel points and drawing the corresponding equilibrium polygons. The scales used for the  $w$  forces are any convenient scales, noting that the pole distance must of course be laid off to the same scale as the forces. The poles  $H_b$  and  $H_c$  were divided by one hundred, thus making the  $\eta_b$  and  $\eta_c$  ordinates hundred times actual when measured to the scale of lengths. The  $w_c$  forces being of both signs it is best to plot their algebraic sums from some initial point of the load line and number the points in the order of the loads, thus 0, 1, 2, 3, etc., to 10. The pole rays are drawn in the same order. Note the check by which the end rays of the  $X_a$  line intersect in a point on the  $y$  axis.

If the  $w_a$  forces were made to act horizontally, then by the method given in Art. 38, the horizontal resultant of these forces would be obtained acting at the intersection of the outer rays. This resultant  $E\Sigma w_a$  would intersect the  $y$  axis in the center of gravity  $O$ . However, the method of finding  $z_o'$  by computation is preferable, as the point  $O$  must be accurately located.

The moment influence line for any point as panel point 4, is now constructed by computing the  $\eta_m$  ordinates from Eq. (52o) as illustrated in Table 52d. The coordinates of point 4 are  $x=54$  ft. and  $y=7.9$  ft. and the  $\eta_a$ ,  $\eta_b$  and  $\eta_c$  ordinates are scaled from the three  $X$  influence lines. The  $\eta_o$  ordinates are obtained from the  $M_{o4}$  influence line which is the ordinary moment influence line for point 4 of a simple beam of span  $l=180$  ft. The table indicates the details of combining these several ordinates to obtain the ordinates which are finally plotted (Figs. 52g), giving the  $M_4$  influence line. The  $M_5$  line is similarly found.

The  $M_4$  influence line may be used to obtain the stress  $S_{3-5}$  in the chord 3-5 with lever  $r=15.21$  ft. Since  $S=M/r$ , this same influence line becomes a stress influence line with a factor  $1/r$ .

The  $M_5$  influence line may thus be regarded as the stress influence line for the chord 4-6 with a factor  $1/r=1\div14.79=0.068$ .

Stress influence lines might also be developed from the formula

$$S=S_o-S_aX_a-S_bX_b-S_cX_c,$$

but this would require computing the stresses  $S_b$  and  $S_c$  in addition to the  $S_a$  stresses already found, and the stresses  $S_A$  and  $S_B$  required to draw the ordinary  $S_o$  line for any member in question.

The influence lines for the web members can best be found from the chord influence lines as described in the theoretical portion of this article.

It is not considered necessary to go further into this problem, as the theory is fully treated and the general method is illustrated by finding a single stress influence line.

The temperature stresses are determined precisely as previously outlined.

## CHAPTER XI

### DESIGN OF STATICALLY INDETERMINATE STRUCTURES

#### ART. 53. METHODS FOR PRELIMINARY DESIGNING

The term indeterminate, according to previous definitions given in Art. 2 and the tests for identification discussed in Art. 3, is always used in the sense that the laws of *pure statics* fail to give a solution when applied to structures involving statically indeterminate or redundant conditions. In all structures of this class the analysis of stresses can be accomplished only by resorting to the theory of elasticity. Hence, indeterminate is not synonymous with impossible only in so far as the application of the laws of statics is concerned.

The complete analysis of a statically indeterminate structure, according to Eqs (7A) and (7H), involves the solution of three separate problems as follows:

1. The determination of all internal stresses  $S_o$ , resulting in the principal system from the externally applied loads  $P$ .
2. The determination of all internal stresses  $S_t$  and  $S_r$  produced in the principal system by the temperature changes and abutment displacements.
3. The determination of elastic deformations in the principal system produced by the several stresses  $S_a$ ,  $S_b$ ,  $S_c$ , etc.,  $S_t$  and  $S_r$  from which the redundant conditions  $X_a$ ,  $X_b$ ,  $X_c$ , etc.,  $X_t$  and  $X_r$  may be evaluated.

Eqs. (7H) and (8D), furnish the solution of these three problems for any indeterminate structure by means of considerations which are of similar character in each problem.

A statically determinate structure can always be analyzed by the methods known in statics, when the live loads and the dead loads of the structure are known. Experience in shop practice supplies approximate data for the weights of structures in common use, but new types of structures, departing from the ordinary forms, necessitate repeated approximations to determine the dead loads before a final analysis for the given live loads becomes possible.

A statically indeterminate structure is likewise incapable of analysis until its dead weight is known with some degree of certainty and will require a preliminary design which is much more difficult to approximate than in the case of determinate structures, because this involves a knowledge of the magnitude of the redundant conditions. These redundant conditions in turn require that the cross-sections of the members be also known.

Fortunately, the *influence* of a system of loads can be made to depend on *relative* cross-sections, thus rendering an approximate solution of the redundants  $X$  possible,



before the *actual cross-sections* are definitely evaluated. This is done by making certain assumptions like adopting a uniform cross-section for all chord members and neglecting the web members entirely, whence the variable  $F$ , involved in  $\rho = l/EF$  or Eq. (42b), is treated as a constant. The  $w$  loads required for constructing the deflection polygon for the loaded chord for any condition  $X=1$  may then be made  $EF$  times the values given by Eq. (36b), using a pole distance of  $EF$ . The details of this process will be discussed later; suffice it to say now that it becomes possible to construct an approximate influence line for any redundant condition without knowing the final cross-sections of the members.

With the aid of these approximate  $X$  influence lines the redundants may be evaluated for any given live loads and some assumed dead loads. Then applying all these loads simultaneously to the principal system, the first approximate values for the stresses  $S$  may be determined from a Maxwell diagram. The redundants  $X$  are applied along with the external forces.

These stresses  $S$  will now serve as a basis for a close approximation of the cross-sections  $F$  from which our new influence lines for the redundants  $X$  may be found in the *usual* manner as illustrated by the problems in Chapter X. A final analysis of the stresses is now possible and from this the final sections are found. If the first assumption for dead load was grossly in error then the first  $X$  influence lines might be used again, employing revised dead loads before the final analysis is made.

This process is on the whole similar to the one above cited for new types of determinate structures, the dead loads for which are not accurately known. The additional difficulty here encountered consists in evaluating the redundants, which depend both on the sections and loads at the same time. Therefore, all such work is likely to be somewhat tedious.

The method of determining approximate values for the redundants in terms of the mutual relations of the sections of the members among themselves, instead of the actual sections, will now be described.

In some cases as for arches with parallel chords it is always permissible to assign a constant section to all chord members and neglect the web system entirely. This is then a very simple case and affords a ready solution for the  $X$  influence lines by computing all  $w$  loads  $EF$  times too large.

When there is only one redundant condition or when there are two or three of these so chosen as to comply with the conditions discussed in Art. 44 then for the above-mentioned case of constant chord sections and disregarding the web system, the redundants may be found analytically from Eq. (42b) whence

$$X_a = \frac{\Sigma S_o S_a \rho}{\Sigma S_a^2 \rho} = \frac{\frac{1}{EF} \Sigma S_o S_a l}{\frac{1}{EF} \Sigma S_a^2 l} = \frac{\Sigma S_o S_a l}{\Sigma S_a^2 l}, \quad \dots \dots \dots (53A)$$

where the stresses  $S_o$  must be obtained from a Maxwell diagram drawn for a maximum case of combined live and assumed dead loads for the principal system. The stresses

$S_a$  are found for the conventional loading  $X_a=1$  from a similar stress diagram, and these are independent of any actual loads. Eq. (53A) shows that whenever any of the variables common to the numerator and denominator become constant, they cease to affect the value of  $X_a$ .

The stress in each member of the principal system may now be found from

$$S = S_o - S_a X_a, \quad . . . . . (53B)$$

and the first approximate sections  $F$  may be evaluated from these stresses.

The approximate effect due to changes in temperature may also be included by finding  $X_{at}$  from Eq. (44c) and Eqs. (8B) and (8C) as

$$X_{at} = \frac{\delta_{at}}{\delta_{aa}} = \frac{\sum S_a \epsilon l}{\sum S_a^2 \frac{\epsilon l}{EF}}, \quad . . . . . (53C)$$

using some assumed constant value for  $F$ .

If for any reason the lengths of the chord members are all equal, then  $l$ , in Eqs. (53A) and (53C), would likewise be eliminated.

A somewhat more comprehensive method, especially when the chord sections are not assumed equal, is obtained by drawing the influence lines for the redundants. This method will now be outlined.

When the redundants are so chosen that the simplified Eqs. (44B) become applicable, then the  $X$  influence lines may be approximated by computing  $w$  loads for relative sections of the members. Thus for any redundant

$$X_a = \frac{\sum P_m \delta_{ma}}{\delta_{aa}} = \frac{\sum P_m \delta_{ma}}{\sum S_a^2 \frac{l}{EF}} = \frac{EF_c \sum P_m \delta_{ma}}{\sum S_a^2 l \frac{F_c}{F}}, \quad . . . . . (53D)$$

where  $F_c$  is some constant chosen about equal to a typical chord section as described below.

The  $w_a$  loads from Eqs. (36B) and (36C), for condition  $X_a=1$ , then become

$$w = \frac{M_a l}{EFr^2}; \quad w_u = \pm \frac{M_a l}{EFr_u r}; \quad \text{and} \quad w_n = \mp \frac{M_a l}{EFr_n r};$$

and multiplying each by  $EF_c$ , then,

$$EF_c w = \frac{M_a l}{r^2} \cdot \frac{F_c}{F}; \quad EF_c w_u = \pm \frac{M_a l}{r r_u} \cdot \frac{F_c}{F}; \quad EF_c w_n = \mp \frac{M_a l}{r r_n} \cdot \frac{F_c}{F}. \quad . . . (53E)$$

$M_a$  is the moment, with lever arm  $r$ , produced by the conventional loading  $X_a=1$ . If a deflection polygon be drawn for these  $EF_cw$  loads with pole distance unity, the ordinates  $\eta$  will represent values  $EF_c\delta_{ma}$  measured to the scale of lengths. Hence the numerator of Eq. (53d) represents the sum of the products  $P\eta$ , and the denominator is  $\Sigma S_a^2 \frac{F_c}{F} = \frac{\Sigma M_a^2 l}{r^2} \cdot \frac{F_c}{F} = EF_c \Sigma M_a w$ , according to Eq. (53e), thus making it possible to construct any  $X$  influence line provided suitable assumptions for the values  $F_c/F$  can be made.

The equation of the  $X$  influence line for a load  $P=1$  then becomes

$$X_a = \frac{EF_c \delta_{ma}}{\Sigma S_a^2 \frac{F_c}{F}} = \frac{EF_c \delta_{ma}}{EF_c \Sigma M_a w_a} \dots \dots \dots (53f)$$

in which  $F_c$  need not be numerically known, but the ratios  $F_c/F$ , for different members of the frame, must be approximated in order to compute the  $EF_cw$  loads from Eqs. (53e).

The value of  $F_c$  should be chosen equal to that of a chord section of most frequent occurrence, which would usually be nearest the crown of an arch or where the chord approaches the horizontal. This will make  $F_c/F=1$  for most chord members and usually that assumption may be made for both top and bottom chord members. The web system may be entirely neglected in the first approximation or if it is thought desirable to include the web members then  $F_c/F$  may be given some constant value ranging from 2 to 10 for these members, depending on the character of the structure.

The  $F_c$  should not be regarded as an average value of the chord sections because the deflection polygon of a frame is governed largely by the chords near the center of the span. Thus, if the depth of an arch is much greater at the springing than at the crown, then the crown sections will govern.

From the approximate  $X$  influence lines the redundant conditions may be evaluated for any case of total loading and the stresses  $S_o$ ,  $S_a$ , etc., can be found by Maxwell diagrams or otherwise. Then Eq. (53b) will furnish the stresses  $S$  from which the sections of the several members are derived. The stresses  $S$  may also be obtained from a single stress diagram by applying all redundants and external loads simultaneously to the principal system. Temperature effect may be included in the redundants at the same time.

Another method of making a preliminary design would result from the use of a Williot-Mohr displacement diagram as used in Art. 50. However, the deflection polygons as found from the  $w$  loads are more easily obtained except for oblique loads  $P$ .

To illustrate the entire procedure of making a preliminary design for a structure involving redundant conditions, the fixed arch in Art. 52 will now be investigated.

**Example.** The data for this arch are given in the example of Art. 52 and need not be repeated here.

The  $EF_cw_a$  loads will be computed from Eq. (53e) making  $F_c/F=1$  and neglecting the web system. The moment  $M_a=1$  and the lengths  $l$ , lever arms  $r$  and ordinates  $z$  are taken from Tables 52A and 52c.



TABLE 53A  
COMPUTATION OF APPROXIMATE LOADS  $EF_c w_a$

Pin Point.	Chord.	$l$ Feet.	$r$ Feet.	$\frac{1}{r^2}$ Feet.	$z$ Feet.	$EF_c w_a = \frac{l}{r^2}$	$zEF_c w_a$
1	0-2	20.73	14.92	0.00449	0.00	0.0931	0.000
3	2-4	19.51	14.84	0.00454	9.99	0.0886	0.885
5	4-6	18.72	14.79	0.00457	17.03	0.0856	1.458
7	6-8	18.25	14.77	0.00458	21.53	0.0836	1.800
9	8-10	18.03	14.79	0.00457	23.69	0.0824	1.952
2	1-3	20.59	14.14	0.00500	22.31	0.1030	2.300
4	3-5	19.33	15.21	0.00432	29.83	0.0835	2.491
6	5-7	18.55	15.25	0.00430	34.99	0.0798	2.792
8	7-9	18.33	15.28	0.00428	38.01	0.0784	2.980
10	$\frac{1}{2}(9-9')$	9.00	15.31	0.00427	39.00	0.0384	1.498
						0.8164	18.156

This makes  $z_o' = \frac{\Sigma zEF_c w_a}{\Sigma EF_c w_a} = \frac{18.156}{0.8164} = 22.24$  ft. from which the origin  $O$  can be located and the ordinates  $y = z - z_o'$  be computed. The remaining  $w$  loads and pole distances are then easily found.

TABLE 53B  
APPROXIMATE  $w$  LOADS AND POLE DISTANCES

Pin Point.	$EF_c w_a$	Coordinates.		$EF_c w_b = xEF_c w_a$	$EF_c w_c = yEF_c w_a$	$xEF_c w_b$	$yEF_c w_c$
		$x$ Feet.	$y$ Feet.				
1	0.0931	81	-22.24	7.541	-2.070	610.82	46.04
2	0.1030	72	+ 0.07	7.416	+0.007	533.95	0.00
3	0.0886	63	-12.25	5.582	-1.085	351.67	13.29
4	0.0835	54	+ 7.59	4.509	+0.634	243.49	4.81
5	0.0856	45	- 5.21	3.852	-0.446	173.34	2.32
6	0.0798	36	+12.75	2.873	+1.017	103.43	12.97
7	0.0836	27	- 0.71	2.257	-0.059	60.94	0.04
8	0.0784	18	+15.77	1.411	+1.236	25.40	19.49
9	0.0824	9	+ 1.45	0.742	+0.120	6.68	0.17
$\frac{1}{2}(10)$	0.0384	0	+16.76	0.000	+0.644	0.00	10.79
Totals..	0.8164 $H_a = 1.633$	.....	.....	36.183	-3.660 +3.658	2109.72 $H_b = 4219.4$	109.92 $H_c = 219.8$

The three influence lines for  $X_a$ ,  $X_b$ , and  $X_c$  may now be drawn precisely as was done in Figs. 52G, by using the values in Table 53B.

Comparing the ordinates found from these influence lines, Fig. 53A, with those previously obtained in Art. 52, it will be seen that the former are fairly close to the correct values, but inclined to be a little large.

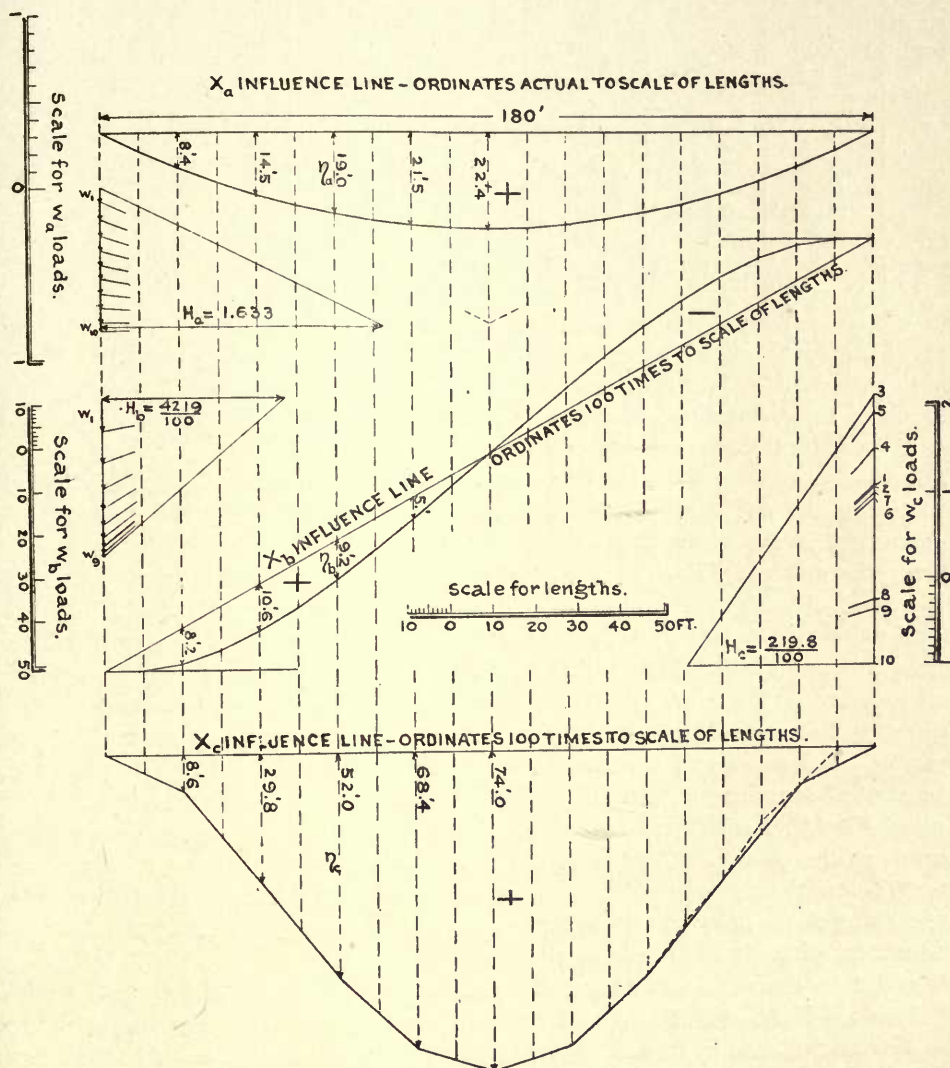


FIG. 53A.

The live load per truss per panel was stipulated at 30 kips and for an assumed dead load of 20 kips the total load would be 50 kips.

Using the ordinates from the influence lines in Fig. 53A and the total load of 50 kips per truss per panel, the redundants  $X_a$ ,  $X_b$  and  $X_c$  are computed in the following Table 53c. For a symmetric loading  $X_b = 0$  and need not be considered.

TABLE 53C  
REDUNDANTS  $X_a$  AND  $X_c$  FOR TOTAL LOADING

Panel Point.	Ordinates.		Panel Load, Kips.	Redundants.		
	$\eta_a$ Feet.	$\eta_c$ Feet.		$X_a$ Kip-feet.	$X_c$ Kips.	
2	8.4	0.086	50	420	4.3	$X_a = 2 \times 3730 = 7460$ k. ft. $X_c = 2 \times 97.9 = 195.8$ kips $A_o = \frac{1}{2} \Sigma P = 225$ kips
4	14.5	0.298	50	725	14.9	
6	19.0	0.520	50	950	26.0	
8	21.5	0.684	50	1075	34.2	
$\frac{1}{2}(10)$	22.4	0.740	25	560	18.5	
Totals . . . .	.....	.....	225	3730	97.9	

The redundants might be obtained for any position of the live load, but since the chords are stressed to their maximum for total loading over the span, and since the web system plays a rather unimportant part in structures of the class here considered, no further investigation of stresses is warranted at this point.

The stresses for the total loading, including the redundants  $X_a$  and  $X_c$  applied as external forces, are now found from a Maxwell stress diagram in Fig. 53B, and from these the preliminary cross-sections of the members are deduced.

From the sums in Table 53A, the value of  $z_o' = 22.24$  ft. This locates the pole  $O$  on the  $y$  axis. The rigid disk, upon which the redundants act, may now be replaced by two rigid members  $\overline{IO}$  and  $\overline{OO}$ . For the symmetric total loading,  $X_b = 0$ , and hence the external loads are  $X_c$  applied at  $O$ ; and a moment  $X_a$  applied anywhere to the disk; a vertical end reaction  $A_o$ ; and the loads  $P$  acting at the several top chord panel points.

In order that the moment  $X_a$  may be incorporated in the stress diagram, it must be resolved into two equal and opposite forces acting on the rigid disk. Since these forces may be applied anywhere on the disk, it is best to choose the lever arm  $l/2$ , thus making the forces  $V = 2X_a/l$  each, one acting upward at the support  $A$  and the other applied downward at the pole  $O$ . The forces  $V$  and  $X_c$ , acting at  $O$ , are then combined into a resultant  $Z$  and from this resultant the stresses in the rigid members  $\overline{IO}$  and  $\overline{OO}$  are found, making it possible now to draw the stress diagram beginning at the reaction  $A$ . The remainder of the work offers no particular difficulty.

It might be desirable to test out the resultant polygon with the aid of Eqs. (52s). From these  $z_o = X_a/X_c = 38.10$  ft. and the ordinate  $\overline{CD}$ , Fig. 53B, determines the intersection of the resultants  $R$ ,  $R_1$  and  $R_2$  in the point  $C$ . The closing line  $\overline{a_1b_1}$  for symmetric loading, is fully located when  $\overline{OD} = z_o$  is given, hence the points  $a_1$  and  $b_1$  are found on the horizontal through  $D$ . The resultant  $R_1$  is obtained by combining  $A_o$  and  $X_c$  at  $a_1$  and  $R_2$  is the resultant of  $B_o$  and  $X_c$  at  $b_1$ . The resultant  $R = \Sigma P$  must be in equilibrium with  $R_1$  and  $R_2$  (see Fig. 52A), hence the three forces must intersect in a point  $C$ .

A further check is obtained by computing the ordinate  $\overline{CD} = lR/4X_c = 103.4$  ft.

The stresses  $S$  are now tabulated and cross-sections  $F$  are determined in Table 53D, using a rather low unit stress of say 9200 lbs. per sq.in., instead of an allowable 15,000



lbs. This then covers extra metal for joints, splices, latticing, etc., and for reduction to net sections for tension members, and for  $l/r$  for columns.

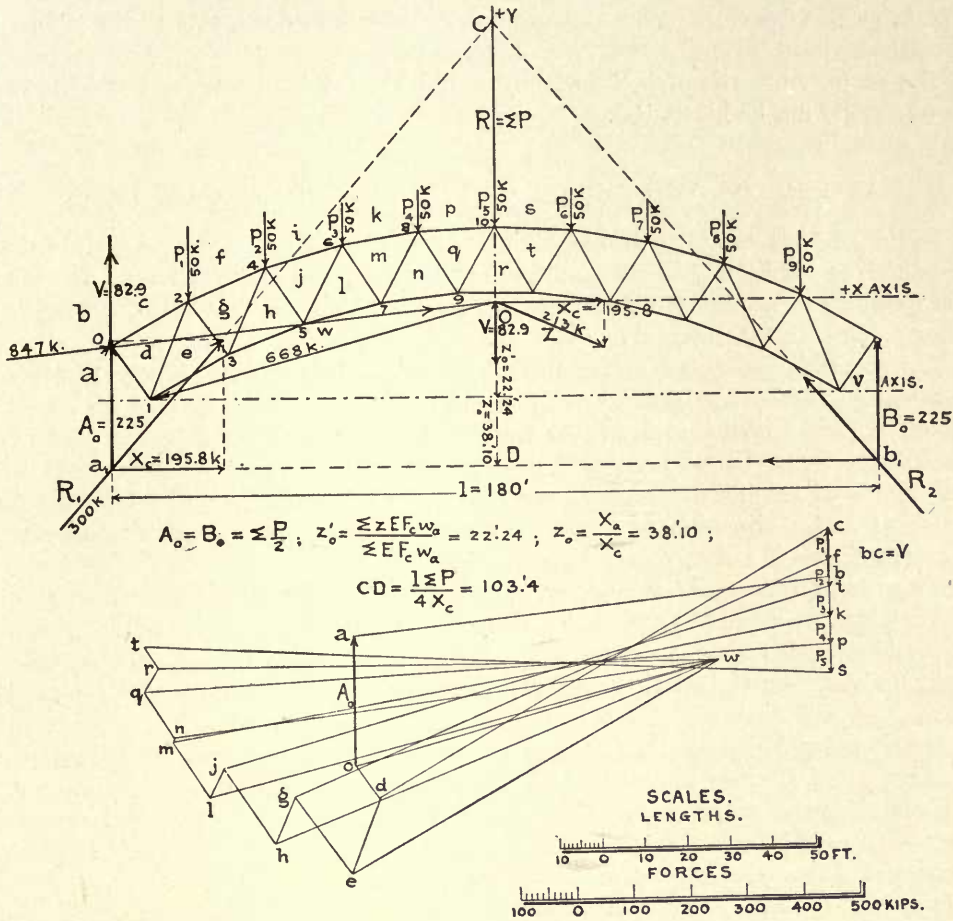


FIG. 53B.

TABLE 53D  
PRELIMINARY STRESSES AND SECTIONS

Top Chord.			Bottom Chord.			Diagonals.			Diagonals.		
Mem.	S Kips.	F Sq.in.	Mem.	S Kips.	F Sq.in.	Mem.	S Kips.	F Sq.in.	Mem.	S Kips.	F Sq.in.
0-2	- 920	100	1-3	748	82	0-1	- 70	8	1-2	-140	14
2-4	-1028	110	3-5	846	94	2-3	+166	18	3-4	- 90	10
4-6	-1114	120	5-7	930	100	4-5	+160	18	5-6	- 55	6
6-8	-1178	124	7-9	970	104	6-7	+117	14	7-8	+ 10	6
8-10	-1210	130	9-9'	988	128	8-9	+ 95	10	9-10	+ 48	6

These cross-sections were used in the example of Art. 52, in making the complete analysis.

Naturally a two-hinged arch or other structure involving one redundant only, would be susceptible to the same method of design above outlined, though the labor would be greatly lessened.

For an unsymmetric arch the angle  $\beta$  would have to be determined and the closing line  $\overline{a_1b_1}$  would not be horizontal.

#### ART. 54. ON THE CHOICE OF THE REDUNDANT CONDITIONS

In the analysis of a structure involving redundancy, it becomes necessary to remove the redundant conditions, whether external or internal, and thereby reduce the indeterminate system to a determinate *principal system* to which the redundant conditions are applied along with the external loading.

The particular reactions or members best suited to represent the redundant conditions designated by  $X_a$ ,  $X_b$ ,  $X_c$ , etc., are those which reduce the given structure to the simplest possible principal system. This will usually offer no difficulty.

However, many cases present themselves wherein it would be difficult to decide which of several possible assumptions would represent the most judicious selection of the redundants in the direction of simplifying the analysis. Therefore, a few suggestions along these lines will not be out of place.

According to the general method just referred to, the elastic deformation of an indeterminate structure subjected to loads  $P$ , will be exactly the same as that of its principal system loaded with loads  $P$ ,  $X_a$ ,  $X_b$ ,  $X_c$ , etc. In each case the deformation is entirely derived from the elastic changes  $\Delta l$  in the lengths of the members of the principal system.

The structural deformation is thus affected by the redundant conditions merely to the extent of altering the stresses in the *necessary members* of the principal system.

Hence, for the same case of loading, the stresses  $S_o$  in the principal system are always diminished by the redundant conditions provided temperature stresses and abutment displacements are excluded.

Generally speaking, any member or reaction of an indeterminate structure may be removed to produce the principal system so long as the latter still remains a stable, determinate structure and does not become subject to infinitesimally small rotation, a condition described in Art. 3, Fig. 3c.

The rule should be to select a principal system of the simplest possible form, always avoiding composite structures, such as the three-hinged arch or a cantilever, whenever a simple beam or truss could as well be used.

Solid web structures should always be transformed into externally determinate beams by assigning the redundant conditions to the supports.

Framed structures, if externally indeterminate, should always be so transformed as to remove the external conditions. The only exception to this rule might be a continuous girder wherein a top chord member over each intermediate pier might be treated as a redundant member.

In the case of the fixed arch, always involving three redundants, several assumptions may be made. First removing one fixed end and thus reducing the arch to a simple cantilever arm acted upon by a moment  $X_a$ , a vertical force  $X_b$  and a horizontal force  $X_c$ . Second, by removing two members adjacent to one end support and one member adjacent to the other end support, thus forming a girder on two determinate supports acted upon by three external forces replacing the three members thus removed.

Also three members may be removed at the crown converting the arch into two cantilever arms with three external forces  $X_a$ ,  $X_b$ , and  $X_c$  applied to the end of each arm to replace the redundant members.

Frequently all the redundant conditions (not exceeding three) may be applied at one point as described in Art. 44. Then for certain assumed directions of the  $X$ 's, the work equations become exceedingly simple and afford excellent graphic solutions. The best of these possible solutions was chosen in Art. 52, where a complete fixed arch problem is solved.

Indeterminate structures, having a vertical axis of symmetry, will always have two  $\delta$ 's bearing double subscripts of like letters, which become equal. Thus  $\delta_{aa} = \delta_{bb}$ , which condition greatly simplifies the determination of  $X_a$  and  $X_b$ , as illustrated in the case of a girder over four supports with the two outer spans equal. See Fig. 43A. In this and similar problems, when the above mentioned symmetry exists, the two influence areas for  $X_a$  and  $X_b$  will also be equivalent but symmetrically placed.

When the redundant conditions are internal then the only way of deriving the principal system is to remove such redundant members and replace them by external forces  $X$ .

Composite structures, or those composed of several determinate frames combined into an indeterminate system, are best treated by assigning the redundant conditions to the reactions and treat as for external redundancy.

## ART. 55. SOLUTION OF THE GENERAL CASE OF REDUNDANCY

In the following it will be assumed that the preliminary design is completed and it is now desired to make the final analysis for stresses due to any causes such as loads, temperature and abutment displacements.

Problems of the general type are usually quite complicated, and since it is important to know the stresses due to loads, to temperature changes and to yielding supports separately, these should always be dealt with in this manner. This is not done merely as a matter of convenience, but it is necessary to know the relation between the load and temperature stresses as a criterion in judging the merits of any particular structure under consideration.

In the general discussion which follows here, only the load effects will be included, while the other matters will be taken up later. Hence the quantities  $\Sigma R \Delta r$  and  $\delta_t$ ,  $S_t$ , etc., will all be neglected, assuming for the present that they are all zero.

To make the case perfectly general, no distinction will be made between external and internal redundancy, hence any of the redundants may be assumed to belong to either class.

For  $n$  redundant conditions, Eqs. (7A), offer a general solution for the stress  $S$  in any



member, the moment  $M$  about any point, the shear  $Q$  on any section or any of the reactions  $R$ , all for the principal system only. The redundant conditions  $X$ , involved in these equations, are treated as external forces applied to the principal system along with the loads  $P$  and their reactions. These redundants may be found from Mohr's work equations (7H) or (8D) of which there will always be as many equations as there are redundants, rendering the solution of the  $X$ 's possible by solving for simultaneous values of  $n$  unknowns  $X$  in  $n$  equations.

It is usually preferable to employ Eqs. (8D) in terms of deflections which are obtained from deflection polygons of the loaded chord, though in principle the solution remains the same whether dealing with conventional stresses or conventional deflections.

In general then for  $n$  redundants, including effects due to temperature changes and yielding supports, Eqs. (7A) give

$$\left. \begin{aligned} S &= S_o - S_a X_a - S_b X_b - \text{etc.} - S_n X_n \pm S_t + S_r \\ M &= M_o - M_a X_a - M_b X_b - \text{etc.} - M_n X_n \pm M_t + M_r \\ R &= R_o - R_a X_a - R_b X_b - \text{etc.} - R_n X_n \pm R_t + R_r \\ Q &= Q_o - Q_a X_a - Q_b X_b - \text{etc.} - Q_n X_n \pm Q_t + Q_r \end{aligned} \right\}, \dots \dots (55A)$$

wherein the quantities  $S_o$ ,  $M_o$ ,  $R_o$  and  $Q_o$  are all linear functions of the externally applied loads  $P$  acting on the principal system as a result of what is known as condition  $X=0$ . The quantities bearing subscripts  $a$ ,  $b$ ,  $c$ , etc., to  $n$ , are constants due to conventional loadings  $X_a=1$ ,  $X_b=1$ ,  $X_c=1$ , etc., to  $X_n=1$ , while the subscript  $t$  refers to temperature effects and the subscript  $r$  to effects produced by yielding supports.

The  $n$  redundants may be obtained from Eqs. (7H) in terms of the constant stresses due to the conventional loadings or from Eqs. (8D) in terms of certain deflection constants obtained from the same conventional loadings. The latter equations are

$$\left. \begin{aligned} \delta_a &= \Sigma P_m \delta_{ma} - X_a \delta_{aa} - X_b \delta_{ab} - X_c \delta_{ac} \text{ etc.} - X_n \delta_{an} - \Sigma R_a \Delta r + \delta_{at} \\ \delta_b &= \Sigma P_m \delta_{mb} - X_a \delta_{ba} - X_b \delta_{bb} - X_c \delta_{bc} \text{ etc.} - X_n \delta_{bn} - \Sigma R_b \Delta r + \delta_{bt} \\ \delta_c &= \Sigma P_m \delta_{mc} - X_a \delta_{ca} - X_b \delta_{cb} - X_c \delta_{cc} \text{ etc.} - X_n \delta_{cn} - \Sigma R_c \Delta r + \delta_{ct} \\ \delta_n &= \Sigma P_m \delta_{mn} - X_a \delta_{na} - X_b \delta_{nb} - X_c \delta_{nc} \text{ etc.} - X_n \delta_{nn} - \Sigma R_n \Delta r + \delta_{nt} \end{aligned} \right\}, \dots \dots (55B)$$

wherein the  $\delta$ 's have the definitions given in Art. 8, and all those bearing double subscripts of like letters are equal by Maxwell's law. Thus

$$\delta_{ma} = \delta_{am}; \delta_{ab} = \delta_{ba}; \delta_{ac} = \delta_{ca}; \delta_{bc} = \delta_{cb}; \text{etc. } \delta_{an} = \delta_{na}; \text{etc.}$$

meaning that the order of the subscripts is immaterial and that only half of the  $\delta$ 's need be determined, or if they are all determined, that they must check.

Hence, either one of the subscripts may be made to refer to the point of application of a load, while the other subscript deals with the conventional loading or condition  $X=1$ . The terms  $R \Delta r$  express the effect due to yielding supports and the  $\delta_t$  quantities

express the effect of temperature changes, both of which will be placed equal to zero for the present, though they will be considered in following articles.

The redundants  $X$  may represent indeterminate reaction conditions or they may be stresses in redundant members, and in either case the displacements  $\delta_a$ ,  $\delta_b$ ,  $\delta_c$ , etc.,  $\delta_n$  are the displacements of the points of application of the respective redundants in the directions of their lines of action. These values  $\delta$  may thus be expressed in terms of the redundants themselves in accordance with Eqs. (7j). When the point of application of a certain redundant is rigid, then its  $\delta=0$ .

For each of the  $n$  redundant conditions there will be one work equation of the form of Eqs. (55B) involving deflections due to conventional loadings. These together with the case of actual loading due to loads  $P$ , will constitute in all  $n+1$  cases of loading on the principal system to solve for *one position* of a moving train of loads.

The aim, in all practical problems of this nature, consists in representing all the required stresses or other functions by influence lines, thus requiring  $n+1$  influence lines to determine each such stress or function. However, the  $n$  influence lines for the  $n$  redundants will be the same for all cases and all stresses or functions of the same structure, while the influence line for the load effect must be separately found for each stress, moment, shear or reaction.

For influence lines the applied load becomes unity and the functions  $\Sigma P_m \delta_m = 1 \cdot \delta_m$ . Each of the  $n$  redundants will furnish a deflection polygon for condition  $X=1$ , drawn for the loaded chord of the principal system. The  $n$  deflection polygons will then furnish all the conventional deflections in Eqs. (55B) for a load  $P=1$ . Also, since the subscripts may be interchanged, one such deflection polygon drawn for  $X_a=1$  will furnish all the double subscript bearing  $\delta$ 's of the first equation.

Thus as a matter of convenience, all of the  $\delta$  coefficients in a single equation can be determined from one deflection polygon drawn for the loaded chord of the principal system. The same might also be accomplished by drawing a Williot-Mohr displacement diagram for the principal system, though this would usually be more laborious.

Therefore, the  $n$  Eqs. (55B) can be solved successively with the aid of  $n$  deflection polygons in accordance with the following form with transposed subscripts and for a single load  $P=1$ .

$$\left. \begin{aligned} \delta_a &= 1 \cdot \delta_{ma} - X_a \delta_{aa} - X_b \delta_{ba} - X_c \delta_{ca} \quad \dots - X_n \delta_{na} = \frac{X_a l_a}{EF_a} \\ \delta_b &= 1 \cdot \delta_{mb} - X_a \delta_{ab} - X_b \delta_{bb} - X_c \delta_{cb} \quad \dots - X_n \delta_{nb} = \frac{X_b l_b}{EF_b} \\ \delta_c &= 1 \cdot \delta_{mc} - X_a \delta_{ac} - X_b \delta_{bc} - X_c \delta_{cc} \quad \dots - X_n \delta_{nc} = \frac{X_c l_c}{EF_c} \\ \delta_n &= 1 \cdot \delta_{mn} - X_a \delta_{an} - X_b \delta_{bn} - X_c \delta_{cn} \quad \dots - X_n \delta_{nn} = \frac{X_n l_n}{EF_n} \end{aligned} \right\} , \dots (55c)$$

where the values of  $\delta_a$ ,  $\delta_b$ ,  $\delta_c$ , etc., were obtained from Eqs. (7j) and may be chosen to represent any of the possible cases of redundancy, as changes in the lengths of redundant members, elastic displacements of redundant supports or angular changes between pairs



of lines according to Art. 9. When the redundants are immovable reactions, then these  $\delta$ 's become zero.

The  $\delta$  coefficients in Eqs. (55c) can thus be obtained from  $n$  deflection polygons drawn as above described and the  $n$  equations solved for simultaneous values of the  $X$ 's thus furnish the values for a complete solution of Eqs. (55A).

Eqs. (55c) are written for a single load  $P=1$  intended specifically for use with influence lines, which are most valuable when dealing with concentrated load systems.

Examples involving dead loads only, or when the live load cannot occupy more than one or two positions, could be solved advantageously without resorting to influence lines according to the very interesting example of a lock gate in Chapter XIV.

For solid web structures and masonry arches, all the above is applicable, remembering that in these cases the redundants must all be external. As soon as the  $X$ 's are found the stresses on any section are readily ascertained.

The solution of the  $n$  simultaneous equations is a matter of considerable labor and may offer some difficulty. The method best suited to problems of the kind here considered is given in connection with the lock gate problem referred to above. See Chapter XIV, Art. 68.

## ART. 56. EFFECT OF TEMPERATURE ON INDETERMINATE STRUCTURES

Determinate systems are not materially affected by temperature changes. But it is not correct to say that the temperature stresses are zero, because any structure which, in consequence of changes in temperature, undergoes such deformations as to change the positions of the points of application of the external forces must thereby create some stresses. These will usually be small and are entirely negligible except possibly in very flat suspension systems or very flat three-hinged arches where the horizontal pull or thrust is a function of the middle ordinate.

For the case of indeterminate structures, wherein the redundant conditions are direct functions of elastic deformations, the general rule implies that stresses always accompany changes in the lengths of structural dimensions, no matter what external cause may have produced such changes.

All temperature changes in externally indeterminate structures will affect the reactions and these in turn set up temperature stresses in the members. The only exception to this case is a continuous girder with supports on the same level and subjected to absolutely uniform temperature throughout. When such a structure is unequally heated then excessive temperature stresses may result, as shown in the examples of Arts. 47 and 48.

On the other hand where the redundancy is entirely internal, no temperature stresses are produced so long as the whole structure retains a uniform temperature throughout. When this uniformity does not exist, then temperature stresses are created, though the reactions may or may not be materially affected.

Hence, in all cases of redundancy, it will be necessary to investigate the question of temperature stresses in a very thorough manner, as in many instances these may assume dangerous proportions.



For this reason also, statically determinate structures should always receive the preference, other considerations being nearly equal.

Internal redundancy is less objectionable than external, and according to the best modern engineering experience, no design should be made to include more than one redundant condition of any kind. This is especially true of steel structures, though to a lesser degree applicable to masonry arches of short spans where the poor conductivity of masonry acts as a protective agency against excessive temperature deformations.

For long-span masonry arches this consideration assumes greater importance. Even though monumental structures of this class have been built and are regarded with pride and admiration from an æsthetic standpoint, they cannot be accepted as representative of the best practice when viewed from the point of modern and progressive engineering.

The general effect of temperature changes on indeterminate systems is thus to produce deformations and resultant stresses of the same kind as those created by externally applied loads in accordance with Eqs. (55A).

Since the temperature effects may be plus or minus in character, depending on the existing conditions, it is always possible to increase the stresses due to the loading by choosing appropriate changes in temperature. For this reason the temperature effect is applied with a plus sign in Eqs. (55A), meaning thereby that the function, whether positive or negative, suffers a numerical increase. Of course some assumptions will produce a decrease, but these are not vital to the problem and require no consideration.

It is always desirable to determine the temperature stresses apart from all other influences so as to furnish a clear conception of their relative importance to the load stresses. This then offers a criterion by which to judge the feasibility of a structure involving redundancy.

The temperature stresses are determined from Eqs. (7H) and (8D) by dropping out all terms depending on  $P_m$ ,  $S_o$  and  $R$ , thus reducing these equations to the following forms, covering all members of the principal system:

$$\left. \begin{aligned} \delta_a &= \epsilon t l_a = \Sigma S_a \epsilon t l - X_{at} \Sigma S_a^2 \rho - X_{bt} \Sigma S_a S_b \rho \dots \text{etc.} \\ \delta_b &= \epsilon t l_b = \Sigma S_b \epsilon t l - X_{at} \Sigma S_a S_b \rho - X_{bt} \Sigma S_b^2 \rho \dots \text{etc.} \end{aligned} \right\}, \dots \dots (56A)$$

or from Eqs. (8D)

$$\left. \begin{aligned} \delta_a &= X_{at} \rho_a = \delta_{at} - X_{at} \delta_{aa} - X_{bt} \delta_{ab} \dots \text{etc.} \\ \delta_b &= X_{bt} \rho_b = \delta_{bt} - X_{at} \delta_{ba} - X_{bt} \delta_{bb} \dots \text{etc.} \end{aligned} \right\} \dots \dots \dots (56B)$$

In both Eqs. (56A) and (56B) the displacements  $\delta_a$  and  $\delta_b$  become zero for external redundancy with immovable supports.

Accordingly the redundant conditions  $X_{at}$ ,  $X_{bt}$ , etc., may be found from either set of the above equations, depending on the method used in finding the load effects from Eqs. (7H), or (8D) since both these and Eqs. (56A) and (56B) involve the same constants.

The stresses  $S_t$  are then easily found from a Maxwell stress diagram drawn for the principal system with the forces  $X_{at}$ ,  $X_{bt}$ , etc., applied as external forces. See also examples in Arts. 47, 48, 49 and 50.

Regarding the assumptions which may be made as a basis for computing temperature stresses, the following conclusions are taken from some experiments on steel arches at Lyons, France, and given in *An. d. ponts et chaus.*, 1893, II, p. 438-444.

For an air temperature in the sun of  $5^{\circ}$  F. higher than the shade temperature, when the latter was  $90^{\circ}$  F., the steel had an average temperature of  $115^{\circ}$  F., while the parts exposed directly to the sun were heated to about  $130^{\circ}$  F. and the shaded portions indicated about  $104^{\circ}$  F. At the same place the coldest winter temperature was about  $-15^{\circ}$  F.

The steel was thus subjected to a mean range of  $-15^{\circ}$  to  $+115^{\circ}=130^{\circ}$  F. giving an average of  $+65^{\circ}$  F. Therefore, such a structure should be designed for a mean temperature of  $65^{\circ}$  F., allowing for uniform changes of  $\pm 65^{\circ}$  F. from this mean.

The difference between maximum and minimum simultaneous temperatures in the steel, amounting to  $26^{\circ}$  F. in these experiments, may cause very serious stresses in certain structures like fixed arches and continuous girders over several supports. In the latter case the entire top chord would elongate relatively to the bottom chord and thus set up an arching effect, relieving the intermediate supports and increasing the two end supports, while a uniform change in temperature would produce no stresses.

Structures over a single span would not be so seriously stressed for unequal temperatures in the two chords. In fact this assumption might work to advantage in the case of arches, though similar conditions for a clear cold day might prove more severe.

The painting of steel structures of the indeterminate class thus assumes considerable importance, since light colors will obviously keep down the temperature while black paint will absorb heat.

Masonry structures are not so severely distorted by temperature changes, but the elasticity of masonry being proportionately lower, the temperature stresses may prove equally dangerous.

## ART. 57. EFFECT OF SHOP LENGTHS AND ABUTMENT DISPLACEMENTS

Every structure is designed for a certain geometric figure for a condition of no stress. This is the figure which the structure should present when at a mean temperature and when carrying no loads of any kind. Naturally the unavoidable errors in the shop lengths of the members as built and the small inaccuracies in the joints and in the location of the supports during erection, preclude the practical possibility of accomplishing this end.

For structures of the determinate class this will have no significance, but for indeterminate types, these errors introduce initial stresses which may assume momentous proportions.

To avoid such stresses requires the utmost care during construction and erection, and even then only a partially satisfactory outcome can be expected.

The difficulties attending the erection of a structure so that no member will be stressed prior to the introduction of the closing link, at the proper temperature, are known to every practical bridge man.

In any event the final member should be inserted at the calculated mean temperature. If this cannot be accomplished, then the exact length which this member



should have must be ascertained by measuring the space which is actually available when the structure is all in place and under no stress. Then applying proper temperature corrections to the entire structure, the *required length* of the final member must be ascertained before attempting to force the latter into its place.

When the end supports are not correctly placed or the entire structure has an error in length, then all the values  $S_o$ ,  $S_a$ , etc., and the redundant conditions will differ from their computed values. If such displacements are in the same direction with a redundant  $X$ , then the stress  $X$  is affected thereby, otherwise the principal system only receives the additional stress.

Should a redundant member possess an erroneous length, then all the members will receive certain initial stresses, while errors in the lengths of principal members would change somewhat the geometric figure, but could not effect the stresses  $S_o$ ,  $S_a$ , etc., of the principal system.

In dealing with abutment displacements it is necessary to distinguish between elastic changes which the supports may undergo as a result of loading, and permanent settlement.

An example of elastic displacement is given in Fig. 45A, where the supporting column  $\overline{CD}$  will be shortened by an amount  $\delta_b$ , which can be determined and then be included in the computations as for any other member of the structure.

However, should the pier at  $C$  undergo permanent settlement, or should one abutment, as  $B$ , be pushed out horizontally or settle vertically, then serious difficulties would arise unless these displacements could be determined beforehand, which is usually quite impossible.

In either case the stresses occasioned by such displacements only, may be found as follows, provided the displacements are known or can be estimated with reasonable accuracy.

If, in Eqs. (55B), the terms involving the temperature effects be dropped, then for internal redundancy, the displacements  $\delta_a$ ,  $\delta_b$ , etc., are evaluated from Eqs. (7J), and the work of the reactions is found as shown in the derivation of Eqs. (7E).

When the redundancy is purely external then the Eqs. (55B) again apply by treating the reactions  $R$  as the reactions of the principal system and evaluating the elastic displacements  $\delta_a$ ,  $\delta_b$ , etc., and the  $\Delta r$  for each reaction  $R$ , using such considerations as given in Art. 12, or estimating these displacements as elastic yielding in the masonry supports, etc. See also examples in Articles 49 and 50.

In any case the combined stresses from all causes are given by Eqs. (55A) and no further comment is necessary here except to emphasize the *inadvisability of adopting externally indeterminate structures whenever immovable supports are not available*. Even for bed rock foundations, this will depend largely on the depth to which the masonry must be carried and also on the quality of masonry used.

When steel towers or pendulum piers are employed to support an indeterminate structure, then the elastic deformation of such supports must be considered in computing the structural stresses.



## CHAPTER XII

### STRESSES IN STATICALLY DETERMINATE STRUCTURES

#### ART. 58. DEAD LOAD STRESSES

(a) **General considerations.** The purpose of taking up the question of stresses in statically determinate structures is not with any intention of covering this subject exhaustively, but merely to present in the briefest possible space the methods which are best suited to the analysis of all ordinary structures.

It was not deemed advisable to take up the present chapter before having treated influence lines and developing the general criteria for the position of loads for maximum and minimum stresses in Chapter IV. The fundamental conceptions there presented are very material to a broader understanding of determinate structures and hence the present order of subjects was considered justifiable.

Since it is desired to treat methods of analysis and not types of structures, only the general case of non-parallel chords will be considered. Whenever a structure is simplified by introducing parallel chords and otherwise simple relations between its dimensions, then naturally the analysis becomes less complicated, until it might be said that the problem is reduced to a mere application of arithmetic. The so-called algebraic methods are, therefore, passed over without further consideration.

Since the dead loads are fixed in position and magnitude, the stresses produced by them in any structure must be absolutely invariable. The live loads, however, owing to their shifting position, may produce a variety of conditions and stresses which may tend to increase or to diminish dead load stresses.

Therefore, every member may be said to be subjected to a maximum and a minimum stress corresponding to the peculiar or critical positions of the live loads. These critical positions are always determined from certain tests or criteria, differing for different members of the same structure according to the principles discussed in Articles 20, 23 and 24.

It was found there that for the chord members the maximum stresses are produced for the case of maximum loading over the entire span, while the minimum stresses in these members result from the minimum total load, which is the dead load.

This condition is very different for the web members, where the dead load rarely produces minimum stresses because different positions of partial live load may produce live load stresses of opposite signs. When these are combined with the dead load

stresses to obtain total stresses, then the minimum total stresses are less than the dead load stresses, while the maximum total stresses exceed the dead load stresses.

When a web member is designed to take only one kind of stress like tension, and this stress is reversed by the live loads, then the panel containing such member must be supplied with a counter web member or the original web member must be differently designed so as to resist both tension and compression. This latter is considered the best modern practice.

Hence, in order that the relation between the dead and live load stresses may be clearly brought out in the analysis, it is always necessary to determine these stresses separately. Also, the methods which apply to the solution of dead load stresses are usually not the best adapted to finding the live load stresses, which presents another reason for dealing with the general subject under separate headings.

However, each method given will be applied directly to all the members of a structure, showing the application both to chords and web members before proceeding further.

(b) **Aug. Ritter's methods of moments (1860).** This method is based on the general theorem of moments. Accordingly for all external forces in the same plane and constituting a system in equilibrium, the sum of the static moments, about any point in this plane, must equal zero.

If now such a set of forces or loads be applied to a frame, Fig. 58A, and these loads, together with the two end reactions  $A$  and  $B$ , form a system in equilibrium, then if the

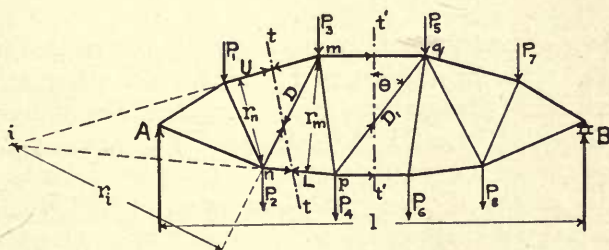


FIG. 58A.

frame be cut by a section  $\bar{u}$ , the stresses in the members cut, if acting as external forces, must maintain equilibrium of all the external forces on either side of the section. If, further, such planes can be passed which do not cut more than three members of the frame, then the stresses in the members cut may be determined one at a time, by taking as the center of moments the intersection of two of the members. The moments of the two intersecting members thus become zero.

The following designations are used:

For member  $U$  the center of moments is  $n$  and the lever arm is  $r_n$ ;

For member  $L$  the center of moments is  $m$  and the lever arm is  $r_m$ ;

For member  $D$  the center of moments is  $i$  and the lever arm is  $r_i$ ;

Also calling  $M$  the sum of the moments of the external forces  $A$ ,  $P_1$  and  $P_2$  to the

left of the section  $\bar{tt}$  and using subscripts  $n$ ,  $m$  and  $i$  to designate the centers about which the moments are taken, then for positive moments in a clockwise direction

$$\left. \begin{aligned} Ur_n + M_n &= 0 & \text{or} & & U &= -\frac{M_n}{r_n} \\ -Lr_m + M_m &= 0 & \text{or} & & L &= +\frac{M_m}{r_m} \\ -Dr_i - M_i &= 0 & \text{or} & & D &= -\frac{M_i}{r_i} \end{aligned} \right\}, \quad . \quad . \quad . \quad . \quad . \quad . \quad (58A)$$

where a positive stress indicates tension and a negative stress indicates compression. Thus a top chord member is always in compression and a bottom chord member is always in tension, while a web member may have either stress depending on its inclination with respect to its center of moments.

Hence, the stress  $S$ , in any member of a determinate frame, may always be expressed in terms of a moment  $M$  and its related lever arm  $r$ , by

$$S = \frac{M}{r}, \quad . \quad . \quad . \quad . \quad . \quad . \quad . \quad . \quad . \quad . \quad . \quad . \quad (58B)$$

which is Ritter's fundamental moment equation so extensively used in the previous chapters.

The centers of moments for the chord members are thus seen to be located opposite the chord in question, while for a web member the center of moments may be anywhere, depending upon the relative inclinations of the two chords composing the panel. The lever arms should be scaled from a large scale drawing or be computed.

When the three members cut by a section intersect in the same point, the method fails. Also, when the chords are parallel the lever arm for the diagonal becomes infinite. Hence the stress in such a diagonal cannot be found by a direct application of Eq. (58B) without some modification.

For the case of chords which are parallel or nearly so, the stress in a web member may be found by first computing the stresses in the chords and then finding the web stresses. This is done by choosing for the center of moments for a web member, any convenient point of one chord and then writing a moment equation, including the other chord of the panel cut among the external forces.

However, there is a simpler method of finding the web stresses in structures with parallel chords and that is from the shear in the panel cut.

Thus in the center panel  $\bar{mq}$  the chords are parallel and the diagonal  $\bar{pq}$  is cut by a section  $\bar{t't'}$ . The lever arm for  $pq$  would be infinite.

Since the sum of the moments of the external forces to the left of the section and of the three members cut must be zero, therefore the sum of the vertical components of these forces and stresses to the left of the section must likewise be equal to zero.

The sum of the vertical components to the left of the section  $\bar{t't'}$  is called the shear  $Q$ .



It is equal to the end reaction  $A$  minus the sum of the panel loads between  $A$  and the section. Thus

$$Q = A - \Sigma_A^P P, \quad . . . . . (58c)$$

where the summation covers only the panel loads to the left of the section and the shear is taken positive upward on the left of the section.

The chords, being horizontal, cannot have a vertical component, hence the only stress in any of the three members cut, which can have a vertical component, is the stress in the diagonal  $pq = D_1$ . The vertical component of  $D_1$  is then  $D_1 \cos \theta$ , and the sum of the vertical components of all forces and members cut on the left of the section  $t't'$  becomes

$$A - \Sigma_t^t P \pm D_1 \cos \theta = 0 = Q \pm D_1 \cos \theta$$

$$\text{or} \quad D_1 = \pm \frac{Q}{\cos \theta} = \pm Q \sec \theta, \quad . . . . . (58d)$$

When  $D_1$  is vertical, then  $\theta = 0$  and the stress becomes equal to the shear.

The above moment equation also admits of a graphic solution which will not be considered here.

(c) **The method of stress diagrams.** The first description of these diagrams seems to have come from Bow, and in 1864 Clerk-Maxwell published a paper "On Reciprocal Figures and Diagrams of Forces" in which he presents a scientific treatment of the subject. Cremona, in 1872, discussed the geometric properties of stress diagrams, showing their general usefulness in connection with graphostatics.

English and American writers, therefore, call such diagrams "*Maxwell stress diagrams*," while in Germany and France they bear Cremona's name.

The Maxwell stress diagram, so called in the present work, serves a most valuable purpose in the graphic analysis of all determinate frames, and is generally applicable to all cases which are susceptible to treatment by Ritter's moment method.

A peculiar relationship exists between a frame and its stress diagram by which each member of the frame is parallel to a line of the diagram and each pin point of the frame is represented by a force polygon in the diagram. It is thus equally possible to construct a stress diagram for a given frame or to construct a frame from a given stress diagram. Hence, the term "*reciprocal figures*" used by Maxwell.

The closed force or funicular polygon, which constitutes the basis for the Maxwell diagram, was known to Stevin, 1608, and Varignon, 1725, and marks the beginning of graphics. Such a polygon may be drawn for any set of forces in equilibrium.

Since all the forces meeting in a pin point must constitute a system in equilibrium, a closed force polygon may be drawn for each such point. Hence a Maxwell diagram is merely a succession of closed force polygons drawn for all the pin points of a frame.

For any given frame, the directions of all forces and members are given or must be assumed before proceeding to an analysis of stresses. Also, if the frame constitutes a system in equilibrium, then the externally applied loads must be in static equilibrium with the supports or reactions, and all these in turn must be in equilibrium with the internal stresses in the members.

Any pin point in equilibrium and acted upon by any number of forces of known directions, may then be represented in the force polygon by a succession of forces and stresses respectively equal and parallel to the forces and stresses meeting in that pin point. Since all directions are known, two magnitudes may be found by inserting the unknown members in such a way as to close the force polygon.

This is the fundamental principle of the Maxwell diagram. It is illustrated in Fig. 58B, where the force  $P$  and stresses  $S_1$  and  $S_2$  are known and the stresses  $S_3$  and  $S_4$  are of unknown magnitudes, but of given positions. All the forces meet in the point  $A$  and are supposed to be in equilibrium.

The method of drawing the stress diagram and nomenclature used in the figure is precisely the same in all cases and affords an easy way of deciding the direction of action of each unknown force.

The clockwise arrow indicates the order in which the forces are assembled in the stress diagram. Passing around the point  $A$  in this direction the first known force reached is  $P$ . Hence the letters  $a, b, c, d, e$  are supplied as shown in the angles between the

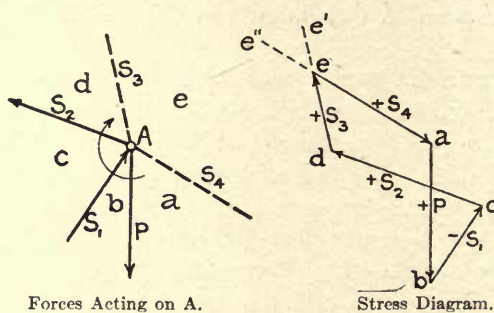


FIG. 58B.

forces, such that the force  $P$  is included between  $a$  and  $b$ . In speaking of the force  $\overline{ab}$  in the stress diagram, we mean a force equal and parallel to the force  $P$  and acting in the given direction from  $a$  to  $b$  in the stress diagram.

Observing this designation, the other known forces are added in their proper order in the stress diagram and made to act in the given directions  $a-b-c-d$  as found by going around the point  $A$  in a clockwise direction. The stress diagram from  $a$  to  $d$  is thus obtained and may now be closed by drawing a line  $\overline{de'} \parallel S_3$  through  $d$  and another line  $\overline{ae''} \parallel S_4$  through  $a$ . The intersection  $e$  thus found completes the force polygon and determines the stresses  $S_3$  and  $S_4$  both in magnitude and direction of action. Thus the arrows around the force polygon must be in the same direction as indicated by the initial given force  $P$ . Accordingly the force  $S_3$  acts in the direction from  $d$  to  $e$  and the force  $S_4$  acts in the direction from  $e$  to  $a$ . All forces in the force polygon are laid off to a certain scale by which the unknown forces are finally determined. A force or stress acting away from the pin point exerts a positive or tensile stress.

It is thus seen that the unknown stresses in two of the members meeting in any pin point may be determined by means of a closed force polygon. However, if a given frame presents no pin point involving only two unknown forces, then the method can-

not be applied except by first finding the forces in excess of two, by some other means. When there are three unknown forces acting on the point, and there are no redundant conditions involved, then Ritter's moment method will always furnish the necessary solution for one of the unknowns, prior to drawing the Maxwell diagram.

The forces in Fig. 58B were arbitrarily assembled in a clockwise direction. A counter clockwise direction might have been chosen with equal right, though the stress diagram would then have occupied a symmetric position with respect to the present case.

To illustrate the method, a simple truss, Fig. 58c, is used. The panel loads  $P$  are each 10 kips and the reactions  $A=B=40$  kips.

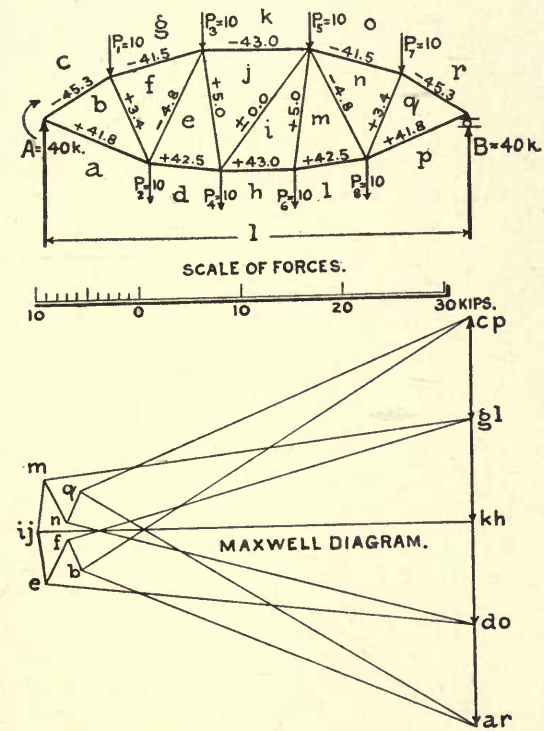


FIG. 58c.

The reactions must always be computed in order to supply the forces which are necessary to establish a system of external forces in absolute equilibrium. The truss diagram is then lettered and the direction of assembling the forces is chosen so as to locate the stress diagram properly on the paper.

A pin point embracing only two unknown members must be selected for a point of beginning and by inspection it is seen that either abutment satisfies this condition. Hence the stress diagram is commenced by drawing the triangle  $\overline{acb}$  in which the vertical upward reaction  $\overline{ac}$  is known and the two forces  $\overline{cb}$  and  $\overline{ba}$  are found. Following around the triangle in the direction  $a-c-b$ , it is seen that the force  $\overline{cb}$  acts toward the point  $A$  and thus



produces negative or compressive stress in the member  $\overline{cb}$ . The stress in  $\overline{ba}$  is found to act away from  $A$ , and is thus positive or tensile.

The construction of the diagram is now continued by assembling the forces around pin point 1, beginning with the first known member  $\overline{bc}$ , then adding the known force  $\overline{cg} = P_1$  and finally closing the figure by drawing  $\overline{gf}$  and  $\overline{fb}$ , which are the two unknowns for point 1.

The members  $\overline{ab}$  and  $\overline{bf}$  being known the closed force polygon for pin point 2 may next be drawn to find the stresses  $\overline{fe}$  and  $\overline{ed}$ .

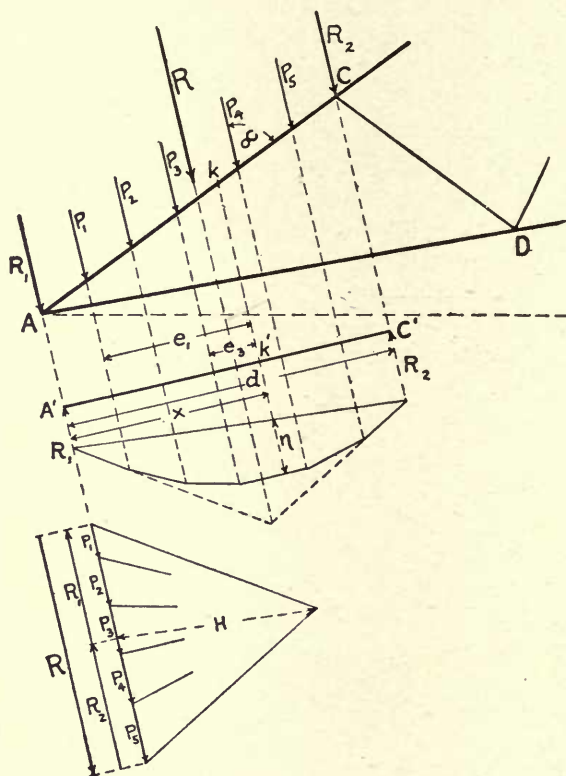


FIG. 58D.

The process is continued, taking the pin points in the following order:  $A-1-2-3-4-5-6-7-8$ . As a final check  $\overline{rp} = B$ .

All the stresses are then scaled from the stress diagram and written on the truss diagram with proper signs,  $-$  for compression and  $+$  for tension.

The present example shows a truss in which the chord stresses are nearly all equal and the web stresses are small. It is similar to the Pauli truss and is economical in design.

A very interesting Maxwell diagram is presented in Fig. 53B, where some of the external loading consists of a moment.

It frequently happens that loads are not applied directly to the pin points, in which

case certain load concentrations must be effected before proceeding to draw a stress-diagram. The members so loaded will usually receive a combination of direct stress and bending as illustrated by the member  $\overline{AC}$ , Fig. 58d, representing a portion of a roof truss.

The parallel loads  $P_1$  to  $P_5$ , acting on the member  $\overline{AC}$ , may be combined (graphically or analytically) into a resultant  $R$  of known position and magnitude, and  $R$  may then be resolved into the components  $R_1$  and  $R_2$ , constituting the pin point concentrations at  $A$  and  $C$  respectively.

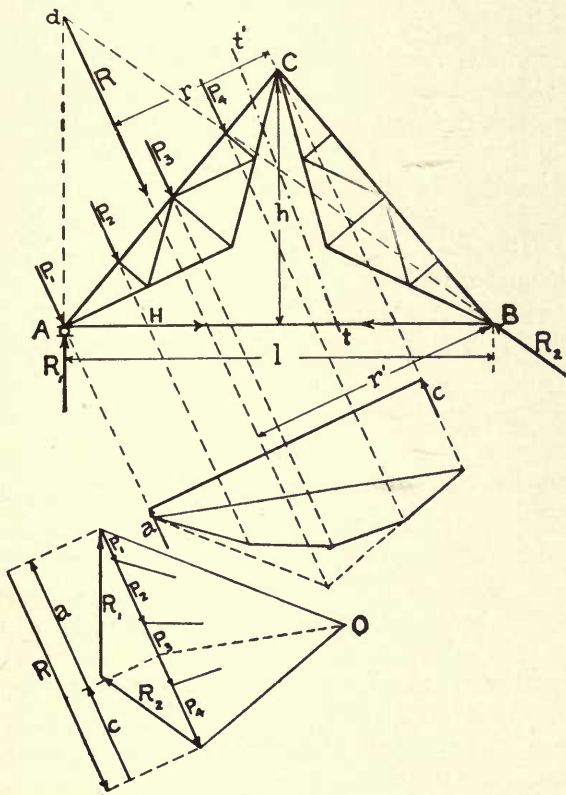


FIG. 58E.

After all loads have been thus concentrated on the several pin points of the structure, the total reactions may be computed in the usual manner, taking into account only the loads  $R_1, R_2$ , etc., which now replace the loads  $P$ , and then the stress diagram is drawn in the usual way and the direct stresses in the members are obtained.

The reactions  $R_1$  and  $R_2$  are the same as for a span  $d$ , taken perpendicular to the direction of the forces, and the bending moment  $M$ , for any point  $k$  distant  $x$  from  $A'$ , may be found from the equilibrium polygon or by computation.

For a direct stress  $-S$ , as obtained from the stress diagram, the total thrust in the member becomes  $N = -S - (R_1 - P_1 - P_2 - P_3) \cos \alpha$  and the moment  $M = R_1 x - P_1 e_1 -$

$P_2e_2 - P_3e_3 = \eta H$ , where  $H$  is the pole distance measured to the scale of forces and  $\eta$  is the ordinate of the equilibrium polygon measured to the scale of lengths.

The unit stresses on the extreme fibers of the column  $\overline{AC}$  then become by Eq. (49M)

$$f = \frac{N}{F} \pm \frac{My}{I},$$

where  $y$  is the distance of the extreme fiber from the gravity axis of the section.

The dead weight of inclined or horizontal members would be considered in this manner, only that for uniform loads the treatment is simplified.

The example given in Fig. 58E belongs to the class previously pointed out, in which not less than three unknown members meet in every pin point, and hence a Maxwell diagram cannot be constructed without first computing one member by Ritter's method of moments.

The resultant  $R$  is found as in the previous figure, and supposing the support at  $A$  to be a roller bearing, the reaction at  $R_1$  must be vertical and  $R_2$  must pass through  $B$  and  $d$ . Hence the reactions of known directions may be found from the force polygon by resolving  $R$  into  $R_1$  and  $R_2$ .

The stress in the member  $\overline{AB}$  is then found by passing a section  $\overline{tt'}$ , cutting only three members. Then with  $C$  as center of moments Eq. (58B) gives

$$\overline{AB} = H = \left( Rr - R_1 \frac{l}{2} \right) \frac{1}{h} = \left( Rr - R_2 \frac{r'}{2} \right) \frac{1}{h} = \frac{R}{h} \left( r - \frac{r'}{2} \right).$$

$R_1$  and  $H$  being now known the Maxwell diagram can be commenced for the pin point  $A$  and continued throughout the truss.

For vertical loads the solution may be conducted analytically.

## ART. 59. LIVE LOAD STRESSES

(a) **The critical positions of a train of moving loads** to produce maximum and minimum stresses in any member of a given determinate structure must be known prior to applying any method for finding the stresses themselves. This question was fully discussed in Arts. 20, 23 and 24, and in the *General Considerations* of Art. 58.

All the methods for the analysis of stresses which follow here presuppose a knowledge of the criteria for the positions of loads. The reader is referred to the articles just mentioned without repeating this discussion here.

(b) **The method of influence lines**, fully treated in Chapters IV and V, may be mentioned as the most universal, answering as it does all questions relating to criteria for positions of loads and magnitudes of stresses for any determinate structure.

The method requires no further explanation here except to point out the types of structures which warrant its application.

In general, the more complicated the geometric figure of a structure, the greater the advisability of employing the method of influence lines, since the geometric relations of the truss dimensions are thereby expressed independently of the loads.



$$S = \pm Q \sec \theta. \quad (59B)$$

The values of  $M$  and  $Q$  for any position of a live load will now be derived and evaluated first from the *sum A line*, and then from a single tabulation of moments.

The critical position of the loads for any particular effect on a certain member is supposed to have been determined in accordance with Arts. 20, 23 and 24.

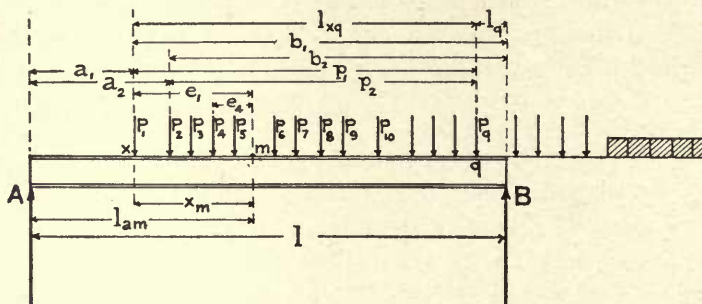


FIG. 59A.

Referring to Fig. 59A and calling  $M_B$  the sum of the moments of all loads on the span about the reaction  $B$  and  $M_m$  the sum of the moments about any point  $m$ ; also calling  $Q_m$  the vertical shear at the point  $m$ ; then for loads 1 to  $q$ , covering a distance  $xq = l_{xq}$

$$M_B = \sum_x^q P b = \sum_x^q P (p + l_q) = \sum_x^q P p + l_q \sum_x^q P; \quad (59c)$$

$$A = \frac{M_B}{l} = \frac{1}{l} \sum_x^q P p + \frac{l_q}{l} \sum_x^q P; \quad (59d)$$

$$Q_m = A - \sum_x^m P; \quad (59e)$$

$$M_m = A l_{am} - \sum_x^m P e = \frac{M_B l_{am}}{l} - \sum_x^m P e, \quad (59f)$$

or

$$M_m = l_{am} \left( A - \frac{\sum_x^m P e}{l_{am}} \right) = l_{am} (A - A_{am}), \quad (59g)$$

wherein  $A_{am} = \sum_x^m P e / l_{am}$  may be defined as the end reaction at  $A$  of the loads 1 to  $m$  covering the distance  $x_m$  of a simple span  $l_{am}$ .

The values  $A$  and  $A_{am}$  may be obtained from a reaction summation influence line, or *sum A line*, drawn for the reaction  $A$  and span  $l$ , according to Art. 22, Figs. 22A and 22B. The ordinates of the *sum A line* may be computed from Eq. (59d), or constructed graphically by the method given in Art. 22.

Such a *sum A line* is shown in Fig. 59B, drawn for a span of 200 feet and using a train of Cooper's E60 loading, consisting of two locomotives followed by a uniform load of 3000 lbs. per linear foot per rail.

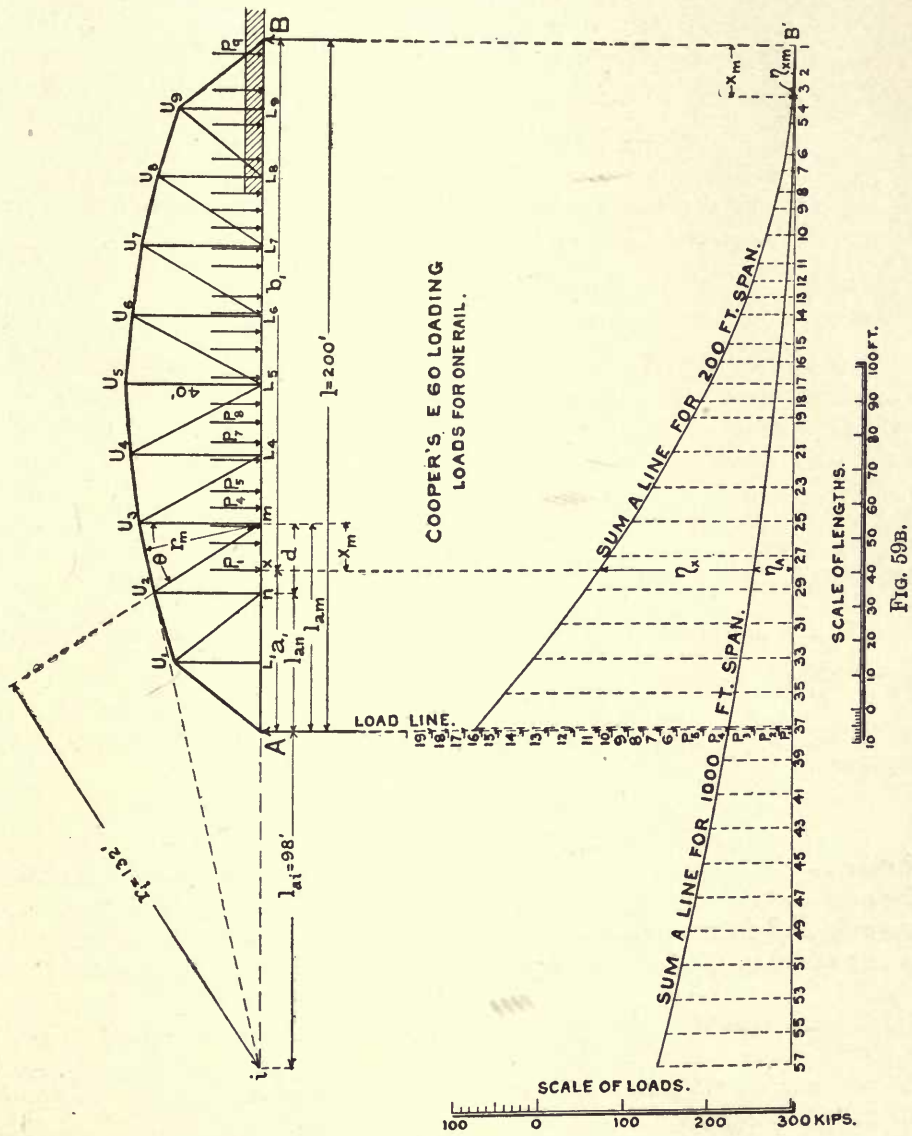
The ordinate  $\eta_x$  under the first load  $P_1$  at  $x$ , represents the end reaction  $A$  for the position of loads indicated, when the span  $AB$  is loaded for a distance  $b_1$  from  $B$ .

The reaction  $A_{am}$ , for the same train covering the distance  $x_m$  from  $m$  on the span  $l_{am}$ , may be obtained from the same *sum A line* as follows: Had the *sum A line*

been drawn for a span  $l_{am}$  then the ordinate at  $x_m$  from  $B'$  would be the required reaction  $A_{am}$ . However, this polygon was actually drawn for a span  $l$ , and hence the ordinate  $\eta_{xm}$  distant  $x_m$  from  $B'$  is  $l/l_{am}$  times too small, therefore,

$$A_{am} = \frac{l \eta_{xm}}{l_{am}}. \quad \dots \quad (59H)$$

This illustrates how a *sum A line* drawn for any span may be used to obtain end reactions for any other span. However, in order to avoid the multiplication of all ordi-





nates by  $l$ , it is best to draw the *sum A line* for a span of 1000 ft., and then derive all ordinates according to Eq. (59H), by which the ordinates of one *A line* are to those of another *A line* in the inverse proportion of the spans for which the lines were drawn.

A portion of such a 1000 ft. *sum A line* is shown in Fig. 59B, from which the actual reactions  $A$  and  $A_{am}$ , for a span  $l=200$  ft., are obtained as

$$A = \frac{1000\eta_A}{l} \quad \text{and} \quad A_{am} = \frac{1000\eta_{xm}}{l_{am}}, \quad . \quad . \quad . \quad . \quad . \quad . \quad (59I)$$

where  $\eta_A$  is the ordinate distant  $b_1$  from  $B'$  and  $\eta_{xm}$  is the ordinate distant  $x_m$  from  $B'$ .

**Any moment  $M_m$  or chord stress** is now readily found from Eq. (59G), using the values from Eq. (59I) as follows:

$$M_m = l_{am}(A - A_{am}) = 1000\eta_A \frac{l_{am}}{l} - 1000\eta_{xm}, \quad . \quad . \quad . \quad . \quad . \quad . \quad (59J)$$

and the stress in any chord member having the point  $m$  for its center of moments with a lever arm  $r_m$ , becomes by Eqs. (59A) and (59J)

$$S = \frac{M_m}{r_m} = \frac{1}{r_m} [1000\eta_A \frac{l_{am}}{l} - 1000\eta_{xm}] \quad . \quad . \quad . \quad . \quad . \quad . \quad (59K)$$

**The web stresses for trusses with non-parallel chords** are derived from moments  $M_i$  of the external forces about the center of moments  $i$  for any particular web member.

Calling the lever arm  $r_i$  for a web member with moment center  $i$  distant  $l_{ai}$  to the left of  $A$ , then for  $x_m < d$  and  $A_{nm} = \Sigma_x^m Pe/d = 1000\eta_{xm}/d$ ,

$$M_i = Al_{ai} - A_{nm}(l_{ai} + l_{an}),$$

$$\text{or} \quad M_i = 1000\eta_A \frac{l_{ai}}{l} - \frac{1000\eta_{xm}}{d} (l_{ai} + l_{an}), \quad . \quad . \quad . \quad . \quad . \quad . \quad (59L)$$

when  $x_m > d$ , a case which happens very rarely, indicating that some loads extend to the left of  $n$ , then

$$M_i = Al_{ai} - A_{nm}(l_{ai} + l_{an}) - \sum_x^n P(l_{ai} + a),$$

$$\text{or} \quad M_i = 1000\eta_A \frac{l_{ai}}{l} - \left( \frac{l_{ai} + l_{an}}{d} \right) \sum_n^m Pe - \sum_x^n P(l_{ai} + a), \quad . \quad . \quad . \quad (59M)$$

wherein the two last terms must be computed. It should be remembered that this last case does not occur more than once or twice, if at all, for a whole analysis and hence involves only a slight amount of work.

In any case Eq. (59A) gives the stress in a web member for non-parallel chords, as

$$S = \frac{M_i}{r_i} \quad . \quad . \quad . \quad . \quad . \quad . \quad (59N)$$

**The web stresses for trusses with parallel chords** are derived from the shear according to Eq. (59E)

Thus the vertical shear to the left of a section through any panel  $\overline{nm}$ , when there are no loads to the left of  $n$ , making  $x_m < d$ , becomes

$$Q_m = A - A_{nm} = \frac{1000\eta_A}{l} - \frac{1000\eta_{xm}}{d}, \quad . . . . . (59o)$$

wherein  $A_{nm}$  is the reaction at  $n$  for the loads in the panel  $\overline{nm}$  extending over a distance  $x_m$  on a span  $d$ .

When  $x_m > d$ , which would be the rare case for one or two loads to the left of  $n$ , then

$$Q_m = A - A_{nm} - \sum_x^n P = \frac{1000\eta_A}{l} - \sum_n^m \frac{Pe}{d} - \sum_x^n P, \quad . . . (59p)$$

where the two last terms would have to be computed for the loads between  $x$  and  $m$  as in the previous case.

The stress in any web member of a truss with parallel chords is then found from Eq. (58d) as

$$S = Q_m \sec \theta, \quad . . . . . (59q)$$

where  $Q_m$  is given from Eqs. (59o) or (59p).

The above demonstration, necessitating the use of one *sum A line* drawn for a span of 1000 ft., was used only for the development of the formulæ. In practice, the *sum A line* is dispensed with by tabulating the ordinates  $1000\eta_A$  for any case of standard loading.

One such table (see Table 59A), will then suffice for the computation of all chord and web stresses in any simple determinate truss for the general case of moving train loads.

Table 59A thus represents the values of  $1000A = 1000\eta_A = M_B =$  the sum of the moments of all loads on the 1000 ft. span about the reaction  $B$ , expressed in kip feet. These moments are readily computed from Eqs. (59c), and (59i), thus

$$M_B = 1000\eta_A = \sum_x^q Pp + l_q \sum_x^q P, \quad . . . . . (59r)$$

where  $l_q$  is the distance the train is moved ahead whenever a new load  $P_q$  is brought on the span.

Eq. (59r), holds until the uniform load reaches the point  $B$ , after which the moments must be figured as for uniformly distributed loads. The table suggests the ease of computation and might be extended over the whole span of 1000 feet, though for purposes of illustration this was not considered necessary.

To facilitate interpolation, the differences in  $M_B$  for one foot were added in a separate column. Interpolations for distances between those given are thus readily performed and these are strictly accurate up to the point where the uniform load is reached. After that there is a slight error because the moment for uniformly distributed loads varies as  $l^2$ . However, the error from this source is entirely negligible.

**Example.** Required the maximum live load stresses in the chord  $\overline{U_2U_3}$ , and in the diagonal  $\overline{U_2L_3}$  of the 200 ft. truss shown in Fig. 59B, using Cooper's E 60 loading.

TABLE 59A  
REACTIONS FOR COOPER'S E-60 LOADING, SPAN OF 1000 FEET.

Wheel No.	Load Length, $b_1$ Feet.	Total Load $\sum_x B P$ Kips.	$M_{B=1000\eta_A}$ Kips.	Diff. for 1 Foot. Kips.	Wheel No.	Load Length, $b_1$ Feet.	Total Load $\sum_x B P$ Kips.	$M_{B=1000\eta_A}$ Kips.	Diff. for 1 Foot. Kips.
1	0	15.0	0.0		26	144	531	41,293.5	523.5
2	8	45.0	120.0	15.0	27	149	546	43,986.0	538.5
3	13	75.0	345.0	45.0	28	154	561	46,753.5	553.5
4	18	105.0	720.0	75.0	29	159	576	49,596.0	568.5
5	23	135.0	1,245.0	105.0	30	164	591	52,513.5	583.5
6	32	154.5	2,460.0	135.0	31	169	606	55,506.0	598.5
7	37	174.0	3,232.5	154.5	32	174	621	58,573.5	613.5
8	43	193.5	4,276.5	174.0	33	179	636	61,716.0	628.5
9	48	213.0	5,244.0	193.5	34	184	651	64,933.5	643.5
10	56	228.0	6,948.0	213.0	35	189	666	68,226.0	658.5
11	64	258.0	8,772.0	228.0	36	194	681	71,593.5	673.5
12	69	288.0	10,062.0	258.0	37	199	696	75,036.0	688.5
13	74	318.0	11,502.0	288.0	38	204	711	78,543.5	703.5
14	79	348.0	13,092.0	318.0	39	209	726	82,146.0	718.5
15	88	367.5	16,224.0	348.0	40	214	741	85,813.5	733.5
16	93	387.0	18,061.5	367.5	41	219	756	89,556.0	748.5
17	99	406.5	20,383.5	387.0	42	224	771	93,373.5	763.5
18	104	426.0	22,416.0	406.5	43	229	786	97,266.0	778.5
19	109	426.0	24,546.0	426.0	44	234	801	101,233.5	793.5
20	114	441.0	26,713.5	433.5	45	239	816	105,276.0	808.5
21	119	456.0	28,956.0	448.5	46	244	831	109,393.5	823.5
22	124	471.0	31,273.5	463.5	47	249	846	113,586.0	838.5
23	129	486.0	33,666.0	478.5	48	254	861	117,853.5	853.5
24	134	501.0	36,133.5	493.5	49	259	876	122,196.0	868.5
25	139	516.0	38,676.0	508.5	50	264	891	126,613.5	883.5

All loads in kips for one rail.



For the chord  $\overline{U_2U_3}$ , the center of moments is at  $m$  and the maximum stress occurs when the span is fully loaded, making  $b_1=l=200$  ft., and  $x_m=l_{am}=60$  ft. Also  $r_m=34.5$  ft.

Then Table 59A gives for 200 ft.,  $1000\eta_A=75036+703.5=75739.5$ , and for  $x_m=60$  ft.,  $1000\eta_{xm}=6948+4\times 228=7860$ , whence by Eq. (59K),

$$S = \frac{1}{r_m} \left[ 1000\eta_A \frac{l_{am}}{l} - 1000\eta_{xm} \right] = \frac{1}{34.5} \left[ 75739.5 \left( \frac{60}{200} \right) - 7860 \right] = 430.78 \text{ kips.}$$

For the diagonal  $\overline{U_2L_3}$  with load divide at  $x_m=10.5$  ft., making  $b_1=140+10.5=150.5$  ft.,  $l_{an}=40$  ft.,  $l_{ai}=98$  ft.,  $d=20$  ft., and  $r_i=132$  ft., and thus  $x_m < d$ , Table 59A gives  $1000\eta_A=43986+1.5\times 553.5=44816.3$  and  $1000\eta_{xm}=120+2.5\times 45=232.5$ .

Hence by Eqs. (59L) and (59N).

$$\begin{aligned} S &= \frac{M_i}{r_i} = \frac{1}{r_i} \left[ 1000\eta_A \frac{l_{ai}}{l} - \frac{1000\eta_{xm}}{d} (l_{ai} + l_{an}) \right] \\ &= \frac{1}{132} \left[ 44816.3 \left( \frac{98}{200} \right) - \frac{232.5}{20} (98 + 40) \right] = 154.21 \text{ kips.} \end{aligned}$$

The minimum stress in  $\overline{U_2L_3}$  may be found by treating the symmetric member  $\overline{L_7U_8}$  in the right half of the span.

Similarly the stress in any member of the truss may be determined for any desired position of the train of loads, all by means of the one Table 59A.

It is believed that the ease and simplicity of applying the above method, together with its universal applicability, should commend itself to the practical designer.

Certainly it does not seem warranted to employ approximate methods when an exact solution is possible without additional labor.

## CHAPTER XIII

### SECONDARY STRESSES

#### ART. 60. THE NATURE OF SECONDARY STRESSES

In the previous chapters a framed structure was regarded as a system of individual members linked together by frictionless pin connections. It was also supposed that the neutral or gravity axes of all members meeting in a panel point actually intersected in one point. The stresses computed on this basis are called *primary stresses*.

Owing to the friction, which always exists in pin-connected joints, and the rigidity introduced by riveted connections, this condition is never fully realized in practice. Hence certain moments or bending effects are always produced in the proximity of the connected ends, which set up bending stresses of variable character and magnitude. These are generally called *secondary stresses* as distinguished from the primary stresses.

All structures involving redundancy are subjected to elastic deformations caused by the loads, temperature, and abutment displacements giving rise to what may be called *additional stresses*. These also exist to a slight degree in determinate structures, especially when their geometric shape is peculiarly subject to large load and temperature deflections as in the case of three-hinged arches. Still other causes, such as erroneous shop lengths of members, wind pressure, and impact and brake effects of moving loads, produce stresses belonging to this class which do not admit of exact determination and can at best be merely estimated.

The first theoretical discussions of secondary stresses were given by Asimont, 1877; Manderla and Engesser, 1879, and Winkler, 1881. Graphic solutions were published by Landsberg, 1885; W. Ritter, 1890; and Mohr, 1891-3. A résumé of most of these is given by C. R. Grimm, C. E., "Secondary Stresses in Bridge Trusses," 1908.

The facts which were revealed by these discussions gave rise to very material improvements in the modern practices of designing structures. Thus, the details of connections at panel points and between floorbeams and truss members have been vastly improved, and particular attention is now being given to a more judicious design of the members themselves, especially those subjected to compressive stress.

It is not the purpose here to treat all the various methods of calculating secondary stresses, but merely to present what appears to the author as the most understandable and usable method. The nature of the problem is such as to preclude the possibility of considering all the complexities involved and yet remain within the limits of practical utility. Hence some approximations must be applied, and justly so, because many of the influences are too small to warrant the labor involved in their analysis, and others are beyond reasonable limits of estimation.

The three primary causes for secondary stresses in bridge members are: the weights of the members themselves producing deflections in all except vertical members and giving rise to bending stresses; the absence of frictionless panel point connections; eccentric connections between members meeting in a common panel point.

Riveted connections are here treated like fixed ends so that the elastic deformations of the structure are supposedly taken up by flexure in the members themselves without producing any changes in the angles at the panel points. While this assumption is not absolutely true, because the bending moments cannot be resisted without producing some elastic angular distortions, yet it is on the side of safety and tends to compensate some other factors which are entirely neglected.

Pin-connected members, according to more recent experience, cannot be regarded as free from bending moments on account of the rather excessive friction which always prevails on the pins. In the case of eye-bars this may add considerable bending stress owing to the slenderness of such members. This should not be construed to mean that pin connections are inferior to riveted joints, but that the former do not possess all the advantages usually attributed to them. The distinct superiority of pins is to be found in the prevention of eccentric transmission of the direct stresses, a condition which is difficult to accomplish in riveted connections.

The excessive bending stresses carried from floor-beam connections to the vertical trusses can hardly be estimated and should be avoided as far as possible by the introduction of flexible connections in preference to the rigid type so much used in the past.

The secondary stresses, which will now be considered, are those caused by the elastic deformations taking place in the plane of the frame itself and due to the three primary causes above enumerated.

#### ART. 61. SECONDARY STRESSES IN THE PLANE OF A TRUSS DUE TO RIVETED CONNECTIONS

Every elastic structure must undergo certain deformation when subjected to loads. If the structural members are rivet-connected at the ends, then this deformation is taken up by the members themselves in the production of certain bending moments which are resisted by the rigid panel connections.

Figs. 61A and 61B show the several possible combinations of single and double flexure with compression and tension as they might occur in any structure.

The straight chord  $\overline{AB}$ , in each case, represents the position of the member on the supposition of frictionless pin connections, while the curved line indicates the member as it would be distorted by the bending moments and axial forces resulting from the fixed riveted connections.

Assuming such a member to be released at the ends by sections passed close to the panel points, then the internal stresses may be replaced by external forces  $P_a$  and  $P_b$ . Each of these may be resolved into two forces and a moment acting at the original fixed ends. Thus  $P_a$  is equivalent to  $S_a$ ,  $A$  and a moment  $M_a$  while  $P_b$  is replaced by  $S_b$ ,  $B$  and a moment  $M_b$ . The conditions of equilibrium require that  $P_a = P_b$  and hence that



$S_a = P_a \cos \theta = S_b = P_b \cos \theta$ ; also  $A = B = P \sin \theta$  and  $M_a + M_b - Al = 0$ . Since  $\theta$  is always very small  $S_a = S_b = P_a = P_b$ , which assumption is entirely permissible.

In the case of compression members the concave side of the elastic curve is always

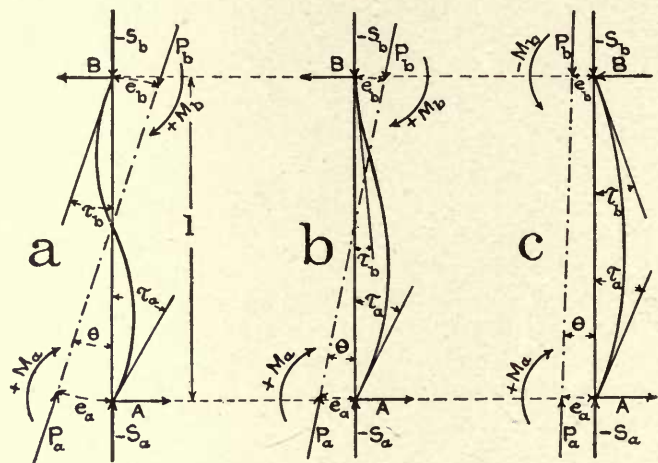


FIG. 61A—Tension Members.

toward the resultant  $P$ , and hence a maximum moment may occur at some point intermediate between  $A$  and  $B$ . For tension members the convex side is toward the force, and the maximum moment must occur at one end of the member.

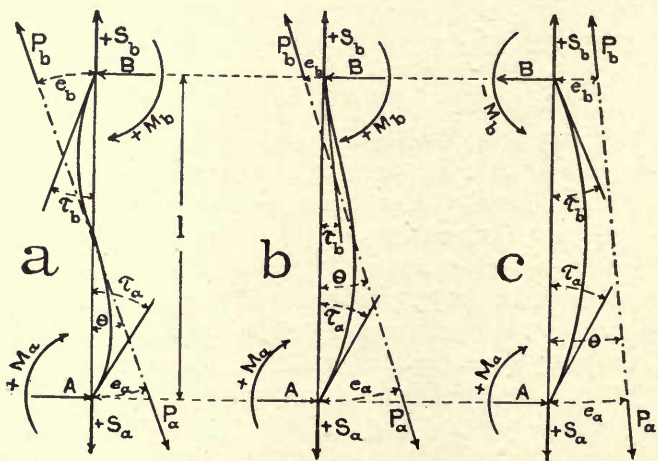


FIG. 61B—Compression Members.

In any case then, the stresses produced in a member by the bending moments  $M_a$  and  $M_b$ , are readily determined provided these moments are known. Of the several

methods proposed for the evaluation of the end moments, the analytic method of Professor Fr. Engesser is probably the most direct and is the one given here.

For any structure of  $m$  members there will be  $2m$  unknown end moments to be evaluated. These are derived from the angular deflections  $\tau$ , which the respective fixed ends of the members undergo as a result of certain distortions  $\Delta\alpha$ ,  $\Delta\beta$ ,  $\Delta\gamma$ , etc., produced in the angles of the frame by the work of the external forces and reactions, as per Eqs. (37D).

The first step in the development of the method is then to derive the relation between the moments  $M_a$  and  $M_b$ , and the deflection angles  $\tau_a$  and  $\tau_b$  for a column on two fixed supports.

The following assumptions are made in the interest of simplifying the theory for practical applications.

Since in well designed members the shear, direct thrust and temperature have a very slight effect on flexure, these factors are neglected. However, for poorly designed members with small moments of inertia and slender dimensions, the deflections due to normal thrust etc., may become very considerable and these assumptions might not hold.

It is further assumed that the axes of all the members are situated in the same plane, and that these axes are centric for all members meeting in a point. Also, that the external loads are all applied at the panel points, neglecting for the present the flexure produced in the members by their own weight.

Since the fixed ends, Fig. 61c, do not of themselves produce any direct thrust or stress in the member  $\overline{AB}$  (not being absolutely fixed in space), therefore, the column involves only two redundant conditions which are the moments  $M_a$  and  $M_b$ . The principal system is then a beam on two supports.

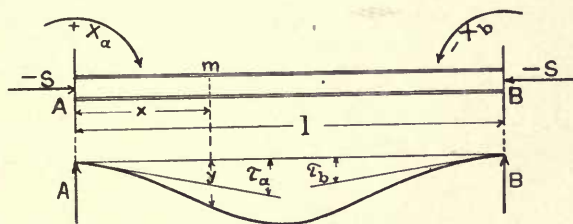


FIG. 61c.

The effect of the direct stress  $S$  is not considered here because for well designed members with comparatively large moments of inertia this was found by Manderla to be entirely negligible. Otherwise a moment  $Sy$  would enter the general moment as given by Eq. (61A).

Eq. (7A) now gives for  $A_o=0$ ,  $A_a=1/l$  and  $A_b=-1/l$ ,

$$A = A_o - A_a X_a - A_b X_b = -\frac{X_a}{l} + \frac{X_b}{l},$$

and the moment  $M_m$ , about any point  $m$ , becomes

$$M_m = Ax + X_a = \frac{x}{l}(X_b - X_a) + X_a, \quad \dots \dots \dots (61A)$$

giving 
$$\frac{\partial M_m}{\partial X_a} = 1 - \frac{x}{l} \quad \text{and} \quad \frac{\partial M_m}{\partial X_b} = \frac{x}{l}.$$

Then according to Eq. (15L), the virtual work of the moment  $M_a$  is

$$\begin{aligned} 1 \cdot \tau_a &= \int_0^l \frac{M_m}{EI} \frac{\partial M_m}{\partial X_a} dx = \frac{1}{EI} \int_0^l \left[ \frac{x}{l} (X_b - X_a) + X_a \right] \left( 1 - \frac{x}{l} \right) dx \\ &= \frac{1}{EI} \left[ \frac{l}{2} X_b - \frac{l}{2} X_a + l X_a - \frac{l}{3} X_b + \frac{l}{3} X_a - \frac{l}{2} X_a \right] = \frac{l}{6EI} (2X_a + X_b). \end{aligned}$$

A similar process will furnish  $\tau_b$  and calling  $X_a = M_a$  and  $X_b = M_b$ , then for any member of single curvature

$$\tau_a = \frac{l}{6EI} (2M_a + M_b) \quad \text{and} \quad \tau_b = \frac{l}{6EI} (2M_b + M_a). \quad \dots \dots \dots (61B)$$

When the moments  $M_a$  and  $M_b$  act in the same direction then the elastic curve will have a point of counterflexure and a similar derivation to the one just given will furnish the values

$$\tau_a = \frac{l}{6EI} (2M_a - M_b) \quad \text{and} \quad \tau_b = \frac{l}{6EI} (2M_b - M_a). \quad \dots \dots \dots (61C)$$

Considering a triangle as the fundamental element of a frame, the distortions  $\Delta\alpha$ ,  $\Delta\beta$  and  $\Delta\gamma$  in the three angles resulting from the changes in the lengths of the members, expressed in terms of unit stresses, were determined in Art. 37. It is now necessary to show the relation between these angle distortions and the deflection angles  $\tau$  at each end of each member forming the triangle.

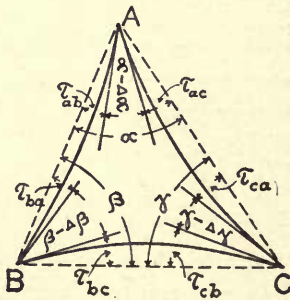


FIG. 61D.

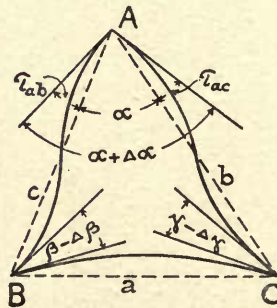


FIG. 61E.

Referring to Figs. 61D and 61E, it is easily seen that

$$\tau_{ab} + \tau_{ac} = \Delta\alpha; \quad \tau_{ba} + \tau_{bc} = \Delta\beta; \quad \tau_{cb} + \tau_{ca} = \Delta\gamma. \quad \dots \dots \dots (61D)$$

Fig. 61D represents an impossible condition because at least one member of the three composing the triangle must undergo double curvature as shown by Fig. 61E and as required by Eq. (37E), whereby

$$\Delta\alpha + \Delta\beta + \Delta\gamma = 0. \quad \dots \dots \dots (61E)$$



The elastic distortions  $\Delta\alpha$ ,  $\Delta\beta$  and  $\Delta\gamma$  are given by Eqs. (37D), and may be considered known for all angles of a frame and for one simultaneous case of loading and stress.

While Eqs. (37D) were derived on the assumption of frictionless pin connections between all members, they are now used to determine the amount of distortion in each angle which is prevented from taking place by virtue of the rigid riveted connections.

Two equations of the form of Eqs. (61C), may be written for each side of a triangle or for each member of a frame. Using the designations indicated by the double subscripts in Fig. 61D, where the first refers to the apex or panel point and the second to the far end of the adjacent member, then by inserting the deflection angles  $\tau$  into Eqs. (61D), the following formulæ are obtained for any triangle  $\overline{ABC}$ :

$$\left. \begin{aligned} 6E\Delta\alpha &= 6E(\tau_{ab} + \tau_{ac}) = \frac{l_c}{I_c} (2M_{ab} + M_{ba}) + \frac{l_b}{I_b} (2M_{ac} + M_{ca}) \\ 6E\Delta\beta &= 6E(\tau_{ba} + \tau_{bc}) = \frac{l_c}{I_c} (2M_{ba} + M_{ab}) + \frac{l_a}{I_a} (2M_{bc} + M_{cb}) \\ 6E\Delta\gamma &= 6E(\tau_{cb} + \tau_{ca}) = \frac{l_a}{I_a} (2M_{cb} + M_{bc}) + \frac{l_b}{I_b} (2M_{ca} + M_{ac}) \end{aligned} \right\} \dots \dots \dots (61F)$$

In the Eqs. (61F), the six moments are unknown, and hence a solution is impossible unless at least three of them may be independently derived from other conditions to be developed later.

According to Eqs. (61D) the sum of the three angle distortions  $\Delta$  for any triangle, must equal the sum of the six deflection angles  $\tau$  and by the condition of Eq. (61E), both sums must then be equal to zero, hence

$$\Delta\alpha + \Delta\beta + \Delta\gamma = \tau_{ab} + \tau_{ac} + \tau_{ba} + \tau_{bc} + \tau_{cb} + \tau_{ca} = 0. \dots \dots \dots (61G)$$

Also, for any apex angles meeting in the same panel point, the sum of the angle distortions  $\Delta$  must equal the sum of the deflection angles  $\tau$ , hence for any panel point

$$\Sigma\Delta = \Sigma\tau, \dots \dots \dots (61H)$$

and therefore, if one of the deflection angles  $\tau$  is known, the others around that panel point may be successively found by applying equations of the form of Eqs. (61D).

For any determinate frame, there will thus be as many unknown deflection angles  $\tau$  as there are panel points, and for  $p$  panel points there will be  $p$  equations of the form of Eqs. (61H), each involving one unknown deflection angle  $\tau$ .

The following values

$$\left. \begin{aligned} \frac{M_{ab}l_c}{6I_c} &= K_{ab}; & \frac{M_{ba}l_c}{6I_c} &= K_{ca} \\ \frac{M_{bc}l_a}{6I_a} &= K_{bc}; & \frac{M_{cb}l_a}{6I_a} &= K_{cb} \\ \frac{M_{ac}l_b}{6I_b} &= K_{ac}; & \frac{M_{ca}l_b}{6I_b} &= K_{ca} \end{aligned} \right\} \dots \dots \dots (61I)$$

are now substituted into Eqs. (61F), as a matter of convenience, to obtain the following formulæ for any triangle  $\overline{ABC}$ , thus

$$E\Delta\alpha = K_{ba} + 2(K_{ac} + K_{ab}) + K_{ca}, \quad . . . . . (61J)$$

$$E\Delta\beta = K_{ab} + 2(K_{bc} + K_{ba}) + K_{cb}, \quad . . . . . (61K)$$

$$E\Delta\gamma = K_{bc} + 2(K_{cb} + K_{ca}) + K_{ac}. \quad . . . . . (61L)$$

Adding these three equations and imposing the condition of Eq. (61E), then for any triangle  $\overline{ABC}$ ,

$$K_{ac} + K_{ab} + K_{bc} + K_{ba} + K_{cb} + K_{ca} = 0. \quad . . . . . (61M)$$

Assuming now that the three quantities  $K_{ac}$ ,  $K_{ab}$  and  $K_{ba}$  are known, then the remaining three may be obtained from the above equations as follows:

$$\text{from Eq. (61J),} \quad K_{ca} = E\Delta\alpha - 2(K_{ac} + K_{ab}) - K_{ba}, \quad . . . . . (61N)$$

$$\text{from Eqs. (61K) and (61M), } K_{bc} = E\Delta\beta + K_{ac} - K_{ba} + K_{ca}, \quad . . . . . (61O)$$

$$\text{from Eqs. (61L) and (61M), } K_{cb} = E\Delta\gamma + K_{ab} + K_{ba} - K_{ca}. \quad . . . . . (61P)$$

By the conditions of static equilibrium, the sum of all the moments about any panel point must be zero, from which  $p$  equations of the following form are obtained, using the values from Eqs. (61I). Thus, for any panel point  $A$

$$\Sigma M_a = \Sigma K_a \frac{6I}{l} = 0, \quad . . . . . (61Q)$$

including all the members meeting in this point. See Fig. 61H and Eq. (61U) for the manner of forming these equations.

The following procedure will furnish a solution for all the bending moments of a frame, using Eqs. (61N) to (61Q): In the first triangle, evaluate three of the quantities  $K$  in terms of the other three, using Eqs. (61N, O, P). Two of the values  $K$  so found, also belong to the adjacent or second triangle and a third value  $K$  in this second triangle may be found from Eq. (61Q), making three values known to find the other three by applying Eqs. (61N, O, P) to the second triangle.

This process is continued throughout the series of triangles up to the last one, where two extra moment condition Eqs. (61Q) become available and these suffice to determine the three first assumed values  $K$ . This is merely a process of successive elimination, eminently suited to the present problem.

When the values  $K$  are thus found then the several moments  $M$  are obtained by substitution into Eqs. (61I). See the example below for symmetric structures with symmetric loading.

The solution of the whole problem is possible, because for any frame with  $m$  members and  $p$  panel points, there will be  $\frac{1}{2}(m-1)$  triangles furnishing  $\frac{3}{2}(m-1)$  equations of the form of Eqs. (61N, O, P) and  $p$  equations of the form of Eq. (61Q) making in all  $\frac{3}{2}(m-1) + p$

available equations from which to find  $2m$  unknown moments  $M$ . Hence, if the problem is determinate, there must be as many equations as there are unknowns and

$$2m = \frac{3}{2}(m-1) + p, \text{ giving } 2p = m + 3 \dots \dots \dots (61R)$$

which by Eq. (3A) is actually true for any determinate frame composed of triangles and, therefore, the solution is possible.

It was previously pointed out that the assumptions regarding the signs of the deflection angles  $\tau$  as illustrated in Fig. 61D, are impossible, and that not all these angles, nor the moments  $M$  in the members of a triangle can have the same algebraic sign on account of the condition imposed by Eq. (61E). Therefore, the computed results must furnish deflection angles  $\tau$  and moments  $M$  of both signs.

However, to avoid complicated rules, it is necessary to adopt some conventional or standard figure and then reverse the assumed deflections wherever the computed angles  $\tau$  are negative. For this reason the conventional figure of distortion is assumed as indicated in Fig. 61F, wherein the members in alternate triangles I, III, V, etc., are made to present a *concave line outward*, indicating *positive moments*  $M$ .

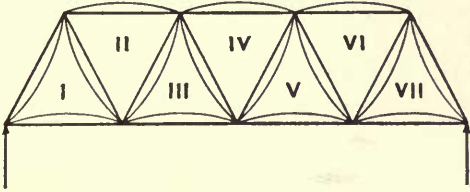


FIG. 61F.

The even triangles II, IV, VI, etc., must then represent negative moments, but in order that Fig. 61F may represent the conventional assumption of all positive moments, the Eqs. (37D) are divided through by minus one when applied to the even triangles with convex lines outward.

Hence, for the odd triangles with positive moments  $M$ , Eqs. (37D) are applied in the form

$$\left. \begin{aligned} E\Delta\alpha &= (f_a - f_b) \cot \gamma + (f_a - f_c) \cot \beta \\ E\Delta\beta &= (f_b - f_c) \cot \alpha + (f_b - f_a) \cot \gamma \\ E\Delta\gamma &= (f_c - f_a) \cot \beta + (f_c - f_b) \cot \alpha \end{aligned} \right\} , \dots \dots \dots (61s)$$

and for the even triangles the negative moments are also made positive by using Eqs. (61s) in the form

$$\left. \begin{aligned} E\Delta\alpha &= (f_b - f_a) \cot \gamma + (f_c - f_a) \cot \beta \\ E\Delta\beta &= (f_c - f_b) \cot \alpha + (f_a - f_b) \cot \gamma \\ E\Delta\gamma &= (f_a - f_c) \cot \beta + (f_b - f_c) \cot \alpha \end{aligned} \right\} , \dots \dots \dots (61t)$$



and then all moments, represented by Fig. 61F, may be considered positive. The subscripts  $a$ ,  $b$ , and  $c$  in Eqs. (61s) and (61t), refer to the sides  $a$ ,  $b$ , and  $c$  opposite the respective angles  $\alpha$ ,  $\beta$ , and  $\gamma$ .

Since the above assumptions do not represent real or possible conditions, some of the moments  $M$ , resulting from the final computation, must develop negative signs. Thus, if  $M_{ac}$  and  $M_{ba}$  in Fig. 61b, should turn out with negative signs, then the real deformations of the triangle would be as represented in Fig. 61g.

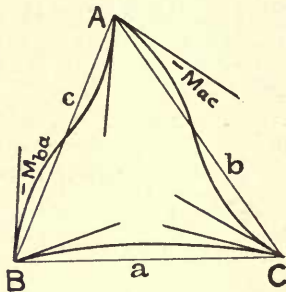


FIG. 61G.

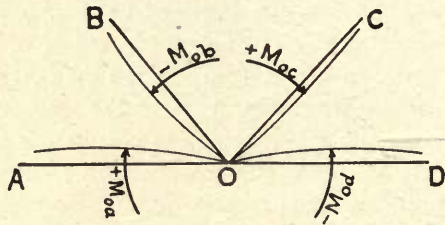


FIG. 61H.

In evaluating Eqs. (61q) for the several panel points, it is necessary to observe the relative signs of the moments in the several members according to the following directions. Thus, for any panel point,  $C$ , Fig. 61h, the clockwise moments should be treated as positive and the counter clockwise moments as negative to obtain the following equation:

$$\Sigma M_o = +M_{oa} - M_{ob} + M_{oc} - M_{od} = 0,$$

or in terms of the values  $K$

$$+K_{oa} \frac{6I_{oa}}{l_{oa}} - K_{ob} \frac{6I_{ob}}{l_{ob}} + K_{oc} \frac{6I_{oc}}{l_{oc}} - K_{od} \frac{6I_{od}}{l_{od}} = 0. \quad \dots \dots \dots (61v)$$

The arithmetic operations required in the solution of problems are somewhat lengthy but not difficult especially when the values  $I$  and  $l$  of the members are well rounded off, which is always permissible in these computations.

The **secondary stress** resulting from the bending moments  $M=6KI/l$ , produced in any member by the riveted connections, may now be found from Navier's law, Eq. (49m), as

$$f_s = \pm \frac{My}{I} = \pm \frac{6Ky}{l}, \quad \dots \dots \dots (61v)$$

where  $y$  is the distance from the gravity axis of the member to the extreme fiber and  $f_s$  is the unit secondary stress caused by the bending of the member due to the moment  $M_a$  or  $M_b$  applied at one end of the member.

The total maximum unit stress in the member is then  $\pm f \pm f_s$ , where  $f=S/F$ , which is the primary unit stress due to the direct loading.

Thus for a compression member, the maximum total stress occurs on the side where  $f_s$  is negative.

The eccentricities  $e$ , Fig. 61A or 61B, produced at either end of any member  $\overline{AB}$  by the secondary moments, may be found from

$$e_a = \frac{M_{ab}}{S_{ab}} = \frac{6I_{ab}K_{ab}}{S_{ab}l_{ab}} \quad \text{and} \quad e_b = \frac{M_{ba}}{S_{ab}} = \frac{6I_{ab}K_{ba}}{S_{ab}l_{ab}} \quad (61w)$$

The secondary stresses here considered may vary in percentage of the primary stresses from 5 to 100 per cent, depending on the type of truss and the details of design employed for the members.

The subject is, therefore, one of considerable importance and cannot be dismissed in the usual manner as taken care of by the safety factor.

The question of maximum secondary stress in any member has not yet received consideration here, though it is a matter of vital importance.

It does not follow that the maximum secondary stress occurs simultaneously with the maximum primary stress for any particular member. The results of computations show this to be quite true for the chords, but not for the web members, though there seems to be no criterion available to indicate the position of a train of loads to produce maximum secondary stress in a member.

The method of influence lines, while not impossible, becomes practically prohibitive on account of the labors involved. The only reasonable treatment which suggests itself is to analyze the structure first for total maximum load and then for a few typical positions for the moving load and from these results select the probable maximum values for each member.

Since the entire truss must be completely solved for each simultaneous position of the live load, this appears to be the only practicable advice to give in view of the immense labors involved in such analyses.

The above method is now illustrated by the solution of a problem.

**Example.** A single-track, through Pratt truss, designed by Messrs. Waddell & Hedrick, in 1899, for the Vera Cruz and Pacific Ry., Mexico, is selected. The truss has six panels with a span of 145 feet, a depth of 30 feet, and the distance between trusses is 17 feet. The equivalent uniform live load for Waddell's class IV was used. The case here investigated is for maximum total load over the entire span.

The cross-sections  $F$  and the moments of inertia  $I$  are computed and tabulated together with the lengths  $l$ , widths  $b$  and distances  $y$  for all the members of the truss. These together with the stresses  $S$ , due to the total maximum load Fig. 61i, are given in Table 61A, where the unit stresses  $f = S/F$  and the functions  $6I/l$  and  $6y/l$  are computed. Impact is not considered.

A live load of 54000 lbs. and a dead load 20800 lbs. per panel were assumed for the computation of the stresses.

While it is not necessary to know how the members were designed as long as  $F$  and  $I$  are given for each, yet it may be of some interest to the reader to have this data. Figs. 61j thus represent the sections of the several members.





TABLE 61A  
DATA FOR THE TRUSS FIG. 61I.

Mem.	$F$ Gross, Sq.in.	$I$ Gross, in. <sup>4</sup>	$l$ in.	$b$ In.	$y$ In.	$S$ Lbs.	$f = \frac{S}{F}$ Lbs. sq.in.	$\frac{6I}{l}$	$\frac{6y}{l}$
AC	15.9	139	290	12.37	6.19	+158,400	+9960	2.88	0.128
CE	15.9	139	290	12.37	6.19	+158,400	+9960	2.88	0.128
EG	26.9	282	290	12.5	6.25	+252,060	+9370	5.84	0.129
BD	26.5	750	290	15.0	7.5	-252,060	-9510	15.52	0.155
DF	29.4	805	290	15.0	7.5	-283,500	-9640	16.66	0.155
AB	33.5	1464	462	16.25	8.34	-245,000	-7310	19.01	0.108
BE	17.6	323	462	12.0	6.0	+156,200	+8875	4.19	0.077
DG	17.6	323	462	12.0	6.0	+ 48,400	+2750	4.19	0.077
BC	13.7	119	360	12.37	6.19	+ 68,000	+4960	1.98	0.103
DE	14.7	288	360	12.0	6.0	- 44,200	-3010	4.80	0.100
FG	14.7	288	360	12.0	6.0	- 6,800	- 460	4.80	0.100

$b$ =width of member in the plane of the truss.  
 $y$ =distance from neutral axis to extreme fiber of section.  
 $I$  is taken about the gravity axis perpendicular to the plane of the truss.

The distortions in all the angles of the several truss triangles are now computed from Eqs. (61s) and Eqs. (61r), using the unit stresses  $f$  from Table 61A and the cotangents of the angles, all as shown in Fig. 61k.

Applying Eqs. (61s) to the odd triangles I, III and V, and Eqs. (61r) to the even triangles II and IV the following values  $E\Delta$  are obtained.

Triangle I. Eqs. (61s):

$$\begin{aligned} E\Delta_{\alpha_1} &= (4960 - 9960)0.0 + (4960 + 7310)1.24 = +15,215 \\ E\Delta_{\beta_1} &= (9960 + 7310)0.806 + (9960 - 4960)0.0 = +13,920 \\ E\Delta_{\gamma_1} &= (-7310 - 4960)1.24 + (-7310 - 9960)0.806 = -29,135 \end{aligned}$$

00

Triangle II. Eqs. (61r):

$$\begin{aligned} E\Delta_{\alpha_2} &= (9960 - 8875)0.806 + (4960 - 8875)1.24 = - 3,980 \\ E\Delta_{\beta_2} &= (4960 - 9960)0.0 + (8875 - 9960)0.806 = - 875 \\ E\Delta_{\gamma_2} &= (8875 - 4960)1.24 + (9960 - 4960)0.0 = + 4,855 \end{aligned}$$

00

**Triangle III.** Eqs. (61s):

$$E\Delta\alpha_3 = (-3010 + 9510)0.0 + (-3010 - 8875)1.24 = -14,737$$

$$E\Delta\beta_3 = (-9510 - 8875)0.806 + (-9510 + 3010)0.0 = -14,818$$

$$E\Delta\gamma_3 = (8875 + 3010)1.24 + (8875 + 9510)0.806 = +29,555$$

---

 00

**Triangle IV.** Eqs. (61t):

$$E\Delta\alpha_4 = (9370 - 2750)0.806 + (-3010 - 2750)1.24 = -1,806$$

$$E\Delta\beta_4 = (-3010 - 9370)0.0 + (2750 - 9370)0.806 = -5,336$$

$$E\Delta\gamma_4 = (2750 + 3010)1.24 + (9370 + 3010)0.0 = +7,142$$

---

 00

**Triangle V.** Eqs. (61s):

$$E\Delta\alpha_5 = (-460 + 9640)0.0 + (-460 - 2750)1.24 = -3,980$$

$$E\Delta\beta_5 = (-9640 - 2750)0.806 + (-9640 + 460)0.0 = -9,986$$

$$E\Delta\gamma_5 = (2750 + 460)1.24 + (2750 + 9640)0.806 = +13,966$$

---

 00

The condition Eq. (61e) must be satisfied for each triangle as indicated above, offering a complete check on the numerical results.

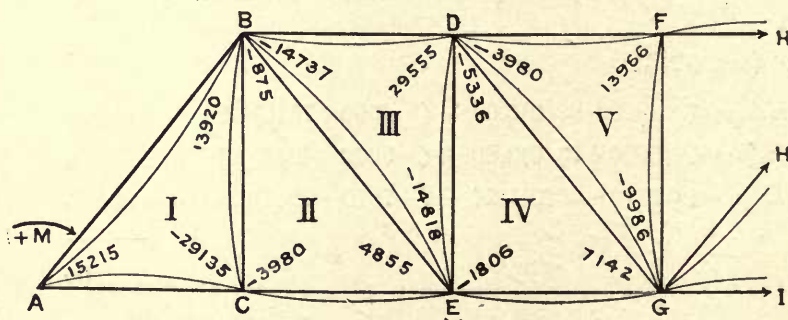


FIG. 61L—Values  $E\Delta$ .

The values  $E\Delta$  are now entered on the diagram Fig. 61L, where the conventional assumptions for the moments  $M$  are indicated according to Fig. 61F. The moment Eq. (61q), is then written out by following the directions given under Eq. (61v).

Using the values for  $6I/l$  from Table 61A in Eq. (61q) the following equations are obtained:

For panel point A,

$$\Sigma M_a = M_{ab} - M_{ac} = K_{ab} \frac{6I_{ab}}{l_{ab}} - K_{ac} \frac{6I_{ac}}{l_{ac}} = 0,$$

and after inserting the values from Table 61A, this gives

$$19.01K_{ab} = 2.88K_{ac} \quad \text{or} \quad K_{ac} = 6.60K_{ab} \quad . \quad . \quad . \quad . \quad . \quad . \quad . \quad . \quad (1)$$

For panel point B,

giving

$$\Sigma M_b = -M_{ba} + M_{bc} - M_{be} + M_{bd} = 0,$$

or

$$\begin{aligned} -19.01K_{ba} + 1.98K_{bc} - 4.19K_{be} + 15.52K_{bd} &= 0, \\ K_{bd} &= 1.23K_{ba} - 0.12K_{bc} + 0.27K_{be}. \quad . \quad . \quad . \quad . \quad . \quad . \quad . \quad (2) \end{aligned}$$

For panel point C,

giving

$$\Sigma M_c = M_{ca} - M_{cb} + M_{ce} = 0,$$

or

$$\begin{aligned} 2.88K_{ca} - 1.98K_{cb} + 2.88K_{ce} &= 0, \\ K_{ce} &= 0.69K_{cb} - K_{ca}. \quad . \quad . \quad . \quad . \quad . \quad . \quad . \quad (3) \end{aligned}$$

For panel point D,

giving

$$\Sigma M_d = -M_{db} + M_{de} - M_{dg} + M_{df} = 0,$$

or

$$\begin{aligned} -15.52K_{db} + 4.80K_{de} - 4.19K_{dg} + 16.66K_{df} &= 0, \\ K_{df} &= 0.932K_{db} - 0.288K_{de} + 0.252K_{dg}. \quad . \quad . \quad . \quad . \quad . \quad . \quad . \quad (4) \end{aligned}$$

For panel point E,

giving

$$\Sigma M_e = -M_{ec} + M_{eb} - M_{ed} + M_{eg} = 0,$$

or

$$\begin{aligned} -2.88K_{ec} + 4.19K_{eb} - 4.80K_{ed} + 5.84K_{eg} &= 0, \\ K_{eg} &= 0.493K_{ec} - 0.72K_{eb} + 0.82K_{ed}. \quad . \quad . \quad . \quad . \quad . \quad . \quad . \quad (5) \end{aligned}$$

For panel point F, noting that for symmetrical loading  $M_{fd} = M_{fh}$ , then

giving

$$\Sigma M_f = -M_{fd} + M_{fg} - M_{fh} = 0,$$

or

$$\begin{aligned} -2 \times 16.66K_{fd} + 4.8K_{fg} &= 0, \\ K_{fg} &= 6.942K_{fd}. \quad . \quad . \quad . \quad . \quad . \quad . \quad . \quad (6) \end{aligned}$$

For panel point G, where for symmetric loading  $M_{ge} = M_{gi}$  and  $M_{gd} = M_{gh}$ , then

giving

$$\Sigma M_g = -M_{ge} + M_{gd} - M_{gf} + M_{gh} - M_{gi} = 0,$$

or

$$\begin{aligned} -5.84K_{ge} + 4.19K_{gd} - 4.80K_{gf} + 4.19K_{gh} - 5.84K_{gi} &= 0, \\ K_{gf} &= -2.433K_{ge} + 1.746K_{gd}. \quad . \quad . \quad . \quad . \quad . \quad . \quad . \quad (7) \end{aligned}$$

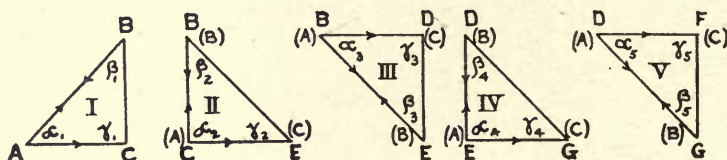


When there is no middle vertical  $\overline{FG}$ , then, for symmetric loading, an equation of the form Eq. (61M) is written out for the center triangle  $\overline{DGH}$  to supply the last condition.

For an unsymmetric truss or unsymmetric loading, the several equations must be extended over all pin points of the structure.

Assuming now that  $K_{ab}$ ,  $K_{ba}$  and  $K_{ac}$ , Fig. 61L, are known, then Eqs. (61N, o, p) will furnish the values  $K_{ca}$ ,  $K_{bc}$  and  $K_{cb}$  for the first triangle  $\overline{ABC}$ , and by applying this process successively to all the triangles it becomes possible to express all the values  $K$  in terms of  $K_{ab}$  and  $K_{ba}$  by including the moment equations (1) to (5) just evaluated. The two last Eqs. (6) and (7) will then serve to find  $K_{ab}$  and  $K_{ba}$ , as will be shown later, and these values substituted back will furnish all the unknowns  $K$ .

In applying Eqs. (61N, o, p) to the several triangles, it is necessary to use the standard lettering employed in the derivation of these formulæ and hence each triangle is sketched in Figs. 61M, to exemplify the process. The angle  $\alpha$  must be so located in a triangle that it is included between the two adjacent known  $K$ 's, and the angle  $\beta$  must be adjacent to the third known  $K$ , while  $\gamma$  is between the adjacent unknown  $K$ 's. This then determines the vertices (A), (B) and (C), shown in parenthesis, for the standard lettering.



FIGS. 61M.

The designations of the angles in Fig. 61K, for the solution of the values  $E\Delta$  were selected so as to comply with the conditions just described. The arrows in the Figs. 61M indicate the values  $K$  found from a previous triangle and from one new moment Eq. (61Q) above evaluated as (1) to (5).

Eqs. (61N, o, p) and Eqs. (1) to (5) thus give:

At panel point A, by Eq. (1):  $K_{ac} = 6.6K_{ab}$ .

$$\triangle I \begin{cases} \text{By Eq. (61N), } K_{ca} = E\Delta\alpha_1 - 2K_{ac} - 2K_{ab} - K_{ba} = 15,215 - 15.2K_{ab} - K_{ba} \\ \text{By Eq. (61o), } K_{bc} = E\Delta\beta_1 + K_{ac} - K_{ba} + K_{ca} = 29,135 - 8.6K_{ab} - 2K_{ba} \\ \text{By Eq. (61p), } K_{cb} = E\Delta\gamma_1 + K_{ab} + K_{ba} - K_{ca} = -44,350 + 16.2K_{ab} + 2K_{ba}. \end{cases}$$

At panel point C, by Eq. (3),  $K_{ce} = 0.69K_{cb} - K_{ca} = -45,816 + 26.4K_{ab} + 2.38K_{ba}$ .

$$II \begin{cases} \text{By Eq. (61N), } K_{ec} = E\Delta\alpha_2 - 2K_{ce} - 2K_{cb} - K_{bc} = 147,217 - 76.6K_{ab} - 6.76K_{ba} \\ \text{By Eq. (61o), } K_{be} = E\Delta\beta_2 + K_{ce} - K_{bc} + K_{ec} = 71,391 - 41.6K_{ab} - 2.38K_{ba} \\ \text{By Eq. (61p), } K_{eb} = E\Delta\gamma_2 + K_{cb} + K_{bc} - K_{ec} = -157,577 + 84.2K_{ab} + 6.76K_{ba}. \end{cases}$$

At panel point  $B$ , by Eq. (2):  $K_{bd} = 1.23K_{ba} - 0.12K_{bc} + 0.27K_{be} = 15,780 - 10.2K_{ab} + 0.83K_{ba}$ .

$$\triangle III \begin{cases} \text{By Eq. (61N), } K_{db} = E\Delta\alpha_3 - 2K_{bd} - 2K_{be} - K_{eb} = -31,502 + 19.4K_{ab} - 3.66K_{ba} \\ \text{By Eq. (61O), } K_{ed} = E\Delta\beta_3 + K_{bd} - K_{eb} + K_{db} = 127,037 - 75.0K_{ab} - 9.59K_{ba} \\ \text{By Eq. (61P), } K_{de} = E\Delta\gamma_3 + K_{be} + K_{eb} - K_{db} = -25,129 + 23.2K_{ab} + 8.04K_{ba}. \end{cases}$$

At panel point  $E$ , by Eq. (5):

$$K_{eg} = 0.493K_{ec} - 0.72K_{eb} + 0.82K_{ed} = 290,203 - 159.9K_{ab} - 16.07K_{ba}.$$

$$\triangle IV \begin{cases} \text{By Eq. (61N), } K_{ge} = E\Delta\alpha_4 - 2K_{eg} - 2K_{ed} - K_{de} = -811,157 + 446.6K_{ab} + 43.28K_{ba} \\ \text{By Eq. (61O), } K_{dg} = E\Delta\beta_4 + K_{cg} - K_{de} + K_{ge} = -501,161 + 263.5K_{ab} + 19.17K_{ba} \\ \text{By Eq. (61P), } K_{gd} = E\Delta\gamma_4 + K_{ed} + K_{de} - K_{ge} = 920,207 - 498.4K_{ab} - 44.83K_{ba}. \end{cases}$$

An panel point  $D$ , by Eq. (4):

$$K_{df} = 0.932K_{db} - 0.288K_{de} + 0.252K_{dg} = -148,414 + 77.80K_{ab} - 0.90K_{ba}.$$

$$\triangle V \begin{cases} \text{By Eq. (61N), } K_{fd} = E\Delta\alpha_5 - 2K_{df} - 2K_{dg} - K_{gd} = 374,963 - 184.2K_{ab} + 8.29K_{ba} \\ \text{By Eq. (61O), } K_{gf} = E\Delta\beta_5 + K_{df} - K_{gd} + K_{fd} = -703,644 + 392.0K_{ab} + 52.22K_{ba} \\ \text{By Eq. (61P), } K_{fg} = E\Delta\gamma_5 + K_{dg} + K_{gd} - K_{fd} = 58,049 - 50.7K_{ab} - 33.95K_{ba}. \end{cases}$$

The moment Eqs. (6) and (7) for panel points  $F$  and  $G$  now furnish independent values for  $K_{fg}$  and  $K_{gf}$  and by combining these with the last two equations of  $\triangle V$ , the values  $K_{ab}$  and  $K_{ba}$  may be found as follows:

$$\text{By Eq. (6), } K_{fg} = 6.942K_{fd} = 2,602,993 - 1278.7K_{ab} + 57.55K_{ba}.$$

$$\text{By Eq. (7), } K_{gf} = -2.433K_{ge} + 1.746K_{gd} = 3,580,226 - 1956.8K_{ab} - 183.57K_{ba}.$$

Substituting these values of  $K_{fg}$  and  $K_{gf}$  into the last two equations of  $\triangle V$ , then,

$$2,544,954 - 1228.0K_{ab} + 91.50K_{ba} = 0,$$

$$4,283,870 - 2348.8K_{ab} - 235.79K_{ba} = 0,$$

from which  $K_{ab} = 1947.5$  and  $K_{ba} = -1676.8$ .

These values of  $K_{ab}$  and  $K_{ba}$  are now substituted into the above twenty equations, furnishing all the values  $K$  as follows:

$$(1) K_{ab} = 1947.5$$

$$(2) K_{ba} = -1676.8$$

$$(3) K_{ac} = 6.6K_{ab} = 12,854$$

$$(4) K_{ca} = 15,215 - 29,602 + 1,677 = -12,710$$

- (5)  $K_{bc} = 29,135 - 16,748 + 3,354 = 15,741$
- (6)  $K_{cb} = -44,350 + 31,549 - 3,354 = -16,155$
- (7)  $K_{cc} = -45,816 + 51,414 - 3,991 = 1,607$
- (8)  $K_{ec} = 147,217 - 149,178 + 11,335 = 9,374$
- (9)  $K_{be} = 71,391 - 81,016 + 3,991 = -5,634$
- (10)  $K_{eb} = -157,577 + 163,979 - 11,335 = -4,933$
- (11)  $K_{bd} = 15,780 - 19,864 - 1,392 = -5,476$
- (12)  $K_{db} = -31,502 + 37,781 + 6,137 = 12,416$
- (13)  $K_{ed} = 127,037 - 146,062 + 16,081 = -2,944$
- (14)  $K_{de} = -25,129 + 45,182 - 13,481 = 6,572$
- (15)  $K_{eg} = 290,203 - 311,405 + 26,946 = 5,744$
- (16)  $K_{ge} = -811,157 + 869,753 - 72,572 = -13,976$
- (17)  $K_{dg} = -501,161 + 513,166 - 32,144 = -20,139$
- (18)  $K_{gd} = 920,207 - 970,634 + 75,171 = 24,744$
- (19)  $K_{df} = -148,414 + 151,515 + 1,509 = 4,610$
- (20)  $K_{fd} = 374,963 - 358,730 - 13,901 = 2,332$
- (21)  $K_{gf} = -703,644 + 763,420 - 87,562 = -27,786$
- (22)  $K_{fg} = 58,049 - 98,738 + 56,927 = 16,238$

Eq. (61m) now furnishes a convenient check on the above numerical results, by taking the sum of all the six values  $K$  for each triangle.

Thus for  $\triangle I$ , the values (1) to (6) give

$$\Sigma K_1 = 30,542 - 30,542 = 0$$

and for  $\triangle II$ , the values (5) to (10) give

$$\Sigma K_2 = 26,722 - 26,722 = 0$$

and for  $\triangle III$ , the values (9) to (14) give

$$\Sigma K_3 = 18,988 - 18,987 = 1$$

and for  $\triangle IV$ , the values (13) to (18) give

$$\Sigma K_4 = 37,060 - 37,059 = 1$$

and for  $\triangle V$ , the values (17) to (22) give

$$\Sigma K_5 = 47,924 - 47,925 = -1$$

The secondary stresses due to the bending at each end of each member are now found from Eq. (61v) as given in the following Table 61b.



TABLE 61B  
SECONDARY STRESSES DUE TO BENDING

Mem.	End.	$\frac{6y}{l}$ in.	K	$\pm f_s = \frac{6Ky}{l}$ Eq. (61v), Lbs. sq.in.	$f = \frac{S}{F}$ Lbs. sq.in.	$e = \frac{6IK}{Sl}$ in.	Mem.	End.	$\frac{6y}{l}$ in.	K	$\pm f_s = \frac{6Ky}{l}$ Eq. (61v), Lbs. sq.in.	$f = \frac{S}{F}$ Lbs. sq.in.	$e = \frac{6IK}{Sl}$ in.
AB	A	0.103	+ 1,948	200	-7310	0.15	ED	E	0.100	- 2,944	294	-3010	0.32
	B	.....	- 1,677	172	-7310	0.13		D	.....	+ 6,572	657	-3010	0.72
AC	A	0.128	+12,854	1645	+9960	0.23	EG	E	0.129	+ 5,744	741	+9370	0.13
	C	.....	-12,710	1627	+9960	0.23		G	.....	-13,976	1803	+9370	0.32
BC	B	0.103	+15,741	1621	+4960	0.46	DG	D	0.077	-20,139	1551	+2750	1.76
	C	.....	-16,155	1664	+4960	0.47		G	.....	+24,744	1905	+2750	2.16
CE	C	0.128	+ 1,607	205	+9960	0.03	DF	D	0.155	+ 4,610	715	-9640	0.28
	E	.....	+ 9,374	1200	+9960	0.17		F	.....	+ 2,332	361	-9640	0.14
BE	B	0.077	- 5,634	434	+8875	0.15	GF	G	0.100	-27,786	2779	- 460	19.62
	E	.....	- 4,933	380	+8875	0.13		F	.....	+16,238	1624	- 460	11.46
BD	B	0.155	- 5,476	849	-9510	0.34							
	D	.....	+12,416	1924	-9510	0.72							

The total stress on the extreme fiber is  $f_s + f$ , noting that no increase was made in  $f$  for buckling effect in compression members.

The actual signs of the values  $K$ , and hence also of the moments  $M = 6KI/l$ , now being determined, the real character of the distortions may be represented diagrammatically in the following Fig. 61N.

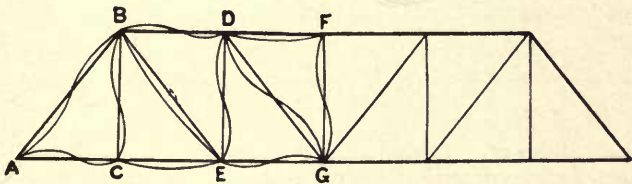


FIG. 61N.

For compression members the most severely stressed fibers will occur on the side where  $f_s$  is negative and for tension members on the side where  $f_s$  is positive. Thus in the compression member  $\overline{AB}$ , the critical stresses occur on the upper side at A and on the lower side at B, while for the tension member  $\overline{AC}$ , these occur on the upper side at A and on the lower side at C.

## ART. 62. SECONDARY STRESSES IN RIVETED CROSS FRAMES OF TRUSSES

The analysis of cross frames, so far as this is possible, presents many obstacles, some of which cannot be overcome owing to the variable character of the external loads.

The bending effect due to all forces acting on a frame, even when direct stresses are neglected, leads to very complicated formulæ of more or less questionable value, and no attempt is made here to discuss the general problem.

A cross frame is usually subjected to the dead load of the bridge floor concentrated on the floor beam; the live load, impact and centrifugal force applied to the floor; wind pressure against the moving load and the vertical trusses; and unequal deflection of the main trusses due to a variety of causes, but particularly to unequal temperature.

The magnitudes of the secondary stresses depend of course on the details of construction and bracing employed in any special frame, so that many different forms would require investigation. However, only two principal types will be discussed and the same formulæ are applicable to both through and deck bridges.

In the following, the unbraced and one type of braced cross frames are considered first for direct loading and then for wind effect.

(a) **Dead and live load effects. Unbraced cross frame with rigid post connections.** The construction, shown in Fig. 62A with lettered dimensions, is analyzed by assuming equality between the unknown bending moments induced in the posts by the symmetric loads  $P$ , as follows:  $M_0 = M_2$  and  $M_1 = M_3$ , positive as indicated when they produce compression on the outer fibers of the posts.

Call  $M$  the bending moment on the floor beam due to symmetrically placed loads  $P$  acting on a simple beam which rests on two supports  $C$  and  $D$ .

Also call  $m_1$  the moment at any point of the post  $\overline{AC}$  distant  $x$  from  $A$ ;  $m_2$  the moment at any point of the strut  $\overline{AB}$ ; and  $m_3$  the moment at any point of the beam  $\overline{CD}$ . Then from Fig. 62A.

$$m_1 = M_1 + \left( \frac{M_0 - M_1}{h} \right) x, \quad m_2 = M_1 \quad \text{and} \quad m_3 = M_0 + M. \quad \dots \quad (62A)$$

Considering only the effect due to bending, by neglecting shear and direct thrust, the virtual work of deformation for the entire frame would be by Eq. (15H)

$$W = \frac{2}{EI_1} \int_0^h m_1^2 dx + \frac{1}{EI_2} \int_0^b m_2^2 dx + \frac{1}{EI_3} \int_0^b m_3^2 dx. \quad \dots \quad (62B)$$

Substituting the values from Eqs. (62A) into Eq. (62B) then

$$W = \frac{2}{EI_1} \int_0^h \left[ M_1 + \left( \frac{M_0 - M_1}{h} \right) x \right]^2 dx + \frac{1}{EI_2} \int_0^b M_1^2 dx + \frac{1}{EI_3} \int_0^b (M_0 + M)^2 dx,$$

which integrated by considering everything constant except  $x$ , gives

$$W = \frac{2}{3EI_1} \left[ M_1 M_0 h + M_0^2 h + M_1^2 h \right] + \frac{M_1^2 b}{EI_2} + \frac{1}{EI_3} \left[ M_0^2 b + 2M_0 \int_0^b M dx + \int_0^b M^2 dx \right], \quad (62C)$$

which is the general expression for any case of loading where  $M$  must be evaluated for each case.

Now since the unknown moments  $M_0$  and  $M_1$  must have such values as will make the first differential derivative of  $W$  with respect to each, equal to zero, then after some reduction

and

$$\left. \begin{aligned} \frac{\partial W}{\partial M_0} &= \frac{M_1 h}{3I_1} + \frac{2M_0 h}{3I_1} + \frac{M_0 b}{I_3} + \frac{1}{I_3} \int_0^b M dx = 0, \\ \frac{\partial W}{\partial M_1} &= \frac{M_0 h}{3I_1} + \frac{2M_1 h}{3I_1} + \frac{M_1 b}{I_2} = 0. \end{aligned} \right\}$$

. . . . . (62D)

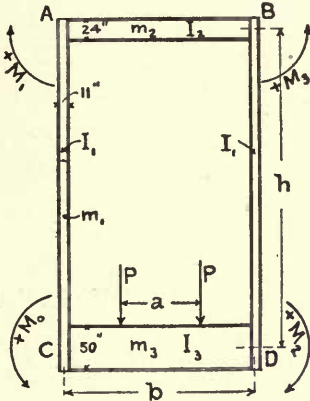


FIG. 62A.

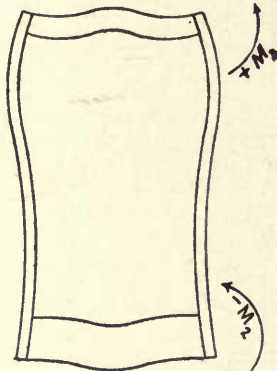


FIG. 62B.

Solving Eqs. (62D) gives

$$\left. \begin{aligned} M_1 &= -M_0 \left( \frac{3I_1 b}{hI_3} + 2 \right) - \frac{3I_1}{hI_3} \int_0^b M dx \\ M_0 &= -M_1 \left( \frac{3I_1 b}{hI_2} + 2 \right), \end{aligned} \right\}$$

. . . . . (62E)

and

from which

$$M_1 = \frac{\frac{3I_1}{hI_3} \int_0^b M dx}{\left( \frac{3I_1 b}{hI_2} + 2 \right) \left( \frac{3I_1 b}{hI_3} + 2 \right) - 1} \quad \dots \dots \dots (62F)$$

For the symmetric loading shown in Fig. 62A, the integral  $M dx$  becomes

$$\int_0^b M dx = -2 \int_0^{\frac{b-a}{2}} P x dx - \int_{\frac{b-a}{2}}^{\frac{b+a}{2}} P \left( \frac{b-a}{2} \right) dx = -\frac{P}{4} (b^2 - a^2),$$

. . . (62G)

and for a uniform load  $p$  per foot of floor beam,

$$\int_0^b M dx = -\frac{pb^3}{12}.$$



$M_0$  and  $M_1$  may thus be found from Eqs. (62E) and (62F), and from these the moments  $m_1$ ,  $m_2$  and  $m_3$ , for any point of the frame, are given by Eqs. (62A).

The maximum fiber stress in the posts must be combined with the direct stress sustained as a truss member.

The upper strut receives a compression of  $(M_0 - M_1)/h$  and a bending moment  $M_1$  over its entire length.

The floor beam will receive a bending moment of  $M_0 + M$  and a direct stress of  $(M_1 - M_0)/h$ .

**Example.** Given the cross frame at  $\overline{DE}$ , Fig. 61I, with the following dimensions:  $h = 28$  ft.,  $b = 17$  ft.,  $a = 7$  ft.,  $P = 59000$  lbs.,  $I_1 = 226$  in.<sup>4</sup> =  $0.0109$  ft.<sup>4</sup>,  $I_2 = 1134$  in.<sup>4</sup> =  $0.0547$  ft.<sup>4</sup>, and  $I_3 = 15262$  in.<sup>4</sup> =  $0.736$  ft.<sup>4</sup>. The style of the frame is as shown in Fig. 62A.

Using the value from Eq. (62G) in Eq. (62F), and substituting the above data, then

$$M_1 = -\frac{\frac{3 \times 0.0109}{28 \times 0.736} \times \frac{59000}{4} (17^2 - 7^2)}{\left(\frac{3 \times 0.0109 \times 17}{28 \times 0.0549} + 2\right) \left(\frac{3 \times 0.0109 \times 17}{28 \times 0.736} + 2\right) - 1} = -1499 \text{ ft.-lbs.},$$

and from Eq. (62E)

$$M_0 = -M_1 \left( \frac{3I_1 b}{hI_2} + 2 \right) = 1499 \left( \frac{3 \times 0.0109 \times 17}{28 \times 0.0549} + 2 \right) = 3541 \text{ ft.-lbs.}$$

For  $y = 5.5$  inches, Eq. (61v) then gives the secondary stress in the post  $\overline{DE}$ .

$$\text{for the upper end } D, f_d = \pm \frac{M_1 y}{I_1} = \frac{1499 \times 12 \times 5.5}{226} = 438 \text{ lbs. per sq.in.};$$

$$\text{for the lower end } E, f_e = \pm \frac{M_0 y}{I_1} = \frac{3541 \times 12 \times 5.5}{226} = 1034 \text{ lbs. per sq.in.}$$

The actual deformation of this frame is indicated in Fig. 62b.

**A braced cross frame with rigid post connections** Fig. 62c, will now be treated as in the previous case.

Neglecting shear and direct stress as before, and dealing only with the effect due to bending, then Eq. (62B) becomes

$$W = \frac{2}{EI_1} \left[ \int_0^{h_1} \left( M_0 + \frac{(M_1 - M_0)x}{h_1} \right)^2 dx + \int_0^e \left( \frac{M_1 x}{e} \right)^2 dx \right] + \frac{1}{EI_3} \int_0^b (M_0 + M)^2 dx.$$

Integrating this expression as above, and then differentiating first with respect to  $M_0$  and then with respect to  $M_1$  and placing these derivatives equal to zero, the following equations are obtained:

$$\frac{\partial W}{\partial M_0} = \frac{h_1}{3I_1} (M_1 + 2M_0) + \frac{bM_0}{I_3} + \frac{1}{I_3} \int_0^b M dx = 0,$$

$$\frac{\partial W}{\partial M_1} = h_1 M_0 + 2h_1 M_1 + 2eM_1 = 0.$$

Solving these two zero equations and noting that  $h=h_1+e$ , then

$$M_1 = -\frac{h_1 M_0}{2h} \quad \text{and} \quad M_0 = -\frac{\int_0^b M dx}{\frac{h_1 I_3}{6h I_1} (4h - h_1) + b}, \quad \dots \quad (62H)$$

wherein  $\int_0^b M dx$  is given by one of Eqs. (62G) and the moments  $M_0$  and  $M_1$  may thus be found.

The stresses in the upper struts then become

$$S_{ab} = -\frac{M_1}{e} \quad \text{and} \quad S_{ef} = \frac{M_1}{e} + \frac{M_1 - M_0}{h_1},$$

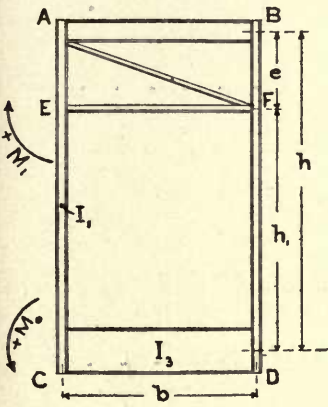


FIG. 62C.

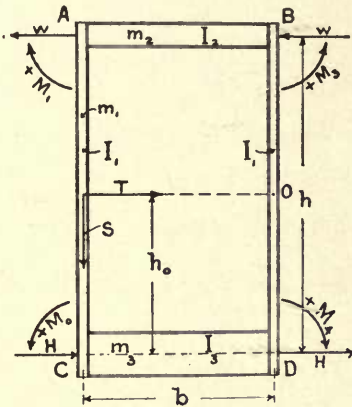


FIG. 62D.

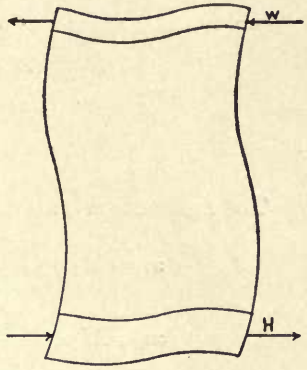


FIG. 62E.

and the stresses in the post will be

$$f_e = \pm \frac{M_1 y}{I_1} \quad \text{and} \quad f_c = \pm \frac{M_0 y}{I_1}.$$

**Example.** Taking dimensions as in the previous example and making  $h_1=19.5$  ft. then  $M_0=4770$  ft.-lbs., and  $M_1=1661$  ft.-lbs. giving  $f_e=1393$  lbs. per sq.in., and  $f_c=485$  lbs. per sq.in.

(b) **Wind effects. Unbraced cross frame with rigid post connections.** The horizontal wind loads on the trusses of a bridge may be carried to the abutments by means of complete horizontal trusses in the planes of the top and bottom chords respectively, provided the end reactions of the top chord wind system can be carried to the abutments by suitable end postal bracing. In this case the intermediate cross frames suffer very little or no distortion and hence carry no bending effects.

However, when the wind pressure along the top chord is carried down to the bottom chord locally at each cross frame, then the latter must be distorted and thus resist bending. In this case the total wind pressure is carried to the abutments through the bottom chord lateral system. The external forces on a cross frame are then as repre-

sented in Fig. 62D. The wind loads  $w$  are transmitted through the posts to the lower lateral system, producing bending effects as shown in Fig. 62E.

Assuming that the wind loads  $w$  are equal and calling  $T$  the tangential stress at the point of counterflexure and  $S$  the normal stress at the same point, then

$$H = w = T. \quad \dots \dots \dots (62i)$$

The general work equation for the frame, considering bending effects only, is the same as Eq. (62B) in which the moments  $m_1$ ,  $m_2$  and  $m_3$  must be evaluated for the wind forces now acting.

The moments of the external forces about  $A$ ,  $B$ ,  $C$ ,  $D$  and  $O$ , from Fig. 62D (counting clockwise moments positive) are respectively

$$\left. \begin{aligned} M_1 &= -T(h-h_0) = -H(h-h_0) \\ M_3 &= -T(h-h_0) - Sb = H(h-h_0) = -M_1 \\ M_0 &= Th_0 = Hh_0 \\ M_2 &= Th_0 - Sb - 2wh = -Hh_0 \text{ because} \\ &\quad -Sb - 2w(h-h_0) = 0 \end{aligned} \right\} \dots \dots \dots (62j)$$

The moments  $m_1$ ,  $m_2$  and  $m_3$  thus become

$$\left. \begin{aligned} m_1 &= M_1 + \left(\frac{M_0 - M_1}{h}\right)x = H(x+h_0-h) \text{ with origin at } A \\ m_2 &= M_1 + \left(\frac{M_3 - M_1}{b}\right)x = H(h-h_0)\left(\frac{2x}{b} - 1\right) \text{ with origin at } A \\ m_3 &= M_0 + \left(\frac{M_2 - M_0}{b}\right)x = Hh_0\left(1 - \frac{2x}{b}\right) \text{ with origin at } C \end{aligned} \right\} \dots \dots (62k)$$

Substituting these values into Eq. (62B) then

$$W = \frac{2H^2}{EI_1} \int_0^h (x+h_0-h)^2 dx + \frac{H^2}{EI_2} \int_0^b (h-h_0)^2 \left(\frac{2x}{b} - 1\right)^2 dx + \frac{H^2 h_0^2}{EI_3} \int_0^b \left(1 - \frac{2x}{b}\right)^2 dx, \\ \text{which gives by integration,} \\ W = \frac{2H^2 h}{3EI_1} (h^2 - 3h_0 h + 3h_0^2) + \frac{H^2 b}{3EI_2} (h-h_0)^2 + \frac{H^2 h_0^2 b}{3EI_3} \dots \dots \dots (62l)$$

Since  $h_0$  must be so chosen that the internal work will be a minimum, this particular value may be obtained by equating to zero the differential derivative of  $W$  with respect to  $h_0$ , thus obtaining

$$\frac{\partial W}{\partial h_0} = \frac{h}{I_1} (6h_0 - 3h) + \frac{b}{I_2} (h_0 - h) + \frac{h_0 b}{I_3} = 0,$$

from which

$$h_0 = \frac{h \left( \frac{3h}{I_1} + \frac{b}{I_2} \right)}{\frac{b}{I_3} + \frac{6h}{I_1} + \frac{b}{I_2}} \dots \dots \dots (62m)$$



Substituting this value of  $h_0$  into Eqs. (62K), will give the moments at all points of the frame and from Eqs. (62J) the stress  $S$  and the moments at the ends of the post may be found.

**Example.** For the cross frame of the first example and a horizontal wind load of  $w=3100$  lbs. the following values are obtained:

$$h_0 = \frac{28 \left( \frac{3 \times 28}{0.0109} + \frac{17}{0.0547} \right)}{\frac{17}{0.736} + \frac{6 \times 28}{0.0109} + \frac{17}{0.0547}} = 14.25 \text{ ft.}$$

Substituting values into Eqs. (62J), then,

$$M_1 = -H(h-h_0) = -3100(28-14.25) = -42,625 \text{ ft.-lbs.}$$

$$M_0 = Hh_0 = 3100 \times 14.25 = 44,175 \text{ ft.-lbs.}$$

$$S = -\frac{2w(h-h_0)}{b} = -\frac{6200(28-14.25)}{17} = -5197 \text{ lbs.}$$

This gives for the stress at the bottom of the post  $\overline{AC}$ ,

$$S = \pm \frac{M_0 y}{I_1} - \frac{S}{F} = \pm \frac{44175 \times 12 \times 5.5}{226} - \frac{5197}{14.7} = \pm 12,899 - 353 \text{ lbs. per sq.in.}$$

**For a braced cross frame with rigid post connections** Fig. 62F, the analysis is conducted in precisely the same manner as in the previous case, making as before,  $H=w=T$ .

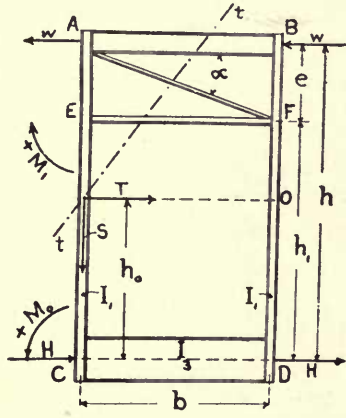


FIG. 62F.

Counting clockwise moments positive, then the moments of the external forces about the points E, C and O are respectively

$$\left. \begin{aligned} M_1 &= -T(h_1-h_0) = -H(h_1-h_0) \\ M_0 &= Th_0 = Hh_0 \\ -Sb-2w(h-h_0) &= 0 \end{aligned} \right\} \dots \dots \dots (62N)$$

The moments at any point  $x$  from  $C$  then become:

$$\left. \begin{array}{l} \text{for } \overline{CE}, \\ \text{for } \overline{EA}, \\ \text{for } \overline{CD}, \end{array} \right\} \begin{array}{l} M_0 + \left( \frac{M_1 - M_0}{h_1} \right) x = H(h_0 - x), \\ M_1 - \frac{M_1}{e}(x - h_1) = H(h_1 - h_0) \left( \frac{x - h_1}{e} \right), \\ M_0 - \frac{2M_0}{b}x = Hh_0 \left( 1 - \frac{2x}{b} \right). \end{array} \quad (620)$$

These values inserted into the general work Eq. (62B) give for the frame

$$W = \frac{2H^2}{EI_1} \int_0^{h_1} (h_0 - x)^2 dx + \frac{2H^2}{EI_1} \int_{h_1}^h (h_1 - h_0) \left( \frac{x - h_1}{e} \right)^2 dx + \frac{H^2 h_0^2}{EI_3} \int_0^b \left( 1 - \frac{2x}{b} \right)^2 dx,$$

from which is obtained after integrating

$$W = \frac{2H^2}{EI_1} \left[ h_1 \left( h_0^2 - h_1 h_0 + \frac{h_1^2}{3} \right) + (h_1 - h_0) \frac{2e}{3} \right] + \frac{H^2 h_0^2 b}{3EI_3}.$$

Taking the first differential derivative with respect to  $h_0$  and equating the same to zero then

$$\frac{\partial W}{\partial h_0} = \frac{1}{I_1} \left[ 2h_1 h_0 - h_1^2 - \frac{2eh_1}{3} + \frac{2h_0 e}{3} \right] + \frac{h_0 b}{3I_3} = 0,$$

from which

$$h_0 = \frac{h_1(2h + h_1)}{2(h + 2h_1) + \frac{bI_1}{I_3}} \quad (62P)$$

**Example.** Given a cross frame as per Fig. 62F, for which  $h = 28$  ft.,  $h_1 = 19.5$  ft.,  $b = 17$  ft.,  $e = 8.5$  ft.,  $I_1 = 226$  in.<sup>4</sup>,  $I_3 = 15262$  in.<sup>4</sup> and  $w = 3100$  lbs. to find  $h_0$ ,  $M_0$  and  $M_1$ . From Eq. (62P)

$$h_0 = \frac{19.5(56 + 19.5)}{2(28 + 39) + \frac{17 \times 226}{15262}} = 10.96 \text{ ft.},$$

and from Eqs. (62N)

$$M_1 = -3100(19.5 - 10.96) = -26,474 \text{ ft.-lbs.}$$

$$M_0 = 3100 \times 19.96 = 33,976 \text{ ft.-lbs.}$$

$$S_{ac} = -\frac{2w(h - h_0)}{b} = -6215 \text{ lbs.}$$

The maximum stress in the post  $\overline{AC}$  is then

$$\frac{\pm M_0 y}{I_1} - \frac{S_{ac}}{F_{ac}} = \pm \frac{33976 \times 12 \times 5.5}{226} - \frac{6215}{14.7} = \pm 9923 - 423 \text{ lbs. per sq.in.}$$

The stresses in the top struts and diagonal are not so easily determined when the double latticed type of bracing is used. In the present case with one diagonal  $\overline{AF}$ , the

stresses are determined by passing a section  $\bar{u}$  through the three members and the point of counterflexure, and taking moments about  $A$ , then,

$$-T(h-h_0)-e\overline{EF}=0, \quad \text{or} \quad \overline{EF}=-\frac{3100(28-10.96)}{8.5}=-6215 \text{ lbs.}$$

The stress in  $\overline{AB}$  is found by taking moments about  $F$ , obtaining,

$$-T(h_1-h_0)-Sb-we+e\overline{AB}=0,$$

whence

$$\overline{AB}=\frac{T(h_1-h_0)+Sb+we}{e}=\frac{3100(19.5-10.95)-6215\times 17+3100\times 8.5}{8.5}=-6325 \text{ lbs.}$$

Also from the vertical shear on the section

$$-S-\overline{AF}\sin\alpha=0, \quad \text{or} \quad \overline{AF}=-\frac{S}{\sin\alpha}=+\frac{6215}{0.449}=13,842 \text{ lbs.}$$

In concluding the subject of cross frames it might be added that good designs should aim at deep floor beams and slender vertical posts, as is clearly indicated by Eq. (62H), which shows that  $M_0$  is diminished when  $I_3$  is increased and increased when  $I_1$  is increased.

It has been stated by Mr. Grimm, "Secondary Stresses in Bridge Trusses," p. 80, that the assumption of fixed connections between floor beams and posts is not verified by investigations. The author suggests an explanation for this by calling attention to the fact that recent tests indicate that compression members as formerly built are not nearly as stiff against buckling as was supposed and furthermore, a slight initial deformation approaching the elastic curve which the stressed member might attain, would almost obviate secondary stresses in the cross frames. That such deformations actually exist, or might be produced in overloaded posts by a permanent set, there can be little doubt, and hence it is quite easy to understand why some of the high theoretical stresses do not appear to exist when the actual stresses are measured with instruments.

ART. 63. SECONDARY STRESSES DUE TO VARIOUS CAUSES

(a) **Bending stresses in the members due to their own weight.** The maximum bending moment, in any member, resulting from its own weight, when supported on frictionless pin bearings at the ends, will occur at the center of the member and is expressed by

$$M_c=\frac{pl^2}{8}\cos\theta, \quad . . . . . (63A)$$

where  $l$  is the length of the member,  $p$  its weight per unit of length and  $\theta$  is the angle which the member makes with the horizontal.

When the member is fixed at the ends and there is no direct stress, the bending moments  $M_0$  at the ends of the member, and  $M_c$  at the center, become respectively

$$M_0=-\frac{pl^2}{12}\cos\theta \quad \text{and} \quad M_c=\frac{pl^2}{24}\cos\theta. \quad . . . . . (63B)$$



In any case these moments produce a unit stress  $f$  on the extreme fibers of the members which is given by Navier's law, Eq. (49M) as

$$f = \pm \frac{My}{I}, \quad . . . . . (63C)$$

where  $y$  is the normal distance from the neutral axis to the extreme fiber.

It is thus seen that  $M$  increases as the square of  $l$  while  $f$  is inversely proportional to  $I$ . Hence, long members of small moment of inertia may receive severe secondary stress due to their own weight.

When the member is in compression or tension, the combined bending stress on the extreme fiber, due to the direct stress and the uniform load, must be investigated. This cannot be accomplished by algebraic summation of the separate bending effects, because axial compression increases the deflection due to cross binding, while axial tension diminishes this deflection. The bending stress, resulting from the simultaneous loading must, therefore, be found.

The analysis for riveted end connections, while very complicated, is not usually necessary. For pin-connected members where the cross bending effect is always more severe, the following approximate solution is given.

**A horizontal compression member**, with centric pin connection at each end, is shown in Fig. 63A. Let  $M_c$  designate the maximum bending moment which, in this case, occurs at the center of the member. Calling  $p$  the weight of the member per unit of length,  $S$  the axial stress,  $l$  the length of the member and  $\delta$  the deflection at the center, then

$$M_c = \frac{pl^2}{8} + S\delta = \frac{l^2}{8} \left( p + \frac{8S\delta}{l^2} \right). \quad . . . . . (63D)$$

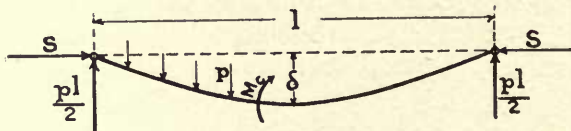


FIG. 63A.

Assuming the effect of the direct stress on the deflection  $\delta$  to be the same in character as that of the uniform load  $p$ , which is not quite true, then

$$\delta = \frac{5M_c l^2}{48EI} = \frac{5l^4}{384EI} \left( p + \frac{8S\delta}{l^2} \right),$$

from which

$$\delta = \frac{\frac{5}{384}pl^4}{48EI - 5Sl^2}. \quad . . . . . (63E)$$

This value of  $\delta$  substituted into Eq. (63D) gives

$$M_c = \frac{6pl^2EI}{48EI - 5Sl^2}. \quad . . . . . (63F)$$

The combined direct and bending unit stress on the extreme fiber of the member then becomes by Eq. (49M)

$$f = \frac{S}{F} \pm \frac{M_c y}{I}, \quad \dots \dots \dots (63G)$$

where  $F$  is the cross-section and  $y$  is the normal distance from the neutral axis to the extreme fiber of the member.

**Horizontal tension members** with pin-connected ends, when similarly treated, lead to the following formulæ:

$$M_c = \frac{pl^2}{8} - S\delta,$$

giving

$$\delta = \frac{\frac{5}{8}pl^4}{48EI + 5Sl^2} \quad \text{and} \quad M_c = \frac{6pl^2EI}{48EI + 5Sl^2} \quad \dots \dots \dots (63H)$$

The combined direct and bending stress on the extreme fiber is again found by Eq. (63G).

**Example.** Given an eye bar  $2 \times 15$  in., making  $F = 30$  sq.in.;  $S = 600,000$  lbs.;  $l = 660$  in.;  $I = 562.5$  in.<sup>4</sup>;  $p = 8.5$  lbs. per in.; and  $E = 29,000,000$  lbs. per sq.in.

Then from Eqs. (63H),  $\delta = 0.4824$  in.; and  $M_c = 173,450$  in. lbs. The stress on the extreme fiber then becomes by Eq. (63G)

$$f = \frac{600,000}{30} \pm \frac{173,450 \times 7.5}{562.5} = 20,000 \pm 2313 \text{ lbs. per sq.in.,}$$

showing that the bending stress alone increases the tension in the lower fiber by 11.5 per cent.

(b) **Secondary stresses in pin-connected structures.** In all usual stress computations the question of how equilibrium is established between the stresses in the several members meeting at a pin or panel point is not considered. It is thus assumed that the individual members extend to the pin centers with full effective sections where the stresses are suddenly balanced in a point.

In reality the case is very different and no such balance in the stresses can be accomplished. The nearest approach to a realization of the ideal condition is in the case of two abutting compression members and then only when there are no bending stresses to be transmitted.

When all the members are connected by pins according to the usual methods of construction, the stresses are transmitted past the panel points in very much the same manner as for riveted connections on account of the frictional resistance on the pins created when the structure is distorted by superimposed loads. The advantages usually claimed for pin connections are not all realized in practice, and while centric connections are best made by this style of panel joint there may be sufficient frictional resistance on the pin to produce secondary bending stresses quite equal to those occurring in riveted joints.

It is thus an erroneous idea to regard a pin-connected structure as free from secondary

stresses. This is never so and the analysis may be even more complicated, though the results are probably more reliable than for riveted structures.

The exact behavior of a member with pin bearings depends on many circumstances, especially the diameters of the pins. When these are sufficiently large the member cannot turn under load, and secondary stresses must result. These may be partially relieved by the vibratory action of the live loads which would probably allow the structure to adjust itself for some mean condition of loading and reduce the secondary stresses to a minimum. However, temperature changes would enter as a disturbing element to prevent such favorable action from establishing permanent relief.

The frictional resistance offered by a pin connection is now analyzed.

Let  $S$  = the stress in any member.

$R$  = the total frictional resistance on the surface of contact between the pin and the member.

$r$  = the radius of the pin.

$\rho$  = the angle of repose, making  $\tan \rho = \mu$  = the coefficient of friction between the two metals.

$c$  = the eccentricity of  $S$  required to resist the moment of the frictional force  $R$ .

$e$  = the actual eccentricity of  $S$  required to resist the bending moment  $M_a$  due to secondary stress.

The line of stress  $S$ , Fig. 63b, is supposed to suffer a displacement  $c$  from the pin center  $A$  of an amount which will make the moment  $Sc$  exactly equal to the opposing moment of the frictional resistance  $R$ .

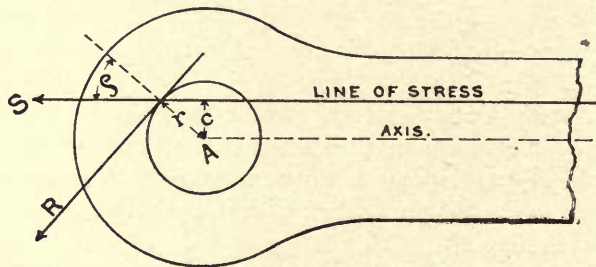


FIG. 63b.

For a frictionless pin the eccentricity  $c$  would be zero and the stress would pass through the pin center.

Hence from the figure

$$Sc = Rr \text{ and } c = r \sin \rho, \dots \dots \dots (63i)$$

showing that  $c$  is independent of the stress  $S$ .

When  $c > e$  no rotation will take place as a result of deformation of the truss due to load effect, and when  $c < e$  the member will turn on the pin and the full amount of bending cannot be developed by the frictional resistance.

The secondary stresses in a pin-connected structure are found in precisely the same manner as shown in Art. 61, for riveted connections, except that for all members where



$c < e$  the limiting value  $c$  will govern and the secondary stress becomes accordingly less. Eq. (61w) gives the value of  $e = 6KI/Sl$ , furnishing the limiting value

$$K = \frac{Slc}{6I} = \frac{Slr \sin \rho}{6I}, \dots \dots \dots (63j)$$

and by Eq. (61v) the limiting secondary stress becomes

$$f_s = \frac{M_{ay}}{I} = \frac{S_{yr} \sin \rho}{I}. \dots \dots \dots (63k)$$

Regarding the values of  $\rho$ , which are purely empiric, no good experimental data seem to be available, though it is preferable to choose rather high values from  $12^\circ$  to  $14^\circ$ , making  $\sin \rho = 0.2$  to  $0.25$ .

(c) **The effect of eccentric connections.** It frequently happens that the line of stress through a member is not coincident with its neutral axis, thus giving rise to eccentric connections.

It might be said that such connections should never be tolerated, and hence their effect in producing secondary stresses would not require investigation. However, there may be rare cases where eccentricity is unavoidable and proper provision must then be made for taking care of the bending stresses thereby produced.

These bending stresses are not merely additional stresses, but the secondary stresses previously found on the assumption of centric connections will be incorrect on account of the changes which must take place in the deflection angles  $\tau$  and the angles  $\alpha, \beta, \gamma$ , etc., between the truss members, as a consequence of the eccentricity.

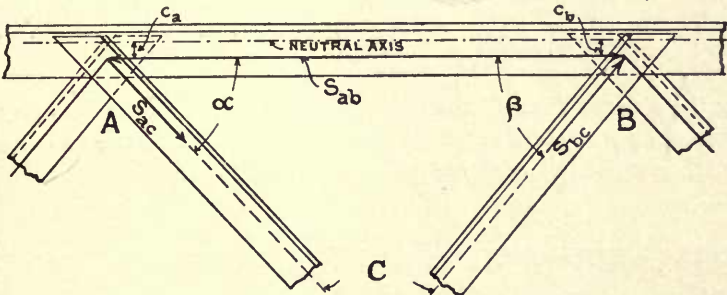


FIG. 63c.

Calling  $c_a$  and  $c_b$  the eccentricities of the stress at the two ends of a member  $\overline{AB}$ , Fig. 63c, then the moments  $M_a = S_{ab}c_a$  and  $M_b = S_{ab}c_b$  will produce deflection angles  $\tau$  by Eqs. (61c), which become

$$\left. \begin{aligned} \tau_a &= \frac{l}{6EI}(2M_a - M_b) = \frac{S_{ab}l}{6EI}(2c_a - c_b) \\ \tau_b &= \frac{l}{6EI}(2M_b - M_a) = \frac{S_{ab}l}{6EI}(2c_b - c_a) \end{aligned} \right\} \dots \dots \dots (63l)$$



and this gives rise to a great variety of cases depending on the type of truss considered. Two cases will be presented for illustration.

- Let  $T$  = the tractive force on one rail under any wheel load  $P$ .
- $f$  = the coefficient of friction between the braked wheel and the rail, usually taken between 0.15 and 0.2, and varying greatly according to weather conditions.

Then the total tractive force, for  $n$  wheels on the bridge, becomes

$$\Sigma_0^n T = f \Sigma_0^n P. \quad \dots \quad (64A)$$

For a through bridge, the compression in the bottom chord members will then be increased by the tractive force producing the additional stress  $-\Sigma_x^l T$ , where  $x$  is the distance from the fixed end of the span to the head of the train.

All top chord and web members remain unaffected. When the train approaches from the roller end the bottom chord receives compression and the stress increases uniformly from the roller end toward the fixed end.

For a deck bridge, as shown in Fig. 64A, the reactions due to a tractive force  $\Sigma T$  becomes:

$$A = \frac{h_0}{l} \Sigma T; \quad B = -\frac{h_0}{l} \Sigma T; \quad H = \Sigma T. \quad \dots \quad (64B)$$

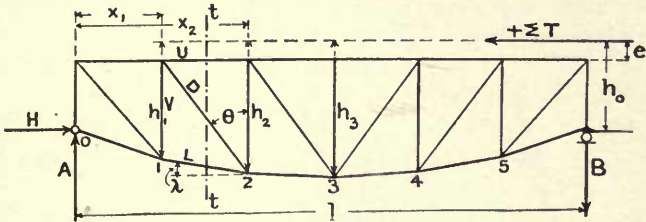


FIG. 64A.

The additional stresses in the members of panel 1-2 are found as follows:

For top chord, 
$$U = -\frac{M_2}{h_2} = \frac{-Ax_2 - H(h_2 - h_0) + h_2 \Sigma_0^x T}{h_2} = \frac{h_0 \Sigma T}{lh_2} (l - x_2) - \Sigma_x^l T$$

For bottom chord, 
$$L = \frac{M_1}{h_1 \cos \lambda} = \frac{Ax_1 - H(h_0 - e) - e \Sigma_0^x T}{h_1 \cos \lambda}$$

For diagonal 
$$D = (A - L \sin \lambda) \sec \theta$$

For vertical 
$$V = A - L \sin \lambda$$

(64c)

The angles  $\lambda$  and  $\theta$  are regarded positive as shown in the figure. The tractive force is taken positive in the direction from right to left, supposing the train to approach the span from the roller end at B.

The maximum value for the additional stress is found for the same position of the train loads as is used to produce maximum primary stress in any particular member.



These additional stresses become less important for long span, massive, structures where the dead load is large in proportion to the live load. For smaller structures, the chord members, adjacent to the hinged end of the span, may receive excessive additional stresses requiring increased area or provision for reversal of stress.

The effect of tractive forces on the floor system is not taken up here.

**When the loaded chord is on a grade,** the total weight  $G$  of the combined dead and live loads on the span exerts a certain component  $G \sin \alpha$  longitudinally along the structure and in a down grade direction, where  $\alpha$  is the grade angle. This component is transmitted to the hinged support and should be considered in designing this bearing, especially if the support happens to be a steel tower.

**(b) Forces acting transversely to a structure.** They are wind pressure, lateral vibrations and centrifugal force on a curved track. These will be separately discussed.

**Wind pressure** is the force due to wind against the total area of all structural elements of both trusses, the floor system and live loads, as presented in elevation. While the wind may have any direction, it is presumed that at times this direction will become normal to the exposed area and thus attain maximum intensity.

Experiments have shown that the normal wind pressure may reach a value of 50 lbs. per sq.ft., which amount is assumed in figuring the wind stresses in the unloaded structure.

Usually it would be unwise to cross a bridge when the wind has sufficient velocity to produce such pressure, and hence the maximum pressure to be assumed for the loaded structure need not exceed about 30 lbs. per sq.ft., applied to the total area of the structure, the moving load, and the portion of the leeward truss which is not covered by the moving load. While both trusses may not receive the full intensity of pressure it is customary to make no deduction on this account.

The wind loads falling on the truss members are considered as concentrated loads acting on the several pin points of the structure, and in estimating the stresses in the web members of the horizontal wind trusses or lateral trusses, these loads are treated as moving loads. The wind pressure on the live load is always considered as a moving load applied to the wind truss of the loaded chord. The total maximum wind load will govern for the chord stresses.

The end reactions of the wind trusses must eventually be carried to the main truss supports through the end portals or sway bracing. Sometimes only one wind truss is used, and then the wind loads of the other chord are carried to this wind truss by sway bracing at each panel point, throwing the entire wind load on the one lateral system.

Since the center of gravity of the wind load on the moving load is always above the plane of the lateral system of the loaded chord, it is necessary to consider the overturning effect of these loads in producing unequal vertical loading of the two main trusses. Figs. 64B show five cases which are met with. In Figs. a, b and c one wind truss is provided and a sway brace at each panel, while in Figs. d and e there are two wind trusses.

Let  $w_1$  = the wind pressure per panel on the live load.

$h_1$  = the lever arm of  $w_1$  to the plane of the horizontal wind truss.

$w_2$  = the wind pressure per panel on the bridge.

$h_2$  = the lever arm of  $w_2$  to the plane of the horizontal wind truss.

Then the overturning moment is

$$\left. \begin{aligned} M &= w_1 h_1 + w_2 h_2 \text{ in Figs. } a \text{ and } b \\ M &= w_1 h_1 - w_2 h_2 \text{ in Fig. } c \\ M &= w_1 h_1 \text{ in Figs. } d \text{ and } e \text{ with two wind trusses} \end{aligned} \right\} \text{with one wind truss} \quad \left. \vphantom{\begin{aligned} M &= w_1 h_1 + w_2 h_2 \text{ in Figs. } a \text{ and } b \\ M &= w_1 h_1 - w_2 h_2 \text{ in Fig. } c \\ M &= w_1 h_1 \text{ in Figs. } d \text{ and } e \text{ with two wind trusses} \end{aligned}} \right\} \dots 64D)$$

and the vertical load  $V$ , acting down on the right-hand truss and up on the left-hand truss, becomes  $V = M/b$ . Depending on the direction of the wind, this leads to positive and negative stresses of equal intensity in each vertical truss. Hence,  $\pm V$  is treated as a live load for the vertical truss to obtain the additional stresses due to overturning effect

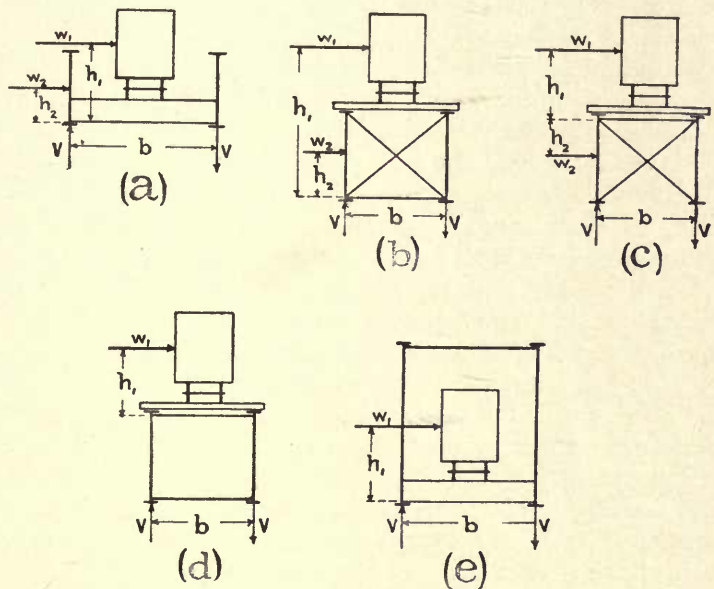


FIG. 64B.

of the wind on the moving live load, though it might be better to determine the stresses separately for the wind loads  $w_1$  and  $w_2$ . Calling  $V_1$  and  $V_2$  the respective vertical wind loads,  $pd$  the live load per panel and  $gd$  the dead load per panel, then for parallel chords the additional wind stresses become  $S_d V_1 / pd + S_l V_2 / gd$ , where  $S_d$  is the dead load and  $S_l$  the live load stress in any member.

It should be noted that the case in Fig. c is most favorable, while the one in Fig. b is most unfavorable in the production of loads  $V$ , and may give rise to stresses amounting to as high as 30 per cent of the primary stresses in certain members.

The stresses in the wind trusses may be found by applying the methods given in Chapter XII, and those occurring in the portal bracing and sway system were analyzed in Art. 62B.

All of these additional stresses resulting from wind pressure in the primary members must finally be combined with the primary stresses to obtain total stresses.



The additional wind stresses increase in importance with the length of the span, and may assume enormous proportions in large structures. It should be mentioned, however, that the frequency in the occurrence of maximum wind stresses is extremely rare, and their simultaneous combination with maximum primary stresses is very improbable.

In view of these considerations it would seem proper to employ higher allowable unit stresses, say such as are permissible for quiescent loading, possibly restricting the total sections of the primary members more nearly to those required only for maximum dead and live loads. For single-track bridges exceeding a span of 200 ft., and for double-track structures of over 350 ft. span, the wind stresses must be fully considered, while for smaller structures the end posts and end chord sections should be appropriately strengthened, making perhaps little allowance in the other members.

**Lateral vibrations**, while they exist, do not appear to produce any serious increase in the primary stresses of a bridge. This is certainly true for highway structures, and in the case of railroad bridges, this effect may be reduced to insignificance by making appropriate provisions to keep the moving loads steady while passing over the span.

The magnitude of the vibratory forces here considered depends on the velocity of the moving load, the character and type of locomotive, the condition of the track and the relative stiffness and rigidity of the floor system and main trusses. Short spans and narrow structures, also skew bridges might receive considerable vibratory stress, especially in the end panels. Coned wheels and loose or spread rails are very objectionable.

It is needless to say that factors of such uncertain constitution and variable nature are not susceptible to analysis, and a direct measurement (even if it could be made) of such additional stresses would merely indicate what might occur in certain cases, but the results from different experiments could not be accurately correlated with the surrounding circumstances.

The remedy thus lies in obviating, so far as possible, the conditions producing deleterious effects rather than in any attempt to estimate their magnitude and weigh down the structure by allowing extra material in the required cross-sections. If this can be done, then the slight additional stresses due to lateral vibrations may safely be neglected. The vertical effect of impact is considered elsewhere in this article.

**Centrifugal force due to curved track.** This problem necessarily deals only with railroad bridges and includes the centrifugal force acting transversely to the structure and producing stresses in the stringers and in the lateral system of the loaded chord; the overturning effect of the centrifugal force producing stresses in the stringers, floor beams and in the main trusses; and the unequal distribution of the vertical loads on the floor and between the main trusses due to the eccentricity of the curved track axis with the straight bridge axis. This latter problem was solved by influence lines in Art. 29, for the case of a skew plate girder on a curve, and will receive no further attention here.

The amount of the centrifugal force acting transversely to the bridge is given by the formula

$$C = \frac{v^2}{gR} P = cP, \quad . . . . . (64E)$$



where  $v$  is the velocity of the moving train;  $P$  is any moving load on the bridge;  $g=32.2$  ft. per second, being the acceleration due to gravity; and  $R$  is the radius of curvature of the track. The units are foot, pound, second. For velocities in miles per hour, and curvature in degrees  $D$ ,  $c=0.0000117v^2D$ .

The following table gives values of  $c=v^2/gR$  for curves of one to ten degrees and velocities which may be regarded as maximum for such curves.

Degree of Curve, $D$	$v$ Miles per Hour.	$c$	Degree of Curve, $D$	$v$ Miles per Hour.	$c$
1	60	0.042	6	50	0.176
2	58	0.078	7	48	0.189
3	56	0.110	8	46	0.198
4	54	0.136	9	44	0.204
5	52	0.158	10	42	0.206

In computing the additional stresses  $S_c$  in the main truss members resulting from centrifugal force, the maximum total stress might be obtained from the train giving the maximum primary stresses rather than from the train moving with the highest velocity. For short spans the maximum combination is likely to occur from passenger trains, while for long spans this may be true for freight trains moving at lower speed.

The methods of finding the stresses in the main trusses and in the lateral system of the loaded chord are precisely the same as given for wind loads.

Since the centrifugal force  $C$  is a linear function  $cP$  of the moving load, therefore the horizontal forces coming on the lateral truss of the loaded chord will, at all points, be  $c$  times the moving load. The same is true of the overturning effect separately considered, where the line of action of  $C$  is above the plane of the lateral truss and passes through the center of gravity of the load  $P$ , which may be assumed at the same level as the center of pressure of the wind load.

The stresses in the lateral truss of the loaded chord will then be found in the ordinary way for loads  $cP$  considered as moving live loads. When these loads  $P$  are uniformly distributed then the stresses found for loads  $cp$  will be  $cp/w$  times those found for the uniform moving wind load  $w$ .

The stresses in the main trusses, due to overturning effect of the centrifugal force  $C$ , are analyzed in the manner previously explained for wind loads. Fig. 64c represents the condition at a panel point assuming the load  $P$  and the centrifugal force  $C$  to be loads per panel and applied at the center of gravity of the moving load.

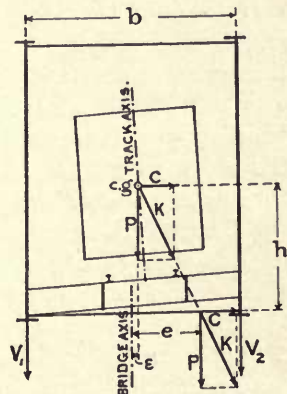


FIG. 64c.

The track is eccentric with the truss and the floor beam is superelevated to suit

the curved track. The resultant  $K$ , of  $P$  and  $C$ , intersects the plane of the lower laterals at a distance  $e$  from the truss axis and may there be resolved into forces  $P$  and  $C = cP$  as they would act on the main and lateral systems.

The reactions  $V_1$  and  $V_2$ , representing the vertical loads which are transmitted to the main trusses, then become

$$V_1 = \frac{P}{2} \left( 1 - \frac{2e}{b} \right) = \frac{P \left( \frac{b}{2} - \varepsilon \right) - Ch}{b} \quad \text{and} \quad V_2 = \frac{P}{2} \left( 1 + \frac{2e}{b} \right) = \frac{P \left( \frac{b}{2} + \varepsilon \right) + Ch}{b}. \quad (64F)$$

With these loads  $V_1$  and  $V_2$ , which vary for each panel point on account of the variable eccentricity  $e$ , the method given in Art. 29 may be advantageously used to find the combined stresses in the main trusses by influence lines and that is the best solution for this problem. It should be noted that the load  $V_1$  becomes maximum for quiescent loading, while  $V_2$  attains maximum for the highest velocity of the train.

(c) **Forces acting vertically on a structure.** This embraces several causes which together exert a more or less severe dynamic influence on the stringers, floor beams and vertical trusses of a bridge, all included under the general term *impact*.

So far as these can be separately enumerated, they may be classified as follows: (1) The true impact due to the instantaneous application of a moving load to a structure at rest; (2) the impact resulting from the unbalanced condition of the engine drivers; irregularities in the surfaces of the rails and imperfections in the rolling stock, etc.; (3) elastic vibrations of the structure which tend to increase the effect of dynamic loads otherwise applied to a rigid body; and (4) vertical centrifugal forces occasioned by the vertical curvature (deflection and camber) of the track.

Owing to the extremely variable conditions and combinations of circumstances, it is practically impossible to analyze separately the magnitudes of these several causes and their resulting effects, though a brief discussion may serve to point out precautionary measures tending to reduce the impact stresses in bridges under traffic. Some very valuable tests have been conducted during late years, both in Europe and America, which give a very good idea of the sum total effect produced on railroad bridges by the moving loads, and from these, formulæ have been deduced which make it possible to provide suitable strength in designing bridges.

The additional stresses, resulting from this combination of causes, are a function of the velocity and magnitude of the moving load, and hence assume minor importance when dealing with highway structures.

**The true impact** due to the instantaneous application of live loads is really not a serious source of additional stresses, because forces are transmitted through a structure with a rapidity approaching the velocity of sound, while the moving train could not exert its effect in so short a space of time.

Theoretically, a load instantaneously applied would produce a dynamic effect twice as great as the static load, but in reality this cannot take place and there will



always be a sufficient lapse of time between the application of the loads and the necessary elastic deformation of the structure to obviate to a great extent this extreme dynamic impulse. The vibrations accompanying the moving loads really constitute the element of danger.

The most unfavorable conditions prevail in short span structures and in the web members subject to a rapid change of stress.

The causes enumerated under (2) and (3) are really of the most serious character, and while much may be accomplished by a careful maintenance of the track and rolling stock, a certain average condition will usually prevail beyond which no remedial measures will be possible or feasible.

In point of design and construction of a railroad bridge the following suggestions may be offered: The bridge and its approaches back for some distance should be straight and when curves are absolutely unavoidable speed restrictions would seem proper. The rails should be long and the joints and tie connections of the best and most rigid construction, carefully maintained. The connections at the abutments require the most attention, avoiding uneven settlements and loose rails. The introduction of continuous roadbed over bridges is very desirable as affording some elasticity to absorb the impact rather than to transmit the same to the structural portions of the floor and trusses. A similar effect is produced by long ties over widely spaced stringers. Very rigid floors and rails directly on stringers may be classed as objectionable.

The greater the proportion of dead to live load and the longer the span, the less will be the effect due to impact.

The avoidance of synchronous vibrations between the moving load and the structure is of the utmost importance and may be practically accomplished by properly stiffening all the members and by providing thorough bracing in the lateral and sway systems.

The effect of vertical centrifugal force might be separately estimated, but the amount is small and the attending conditions are too uncertain to warrant this.

As early as 1859, Gerber proposed a general formula providing a certain reduction in the allowable unit stresses to cover these several sources of dynamic impact. This formula is

$$f = f' \left( \frac{S_l + S_d}{3S_l + S_d} \right),$$

wherein  $f'$  is about the elastic limit of the material and  $S_l$  and  $S_d$  are the respective live and dead load stresses in any member.

The following formulæ are at present in use and give the factor  $\phi$  by which the live load stress should be multiplied, so as to include the dynamic effects considered under the present heading. Calling  $S_l$  the live load stress,  $S_d$  the dead load stress and  $l$  the strength of span for chord members, or the loaded distance producing maximum stress in a web member, then  $\phi$  is given as follows:



- (1) C. C. Schneider, 1887, railroad bridges,

$$\phi = 1 + \frac{300}{l+300} = \frac{l+600}{l+300}$$

- (2) C. C. Schneider, electric roads,

$$\phi = 1 + \frac{150}{l+300} = \frac{l+450}{l+300}$$

- (3) J. A. L. Waddell, railroad bridges,

$$\phi = 1 + \frac{400}{l+500} = \frac{l+900}{l+500}$$

- (4) J. A. L. Waddell, highway bridges,

$$\phi = 1 + \frac{100}{l+150} = \frac{l+250}{l+150}$$

- (5) H. S. Pritchard, 1899, railroad bridges,

$$\phi = 1 + \frac{S_l}{S_l + S_d} = \frac{2S_l + S_d}{S_l + S_d}; \text{ for counters } \phi = 2$$

- (6) J. Melan, railroad bridges,

$$\phi = 1.14 + \frac{24}{l+30} = \frac{1.14l + 58}{l+30}$$

- (7) J. Melan, secondary roads,

$$\phi = 1.10 + \frac{18}{l+30} = \frac{1.1l + 51}{l+30}$$

- (8) F. Engesser, railroad bridges,

$$\phi = 1.67 + \frac{(65-l)^2}{10,000}; \text{ for } l > 65, \quad \phi = 1.67$$

- (9) F. Engesser, highway bridges,

$$\phi = 1.50 + \frac{(33-l)^2}{3300}; \text{ for } l > 33, \quad \phi = 1.50$$

- (10)\* American Railway Eng'r and Maintenance of Way Ass'n, 1910,

$$\phi = \frac{l^2 + 40,000}{l^2 + 20,000}$$

. . . (64G)

Table 64A gives values of  $\phi$  as obtained from each of the above ten formulæ for a few even lengths  $l$ .

Only those values of  $\phi$  are comparable which are intended for the same class of structures as (1), (3), (5), (6), (8) and (10). It is clearly seen that formula (10) gives the highest values for short spans  $l$  and the lowest values for long spans, noting that in

\* Where  $l$  is the span length and all members receive the same impact.

this formula  $l$  represents the length of span and not the loaded distance as in formulæ (1) to (9).

TABLE 64A.  
VALUES OF  $\phi$  AS FOUND FROM THE VARIOUS Eqs. (64g)

$l$ Feet.	(1)	(2)	(3)	(4)	(5)	(6)	(7)	(8)	(9)	(10)
10	1.97	1.48	1.78	1.63	Cannot	1.73	1.55	1.97	1.66	1.99
50	1.86	1.43	1.73	1.50	be	1.44	1.33	1.69	1.50	1.89
100	1.75	1.38	1.67	1.40	solved	1.32	1.24	1.67	1.50	1.67
200	1.60	1.30	1.57	1.28	without	1.24	1.18	1.67	1.50	1.33
300	1.50	1.25	1.50	1.22	knowing	1.21	1.16	1.67	1.50	1.18
400	1.43	1.21	1.44	1.18	the	1.20	1.14	1.67	1.50	1.11
500	1.38	1.19	1.40	1.15	stresses	1.18	1.13	1.67	1.50	1.07
600	1.33	1.17	1.36	1.13		1.18	1.13	1.67	1.50	1.05

The American Railway Engineer and Maintenance of Way Association formulæ is undoubtedly entitled to the greatest confidence, being based on very extensive experiments which were carried out by the committee on impact tests under actual conditions of traffic. The formula is not as yet officially adopted by the association.

However, no allowance was made for secondary stresses in the members and hence the formula (10) may be said to include more than actual impact effect which is probably true of all the Eqs. (64g).

(d) **Fatigue of the material.** Based on the classic experiments of Wöhler (1859-1870) which were continued by Professor J. Bauschinger, a formula was proposed by Launhardt (1873) and later modified by Weyrauch, aiming to apply the principles of the fatigue of material to the design of bridge members.

Wöhler's law states that for a large number of repeated load applications, rupture of a material is produced under stress which is below the ordinary (static) breaking strength of that material. The conditions under which Wöhler's experiments were made differ so radically from those attending the actual operating conditions of bridges, that it is questionable whether anyone is justified in applying the Launhardt-Weyrauch formulæ to bridge designs.

Wöhler's load repetitions followed in quick succession and were continued without interruption (several million times) until failure was produced. Bridge members are subjected to a repetition of stress which is always followed by a rather long period of rest, and few structures, even under the heaviest traffic, are retained in service long enough to receive several million applications of the moving load. Also, a well-designed bridge is never calculated for stresses approaching even the elastic limit, while Wöhler bases all his observations on stresses exceeding this limit.

In addition to these facts, modern experiments made under conditions which correspond quite closely with bridge practice, though limited in extent, point uniformly against the existence of fatigue in bridges.

The above mentioned Launhardt-Weyrauch formulæ have been extensively used

in designing bridge members and are still retained in many specifications. However, this practice does not seem justifiable, especially when allowance is made for impact and secondary stresses generally.

The fatigue formulæ undoubtedly served a good purpose in the days when so many important factors were neglected, but at the present time the aim should be to make proper allowance for all the known stress elements and thereby reduce the "factor of ignorance" to a minimum.

(e) **Unusual load effects** may be produced by loads of unusual magnitude applied at rare intervals or by loads which occur under unusual circumstances.

It is possible that the maximum combination of moving loads, wind pressure and temperature effects may take place, under which the structure might be stressed to its utmost capacity, while under ordinary conditions of traffic the stresses would be far below those for which the design was made. The maximum load basis for a design is then an unusual load effect for the average use of a structure.

At times it may be necessary to transport some abnormal piece of freight or a train of locomotives, which would exceed the loads assumed in the computations. This may be done without danger even if the members are stressed quite near the elastic limit, provided the design is made with some forethought. For most ordinary structures such a practice might prove very disastrous.

It should be observed that, while the stress in any member for a particular position of a moving load is exactly proportional to the intensity of this load, the combination of maximum and minimum stresses for such member, which fixes the required cross-section, might not be thus proportional. In the case of chord members, all governing stresses are proportional to the loads because the critical positions of the loads are alike for all chords, that is, for maximum chord stress the whole span is fully loaded while the minimum chord stress occurs for dead load only.

Hence, the chord sections are directly proportional to the total moving load, while most of the web sections are not so proportional and increase more rapidly than the loads. This is particularly the case with all counter web members wherein the stress is the difference between that produced by the moving load and that due to the dead load. It also applies to the sections of such web members as are subject to stress reversal.

This is an important item in making provision for a future increase in train loads, where 25 to 50 per cent additional carrying capacity might easily be secured by providing a slight increase in the counters and web members having stress reversals. Many old structures would still be usable for considerable overload had such provision been made in their design.

The best way to provide for such overload in view of future increase in train loads, is to design the structure for the given case of loading and allowable unit stresses and then to increase the sections of the counters, and web members with stress reversals, for the desired overload, which of course could not exceed a reasonable amount according to the limitations imposed by the chord sections.

A structure so designed might then carry say 30 per cent overload without imposing unduly on certain few web members, while the ordinary structure would fail by the buckling of these members long before the chords had received any serious stresses.



In the same way a highway bridge may be designed to carry an occasional overload of a certain heavy road roller, etc., without increasing the sections of the chords and main web members, but by providing for the extra counter stresses due to the excess load.

To the second class of unusual load effects belong derailments, collisions with drift-wood during times of high water and possible settlements of piers or abutments.

The absolute prevention of such occurrences may be classified with the impossible. However, the ultimate destruction of a structure when they do occur may be safeguarded by applying certain precautionary measures which should never be overlooked.

Thus the bridge floor should be made sufficiently strong to allow a derailed train to pass over without breaking through, and the wheels should be guided between guard rails or by other means to prevent collision with the main truss members, necessitating certain clearances for through bridges to accomplish this. In the case of deck bridges it may be advisable to utilize the top chord as a barrier or protection to prevent the train from leaving the structure.

The design of the floor should, therefore, aim at the use of solid web, riveted girders and braces in preference to built-up frames, and the soft, ductile varieties of steel are more desirable than the harder, brittle varieties.

In cases where high water may reach the bottom chord, slender eye-bar members are decidedly objectionable.

#### ART. 65. CONCLUDING REMARKS

(a) **Features in design intended to diminish secondary and additional stresses.** The following suggestions should be given careful consideration:

Skew structures and bridges on curves should never be built except in very rare cases where no other disposition is possible. These types should be regarded as measures of last resort.

The axes of all members of a truss should be in the same plane and should intersect in a point at all connections.

Special attention should be directed toward a careful design of all connections with a view of reducing the secondary stresses. Thick gusset plates and large diameter rivets materially reduce the sizes of these plates and are thus desirable from this aspect.

The widths of members, in the plane of the truss, should not be chosen larger than is absolutely required to secure proper connections and stiffness against buckling in compression members. It may thus be desirable to taper compression members from the center toward both ends.

The cross-sections of members should be so chosen that the material is concentrated as far from the neutral axis as possible, thus securing the largest moments of inertia for the smallest over all dimensions. The cross form is thus the least advantageous, while a square box form is most desirable. In rare instances the cross form may be acceptable, when the width of a member is determined by other conditions. Secondary stresses occurring simultaneously in the plane of the truss and in a cross frame are additive in members of the box type while in the cross form they are not additive, a consideration which may become important at times.

The secondary stresses may be reduced to a certain degree by shortening all tension members and lengthening all compression members by amounts  $\Delta l$ , determined for the case of maximum total load. This practice is generally followed and provides a camber in the unloaded structure which exactly disappears under the full load when the structure assumes its true geometric shape.

The plane of the lateral system should coincide with that of the chords and the plane of the floor should be as close as possible to that of the lateral system.

The web members of the lateral systems should present considerable stiffness against buckling, making  $l/r$  not greater than 140 for all these members, whether in compression or tension.

The end portals, or cross frames, should be heavy to carry the wind reactions and dynamic effects to the supports.

Floor beams should be made deep to reduce secondary stresses in the cross frames. When this cannot be done then flexible connections should be provided between the truss members and the beams, a type which is best suited to large bridges, while riveted connections are desirable for small spans.

The stringers should be made heavy and continuous and should be designed to transmit the tractive forces to the panel points of the loaded chord instead of to the floor beams by inserting proper tie members between the stringers. Long ties over widely spaced stringers tend to relieve impact vibrations.

The use of pin connections is not admissible for bridges of less than 200 ft. span, and even in larger structures the advantages to be gained may not be so easily demonstrated. Some benefits may be derived from pins for the web system but certainly not for the compression chord.

According to prevalent practice in designing pins, the diameters are usually so large that the friction produces secondary stresses quite equal to those resulting from riveted connections. Perhaps this condition might be remedied.

Also pin-connected columns are not as stiff as those with riveted ends, though the great convenience offered by pin connections during erection and the saving of material and other advantages in point of design, speak greatly in their favor.

The advisability of using the higher classes of steel for the main truss members of large structures and employing soft steel for the floor system was previously mentioned.

In choosing between different styles of trusses, those of the statically determinate class should always receive preference, other things being equal. The primary stresses will usually be less than in similar indeterminate systems, especially when temperature stresses are included. Yet the deformations and secondary stresses may be less and frequently the connections may be simpler for the indeterminate types.

The use of light-colored paints is advisable to reduce temperature effects, especially in structures involving redundant conditions.

(b) **Final combination of stresses as a basis for designing.** If the several stresses resulting in a bridge member from all causes could be absolutely known, then there is no good reason why a design should not be based on a unit stress of say four-fifths the elastic limit of the material and still allow ample leeway for some deterioration and unusual effects.

The low unit stresses of one-third to one-half the elastic limit, generally employed



are intended to cover, more or less blindly, the unknown stresses, on the presumption that these are in a way proportional to the known primary stresses. In reality, few, if any, of the secondary and additional stresses are directly related to the primary stresses, but are produced by totally different causes.

Our knowledge of the properties of material, while of a purely empiric nature, undoubtedly approaches the truth as closely as the knowable accuracy of the moving loads would require. The behavior of full-size bridge members has also been investigated to an extent which should make it possible to design such members with a reasonable expectancy of developing a strength commensurate with that observed on test specimens. This was perhaps not possible in the past, but should be expected when the results of the elaborate tests of the American Society for Testing Materials become available.

If the stresses in the members of a structure are determined with similar exactness and combined into totals representing the maximum and minimum stresses for each member as a result of all known material causes, and on a basis of *equivalent quiescent loads*, then there is no valid argument why the safe unit working stress  $f$  should not be taken at least equal to two-thirds the elastic limit of the material.

If also the main members and counters, subjected to reversals of stress, are designed for a 30 per cent overload, then such a structure should still be usable even for a 30 per cent increase in the assumed moving loads.

Furthermore, since the combined effect of the maximum values of all the known primary, secondary and additional stresses is one of very rare occurrence, this provides still greater safety and subjects the structure to a less severe average usage than that intended by the maximum combination of all loads.

Assuming then that the following stresses have been computed, or approximately estimated when no other means is afforded, then the required area for any member may be determined from the formulæ given below.

Let  $S_d$ =the stress in any member due to dead load.

$S_l$ =max. stress in this member due to moving load.

$S'_l$ =min. stress in this member due to moving load.

$S_w$ =the max. wind stress due to  $w_1$  and  $w_2$ , Art. 64b.

$S_T$ =the stress due to tractive forces, Art. 64a.

$S_t$ =the temperature stress when redundant conditions exist.

$S_c$ =the stress due to centrifugal force from curved track, Art. 64b.

$\phi$ =the impact coefficient or moving load factor Eq. (64g).

$l$ =the length of a member in inches.

$r$ =the least radius of gyration in inches.

$f$ =the allowable unit stress = two-thirds the elastic limit of the material.

$M_s$ =the bending moment produced by rigidity of joints, weight of the member, eccentricity, etc., representing the total secondary stress, Arts. 61, 62, 63.

Then the required area  $F$  for any tension member becomes:

$$F = \frac{1}{f} [S_d + \phi S_l + S_w + S_T + S_t + S_c] + \frac{M_s y}{f r^2} \dots \dots \dots (65A)$$



Whenever the area  $My/fr^2$  can be added to the area given by the first term of Eq. (65A) to obtain  $F$  without materially altering  $y$  and  $r$ , then it may be done, otherwise a new section must be chosen to satisfy the equation. Also, that combination of the stresses in the parenthesis which gives maximum must be used.

Eq. (65A) will also apply to any compression member when  $f$  is reduced for buckling effect according to a modified form of Mr. T. H. Johnson's formula, for values of  $l/r < 120$ :

For hinged ends and soft steel of 30,000 lbs. per sq.in. elastic limit,

$$\left. \begin{aligned} f &= 20,000 - 88 \frac{l}{r} \\ f &= 20,000 - 71 \frac{l}{r} \end{aligned} \right\} \dots \dots \dots (65B)$$

for flat ends,

For hinged ends and medium steel of 35,000 lbs. per sq.in. elastic limit,

$$\left. \begin{aligned} f &= 24,000 - 105 \frac{l}{r} \\ f &= 24,000 - 85 \frac{l}{r} \end{aligned} \right\} \dots \dots \dots (65C)$$

for flat ends,

When  $S'_l$  is opposite in sign from  $S_d$  and  $S_l$ , then the member must be capable of carrying an additional stress  $1.3\phi'S'_l$  in the place of  $\phi S_l$ , using the maximum combination of the same sign as  $S'_l$  in Eq. (65A). In this case, which is one of stress reversal, the factor 1.3 should also be applied to the stress  $\phi S_l$ . The impact factors  $\phi$  and  $\phi'$  being determined by one of the formulæ in Eqs. (64G) for the load lengths producing the respective stresses  $S_l$  and  $S'_l$ . However, this should not be construed to mean that the area must be designed to carry the total loads  $1.3\phi'S'_l + 1.3\phi S_l$  as if simultaneously applied.

Aside from the additional 30 per cent in the live load stresses, members with stress reversals may not require any increase in area, though the design should always be made so as to provide for the two kinds of stress.

## CHAPTER XIV

### MITERING LOCK GATES

#### ART. 66. THE NATURE OF THE PROBLEM

A mitering lock gate is in principle a three-hinged arch, so placed that the hinges have vertical axes, and the arch elements are acted upon normally by horizontal water loads. Each half arch is called a gate leaf and the hinges are replaced by compression joints adjacent to the *quoin* ends and *miter* post, see Figs. 67A and 68A.

Each leaf is designed to swing about a vertical axis at the quoin end, thus permitting the gate to be opened when the pressures on up- and downstream sides are equalized, a condition which prevails when the gate is swung in air or when the water level is equal on both sides.

The fastening on the top of the quoin post is called *anchorage*, and is usually in tension while the gate is open. At the same time the entire weight of a leaf is supported on a *pintle* located at the foot of the quoin post. See Figs. 68A.

The maximum stresses on the anchorage and the pintle are encountered when the gate is swung in air, while the maximum stresses in the structural elements of the gate occur when the gate is closed against a full head of water on the upstream side with no water on the downstream side, which is the case when the lock chamber is empty.

The ordinary working condition of a pair of gate leaves is less severe, being due to a full head of water on the upstream side and a counter pressure on the downstream side produced by the water inside the lock and sufficient to float the largest vessels for which the lock is intended. These two water levels are usually called the *upper* and *lower pool* levels.

In order that a closed gate may act as a barrier or structural element against a water head, the bottom horizontal girder is made to bear against a horizontal miter sill extending over the full length of each leaf. The amount of pressure exerted by each leaf against this miter sill is somewhat problematic, depending on the adjustment of the sill to the gate. Usually this adjustment is so made that the pressure is just sufficient to make a water-tight joint, though it may approach zero or may be made to take the entire reaction due to the full head of water.

Hence, a variety of conditions may occur, ranging from zero sill pressure to the full hydrostatic head. Usually these two extreme assumptions are made and the resulting stresses in the gate are found for each case. The actual condition during operation may then be assumed at some intermediate state of sill contact which can only be surmised but never absolutely known.



The structural elements of a single gate leaf consist of a series of horizontal girders connected vertically by a sheathing or skin plate and a number of vertical intermediate braces or stiffening girders. The horizontal girders of both leaves thus constitute a series of three-hinged arches transmitting the water pressure through the quoin hinges to the lock walls. The vertical system of stiffeners may be regarded as a set of trusses connected with the horizontal arches and thus constituting a series of vertical continuous girders, the supports of which are the elastic horizontal girders.

If the horizontal girders were designed to carry exactly their proportionate water loads and at the same time be allowed to deflect in proportion to these loads, then for no contact between the miter sill and the vertical stiffeners, the entire work would fall on the horizontal girders and the vertical stiffeners would do no work and would thus be superfluous.

However, for practical reasons, the top horizontal girders are always designed much stronger than is actually required for the water load and also the other girders are not all different, owing to commercial sizes of rolled shapes and the saving in manufacture resulting from duplication of like parts. Also, some sill pressure must be provided to accomplish water tightness of the gate. Therefore, the vertical system of stiffeners must necessarily do a certain amount of work in distributing these inequalities between the horizontal girders and the vertical stiffening system. The reactions, which the horizontal girders thus present to each vertical girder, may be considered as redundant reactions of a vertical continuous girder on  $n$  flexible horizontal supports, where  $n$  is the number of horizontal arch girders.

The vertical girders are not very definite structural elements, being made up of a rather disconnected system of web bracing between the horizontal arches. The total vertical stiffness of a gate is thus produced by the combined effect of the sheathing plates, the quoin and miter posts and the intermediate vertical girders. If these were all combined in one vertical system so as to represent one vertical girder for a gate leaf, then the average stiffener per foot of gate could be approximated by dealing with an average vertical section of the gate leaf. Such a hypothetical vertical girder could then be treated as a continuous girder, on  $n$  horizontal supports consisting of  $n$  three-hinged arches.

The problem would thus be to find the magnitudes of these  $n$  redundant supports  $X_1$  to  $X_n$  of the vertical girder for a certain water load (usually the maximum) together with the elastic displacements  $\delta_1$  to  $\delta_n$  of the  $n$  supports.

Since the contact at the miter sill cannot be absolutely adjusted, it is best to investigate two cases; one with full contact against the miter sill, giving the maximum sill pressure; and the other where the miter sill pressure is just zero and there is theoretically no contact.

It is certain that all possible cases must be included between these two extremes. However, in practice it is customary to design the bottom horizontal girder to carry the total water load without sill contact and to design the sill amply strong to carry the same full load, but to adjust the gate so that the sill pressure is only sufficient to make a water-tight joint.

The author has proposed details of construction obviating such duplication of



strength in the gate and miter sill by the introduction of a flexible sill connection whereby the water pressure against the sill can never exceed a certain allowable quantity.

### ART. 67. THE THEORY OF THE ANALYSIS

**The principal system.** The problem is analyzed according to the solution of the general case of redundancy presented in Art. 55, using the graphic method for all deflection polygons. Since there are only two cases of loading requiring investigation it is best to employ the general Eqs. (55A) and (55B) necessitating two solutions, each involving  $n$  equations of  $n$  unknown quantities  $X$ .

The effect of temperature will be neglected in the present, though it could be determined in accordance with Art. 56.

To make the problem perfectly definite, it is first necessary to decide on the *principal system* with its determinate reactions, and then to apply the redundant forces along with the external loads following the general scheme illustrated in Figs. 7A to 7E, Art. 7.

**The case of full contact at miter sill** is illustrated in Figs. 67A and B.

Fig. 67A shows a lock gate in plan, with the water loads  $p$ , per linear foot, applied to the upstream surface. The resultants  $R$ , of the loads  $p$  on each leaf, give rise to arch thrusts  $R'$  and  $R''$  at the quoin ends and a horizontal thrust  $H$  acting between the miter posts. The gate is supposed to undergo elastic deformations, as indicated by the dotted deflection curves. The lock walls take up the arch thrusts.

Each horizontal girder receives a total load  $P$  which is proportional to the depth of water below the surface. These loads are easily computed for all the horizontal girders and are assumed to be known.

Fig. 67B shows a projected elevation of the gate with the several loads  $P$  applied to the respective horizontal girders. The bottom girder rests against the miter sill over its entire length.

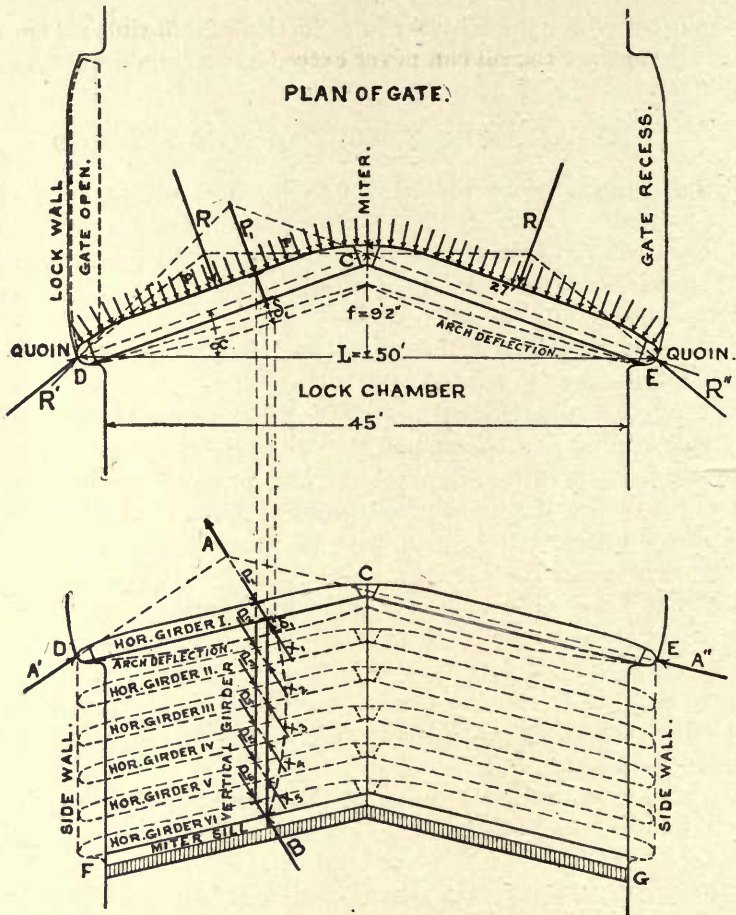
The vertical girder  $AB$  represents an element one foot thick lengthwise of the gate leaf and may be regarded as a plate girder whose chords are portions of the sheathing plate and all material making up the average vertical stiffness of the leaf, while its web may be neglected.

This vertical girder is now treated as the *principal system* and the problem consists of determining the stresses in, and the deflection of, this girder.

The determinate supports for this vertical girder (or principal system) are the sill reaction  $B$ , which is immovable in the present case, and the reaction  $A$  offered by the top horizontal arch girder. All the other horizontal girders 2 to  $n$  (shown by dotted lines) are now considered removed and the redundant reactions  $X$  which they present to the vertical girder are shown as external forces  $X_1$  to  $X_n$ .

The principal system is thus the vertical girder on two determinate supports  $A$  and  $B$ , with  $A$  elastic and  $B$  immovable. The external loads on the principal system are the water loads  $P$  and the redundant reactions  $X$ .

The yielding condition of the support  $A$  may be obviated by introducing another redundant reaction  $X_1$  and including the top horizontal arch as a part of the principal system with immovable supports at the quoin ends  $D$  and  $E$ . The reaction  $A$  is then



FIGS. 67A, B—Principal System, Full Loading, for Case of Full Contact at Miter Sill.

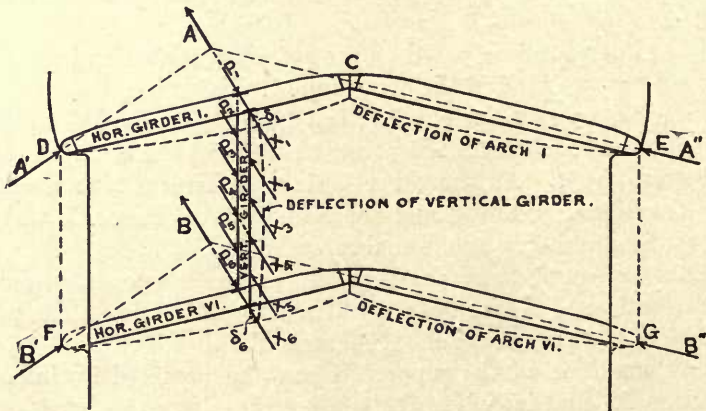


FIG. 67C—Principal System, Full Loading, for Case without Contact at Miter Sill.

regarded as the resultant of the immovable reactions  $A'$  and  $A''$ , and the deflection  $\delta_1$  of the point of application of  $X_1$ , can then be evaluated in terms of  $X_1$ , making  $\delta_1 = \delta_{1-1} X_1$ . The deflection curve of the vertical girder is indicated by a heavy dotted line.

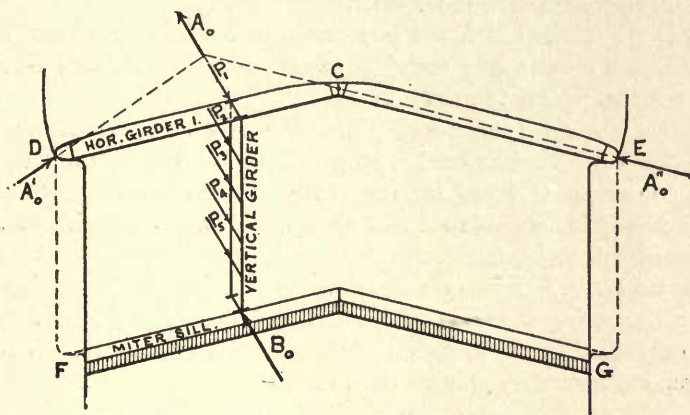


FIG. 67D—Principal System, Condition  $X=0$ . For Case of Full Contact at Miter Sill.

The case without contact at the miter sill is illustrated in Fig. 67c, where the principal system consists of the vertical girder  $AB$  supported on two yielding supports. Hence, by taking in the top and bottom horizontal arches as part of the principal system the fixed reactions became the four points  $D$ ,  $E$ ,  $F$  and  $G$ , while the elastic supports  $A$  and

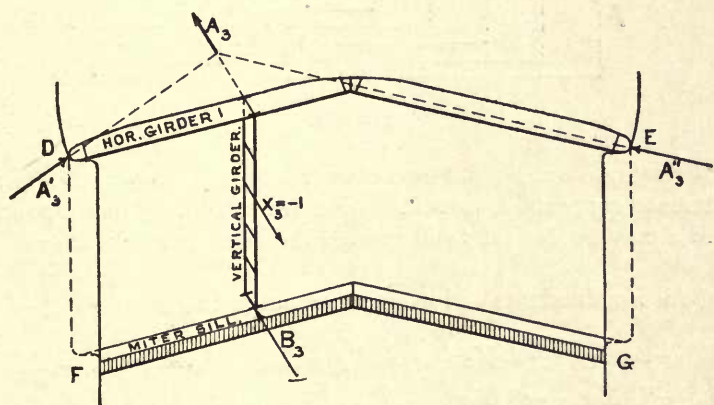


FIG. 67E—Principal System, Condition  $X_3=1$ . For Case of Full Contact at Miter Sill.

$B$  undergo certain deflections  $\delta_1$  and  $\delta_6$ , which are evaluated in terms of the redundants  $X_1$  and  $X_6$ . The reaction  $B$  is the resultant of the arch thrusts  $B'$  and  $B''$ .

This case presents no new difficulty except to add one redundant condition  $X_3$ .



and another water load  $P_n$  to those involved in the previous case. No further consideration is, therefore, given to the case without sill contact.

The conventional loadings of the principal system are illustrated in Figs. 67D and E, for the case of full contact at the miter sill.

In Fig. 67D the condition  $X=0$  is represented. This embraces the total water loads on the principal system and the determinate reactions  $A_o$  and  $B_o$  resulting therefrom, when all the redundants  $X$  are removed.

Fig. 67E shows, for example, the condition  $X_3=1$ , where all loads are removed from the principal system except a unit load applied in the place of  $X_3$  and acting in a direction opposite to the direction assumed for the redundant reaction  $X_3$ . Similarly all other conventional loadings from  $X_1=1$  to  $X_n=1$  are applied one at a time. It was not deemed necessary to show them all by figures.

The external forces. Eqs. (55A) may now be applied to the principal system as above illustrated, choosing the case of  $n$  horizontal arches with, or without, miter sill contact. The only distinction between the two cases is that  $X_n=0$  for full contact, otherwise the general formulæ apply to both cases.

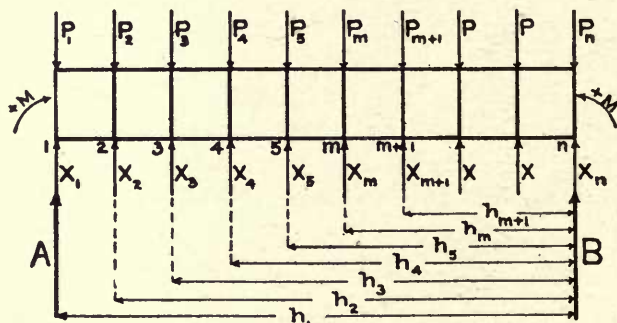


FIG. 67F.

Let Fig. 67F represent a general case of  $n$  redundants, showing the principal system on two determinate supports  $A$  and  $B$ . Also, let  $m$  be any panel point about which the moment  $M_m$  may be desired to determine the stresses in the chords of the vertical girder.

Eqs. (55A) for  $n$  redundants and moments about  $m$  become:

$$\left. \begin{aligned} A &= A_o - A_1 X_1 - A_2 X_2 - A_3 X_3 \quad \dots - A_m X_m \quad \dots - A_n X_n \\ B &= B_o - B_1 X_1 - B_2 X_2 - B_3 X_3 \quad \dots - B_m X_m \quad \dots - B_n X_n \\ M_m &= M_{mo} - M_{m1} X_1 - M_{m2} X_2 - M_{m3} X_3 \quad \dots - M_{mm} X_m \quad \dots - M_{mn} X_n \end{aligned} \right\} \quad (67A)$$

The lettered constants in Eqs. (67A) are evaluated as follows:

Condition.	<i>A</i>	<i>B</i>	<i>M<sub>m</sub></i>
$X=0$	$A_0 = \frac{1}{h_1} \Sigma_1^n Ph$	$B_0 = \frac{1}{h_1} \Sigma_1^n P(h_1 - h)$	$M_{m0} = \left(1 - \frac{h_m}{h_1}\right) \Sigma_1^n Ph - \frac{h_m}{h_1} \Sigma_1^m Ph + h_m \Sigma_1^m P$
$X_1=1$	$A_1 = \frac{1 \cdot h_1}{h_1} = 1$	$B_1 = 0$	$M_{m1} = h_m \left(1 - \frac{h_1}{h_1}\right) = 0$
$X_2=1$	$A_2 = \frac{1 \cdot h_2}{h_1}$	$B_2 = \frac{1(h_1 - h_2)}{h_1}$	$M_{m2} = h_m \left(1 - \frac{h_2}{h_1}\right)$
$X_3=1$	$A_3 = \frac{1 \cdot h_3}{h_1}$	$B_3 = \frac{1(h_1 - h_3)}{h_1}$	$M_{m3} = h_m \left(1 - \frac{h_3}{h_1}\right)$
$X_m=1$	$A_m = \frac{1 \cdot h_m}{h_1}$	$B_m = \frac{1(h_1 - h_m)}{h_1}$	$M_{mm} = h_m \left(1 - \frac{h_m}{h_1}\right)$
$X_{m+1}=1$	$A_{m+1} = \frac{1 \cdot h_{m+1}}{h_1}$	$B_{m+1} = \frac{1(h_1 - h_{m+1})}{h_1}$	$M_{m,m+1} = h_{m+1} \left(1 - \frac{h_m}{h_1}\right)$
$X_n=1$	$A_n = 0$	$B_n = \frac{1(h_1 - h_n)}{h_1} = 1$	$M_{nn} = A_n(h_1 - h_m) = 0$

The tabular values substituted into Eqs. (67A) give after considerable reduction:

$$\left. \begin{aligned}
 A &= \frac{1}{h_1} \Sigma_1^n (P - X)h \\
 B &= \frac{1}{h_1} \Sigma_1^n (P - X)(h_1 - h) \\
 M_m &= \left(1 - \frac{h_m}{h_1}\right) \Sigma_m^n (P - X)h - \frac{h_m}{h_1} \Sigma_1^m (P - X)h + h_m \Sigma_1^m (P - X) \\
 &= \frac{h_m}{h_1} \Sigma_1^m (P - X)(h_1 - h) + \left(1 - \frac{h_m}{h_1}\right) \Sigma_m^n (P - X)h
 \end{aligned} \right\} \dots (67B)$$

The last of Eqs. (67B) for  $m=1$  and  $h_m=h_1$ , gives  $M_A=0$ ; and for  $m=n$  and  $h_m=h_n=0$ , gives  $M_B=0$ , which results must follow from the conditions of equilibrium.

The same expression for  $M_m$  may also be obtained by taking the moments about  $m$  of all the external forces to either side of a section through  $m$ .

**The redundant reactions  $X$ .** The general work Eqs. (55B), when the effect of temperature is neglected, will furnish  $n$  equations for finding  $n$  redundant reactions  $X$ , as follows:

$$\left. \begin{aligned}
 X_1\delta_{1-1} + X_2\delta_{1-2} + X_3\delta_{1-3} + X_4\delta_{1-4} + \text{etc.}, + X_n\delta_{1n} + \delta_1 &= \Sigma_1^n P_m\delta_{1m} \\
 X_1\delta_{2-1} + X_2\delta_{2-2} + X_3\delta_{2-3} + X_4\delta_{2-4} + \text{etc.}, + X_n\delta_{2n} + \delta_2 &= \Sigma_1^n P_m\delta_{2m} \\
 X_1\delta_{3-1} + X_2\delta_{3-2} + X_3\delta_{3-3} + X_4\delta_{3-4} + \text{etc.}, + X_n\delta_{3n} + \delta_3 &= \Sigma_1^n P_m\delta_{3m} \\
 \text{etc.}, \quad \text{etc.}, \quad \text{etc.}, \quad \text{etc.}, \quad \text{etc.}, \quad \text{etc.}, \quad \text{to} & \\
 X_1\delta_{n1} + X_2\delta_{n2} + X_3\delta_{n3} + X_4\delta_{n4} + \text{etc.}, + X_n\delta_{nn} + \delta_n &= \Sigma_1^n P_m\delta_{mn}
 \end{aligned} \right\}, \dots (67C)$$

wherein the subscript  $m$  has all values successively from 1 to  $n$ . In all cases of double subscripts the first one always indicates the point of application of the conventional

load while the second one refers to the location of the deflection. It should also be remembered that all deflections  $\delta$ , with like double subscripts, are always equal; thus  $\delta_{2-6} = \delta_{6-2}$  and  $\delta_{m5} = \delta_{5m}$ , etc.

The double subscript bearing  $\delta$ 's are found from deflection polygons drawn for the principal system, and for each case of conventional loading, requiring  $n$  such deflection polygons for  $n$  redundants. Thus, the several *double-subscript-bearing* deflection ordinates  $\delta$  of the first of Eqs. (67c) are all obtained from a deflection polygon drawn for condition  $X_1 = 1$  acting on the principal system.

The deflections  $\delta_1, \delta_2, \delta_3$  to  $\delta_n$  are the actual displacements of the points 1 to  $n$ , of the principal system. Since these points are the points of support offered by the horizontal arch girders to the vertical girder, they represent the deflections really produced in the arch girders by the redundant reactions  $X_1$  to  $X_n$  respectively. Hence  $\delta_1, \delta_2, \delta_3$  to  $\delta_n$  cannot be determined until the redundants  $X_1$  to  $X_n$  are known, though they may be expressed in terms of the latter without increasing the number of unknowns.

Let  $d_1$  = the deflection of horizontal girder I at the point of support of  $X_1$  and due to the conventional load  $X_1 = 1$ .

$d_2$  = the deflection of horizontal girder II at the point of support of  $X_2$  and due to the conventional load  $X_2 = 1$ . Similarly for  $d_3$  to  $d_n$ . When several horizontal girders are of like sections then their deflections  $d$  become equal, thus obviating the necessity for drawing  $n$  such deflection polygons.

When the conventional deflections  $d_1, d_2, d_3$  to  $d_n$  are known, then the actual deflections  $\delta_1, \delta_2, \delta_3$  to  $\delta_n$ , due to the redundant reactions  $X_1$  to  $X_n$ , become (by the law of proportionality between cause and effect):

$$\delta_1 = d_1 X_1; \delta_2 = d_2 X_2; \delta_3 = d_3 X_3; \text{ etc., to } \delta_n = d_n X_n. \quad (67D)$$

It should be noted that in the particular case here considered, the deflection  $d_1 = \delta_{1-1}$  because the vertical girder is not deflected by the load  $X_1 = 1$  while the total displacement of the principal system at point 1 is that due to the deflection of the horizontal arch, and the vertical girder merely moves with the arch. Similarly when there is no sill contact then  $d_n = \delta_{nn}$ . These conditions make it possible to draw the deflection polygons for  $X_1 = 1$  and  $X_n = 1$  for the vertical girder.

The conventional loading for the principal system (being the vertical girder of 1 ft. thickness measured lengthwise of the horizontal girder) is taken as a unit force of say one kip = 1000 lbs. The corresponding conventional loading for the horizontal arch girders should then be one kip per foot of wetted length of the arch. Whatever loads are used, this ratio between the conventional loads of the horizontal and vertical systems must be maintained.

The values from Eqs. (67d) are substituted into Eqs. (67c), which latter are then solved by any process of elimination to obtain the  $n$  redundants  $X$ .

When these redundants  $X$  are thus evaluated for any particular case of water loads  $P_1$  to  $P_n$ , then the functions  $A, B, M_m$  and  $\delta_1$  to  $\delta_n$  may all be obtained by substitutions in Eqs. (67B) and (67D), and the problem is considered solved.



The moment  $M_m$ , will in turn furnish the chord stress in the vertical girder for the center of moments  $m$ . The reaction  $B$  will represent the pressure against the miter sill which must be considered in designing this sill.

ART 68. EXAMPLE—UPPER GATE, ERIE CANAL LOCK NO. 22

The example originally chosen for analysis was one of the huge Panama Canal lock gates with sixteen horizontal arches. After completing the drawings and computations it was deemed advisable to use a smaller gate for illustrative purposes as the theory would be less obscured by the rather extensive tabulated computations. Accordingly one of the small 1909 steel gates of the Erie Canal was used.

Figs. 68A show one leaf of this gate in elevation and two sections. There are six horizontal girders and the upstream side is covered by a  $\frac{3}{8}$ -inch sheathing plate, while the downstream side is open.

The material is soft steel with a modulus of elasticity  $E=29,000$  kips per sq.in. The quoin and miter-post cushions are made of white oak which when saturated with water becomes quite soft. According to the best available data, the modulus  $E_1$ , for such material, may be taken at about 30 kips per sq.in.

The cross-sections of the horizontal girders are shown in Figs. 68B, from which it is seen that girders II to V are exactly alike, so that there are only two different types of horizontal girders requiring analysis.

Since the sheathing plate is continuous between the girders, a certain portion of this plate will act with the flange material of each horizontal girder. It is difficult to say just how much of the sheathing will actually act in that manner, but in the present analysis a width of sixteen inches is thus included with the upstream flanges of the horizontal girders except for girder I, where the sheathing stops at the girder web, and only eight inches are included here.

The cross-sections  $F$  and moments of inertia  $I$ , of these horizontal girder sections, are computed from Figs. 68B and given in Table 68A.

TABLE 68A  
VALUES OF  $F$  AND  $I$  FOR THE HORIZONTAL GIRDERS.

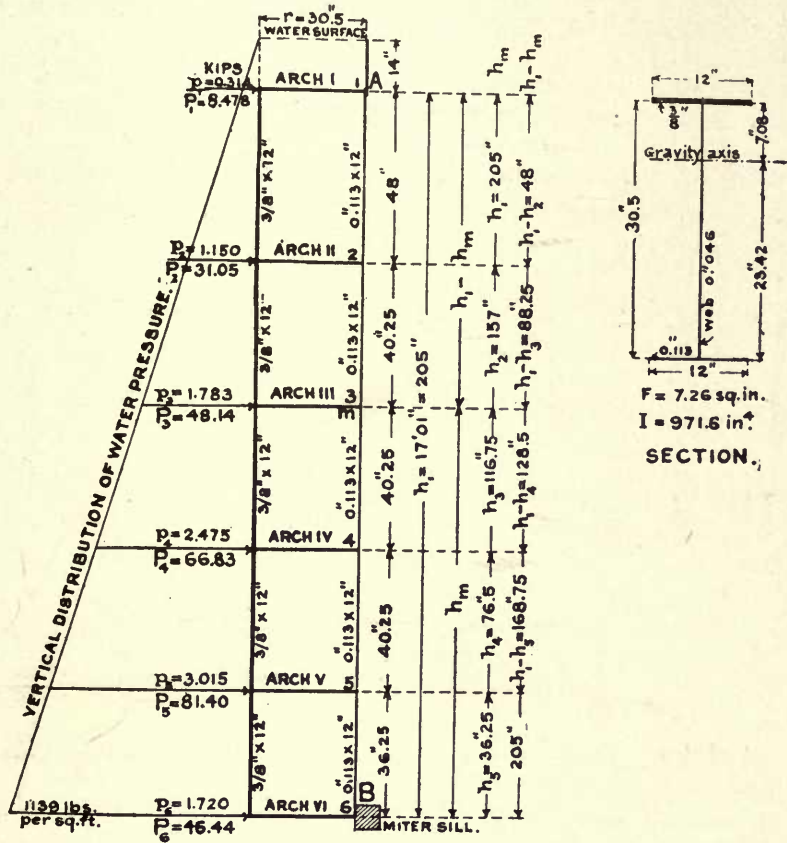
At Points	Girder I.		Girders II to V.	
	$F$ sq.in.	$I$ in. <sup>4</sup>	$F$ sq.in.	$I$ in. <sup>4</sup>
2 and 10	26.45	3740.6	30.96	4054.6
3 to 9	26.91	4120.1	31.30	4466.0

Fig. 68C shows the average vertical girder and the water loads for the gate. This girder is made up of the material which gives vertical stiffness to the gate and includes the sheathing plate on the upstream surface and such plates and angles as



extend vertically over the downstream surface. The total web may be considered as made up of three  $\frac{3}{8}$ -inch plates, one in the center of the leaf and one each at the quoin and miter posts.

The total volume of this material is then divided by the length of the gate leaf (24.3 ft.) giving the average section of the vertical girder per horizontal foot of the gate



The loads  $p$  are the water pressures in kips per foot of horizontal arch.  
The loads  $P = 27p$  are the total pressures for the horizontal girders.

FIG. 68c.

as shown in Fig. 68c. The vertical girder is thus considered as an average strip of the gate, one foot thick lengthwise of the leaf.

The water loads  $p$  are the actual pressures (in kips) per horizontal foot of gate and extend vertically from center to center of the panels between the arches. The loads  $P = 27p$  are the total pressures for the horizontal girders of wetted length 27 ft. Hence  $\sum_1^6 P$  would be the total water pressure on one gate leaf, while  $\sum_1^6 p$  would be the total load on the vertical girder with an exposed surface of  $1 \cdot h_0$ .



The deflections  $d$  of the horizontal arches are now found for the conventional loading according to the previous article. This loading should be one kip per horizontal foot of wetted length of the arch, corresponding to a conventional loading of one kip for the vertical girder one foot wide horizontally. However, in the present problem a conventional load of  $q=1/l=1/27=0.037$  kip will be used for the horizontal girders, giving deflections  $1/l$  times too small. That is, the conventional load should have been  $l$  kips on each leaf, uniformly distributed, but instead of this one kip was distributed over each leaf of 27 feet wetted length.

The deflection of a three-hinged arch under a uniformly distributed load is made up of a direct cross bending of the beam or half arch, and a deflection of the arch crown due to axial compression, as shown in Fig. 68*b*.

Let  $N_{av}$  be the average axial thrust in the half arch of length  $l$  and cross section  $F$ . Also, let  $d_c$  be the deflection at the crown normally to  $\overline{DC}$  due to a shortening  $\Delta l$  in the length  $l$  as a result of the compression  $N_{av}$ .

Then

$$\Delta l = \frac{N_{av} l}{EF} \quad \text{and} \quad d_c = \frac{\Delta l}{\tan \alpha} = \frac{N_{av} l}{EF \tan \alpha} \quad \dots \dots \dots (68A)$$

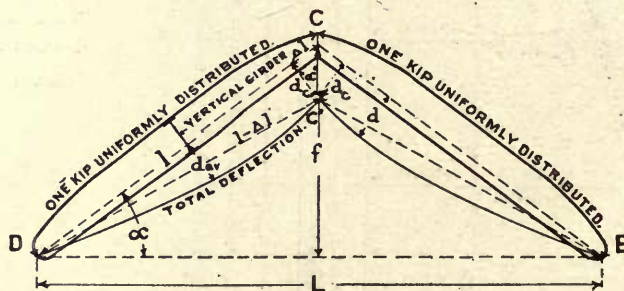


FIG. 68*b*.

The effect of  $d_c$  on the arch is merely to lower the crown to  $C'$ , leaving the beams  $\overline{DC}$  and  $\overline{CE}$  otherwise unchanged and producing the dotted deflection line  $\overline{DC'E}$ . With this must be combined the deflection due to bending and shear in the beam, finally producing the deflection curve  $\overline{DC'E}$ , with ordinates  $d$  measured normally to the girder  $\overline{DC}$ . The bending deflection will be determined from the bending moments, by the method given in Art. 39 for solid web beams.

Before proceeding to this it may be well to say a few words regarding the particular deflection  $d$  which is to be used in the solution of the problem, since this point may involve a considerable element of doubt.

In the first place the deflections must be determined in the direction normally to the girder  $\overline{DC}$ , because that is the direction of action of the water loads  $P$  and of the redundant reactions  $X$ . Ordinarily the deflections for any three-hinged arch would be taken normally to the span  $\overline{DE}$ .

The principal system was chosen as an element of average vertical cross-section of the gate and the deflection properly belonging to such a hypothetical vertical girder

would necessarily be an average deflection. Hence, the value of  $d$  which is actually used is obtained by dividing the area  $\overline{DCC'}$ , of the deflection curve  $\overline{DC'}$ , by the length  $l$  of the leaf. This average deflection  $d_{av}$ , is shown in Fig. 68D under the assumed vertical girder. See also Figs. 68F.

The bending moments for the various points of a horizontal girder, due to the load  $q=0.037$  kip per foot of wetted length, are now determined by drawing a resultant polygon through the girder and then taking the moments of the resultant normal thrust about the center of gravity of the section, as shown in Fig. 68E.

The loads  $q_1$  to  $q_{27}$  are first combined into a force polygon furnishing the resultant  $R$  and the reactions  $R'$  and  $H$ , which latter can be determined when the points  $D$  and  $C$  through which the resultant polygon shall pass, are fixed. The point  $C$  is taken in the center of the joint and the point  $D$  is taken so that the resultant  $R'$  is normal to the hollow quoin. The resultant polygon is then easily drawn and the offsets  $v$ , between it and the gravity axis of the girder, are thus found. The axial thrusts  $N$  are then scaled from the force polygon and from these and the eccentricities  $v$  the moments  $M=Nv$  are computed in Table 68B.

The elastic loads  $w=M\Delta x/I$  are also determined and from these the required deflection polygon is drawn.

TABLE 68B

ELASTIC LOADS  $w$  FOR HORIZONTAL GIRDERS.

Pt.	$N$ Kips.	$v$ Inches.	$M=Nv$ Kip in.	Horizontal Girder I.				Horizontal Girders II to V.			
				$I$ in. <sup>4</sup>	$\frac{M}{I}$	$\Delta x$ Inches	$w=\frac{M\Delta x}{I}$	$I$ in. <sup>4</sup>	$\frac{M}{I}$	$\Delta x$ Inches.	$w=\frac{M\Delta x}{I}$
D, 1	1.38	0.0	0.00		0.0	40.00	0.0126		0.0	40.00	0.0116
2	1.396	1.7	2.373	3740.6	0.00063	24.00	0.0377	4054.6	0.00058	24.00	0.0348
3	1.40	7.4	10.360	4120.1	0.00251	32.64	0.1142	4466.0	0.00232	32.64	0.1054
4	1.40	13.2	18.480	4120.1	0.00449	32.64	0.1643	4466.0	0.00414	32.64	0.1514
5	1.40	16.4	22.960	4120.1	0.00558	32.64	0.1877	4466.0	0.00514	32.64	0.1728
6	1.40	17.4	24.360	4120.1	0.00591	32.64	0.1845	4466.0	0.00545	32.64	0.1697
7	1.40	15.8	22.120	4120.1	0.00537	32.64	0.1542	4466.0	0.00495	32.64	0.1421
8	1.40	12.0	16.800	4120.1	0.00408	32.64	0.1000	4466.0	0.00376	32.64	0.0920
9	1.40	6.0	8.394	4120.1	0.00204	24.00	0.0266	4466.0	0.00188	24.00	0.0246
10	1.395	0.5	0.698	3740.6	0.00018	33.00	0.0030	4054.6	0.00017	33.00	0.0028
C, 11	1.375	0.0	0.0		0.0	316.84	0.9848		0.0	316.84	0.9072

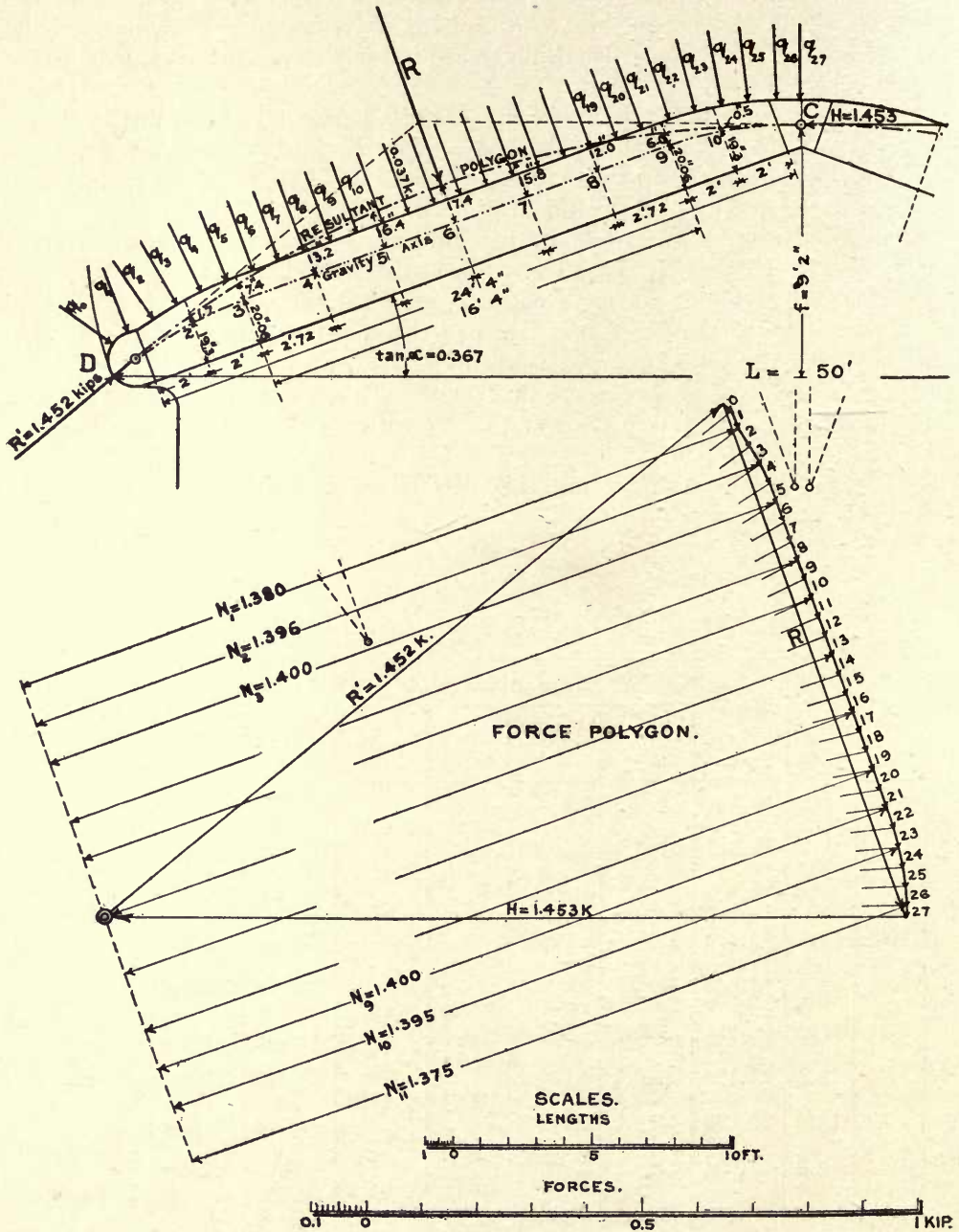


FIG. 68E.



There are two different kinds of horizontal girders, thus making two such deflection polygons necessary, one for Girder I and one for Girders II to V. The sections are given in Figs. 68B and Table 68A. The increments  $\Delta x$  are measured along the span  $\overline{DC}$  such that  $\Sigma \Delta x = l$ . All dimensions are now taken in inches and loads in kips.

According to Art. 39, an equilibrium polygon drawn for the elastic loads  $w$  with a pole distance equal to  $E=29,000$  kips, will represent the deflection polygon for the moments  $M$ , with ordinates measured to the scale of lengths of the drawing.

In Figs. 68F, the pole distances were made equal to  $H=E/20,000=1.45$ , giving deflections 20,000 times actual to the scale of lengths.

The moment deflection polygon is constructed by plotting the values  $M/I$ , from Table 68B, as ordinates at the points 1 to 11, using any convenient scale, then finding the centers of gravity  $g$  of the several trapezoidal areas of this  $M/I$  polygon and applying the loads  $w_1$  to  $w_{10}$  at these centers. The equilibrium polygon drawn for the  $w$  forces is then the moment deflection polygon, with deflections measured parallel to the direction taken for the  $w$  loads, in this case perpendicular to the chord of the girder.

The scale for the loads and the force polygon is immaterial so long as it is convenient and the pole distance  $H$  must be laid off to the scale of loads. The pole  $O$  may be anywhere to suit a convenient closing line  $\overline{D'C'}$ .

The actual moment deflection of girder I at point 6 is thus

$$\frac{3'.15 \times 12}{20000} = 0.00189 \text{ inch.}$$

The actual deflection due to shear at the same point 6, which is the point of maximum moment, is by Eq. (39D),

$$d_6' = \frac{5M_6}{2EF_1} = \frac{5 \times 24.36}{2 \times 29000 \times 30 \times 0.375} = 0.00019 \text{ inch,}$$

where  $F_1$  is the area of the web plate and  $M_6$  is taken from Table 68B.

The deflection for point 6, due to shear alone, is thus about 10 per cent of the deflection for the same point and due to moments. Hence, all the deflection ordinates are increased 10 per cent to obtain the combined moment and shear deflection polygon.

The crown deflection  $d_c$ , Eq. (68A), due to rib shortening by axial thrust, is now found.

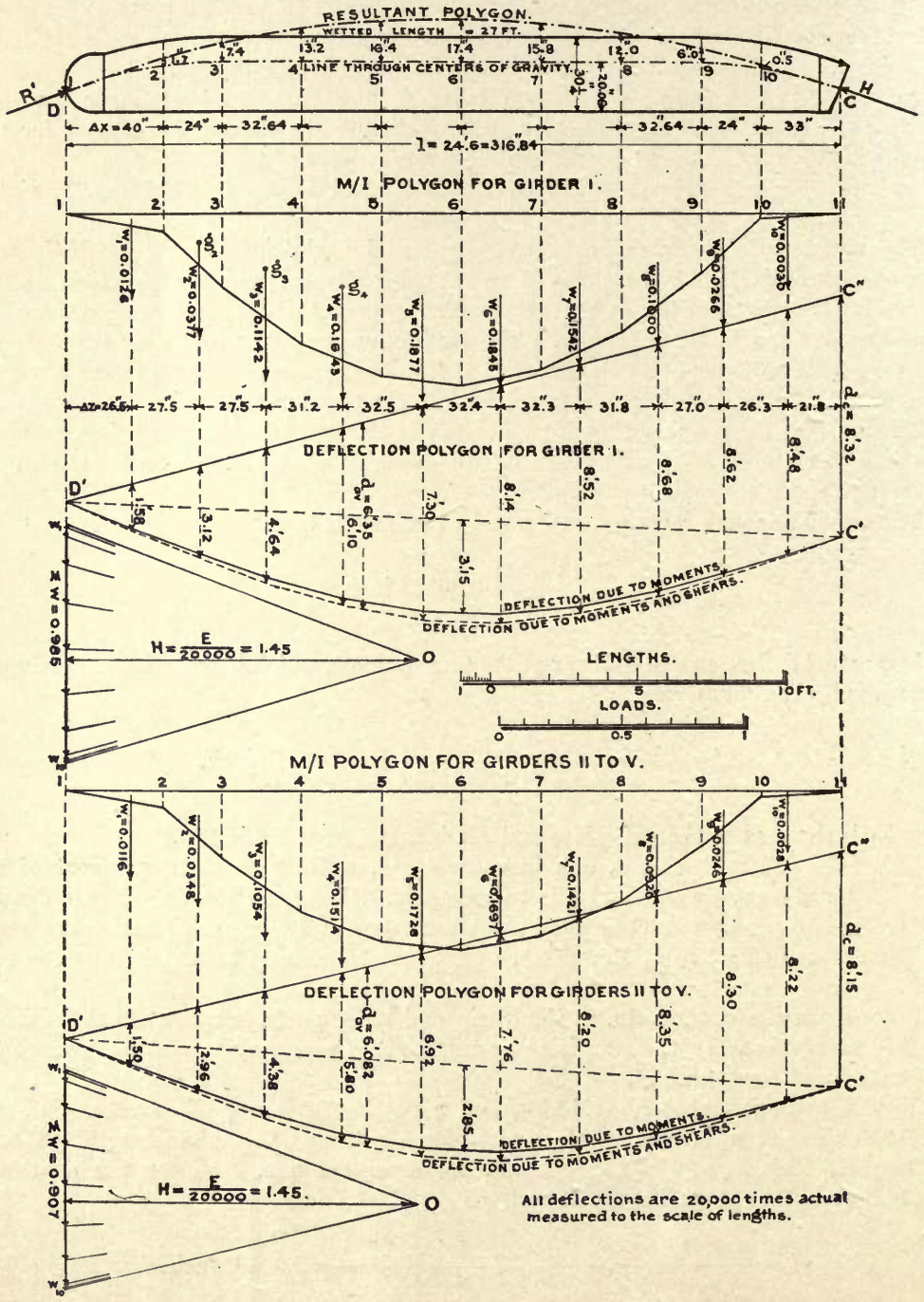
Since a portion of the gate, at the quoin and miter posts, is made of oak, which is probably saturated when the gate is in operation, it is necessary to make allowance for this condition in computing  $\Delta l$ .

For an average thrust  $N=1.4$  kips, and a net  $l=292$  inches,  $F'=26.91$  sq.in., and  $E=29,000$  kips per sq.in. for the steel part of the gate and  $l'=24.8$  inches,  $F'=24 \times 36 = 864$  sq.in., and  $E_1=30$  kips per sq.in. for saturated oak, then for  $\tan \alpha = 0.367$ , Eq. (68A) gives for the steel and oak portions

$$d_c = \frac{1.4 \times 292}{29000 \times 26.91 \times 0.367} + \frac{1.4 \times 24.8}{30 \times 864 \times 0.367} = 0.00499 \text{ inch,}$$

DEFLECTION POLYGONS OF HORIZONTAL GIRDERS

For Conventional Loading of One Kip Uniformly Distributed Over Wetted Length



All deflections are 20,000 times actual measured to the scale of lengths.

FIGS. 68F.

and 20,000 times actual in feet becomes

$$d_c = 0.00499 \left( \frac{20,000}{12} \right) = 8.32 \text{ feet.}$$

This crown deflection  $d_c = 8.32$  ft. is now incorporated in the deflection polygon for Girder I, Fig. 68F, by laying off the ordinate  $\overline{C''C'''} = d_c$  and then drawing the final closing line  $\overline{D'C'''}$  to complete the deflection polygon. The ordinates written in this diagram represent deflections 20,000 times actual in feet.

In similar manner the deflection polygon for girders II to V is drawn.

The actual moment deflection at point 6 is now  $\frac{2'.85 \times 12}{20,000} = 0.00171$  inch, and the actual deflection due to shear at the same point is

$$d_6' = \frac{5M_6}{2EF_1} = \frac{5 \times 24.36}{2 \times 29000 \times 30 \times 0.375} = 0.00019 \text{ inch,}$$

being about 11 per cent of that due to moments. Hence, the deflection ordinates are increased 11 per cent to obtain the combined moment and shear deflection polygon.

The crown deflection  $d_c$  is found as before, and all numerical values are the same except the cross-section  $F$  of the girder, which is now 31.3 sq.in. Hence

$$d_c = \frac{1.4 \times 292}{29000 \times 31.3 \times 0.367} + \frac{1.4 \times 24.8}{30 \times 864 \times 0.367} = 0.00490 \text{ inch,}$$

or 20,000 times actual in feet gives  $d_c = 8.15$  feet.

This value of  $d_c$  is now used to complete the deflection polygon for girders II to V.

The average deflection  $d_{av}$  for each girder is now computed from the ordinates taken from the deflection polygons Figs. 68F, and the distances  $\Delta z$  between these ordinates. The values  $\Delta z$  were taken in inches and the areas finally divided by the length  $l$  in inches, which eliminates the unit of length. The computations are given in the following table:

TABLE 68C  
DEFLECTIONS  $d_{av}$  FOR THE HORIZONTAL GIRDERS.

$\Delta z$  Inches.	Horizontal Girder I.		Horizontal Girders II to V.	
	$d$ * Feet.	Areas $d\Delta z$ .	$d$ * Feet.	Areas $d\Delta z$ .
26.5	0 + 1.58	20.94	0 + 1.50	19.88
27.5	1.58 + 3.12	64.63	1.50 + 2.96	61.33
27.5	3.12 + 4.64	106.70	2.96 + 4.38	100.93
31.2	4.64 + 6.10	167.54	4.38 + 5.80	158.81
32.5	6.10 + 7.30	217.75	5.80 + 6.92	206.70
32.4	7.30 + 8.14	250.13	6.92 + 7.76	237.82
32.3	8.14 + 8.52	269.06	7.76 + 8.20	257.75
31.8	8.52 + 8.68	273.48	8.20 + 8.35	263.15
27.0	8.68 + 8.62	233.55	8.35 + 8.30	224.78
26.3	8.62 + 8.48	224.86	8.30 + 8.22	217.24
21.8	8.48 + 8.32	183.12	8.22 + 8.15	178.43
316.8	Total.....	2011.76	Total.....	1926.82

\* The deflection ordinates  $d$  are 20,000 times actual in feet.



This gives for horizontal girder I,

$$d_{av} = \frac{2011.76}{316.8} = 6.35 \text{ feet, or actually } \frac{6.35 \times 12}{20000} = 0.00381 \text{ inch,}$$

and for girders II to V,

$$d''_{av} = \frac{1926.82}{316.8} = 6.082 \text{ feet, or actually } \frac{6.082 \times 12}{20000} = 0.00365 \text{ inch,}$$

which values will be used in Eqs. (67D) to obtain the deflections  $\delta_1$  to  $\delta_5$ , observing that  $d''_{av}$  for arches II, III, IV and V is the same quantity.

Attention is called to a slight oversight on Figs. 68F, where the deflection ordinates should have been measured at the numbered points 2 to 10, instead of on the lines of the  $w$  loads. The effect on the results is scarcely appreciable and therefore, the error was not corrected.

**The conventional deflections  $\delta$  of the principal system** are determined graphically in Figs. 68G and 68H, for the case of full contact at the miter sill. This requires drawing a deflection polygon for the principal system for each of the five cases of conventional loading.

The conventional loading for the horizontal arches was made equal to 1 kip, uniformly distributed over the wetted length of a gate leaf, being  $1/l = 1/27 = 0.037$  kip per foot of arch. Hence the same load  $1/l = 0.037$  kip must be employed as the conventional load for the principal system.

The deflection of the principal system is made up of the deflection of the vertical girder and the elastic displacements of the two determinate supports  $A$  and  $B$ . For full contact at the miter sill the  $B$  support is assumed as being immovable and the  $A$  support is subject to the elastic displacement of the top horizontal arch caused by a conventional load  $X = 1/l$  acting on the principal system. The elastic displacement of the point  $A$  is determined from the deflection  $d_{av}$  just found for the top horizontal arch.

For the condition  $X_1 = 1/l$ , there are no moments produced in any part of the vertical girder and hence the deflection polygon for this case of loading would show no bending effect of the vertical girder, but merely an elastic displacement of the  $A$  support which was previously found to be  $\delta_{1-1} = d_{av}$  for the top horizontal girder. Hence, this conventional deflection polygon is easily drawn and becomes a triangle  $aa'b$ , Fig. 68G, wherein the ordinate  $aa' = d_{av} = \delta_{1-1}$  for the top horizontal girder. This deflection line also furnishes the values  $\delta_{1-2}$ ,  $\delta_{1-3}$ ,  $\delta_{1-4}$  and  $\delta_{1-5}$ , which are respectively equal to  $\delta_{2-1}$ ,  $\delta_{3-1}$ ,  $\delta_{4-1}$  and  $\delta_{5-1}$ . The latter are the end ordinates at  $A$  of the several deflection polygons to be drawn for the conditions  $X_2 = 1/l$  to  $X_5 = 1/l$ .

Hence, the deflections of the *principal system* are easily found when the deflection lines of the *vertical girder* are once drawn for each of the several conventional loadings.

The deflection lines for the vertical girder are drawn, again using the method for plate girders, Art. 39. However, no allowance is made for shear because the web is too insignificant.

A set of  $w$  loads is now computed for each of the loadings  $X_2 = 1/l$  to  $X_5 = 1/l$ , and observing that the moment of inertia  $I = 971.6 \text{ in.}^4$ , for the vertical girder, is constant, it is preferable to make these loads equal to  $M\Delta x$  for a pole distance  $H = EI$ , which would give actual deflections to the scale of lengths.

For simplicity in determining the moments  $M$  and the  $w$  loads, the conventional loads  $X=1$  are used, giving moments 27 times too large. The deflections for the loads  $X=1/l$  are then obtained from

$$\delta = \frac{M \Delta x}{27EI}, \text{ using a pole distance}$$

$$H = 27EI = 27 \times 29000 \times 971.6 = 760,762,800,$$

where the dimensions are kips and inches, giving actual deflections in inches to the scale of lengths. Instead, however, the pole was made  $H = 27EI/30,000 = 25,360$  for deflections 30,000 times actual to the scale of lengths, and  $w$  loads 27 times actual.

TABLE 68D  
ELASTIC LOADS  $w$  FOR VERTICAL GIRDERS

$\Delta x$ inches.	$w$ loads for $X_2=1$ Kip.		$w$ loads for $X_3=1$ Kip.	
	$M$ for $X_2=1$ Kip. Kips and inches.	$w = M \Delta x$	$M$ for $X_3=1$ Kip. Kips and inches.	$w = M \Delta x$
48.00	$A_2=0.2341$ $B_2=0.7659$ $M_1=0.7659 \times 0.00 = 0.0$	$w_1 = 882.0$	$A_3=0.4305$ $B_3=0.5695$ $M_1=0.0$	$w_1 = 655.2$
40.25	$M_2=0.2341 \times 157.0 = 36.75$	$w_2 = 1289.6$	$M_2=0.5695 \times 48.00 = 27.3$	$w_2 = 1561.7$
40.25	$M_3=0.2341 \times 116.75 = 27.33$	$w_3 = 910.5$	$M_3=0.5695 \times 88.25 = 50.3$	$w_3 = 1674.4$
40.25	$M_4=0.2341 \times 76.5 = 17.91$	$w_4 = 539.4$	$M_4=0.4305 = 76.50 = 32.9$	$w_4 = 976.1$
36.25	$M_5=0.2341 \times 36.25 = 8.49$	$w_5 = 153.9$	$M_5=0.4305 \times 36.25 = 15.6$	$w_5 = 282.8$
	$M_6=0.2341 \times 0.0 = 0.0$	$\Sigma w = 3775.4$	$M_6=0.0$	$\Sigma w = 5150.2$

$\Delta x$ inches.	$w$ loads for $X_4=1$ Kip.		$w$ loads for $X_5=1$ Kip.	
	$M$ for $X_4=1$ Kip. Kips and inches.	$w = M \Delta x$	$M$ for $X_5=1$ Kip. Kips and inches.	$w = M \Delta x$
48.00	$A_4=0.627$ $B_4=0.373$ $M_1=0.0$	$w_1 = 429.6$	$A_5=0.823$ $B_5=0.177$ $M_1=0.0$	$w_1 = 204.0$
40.25	$M_2=0.373 \times 48.0 = 17.9$	$w_2 = 1022.4$	$M_2=0.177 \times 48.00 = 8.5$	$w_2 = 485.0$
40.25	$M_3=0.373 \times 88.25 = 32.9$	$w_3 = 1626.1$	$M_3=0.177 \times 88.25 = 15.6$	$w_3 = 770.8$
40.25	$M_4=0.373 \times 128.5 = 47.9$	$w_4 = 1420.8$	$M_4=0.177 \times 128.5 = 22.7$	$w_4 = 1058.6$
36.25	$M_5=0.627 \times 36.25 = 22.7$	$w_5 = 411.4$	$M_5=0.177 \times 168.75 = 29.9$	$w_5 = 541.9$
	$M_6=0.0$	$\Sigma w = 4910.3$	$M_6=0.0$	$\Sigma w = 3060.3$



The several conventional deflection polygons, for loadings  $X=1/l=0.037$  kip, are now drawn as illustrated in Figs. 68G and 68H. The factor 30,000 was introduced to obtain diagrams of convenient size to the scale of the drawing, and it is worthy of comment that the highest desirable accuracy may be obtained from small drawings by an appropriate choice of the scale and this factor. The scale employed for the force polygon is entirely immaterial so long as it is convenient, noting that the  $w$  loads and the pole must be measured to the same scale. The pole distance remains the same for all the diagrams and is 25,360  $w$  units.

The moment diagrams were drawn for the conventional loadings  $X=1$  to correspond with the moments in Table 68D, and serve merely to locate the centers of gravity  $g_1, g_2$ , etc., which are the points of application for the  $w$  loads.

The value  $d_{av}=0.00381$  inch, as previously found for the top horizontal arch, now furnishes  $\delta_{1-1}=30,000 d_{av}=114.3$  inches, from which the deflection line for  $X_1=1/l$  is drawn. This diagram then furnishes the deflections  $\delta_{1-2}=\delta_{2-1}$ ,  $\delta_{1-3}=\delta_{3-1}$ ,  $\delta_{1-4}=\delta_{4-1}$  and  $\delta_{1-5}=\delta_{5-1}$ , which are necessary in fixing the closing lines of the several other deflection polygons.

With this explanation the drawings should be readily understandable and will furnish all the deflections  $\delta$  required in solving Eqs. (67c).

The problem is solved completely for the case of *full contact* at the miter sill, and the method of deriving the deflections for the case of *no sill contact* is shown in Figs. 68H.

When there is no sill contact then the bottom support of the vertical girder becomes the bottom horizontal arch in the same manner as the principal system was previously formed for the top support at  $A$ , requiring now the determination of  $d'_{av}$  for the bottom arch (for a loading  $q=0.037$  k. per foot of arch) as was done for the other arches. This  $d'_{av}$  then gives  $\delta_{6-6}=30,000 d'_{av}$  for the principal system and furnishes the means of drawing the deflection polygon for condition  $X_6=1/l$  from which  $\delta_{6-5}=\delta_{5-6}$ ,  $\delta_{6-4}=\delta_{4-6}$ , etc., are obtained. These deflections then serve to complete the conventional deflection polygons for the case of *no contact* at the miter sill in the manner shown for the two conditions  $X_4=1/l$  and  $X_5=1/l$  in Figs. 68H. Hence, all the work previously accomplished in solving the case for *full contact* is also usable for the case of *no contact*, though the final deflections  $\delta$  are different in the two problems.

**The formation of the final equations** for the solution of the redundants  $X$  is now possible by introducing the numerical values for all the deflections  $\delta$  into Eqs. (67c), remembering that these were all taken 30,000 times actual, which in no wise interferes with their use in the equations.

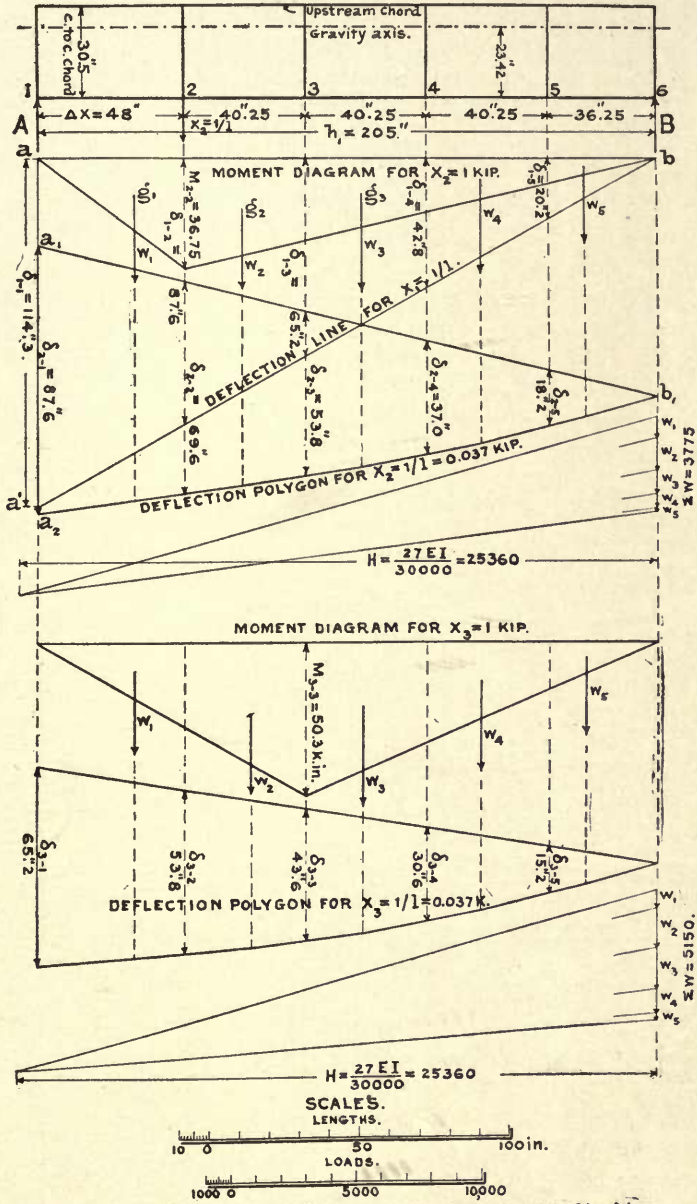
The numerical terms  $\Sigma p_m \delta_{1m}$ ,  $\Sigma p_m \delta_{2m}$ , etc., must first be computed for the actual water loads  $p$  per foot of the horizontal arches. These loads are given on the diagram Fig. 68C and represent the actual water pressures on the girders for vertical depths extending from center to center of the respective spaces between arches. Thus the load  $p_1$  is the water pressure per horizontal foot of arch and over a depth extending from the water surface down to a line 24 inches below the top arch. The load  $p_2$  is the pressure per horizontal foot of the arch included between the depths 38 inches and 82.12 inches below the surface, and so on for each girder.

The double-subscript-bearing deflections are taken from the deflection polygons in



DEFLECTION POLYGONS FOR THE PRINCIPAL SYSTEM

FOR FULL CONTACT AT MITER.  
THE CONVENTIONAL LOAD =  $1/l = 1/27 = 0.037$  KIP CON.



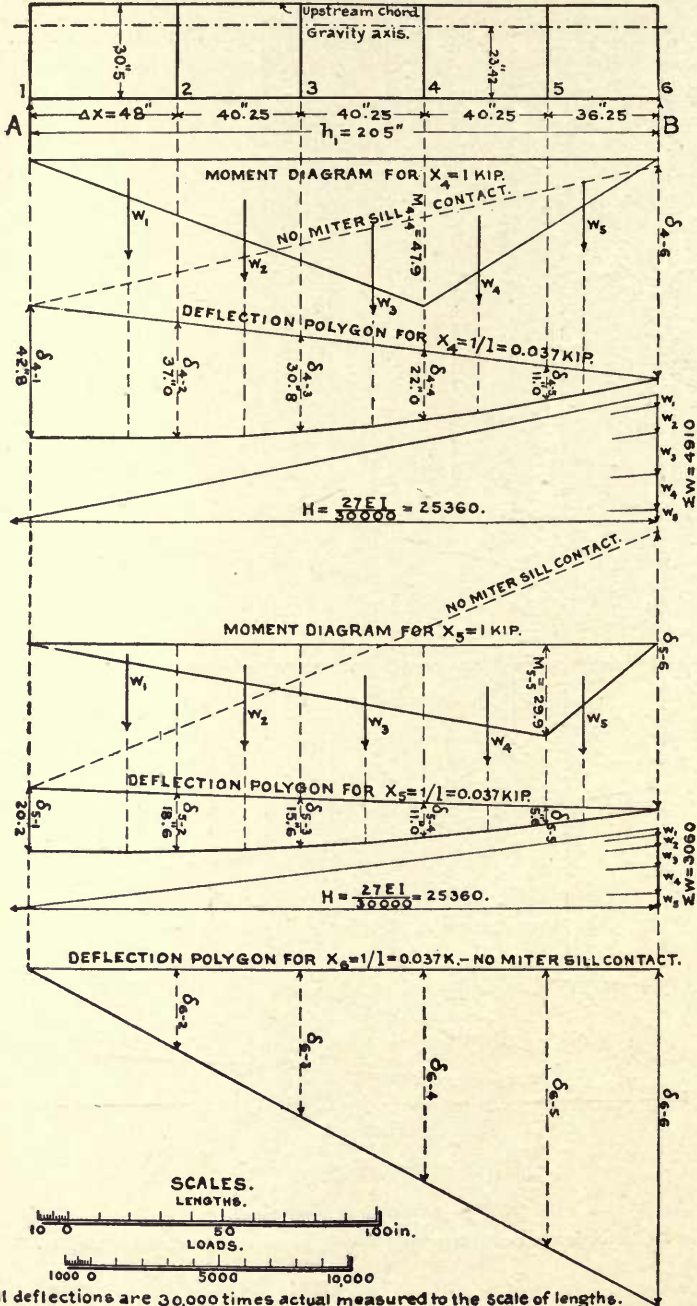
All deflections are 30,000 times actual measured to the scale of lengths.

FIGS. 68G.

DEFLECTION POLYGONS FOR THE PRINCIPAL SYSTEM

FOR FULL CONTACT AT MITER.

THE CONVENTIONAL LOAD =  $1/l = 1/27 = 0.037$  KIP CONCENTRATED.



FIGS. 68H.

Figs. 68G to H, using the values 30,000 times actual, in inches. The deflections  $\delta_1$  to  $\delta_5$  are obtained according to Eqs. (67D), using 30,000 times the deflection  $d_{av}$ , found for the horizontal arches.

All these numerical values are now entered in Table 68E, and the sum products  $\Sigma p_m \delta_{am}$  are computed, giving all required data for writing out the general equations for the redundants.

TABLE 68E  
COMPUTATION OF THE TERMS  $K = \Sigma p_m \delta_{am}$  FOR EQS. (67c)

Pt. <i>m</i>	<i>p<sub>m</sub></i> Kips.	$\delta_{1m}$	$p_m \delta_{1m}$	$\delta_{2m}$	$p_m \delta_{2m}$	$\delta_{3m}$	$p_m \delta_{3m}$	$\delta_{4m}$	$p_m \delta_{4m}$	$\delta_{5m}$	$p_m \delta_{5m}$	$\delta = d_{av} X$ Eq. (67D)
1	0.314	114.3	35.890	87.6	27.506	65.2	20.473	42.8	13.439	20.2	6.343	114.3X <sub>1</sub>
2	1.150	87.6	99.590	69.6	80.040	53.8	61.870	37.0	42.550	18.4	21.160	109.5X <sub>2</sub>
3	1.783	65.2	116.252	53.8	95.925	43.6	77.739	30.7	54.738	15.4	27.458	109.5X <sub>3</sub>
4	2.475	42.8	105.930	37.0	91.575	30.7	75.983	22.0	54.450	11.0	27.225	109.5X <sub>4</sub>
5	3.015	20.2	60.903	18.4	55.476	15.4	46.431	11.0	33.165	5.6	16.884	109.5X <sub>5</sub>
		$\Sigma p_m \delta_{1m} =$	418.565	$\Sigma p_m \delta_{2m} =$	350.522	$\Sigma p_m \delta_{3m} =$	282.496	$\Sigma p_m \delta_{4m} =$	198.342	$\Sigma p_m \delta_{5m} =$	99.070	

The summations cover all the redundants from 1 to 5 and the subscript *m* has all successive values from 1 to 5. All the values  $\delta$  are 30,000 times actual in inches.

#### FINAL EQUATIONS FOR THE REDUNDANTS

$$\begin{aligned}
 \text{Eq. (1)} \quad & X_1 \delta_{1-1} + X_2 \delta_{1-2} + X_3 \delta_{1-3} + X_4 \delta_{1-4} + X_5 \delta_{1-5} + \delta_1 = \Sigma p_m \delta_{1m} = K_1 \\
 \text{Eq. (2)} \quad & X_1 \delta_{2-1} + X_2 \delta_{2-2} + X_3 \delta_{2-3} + X_4 \delta_{2-4} + X_5 \delta_{2-5} + \delta_2 = \Sigma p_m \delta_{2m} = K_2 \\
 \text{Eq. (3)} \quad & X_1 \delta_{3-1} + X_2 \delta_{3-2} + X_3 \delta_{3-3} + X_4 \delta_{3-4} + X_5 \delta_{3-5} + \delta_3 = \Sigma p_m \delta_{3m} = K_3 \\
 & \text{etc.} \qquad \qquad \text{etc.}
 \end{aligned} \quad (68B)$$

After substituting the numerical values from Table 68E, the following equations are obtained:

$$\begin{aligned}
 (1) \quad & 114.3X_1 + 87.6X_2 + 65.2X_3 + 42.8X_4 + 20.2X_5 + 114.3X_1 = 418.56 \\
 (2) \quad & 87.6X_1 + 69.6X_2 + 53.8X_3 + 37.0X_4 + 18.4X_5 + 109.5X_2 = 350.52 \\
 (3) \quad & 65.2X_1 + 53.8X_2 + 43.6X_3 + 30.7X_4 + 15.4X_5 + 109.5X_3 = 282.50 \\
 (4) \quad & 42.8X_1 + 37.0X_2 + 30.7X_3 + 22.0X_4 + 11.0X_5 + 109.5X_4 = 198.34 \\
 (5) \quad & 20.2X_1 + 18.4X_2 + 15.4X_3 + 11.0X_4 + 5.6X_5 + 109.5X_5 = 99.07
 \end{aligned} \quad (68c)$$

The terms are now collected in the above equations and the solution is carried out in the following tabular forms:



TABLE 68F—SOLUTION OF THE EQUATIONS

Operations.	Coefficients of the X's.					Numerical Term K.
	X <sub>1</sub>	X <sub>2</sub>	X <sub>3</sub>	X <sub>4</sub>	X <sub>5</sub>	
Eq. (1).....	228.6	87.6	65.2	42.8	20.2	418.56
Eq. (2).....	87.6	179.1	53.8	37.0	18.4	350.52
$\frac{87.6}{228.6}$ [Eq. (1)] = 0.383[Eq. (1)]		33.55	24.97	16.39	7.74	160.31
Eq. (2) <sub>1</sub> = Eq. (2) - 0.383[Eq. (1)]		145.55	28.83	20.61	10.66	190.21
Eq. (3).....	65.2	53.8	153.1	30.7	15.4	282.50
$\frac{65.2}{228.6}$ [Eq. (1)] = 0.285[Eq. (1)]		24.97	18.58	12.20	5.76	119.29
Eq. (3) <sub>1</sub> = Eq. (3) - 0.285[Eq. (1)]		28.83	134.52	18.50	9.64	163.21
$\frac{28.83}{145.55}$ [Eq. (2) <sub>1</sub> ] = 0.198[Eq. (2) <sub>1</sub> ]			5.71	4.08	2.11	37.66
Eq. (3) <sub>2</sub> = Eq. (3) <sub>1</sub> - 0.198[Eq. (2) <sub>1</sub> ]			128.81	14.42	7.53	125.55
Eq. (4).....	42.8	37.0	30.7	131.5	11.0	198.34
$\frac{42.8}{228.6}$ [Eq. (1)] = 0.187[Eq. (1)]		16.39	12.20	8.00	3.78	78.27
Eq. (4) <sub>1</sub> = Eq. (4) - 0.187[Eq. (1)]		20.61	18.50	123.50	7.22	120.07
$\frac{20.61}{145.55}$ [Eq. (2) <sub>1</sub> ] = 0.142[Eq. (2) <sub>1</sub> ]			4.08	2.92	1.51	27.01
Eq. (4) <sub>2</sub> = Eq. (4) <sub>1</sub> - 0.142[Eq. (2) <sub>1</sub> ]			14.42	120.58	5.71	93.06
$\frac{14.42}{128.81}$ [Eq. (3) <sub>2</sub> ] = 0.112[Eq. (3) <sub>2</sub> ]				1.62	0.84	14.06
Eq. (4) <sub>3</sub> = Eq. (4) <sub>2</sub> - 0.112[Eq. (3) <sub>2</sub> ]				118.96	4.87	79.00
Eq. (5).....	20.2	18.4	15.4	11.0	115.1	99.07
$\frac{20.2}{228.6}$ [Eq. (1)] = 0.0884[Eq. (1)]		7.74	5.76	3.78	1.78	37.00
Eq. (5) <sub>1</sub> = Eq. (5) - 0.088[Eq. (1)]		10.66	9.64	7.22	113.32	62.07
$\frac{10.66}{145.55}$ [Eq. (2) <sub>1</sub> ] = 0.0732[Eq. (2) <sub>1</sub> ]			2.11	1.51	0.78	13.92
Eq. (5) <sub>2</sub> = Eq. (5) <sub>1</sub> - 0.073[Eq. (2) <sub>1</sub> ]			7.53	5.71	112.54	48.15
$\frac{7.53}{128.81}$ [Eq. (3) <sub>2</sub> ] = 0.0585[Eq. (3) <sub>2</sub> ]				0.84	0.44	7.34
Eq. (5) <sub>3</sub> = Eq. (5) <sub>2</sub> - 0.058[Eq. (3) <sub>2</sub> ]				4.87	112.10	40.81
$\frac{4.87}{118.96}$ [Eq. (4) <sub>3</sub> ] = 0.041[Eq. (4) <sub>3</sub> ]					0.20	3.23
Eq. (5) <sub>4</sub> = Eq. (5) <sub>3</sub> - 0.041[Eq. (4) <sub>3</sub> ]					111.90	37.58

$$X_5 = \frac{37.58}{111.9} = 0.3358$$

The solution of the equations is completely given in Table 68F, which also illustrates the method. The successive operations are expressed in the first column in unmistakable language, and the order of performing the computations is to work down the table first entering the given equations, then obtaining the products  $f$  [Eq. (1)] down through each sub-table, and finally making the subtractions. At this point apply the following checks: Note that the symmetric values must be the same and that the terms included between the double-ruled lines and those in the columns headed  $K$  are not checked. Therefore, check the latter terms by repeating the numerical work and check the symmetric terms by inspection. Then proceed with the work of obtaining the products  $f''$  [Eq. (2)<sub>1</sub>] and repeat the same programme above outlined.

The final Eq. (5)<sub>4</sub> gives the value of  $X_5=0.3358$  kip per horizontal foot of horizontal girder V. The other redundants are then determined from the equations in the last sub-table of Table 68F by successive substitutions as indicated in the following Table 68G.

TABLE 68G  
THE VALUES X BY SUBSTITUTION

Terms.	$X_1$	$X_2$	$X_3$	$X_4$	$X_5$
$K=$	99.07	62.07	48.15	40.81	37.58
$X_5C_5$	-38.65	-38.02	-37.79	-37.64	
$X_4C_4$	- 7.16	- 4.70	- 3.72	-37.64	$X_5 = \frac{37.58}{111.9}$
$X_3C_3$	-13.58	- 8.50	-41.51	3.17	=0.3358
$X_2C_2$	-18.73	-51.22	6.64	$X_4 = \frac{3.17}{4.87}$	
	-78.12	10.85	$X_3 = \frac{6.64}{7.53}$	=0.6509	
	20.95	$X_2 = \frac{10.85}{10.66}$	=0.8818		
	$X_1 = \frac{20.95}{20.2}$	= 1.0178			
	=1.0371 kips per horizontal foot of gate.				

$C$  = the coefficients from the last of Tables 68F.

The redundants  $X$  are thus expressed in kips per horizontal foot of gate, representing the *average intensity* of these forces for the *average vertical stiffness* of a gate leaf.

The reactions **A** and **B** and the moments **M** for this average vertical girder, may now be found from Eqs. (67B) employing the values in the following table.





An approximate idea of the deflection curve at any vertical  $m$  other than the average, may be obtained by assuming that the same proportionately exists between the deflections  $d_{av}$  and  $d_m$  as between  $\delta_1$  and  $\delta_m$ , etc., where the point  $m$  designates any vertical section of the gate. Thus in Fig. 68f, for a vertical girder at point 8, the deflection  $d_8=8.68$  ft. for the top horizontal arch while  $d_{av}$  for that arch was 6.35 ft., giving a ratio  $d_8/d_{av}=8.68/6.35=1.367$ . For the arches II to V the ratio between similar ordinates becomes  $d_8/d_{av}=8.35/6.082=1.373$ .

Hence, in considering a vertical girder at point 8, where the deflections in the horizontal arches are about 37 per cent greater than the average, the effect on all the conventional deflections would be to increase them approximately by the same constant percentage. This would be equivalent to multiplying Eqs. (68c) by a constant 1.37 and since the water loads  $p$  remain unchanged the resulting redundants  $X$  would not be materially different than for the average vertical girder.

However, the deflections  $\delta_1$  to  $\delta_5$  would be increased throughout by the same 37 percent.

Since the ratio  $d_m/d_{av}$  is not necessarily constant, though nearly so in the present example, this proposition cannot be accepted for more than it is worth, and approximate results only can be expected.

Where a rigid determination is desirable, it would be necessary to repeat the whole computation for the actual deflections of another principal system with vertical girder at point 8. This would not involve very much labor, however, beyond solving Eqs. (68c) for a new set of numerical coefficients.

**A summary of the steps employed** in the solution of the above problem is given in closing this subject.

**Horizontal arches.** Draw a moment deflection polygon for each of the different arches, using a conventional load of one kip uniformly distributed over the wetted length of each leaf. These deflections are then combined with the arch deformation for axial thrust or rib shortening for the same loading, to obtain the total displacements of the several points of the arches with respect to the fixed quoin post supports.

These total displacements are then averaged for one gate leaf by dividing the area of the displacement polygon by the straight length of the girder, giving the deflection  $d_{av}$  for each arch. Then  $\delta=d_{av}X$ , and for the top arch  $d_{av}=\delta_{1-1}$ , while for the bottom arch  $d'_{av}=\delta_{nn}$  when there is no sill contact and  $d'_{av}=0$  when full sill contact is assumed.

**The principal system.** Draw conventional deflection polygons for the principal system, using conventional loads of  $1/l$  kips for each condition  $X=1/l$  where  $l$  is the wetted length of one gate leaf as above. This gives the conventional deflections of all panel points of the vertical girder for each condition of loading, remembering that the vertical girder represents a strip of gate one foot thick and of average cross-section.

The water loads  $p$  per horizontal foot of gate for each arch, are then used as the actual loads in computing the numerical terms  $\Sigma p_m \delta_{am}$  for each condition  $X=1/l$ . The resulting values  $X$  are then the redundant reactions of the average vertical girder against the horizontal arches per linear foot of the latter.

When the vertical girder is a truss frame instead of a plate girder, then the method of deflections given in Art. 36 must be used, neglecting the effect of the web members, as the nature of the problem does not warrant the extreme accuracy implied when the web system is considered.

## CHAPTER XV

### FIXED MASONRY ARCHES

#### ART. 69. GENERAL CONSIDERATIONS

The fixed arch is statically indeterminate in the third degree, or, as commonly expressed, it involves three redundant conditions, provided the arch ring may be treated as an elastic body.

According to the theory of elastic deformation, these redundant conditions are determined from the elastic properties of the material, while for the older "line of thrust" method the redundants are merely approximated by assigning certain assumed conditions to be fulfilled by the line of thrust.

**A line of thrust** is defined as an equilibrium polygon for any case of simultaneous loads acting on the arch ring. Hence, for any section, the adjacent elements of the line of thrust will represent the resultant of all the external forces on either side of the section, including the reactions. From this it follows that the sum of the moments of all external forces about any point on the line of thrust, or resultant polygon, must always be zero.

Therefore, if the external redundant reactions were known, then the real resultant polygon could be drawn, but since the redundants can be found only from the theory of elasticity, the line of thrust method fails to give a direct solution.

A resultant polygon may always be drawn through three given points, as will be shown later. Hence, by successive trials, a resultant polygon may be approximated so as to fulfill certain requirements which are now discussed. The line of thrust is henceforth called the *resultant polygon*, this being a more appropriate designation.

The theory of elasticity fixes the position of the resultant polygon in terms of the modulus  $E$  of the material and the elastic deformation of the arch ring. According to the older method an infinite number of resultant polygons may be constructed for the same arch and same loading, and it becomes a question to decide which of all possible lines is the most probable.

Hagen (1844 and 1862), according to his "theory of the most favorable distribution of stress," defines the most probable resultant polygon as the one for which the vertical projections of the minimum distances, between the sides of this polygon and the bounding lines of the arch ring, become equal.

Culmann (1866) advanced the theory that of all the possible resultant polygons, the most probable one must approach the arch center line in such manner as to reduce the stresses in the critical sections to a minimum. Carvallo (1853) and Durand-Claye (1867) adopted this theory with slight modifications.



The theory of elastic deformation was introduced by Navier in 1826, by his analysis of the stresses on an arch section, in which he assumes a combined thrust and bending moment distributed over the section. According to Navier, the stress on the extreme fiber of any arch section becomes

$$f = \frac{N}{F} \pm \frac{My}{I} = \frac{N}{F} \pm \frac{M}{W}, \quad . . . . . (69A)$$

where  $N$  is the normal thrust on the section,  $M$  the bending moment,  $F$  the area,  $y$  the distance from the neutral axis to the extreme fiber and  $I$  and  $W$  the moments of inertia and of resistance, respectively, of the cross-section. The formula when applied to curved beams, or arches, is not strictly accurate, but when the radius of curvature is large in comparison with the depth of the arch ring, a condition which always obtains in ordinary arches, then the error due to omitting curvature is extremely small and is never considered.

The experiments of Bauschinger (1834–93), Koepeke (1877), and the Austrian Society of Engineers and Architects (1895), have substantiated the correctness of the theory of elasticity within knowable limits of the elastic properties of building materials.

Nearly all modern writers on this subject adopt Navier’s law as the basis of investigation. The various arch theories by Winkler (1867), Mohr (1870), Belpaire (1877), J. Weyrauch (1878), F. Engesser (1880), Mueller-Breslau (1880), and those of American writers, differ principally in manner of presenting the subject. Each author has contributed something in the direction of rendering the theory of elasticity more usable, and this is especially desirable even at the present time.

Professor Winkler was the first to prove that the *most favorable resultant polygon* in an unsymmetric arch must intersect the arch center line in at least three points, while for symmetric arches four such intersections are necessary. He also proved that according to the theory of elasticity the *most probable resultant polygon* is the one for which the residual departures from the arch center line become a minimum, according to the method of least squares. This then furnishes the real criterion with which to judge an arch design in connection with certain other limitations to be discussed later.

The common graphic solution is nothing more than the application of the principles of the three-hinged arch to the fixed arch by assuming the location of the hinged points, at the crown and springing. The location of these hinged points may be altered until such a resultant polygon is found as will approach the arch center line in the manner required by the theory of elasticity.

The most probable resultant polygon, when found, must remain within the middle third of the ring, when tensile stress is not permissible. This follows from Eq. (69A). Hence, it is clear that the most economic masonry arch is one for which the center line coincides most closely with the resultant polygon drawn for the case of average or half total live load, provided the arch ring has sufficient thickness at all points to prevent excessive unit stresses due to unsymmetric loading. This idea will be followed out in treating of methods for preliminary designs.

Formerly an arch problem was considered solved, when, for a given span, rise and loading, a resultant polygon could be found which, for the critical position of the live load, remained entirely within the middle third of the ring. However, this is far from



constituting an acceptable solution, as will be shown in the following. The fact that most arches have stood so well is no defense of this method of designing, especially when it is understood that the usual factor of safety employed in such designs ranges between ten and sixty, rarely going below twenty.

Furthermore, solid spandrel arches are usually designed with very high safety without considering the additional carrying capacity of the masonry in the spandrel, which is often sufficient to sustain the loads without regard to the ring.

The author adds the criticism that few fixed arches exist which are not disfigured by unsightly cracks and this, in conjunction with the very wasteful expenditure of material necessitated by low unit stresses, constitutes a fertile field for doubt regarding the expediency and justification of building fixed arches in this progressive age.

While it is freely admitted that these masonry structures, many of which are monumental in character, have stood well, and will undoubtedly continue to stand, every engineer must agree that a cracked arch is neither an achievement nor the ultimate aim of his ambition, to say nothing of the dissatisfaction which such a blemish constitutes to both engineer and owner.

Practically, the objections to fixed masonry arches may seem trivial and mostly a matter of sentiment, while theoretically they are important. The remedy for all these objections is to introduce hinged joints during construction or preferably for all time. This has been practiced in Germany since 1880, and has given excellent satisfaction, though many fixed arches are still being built. This will continue to be the case so long as we do not come to recognize that "new truths are better than old errors." \*

The theory of elasticity is most applicable to arches of small depth of ring and high rise, and the analysis of stresses will be more accurate the nearer the shape of the arch center line coincides with the resultant polygon for average loading.

This is true when dealing with the arch ring alone, as the ring is the only portion of an arch which could be expected to follow the laws of elastic deformation. Hence, in order that the theory shall be at all applicable, the relation between the arch ring and its spandrel filling must be such as to allow the ring perfect freedom to undergo elastic deformations.

The style of structure which best satisfies this requirement is one where the arch ring supports the roadway on a succession of piers, producing what is called an open spandrel filling. Even here the roadway should be provided with expansion at one end.

Any other style of spandrel will introduce further redundants which are wholly beyond analysis, because the spandrel is then subjected to bending and direct stress the same as the ring.

Therefore, to apply the theory of elasticity or in fact any theory, to a solid spandrel fixed arch is, in the author's opinion, a mere waste of time which should be expended in a more profitable pursuit. In the following, nothing but open spandrel arch bridges are dealt with.

While the theory of elasticity is undoubtedly the only trustworthy basis for the

---

\* See paper by the author on Three-Hinged Masonry Arches, Trans. Am. Soc. C. E., Vol. XL, 1898, p. 31.

analysis of fixed arches, and should always be employed in designing structures of any importance, it does not follow that the older methods of investigation, and many of the empiric rules in common use, are all worthless. On the contrary, the preliminary design can be carried out most efficiently by the aid of these simpler methods, and the final design should then be tested by the application of the more exact method of the theory of elasticity.

The theory of fixed arches has reached a status of perfection quite in keeping with the nature of the problem, the still existing uncertainty being a function of the material and other circumstances, depending on the rigidity of the abutment foundations, conditions of erection, etc., all of which can never be definitely known nor be entirely eliminated in the best designs.

When the loading is not known with considerable accuracy, as for arches sustaining high earth banks, the design must necessarily remain more or less indefinite, though the elastic property of the superimposed earth assists greatly in distributing pressures and rendering conditions more favorable. Also in dealing with small arches, such as culverts and road crossings, the resultant polygon theory will probably continue to be the only method of approximate analysis.

#### ART. 70. MODERN METHODS OF CONSTRUCTION

Many difficulties are encountered in the construction of fixed masonry arches, owing particularly to insufficient elasticity in masonry. The natural deformations in the arch, caused by shrinkage of the masonry or concrete, due to the setting process, stress and temperature, usually cause cracks, which, while rarely of a serious character, are reasons for discouragement to the engineer, who has probably applied every known precaution to prevent their occurrence.

So long as there are no abutment displacements after completion of an arch, the above difficulties may be fairly well controlled. However, when an arch was designed for certain allowable unit stress on the extreme fiber at the critical points, then, if the structure is to be regarded safe for all time, the original stress must not be exceeded even when the material increases in strength (as by setting of the cement) or when the arch or its abutments undergo slight elastic or permanent displacements. For this there is absolutely no assurance, though it is an essential necessity in the general assumption.

If an arch ring could be built in such manner that its resultant polygon would pass through the center of the ring at the crown and springing points at the time of releasing the falsework, a large proportion of the redundant stress could be prevented. In other words, the bending moments at the critical points would then be almost zero for symmetric loading, reserving the strength for the unsymmetric live load and other contingencies affecting the shape of the arch ring.

By the ordinary process of construction, the arch is commenced at the abutments and the load is gradually applied to the falsework, thus distorting the latter and causing bending stresses in the completed portion of the ring. The final settling of the ring, produced by the contraction of the mortar or concrete, as a result of compression and shrinkage during setting, even when the abutments remain immovable, are sufficient



to create serious initial stresses, thus destroying to a large extent the usefulness of the structure and frequently cracking the arch.

Several methods have come into use by which these initial arch stresses may be more or less completely prevented. One of the oldest of these consisted in setting the arch stones on the entire falsework, spacing the joints by small strips of wood, and lastly filling all the joints simultaneously with mortar. This is still a very good programme for construction of small arches, but not so well adapted to large structures, owing to the excessive stresses produced in the falsework, frequently causing considerable settlement before the ring can be closed. However, the falsework could be wedged up just previous to filling the joints.

Another method, frequently employed in the construction of brick and concrete arches, is to close a complete ring adjacent to the falsework, and after allowing this course to set firmly, the remainder of the arch is completed, thus carrying the load by the first ring rather than by the falsework. By this means the settlement during construction becomes very slight, but, as is readily seen, the intrados is excessively stressed, a condition which cannot be averted and which is highly objectionable.

A programme of construction frequently followed on large arches is to commence work simultaneously at two, four or six points of the ring and closing at three, five or seven points, respectively. The larger the span the greater the number of points of commencement.

The most modern method consists of the introduction of temporary flexible or hinged joints at the crown and springing and following the last-mentioned programme of construction. These flexible joints are made of stone with curved roller-like surfaces; or iron blocks may be used. By this means the resultant polygon becomes determinate during the period of construction. After the falsework is removed and the structure has assumed a normal condition of stress, these open joints are grouted with cement mortar.

Sheet lead or lead blocks have also been used for this purpose, allowing sufficient surface of contact on the arch center line to carry the pressure without causing the lead to flow. A safe allowable pressure for lead is from 1000 to 1500 lbs. per sq. in.

The author would recommend an alloy of lead with from 5 to 10 per cent of copper added, thus permitting an allowable unit stress of about 2500 lbs. per sq. in. The last mentioned method gives very good results in preventing cracks and excessive stresses, during construction, but subsequent abutment displacements or other changes cannot be compensated and still remain as a serious objection to this class of structure. Eventual settlements in foundation masonry, contraction of mortar or concrete due to setting and drying out; compression due to loading, elastic deformations caused by temperature and load effects—all these influences are ever present to create stresses which, in spite of all precautions during construction, may attain dangerous proportions and make it utterly impossible to estimate the ultimate strength of a fixed masonry arch.

However, it should be remembered that, for masonry arches, the live load is generally a small fraction of the dead load, and for this reason an arch which is sufficiently strong to sustain its own weight permanently will carry temporary live loads with perfect safety.



Masonry arches possess the redeeming feature that when stressed to the breaking limit the masonry generally chips near the surface, thus relieving the stress and allowing the resultant polygon to return to a more favorable position. In this manner an arch which has become distorted may readjust itself to a new condition of stress.

Hence fixed masonry arches, in view of their past history, cannot be condemned on account of insufficient safety which they afford, but because masonry is not a suitable material from the criterion of inability to withstand elastic deformations well. A fixed plate girder arch would be a far more rational structure than a fixed masonry arch, though the former would require frequent painting and even then might deteriorate and thus outlive its usefulness earlier than the masonry structure. But from an engineering standpoint the plate girder would probably be more satisfactory because it would not open up cracks and thus bring discredit to the designer and builder.

In this connection it may be of interest to recall the recommendations proposed by the Austrian Society of Engineers and Architects, which, if strictly carried out, would limit the application of fixed masonry arches to comparatively short spans with bed rock foundations. These recommendations require the fulfillment of the following conditions:

1. The abutments must be perfectly rigid.
2. The falsework must retain its form during the period of construction of the arch ring.
3. The masonry must be of the best quality.
4. The construction of the arch ring must be most carefully conducted.
5. The falsework must not be released until the cement has thoroughly set.
6. When the falsework is finally released, it must be done gradually and uniformly.
7. To this the author adds that the arch ring should be closed at the lowest possible temperature.

The use of sand jacks or sand pots, which was introduced in 1854 during the construction of the Austerlitz Bridge, in Paris, offers a very novel and efficient means of releasing falsework.

The necessity of these recommendations is clearly understood after what has been said regarding the theory of fixed masonry arches and its practical applications and limitations.

The two first conditions can be realized only when rock foundations are available. The other requirements can generally be fulfilled by exercising proper care and by permitting nothing other than first-class materials and workmanship.

From the above review of the subject and actuated by many years of practical experience, the author ventures the following opinion as to the general advisability of adopting the fixed type of masonry arch for any particular case in hand: If the span  $l$  is moderate and the rise  $h$  comparatively high, such that  $l/h$  will be between two and four, then for bed rock foundation and open spandrels the fixed masonry arch may be chosen as an appropriate type of structure. The design for such a bridge should be based on a factor of safety of at least ten, allowing no tension unless carried by steel reinforcement, and after the preliminary design is completed it should receive a final analysis according to the theory of elasticity.

When all this is followed by a most careful and approved system of construction, it may frequently happen that the results will not prove entirely satisfactory to the engineer. However, such a structure will be certain to last well, to cost little or nothing for maintenance, and to be safe practically for all time, even though small cracks may appear at any time after removing the falsework.

On the other hand, when the spandrel filling must for some reason be made solid, and bed rock foundations are not available, also when the span is great and the rise small, a fixed masonry arch should never be built. A hinged arch is the only rational solution for such a case in the light of modern engineering experience, and that type can be employed only when the spandrels can be so arranged as to allow of proper expansion or rotation at the hinged points.

All this applies strictly to bridges and not to small arched culverts and floors where the hinged type is in many ways impracticable and the fixed type, preferably of reinforced concrete, has given good satisfaction.

It is thus seen that the successful construction of a large masonry arch may justly be considered a masterpiece of engineering achievement and requires far more intimate knowledge and experience than is required for a steel structure of the same span.

Masonry and concrete are materials which are solely adapted to carrying compressive stress. Hence, it is rational to reinforce this material to better resist tensile stress by the introduction of steel, but this should be confined within proper limits and with the sole aim of developing thereby the otherwise latent capacity of the material to do work in compression.

When, therefore, steel is used to reinforce concrete in compression, the result is bound to be wasteful, unprecedented, and a monument to engineering misconception. Designs of this kind should be discountenanced, both from an æsthetic as well as from an engineering standpoint, because they imply a misapplication of the true purpose of both masonry and steel.

## ART. 71. PRELIMINARY DESIGNS

On the supposition that a fixed masonry arch is feasible only when the foundations are rigid, it is fair to assume that the fixed conditions will remain unchanged even though the transmission of stress may call forth very slight elastic changes in the abutments.

In any problem the given data are usually the live load to be carried, the clear span and the clear rise of the intrados and the allowable unit stress. The elevation of the roadway is also known.

The preliminary design would then include a reasonably accurate determination of the thickness and shape of the arch ring at all points over the span.

To accomplish this, it is necessary first to decide on the general outlines of the bridge, particularly on the design of the spandrel filling and the roadway, which should be completely detailed before proceeding to the design of the arch ring. By this means a large portion of the dead load can be accurately estimated, leaving the bare arch ring as the only variable portion of the dead load.



Since the dead load for masonry arches is usually large compared with the live load this procedure is clearly indicated.

The next step should be to determine the axis of the arch ring so that it will coincide with the resultant polygon for an average load, which latter is taken as the dead load plus half the uniformly distributed live load. In preliminary designs the live load, whatever it may be, is always taken as uniformly distributed.

The shape of the arch center line thus obtained will be the one yielding the most economic sections for the unsymmetric maximum and minimum live loads.

However, this center line cannot be directly found because the resultant polygon upon which it depends must be determined before the dimensions of the arch ring and its weight are definitely known.

Hence, this part of the problem must be solved by successive approximations and trials. We must seek to find such an arch ring for which the resultant polygon will coincide approximately with the center line.

With the aid of approximate formulæ, the thicknesses of the arch ring at the crown and abutments are determined, and from these the radius of curvature at the crown is approximated to find the first arch center line. The weight of this arch ring is now estimated and combined with the weight of roadway and half live load, and a resultant polygon is then drawn through the centers of the crown and springing sections. This then gives a criterion as to the modifications required to make a second approximation for a correct center line. This process is continued until a center line is found which coincides closely with the resultant polygon.

The maximum stress for unsymmetric loading is now estimated from another resultant polygon drawn for the critical quarter points and this then furnishes the criterion for the thickness of the arch ring. If this stress is sufficiently close to the allowable stress, the preliminary design may be accepted and the final rigid analysis may then be undertaken. Otherwise further alterations in the dimensions must be made until the preliminary design is sufficiently close to the assigned requirements.

The approximate formulæ and method of conducting this investigation will now be given, and this will constitute a complete solution as far as is possible by the use of the older, resultant polygon method.

Fig. 71A represents a symmetric arch ring of unit thickness. If the arch were slightly unsymmetric, the present solution might answer for the symmetric portion and the resultant polygon could afterward be extended into the unsymmetric portion which was omitted in the first analysis. However, this could not be done in the final rigid analysis by the theory of elasticity and should never be considered for badly unsymmetric structures.

All pressures and loads will be expressed in terms of cubic feet of masonry per square foot of surface, so that all areas on the drawing represent true relations of loads from which actual weights are obtained by multiplying the areas by the weight of one cubic foot of masonry. This is the most convenient unit for graphic solutions, as it does away with estimating the weight of the arch ring and spandrel filling.

The following data are supposed to be given: The system of loading; width of roadway; span and rise of intrados; and the allowable unit stresses of the masonry or concrete.





For the unsymmetric live load, extending over half the span to the center, the following value of  $D_0$  is obtained:

where

$$\left. \begin{aligned} D_0 &\geq \sqrt{G + 0.31ph_0} - G \\ G &= \frac{1}{2} \left( q + \frac{p}{2} + \frac{h_0}{10} \right) \end{aligned} \right\} \text{ for feet or meters, . . . . . (71B)}$$

When the value from Eq. (71B) exceeds that given by Eq. (71A) then the larger dimension should be adopted.

It is clearly seen that the full allowable unit stress  $f$  could not be taken in the above formulæ, because this average case of loading will stress the arch ring only about half as much as when the resultant polygon passes through the middle third points. In all arch designs where tensile stresses are prohibitive, this condition will govern.

The next step is to choose a preliminary shape for the intrados such that, for the case of dead load plus half live load over the whole span, the resultant polygon will exactly coincide with the arch center line.

At this point all theory fails and the judgment and experience of the engineer must guide in making a suitable first approximation. However, the following practical suggestions will serve a valuable purpose.

Theoretically the intrados can never be a true circle nor a true parabola for any arch which is made to follow the resultant polygon, as above required, for economic reasons.

The resultant polygon becomes a parabola when the total load is uniform per foot of arch. This can never happen in a real arch, even if the spandrel filling were neglected, because the stresses in the arch ring increase from the crown toward the abutments, thus necessitating a variable thickness of ring, increasing with the stress.

On the other hand the resultant polygon becomes a circle when the superimposed load at the springing points becomes infinite, a condition which is never attainable.

Hence an arch of economic design and shape to fit the resultant polygon for average loading will have an intrados which is neither a circle nor a parabola, but a curve lying between these two.

Having thus established the limits between which the true intrados must be situated and knowing from experience that the true line falls nearer to the mean of the two curves than to either one of them, for all open spandrel arches, it becomes an easy matter to approximate the intrados.

Hence, for open spandrels with roadway supported on piers or columns, the intrados may safely be taken half way between the circle and the parabola, both drawn through the three given points of the intrados.

The radius of the circle is given by the formula

$$r = \frac{l_0^2}{8h_0} + \frac{h_0}{2}, \quad . . . . . (71c)$$

and the parabola passing through the same three points is

$$y = \frac{4h_0x^2}{l_0^2}, \quad . . . . . (71d)$$

which gives the coordinates  $y = h_0/4$  and  $x = l_0/4$  for the quarter points, see Fig. 71A.







If this resultant polygon remains within the middle third at every point and crosses the axial line in at least three points, then the design is acceptable. If the polygon does not touch the middle third point at the two critical sections  $m$  and  $s$ , Fig. 71A, then the ring is too thick. If the polygon goes outside the middle third at one of these sections and remains inside at the other, then the point  $n$  should be shifted and a new polygon should be passed through  $a$ ,  $b$ , and  $n$ . However, if the resultant polygon passes outside the middle third at both critical sections, then the arch ring must be made thicker and the investigation is then repeated.

Lastly the stresses at the four sections  $a$ ,  $m$ ,  $n$ , and  $b$  must not exceed the allowable unit stress as given by Eq. (69A).

When all these requirements are fulfilled, the crown section should be tested for full live load over the entire span, which is easily done from the loads already found for the half span, since this is a case of symmetric loading.

This then constitutes a complete design according to the ordinary graphic method, and the arch ring so found should now be subjected to a rigid analysis according to the theory of elasticity which follows.

The above outline will be exemplified more fully when presenting a problem at the close of this chapter.

The criterion for position of moving loads to produce maximum and minimum stress is discussed in another place.

## ART. 72. DETERMINATION OF THE REDUNDANT CONDITIONS BY THE THEORY OF ELASTICITY

**Introductory.** A fixed, solid web arch must be treated as a structure with three external redundant conditions according to Eq. (3c) and Fig. 3f. Hence there is very little difference between a fixed framed arch and a fixed solid web or masonry arch, since the complications arising from external redundancy are alike in both cases while the internal stresses must be found by the methods peculiar to frames and isotropic bodies, respectively.

The method of treating the external redundant conditions involves the use of deflection polygons for the determinate principal system, and in this connection a further difference exists in the manner of determining the elastic loads for the two types of fixed arches.

The elastic loads  $w$  for a framed structure are easily expressed in terms of the geometric relations existing between the members and the angles composing the frame. For isotropic bodies the elastic loads are functions of the cross-sections obtained by integration and expressed in terms of moments.

Hence, with due regard to these differences, which are easily distinguished, both framed and solid web, fixed arches may be analyzed in precisely the same manner. However, the general subject of solid web and masonry arches involves many considerations not met with in framed arches. For this reason the solid web arch will be treated in full detail in the following articles.

Regarding the reliability of the method, which is based on the theory of elasticity,

the author would add here that for steel arches, either framed or solid web, the method is entitled to full confidence, while for stone and concrete it is reliable when the design is based on the condition that tensile stress does not occur. In attempting to design in concrete for *equal* tensile and compressive stress by reinforcing with steel, the method must be regarded as more or less approximate, since it involves the modulus  $E$  of the material, which is quite uncertain owing to the heterogenous character of masonry and concrete generally, and especially when the latter is combined with steel. The introductory remarks of Art. 52 are especially applicable here.

**General relations of the external forces to the principal system.** The considerations under this heading, in Art. 52, are again applied to the analysis of the solid web arch, and the principal system is chosen as a determinate beam on two supports.

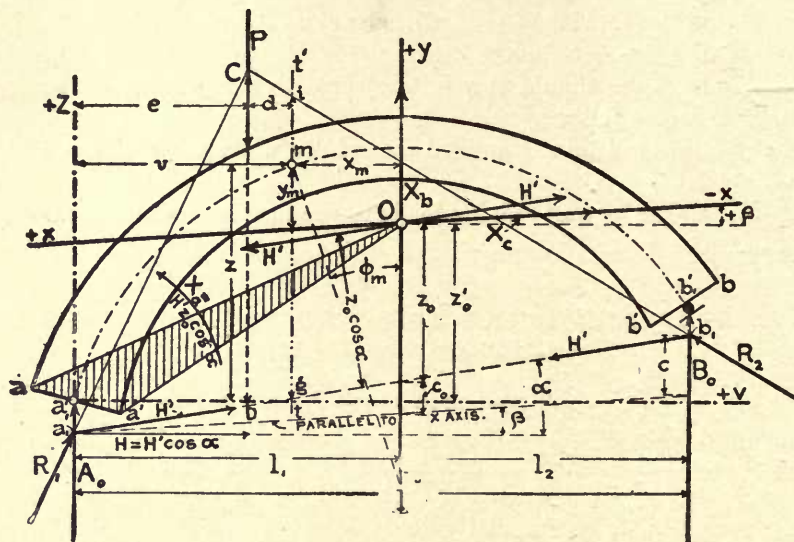


FIG. 72A.

Fig. 72A shows the *principal system* for an unsymmetric arch with the redundant conditions acting as external forces on the left-hand abutment. Similar redundants act on the right-hand abutment, and these are equal and opposite to the set shown for the left-hand end. See Figs. 52B and 52C.

The arch ring  $\overline{aa'bb'}$ , loaded with a single load  $P$ , is referred to coordinate axes  $(x, y)$  choosing the  $y$  axis vertical and the  $x$  axis making some angle  $\beta$  with the horizontal. The origin  $O$  is supposed to be known and is fixed by certain geometric relations to be established later.

The ordinate  $y_m$ , of any point  $m$  of the gravity axis or axial line of the arch ring, is measured vertically from the  $x$  axis, while the abscissa  $x_m$ , of this point, is measured horizontally from the  $y$  axis instead of parallel to the  $x$  axis. This is a mere matter of convenience.

The span  $\overline{AB} = l$  is taken as the line joining the intersections between the axial line



and the verticals through  $a'_1$  and  $b'_1$ . The support at  $a'_1$  is assumed as hinged while the one at  $b'_1$  is made movable for the principal system.

The single load  $P$  then produces reactions  $R_1$  and  $R_2$ , intersecting in the point  $C$  and passing respectively through the unknown points  $a_1$  and  $b_1$  on the verticals through the supports  $a'_1$  and  $b'_1$ . The triangle  $\overline{a_1Cb_1}$  thus becomes a resultant polygon with the closing line  $\overline{a_1b_1}$ . The reaction  $R_1$  may be resolved into the vertical component  $A_o$  and the haunch thrust  $H'$  along  $\overline{a_1b_1}$ . The reaction  $R_2$  may be similarly resolved into the vertical reaction  $B_o$  and the thrust  $H'$ , which latter is equal and opposite to  $H'$  acting at  $a_1$ .

The vertical reactions  $A_o$  and  $B_o$  are the same as for a simple beam of span  $l$  on determinate supports. Hence,

$$A_o = \frac{P}{l}(l-e) \quad \text{and} \quad B_o = \frac{Pe}{l} \quad \dots \dots \dots (72A)$$

Also, the moment for any point  $m$  of the simple beam, equals

$$M_{om} = KH = KH' \cos \alpha \quad \text{or} \quad K = \frac{M_{om}}{H} = \frac{M_{om}}{H' \cos \alpha}, \quad \dots \dots \dots (72B)$$

where  $K$  is the ordinate  $\overline{ig}$  through  $m$ , and  $H$  is the horizontal component of  $H'$ .

Therefore, the resultant polygon  $\overline{a_1Cb_1}$  becomes fixed whenever  $H'$  and the closing line  $\overline{a_1b_1}$  are found.

The origin  $O$  is connected to the arch along  $\overline{aa'}$  by the rigid disc  $\overline{aa'O}$  and to this origin are applied two equal and opposite forces  $H'$ , which are equal and parallel to the original haunch thrust acting at  $a_1$ . The equilibrium of the principal system and of the fixed arch thus remains undisturbed.

Suppose now that all the external forces to the left of a section  $\overline{u'u'}$  act on the principal system only, and that the three forces  $H'$  and the vertical reaction  $A_o$  are applied to the rigid disc and are thence transmitted to the principal system. Then the force  $H'$  at  $a_1$  and the opposing force  $H'$  acting at  $O$ , form a couple with lever arm  $z_o \cos \alpha$ , producing a moment  $X_a = H'z_o \cos \alpha$ . The other force  $H'$ , acting at  $O$  and to the right, may be resolved into two components  $X_b$  and  $X_c$ , where  $X_b$  is vertical along the  $y$  axis, and  $X_c$  acts along the  $x$  axis. The external forces to the left of the section and applied to the principal system are then  $P$ ,  $A_o$ ,  $X_b$ ,  $X_c$ , and a moment  $X_a = H'z_o \cos \alpha = Hz_o$ . Of these the two forces  $X_b$  and  $X_c$  and the moment  $X_a$  constitute the redundant conditions while the forces  $P$  and  $A_o$  are known, and all are applied to the principal system to the left of the section  $\overline{u'u'}$ . A similar set of external forces (not shown) acts on the principal system to the right of this section.

The moment of all the external forces about any point  $m$  of any structure, involving three external redundant conditions, is given by Eq. (7A) as

$$M_m = M_{om} - M_a X_a - M_b X_b - M_c X_c, \quad \dots \dots \dots (72C)$$

wherein

$M_{om} = A_o(l_1 - x_m) - Pd$  = the moment about  $m$  due to the load  $P$  acting on the principal system, This is condition  $X=0$ .



$M_a=1$  is the moment about  $m$  due to the moment  $X_a=1$  applied to the principal system. Condition  $X_a=1$ .

$M_b=1 \cdot x_m$  is the moment about  $m$  due to the force  $X_b=1$  acting on the principal system. Condition  $X_b=1$ .

$M_c=1 \cdot y_m \cos \beta$  is the moment about  $m$  due to the force  $X_c=1$  acting on the principal system. Condition  $X_c=1$ .

Substituting these values into Eq. (72c), gives the following fundamental moment equation for fixed arches:

$$M_m = M_{om} - 1 \cdot X_a - x_m X_b - y_m \cos \beta X_c. \quad (72d)$$

Before  $M_m$  can be determined for any point  $m$  of the arch, the three redundants  $X_a$ ,  $X_b$ , and  $X_c$  must be evaluated from three simultaneous work equations of the form of Eqs. (44B) which may be made to apply to the present problem by so locating the  $(x, y)$  axes that  $\delta_{ab} = \delta_{ba} = 0$ ,  $\delta_{ac} = \delta_{ca} = 0$  and  $\delta_{bc} = \delta_{cb} = 0$ .

The Redundant conditions for a single load  $P=1$  then become

$$X_a = \frac{1 \cdot \delta_{mc}}{\delta_{aa}}; \quad X_b = \frac{1 \cdot \delta_{mb}}{\delta_{bb}}; \quad X_c = \frac{1 \cdot \delta_{mc}}{\delta_{cc}}, \quad (72e)$$

for fixed abutments and omitting temperature effects.

Neglecting the term involving the axial thrust  $N$  in Eq. (15x) the deflections in Eqs. (72e) may be expressed as virtual work in terms of the moments  $M_{om}$ ,  $M_a=1$ ,  $M_b=x$  and  $M_c=y \cos \beta$ , as follows:

$$\left. \begin{aligned} \delta_{ma} &= \int \frac{M_{om} M_a du}{EI} = \int \frac{M_{om} du}{EI}; & \delta_{aa} &= \int \frac{M_a^2 du}{EI} = \int \frac{du}{EI} \\ \delta_{mb} &= \int \frac{M_{om} M_b du}{EI} = \int \frac{M_{om} x du}{EI}; & \delta_{bb} &= \int \frac{M_b^2 du}{EI} = \int \frac{x^2 du}{EI} \\ \delta_{mc} &= \int \frac{M_{om} M_c du}{EI} = \int \frac{M_{om} y \cos \beta du}{EI}; & \delta_{cc} &= \int \frac{M_c^2 du}{EI} = \int \frac{y^2 \cos^2 \beta du}{EI} \end{aligned} \right\} \quad (72f)$$

Introducing the elastic loads

$$\frac{du}{EI} = w_a, \quad x \frac{du}{EI} = w_b, \quad \text{and} \quad y \frac{du}{EI} = w_c, \quad (72g)$$

into Eqs. (72f), then substituting these values into Eqs. (72e) and replacing the integrations by summations, then

$$X_a = \frac{\delta_{ma}}{\delta_{aa}} = \frac{\Sigma M_{om} w_a}{\Sigma w_a}; \quad X_b = \frac{\delta_{mb}}{\delta_{bb}} = \frac{\Sigma M_{om} w_b}{\Sigma x w_b}; \quad X_c = \frac{\delta_{mc}}{\delta_{cc}} = \frac{\Sigma M_{om} w_c}{\Sigma y \cos \beta w_c}. \quad (72h)$$

The modulus  $E$ , being involved in both numerator and denominator, of Eqs. (72h), has no effect on the redundants except when temperature and reaction displacements are included.

If the axial thrust is to be considered, then the deflections due to this effect alone

and for  $N_a=0$ ,  $N_b=1 \cdot \sin \phi$  and  $N_c=1 \cdot \cos \phi$ , according to Eq. (15N), become for  $du=dx/\cos \phi$ :

$$\left. \begin{aligned} \delta_{aa}=0; \quad \delta_{bb} &= \int \frac{N_b^2 du}{EF} = \int_0^l \frac{\sin^2 \phi \, dx}{EF \cos \phi} \\ \delta_{cc} &= \int \frac{N_c^2 du}{EF} = \int \frac{\cos^2 \phi \, du}{EF} = \int_0^l \frac{\cos \phi \, dx}{EF} \end{aligned} \right\} \dots \dots \dots (72J)$$

These values added for total effect including axial thrust in the determination of the redundants will change Eqs. (72H) to the following:

$$X_a = \frac{\Sigma M_{om} w_a}{\Sigma w_a}; \quad X_b = \frac{\Sigma M_{om} w_a}{\Sigma x w_b + \Sigma \frac{\sin^2 \phi \, dx}{EF \cos \phi}}; \quad X_c = \frac{\Sigma M_{om} w_c}{\Sigma y \cos \phi w_c + \Sigma \frac{\cos \phi \, dx}{EF}} \quad (72K)$$

Eqs. (72H) and (72K) being written for a single load  $P=1$  represent the equations of the influence lines of the redundants.

If axial thrust is to be considered in Eqs. (72K) it will be well to compute the two functions in the denominators and thus include them in the pole distances when drawing the  $X_b$  and the  $X_c$  influence lines.

It should be pointed out that in general, axial thrust becomes important for very flat arches, in which case the function  $\Sigma \sin^2 \phi \, dx / EF \cos \phi$  becomes very small, while  $\Sigma \cos \phi \, dx / EF$  becomes large. Hence it is never necessary to include the thrust function in determining  $X_b$ , while for  $X_c$  it may take on considerable proportions.

**Regarding the curvature of an arch**, which is involved in the integral  $\int du$  and which could be fully considered should the necessity arise, it must be remembered that the depth of the arch ring is, almost without exception, very small compared with the radius of curvature of the axial line, and no appreciable error is committed when this effect is entirely neglected. Some comparative analyses have been worked out by various investigators, which show quite conclusively that this error is smaller than the knowable accuracy of the strength of materials, to say nothing about temperature stresses and abutment displacements, which may be estimated but never become known.

For these reasons, which are considered ample, the question of axial curvature will not be treated here.

**The location of the coordinate axes** was to be so chosen that the displacements  $\delta_{ab}=\delta_{ac}=\delta_{bc}=0$ , thus permitting the use of the simplified Eqs. (44B) instead of the involved form of Eqs. (8D).

According to Eq. (15N) and noting that  $N_a=0$ , these displacements become

$$\left. \begin{aligned} \delta_{ab} &= \int \frac{M_a M_b du}{EI} = \int \frac{x du}{EI} = \Sigma x w_a = \Sigma w_b = 0 \\ \delta_{ac} &= \int \frac{M_a M_c du}{EI} = \int \frac{y du}{EI} = \Sigma y w_a = \Sigma w_c = 0 \\ \delta_{bc} &= \int \frac{M_b M_c du}{EI} = \int \frac{xy du}{EI} = \Sigma xy w_a = 0 \end{aligned} \right\} \dots \dots \dots (72L)$$

If the coordinate axes are located so as to comply with the conditions of Eqs. (72L) then the origin of these axes must be the center of gravity of the elastic loads  $w_a$  because  $\Sigma xw_a=0$  and  $\Sigma yw_a=0$ . Also the axes must be conjugate in order that the centrifugal moment  $\Sigma xyw_a=0$ .

The manner of computing the elastic loads and then of finding the positions of the axes with respect to any unsymmetric arch ring follows here.

### ART. 73. COORDINATE AXES AND ELASTIC LOADS

**Unsymmetric arches.** The elastic loads  $w_a$  depend on the geometric shape of the arch sections while the loads  $w_b=xw_a$  and  $w_c=yw_a$  are seen to be functions of the  $w_a$  loads and of the coordinates of the axial points of the arch. Hence the  $w_a$  loads may be found for any arch ring of given sections while the  $w_b$  and  $w_c$  loads require for their determination a careful location of the coordinate axes in compliance with the conditions given by Eqs. (72L).

The first step is then to evaluate the  $w_a$  loads for finite distances  $\Delta u$ , which is done

by dividing up the arch ring into an even number of lengths and after computing  $EI$  for each section, the values

$W_a = \int w_a = \int_0^{\Delta u} \frac{du}{EI}$  are found by summation according to Simpson's rule. This will answer all practical purposes and will be the more accurate the shorter the lengths  $\Delta u$  or the greater the number of sections taken.

The manner in which this is done will now be illustrated, as the accuracy

of the analysis depends almost entirely on the values  $W_a$ . See Fig. 73A.

Instead of dividing the axial line into small lengths  $\Delta u$ , it is preferable to make these spaces equal horizontally, so that  $\Delta u = \Delta x / \cos \phi$ , where  $\phi$  is the angle which the normal section makes with the vertical. The Eqs. (72G) then become

$$w_a = \frac{\Delta u}{EI} = \frac{\Delta x}{EI \cos \phi}; \quad w_b = xw_a = \frac{x\Delta x}{EI \cos \phi}; \quad \text{and} \quad w_c = yw_a = \frac{y\Delta x}{EI \cos \phi}. \quad (73A)$$

Each half of the arch is now spaced off into an even number of spaces  $\Delta x$ , beginning at the crown. When the spaces  $\Delta u$  appear to get too large they may be shortened toward the haunches of the arch, but it is best to keep as many as possible of the  $\Delta x$  alike.

Now tabulate the depths  $D$  of the arch ring and angles  $\phi$  for the axial points from  $A$  to  $B$  and figure the reciprocal values of  $EI \cos \phi$  for each. If the section is one of a steel girder the real moment of inertia is to be used while for a masonry arch it is best to take a section of width unity and depth  $D$  making  $I = D^3/12$ .

Simpson's rule is now employed to sum the values  $w_a$  in order to obtain finite values for  $\int w_a = \int \frac{du}{EI} = \int \frac{dx}{EI \cos \phi}$  for the lengths  $\Delta x$ ,  $\Delta x'$ , and  $\Delta x''$ .

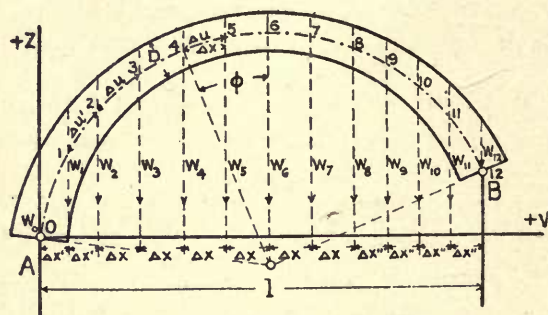


FIG. 73A.



The quantities  $1/EI \cos \phi$  are treated as parallel ordinates to some irregular curve and the volume of length  $l$ , which is divided into an even number  $n$  of equal spaces  $\Delta x$ , is then given from

$$\sum_0^l W_a = \frac{\Delta x}{3} [w_0 + 4w_1 + 2w_2 + 4w_3 + 2w_4 \text{ to } 4w_{n-1} + w_n], \dots \dots \dots (73B)$$

One such compression can be written for any even number of equal spaces  $\Delta x$ ,  $\Delta x'$ , or  $\Delta x''$ .

To find  $W_a = \int w_a$  for each of the sections, Simpson's rule for three quantities is then applied. This is the well-known prismoidal formula for volume and is used here to figure volumes between successive mean areas taking the originally computed values  $w$  for the middle terms.

Since the loads  $W_a$  are wanted for the points  $m$  themselves and not between these, we interpolate mean values between consecutive pairs of computed values and then figure the sums  $W_a$ , using the computed  $W_a$  as the middle term in the formula.

Thus the formula,

$$w_{a3} = \frac{\Delta x}{6} [w_2 + 4w_3 + w_4], \dots \dots \dots (73C)$$

as here applied, becomes

$$w_{a3} = \frac{\Delta x}{6} \left[ \frac{w_2 + w_3}{2} + 4w_3 + \frac{w_3 + w_4}{2} \right], \dots \dots \dots (73D)$$

when the interpolated means are used. This gives a much better check on Eq. (73B) than could be obtained by the use of Eq. (73C).

Beginning at  $A$ , and making  $\frac{w_0 + w_1}{2} = w_{0-1}$ ,  $\frac{w_1 + w_2}{2} = w_{1-2}$ , etc., the several values of  $W_a$  are as follows:

$$\begin{aligned} \frac{1}{2} W_{a0} &= \frac{\Delta x'}{6} [2w_0 + w_{0-1}] = \text{half load for an end section} \\ W_{a1} &= \frac{\Delta x'}{6} [w_{0-1} + 4w_1 + w_{1-2}] \\ W_{a2} &= \frac{\Delta x'}{6} [w_{1-2} + 2w_2] + \frac{\Delta x}{6} [2w_2 + w_{2-3}] \\ W_{a3} &= \frac{\Delta x}{6} [w_{2-3} + 4w_3 + w_{3-4}] \\ W_{a4} &= \frac{\Delta x'}{6} [w_{3-4} + 4w_4 + w_{4-5}] \\ \text{etc.,} &\qquad \qquad \text{etc.} \\ W_{a8} &= \frac{\Delta x}{6} [w_{7-8} + 2w_8] + \frac{\Delta x''}{6} [2w_8 + w_{8-9}] \\ \text{etc.,} &\qquad \qquad \text{etc.} \\ \frac{1}{2} W_{a12} &= \frac{\Delta x''}{6} [w_{11-12} + 2w_{12}] \end{aligned}$$

}

$$\dots \dots \dots (73E)$$

and as a final check the sum of all  $W_a$  loads must be by Eq. (73B)

$$\Sigma_0^l W_a = \int_0^l w_a = \frac{\Delta x'}{6} [w_0 + 4w_1 + w_2] + \frac{\Delta x}{3} [w_2 + 4w_3 + 2w_4 + 4w_5 + 2w_6 + 4w_7 + w_8] + \frac{\Delta x''}{3} [w_8 + 4w_9 + 2w_{10} + 4w_{11} + w_{12}]$$

Having thus found the elastic loads  $W_a = \int \frac{dx}{EI \cos \phi} = \int_0^{\Delta x} w_a$ , these are now used to determine the center of gravity  $O$  and the angle  $\beta$  which the  $x$  axis makes with the horizontal. The  $y$  axis was taken vertically and is thus fixed as soon as the origin is located.

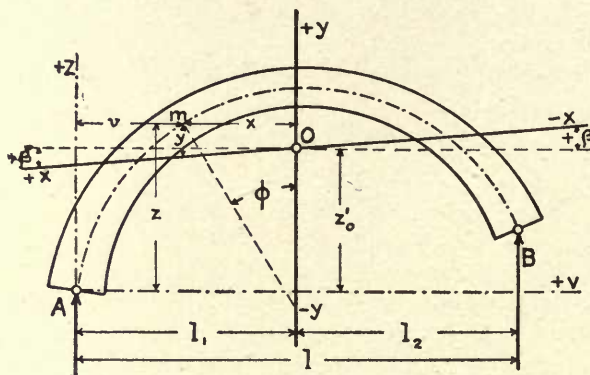


FIG. 73B.

The center of gravity  $O$  is located with respect to any assumed rectangular axes  $(z, v)$ , Fig. 73B, with origin at the axial point  $A$  the same as shown in Fig. 73A. It is most convenient to assume the  $z$  axis vertical and the  $v$  axis horizontal. The coordinates  $(z, v)$  are found for each of the several axial points  $m$  previously used for the computation of the  $W_a$  loads, and all are tabulated together. Finally the moments  $zW_a$  and  $vW_a$  are found and from these the coordinates  $l_1$  and  $z_o'$  of the origin  $O$  are obtained from

$$l_1 = \frac{\Sigma v W_a}{\Sigma W_a}; \quad \text{and} \quad z_o' = \frac{\Sigma z W_a}{\Sigma W_a}. \quad (73F)$$

This also fixes the  $y$  axis which is parallel to the vertical  $z$  axis through the center of gravity  $O$ . The  $x$  axis, while passing through  $O$ , makes some angle  $\beta$  with the horizontal such that  $\Sigma xy W_a = 0$ , according to the last of Eqs. (72L).

The  $(x, y)$  coordinates may be derived from the  $(z, v)$  coordinates when the angle  $\beta$  is determined. Taking  $\beta$  positive when measured to the right of the origin and above the horizontal, as shown in Fig. 73B, then

$$x = l_1 - v \quad \text{and} \quad y = z - z_o' + x \tan \beta. \quad (73G)$$

The angle  $\beta$  is found by substituting the value of  $y$  from Eq. (73G) into the condition equation  $\Sigma xyW_a=0$ , giving, as in Eq. (52j),

$$\tan \beta = -\frac{\Sigma xzW_a}{\Sigma x^2W_a} \quad \dots \quad (73H)$$

The abscissæ  $x$  being known from Eqs. (73G) the values  $\Sigma xzW_a$  and  $\Sigma x^2W_a$  are readily found and  $\tan \beta$  is then obtained from Eq. (73H) and the new axes and  $(x, y)$  coordinates are thus determined.

**For symmetric arches** the above calculations are greatly simplified and the coordinate axes are readily located as follows: The  $y$  axis, being the axis of symmetry, is practically given when the shape of the arch is given, and the angle  $\beta=0$  because for symmetric forces the centrifugal moment  $\int xyW_a=0$  for any pair of rectangular gravity axes.

Hence the  $y$  axis and the direction of the  $x$  axis are given and the origin  $O$  is located by computing the ordinate  $z_o'$  from any assumed horizontal  $v$  axis, giving for symmetric arches,

$$z_o' = \frac{\Sigma zW_a}{\Sigma W_a}; \quad \beta=0; \quad \text{and} \quad y=z-z_o'. \quad \dots \quad (73J)$$

In any case the  $W_a$ ,  $W_b$ , and  $W_c$  loads are now readily figured and from these the equations for the influence lines for the redundant conditions  $X_a$ ,  $X_b$ , and  $X_c$  are evaluated.

Solid web circular arches which are only *very slightly* unsymmetric may be approximately analyzed by extending the short half to a point of symmetry and treating the structure as a symmetric arch. However, when the difference in the elevations of the springing points is appreciable, such approximations should not be made.

The center of gravity  $O$  may be found graphically by combining the  $W_a$  loads into two equilibrium polygons, for the loads acting first vertically and then horizontally through the centers of gravity of the arch sections. The two resultants thus obtained will intersect in the required point  $O$ . The moments of inertia  $\Sigma x^2W_a$  and  $\Sigma y^2W_a$  may be obtained from the same polygons by Professor Mohr's method.

#### ART. 74. INFLUENCE LINES FOR $X_a$ , $X_b$ , $X_c$ , AND $M_m$

Having located the coordinate axes  $(x, y)$  to fulfill the requirements  $\delta_{ab}=\delta_{ac}=\delta_{bc}=0$ , the Eqs. (72E) and (72H) now become applicable to the present problem, giving

$$\left. \begin{aligned} X_a &= \frac{\Sigma M_{om}W_a}{\Sigma W_a} = \frac{1 \cdot \delta_{ma}}{\Sigma W_a} = \frac{\delta_{ma}}{H_a} = \eta_{am} \\ X_b &= \frac{\Sigma M_{om}W_b}{\Sigma xW_b} = \frac{1 \cdot \delta_{mb}}{\Sigma xW_b} = \frac{\delta_{mb}}{H_b} = \eta_{bm} \\ X_c &= \frac{\Sigma M_{om}W_c}{\cos \beta \Sigma yW_c} = \frac{1 \cdot \delta_{mc}}{\cos \beta \Sigma yW_c} = \frac{\delta_{mc}}{H_c} = \eta_{cm} \end{aligned} \right\} \dots \quad (74A)$$

These Eqs. (74A) which are written for a load  $P_m=1$ , thus represent the equations for the influence lines of the redundants  $X_a$ ,  $X_b$ , and  $X_c$ .



For  $X_a=1$ , the first of Eqs. (74A) gives  $1 \cdot \Sigma W_a = 1 \cdot \delta_{ma} = \Sigma M_{om} W_a$ . Therefore, the special moment  $M_{om}$  equals unity and this equals the moment  $X_a=1$  acting on the principal system, which would follow from Maxwell's law. Hence, an equilibrium polygon drawn for the loads  $W_a$  with pole unity, would give the deflection polygon for  $\delta_{ma}$  due to a moment  $X_a=1$  applied to the principal system. Also, the ordinates of a similar equilibrium polygon drawn with a pole  $H_a = \Sigma W_a$  would represent the ordinates  $\eta_{am}$ , of the  $X_a$  influence line, measured to the scale of lengths of the drawing.

The influence lines for  $X_b$  and  $X_c$  are similarly found from equilibrium polygons drawn for the elastic loads  $W_b$  and  $W_c$  with pole distances respectively equal to  $\Sigma x W_b = H_b$  and  $\cos \beta \Sigma y W_c = H_c$ . When axial thrust is to be considered then the pole distance  $H_c = \cos \beta \Sigma y W_c + \Sigma \cos^2 \phi du / EF = \cos \beta \Sigma y W_c + \Sigma \cos \phi dx / EF$  from Eq. (72κ).

The  $M_m$  influence line for moments about any point  $m$  of the axial line and a moving load  $P_m=1$ , is now derived from Eq. (72D). Accordingly the ordinates  $\eta_m$ , of the  $M_m$  influence line, must represent the algebraic summation of the influences due to  $M_{om}$ ,  $X_a$ ,  $X_b$ , and  $X_c$  expressed by the equation

$$\eta_m = M_m = M_{om} - X_a - x_m X_b - y_m \cos \beta X_c \quad . \quad . \quad . \quad (74B)$$

The influence line for  $M_{om}$  is the ordinary moment influence line drawn for the point  $m$  and for a simple beam on two determinate supports at  $a'_1$  and  $b'_1$ , Fig. 72A. It is a different line for each axial point  $m$ .

The influence lines for  $X_a$ ,  $X_b$ , and  $X_c$  remain the same for the same structure, but the ordinates of the  $X_b$  and  $X_c$  lines, according to Eq. (74B), require multiplication by the variable coordinates  $x$  and  $y \cos \beta$ , which differ for each axial point  $m$ .

Hence the  $M_m$  influence line is best constructed by computing the ordinates  $(X_a + x_m X_b + y_m \cos \beta X_c)$  for the particular values of  $x_m$  and  $y_m \cos \beta$  and plotting these ordinates negatively from the  $M_{om}$  influence line.

The  $M_m$  line, so found, will serve to determine the bending moment for the axial point  $m$  due to any position of a system of concentrated loads.

The normal thrust  $N_m$ , and stresses on any normal arch section through  $m$ , are then computed as described in Art. 49 and further discussed below by involving the moments about the kernel points  $e$  and  $i$ .

## ART. 75. TEMPERATURE STRESSES

The effect of a uniform rise in temperature is to expand the principal system uniformly in all directions. But since a uniform vertical expansion is not resisted by the fixed abutments, it may be assumed that the whole temperature stress is produced by horizontal expansion. This manifests itself by a bending moment extending over the entire arch ring, and produced by resisting abutments.

Thus for a rise in temperature, the extreme elements of the extrados at the crown are in tension while at the haunches they are in compression, when the arch is not otherwise loaded. The simultaneous condition of the intrados elements is exactly the reverse.

In Eqs. (72E) the temperature term was neglected. It is now separately considered without regard to the effect of the loads  $P$ .

According to Eqs. (44c), which apply to the present problem, the redundant temperature stresses, for rigid abutments, become:

$$X_{at} = \frac{\delta_{at}}{\delta_{aa}} = 0; \quad X_{bt} = \frac{\delta_{bt}}{\delta_{bb}} = 0; \quad \text{and} \quad X_{ct} = \frac{\delta_{ct}}{\delta_{cc}} \quad . \quad . \quad . \quad . \quad (75A)$$

The first two are placed equal to zero because uniform temperature changes cannot produce rotation nor vertical deflection of the principal system, which latter is here regarded as a simple beam on two supports.

The distance over which the change  $\delta_{ct}$  is cumulative must be the projection of the span  $l$  on the  $x$  axis, hence  $\delta_{ct} = \epsilon t l / \cos \beta$  and from Eqs. (72F)  $\delta_{cc} = \Sigma y \cos^2 \beta W_c$ , giving for the last of Eqs. (75A):

$$X_{ct} = \frac{\delta_{ct}}{\delta_{cc}} = \frac{\epsilon t l}{\cos^2 \beta \Sigma y W_c}, \quad \text{where} \quad W_c = y W_a = \frac{y A x}{EI \cos \phi} \quad . \quad . \quad . \quad (75B)$$

The moment about any axial point  $m$  due to temperature alone, may now be found from Eq. (72D), wherein  $M_{om} = 0$ ,  $X_{at} = 0$ ,  $X_{bt} = 0$ , and  $X_{ct}$  is given from Eq. (75B). Then

$$-M_{mt} = y_m \cos \beta X_{ct} = y_m \frac{\epsilon t l}{\cos^2 \beta \Sigma y W_c} \quad . \quad . \quad . \quad . \quad (75C)$$

According to Eq. (75C) the only variable affecting the moment  $M_{mt}$  is the ordinate  $y_m$ . Hence for  $y_m = 0$ ,  $M_{mt} = 0$  and for  $y_m$  maximum,  $M_{mt}$  becomes maximum. The points where the  $x$  axis intersects the axial line are thus points of zero moment for temperature effects, while the crown and haunch points receive maximum effects.

The temperature effects must finally be combined with the dead and live load stresses to obtain absolute maxima and minima.

It is a well-established fact that when masonry arches open up cracks this generally occurs during the coldest winter weather. This is because masonry or concrete is scarcely ever placed during freezing temperatures, but generally in the warmest summer months. Hence, the variations in temperature from that existing at the time of closing the arch ring are nearly always greater in the negative direction. Thus, if the ring was closed at 70° F. the completed structure might at some future period attain a temperature of perhaps 90°, but it is quite certain to fall to about -10° if the climate is severe. This then would subject the arch to temperature stresses resulting from +20° and -80° from the closing temperature.

When it is considered that a lowering in temperature will induce tensile stresses in the spandrels and thus cause rupture at the points of least strength, it is clear why this phenomenon is of such frequent occurrence. Rising temperature would tend to increase the compressive stresses, but probably not to any alarming extent.



## ART. 76. STRESSES ON ANY NORMAL ARCH SECTION

This subject is fully discussed in Art. 49 and illustrated by Fig. 49B and will not be repeated here except in so far as to show the application of Eqs. (49s) to the fixed masonry arch.

For any rectangular arch section the kernel points  $e$  and  $i$  are located on opposite sides of the axial line at equal distances  $k = D/6$  from the axis. The kernel point  $i$  for the intrados is situated above the gravity axis, while the kernel point  $e$  for the extrados is below this axis as shown in Fig. 49B.

The moments  $M_e$  and  $M_i$  are found from Eq. (74B) in which the coordinates of the axial point  $m$  are replaced by the coordinates  $(x_e, y_e)$  for an extrados kernel point and by the coordinates  $(x_i, y_i)$  for an intrados kernel point. This is permissible because this equation is perfectly general and is true for any point in the plane of the structure.

The moment equations for the kernel points  $e$  and  $i$ , of any normal section, are thus

$$\left. \begin{aligned} M_e &= M_{oe} - [X_a + x_e X_b + y_e \cos \beta X_c] \\ M_i &= M_{oi} - [X_a + x_i X_b + y_i \cos \beta X_c] \end{aligned} \right\} \dots \dots \dots (76A)$$

Designating all influence line ordinates by  $\eta$  and using proper subscripts as a distinctive feature, then the ordinates of the kernel point moment influence lines may be expressed as

$$\left. \begin{aligned} \eta_e &= \eta_{oe} - [\eta_a + x_e \eta_b + y_e \cos \beta \eta_c] \\ \eta_i &= \eta_{oi} - [\eta_a + x_i \eta_b + y_i \cos \beta \eta_c] \end{aligned} \right\}, \dots \dots \dots (76B)$$

wherein  $\eta_o$ ,  $x$ , and  $y$  are special for each normal arch section  $\overline{u'}$  while the ordinates  $\eta_a$ ,  $\eta_b$ , and  $\eta_c$  are the same for all influence lines but differ for each point of the span.

When the kernel moments are known for any rectangular section and due to any position of a moving train of loads, the stresses on the extreme fibers of the arch section and the normal thrust  $N$  and its distance  $v$  from the axial line, may be determined from Eqs. (49s) thus:

$$\left. \begin{aligned} f_e &= -\frac{6M_e}{D^2}; & f_i &= \frac{6M_i}{D^2}; \\ N &= \frac{3}{D}(M_e - M_i); & v &= \frac{M_e + M_i}{2N}; \\ k &= \frac{D}{6}; & F &= 1 \cdot D; & \text{and} & I &= \frac{1 \cdot D^3}{12} \end{aligned} \right\}, \dots \dots \dots (76c)$$

where  $D$  is the depth and  $F$  is the area of a normal arch section of unit thickness.



In Eqs. (76c)  $M_e$  and  $M_i$  have opposite signs when  $N$  acts between the two kernel points  $e$  and  $i$ . The stresses  $f_e$  and  $f_i$  take their signs from  $M_e$  and  $M_i$  respectively, and compression is regarded as a negative stress. The offset  $v$  is positive when measured from the gravity axis toward the extrados and when so applied determines a point on the resultant polygon for that section.

It is not necessary to draw the  $M_m$  influence lines because the  $M_e$  and  $M_i$  lines cannot be derived from the  $M_m$  line, nor is it possible to determine  $N$  and  $v$  when  $M_m$  alone is known except by constructing a resultant polygon.

Hence the stresses on any arch section are best found from the kernel point moments  $M_e$  and  $M_i$  of that section. If the redundants  $X_a$ ,  $X_b$ , and  $X_c$  are evaluated from their respective influence lines for a certain position of a train of loads, then the kernel moments, for any section, may be computed from Eqs. (76A). However, it is preferable to conduct the entire solution by means of influence lines, as will be illustrated later.

Since different portions of the arch ring are situated in the four quadrants of the coordinate axes, it may be well to show how to pass from the coordinates of any axial point  $m$  to those of the kernel points of the normal section through  $m$ .

For a rectangular arch section  $k_e = k_i = D/6$ , so that the following relations may be written out, from Fig. 76A, in terms of the lettered variable dimensions  $D$  and  $\phi$  for each point, thus:

$$\left. \begin{array}{ll}
 \text{For point } A, & \left. \begin{array}{ll} x_e = x - \frac{D}{6} \sin \phi & \text{and} & -y_e = -y - \frac{D}{6} \cos \phi \\ x_i = x + \frac{D}{6} \sin \phi & \text{and} & -y_i = -y + \frac{D}{6} \cos \phi \end{array} \right\} \\
 \text{For point } m, & \left. \begin{array}{ll} x_e = x - \frac{D}{6} \sin \phi & \text{and} & y_e = y - \frac{D}{6} \cos \phi \\ x_i = x + \frac{D}{6} \sin \phi & \text{and} & y_i = y + \frac{D}{6} \cos \phi \end{array} \right\} \\
 \text{For point } n, & \left. \begin{array}{ll} x_e = 0 & \text{and} & y_e = y - \frac{D}{6} \\ x_i = 0 & \text{and} & y_i = y + \frac{D}{6} \end{array} \right\} \quad \dots (76D) \\
 \text{For point } m', & \left. \begin{array}{ll} -x_e = -x + \frac{D}{6} \sin \phi & \text{and} & y_e = y - \frac{D}{6} \cos \phi \\ -x_i = -x - \frac{D}{6} \sin \phi & \text{and} & y_i = y + \frac{D}{6} \cos \phi \end{array} \right\} \\
 \text{For point } B, & \left. \begin{array}{ll} -x_e = -x + \frac{D}{6} \sin \phi & \text{and} & -y_e = -y - \frac{D}{6} \cos \phi \\ -x_i = -x - \frac{D}{6} \sin \phi & \text{and} & -y_i = -y + \frac{D}{6} \cos \phi \end{array} \right\}
 \end{array} \right\}$$



the critical sections must be investigated while all other sections are of minor importance and usually receive no consideration.

Unfortunately the theory of elasticity does not afford a direct solution for finding the critical sections. The critical sections might be located after a number of sections all along the arch ring had been examined, and the points of greatest maxima would correspond to the critical sections. However, this would involve much labor and from the nature of the case is not warranted, since the stresses in an arch ring always change gradually and not abruptly. An approximate knowledge of the location of the critical sections is, therefore, all that is required and this may be had from a discussion of the moment equation.

Thus the general equation for moments about any point  $m$  by Eq. (74B) is

$$M_m = M_{om} - [X_a + x_m X_b + y_m \cos \beta X_c]$$

wherein the parenthetic quantity may be positive or negative, depending on the location of the point  $m$ .

Since the stresses are direct functions of  $M_e$  and  $M_i$  for a given section, then these moments and stresses attain maximum values simultaneously:

1. For  $X_a$  negative and  $X_b$  and  $X_c$  both positive, when  $y_m=0$  or when  $x_m=0$ . This would locate three critical sections, one at the crown for  $x_m=0$ , and two on the  $x$  axis for  $y_m=0$ .

2. For  $X_a$ ,  $X_b$ , and  $X_c$  all positive,  $M_m$  may become maximum when  $y_m$  has its greatest negative value or when both  $x_m$  and  $y_m$  have their greatest negative values. This locates two other critical points, one in each abutment.

Hence, there are five critical sections in every arch which must be carefully examined for maximum and minimum stresses, and the positions of the moving loads for these limiting stresses are given from the influence lines drawn for the five critical sections. In the case of symmetric arches, only three critical sections require investigation.

The two critical sections for  $y=0$  fall very close to the quarter points of the arch, a fact which is important in making preliminary designs by the method of resultant polygons. The load divide may then be approximately located in the manner given for three-hinged arches by treating the crown as a hinged point.

The maximum stresses are not appreciably altered by taking the quarter point critical sections a little to one side or the other of the real theoretical point, while the stresses are greatly affected by the shape of the axial line of the arch ring.

*Thus for maximum economy, the axial line should be a line of zero moments for the case of average loading. That is  $M_m$  should be zero for every point of the axis of the ring when the arch is carrying a dead load and half the maximum live load over the whole span.*



## ART. 78. RESULTANT POLYGONS

The resultant polygon for any case of applied loads  $P$  may be located by finding the corresponding values of  $X_a$ ,  $X_b$ , and  $X_c$  from the three influence lines for these redundants, having previously located the  $(x, y)$  axes.

The redundants  $X_c$  and  $X_b$ , Fig. 78A, were taken as the components of  $H'$ , respectively coincident with the  $x$  and  $y$  axes. The angle  $\beta$ , which the  $x$  axis makes with the horizontal, is given by Eq. (73H) and the  $y$  axis was taken vertically. Hence the horizontal component  $H$ , of  $X_c$ , is

$$\left. \begin{aligned} H &= X_c \cos \beta \quad \text{and, from Fig. 72A,} \\ \tan \alpha &= \tan \beta + \frac{X_b}{H} \\ H' &= \frac{H}{\cos \alpha} = \frac{X_c \cos \beta}{\cos \alpha} \\ z_o &= \frac{X_a}{H' \cos \alpha} = \frac{X_a}{H} \\ c &= \frac{X_b l}{H} = l (\tan \alpha - \tan \beta) \\ c_o &= \frac{X_b l_1}{H} = l_1 (\tan \alpha - \tan \beta) \\ X_a &= X_c z_o \cos \beta = X_b z_o \frac{l}{c} \end{aligned} \right\} \dots \dots \dots (78A)$$

These dimensions fix the closing line  $\overline{a_1 b_1}$  on the two end verticals of the abutments, also the haunch thrust  $H'$ , all in terms of  $X_a$ ,  $X_b$ , and  $X_c$ .

The reactions  $R_1$  and  $R_2$  may be found from the vertical reactions  $A_o$  and  $B_o$  and the thrust  $H'$ . The vertical reactions are those due to loads  $P$  acting on a simple beam  $\overline{a_1 b_1}$  and may be computed from Eqs. (72A) as  $A_o = \Sigma(l - e) P/l$  and  $B_o = \Sigma P e/l$ . The reactions  $R_1$  and  $R_2$  must then intersect on the line of the resultant  $R$  of all the applied loads  $P$ .

A force polygon, Fig. 78A, is drawn by laying off all the loads  $P$  in proper succession, dividing this load line into the parts  $A_o$  and  $B_o$  and at the dividing point drawing a line parallel to  $\overline{a_1 b_1}$  of length equal to  $H'$ . This determines the pole of the force polygon from which the reactions  $R_1$  and  $R_2$  and the resultant polygon through  $a_1$  and  $b_1$  are easily drawn. See also the force polygon in Fig. 52A, showing how the pole  $O$  is located when  $H'$ ,  $A_o$ , and  $B_o$  are given.

The resultant polygon thus found must intersect the arch center line at least three times for unsymmetric loading on an unsymmetric arch, and four times for a symmetric arch, provided the arch center line was so chosen as to be coincident with the resultant polygon drawn for the case of average loading. This *average loading* consists of the total dead load, plus half the live load uniformly distributed over the entire span. It

will be so understood whenever average loading is referred to in connection with arch designs.

The most favorable resultant polygon is the one which coincides with the axial line of the arch ring. Hence the most economic shape for an arch is the one for which the axial line is chosen to be the resultant polygon drawn for the case of average loading as just defined. The live load, in its critical positions, will then produce minimum values for the moment  $M_m = N_m v$  by making the offsets  $v$ , between the axial line and the resultant polygon, all minimum. The absolute minimum for  $M_m = N_m v$  can occur

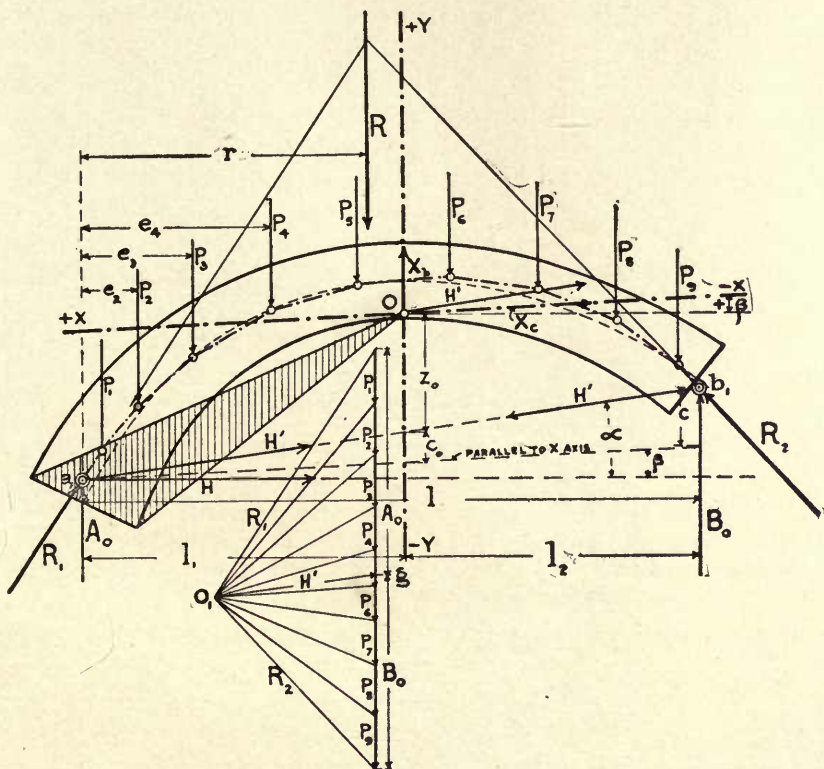


FIG. 78A.

only for  $v=0$  at all arch sections, and this condition can be produced only for one case of loading, which is taken as the *average loading*, when maximum economy is to be achieved in the design.

For all cases of live loads other than the *average*, the moments  $M_m = N_m v$  could never become zero for all points of the axial line, though these moments would be minimum for an arch properly designed for the average loading.

## ART. 79. EXAMPLE—150 FT. CONCRETE ARCH

(a) **Given data and preliminary design.** The data. Required to design a single track railway arch of 150 ft. clear span and 50 ft. clear rise with profile of surface and foundations as shown in Fig. 79B. The loading to be Cooper's E60, allowing full impact according to formula (1), Eqs. (64G),  $300 \div [l + 300]$ , where  $l$  is the portion of span covered by loads, for any case of loading.

The material shall be concrete, mixed in the proportion of one part American Portland cement to two parts sand to four parts crushed granite or limestone. Cubes of 12 inches on each side, at the age of 6 months, shall sustain a compressive stress of not less than 3600 lbs. per sq. in. and briquettes 90 days old, mixed one part cement to two parts sand, shall not break below 300 lbs. per sq. in. in tension.

Accordingly the weight of one cu. ft. of concrete is assumed at 140 lbs., and for stresses between 100 and 600 lbs. per sq. in.  $E = 3,670,000$  lbs. per sq. in., and

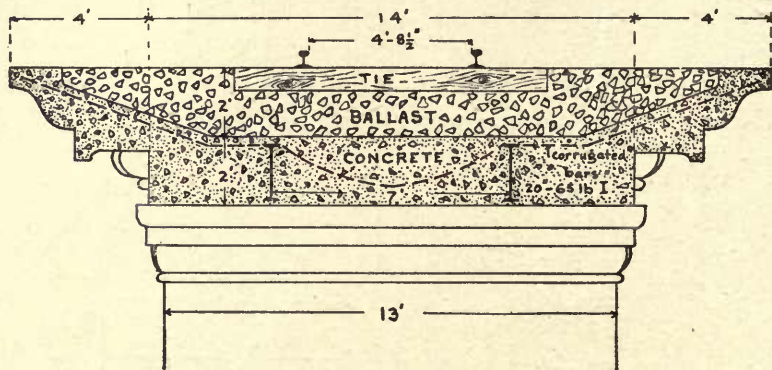


FIG. 79A—Pier of Roadway 3'×13'.

$\epsilon = 0.0000054$  per  $1^\circ$  F. The allowable unit compressive stress will be 500 lbs. per sq. in. or 515 cu. ft. of concrete per sq. ft. of surface. All pressures will be expressed in cu. ft. per sq. ft., a unit which is very convenient and nearly the same as lbs. per sq. in. Thus if  $\gamma = 144$  lbs., then lbs. per sq. in. = cu. ft. per sq. ft.

**Design of roadway.** It is proposed to place the track on a floor built of concrete and reinforced by rolled I-beams of sufficient strength to carry the whole wheel loads over spans 10 ft. in length. This floor system is supported by concrete piers 3 ft. thick and 13 ft. wide and these in turn transmit the loads to the arch ring. This floor is shown in section Fig. 79A.

Each I-beam must carry two 30,000 lb. wheel loads spaced five feet apart and producing a maximum bending moment of

$$M = 30,000 \times 60 - 30,000 \times 30 = 900,000 \text{ in. lbs.}$$

Allowing 97 per cent impact for a 10 ft. span, this moment becomes 1,733,000 in. lbs., and for an allowable unit stress of 16,000 lbs., the required section modulus is



$M/16,000=111$  in inches. One 20-inch I, 65 lbs., has a section modulus of 117, which is ample.

<b>Weight of floor.</b>	2 ft. of ballast at 120 lbs. per cu. ft.	3850 lbs.
	Concrete.....	5000 "
	2 I-beams and cor. bars.....	150 "
	2 rails.....	200 "

Total per foot. of roadway .....9200 lbs.

Total per sq. ft. of arch ring  $q=710$  lbs.  $=5.07$  cu. ft.

**Live loads.** E60 loading for 150 ft. span, all locomotives, gives 8400 lbs. per ft. of one track, and this, distributed over a 13 ft. wide arch, gives 640 lbs. per sq. ft. Adding 67 per cent. impact for 150 ft. span, then the total live load  $p$  becomes  $1.67 \times 640 = 1070$  lbs. per sq. ft.  $=7.64$  cu. ft. concrete per sq. ft.

**Preliminary design by resultant polygons.** The methods outlined in Art. 71 are applied here and the design is shown in Fig. 79B.

Taking dimensions above given and assuming that the stress for dead load plus half uniform live load will be about 0.4 of the allowable, then Eq. (71A) gives

$$D_0 = \frac{\frac{0.14l_0^2}{h_0} \left( q + \frac{p}{2} + \frac{h_0}{10} \right)}{0.4f - \frac{0.14l_0^2}{h_0}} = 6.12 \text{ feet,} \quad \dots \quad (79A)$$

and Eqs. (71B) give  $D_0=6.00$  ft. which value is accepted for the crown thickness of the arch.

Eq. (71c) gives 81.25 ft. for the radius of the intrados at the crown, and the quarter point for the parabola passing through the same three points at crown and springing, is from Eq. (71d)

$$y = \frac{h_0}{4} = 12.5 \text{ feet} \quad \text{and} \quad x = \frac{l_0}{4} = 37.5 \text{ feet.}$$

The point on the parabola is plotted at  $s$ , Fig. 79B, and the point  $s'$  is on the circle drawn with radius 81.25 ft. The point  $s''$ , midway between  $s$  and  $s'$ , is chosen and a three-center curve is drawn through  $s''$  and the given crown and springing points.

The thickness of the arch at the point  $s''$  is found to be 6.9 ft., using Eq. (71E).

The remainder of the ring is drawn according to good judgment and the thickness at the springing was taken at 10 ft.

The arch ring is now divided up into an even number of sections as described in Art. 73, so that the same subdivisions may be used throughout the final analysis. The dead loads are then computed and tabulated together with the live loads as required for the construction of the resultant polygons. All this is given in Table 79A.



TABLE 79A

DEAD LOADS AND EQUIVALENT UNIFORM LIVE LOADS

Ordinates <i>V</i> from <i>A</i>  ft.	Length on Axis, <i>4u</i>  ft.	<i>D</i>  ft.	DEAD LOADS IN CUBIC FEET.				Live Load, <i>P</i>  cu.ft.	$Q + \frac{P}{2}$  cu.ft.	<i>Q + P</i>  cu.ft.
			Arch Sections, sq.ft.	Piers, sq.ft.	Road- way, sq.ft.	Total <i>Q</i> , cu.ft.			
0- 0.0	.....	10.00							
1- 5.9	20.80	9.30	193.44	108.00	65.91	<i>Q</i> <sub>1</sub> =367.35	99.32	<i>P</i> <sub>1</sub> =417.01	<i>P'</i> <sub>23</sub> =466.67
2-12.4	.....	8.60							
3-18.9	18.10	8.00	145.40	64.80	65.91	<i>Q</i> <sub>3</sub> =276.11	99.32	<i>P</i> <sub>3</sub> =325.77	<i>P'</i> <sub>21</sub> =375.43
4-25.4	.....	7.60							
5-31.9	16.00	7.20	115.47	42.00	65.91	<i>Q</i> <sub>5</sub> =223.38	99.32	<i>P</i> <sub>5</sub> =273.04	<i>P'</i> <sub>19</sub> =322.70
6-38.4	.....	6.90							
7-44.9	14.40	6.64	95.82	21.00	65.91	<i>Q</i> <sub>7</sub> =182.73	99.32	<i>P</i> <sub>7</sub> =232.39	<i>P'</i> <sub>17</sub> =282.05
8-51.4	.....	6.46							
9-57.9	13.84	6.30	87.33	14.80	65.91	<i>Q</i> <sub>9</sub> =168.04	99.32	<i>P</i> <sub>9</sub> =217.70	<i>P'</i> <sub>15</sub> =267.36
10-64.4	.....	6.20							
11-71.9	15.02	6.10	91.62	6.00	76.05	<i>Q</i> <sub>11</sub> =173.67	114.60	<i>P</i> <sub>11</sub> =230.97	<i>P'</i> <sub>13</sub> =288.27
12-79.4	.....	6.00							
					Totals	1391.28	611.20	1696.88	2002.48

Above loads are all for an arch ring one foot thick.

The resultant polygon for the symmetric loading  $Q + \frac{1}{2}P$ , given in Table 79A as loads *P*<sub>1</sub> to *P*<sub>11</sub>, may now be drawn so as to pass through the center of the arch ring at the joint *a* and at the crown *n*. This polygon is shown in Fig. 79B, as a fine line almost coincident with the center line, and the shape of the arch ring is thus found to be acceptable. Had this coincidence not been so close then the shape of the arch would require modification.

For the above case of symmetric shape and loading, the resultant polygon for the half span only is required, which is best constructed by computing the horizontal thrust instead of finding it graphically. This is done by computing the moments of the forces *P*<sub>1</sub> to *P*<sub>11</sub> about *n* and dividing the sum of these moments by *R*=Σ*P* to obtain the lever arm *x* of *R*. The vertical component of the reaction at *A* is equal to *R* and hence *H* is found by taking moments about *n* of all the external forces to the left of *n*. This gives

$$H=Q\frac{\left(\frac{l}{2}-x\right)}{h}=\frac{1696.88(79.4-45.83)}{50.4}=1130.2 \text{ cu.ft.}$$

The force polygon is thus easily constructed and the resultant polygon is then drawn through the two section centers 0 and the crown.

The resultant polygon for maximum one-sided loading, is now constructed. To do this the load divide for the quarter point *m* is found as indicated in Fig. 79B by drawing lines *am* and *bn* which intersect in the required point *i*.

The full load *p*=7.64 cu.ft. per foot is allowed to cover the span from the right up to the point *i* and the left portion is acted on by dead loads only. The loads *Q*<sub>1</sub> to *Q*<sub>9</sub> and *P'*<sub>11</sub> to *P'*<sub>23</sub>, from Table 79A, are now united into a force polygon with assumed pole



distance  $H'_1$  and an equilibrium polygon  $\overline{a'cb'}$  is drawn for the purpose of finding the reactions  $R'_1$  and  $R'_2$  and the correct pole  $O_3$ .

It is then required to pass a resultant polygon through the three points  $a$ ,  $n$  and  $b$ , where  $a$ , and  $b$  are middle third points and  $n$  is  $D/8$  above the axial line. This is done as follows: project the points  $a$ ,  $n$  and  $b$  down vertically on the equilibrium polygon, giving the points  $a'$ ,  $c$  and  $b'$  respectively. Draw  $\overline{a'c}$  and  $\overline{b'c}$ . Then in the force polygon make  $\overline{O_2c'} \parallel \overline{a'c}$  and  $\overline{O_2c''} \parallel \overline{b'c}$  thus establishing the points  $c'$  and  $c''$ . Now draw the lines  $\overline{c'O_3} \parallel \overline{an}$ , and  $\overline{c''O_3} \parallel \overline{bn}$  giving the intersection  $O_3$  as the required pole and the line  $\overline{O_3T} \parallel \overline{ab}$  will be the true pole distance. An equilibrium polygon drawn through the point  $a$ , using the force polygon  $O_3MN$ , will then pass through the other two points  $n$  and  $b$ . The loads are divided at  $T$  into the reactions  $A_o = \overline{MT}$  and  $B_o = \overline{NT}$  as per Eqs. (72A) and  $\overline{O_3M} = R'_1$  and  $\overline{O_3N} = R'_2$ .

By the construction given in Fig. 79B, the correct pole  $H' = 1220$  cu.ft., and the required resultant polygon  $\overline{anb}$  are found. The polygon intersects the arch center line in three points and remains just inside the middle third of the arch ring at all critical sections.

It is seen by inspection that a more favorable resultant polygon could not be drawn, hence the solution is considered completed provided the stresses resulting from this loading do not exceed the allowable limits.

The stresses are now found from Eq. (69A) which, for a rectangular section of depth  $D$  and width unity, becomes

$$f = \frac{N}{D} \left( 1 \pm \frac{6v}{D} \right), \quad \dots \dots \dots (79B)$$

where  $v$  is the lever arm of the normal  $N$  about the axial point of the section.

TABLE 79B  
STRESSES FOUND FROM PRELIMINARY DESIGN

Section.	V ft.	D ft.	UNSYMMETRIC LOAD $Q+P$ .				LOADS $Q+P$ OVER WHOLE SPAN.			
			$N$ cu.ft.	$v$ ft.	$f_e$ cu.ft.	$f_i$ cu.ft.	$N$ cu.ft.	$v$ ft.	$f_e$ cu.ft.	$f_i$ cu.ft.
$a$	0.0	10.00	1980	1.67	396.0	0.0	2372	0	237.2	237.2
$m$	41.3	6.77	1390	1.13	0.0	410.7				
$n$	79.4	6.00	1220	0.75	406.6	0.0	1266	0	422.0	422.0
$-$	94.4	6.20	1234	1.03	398.0	0.0				
$b$	158.8	10.00	2290	1.67	0.0	458.0	2372	0	237.2	237.2

It is thus seen that the stresses are all well on the safe side and the preliminary design is, therefore, acceptable. Had it been impossible to construct a resultant polygon for the unsymmetric loading, which would remain within the middle third of the arch ring, then the thickness of the ring would have to be altered accordingly. Also, if the unit stresses had exceeded the allowable limits the thickness of the arch would have to be increased.

The structure thus designed and found adequate to carry the required loads safely is now subjected to a rigid analysis by applying the foregoing formulæ, derived from the theory of elasticity.

(b) Analysis of the preliminary design by the theory of elasticity treating the structure as symmetric. The computations are all given in tabular form, thus illustrating more clearly the method of conducting such analyses and furnishing a record of the numerical work which is well suited for reference and checking.

The computations for the elastic loads  $W$ , and the location of the  $(x, y)$  axes are carried out in Table 79c, following closely the method described in Art. 73.

The original subdivisions of the arch ring are still retained and each space is again divided into two, making 24 sections in the whole ring between  $a$  and  $b$ .

The programme carried out in the table is as follows: Compute the loads  $W_a$  from Eq. (73A) then determine  $z_o'$  and transform the original  $(v, z)$  axes to the  $(x, y)$  axes according to Eqs. (73J). Finally compute the  $W_b$  and  $W_c$  loads by Eqs. (73A), and the pole distances  $H_a, H_b$  and  $H_c$  from Eqs. (74A). This then furnishes all the data for constructing the  $X_a, X_b$  and  $X_c$  influence lines.

The  $y$  axis is known to be the axis of symmetry and must, therefore, pass through the crown joint  $n$  or 12. The location of the  $x$  axis is found by computing the ordinate  $z_o'$  of the origin  $O$  from some assumed  $v$  axis which was taken 26.4 ft. below the springing points 0 and 24, Fig. 79b.

In Table 79c, the dimensions  $D, z$  and  $\sec \phi$  are tabulated from the drawing and from these the values  $1/I, w_a$  and  $zw_a$  are derived. The abscissæ  $x$  and increments  $\Delta x$  are also taken from the drawing, and the other values result from performing the operations indicated in the headings. It should be noted that the constant modulus  $E$  was not considered in computing the elastic loads  $W$  so that all these loads are  $E$  times actual.

The secants are computed from

$$\sec \phi = \frac{R}{z+33.5} = \frac{115.8}{z+33.5} \text{ for points between } a \text{ and } m,$$

$$\sec \phi = \frac{77.7}{z+0.9} \text{ for points between } m \text{ and } n.$$

The sums  $\Sigma w_a = W_a, \Sigma zw_a = zW_a$ , etc., are computed by Simpson's rule for distance increments  $\Delta x$ , according to Eqs. (73E).

The ordinate  $z_o'$ , of the center of gravity or origin of coordinates, is then found to be  $\Sigma zw_a / \Sigma W_a = 64.72$  ft. Also, the sum  $\Sigma xzW_a = 0$  when extended over the whole arch, hence  $\tan \beta = 0$ , making  $y = z - z_o'$ .

The functions  $xw_a, x^2w_a, yw_a$  and  $y^2w_a$  are now figured and from these the sums  $\Sigma xw = W_b, \Sigma x^2w_a = xW_b, \Sigma yw_a = W_c$  and  $\Sigma y^2w_a = yW_c$  are again derived by applying Simpson's rule for the distance increments  $\Delta x$ . It should be noted that for the whole arch ring  $\Sigma W_b = 0$  and  $\Sigma W_c = 0$ , serving as a check on the computations. If these sums do not become zero, then errors have occurred which must be rectified. Small discrepancies will always be found owing to insufficient accuracy in the data and not carrying sufficient decimals. These may be adjusted by proportionate distribution. However, this must



TABLE 79C

COMPUTATIONS FOR THE LOCATION OF THE X, Y AXES AND FOR THE W FORCES AND POLE DISTANCES.—  
SYMMETRIC ARCH

Pt.	D ft.	z ft.	$\frac{1}{I} = \frac{12}{D^3}$ ft.	$\frac{w_a}{I \cos \phi}$	$zw_a$	$\Delta x$	$W_a = \Sigma w_a$	$\Sigma zw_a =$ $zW_a$	x	$y =$ $z - z_o'$	$xw_a$	$\Sigma xw_a =$ $W_b$	$x^2w_a$	$\Sigma x^2w_a =$ $xW_b$	$yw_a$	$\Sigma yw_a =$ $W_c$	$y^2w_a$	$\Sigma y^2w_a =$ $yW_c$
0	10.00	26.4	0.0120	1.933	0.0232	0.612	0.0694	1.9385	79.4	-38.32	1.8421	5.43	146.3	426.1	-0.889	-2.55	34.07	94.5
1	9.30	35.2	0.0149	1.686	0.0251	0.884	0.1565	5.5348	73.5	-29.52	1.8449	7.47	135.6	882.8	-0.741	-4.60	21.87	136.8
2	8.60	43.3	0.0189	1.508	0.0285	1.234	0.1855	8.0413	67.0	-21.42	1.9095	11.45	127.9	830.6	-0.610	-3.97	13.08	86.5
3	8.00	50.0	0.0234	1.387	0.0325	1.625	0.2106	10.5370	60.5	-14.72	1.9663	12.72	119.0	769.4	-0.478	-3.09	7.04	46.7
4	7.60	55.8	0.0273	1.297	0.0354	1.975	0.2306	12.8714	54.0	-8.92	1.9116	12.43	103.2	671.6	-0.316	-2.05	2.82	19.4
5	7.20	60.8	0.0321	1.228	0.0394	2.395	0.2558	15.5508	47.5	-3.92	1.8715	12.12	88.9	576.3	-0.154	-1.00	0.61	4.8
6	6.90	65.1	0.0365	1.174	0.0429	2.793	0.2784	18.1245	41.0	+0.38	1.7589	11.39	72.1	468.1	+0.016	+0.10	0.006	0.8
7	6.64	68.7	0.0410	1.116	0.0458	3.146	0.2971	20.3972	34.5	3.98	1.5801	10.23	54.5	354.5	0.182	1.17	0.73	5.2
8	6.46	71.6	0.0445	1.072	0.0477	3.415	0.3101	22.1901	28.0	6.88	1.3356	8.67	37.4	244.5	0.328	2.12	2.26	14.9
9	6.30	73.8	0.0480	1.040	0.0499	3.683	0.3238	23.8845	21.5	9.08	1.0729	6.95	23.1	151.4	0.453	2.92	4.11	26.6
10	6.20	75.3	0.0503	1.020	0.0513	3.863	0.3594	27.0597	15.0	10.58	0.7695	5.32	11.5	81.7	0.543	3.80	5.74	40.3
11	6.10	76.5	0.0528	1.004	0.0530	4.055	0.3980	30.4219	7.5	11.78	0.3975	2.97	3.0	24.0	0.624	4.66	7.35	54.6
12	6.00	76.8	0.0555	1.000	0.0555	4.262	0.2066	15.8531	0.0	12.08	0.0000	0.25	0.0	1.9	0.670	2.49	8.10	29.9
						Totals	3.2818	212.4048				107.40		5482.9		-17.26 +17.26		560.9

$$z_o' = \frac{\Sigma zw_a}{\Sigma W_a} = \frac{212.4048}{3.2818} = 64.72 \text{ ft.}, \quad \tan \beta = 0.0, \quad y = z - z_o' = z - 64.72.$$

The constant  $E$  was omitted from all  $w_a$  loads making all elastic loads,  $E$  times actual.



be confined to small errors not exceeding  $\frac{1}{2}$  per cent. Mistakes must be corrected and not distributed.

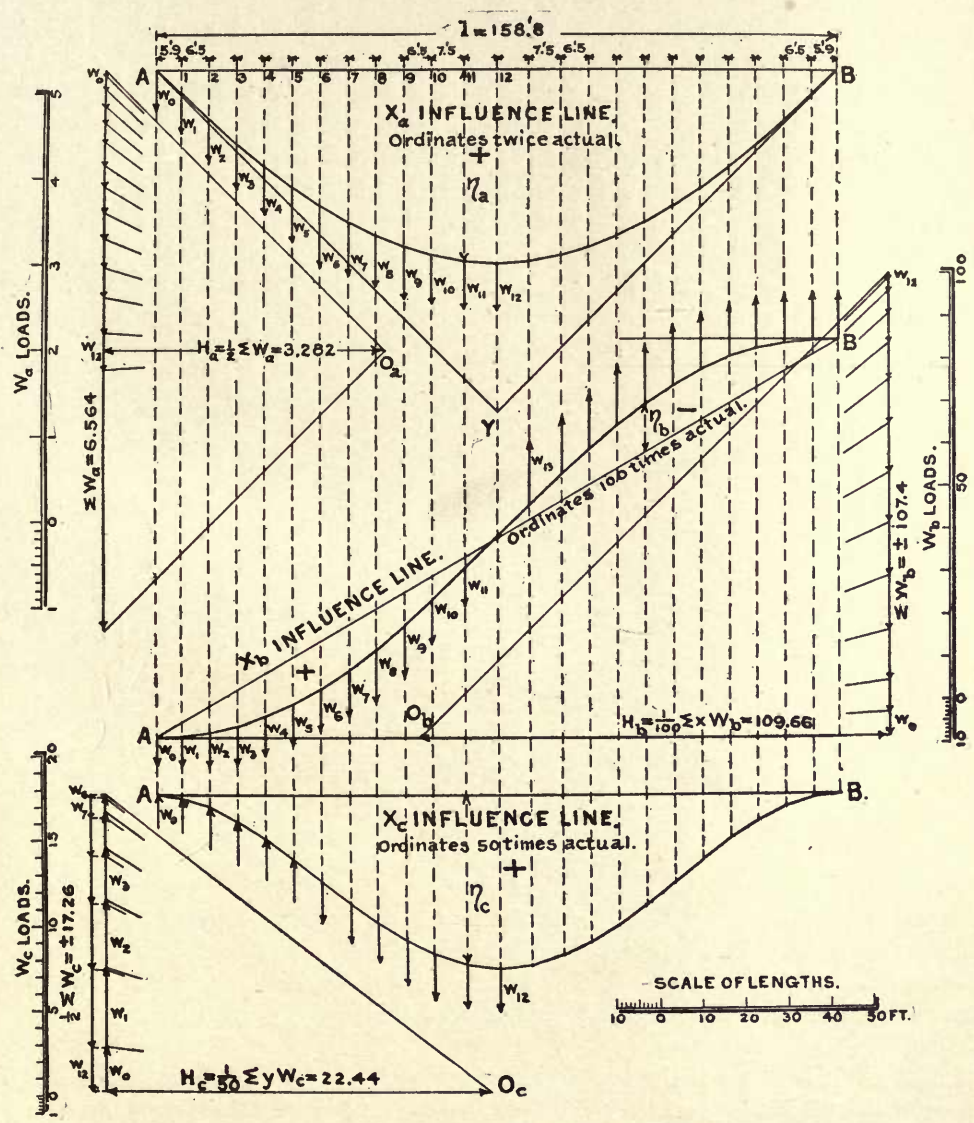


FIG. 79c.—X Influence Lines for Symmetric Arch.

The influence lines for  $X_a$ ,  $X_b$ , and  $X_c$  were drawn in Fig. 79c, using the results from Table 79c, and neglecting the effect  $\sum \cos \phi \Delta x / EF$  due to the axial thrust  $N$  on the pole distance  $H_c$  of the  $X_c$  influence line. If this effect is to be considered then the value  $\sum \cos \phi \Delta x / EF$  would be determined in the manner later indicated in Table 79m, omitting

the constant  $E$ , since it was also omitted in computing the values  $w_a$ . This is permissible because  $E$  being involved as a reciprocal factor in all elastic loads, as per Eqs. (72G), may be considered as canceled in Eqs. (72K). It must be remembered, however, that the elastic loads are then actually  $E$  times too large, a point which must be considered in computing temperature effects by Eqs. (75B).

The  $X$  influence lines are the equilibrium polygons for the  $W$  loads when certain pole distances are employed in the respective force polygons. It is generally convenient to draw these diagrams so that the influence line ordinates may appear a certain number of times actual when scaled to the scale of lengths of the drawing.

The  $X_a$  influence line is the equilibrium polygon for the  $W_a$  loads when the pole distance is made equal to  $H_a = \Sigma W_a = 6.564$ , as given by Table 79c. In the present case the pole was made  $\frac{1}{2} \Sigma W_a$  so that the ordinates  $\eta_a$  of the  $X_a$  influence

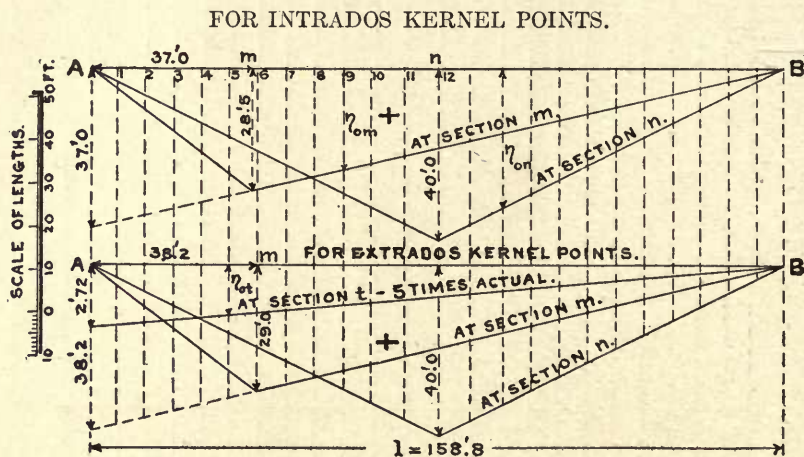


FIG. 79D.— $M_o$  Influence Lines for Symmetric Arch.

line become twice actual to the scale of lengths. The scale of the force polygon is chosen so as to give a reasonably large figure and to permit of accurate construction of the equilibrium polygon, otherwise the scale of loads need not bear any specified relation to the scale of ordinates. As a check on the drawing, the outer rays of this influence line must intersect on the  $y$  axis, in fact this is the graphic method of locating this axis.

The  $X_b$  influence line is the equilibrium polygon for the  $W_b$  loads when the pole distance is made equal to  $H_b = \Sigma x W_b = 2 \times 5482.9 = 10965.8$ , from Table 79c. As this pole is very large in comparison with the  $\Sigma W_b = \pm 107.4$ , it is advisable to take  $H_b = 0.01 \Sigma x W_b = 109.66$ , making the ordinates  $\eta_b$  one hundred times actual to the scale of lengths. The scale of the  $W_b$  loads was again chosen as a matter of convenience. The closing line  $\overline{AB}$  divides the influence line into a positive and a negative area.

The  $X_c$  influence line is the equilibrium polygon for the  $W_c$  loads when the pole is made equal to  $H_c = \cos \beta \Sigma y W_c = 2 \times 560.9 = 1121.8$ . Here also, the pole is too large



to furnish a well shaped force polygon and hence the pole was made  $H_c = 0.02 \Sigma y W_c$ , giving influence line ordinates  $\eta_c$  fifty times actual to the scale of lengths. The scale of  $W_c$  loads is also chosen as a matter of convenience.

The  $M_o$  influence lines are ordinary moment influence lines drawn for the simple span  $AB$  and the several kernel points of the critical sections, Fig. 79D. The ordinates may be made actual to the scale of lengths or, as in the case of the  $M_{oi}$  line, the ordinates were made five times actual.

The  $M_i$  and  $M_e$  influence lines for the kernel points of the critical sections are drawn by plotting the coordinates computed according to Eqs. (76E). See Fig. 79E and Tables 79E and 79F.

The coordinates of the kernel points  $i$  and  $e$  of the three critical sections at  $t$ ,  $m$  and  $n$  of the arch ring, are computed from the coordinates  $(x, y)$  of the axial points, using Eqs. (76D) as given in Table 79D.

TABLE 79D  
DATA RELATING TO THE CRITICAL SECTIONS

Point.	D ft.	$\phi$	AXIAL POINT.		$\frac{D}{6} \sin \phi$ ft.	$\frac{D}{6} \cos \phi$ ft.	KERNEL POINTS.			
			$x$ ft.	$y$ ft.			$x_i$ ft.	$y_i$ ft.	$x_e$ ft.	$y_e$ ft.
$t$	9.75	$56^\circ 30'$	78.05	-36.19	1.36	0.89	79.4	-35.3	76.7	-37.1
$m$	6.90	$30^\circ 30'$	41.8	0.0	0.62	0.99	42.4	+ 0.99	41.2	- 0.99
$n$	6.00	$0^\circ 00'$	0.0	+12.08	0.00	1.00	0.0	+13.08	0.0	+11.08

From the coordinates of the kernel points Table 79D, and the ordinates in Tables 79E and 79F, taken from the  $X_a$ ,  $X_b$ ,  $X_c$  and  $M_o$  influence lines,  $\eta_e$  and  $\eta_i$  are computed for each section of the span and for the critical sections  $t$ ,  $m$  and  $n$ .

Thus, for the section at  $m$ , Eqs. (76B) may be written

$$\left. \begin{aligned} \eta_{me} &= \eta_{oe} - [\eta_a + x_{me}\eta_b + y_{me}\eta_c] \\ \eta_{mi} &= \eta_{oi} - [\eta_a + x_{mi}\eta_b + y_{mi}\eta_c] \end{aligned} \right\} \dots \dots \dots (79c)$$

The computations are all indicated in the headings of the tables and no further comment is necessary here.

With the use of  $M_i$  and  $M_e$  influence lines for the three critical sections of a symmetric arch, the stresses in these sections may be found for any possible case of loading.

The resultant polygon for any particular case of simultaneous loading, is located when the redundants  $X_a$ ,  $X_b$  and  $X_c$  are known. Eqs. (78A) then give the necessary dimensions from which the resultant polygon may be drawn.

Table 79G gives the computations for the resultant polygon for the case of average loading  $Q + \frac{1}{2}P$ , over the entire span. This is the case for which the resultant polygon should coincide with the axis and the results are comparable with those on Fig. 79B.



The lettered dimensions in the table are all shown in Fig. 78A, but the resultant polygon is not drawn for this case.

The influence line ordinates  $\eta_a$ ,  $\eta_b$  and  $\eta_c$  are taken from Fig. 79c and the sums of the products of the loads and ordinates give the respective redundants  $X$  from which  $z_o$ ,  $c$  and  $c_o$ , also  $A_o$  and  $B_o$  are readily found by Eqs. (78A).

TABLE 79E

MOMENT INFLUENCE LINES FOR EXTRADOS KERNEL POINTS.—SYMMETRIC ARCH

Pt.	$\eta_a$	$\eta_b$	$\eta_c$	SECTION $t$				SECTION $m$ .				SECTION $n$ .		
				$\eta_t = \eta_o - [\eta_a + 76.7\eta_b - 37.1\eta_c]$				$\eta_m = \eta_o - [\eta_a + 41.2\eta_b - 0.99\eta_c]$				$\eta_n = \eta_o - [\eta_a + 11.1\eta_c]$		
	ft.	ft.	ft.	$\eta_o$	76.7 $\eta_b$	-37.1 $\eta_c$	$\eta_t$	$\eta_o$	41.2 $\eta_c$	0.99 $\eta_c$	$\eta_m$	$\eta_o$	11.1 $\eta_c$	$\eta_n$
0	0.0	0.0	0.0					0.0	0.0	0.0	0.0	0.0	0.0	0.0
1	2.9	0.031	0.014	2 61	2.38	- 0.52	-2.15	4.5	1.28	-0.01	0.33	2.9	0.14	-0.14
2	6.0	0.062	0.056					9.4	2.55	-0.05	0.90	6.3	0.62	-0.32
3	8.8	0.086	0.120	2 39	6.59	- 4.45	-8.55	14.2	3.54	-0.12	1.98	9.5	1.33	-0.63
4	11.4	0.102	0.200					19.1	4.20	-0.20	3.70	12.8	2.22	-0.82
5	13.9	0.110	0.296	2 17	8.44	-10.98	-9.19	24.0	4.53	-0.29	5.86	16.0	3.29	-1.19
6	16.0	0.111	0.396					29.0	4.57	-0.39	8.82	19.3	4.40	-1.10
7	17.8	0.105	0.496	1.95	8.05	-18.40	-5.50	27.5	4.33	-0.49	5.86	22.6	5.51	-0.71
8	19.4	0.095	0.588					25.9	3.91	-0.58	3.17	25.9	6.53	-0.03
9	20.7	0.079	0.672	1.73	6.06	-24.93	-0.10	24.2	3.25	-0.67	0.92	29.1	7.46	-0.94
10	21.7	0.058	0.734					22.7	2.39	-0.73	-0.66	32.3	8.15	2.45
11	22.4	0.030	0.782	1.48	2.30	-29.01	+5.69	21.0	1.24	-0.77	-1.87	36.0	8.68	4.92
12	22.6	0.000	0.800					19.2	0.00	-0.79	-2.70	40.0	8.88	8.52
13	22.4	-0.030	0.782	1 23	-2.30	-29.01	10.14	17.4	-1.24	-0.77	-2.99	36.0	8.68	4.92
14	21.7	-0.058	0.734					15.6	-2.39	-0.73	-2.98	32.3	8.15	2.45
15	20.7	-0.079	0.672	0.98	-6.06	-24.93	11.27	14.0	-3.25	-0.67	-2.78	29.1	7.46	0.94
16	19.4	-0.095	0.588					12.4	-3.91	-0.58	-2.51	25.9	6.53	-0.03
17	17.8	-0.105	0.496	0.77	-8.05	-18.40	9.42	10.8	-4.33	-0.49	-2.18	22.6	5.51	-0.71
18	16.0	-0.111	0.396					9.3	-4.57	-0.39	-1.74	19.3	4.40	-1.10
19	13.9	-0.110	0.296	0.55	-8.44	-10.98	6.07	7.7	-4.53	-0.29	-1.38	16.0	3.29	-1.19
20	11.4	-0.102	0.200					6.1	-4.20	-0.20	-0.90	12.8	2.22	-0.82
21	8.8	-0.086	0.120	0.32	-6.59	- 4.45	2.56	4.6	-3.54	-0.12	-0.54	9.5	1.33	-0.63
22	6.0	-0.062	0.056					3.1	-2.55	-0.05	-0.30	6.3	0.62	-0.32
23	2.9	-0.031	0.014	0.10	-2.38	- 0.52	0.10	1.5	-1.28	-0.01	-0.11	2.9	0.14	-0.14
24	0.0	0.0	0.0					0.0	0.0	0.0	0.0	0.0	0.0	0.0

All ordinates  $\eta$  in above table are expressed in feet.

Table 79H presents the case of unsymmetric loading shown in Fig. 79B. The results are plotted in Fig. 79F, and the resultant polygon is finally drawn in accordance with the method given in Art. 78.

The arch being symmetric  $\beta=0$  and  $l_1=l_2$  hence with the values of  $X_o$ ,  $X_b$  and  $X_c$  from Table 79H, the resulting data in that table were found.

In Fig. 79F the arch ring and the  $(x, y)$  axes are given to locate the points  $a$  and  $b$  on the verticals through the end supports and then to draw the resultant polygon.

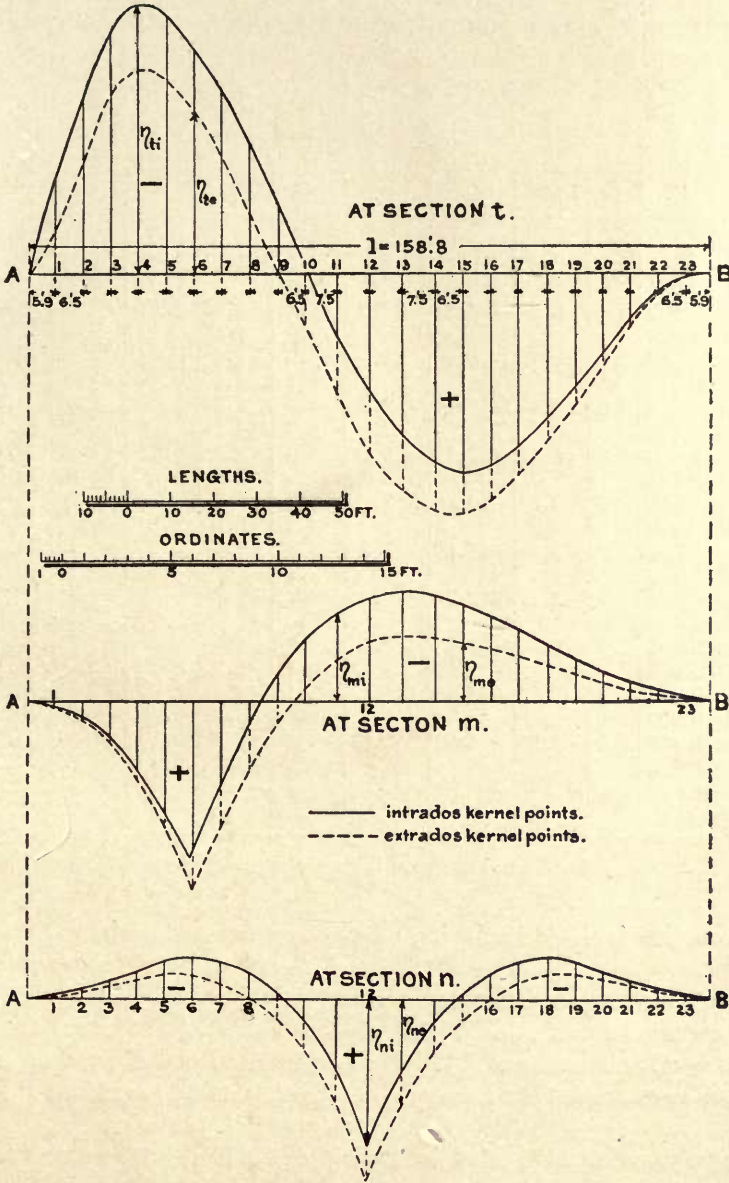


FIG. 79E.—*M* Influence Lines for the Kernel Points. Symmetric Arch.

TABLE 79F

MOMENT INFLUENCE LINES FOR INTRADOS KERNEL POINTS.—SYMMETRIC ARCH

Pt.	$\eta_a$ ft.	$\eta_b$ ft.	$\eta_c$ ft.	SECTION $t$ .				SECTION $m$ .				SECTION $n$ .		
				$\eta = \eta_o - [\eta_a + 79.4\eta_b - 35.3\eta_c]$				$\eta_m = \eta_o - [\eta_a + 42.4\eta_b + 0.99\eta_c]$				$\eta_n = \eta_o - [\eta_a + 13.1\eta_c]$		
				$\eta_o$	$79.4\eta_b$	$-35.3\eta_b$	$\eta_t$	$\eta_o$	$42.4\eta_b$	$0.99\eta_c$	$\eta_m$	$\eta$	$13.1\eta_c$	$\eta_n$
0	0.0	0.0	0.0					0.0	0.0	0.0	0.0	0.0	0.0	0.0
1	2.9	0.031	0.014	0.0	2.46	- 0.49	- 4.87	4.5	1.31	0.01	0.28	2.9	0.18	-0.18
2	6.0	0.062	0.056					9.4	2.63	0.05	0.72	6.3	0.73	-0.43
3	8.8	0.086	0.120	0.0	6.83	- 4.24	-11.39	14.3	3.65	0.12	1.73	9.5	1.57	-0.87
4	11.4	0.102	0.200					19.3	4.32	0.20	3.38	12.8	2.62	-1.22
5	13.9	0.110	0.296	0.0	8.73	-10.45	-12.18	24.2	4.66	0.29	5.35	16.0	3.88	-1.78
6	16.0	0.111	0.396					28.1	4.71	0.39	7.00	19.3	5.19	-1.89
7	17.8	0.105	0.496	0.0	8.34	-17.51	- 8.63	26.6	4.45	0.49	3.86	22.6	6.50	-1.70
8	19.4	0.095	0.588					25.0	4.03	0.58	0.99	25.9	7.70	-1.20
9	20.7	0.079	0.672	0.0	6.27	-23.72	- 3.25	23.5	3.35	0.67	-1.22	29.1	8.80	-0.21
10	21.7	0.058	0.734					22.0	2.46	0.73	-2.89	32.3	9.61	0.99
11	22.4	0.030	0.782	0.0	2.38	-27.60	+ 2.82	20.3	1.27	0.77	-4.14	36.0	10.24	3.36
12	22.6	0.000	0.800					18.6	0.00	0.79	-4.79	40.0	10.48	6.92
13	22.4	-0.030	0.782	0.0	-2.38	-27.60	7.58	16.8	-1.27	0.77	-5.10	36.0	10.24	3.36
14	21.7	-0.058	0.734					15.1	-2.46	0.73	-4.87	32.3	9.61	0.99
15	20.7	-0.079	0.672	0.0	-6.27	-23.72	9.29	13.6	-3.35	0.67	-4.42	29.1	8.80	-0.21
16	19.4	-0.095	0.588					12.0	-4.03	0.58	-3.95	25.9	7.70	-1.20
17	17.8	-0.105	0.496	0.0	-8.34	-17.51	8.05	10.6	-4.45	0.49	-3.24	22.6	6.50	-1.70
18	16.0	-0.111	0.396					9.1	-4.71	0.39	-2.58	19.3	5.19	-1.89
19	13.9	-0.110	0.296	0.0	-8.73	-10.45	5.28	7.5	-4.66	0.29	-2.03	16.0	3.88	-1.78
20	11.4	-0.102	0.200					6.0	-4.32	0.20	-1.28	12.8	2.62	-1.22
21	8.8	-0.086	0.120	0.0	-6.83	- 4.24	2.27	4.4	-3.65	0.12	-0.87	9.5	1.57	-0.87
22	6.0	-0.062	0.056					3.0	-2.63	0.05	-0.42	6.3	0.73	-0.43
23	2.9	-0.031	0.014	0.0	-2.46	- 0.49	0.05	1.4	-1.31	0.01	-0.20	2.9	0.18	-0.18
24	0.0	0.0	0.0					0.0	0.0	0.0	0.0	0.0	0.0	0.0

All ordinates in above table are expressed in feet.

The construction is made by laying off  $z_o$  down from the origin  $O$  on the  $y$  axis to obtain the point  $s$ . Then lay off  $-c_o$  up from  $s$  to determine  $s'$  on the  $y$  axis. Through  $s'$  draw a line parallel to the  $x$  axis and where this line intersects the vertical at  $A$  gives the point  $a$  on the resultant  $R'_1$ . The line  $\overline{as}$  prolonged to intersect the vertical at  $B$  gives the point  $b$  on the resultant  $R'_2$ . Knowing  $A_o$ ,  $B_o$  and  $H'$ , the resultants  $R'_1$  and  $R'_2$  can now be drawn, and their intersection must fall on the resultant  $R$ , distant  $r$  from the  $z$  axis.

The force polygon is constructed by laying off the load line  $\overline{MN}$  and then finding  $T$ , which is the point of division between  $A_o$  and  $B_o$ . Through  $T$  draw  $\overline{OT} \parallel \overline{ab}$  and lay off the force  $H'$ , thus locating the pole  $O_1$ , and giving the reactions  $R'_1$  and  $R'_2$ . The equilibrium polygon drawn through  $a$  and with pole  $O_1$  will then pass through  $b$  as a final check. The resultant polygon for unsymmetric loading intersects the axial line three times, as it should.



TABLE 79G  
COMPUTATION OF THE RESULTANT POLYGON FOR LOADS  $Q + \frac{1}{2}P$  OVER SPAN. SYMMETRIC ARCH.

Point.	$\eta_a$ ft.	$\eta_b$ ft.	$\eta_c$ ft.	Dead Loads, $Q$ cu.ft.	Live Loads, $\frac{P}{2}$ cu.ft.	Total Loads, $Q + \frac{P}{2}$ cu.ft.	$\eta \left( Q + \frac{P}{2} \right)$ for			RESULTING DATA.
							$X_a$	$X_b$	$X_c$	
1	2.9	0.031	0.014	367.4	49.65	417.0	1209.3	12.93	5.84	<p>For <math>l = 158.8</math> ft.; <math>l_1 = l_2 = 79.4</math> ft.; <math>\cos \beta = 1</math>; <math>\tan \alpha = 0</math>.  Then <math>H = H' = X_c = 1135.9</math> cu.ft.  <math>z_o = \frac{X_a}{H} = 38.19</math> ft.  <math>c_o = \frac{l}{H} X_b = 0</math> and <math>c_o = \frac{l_1}{H} X_b = 0</math>.  <math>r = \frac{l}{2} = 79.4</math> ft. = lever arm of <math>R</math>.  <math>A_o = B_o = \frac{R}{2} = 1696.9</math> cu.ft.  <math>R_1 = \sqrt{H^2 + A_o^2} = 2041.5</math>.</p>
3	8.8	0.086	0.120	276.1	49.65	325.8	2867.0	28.02	39.10	
5	13.9	0.110	0.296	223.4	49.65	273.0	3794.7	30.03	80.81	
7	17.8	0.105	0.496	182.7	49.65	232.4	4136.7	24.40	115.27	
9	20.7	0.079	0.672	168.0	49.65	217.7	4506.4	17.20	146.29	
11	22.4	0.030	0.782	173.7	57.30	231.0	5174.4	6.93	180.64	
13	22.4	-0.030	0.782	173.7	57.30	231.0	5174.4	-6.93	180.64	
15	20.7	-0.079	0.672	168.0	49.65	217.7	4506.4	-17.20	146.29	
17	17.8	-0.105	0.496	182.7	49.65	232.4	4136.7	-24.40	115.27	
19	13.9	-0.110	0.296	223.4	49.65	273.0	3794.7	-30.03	80.81	
21	8.8	-0.086	0.120	276.1	49.65	325.8	2867.0	-28.02	39.10	
23	2.9	-0.031	0.014	367.4	49.65	417.0	1209.3	-12.93	5.84	
						3393.8	43377.0	+119.51	1135.9	
						$= R$	$= X_a$	-119.51	$= X_c$	
								$X_b = 0$ .		

TABLE 79H

COMPUTATION OF THE RESULTANT POLYGON FOR LOADS  $P$  OVER THE HALF SPAN 11 TO 24.  
SYMMETRIC ARCH.

Pt.	$\eta_a$ ft.	$\eta_b$ ft.	$\eta_c$ ft.	Dead Loads $Q$ cu.ft.	Live Loads, $P$ cu.ft.	Total Loads, $Q + P$ cu.ft.	$\eta(Q + P)$ for			Moments of $Q + P$ about $A$ .		RESULTING DATA.
							$X_a$	$X_b$	$X_c$	$r$ ft.	$r(Q + P)$	
1	2.9	0.031	0.014	367.4	0.0	367.4	1065.5	11.39	5.14	5.9	2167.7	For $l = 158.8$ ft.; $l_1 = l_2 = 79.4$ ft., $\cos \beta = 1$ . Then $H = X_c \cos \beta = 1225.42$ cu.ft. $\tan \alpha = \tan \beta + \frac{X_b}{H}$ $H' = \frac{H}{\cos \alpha} = 1226.2$ cu.ft. $X_a = \frac{X_c}{H} = 37.45$ ft. $z_o = \frac{l}{H} X_b = -5.29$ ft. $c = \frac{l_1}{H} X_b = -2.64$ ft. $r = \frac{M}{R} = \frac{302142.9}{3508.3} = 86.12$ ft. $B_o = \frac{M}{l} = \frac{302142.9}{158.8} = 1902.66$ cu.ft. $A_o = R - B_o = 3508.3 - B_o = 1605.64$ cu.ft.
3	8.8	0.086	0.120	276.1	0.0	276.1	2429.7	23.74	33.13	18.9	5218.3	
5	13.9	0.110	0.296	223.4	0.0	223.4	3105.3	24.57	66.13	31.9	7126.5	
7	17.8	0.105	0.496	182.7	0.0	182.7	3252.1	19.18	90.62	44.9	8203.2	
9	20.7	0.079	0.672	168.0	0.0	168.0	3477.6	13.27	112.90	57.9	9727.2	
11	22.4	0.030	0.782	173.7	114.6	288.3	6457.9	8.65	225.45	71.9	20728.8	
13	22.4	-0.030	0.782	173.7	114.6	288.3	6457.9	-8.65	225.45	86.9	25053.3	
15	20.7	-0.079	0.672	168.0	99.3	267.3	5533.1	-21.12	179.63	100.9	26970.6	
17	17.8	-0.105	0.496	182.7	99.3	282.0	5019.6	-29.61	139.87	113.9	32119.8	
19	13.9	-0.110	0.296	223.4	99.3	322.7	4485.5	-35.50	95.52	126.9	40950.6	
21	8.8	-0.086	0.120	276.1	99.3	375.4	3303.5	-32.28	45.05	139.9	52518.5	
23	2.9	-0.031	0.014	367.4	99.3	466.7	1353.4	-14.47	6.53	152.9	71358.4	
				3508.3		45941.1	+100.80	1225.42			302142.9	
				$= R$		$= X_a$	-141.63	$= X_c$			$= M$	

$X_b = -40.83$

SYMMETRIC ARCH.

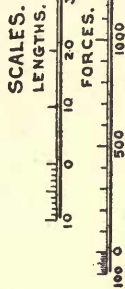
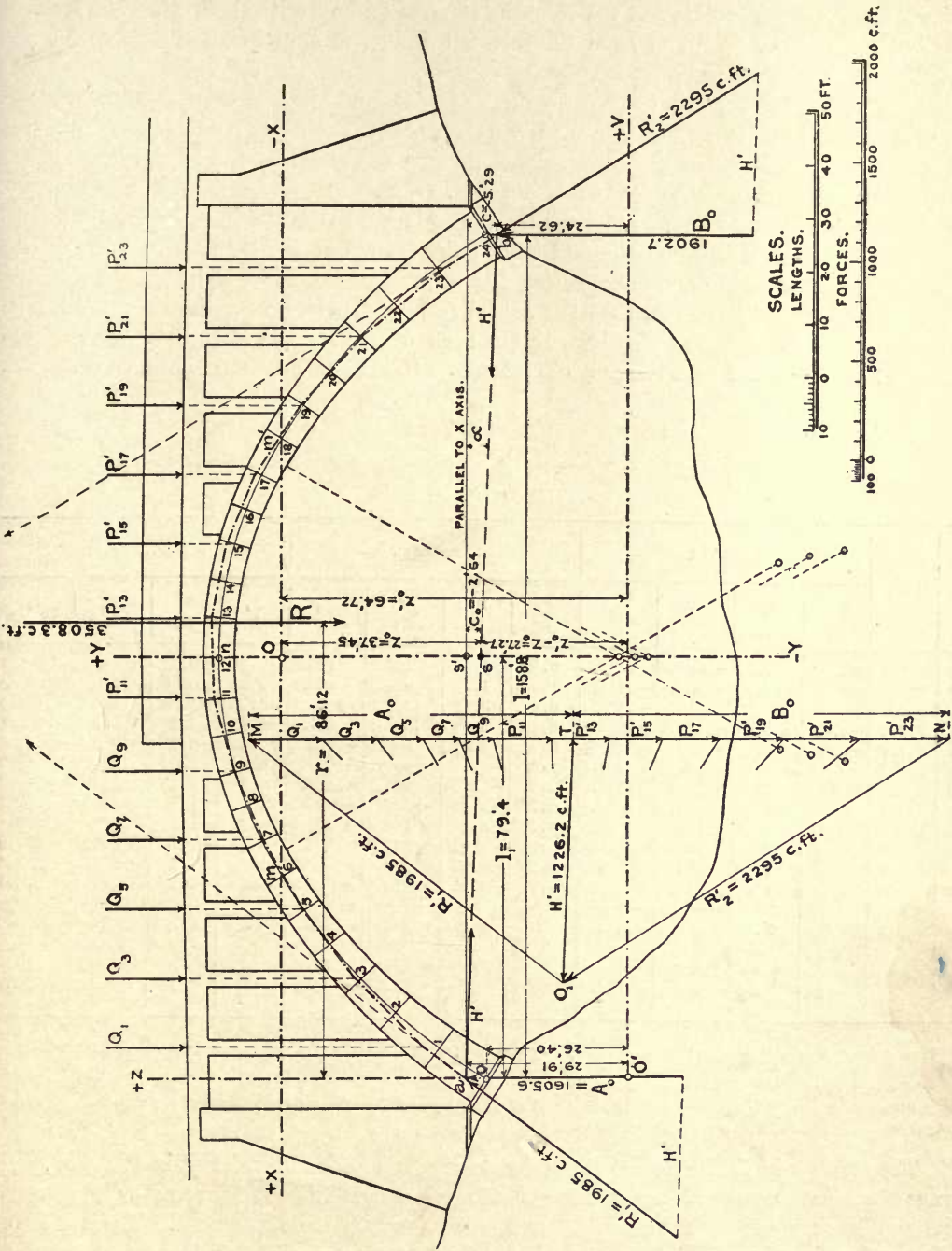


Fig. 79F.



The moments  $M_e$  and  $M_i$  and the resulting stresses on any critical section, and for any case of loading, may be found from the moment influence lines Fig. 79E, drawn for the kernel points of the critical sections.

The stresses for the two cases of loading,  $Q + \frac{1}{2}P$  and the one-sided load  $Q + P$ , are computed in Tables 79I and 79J, using the influence line ordinates from Tables 79E and 79F, or from the diagrams Fig. 79E. At the bottom of the tables the values  $R$ ,  $N$ ,  $v$ ,  $f_e$  and  $f_i$  are computed for each section, using Eqs. (76c).

The sections  $t$  and  $t'$ , at the abutments, are so located that the intrados kernel points  $i$  fall on the verticals through the end axial points, thus avoiding negative  $\eta_o$  values in Eqs. (79c), and other difficulties affecting the  $X$  influence lines.

It is seen from Table 79I, that the actual resultant polygon for the case of average loading really coincides very closely with the arch center line as designed. The offsets  $v$  being + and - show that the polygon intersects the center line four times, as it should.

TABLE 79I  
MOMENTS  $M_e$  AND  $M_i$  FOR THE CRITICAL SECTIONS, LOADS  $Q + \frac{P}{2}$   
SYMMETRIC ARCH

Pt.	Loads $Q + \frac{P}{2}$ cu.ft.	SECTION $t$ .				SECTION $m$ .				SECTION $n$ .			
		$\eta_e$ ft.	$\eta_i$ ft.	$M_e$	$M_i$	$\eta_e$ ft.	$\eta_i$ ft.	$M_e$	$M_i$	$\eta_o$ ft.	$\eta$ ft.	$M_e$	$M_i$
1	417.0	-2.15	-4.87	-896.6	-2030.8	0.33	0.28	137.6	116.8	-0.14	-0.18	-58.4	-75.1
3	325.8	-8.55	-11.39	-2785.6	-3710.9	1.98	1.73	645.1	563.6	-0.63	-0.87	-205.3	-283.4
5	273.0	-9.19	-12.18	-2508.9	-3325.1	5.86	5.35	1599.8	1460.6	-1.19	-1.78	-324.9	-485.9
7	232.4	-5.50	-8.63	-1278.2	-2005.6	5.86	3.86	1366.9	897.1	-0.71	-1.70	-165.0	-395.1
9	217.7	-0.10	-3.25	-21.8	-707.5	0.92	-1.22	200.3	-265.6	+0.94	-0.21	+204.6	-45.7
11	231.0	+5.69	+2.82	+1314.4	+651.4	-1.87	-4.14	-432.0	-956.3	4.92	+3.36	1136.5	+776.2
13	231.0	10.14	7.58	2342.3	1751.0	-2.99	-5.10	-690.7	-1178.1	4.92	+3.36	1136.5	+776.2
15	217.7	11.27	9.29	2453.5	2022.4	-2.78	-4.42	-605.2	-962.2	+0.94	-0.21	+204.6	-45.7
17	232.4	9.42	8.05	2189.2	1870.8	-2.18	-3.24	-506.6	-753.0	-0.71	-1.70	-165.0	-395.1
19	273.0	6.07	5.28	1657.1	1441.4	-1.38	-2.03	-376.7	-554.2	-1.19	-1.78	-324.9	-485.9
21	325.8	2.56	2.27	834.0	739.6	-0.54	-0.87	-175.9	-283.4	-0.63	-0.87	-205.3	-283.4
23	417.0	0.10	0.05	41.7	20.9	-0.11	-0.20	-45.9	-83.4	-0.14	-0.18	-58.4	-75.1
$R =$	3393.5	$D =$	9'.75	+3341.1	-3282.4	$D =$	6'.90	+1116.7	-1998.1	$D =$	6'.00	+1175.0	-1018.0
			$N =$	2037.9			$N =$	1354.3			$N =$	1096.5	
			$v =$	+0'.014			$v =$	-0'.325			$v =$	+0'.071	
			$f =$	-210.9	-207.2		$f =$	-140.8	-251.8		$f =$	-195.9	-169.7

$$\text{Eqs. (76c), } N = \frac{3}{D}(M_e - M_i); \quad v = \frac{M_e + M_i}{2N}; \quad f_e = -\frac{6M_e}{D^2}; \quad f_i = \frac{6M_i}{D^2}; \quad v \text{ is positive when measured from the axis}$$

toward the extrados.

All loads in above table are expressed in cubic feet of masonry and the stresses are cubic feet per square foot. Cubic feet per square foot  $\times 0.972$  = pounds per square inch.

The stresses in Table 79J are those due to the case of loading shown in Fig. 79F, and hence the offsets  $v$  are those which the resultant polygon in that figure actually present. The smallness of the scale, however, prevents a very close agreement. The resultant polygon for the unsymmetric loading is seen to intersect the center line three times as it should, since two values  $v$  are negative and three positive.

TABLE 79J

MOMENTS  $M_e$  AND  $M_i$  FOR CRITICAL SECTIONS. TOTAL DEAD AND ONE-SIDED LIVE SYMMETRIC ARCH

Pt.	Loads $Q$ and $P'$ , cu.ft.	SECTION $l$ .				SECTION $m$ .				SECTION $n$ .			
		$\eta_e$ ft.	$\eta_i$ ft.	$M_e$	$M_i$	$\eta_e$ ft.	$\eta_i$ ft.	$M_e$	$M_i$	$\eta_e$ ft.	$\eta_i$ ft.	$M_e$	$M_i$
1	$Q_1=367.4$	- 2.15	- 4.87	- 789.9	-1789.2	0.33	0.28	121.2	102.9	-0.14	-0.18	- 51.4	- 66.1
3	$Q_3=276.1$	- 8.55	-11.39	-2360.7	-3144.8	1.98	1.73	546.7	477.6	-0.63	-0.87	- 173.9	-240.2
5	$Q_5=223.4$	- 9.19	-12.18	-2053.0	-2721.0	5.86	5.35	1309.1	1195.2	-1.19	-1.78	- 265.8	-397.6
7	$Q_7=182.7$	- 5.50	- 3.63	-1004.9	-1576.7	5.86	3.86	1070.6	705.2	-0.71	-1.70	- 129.7	-310.6
9	$Q_9=168.0$	- 0.10	- 3.25	- 16.8	- 546.0	0.92	-1.22	154.6	- 205.0	+0.94	-0.21	+ 157.9	- 35.3
11	$P_{11}'=288.3$	+ 5.69	+ 2.82	+1640.4	+ 813.0	-1.87	-4.14	-539.1	-1193.6	4.92	+3.36	1418.4	+968.7
13	$P_{13}'=288.3$	10.14	7.58	2923.4	2185.3	-2.99	-5.10	-862.0	-1470.3	4.92	+3.36	1418.4	+968.7
15	$P_{15}'=267.3$	11.27	9.29	3012.5	2483.2	-2.78	-4.42	-743.1	-1181.5	+0.94	-0.21	+ 252.3	- 56.1
17	$P_{17}'=282.0$	9.42	8.05	2656.4	2270.1	-2.18	-3.24	-614.8	- 913.7	-0.71	-1.70	- 200.2	-479.4
19	$P_{19}'=322.7$	6.07	5.28	1958.8	1703.8	-1.38	-2.03	-445.3	- 653.0	-1.19	-1.78	- 384.0	-574.4
21	$P_{21}'=375.4$	2.56	2.27	961.0	852.2	-0.54	-0.87	-202.7	- 326.6	-0.63	-0.87	- 236.5	-326.6
23	$P_{23}'=466.7$	0.10	0.05	46.0	23.3	-0.11	-0.20	- 51.3	- 93.3	-0.14	-0.18	- 65.3	- 84.0
$R=$	3508.3	$D=$	9'.75	+6973.9	+ 453.2	$D=$	6'.90	-256.1	-3556.1	$D=$	6'.00	+1740.2	-632.9
			$N=$	2006.4			$N=$	1434.8			$N=$	1186.6	
			$v=$	+1'.851			$v=$	-1'.328			$v=$	+0'.467	
			$f=$	- 440.2	+ 28.5		$f=$	+ 32.3	- 448.2		$f=$	- 290.0	-105.5

Pt.	Loads $Q$ and $P'$ , cu.ft.	SECTION $m'$ .				SECTION $l'$ .			
		$\eta_e$ ft.	$\eta_i$ ft.	$M_e$	$M_i$	$\eta_e$ ft.	$\eta_i$ ft.	$M_e$	$M_i$
1	$Q_1=367.4$	-0.11	-0.20	- 40.4	- 73.5	0.10	0.05	36.7	18.3
3	$Q_3=276.1$	-0.54	-0.87	- 149.1	- 240.2	2.56	2.27	706.8	626.7
5	$Q_5=223.4$	-1.38	-2.03	- 308.3	- 453.5	6.07	5.28	1356.0	1179.6
7	$Q_7=182.7$	-2.18	-3.24	- 398.3	- 591.9	9.42	8.05	1721.0	1470.7
9	$Q_9=168.0$	-2.78	-4.42	- 467.0	- 742.6	11.27	9.29	1893.4	1560.7
11	$P_{11}'=288.3$	-2.99	-5.10	- 862.0	-1470.3	10.14	7.58	2923.4	2185.3
13	$P_{13}'=288.3$	-1.87	-4.14	- 539.1	-1193.6	5.69	2.82	1640.4	813.0
15	$P_{15}'=267.3$	+0.92	-1.22	+ 245.9	- 326.0	-0.10	- 3.25	- 26.7	- 868.7
17	$P_{17}'=282.0$	5.86	+3.86	1652.5	+1088.5	-5.50	- 8.63	-1551.0	-2433.7
19	$P_{19}'=322.7$	5.86	5.35	1891.0	1726.4	-9.19	-12.18	-2965.6	-3930.5
21	$P_{21}'=375.4$	1.98	1.73	743.3	649.4	-8.55	-11.39	-3210.5	-4275.8
23	$P_{23}'=466.7$	0.33	0.28	154.0	130.7	-2.15	- 4.87	-1003.4	-2272.8
$R=$	3508.3	$D=$	6'.90	+1922.5	-1496.6	$D=$	9'.75	+1520.5	-5927.2
			$N=$	1485.3			$N=$	2291.4	
			$v=$	+0'.144			$v=$	-0'.962	
			$f=$	- 242.3	- 188.7		$f=$	- 96.0	- 374.1

The influence line ordinates  $\eta$  for points  $m'$  and  $l'$  are symmetric with those of points  $m$  and  $l$ . See note, foot of Table 79i.



By referring to Fig. 79E, it is seen that this position of loading gives maximum stresses for the section  $l$  and almost maximum for section  $m$ , but not for the other sections. In the present instance the effects at the five critical sections were found for one position of the moving load, giving a simultaneous condition of stress, but not maximum stresses at all sections.

The maximum stresses for each of the critical sections must be computed for special positions of the moving train as illustrated in Table 79K, for the crown section.

In the general investigation of stresses it is best to obtain the dead load moments separately for each section and combine these with the live load moments which are found without regard to impact and then increased for impact prior to adding the dead load moments, as shown in Table 79K.

TABLE 79K  
INVESTIGATION FOR MAXIMUM STRESSES AT THE CROWN SECTION "n."  
SYMMETRIC ARCH

Point.	Dead Loads $Q$ cu.ft.	Total Dead Load Moments				No. Wheel from Head of Train.	Live Loads, cu.ft.	Max. + Live Load Moments.			
		$\eta_e$ ft.	$\eta_i$ ft.	$M_e$	$M_i$			$\eta_e$ ft.	$\eta_i$ ft.	$M_e$	$M_i$
1	367.4	-0.14	-0.18	- 51.4	- 66.1	1	16.5	0.00	-1.19	0.0	- 19.6
3	276.1	-0.63	-0.87	-173.9	-240.2	2	33.0	1.30	+0.10	42.9	+ 3.3
5	223.4	-1.19	-1.78	-265.8	-397.6	3	33.0	2.55	1.10	84.2	36.3
7	182.7	-0.71	-1.70	-129.7	-310.6	4	33.0	4.10	2.55	135.3	84.2
9	168.0	+0.94	-0.21	+157.9	- 35.3	5	33.0	6.10	4.45	201.3	146.9
11	173.7	4.92	+3.36	854.6	+583.6	6	21.4	6.40	4.80	137.0	102.7
13	173.7	4.92	+3.36	854.6	+583.6	7	21.4	4.40	2.80	94.2	59.9
15	168.0	0.94	-0.21	157.9	- 35.3	8	21.4	2.55	1.00	54.6	21.4
17	182.7	-0.71	-1.70	-129.7	-310.6	9	21.4	1.30	0.00	27.8	0.0
19	223.4	-1.19	-1.78	-265.8	-397.6	10	0.0	0.00	-1.19	0.0	0.0
21	276.1	-0.63	-0.87	-173.9	-240.2						
23	367.4	-0.14	-0.18	- 51.4	- 66.1						
$R=$ 2782.6		$D=$ 6'.00		+783.4	-932.4			Max. + L.L. =		+777.3	+435.1
			$N=$ 857.9					84% impact =		652.9	+365.5
			$v=$ -0'.087					Total D.L. =		783.4	-932.4
			$f=$ -130.6	-155.4				Total max. + $M=$		2213.6	-131.8
								max. $N=$		1190.8	$v=$ -0'.88
								max. $f=$		-369.0	- 22.9

All stresses  $f$  are in cubic feet per square foot. Multiply by 0.972 to reduce to pounds per square inch. Impact for 56 feet is  $\frac{300}{300+56}=0.84$ .

The live load moments are found by placing the train of wheel loads for Cooper's E 60 loading over the positive portions of the  $M_e$  and  $M_i$  influence lines for the section in question to obtain the simultaneous maximum positive moments for the kernel points. Similarly the negative portions of these influence lines will yield the maximum negative moments for the same section.



Since the loads are distributed over a roadbed 13 feet in width the train of wheel loads, for the present purpose, is obtained by dividing the standard axle loads by 13, and also converting the loads into cubic feet of masonry, all as shown in Fig. 79g. The load diagram must of course be drawn to the same horizontal scale as the influence lines, which is not the case in the figures as here reproduced.

The wheel loads, in kips, are converted into cubic feet of masonry by multiplying kips by  $1000/140 = 7.14$ .

The maximum stresses at the crown section  $n$  are computed in Table 79κ. The dead load moments are first found and these are combined with the live load moments which latter are increased for impact. The maximum stresses are found from the total maximum moments.

The live load diagram Fig. 79G, was placed over the influence line for section  $n$ , Fig. 79E, so that the first load came at the point 8, which is the zero point for positive ordinates. One locomotive then covered the distance from point 8 to 16, and the remainder of the span was considered empty. The same position was used for both  $M_e$  and  $M_i$  moments, because Eqs. (76c) apply only to simultaneous kernel moments.

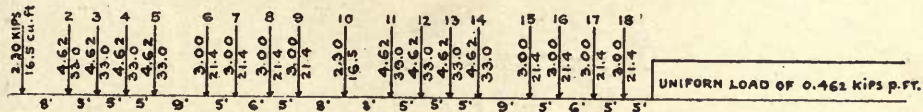


FIG. 79g.—Cooper's E 60 Loading for an Arch Ring One Foot Thick.

Comparing the result for  $max. f_e = -369$  cu.ft., obtained here with the value given in Table 79j as  $-290$  cu.ft., the relative effect of the two cases of loading is clearly seen.

Each of the critical sections should be examined in the manner shown in Table 79κ, and the positive as well as negative influence line areas should be considered as separate cases.

The temperature stresses are easily determined according to the method given in Art. 75.

Referring back to the given data,  $E = 3,670,000$  lbs. per sq.in.  $= 3,755,720$  cu.ft. per sq.ft.;  $\epsilon = 0.000,005,4$  per  $1^\circ$  F;  $t = -80^\circ$ ;  $l = 158.8$  ft; and  $\cos \beta = 1$ , then  $\epsilon t l = -0.0686$  ft., and by Eq. (75c)

$$M_{mt} = -y_m \frac{\epsilon t l E}{\cos^2 \beta \Sigma y W_c} = + \frac{0.0686 \times 3,775,720}{1121.8} y_m = 230.9 y_m,$$

where the value  $\cos^2 \beta \Sigma y W_c$  is taken from Table 79c for  $W_c$  loads which are  $E$  times actual.

The stresses on any section are then found by evaluating the kernel moments for temperature and combining these with the kernel moments previously found for the case of maximum loading.

Thus, for the haunch section  $t$ , Table 79D gives  $D=9'.75$ ,  $y_e=-37'.1$  and  $y_i=-35'.3$  and maximum  $M_e$  and  $M_i$  are taken from Table 79J as follows:

$$M_{et} = -37.1 \times 230.9 = -8566.4$$

$$M_e \text{ from Table 79J} = +6973.9$$

$$\text{Total } M_e = -1592.5$$

$$\text{giving } f_e = + \frac{6 \times 1592.5}{9.75^2} = +100.5 \text{ cu.ft.}$$

Also,

$$M_{it} = -35.3 \times 230.9 = -8150.8$$

$$M_i \text{ from Table 79J} = +453.2$$

$$\text{Total } M_i = -7697.6$$

$$\text{giving } f_i = - \frac{6 \times 7697.6}{9.75^2} = -458.8 \text{ cu.ft.}$$

Similarly for the crown section  $n$  where  $D=6'.0$ ,  $y_e=11'.08$  and  $y_i=13'.08$ , then for the maximum moments from Table 79K

$$M_{en} = 10.08 \times 230.9 = +2558.4$$

$$M_e \text{ from Table 79K} = +2213.6$$

$$\text{Total } M_e = +4772.0 \text{ or } f_e = -795.3 \text{ cu.ft.,}$$

and

$$M_{in} = 13.08 \times 230.9 = +3020.2$$

$$M_i \text{ from Table 79K} = -131.8$$

$$\text{Total } M_i = +2888.4 \text{ or } f_i = +481.4 \text{ cu.ft.}$$

It is readily seen that these stresses are excessive and would undoubtedly cause cracks on the tension elements occurring in the intrados at the crown and in the extrados at the haunches.

(c) **Analysis as under (b), treating the structure as unsymmetric.** It is presumed that for good and sufficient reasons the  $B$  abutment had to be founded on a lower stratum of rock, a condition which developed after the original design for the symmetric arch was accepted. The question to be answered here is whether such a change in the location of a foundation would seriously alter the resulting stresses and necessitate a change in the design.

The location of the  $(x, y)$  axes and computation of the elastic loads is given in Tables 79L and 79M, following the method outlined in Art. 73, and using the same data as in the previous case of the symmetric arch with the addition of two sections at the right-hand end, producing the unsymmetric condition illustrated in Fig. 79H..

The  $(z, v)$  axes are located through the axial points of the haunches, which is the same position previously chosen for these axes in dealing with the symmetric condition.

The dimensions  $D$ ,  $v$  and  $z$  are tabulated in Table 79L, and from these the values  $1/I$ ,  $\sec \phi$ ,  $w_a$ ,  $vw_a$  and  $zw_a$  are computed, using the formulæ for  $\sec \phi$  above given, p. 331.



TABLE 79L.—COMPUTATIONS FOR THE LOCATION OF THE X, Y AXES. UNSYMMETRIC ARCH

Pt.	D ft.	COORDINATES.		$\frac{1}{I} = \frac{12}{D^3}$ ft. <sup>4</sup>	$\sec \phi$	$w_a = \frac{1}{I \cos \phi}$	$vw_a$	$zw_a$ ft.	$W_a = \Sigma w_a$	$\Sigma vw_a = vW_a$	$\Sigma zw_a = zW_a$	$x = l_1 - v$ ft.	$xz$	$x^2$
		v ft.	z ft.											
0	10.00	0.0	+ 26.4	0.0120	1.933	+ 0.0232	+ 0.00	+ 0.612	0.0694	0.0727	1.9385	+ 81.27	+ 2145.6	+ 6604.8
1	9.30	5.9	35.2	0.0149	1.686	0.0251	0.148	0.884	0.1566	0.9553	5.5348	75.37	2653.0	5680.6
2	8.60	12.4	43.3	0.0189	1.508	0.0285	0.353	1.234	0.1855	2.3230	8.0413	68.87	2982.1	4743.1
3	8.00	18.9	50.0	0.0234	1.387	0.0325	0.614	1.625	0.2106	4.0028	10.5370	62.37	3118.5	3890.0
4	7.60	25.4	55.8	0.0273	1.297	0.0354	0.899	1.975	0.2307	5.8818	12.8714	55.87	3117.5	3121.5
5	7.20	31.9	60.8	0.0321	1.228	0.0394	1.257	2.395	0.2558	8.1853	15.5508	49.37	3001.7	2437.4
6	6.90	38.4	65.1	0.0365	1.174	0.0429	1.647	2.793	0.2784	10.7553	18.1245	42.87	2790.8	1837.8
7	6.64	44.9	68.7	0.0410	1.116	0.0458	2.056	3.146	0.2971	13.3523	20.3972	36.37	2498.6	1322.8
8	6.46	51.4	71.6	0.0445	1.072	0.0477	2.452	3.415	0.3102	15.9548	22.1901	29.87	2138.7	892.2
9	6.30	57.9	73.8	0.0480	1.040	0.0499	2.889	3.683	0.3238	18.7608	23.8845	23.37	1724.7	546.1
10	6.20	64.4	75.3	0.0503	1.020	0.0513	3.304	3.863	0.3594	23.2158	27.0597	16.87	1270.3	284.6
11	6.10	71.9	76.5	0.0528	1.004	0.0530	3.811	4.035	0.3980	28.6381	30.4219	9.37	716.8	87.8
12	6.00	79.4	76.8	0.0555	1.000	0.0555	4.407	4.262	0.4132	32.8044	31.7063	+ 1.87	143.6	3.5
13	6.10	86.9	76.5	0.0528	1.004	0.0530	4.606	4.035	0.3980	34.5688	30.4219	- 5.63	- 430.7	31.7
14	6.20	94.4	75.3	0.0503	1.020	0.0513	4.843	3.863	0.3594	33.8520	27.0597	- 13.13	- 988.7	172.4
15	6.30	100.9	73.8	0.0480	1.040	0.0499	5.035	3.683	0.3238	32.6611	23.8845	- 19.63	- 1448.7	385.3
16	6.46	107.4	71.6	0.0445	1.072	0.0477	5.123	3.415	0.3102	33.2925	22.1901	- 26.13	- 1870.9	682.8
17	6.64	113.9	68.7	0.0410	1.116	0.0458	5.217	3.146	0.2971	33.8210	20.3972	- 32.63	- 2241.7	1064.7
18	6.90	120.4	65.1	0.0365	1.174	0.0429	5.165	2.793	0.2784	33.5010	18.1245	- 39.13	- 2547.4	1531.1
19	7.20	126.9	60.8	0.0321	1.228	0.0394	5.000	2.395	0.2558	32.4288	15.5508	- 45.63	- 2774.3	2082.1
20	7.60	133.4	55.8	0.0273	1.297	0.0354	4.722	1.975	0.2307	30.7393	12.8714	- 52.13	- 2908.8	2717.5
21	8.00	139.9	50.0	0.0234	1.387	0.0325	4.547	1.625	0.2106	29.4381	10.5370	- 58.63	- 2931.5	3437.5
22	8.60	146.4	43.3	0.0189	1.508	0.0285	4.172	1.234	0.1855	27.1318	8.0413	- 65.13	- 2820.1	4241.9
23	9.30	152.9	35.2	0.0149	1.686	0.0251	3.838	0.884	0.1566	23.4407	5.4596	- 71.63	- 2521.4	5130.9
24	11.00	158.8	26.4	0.0090	1.933	0.0174	2.763	0.459	0.1042	16.5110	2.7888	- 77.53	- 2046.8	6010.9
25	13.20	164.7	15.5	0.0055	2.364	0.0129	2.125	0.200	0.0784	12.9009	1.2086	- 83.43	- 1293.7	6960.6
26	14.70	170.6	0.0	0.0038	3.457	0.0131	2.235	0.000	0.0407	6.5370	0.0983	- 89.33	0.0	7979.8
										6.7148	545.7264	426.8917		

REMARKS

$$l_1 = \frac{\Sigma vW_a}{\Sigma W_a} = \frac{545.7264}{6.7148} = 81.272 \text{ ft.} \quad z_o' = \frac{\Sigma zW_a}{\Sigma W_a} = \frac{426.8917}{6.7148} = 63.574 \text{ ft.}$$

$$\tan \beta = -\frac{\Sigma xzW_a}{\Sigma x^2W_a} = -\frac{620.3}{11953.1} = -0.0519. \quad \tan \beta \text{ is obtained from values in Table 79M.}$$

All elastic loads  $W$  are  $E$  times actual.



TABLE  
COMPUTATION OF W FORCES AND POLE

Pt.	$w_a$	$xzw_a$	$x^2w_a$	$\Sigma xzw_a$ $=xzW_a$	$\Sigma x^2w_a$ $=xW_b$	Eq. (73G), $y=z-z_0'+x \tan \beta$			$xw_a$
						$x \tan \beta$	$z-z_0'$	$y$ ft.	
0	0.0232	49.8	153.2	155.1	446.6	-4.22	-37.17	-41.39	1.885
1	0.0251	66.6	142.6	414.5	885.0	-3.91	-28.37	-32.28	1.892
2	0.0285	85.0	135.2	551.2	877.8	-3.57	-20.27	-23.84	1.963
3	0.0325	101.4	126.4	656.0	817.5	-3.24	-13.57	-16.81	2.027
4	0.0354	110.4	110.5	716.8	718.8	-2.90	- 7.77	-10.67	1.978
5	0.0394	118.3	96.0	765.2	622.3	-2.56	- 2.77	- 5.33	1.945
6	0.0429	119.7	78.8	774.2	511.5	-2.22	+ 1.53	- 0.69	1.839
7	0.0458	114.4	60.6	739.5	393.9	-1.89	5.13	+ 3.24	1.666
8	0.0477	102.0	42.6	661.0	278.3	-1.55	8.03	6.48	1.425
9	0.0499	86.1	27.3	556.8	178.8	-1.21	10.23	9.02	1.166
10	0.0513	65.2	14.6	450.6	102.8	-0.88	11.73	10.85	0.865
11	0.0530	38.0	4.6	283.2	38.0	-0.49	12.93	12.44	0.497
12	0.0555	8.0	0.2	51.2	5.2	-0.10	13.23	13.13	0.104
13	0.0530	- 22.8	1.7	-168.6	16.3	+0.29	12.93	13.22	-0.298
14	0.0513	- 50.7	8.8	-349.1	62.8	0.68	11.73	12.41	-0.674
15	0.0499	- 72.3	19.2	-467.3	126.4	1.02	10.23	11.25	-0.980
16	0.0477	- 89.2	32.6	-577.8	213.4	1.36	8.03	9.39	-1.246
17	0.0458	-102.7	48.8	-663.6	317.5	1.69	5.13	6.82	-1.494
18	0.0429	-109.3	65.7	-706.6	426.6	2.03	1.53	3.56	-1.679
19	0.0394	-109.3	82.0	-706.8	531.7	2.37	- 2.77	- 0.40	-1.798
20	0.0354	-103.0	96.2	-668.5	625.8	2.71	- 7.77	- 5.06	-1.845
21	0.0325	- 95.3	111.7	-615.4	722.4	3.04	-13.57	-10.53	-1.906
22	0.0285	- 80.4	120.9	-521.2	784.9	3.38	-20.27	-16.89	-1.856
23	0.0251	- 63.3	128.8	-388.0	782.1	3.72	-28.37	-24.65	-1.798
24	0.0174	- 35.6	104.6	-214.3	621.6	4.02	-37.17	-33.15	-1.349
25	0.0129	- 16.7	89.8	- 99.6	544.1	4.33	-48.07	-44.74	-1.076
26	0.0131	0.0	104.5	- 8.2	301.0	4.64	-63.57	-58.93	-1.170
				+620.3	11953.1				

All elastic loads W

The sums  $\Sigma w_a=W_a$ ,  $\Sigma vw_a=vW_a$  and  $\Sigma zw_a=zW_a$  are now computed by Simpson's rule according to Eqs. (73E), using the lengths  $\Delta v$  for the horizontal distances between the arch sections.

Eqs. (73F) then give the coordinates  $l_1$ ,  $z_o'$  of the new origin  $O$  with respect to the  $(v, z)$  axes. Thus

$$l_1 = \frac{\Sigma vW_a}{\Sigma W_a} = \frac{545.7264}{6.7149} = 81.272 \text{ feet,}$$
$$z_o' = \frac{\Sigma zW_a}{\Sigma W_a} = \frac{426.8917}{6.7148} = 63.574 \text{ feet,}$$

and  $x=l_1-v$ .

79M

## DISTANCES. UNSYMMETRIC ARCH

$\Delta x$	$\Sigma xw_a = W_b$	$yw_a$	$\Sigma yw_a = W_c$	$y^2$	$y^2w_a$	$\Sigma y^2w_a = yW_s$	$\frac{\cos \phi}{D}$	$\frac{\Sigma \cos \phi \Delta x}{D}$	Point.
ft.									
5.9	5.56	-0.960	- 2.76	1713.1	39.74	110.5	0.052	0.158	0
6.5	11.77	-0.810	- 5.04	1042.0	26.15	163.4	0.064	0.394	1
6.5	12.77	-0.679	- 4.43	568.3	16.20	106.8	0.077	0.500	2
6.5	13.13	-0.546	- 3.54	282.6	9.18	60.6	0.090	0.583	3
6.5	12.88	-0.378	- 2.47	113.8	4.03	27.4	0.101	0.657	4
6.5	12.61	-0.210	- 1.36	28.4	1.12	8.3	0.113	0.732	5
6.5	11.92	-0.030	- 0.13	0.5	0.02	1.0	0.123	0.799	6
6.5	10.80	+0.148	+ 0.95	10.5	0.48	3.7	0.135	0.872	7
6.5	9.26	0.309	1.99	42.0	2.00	13.3	0.144	0.930	8
6.5	7.56	0.450	2.90	81.4	4.06	26.3	0.153	0.987	9
6.5	5.99	0.557	3.89	117.7	6.04	42.6	0.158	1.110	10
7.5	3.71	0.659	4.91	154.8	8.20	61.0	0.163	1.225	11
7.5	0.73	0.729	5.39	172.4	9.57	70.7	0.167	1.250	12
7.5	- 2.22	0.701	5.22	174.8	9.26	68.8	0.163	1.225	13
6.5	- 4.65	0.637	4.45	154.0	7.90	55.3	0.158	1.110	14
6.5	- 6.35	0.561	3.62	126.6	6.32	40.8	0.153	0.987	15
6.5	- 8.08	0.448	2.89	88.2	4.21	27.4	0.144	0.930	16
6.5	- 9.66	0.312	2.01	46.5	2.13	14.1	0.135	0.872	17
6.5	- 10.86	0.153	0.99	12.7	0.54	4.1	0.123	0.799	18
6.5	- 11.63	-0.016	- 0.08	0.2	0.01	0.8	0.113	0.732	19
6.5	- 11.98	-0.179	- 1.16	25.6	0.91	6.9	0.101	0.657	20
6.5	- 12.31	-0.342	- 2.21	110.9	3.60	24.4	0.090	0.583	21
6.5	- 12.05	-0.481	- 3.14	285.3	8.13	54.2	0.077	0.500	22
6.5	- 10.94	-0.619	- 3.75	607.6	15.25	92.6	0.064	0.393	23
5.9	- 8.03	-0.577	- 3.44	1098.9	19.12	114.2	0.047	0.275	24
5.9	- 6.53	-0.577	- 3.52	2001.7	25.82	158.7	0.032	0.187	25
5.9	- 3.40	-0.772	- 2.18	3472.7	45.49	124.5	0.020	0.064	26
	+118.69		+39.21			1482.4		19.511	
	-118.69		-39.21		$\cos \beta \Sigma yW_c = 1480.6$				

are  $E$  times actual.

When the ordinates  $x$  are found then the quantities  $xw_a$  and  $x^2w_a$  and their sums  $\Sigma xw_a$  and  $\Sigma x^2w_a$  are determined in Table 79M, using Simpson's rule in summing for the horizontal increments  $\Delta x$ .

Eq. (73H) then gives

$$\tan \beta = -\frac{\Sigma xw_a}{\Sigma x^2w_a} = -\frac{620.3}{11953.1} = -0.0519.$$

Eq. (73G) now furnishes the ordinates  $y$  and from these the quantities  $yw_a$  and  $y^2w_a$  are computed. As a check  $\Sigma W_b = 0$  and  $\Sigma W_c = 0$ , and any small discrepancies must be adjusted.

UNSYMMETRIC ARCH

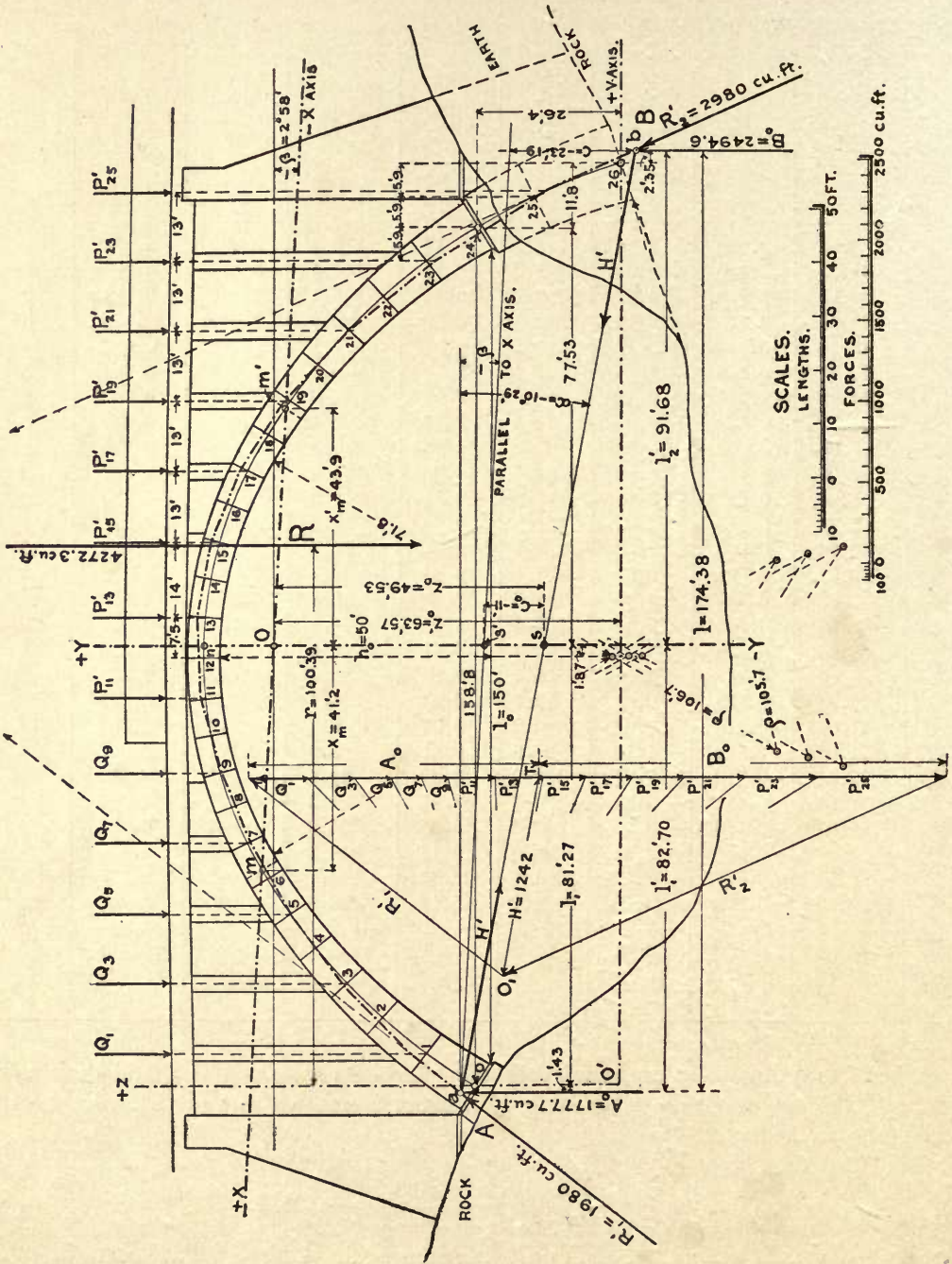


Fig. 79H.



The  $W$  loads were again derived without including  $E$  so that these loads are all  $E$  times actual, a fact which should not be overlooked if temperature stresses are to be found from Eq. (75c).

In Table 79M the quantities  $\cos \phi \Delta x/D$  are given, showing that the pole distance  $H_c = \cos \beta \Sigma y W_c + \Sigma \cos \phi \Delta x/D$  from Eq. (72k), would be increased by 1.3 per cent if axial thrust is included in the determination of  $X_c$ . This would tend to diminish  $X_c$ , and the ordinates of the  $X_c$  influence line.

**The influence lines for  $X_a$ ,  $X_b$  and  $X_c$**  are shown in Fig. 79I, noting that the length of span  $l$ , is now taken as the horizontal distance between the intrados kernel points of the haunch sections. This was done to obviate the negative  $M_o$  moments otherwise encountered here and leading to complications which are rather far reaching. In the previous case of symmetric arch, the real haunch sections could not be examined because the span was chosen as the distance between the verticals through the axial points and the section  $t$  was accordingly taken as the nearest approach to the haunch section. It is thus interesting to note the two methods of treating this matter. The length does not enter into the computations, but must be considered in drawing all the influence lines.

The detailed description of the method of drawing these influence lines need not be repeated here, and the reader is referred back to the treatment of the symmetric arch in the first part of this article.

Axial thrust was not included in Fig. 79I, thus making all the results of both investigations comparable. However, the effect is so small that it may be regarded as a negligible quantity in the present case.

Having located the coordinate axes, this determines the critical sections, and the data required for the computation of the ordinates for the  $M_e$  and  $M_i$  influence lines are given in Table 79N.

TABLE 79N.—DATA RELATING TO THE CRITICAL SECTIONS—UNSYMMETRIC ARCH

Point	$D$ ft.	$\phi$	Coordinates, Axial Point.		$\frac{D}{6} \sin \phi$ ft.	$\frac{D}{6} \cos \phi$ ft.	Coordinates Extrados Kernel Points.			Coordinates Intrados Kernel Points.		
			$x$ ft.	$y$ ft.			$x_e$ ft.	$y_e$ ft.	$\cos \beta y_e$ ft.	$x_i$ ft.	$y_i$ ft.	$\cos \beta y_i$ ft.
$A$	10.0	58° 51'	+81.27	-41.39	1.43	0.86	+79.85	-42.25	-42.20	+82.70	-40.53	-40.48
$m$	6.9	31 04	+41.20	0.00	0.59	1.00	+40.61	- 1.00	- 1.00	+41.79	+ 1.00	+ 1.00
$n$	6.0	0 00	0.00	+13.25	0.00	1.00	0.00	+12.25	+12.23	0.00	+14.25	+14.23
$m'$	7.2	34 58	-43.90	0.00	0.69	0.98	-43.21	- 0.98	- 0.98	-44.59	+ 0.98	+ 0.98
$B$	14.7	73 11	-89.33	-58.93	2.35	0.71	-86.98	-59.64	-59.56	-91.68	-58.22	-58.14

$\beta = 2^\circ 58'$  and  $\cos \beta = 0.9987$  from Table 79L

**The  $M_o$  influence lines** for the kernel points of the several critical sections are shown in Fig. 79J, the data for the construction of these being taken from Table 79N. It should be noted that for the haunch sections  $A$  and  $B$ ,  $M_{oi} = 0$ .

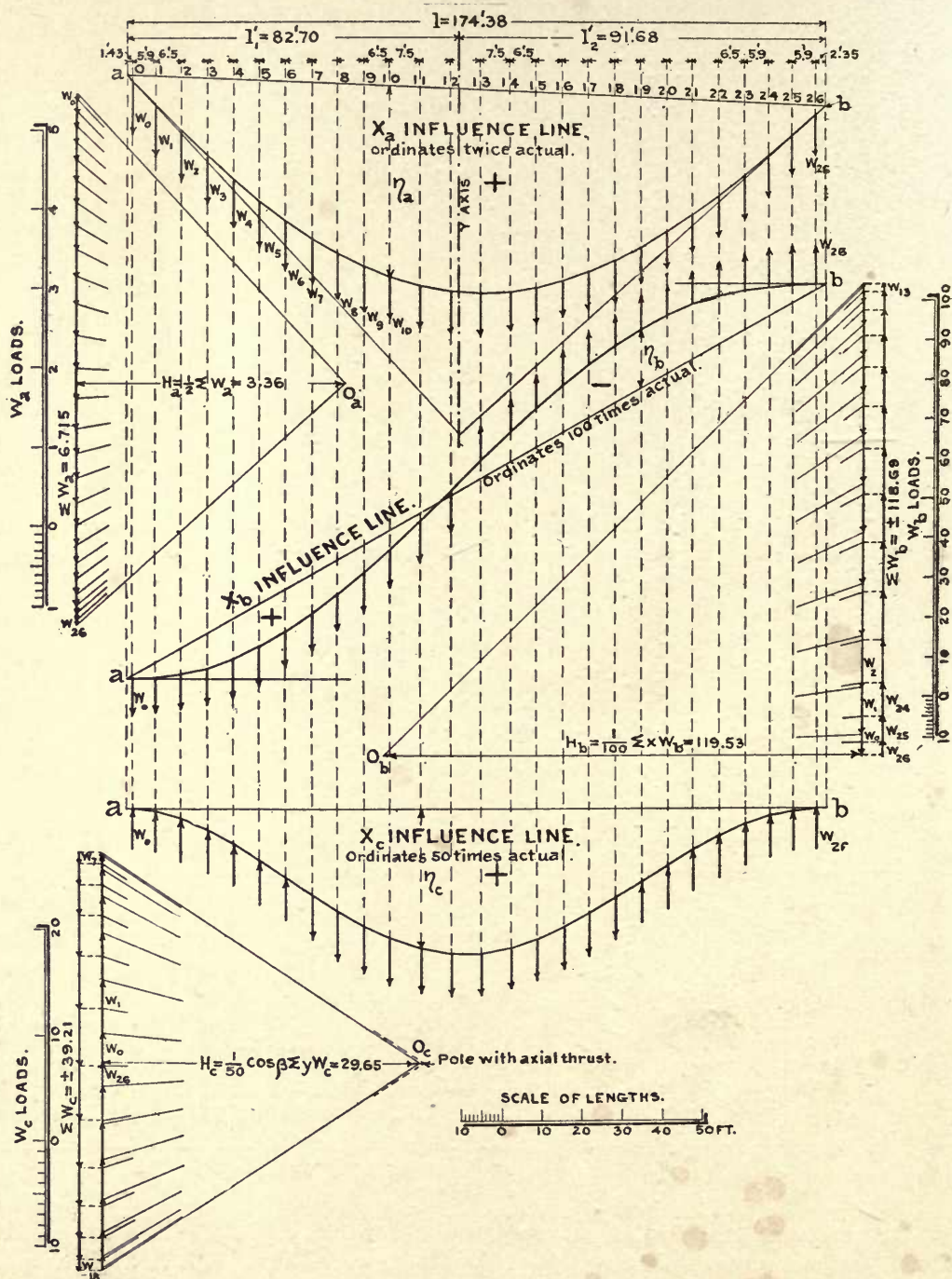


FIG. 791.—X Influence Lines for Unsymmetric Arch



From the coordinates of the kernel points in Table 79N, and the ordinates in Tables 79O and 79P, taken from the  $X_a$ ,  $X_b$ ,  $X_c$  and  $M_o$  influence lines, Figs. 79I and 79J, the  $\eta_e$  and  $\eta_i$  are computed for the odd points and for the five critical sections according to Eqs. (76B). The operations are all indicated in the headings of Tables 79O and 79P, thus requiring no further description here.

These ordinates, plotted in Fig. 79K, furnish the  $M_e$  and  $M_i$  influence lines from which the moments and stresses for any position of the live loads may be found for each of the five critical sections. In practice it is well to compute all the ordinates  $\eta$  instead of merely the odd ones as given here.

#### FOR INTRADOS KERNEL POINTS.

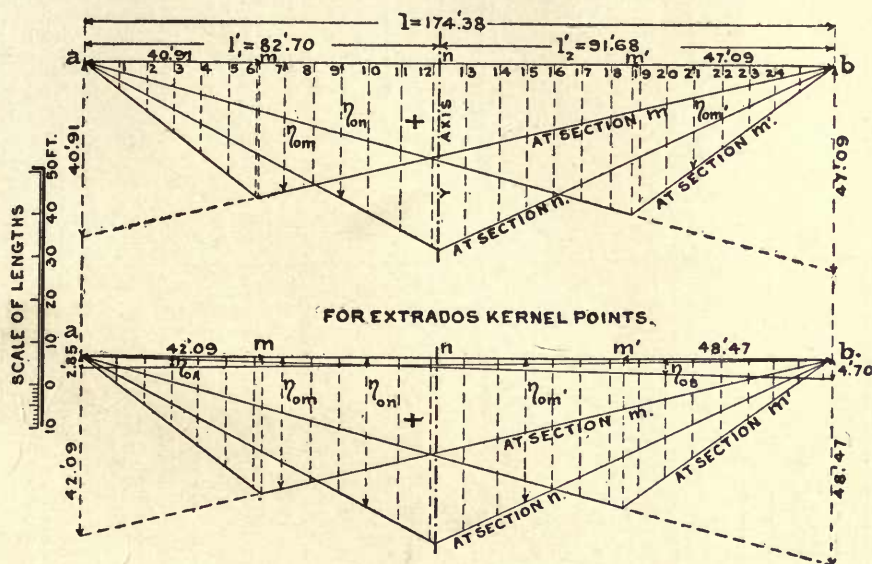


FIG. 79J.— $M_o$  Influence Lines for Unsymmetric Arch.

Table 79Q, gives the computations for the resultant polygon for the same case of loading previously used in Table 79H, adding one additional load  $P_{25}$  at a point on the right abutment. The results of this computation are shown in Fig. 79H, where the resultant polygon is drawn through the points  $a$  and  $b$  which are located on the verticals through the intrados kernel points of the  $A$  and  $B$  sections.

It should be noted that  $c$  and  $c_o$  are both negative, indicating that they must be measured up from the line  $\overline{ab}$  when found. Hence  $z_o$  is measured down on the  $y$  axis to locate the point  $s$  and  $-c_o = ss'$  is then laid off upward from  $s$ . The line  $\overline{as'} \parallel x$  axis, locates the point  $a$  at the left abutment and the line  $\overline{as}$  prolonged fixes the point  $b$  at the right abutment. The force polygon is then easily constructed by laying off the reactions  $A_o$  and  $B_o$  and finding the pole  $O_1$  by drawing the line  $\overline{O_1T} \parallel \overline{ab}$  and equal in length to  $H'$ .



TABLE 79Q.—MOMENT INFLUENCE LINES FOR

Point.	$\eta_a$ ft.	$\eta_b$ ft.	$\eta_c$ ft.	SECTION A. $\eta_A = \eta_o - [\eta_a + 79.85\eta_b - 42.2\eta_c]$				SECTION m. $\eta_m = \eta_o - [\eta_a + 40.6\eta_b - 1.0\eta_c]$		
				$\eta_o$	$79.85\eta_b$	$-42.2\eta_c$	$\eta_A$	$\eta_o$	$+40.6\eta_b$	$\eta_m$
1	3.5	0.036	0.012	2.74	2.87	- 0.51	- 3.12	5.2	1.46	0.26
3	9.8	0.082	0.100	2.52	6.55	- 4.22	- 9.61	15.2	3.33	2.17
5	15.2	0.102	0.252	2.31	8.14	-10.63	-10.40	25.1	4.14	6.01
7	19.7	0.092	0.424	2.10	7.35	-17.89	- 7.06	31.0	3.74	7.98
9	22.9	0.064	0.580	1.88	5.11	-24.48	- 1.65	28.0	2.60	3.08
11	25.0	0.014	0.692	1.64	1.12	-29.20	+ 4.72	24.5	0.57	-0.38
13	25.5	-0.044	0.720	1.40	- 3.51	-30.38	9.79	21.0	-1.79	-1.99
15	24.5	-0.100	0.652	1.18	- 7.99	-27.51	12.18	17.4	-4.06	-2.39
17	22.1	- 0.132	0.520	0.97	-10.54	-21.94	11.35	14.2	-5.36	-2.02
19	18.7	-0.148	0.360	0.75	-11.62	-15.19	8.86	11.1	-6.01	-1.23
21	14.3	-0.136	0.196	0.53	-10.86	- 8.27	5.36	8.0	-5.52	-0.58
23	9.1	-0.100	0.070	0.32	- 7.99	- 2.95	2.16	4.8	-4.06	-0.17
25	3.9	-0.046	0.016	0.13	- 3.67	- 0.68	0.58	2.0	-1.87	-0.01

All ordinates in above

TABLE 79R.—MOMENT INFLUENCE LINES FOR

Point.	$\eta_a$ ft.	$\eta_b$ ft.	$\eta_c$ ft.	SECTION A. $\eta_A = 0 - [\eta_a + 82.7\eta_b - 40.5\eta_c]$			SECTION m. $\eta_m = \eta_o - [\eta_a + 41.8\eta_b + 1.0\eta_c]$			
				$82.7\eta_b$	$-40.5\eta_c$	$\eta_A$	$\eta_o$	$41.8\eta_b$	$1.0\eta_c$	$\eta_m$
1	3.5	0.036	0.012	2.98	- 0.49	- 5.99	5.4	1.50	0.01	0.39
3	9.8	0.082	0.100	6.78	- 4.05	-12.53	15.4	3.43	0.10	2.07
5	15.2	0.102	0.252	8.44	-10.21	-13.43	25.2	4.26	0.25	5.49
7	19.7	0.092	0.424	7.61	-17.17	-10.14	30.0	3.85	0.42	6.03
9	22.9	0.064	0.580	5.29	-23.49	- 4.70	27.0	2.68	0.58	0.84
11	25.0	0.014	0.692	1.16	-28.03	+ 1.87	23.8	0.59	0.69	-2.48
13	25.5	-0.044	0.720	- 3.64	-29.16	7.30	20.2	-1.84	0.72	-4.18
15	24.5	-0.100	0.652	- 8.27	-26.41	10.18	17.0	-4.18	0.65	-3.97
17	22.1	-0.132	0.520	-10.92	-21.06	9.88	14.0	-5.52	0.52	-3.10
19	18.7	-0.148	0.360	-12.24	-14.58	8.12	11.0	-6.18	0.36	-1.88
21	14.3	-0.136	0.196	-11.25	- 7.94	4.89	7.8	-5.68	0.20	-1.02
23	9.1	-0.100	0.070	- 8.27	- 2.84	2.01	4.8	-4.18	0.07	-0.19
25	3.9	-0.046	0.016	- 3.80	- 0.65	0.55	2.0	-1.92	0.02	0.00

All ordinates in above

It is seen that the resultant polygon intersects the axial line four times, showing consistency with Professor Winkler's theorem.

As a final check, the normal thrusts  $N$ , offsets  $v$  and stresses  $f$  are computed in Table 79R for the same case of loading used in Table 79Q, and the close agreement of the results shows both solutions to be satisfactory. The only stresses, however, which are maximum, are those on the section A, the others are simply for the simultaneous case of loading and have no special interest.

The stresses on the haunch section A are thus found to be  $f_e = -549$  and  $f_i = +152.9$

## EXTRADOS KERNEL POINTS—UNSYMMETRIC ARCH

SECTION <i>n</i> . $\eta_n = \eta_o - [\eta_a + 12.23\eta_c]$			SECTION <i>m'</i> . $\eta_{m'} = \eta_o - [\eta_a - 43.2\eta_b - 0.98\eta_c]$				SECTION <i>B</i> . $\eta_B = \eta - [\eta_o - 87.0\eta_b - 59.56\eta_c]$				Point.
$\eta_o$	$12.23\eta_c$	$\eta_n$	$\eta_o$	$-43.2\eta_b$	$-0.98\eta_c$	$\eta_{m'}$	$\eta_o$	$-87.0\eta_b$	$-59.56\eta_c$	$\eta_B$	
3.7	0.14	+0.05	1.9	-1.56	-0.01	-0.03	0.18	- 3.13	- 0.71	0.52	1
10.6	1.22	-0.42	5.5	-3.54	-0.10	-0.66	0.54	- 7.13	- 5.96	3.83	3
17.2	3.08	-1.08	9.1	-4.41	-0.25	-1.44	0.89	- 8.88	-15.01	9.58	5
24.2	5.19	-0.69	13.0	-3.97	-0.41	-2.32	1.24	- 8.00	-25.25	14.79	7
31.1	7.10	+1.10	16.4	-2.76	-0.57	-3.17	1.59	- 5.57	-34.54	18.80	9
38.5	8.46	5.04	20.3	-0.60	-0.68	-3.42	1.99	- 1.22	-41.22	19.43	11
40.8	8.80	6.50	24.6	+1.90	-0.71	-2.09	2.38	+ 3.83	-42.88	15.93	13
34.2	7.97	+1.73	28.4	4.32	-0.64	+0.22	2.76	8.70	-38.83	8.39	15
28.1	6.36	-0.36	32.0	5.70	-0.51	4.71	3.10	11.48	-30.97	0.49	17
22.0	4.40	-1.10	33.4	6.39	-0.35	8.66	3.47	12.88	-21.44	- 6.67	19
15.6	2.40	-1.10	23.7	5.88	-0.20	3.72	3.82	11.83	-11.67	-10.64	21
9.5	0.85	-0.45	14.4	4.32	-0.07	+1.05	4.17	8.70	- 4.17	- 9.46	23
4.0	0.20	-0.10	5.8	1.99	-0.02	-0.07	4.50	4.00	- 0.95	- 2.45	25

table are expressed in feet.

## INTRADOS KERNEL POINTS—UNSYMMETRIC ARCH

SECTION <i>n</i> . $\eta_n = \eta_o - [\eta_a + 14.23\eta_c]$			SECTION <i>m'</i> . $\eta_{m'} = \eta_o - [\eta_a - 44.6\eta_b + 0.98\eta_c]$				SECTION <i>B</i> . $\eta_B = 0 - [\eta_a - 91.7\eta_b - 58.14\eta_c]$			Point.
$\eta_o$	$14.23\eta_c$	$\eta_n$	$\eta_o$	$-44.6\eta_b$	$0.98\eta_c$	$\eta_{m'}$	$-91.7\eta_b$	$-58.14\eta_c$	$\eta_B$	
3.7	0.17	+0.03	1.8	-1.61	0.01	-0.09	-3.30	- 0.70	+ 0.50	1
10.6	1.42	-0.62	5.4	-3.66	0.10	-0.84	-7.52	- 5.81	3.53	3
17.2	3.58	-1.58	8.9	-4.55	0.25	-2.00	-9.35	-14.65	8.80	5
24.2	6.03	-1.53	12.4	-4.10	0.41	-3.61	-8.44	-24.65	13.39	7
31.1	8.25	-0.05	16.0	-2.85	0.57	-4.62	-5.87	-33.72	16.69	9
38.5	9.85	+3.65	19.6	-0.62	0.68	-5.46	-1.28	-40.23	16.51	11
40.8	10.24	5.06	23.8	+1.96	0.71	-4.37	+4.03	-41.86	12.33	13
34.2	9.28	0.42	27.8	4.46	0.64	-1.80	9.17	-37.91	4.24	15
28.1	7.40	-1.40	31.2	5.88	0.51	+2.71	12.10	-30.23	- 3.97	17
22.0	5.12	-1.82	33.4	6.60	0.35	7.75	13.57	-20.93	-11.34	19
15.6	2.84	-1.54	24.2	6.06	0.20	3.64	12.47	-11.40	-15.37	21
9.5	0.99	-0.59	14.6	4.46	0.07	0.97	9.17	- 4.07	-14.20	23
4.0	0.23	-0.13	6.0	2.05	0.02	0.03	4.22	- 0.93	- 7.19	25

table are expressed in feet.

cu.ft., which are quite excessive as compared to those previously obtained for section *t* of the symmetric arch, where  $f_e = -440$  and  $f_i = +28.5$  cu.ft.

If the investigation of stresses were extended to all the critical sections it would be found that the dimensions found safe for the symmetric arch are now quite insufficient when the arch is treated as an unsymmetric structure using the same axial line as before. The shape of the ring might be so adjusted as to reduce the stresses within the required limits by computing a resultant polygon for the average loading  $Q + \frac{1}{2}P$ , and shifting the axial line by the amounts  $\pm v$  obtained for the several critical sections.



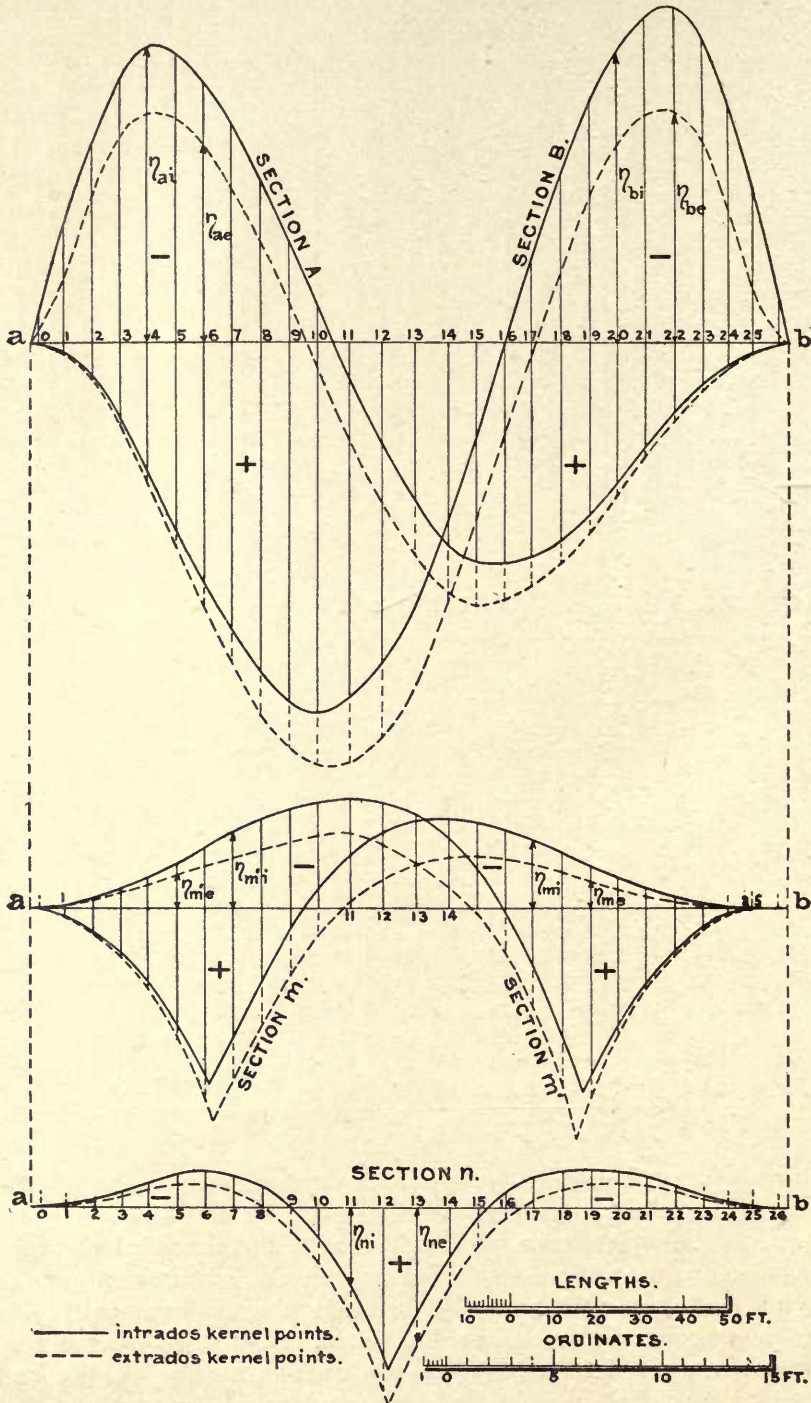


Fig. 79K.—M Influence Lines for the Kernel Points. Unsymmetric Arch.



TABLE 79Q.  
THE RESULTANT POLYGON FOR LOADS  $Q+P$ —UNSYMMETRIC ARCH

Point.	$\eta_a$ ft.	$\eta_b$ ft.	$\eta_c$ ft.	Dead Loads. $Q$ cu.ft.	Live Loads. $P$ cu.ft.	Total Loads. cu.ft.	$\eta(Q+P)$ for			Moments about $a$	
							$X_a$	$X_b$	$X_c$	$r$ ft.	$r(Q+P)^*$
1	3.5	0.036	0.012	367.4	0.0	367.4	1285.9	13.23	4.40	5.9	2167.7
3	9.8	0.082	0.100	276.1	0.0	276.1	2705.8	22.64	27.61	18.9	5218.3
5	15.2	0.102	0.252	223.4	0.0	223.4	3395.7	22.82	56.30	31.9	7126.5
7	19.7	0.092	0.424	182.7	0.0	182.7	3599.2	16.81	77.46	44.9	8203.2
9	22.9	0.064	0.580	168.0	0.0	168.0	3847.2	10.75	97.44	57.9	9727.2
11	25.0	0.014	0.692	173.7	114.6	288.3	7207.5	4.03	199.50	71.9	20728.8
13	25.5	-0.044	0.720	173.7	114.6	288.3	7344.8	-12.68	207.59	86.9	25053.3
15	24.5	-0.100	0.652	168.0	99.3	267.3	6548.9	-26.73	174.28	100.9	26970.6
17	22.1	-0.132	0.520	182.7	99.3	282.0	6232.2	-37.22	146.64	113.9	32119.8
19	18.7	-0.148	0.360	223.4	99.3	322.7	6034.5	-47.76	116.17	126.9	40950.6
21	14.3	-0.136	0.196	276.1	99.3	375.4	5368.2	-51.05	73.58	139.9	52518.5
23	9.1	-0.100	0.070	367.4	99.3	466.7	4247.0	-46.67	32.67	152.9	71358.4
25½	3.5	-0.040	0.012	680.0	84.0	764.0	2674.0	-30.56	9.17	165.9	126747.6
						4272.3 = $R$	60490.9 = $X_a$	-162.39 = $X_b$	1222.81 = $X_c$		428890.5 = $M$

$l=174'.38, \quad l_1=82'.7, \quad l_2=91'.68 \qquad \tan \beta = -0.0519, \quad \cos \beta = 0.9987$

Then  $H = X_c \cos \beta = 1221.22$  cu.ft.  $\tan \alpha = \tan \beta + \frac{X_b}{H} = -0.1849$

$$H' = \frac{H}{\cos \alpha} = 1242 \text{ cu.ft.}$$
$$c = \frac{l}{H} X_b = -23.19 \text{ ft.}$$
$$r = \frac{M}{R} = 100.388 \text{ ft.}$$

$$z_o = \frac{X_a}{H} = 49.53 \text{ ft.}$$
$$c_o = \frac{l_1}{H} X_b = -11.00 \text{ ft.}$$
$$B_o = \frac{R(r+1.43)}{l} = 2494.6 \text{ cu.ft.}$$

$A_o = R - B_o = 1777.7$  cu.ft.

The investigation for temperature is not repeated here except to evaluate the moment Eq. (75c) for this case using the same data just given for the symmetric arch.

For  $\cos \beta = 0.9987$  span  $l = 174.4$  ft., and  $\Sigma y W_c = 1482.6$  from Table 79m, then

$\epsilon t l = -0.0752$  ft. and

$$M_{mt} = \frac{0.0752 \times 3,775,720}{1478.8} y_m = +146.0 y_m,$$

from which the temperature stresses for any section are readily obtained by computing the moments about the two kernel points of the section.

A complete investigation of the stresses in any arch would then consist in finding the kernel moments due to the dead loads, the kernel moments due to the train of concentrated live loads, Fig. 79g, making proper allowance for impact; and finally the kernel moments due to temperature effects; all for each of the five critical sections. These moments for the same section are algebraically combined into the total  $M_e$  and  $M_i$  moments and from them and Eqs. (76c) the maximum stresses are found.

TABLE 79R  
COMPUTATION OF MOMENTS AND STRESSES ON THE CRITICAL SECTIONS  
FOR LOADS  $Q+P$ —UNSYMMETRIC ARCH

Point.	Loads $Q+P$ cu.ft.	SECTION A.				SECTION m.				SECTION n.			
		$\eta_e$ ft.	$\eta_i$ ft.	$M_e$	$M_i$	$\eta_e$ ft.	$\eta_i$ ft.	$M_e$	$M_i$	$\eta_e$ ft.	$\eta_i$ ft.	$M_e$	$M_i$
1	367.4	- 3.12	- 5.99	-1146.3	-2200.7	0.25	0.39	91.9	143.3	+0.05	+0.03	+ 18.4	+ 11.0
3	276.1	- 9.61	-12.53	-2653.3	-3459.5	2.17	2.07	599.1	571.5	-0.42	-0.62	- 116.0	- 171.2
5	223.4	-10.40	-13.43	-2323.4	-3000.3	6.01	5.49	1342.6	1226.5	-1.08	-1.52	- 241.3	- 339.6
7	182.7	- 7.06	-10.14	-1289.9	-1852.6	7.98	6.03	1457.9	1101.7	-0.69	-1.53	- 125.1	- 279.5
9	168.0	- 1.65	- 4.70	- 277.2	- 789.6	3.08	0.84	517.4	141.1	+1.10	-0.05	+ 184.8	- 8.4
11	288.3	+ 4.72	+ 1.87	+1360.8	+ 539.1	-0.38	-2.48	- 109.5	- 715.0	5.04	+3.65	1453.0	+1052.3
13	288.3	9.79	7.30	2822.4	2104.6	-1.99	-4.18	- 573.7	-1205.1	6.50	5.06	1874.1	1458.9
15	267.3	12.18	10.18	3255.7	2721.1	-2.39	-3.97	- 638.8	-1051.2	+1.73	+0.42	+ 462.4	+ 112.3
17	282.0	11.35	9.88	3200.7	2786.2	-2.02	-3.10	- 569.6	- 874.2	-0.36	-1.40	- 101.5	- 394.8
19	322.7	8.86	8.12	2859.1	2620.3	-1.23	-1.88	- 396.9	- 606.7	-1.10	-1.82	- 355.0	- 587.3
21	375.4	5.36	4.89	2012.1	1835.7	-0.58	-1.02	- 217.7	- 382.9	-1.10	-1.54	- 412.9	- 578.1
23	466.7	2.16	2.01	1008.1	938.1	-0.17	-0.19	- 79.4	- 88.7	-0.45	-0.59	- 210.0	- 275.4
25½	764.0	0.42	0.40	320.9	305.6	-0.01	0.00	- 7.6	- 0.0	-0.08	-0.11	- 61.1	- 84.0
Totals	4272.3	$D=$	10'.0	+9149.7	+2548.0	$D=$	6'.90	+1415.7	-1739.7	$D=$	6'.00	+2369.8	- 83.9
			$N=$	1980.5			$N=$	1372.0			$N=$	1226.9	
			$v=$	+2'.953			$v=$	-0'.119			$v=$	+0'.932	
			$f=$	- 549.0	+ 152.9		$f=$	- 178.4	- 219.7		$f=$	- 395.0	- 14.0

Point.	Loads. $Q+P$ cu ft.	SECTION m'.				SECTION B.			
		$\eta_e$ ft.	$\eta_i$ ft.	$M_e$	$M_i$	$\eta_e$ ft.	$\eta_i$ ft.	$M_e$	$M_i$
1	367.4	-0.03	-0.09	- 11.0	- 33.0	0.52	0.50	191.0	183.7
3	276.1	-0.66	-0.84	- 182.2	- 231.9	3.83	3.53	1057.5	974.6
5	223.4	-1.44	-2.00	- 321.7	- 446.8	9.58	8.80	2140.2	1965.9
7	182.7	-2.32	-3.61	- 323.9	- 659.5	14.79	13.39	2702.0	2446.4
9	168.0	-3.17	-4.62	- 532.6	- 776.2	18.80	16.69	3158.4	2803.9
11	288.3	-3.42	-5.46	- 986.0	-1574.1	19.43	16.51	5601.7	4759.8
13	288.3	-2.09	-4.37	- 602.5	-1259.9	15.93	12.33	4592.6	3554.7
15	267.3	+0.22	-1.80	+ 58.7	- 481.1	8.39	4.24	2242.6	1133.4
17	282.0	4.71	+2.71	1328.2	+ 764.2	0.49	- 3.97	138.2	-1119.5
19	322.7	8.66	7.75	2794.6	2500.9	- 6.67	-11.34	-2152.4	-3659.4
21	375.4	3.72	3.64	1396.5	1365.4	-10.64	-15.37	-3994.3	-5769.9
23	466.7	+1.05	0.97	+ 490.1	452.7	- 9.46	-14.20	-4415.0	-6627.1
25½	764.0	-0.05	0.02	- 38.2	15.3	- 1.76	- 6.80	-1344.6	-5195.2
Totals	4272.3	$D=$	7'.20	+3070.0	- 374.0	$D=$	14'.7	+9917.9	-4548.7
			$N=$	1435.0			$N=$	2952.4	
			$v=$	+0'.940			$v=$	+0'.909	
			$f=$	- 355.3	- 43.3		$f=$	- 274.7	- 126.0

Eqs. (76c,  $N = \frac{3}{D}(M_e - M_i)$ ;  $v = \frac{M_e + M_i}{2N}$ ;  $f_e = -\frac{6M_e}{D^2}$ ;  $f_i = \frac{6M_i}{D^2}$ ;  $v$  is positive when measured from the axis toward the extrados. All loads in above table are expressed in cubic feet of masonry and the stresses are cubic feet per square foot. Cubic feet per square foot  $\times 0.972$  = pounds per square inch.

## BIBLIOGRAPHY

---

### THEORY OF ELASTICITY

- HOKE. Philosophical tracts and collections, 1678. Hooke's law of proportionality between stress and strain.
- BERNOULLI, 1667-1748, was the first to give an analytic solution for the elastic curve.
- EULER. Methodus invenendi lineas curvas, 1741-4.
- COULOMB. Mémoires de l'académie des Sciences, 1784.
- LAGRANGE. Mécanique analytique, Paris, 1788.
- YOUNG. A course of lectures on natural philosophy and mechanical arts, 1807. Gives Young's modulus of elasticity  $E$ .
- NAVIER. Mémoire sur la flexion des verges élastiques courbes, 1827. Law of distribution of stress on any section subjected to bending.
- POISSON. Mémoire de l'Académie des Sciences, VIII, 1829.
- CLAPEYRON. Sur l'équilibre interieur des corps solides homogènes. Mémoires des savants étrangers, IV, 1833.
- LAMÉ. Leçons sur la théorie mathématique de l'élasticité, 1852.
- DE SAINT-VENANT. Mémoires des savants étrangers, XIV, 1856.
- MENABREA. Nouveau principe sur la distribution des tensions dans les systèmes élastiques. Comptes rendus, 1858.
- CASTIGLIANO. Théorie de l'équilibre des systèmes élastiques, 1879.
- FRAENKEL. Das Prinzip der kleinsten Arbeit, etc., Zeitsch. des Arch.- und Ing.-Vereins, Hannover, 1882.
- MOHR. Ueber die Darstellung des Spannungszustandes und des Deformationszustandes eines Koerperelementes. Civilingenieur, 1882.
- MOHR. Ueber die Elastizitaet der Deformationsarbeit. Zeitschr. des Arch.- und Ing.-Vereins, Hannover, 1886.
- MOHR. Welche Umstaende bedingen die Elastizitaetsgrenze und den Bruch eines Materials. Zeitschr. des Vereins deutscher Ing., 1900.

### GRAPHOSTATICS

- PONCELET. Cours de Mécanique industrielle, 1826-9.
- CULMANN. Graphische Statik, 1866.
- CLERK MAXWELL. On reciprocal figures and diagrams of forces. Phil. Mag., 1864.
- WINKLER. Vortrag ueber die Berechnung von Bogenbruecken, Mitth. des Arch.- und Ing.-Vereins, Boehmen, 1868. Introduces influence lines.



- MOHR. Beitrag zur Theorie der Holz und Eisenkonstruktionen. Zeitschr. des Arch.- und Ing. Vereins, Hannover, 1868. Introduces influence lines.
- CREMONA. Le figure reciproche nella Statica Grafica, 1872.
- MOHR. Die graphische Statik und das graphische Rechnen. Civiling., 1875.
- WILLIOT. Notions pratiques sur la statique graphique. Génie Civil, Oct., 1877.
- MUELLER-BRESLAU. Die graphische Statik der Baukonstruktionen, 1881-1905.
- MOHR. Ueber Geschwindigkeitspläne und Beschleunigungspläne. Civiling., 1887.
- W. RITTER. Anwendungen der graphischen Statik, 1890-1906.

## GENERAL TREATISES

- SCHWEDLER. Theorie der Brueckenbalkensysteme. Zeitschr. fuer Bauwesen, 1851.
- A. RITTER. Elementare Theorie und Berechnung eiserner Dach- und Brueckenkonstruktionen, 1863.
- CLERK MAXWELL. On the calculation of the equilibrium and stiffness of frames. Phil. Mag., 1864.
- MOHR. Beitrag zur Theorie des Fachwerks. Zeitschr. des Arch.- und Ing.-Vereins, Hannover, 1870, 1874, 1875, 1877.
- WEYRAUCH. Theorie und Berechnung der Kontinuierlichen und einfachen Traeger, 1873.
- WINKLER. Vortraege ueber Brueckenbau, 1873-1884.
- FRAENKEL. Anwendung der Theorie des augenblicklichen Drehpunktes auf die Bestimmung der Formaenderung von Fachwerken. Civiling., 1875.
- FRAENKEL. Ueber die unguenstigste Einstellung eines Systemes von Einzellasten auf Fachwerktraeger mit Hilfe von Influenzkurven. Civiling., 1876.
- FOEPPL. Theorie des Fachwerks, 1880.
- MUELLER-BRESLAU. Graphische Statik der Baukonstruktionen. 1881-1908.
- SWAIN. On the application of the principle of virtual velocities to the determination of the deflection and stresses of frames. Jour. Franklin Inst., 1883.
- MELAN. Beitrag zur Berechnung statischunbestimmter Stabsysteme. Zeitschr., des Oestr. Arch. und Ing. Vereins, 1884.
- LAND. Die Gegenseitigkeit elastischer Formaenderungen, etc. Wochenblatt fuer Baukunde, Jan., 1887.
- LAND. Beitrag zur Ermittlung der Biegungslinien ebener und elastischer Stabwerke. Civiling., 1889.
- L. v. TETMAJER. Angewandte Elastizitaets und Festigkeitslehre. 1888, 1902.
- MUELLER-BRESLAU. Festigkeitslehre, 1893.
- LANDSBERG. Beitrag zur Theorie des raemlichen Fachwerks. Zentr. der Bauverwaltung. 1898 and 1903.
- MEHRTENS. Statik der Baukonstruktionen. 3 vol., 1903-5.
- MOHR. Abhandlungen aus dem Gebiete der technischen Mechanik. 1905.
- KECK-HOTOPP. Elastizitaetslehre, 1905.
- Handbuch der Ingenieurwissenschaften. Der Brueckenbau.

## SECONDARY AND ADDITIONAL STRESSES

- ENGESSER. Ueber die Durchbiegung von Fachwerktraegern und die hierbei auftretenden zusaetzlichen Spannungen. Zeitschr. fuer Baukunde, 1879.
- ASIMONT. Hauptspannung und Sekundaerspannung. Zeitschr. fuer Baukunde, 1880.
- MANDERLA. Die Berechnung der Sekundaerspannungen, etc., Allgemeine Bauzeitung, 1880.
- MUELLER-BRESLAU. Ueber Biegungsspannungen in Fachwerken. Allgemeine Bauzeitung, 1885.

- LANDSBERG. Ebene Fachwerksysteme mit festen Knotenpunkten, etc. Centralb. der Bauverwaltung, 1885.
- LANDSBERG. Beitrag zur Theorie des Fachwerks. Zeitschr. des Arch.- und Ing.-Vereins, Hannover, 1885 and 1886.
- MUELLER-BRESLAU. Zur Theorie der Biegungsspannungen in Fachwerktraegern. Zeitschr. des Arch.- und Ing.-Vereins, Hannover, 1886.
- WINKLER. Querkonstruktionen. Zeitschr. des Arch.- und Ing.-V., Hannover, 1886.
- Handbuch der Ingenieurwissenschaften, Vol. II, 1890.
- MOHR. Die Berechnung der Fachwerke mit starren Knotenverbindungen. Civiling., 1891 and 1892.
- ENGESSER. Die Zusatzkrafte und Nebenspannungen eiserner Fachwerke, 1892-3.
- HIROI. Statically Indeterminate Bridge Stresses, 1905.
- MEHRTENS. Statik der Baukonstruktionen, Vol. III, 1905.
- MOHR. Abhandlungen aus dem Gebiete der technischen Mechanik, 1906.
- GRIMM. Secondary Stresses in Bridge Trusses, 1908.

## SPECIAL TREATISES ON ARCHES

- LAMÉ and CLAPEYRON. Journal des Voies de Communication, 1826. This contains the first application of force and equilibrium polygons to fixed arches.
- PONCELET. Memorial de l'officier du génie, 1835.
- GERSTNER. Handbuch der Mechanik, 1831. Line of thrust method.
- MOSELEY. Phil. Mag., 1833. Discussion of most probable position of line of thrust.
- HAGEN. Ueber Form und Staerke gewoelbter Bogen, 1844.
- SCHWEDLER. Theorie der Stuetzlinie. Zeitschr. fuer Bauwesen, 1859.
- CULMANN. Die graphische Statik, 1866.
- FRAENKEL. Berechnung eiserner Bogenbruecken. Civiling., 1867, 1875.
- MOHR. Beitrag zur Theorie der elastischen Bogentraeger. Zeitschr. des Arch.- und Ing.-Ver., Hannover, 1870, 1874, 1881.
- WINKLER. Beitrag zur Theorie der elastischen Bogentraeger. Zeitschr. des Arch.- und Ing.-Ver., Hannover, 1879.
- WEYRAUCH. Theorie der elastischen Bogentraeger. Zeitschr. fuer Baukunde, 1878.
- ENGESSER. Theorie und Berechnung der Bogenfachwerktraeger, 1880.
- MUELLER-BRESLAU. Theorie und Berechnung der eiserner Bogenbruecken, 1880.
- W. RITTER. Der elastische Bogen berechnet mit Hilfe der graphischen Statik, 1886.
- MUELLER-BRESLAU. Graphische Statik der Baukonstruktionen, 1892, 1907.
- WEYRAUCH. Die elastischen Bogentraeger, 1897.
- TOLKMITT. Leitfaden fuer das Entwerfen gewoelbter Bruecken, 1895.
- MEHRTENS. Statik der Baukonstruktionen, 3 vols., 1903-5.
- Handbuch der Ingenieurwissenschaften, Vol. I, 1904.







# INDEX

## A

	PAGE
Abutment displacements, fixed framed arches. . . . .	188
for general case of redundancy. . . . .	208
in two-hinged arches, . . . . .	156, 165, 168
stresses due to. . . . .	32
Additional stresses due to dynamic influences. . . . .	256
Arches, bibliography of special treatises on. . . . .	361
fixed framed. . . . .	178, 197
fixed solid web or masonry. . . . .	298
three-hinged. . . . .	72, 78
two-hinged. . . . .	153, 166, 176
without hinges. . . . .	178, 298

## B

Beams, deflection of. . . . .	117, 118, 123, 125, 126
work of deformation for. . . . .	41
Betti's law. . . . .	28
Bibliography of treatises, etc. . . . .	359

## C

Cantilever bridges by influence lines. . . . .	67
Castigliano's law, derivative of work equation. . . . .	30, 31
Centrifugal force due to curved track. . . . .	260
Changes in the angles of a triangle due to stress. . . . .	107
Choice of the redundant conditions. . . . .	202
Clapeyron's law. . . . .	2, 14
Column formulæ. . . . .	270
Combination of stresses as a basis for design- ing. . . . .	268
Continuous girder over four supports. . . . .	130
three supports. . . . .	129, 143, 148
Critical loading for max. moments, direct loading. . . . .	59
Critical loading for max. moments, indirect loading. . . . .	60
Critical loading for max. shear, direct loading. . . . .	62
, indirect loading . . . . .	62

## D

	PAGE
Dead-load stresses in determinate structures . . . . .	210
Definitions of terms used throughout this work. . . . .	vii
Deflection influence lines. . . . .	49
of a solid web beam. . . . .	117
polygons according to Prof. Laud . . . . .	107
polygons according to Prof. Mohr, . . . . .	100, 104
polygons for determinate structures. . . . .	99
polygons for the loaded chord. . . . .	104
Deformations. . . . .	11
Deformation, work due to. . . . .	1, 29
Derivative of the work equation; Castigliano's law. . . . .	30, 31
Designing, combination of stresses as a basis for. . . . .	268
Determinate structures, dead load stresses in. . . . .	210
displacements of . . . . .	18
displacement influence lines for. . . . .	122
influence lines for. . . . .	46, 65
stresses in . . . . .	210, 218
Direct and indirect loading. . . . .	47, 48, 50
Displacement influence lines, determinate structures. . . . .	122
for a cantilever. . . . .	124
for a simple beam or truss. . . . .	123, 125, 126
Displacements, horizontal. . . . .	114
of points for determinate structures. . . . .	18
Distortion of a statically determinate frame by graphics. . . . .	87
Distortions due to changes in the lengths of members. . . . .	87
Double intersection trusses by influence lines. . . . .	65
Dynamic impact. . . . .	262
work of deformation due to. . . . .	43
influences. . . . .	256

E		PAGE
Eccentric connections, stresses produced by...	255	
Effects due to unusual loads.....	266	
Effect of shop lengths on determinate structures	256	
indeterminate struc-		
tures.....	208	
Elastic deformations.....	11	
Elastic loads $w$ in terms of angle changes.	109, 111	
Equation of an influence line.....	47	
Equations, solution of simultaneous.....	295	
Externally indeterminate, definition of .....	6	
External redundant, influence line for one.	128, 140	
F		
Fatigue of material.....	265	
Features in design intended to diminish second-		
ary stresses.....	267	
Fixed framed arches.....	178	
effect of abutment dis-		
placements.....	188	
example .....	189	
influence lines for the re-		
dundants.....	184	
location of the coordinate		
axes.....	182	
resultant polygon for....	187	
stress influence lines for..	185	
temperature stresses in ..	188	
Fixed masonry arches.....	298	
coordinate axes and		
elastic loads, 314, 331, 346		
critical sections.....	322	
determination of the		
redundants .....	309	
example of symmetric..	326	
example of unsymmet-		
ric.....	346	
influence lines for the		
redundants. 317, 333, 351		
maximum stresses,		
322, 344, 357		
modern methods of con-		
struction.....	301	
preliminary design for,		
304, 326		
resultant polygons,		
324, 335, 357		
stresses on any normal		
section.....	320, 344	
temperature stresses in,		
318, 345, 357		
Framed structures, theorems, laws and formulæ		PAGE
for.....	11	
G		
General case of redundancy.....	203	
Girder continuous over four supports.....	130	
three supports. 129, 143, 148		
fixed at one end, supported at the other.	140	
Glossary of terms.....	vii	
Graphostatics, bibliography.....	359	
H		
Horizontal displacements.....	114	
I		
Impact due to dynamic effects.....	262	
formulæ.....	264	
Indeterminate, externally.....	6	
internally.....	6	
Indeterminate straight beams, work of defor-		
mation.....	41	
structures by Maxwell's law....	24	
by Mohr's work equa-		
tion.....	19	
effect of abutment		
displacements. 32, 208		
effect of shop lengths	208	
effect of temperature	206	
influence lines for,		
127, 140		
influence line for one		
redundant .....	127	
stress influence lines		
for.....	137, 139, 140	
Influence line, equation for.....	47	
defined.....	46	
for cantilever bridges.....	67	
deflections.....	49	
determinate structures,		
46, 65, 218		
direct loading.....	48	
displacements of determinate		
structures.....	122	
double intersection trusses ..	65	
indeterminate structures. 127, 140		
indirect loading.....	50	
moments.....	49, 50	
one external redundant. 128, 140		
one internal redundant .....	128	
one redundant condition....	127	
shear.....	49, 50	

	PAGE
Influence line for skew plate girder on curved	
double track.....	80
stresses in truss members...	52
reactions.....	48, 50
redundants in fixed masonry	
arches.....	317, 333
three-hinged arches.....	72
three-hinged masonry arches	78
three-hinged solid web	
arches.....	78
trusses with subdivided	
panels.....	83
two redundant conditions...	130
Internal redundant, influence lines for one....	128
Internally indeterminate.....	6, 7
Introduction.....	1
Isotropic bodies, theorems, laws and formulæ	
for.....	34

K

Kernel moment influence areas for three-hinged solid web arch.....	79
Kernel moment influence areas for two-hinged solid web arches.....	159

L

Lateral trusses, stresses due to wind, etc..	258, 261
vibrations.....	260
Least work, theorem of.....	29
Live load stresses.....	218, 219
author's method.....	219
Load divide for a truss.....	51
Loading, direct and indirect.....	47, 48, 50

M

Masonry arches, see under Arches.	
Maxwell's theorem of reciprocal displacements.	27
Menabrea's law of least work.....	29, 31
Mitering lock gates.....	271
example.....	279
theory of the analysis....	273
Mohr's rotation diagram.....	89
work equations.....	16, 17
Moment influence lines.....	49, 50
Moving load stresses.....	218, 219
Multiple redundancy.....	132, 137
simplification of influence	
lines for.....	132, 135

N

Nature of secondary stresses.....	226
-----------------------------------	-----

P

	PAGE
Plate girder continuous over four supports...	130
over three supports,	
129, 143, 148	
deflection of.....	117
fixed at one end and supported at	
the other.....	140
Positions of a moving load for max. moments...	57
for max. shears.....	62
Preface.....	v
Principle of virtual velocities.....	2, 16
work.....	1, 15

R

Reaction conditions.....	5
influence lines.....	48, 50
summation influence lines.....	54
Redundancy, simplification of influence lines	
for.....	132, 135
solution of the general case of...	203
stress influence lines for struc-	
tures involving same.	137, 139, 140
Redundant conditions.....	5
influence lines for one...	128
influence lines for two...	130
on the choice of.....	202
Ritter's method of moments.....	211
Rotation diagram, Mohr's.....	89
of a rigid frame about a fixed point..	89

S

Secondary and additional stresses, bibliog-	
raphy.....	360
Secondary stresses.....	226
as effected by certain de-	
signs.....	267
concluding remarks on.....	267
due to riveted connections,	
227, 235	
due to various causes.....	251
in members due to eccentric	
connections.....	255
in members due to their own	
weight.....	251
in pin-connected structures.	253
in riveted cross-frames, load	
effects.....	244
in riveted cross-frames, wind	
effects.....	247
the nature of.....	226
Shear influence lines.....	49, 50
Shearing stress, work of deformation due to..	38









THIS BOOK IS DUE ON THE LAST DATE  
STAMPED BELOW

AN INITIAL FINE OF 25 CENTS  
WILL BE ASSESSED FOR FAILURE TO RETURN  
THIS BOOK ON THE DATE DUE. THE PENALTY  
WILL INCREASE TO 50 CENTS ON THE FOURTH  
DAY AND TO \$1.00 ON THE SEVENTH DAY  
OVERDUE.

SEP. 28 1932

JUN 22 1940

OCT 26 1932

APR 29 1942 U

MAY 3 1943

APR 28 1947

DEC 10 1932 14 DAYS AFTER RECEIPT

NON-RENEWABLE

MAR 13 1934

JAN 30 1978

APR 23 1937

REC. ILL FEB 22 1978

MAR 23 1933

LD 21-50m-8,32



YD 02782

215133

TG 260

M7

UNIVERSITY OF CALIFORNIA LIBRARY

